NUREG/IA-0213, Vol. 2
IRSN/DPAM 2005-275
NSI RRC KI 3230

International Agreement Report

Experimental Study of Narrow Pulse Effects on the Behavior of High Burnup Fuel Rods with Zr-1%Nb Cladding and UO_2 Fuel (VVER Type) under Reactivity-Initiated Accident Conditions: Test Conditions and Results

Prepared by
L. Yegorova, K. Lioutov, N. Jouravkova
Nuclear Safety Institute of Russian Research Centre "Kurchatov Institute"
Kurchatov Square 1, Moscow 123182, Russian Federation

O. Nechaeva, A. Salatov
A.A. Bochvar All-Russian Research Institute of Inorganic Materials
Rogov Street 5, Moscow 123182, Russian Federation

V. Smirnov, A. Goryachev
State Research Centre "Research Institute of Atomic Reactors"
Dimitrovgrad 433510, Russian Federation

V. Ustinenko, I. Smirnov
Russian Federal Nuclear Centre "All-Russian Research Institute of Experimental Physics"
Sarov 607200, Russian Federation

Office of Nuclear Regulatory Research
U.S. Nuclear Regulatory Commission
Washington, DC 20555-0001

March 2006

Prepared for
U.S. Nuclear Regulatory Commission (United States),
Institute for Radiological Protection and Nuclear Safety (France),
and Joint Stock Company "TVEL" (Russian Federation)

Published by
U.S. Nuclear Regulatory Commission

AVAILABILITY OF REFERENCE MATERIALS IN NRC PUBLICATIONS

NRC Reference Material

As of November 1999, you may electronically access NUREG-series publications and other NRC records at NRC's Public Electronic Reading Room at http://www.nrc.gov/reading-rm.html. Publicly released records include, to name a few, NUREG-series publications; *Federal Register* notices; applicant, licensee, and vendor documents and correspondence; NRC correspondence and internal memoranda; bulletins and information notices; inspection and investigative reports; licensee event reports; and Commission papers and their attachments.

NRC publications in the NUREG series, NRC regulations, and *Title 10, Energy*, in the Code of *Federal Regulations* may also be purchased from one of these two sources.

1. The Superintendent of Documents
   U.S. Government Printing Office
   Mail Stop SSOP
   Washington, DC 20402–0001
   Internet: bookstore.gpo.gov
   Telephone: 202-512-1800
   Fax: 202-512-2250
2. The National Technical Information Service
   Springfield, VA 22161–0002
   www.ntis.gov
   1–800–553–6847 or, locally, 703–605–6000

A single copy of each NRC draft report for comment is available free, to the extent of supply, upon written request as follows:

Address: Office of the Chief Information Officer,
Reproduction and Distribution
Services Section
U.S. Nuclear Regulatory Commission
Washington, DC 20555-0001
E-mail: DISTRIBUTION@nrc.gov
Facsimile: 301–415–2289

Some publications in the NUREG series that are posted at NRC's Web site address http://www.nrc.gov/reading-rm/doc-collections/nuregs are updated periodically and may differ from the last printed version. Although references to material found on a Web site bear the date the material was accessed, the material available on the date cited may subsequently be removed from the site.

Non-NRC Reference Material

Documents available from public and special technical libraries include all open literature items, such as books, journal articles, and transactions, *Federal Register* notices, Federal and State legislation, and congressional reports. Such documents as theses, dissertations, foreign reports and translations, and non-NRC conference proceedings may be purchased from their sponsoring organization.

Copies of industry codes and standards used in a substantive manner in the NRC regulatory process are maintained at—

The NRC Technical Library
Two White Flint North
11545 Rockville Pike
Rockville, MD 20852–2738

These standards are available in the library for reference use by the public. Codes and standards are usually copyrighted and may be purchased from the originating organization or, if they are American National Standards, from—

American National Standards Institute
11 West 42nd Street
New York, NY 10036–8002
www.ansi.org
212–642–4900

Legally binding regulatory requirements are stated only in laws; NRC regulations; licenses, including technical specifications; or orders, not in NUREG-series publications. The views expressed in contractor-prepared publications in this series are not necessarily those of the NRC.

The NUREG series comprises (1) technical and administrative reports and books prepared by the staff (NUREG–XXXX) or agency contractors (NUREG/CR–XXXX), (2) proceedings of conferences (NUREG/CP–XXXX), (3) reports resulting from international agreements (NUREG/IA–XXXX), (4) brochures (NUREG/BR–XXXX), and (5) compilations of legal decisions and orders of the Commission and Atomic and Safety Licensing Boards and of Directors' decisions under Section 2.206 of NRC's regulations (NUREG–0750).

DISCLAIMER: Where the papers in these proceedings have been authored by contractors of the U. S. Government, neither the U.S. Government nor any agency thereof, nor any U.S. employee makes any warranty, expressed or implied, or assumes any legal liability or responsibility for any third party's use or the results of such use, of any information, apparatus, product, or process disclosed in these proceedings, or represents that its use by such third party would not infringe privately owned rights. The views expressed in these proceedings are not necessarily those of the U. S. Regulatory Commission.

NUREG/IA-0213, Vol. 2
IRSN/DPAM 2005-275
NSI RRC KI 3230

International Agreement Report

Experimental Study of Narrow Pulse Effects on the Behavior of High Burnup Fuel Rods with Zr-1%Nb Cladding and UO_2 Fuel (VVER Type) under Reactivity-Initiated Accident Conditions: Test Conditions and Results

Prepared by
L. Yegorova, K. Lioutov, N. Jouravkova
Nuclear Safety Institute of Russian Research Centre "Kurchatov Institute"
Kurchatov Square 1, Moscow 123182, Russian Federation

O. Nechaeva, A. Salatov
A.A. Bochvar All-Russian Research Institute of Inorganic Materials
Rogov Street 5, Moscow 123182, Russian Federation

V. Smirnov, A. Goryachev
State Research Centre "Research Institute of Atomic Reactors"
Dimitrovgrad 433510, Russian Federation

V. Ustinenko, I. Smirnov
Russian Federal Nuclear Centre "All-Russian Research Institute of Experimental Physics"
Sarov 607200, Russian Federation

Office of Nuclear Regulatory Research
U.S. Nuclear Regulatory Commission
Washington, DC 20555-0001

March 2006

Prepared for
U.S. Nuclear Regulatory Commission (United States),
Institute for Radiological Protection and Nuclear Safety (France),
and Joint Stock Company "TVEL" (Russian Federation)

Published by
U.S. Nuclear Regulatory Commission

ABSTRACT

This volume of the report contains a detailed description of calculation and test results obtained in the fast-pulse-graphite-reactor (BIGR) tests of twelve fuel rods refabricated from the VVER-440 and VVER-1000 high burnup fuel elements (50, 60 MW d/kg U).

The BIGR data base includes the following types of fuel rod characterization:

- material and geometrical parameters of VVER-440 and VVER-1000 commercial fuel elements before the base irradiation in the nuclear power plant (NPP);
- parameters of fuel cycles and characteristics of commercial fuel elements after the base irradiation;
- characteristics of twelve refabricated fuel rods before the BIGR pulse tests;
- parameters of the BIGR power pulses;
- characteristics of refabricated fuel rods during and after the BIGR tests.

FOREWORD

This two-volume report provides results of a cooperative research program involving the Russian Research Center–Kurchatov Institute, the French Institute for Radiological Protection and Nuclear Safety (IRSN), and the United States Nuclear Regulatory Commission (NRC). The research addresses the behavior of high-burnup nuclear fuel under postulated reactivity-initiated accident (RIA) conditions, based on experimental results from the Russian fast-pulse graphite reactor, known as BIGR.

The Kurchatov Institute initiated its RIA test program in 1983, several years before the accident at Chernobyl. That accident, which resulted from a rapid increase in reactivity, demonstrated that severe fuel damage may occur too quickly to be easily mitigated. However, the consequences of such an event can be reduced by thorough understanding and design.

Information concerning Russian reactivity insertion experiments in the Impulse Graphite Reactor (IGR) was first revealed to western observers in 1992. Differences between IGR and other fuel behavior tests were initially attributed to differences in Russian fuel designs and the larger pulse width of the IGR test reactor. However, the test rods used in the IGR were taken from zirconium-niobium clad uranium dioxide (UO_2) fuel rods that were commercially irradiated in pressurized, light-water-reactors. This type of cladding material is used throughout the world, and generated great interest. The IRSN and NRC recognized the value of this test program and, in 1995, joined with the Kurchatov Institute in assessing and interpreting the IGR data. Then, in July 1999, the agencies jointly published the results in a three-volume compendium, identified as NUREG/IA-0156, "Data Base on the Behavior of High Burnup Fuel Rods with Zr-1%Nb Cladding and UO_2 Fuel (VVER Type) Under Reactivity Accident Conditions."

More recently, the Kurchatov Institute addressed the issue of the broad pulse width effects in the IGR with a series of narrow pulse width experiments in the BIGR fast-pulse graphite reactor. The work was performed in cooperation with other Russian institutes and support of the Russian fuel vendor (Joint Stock Company "TVEL"). Pulses produced by the two test reactors span an extraordinary range, from 3 milliseconds in BIGR to over 700 milliseconds in IGR, and bound the expected pulse widths for postulated RIA events in commercial light-water reactors. Taken together, these test results show that cladding with very light corrosion is remarkably resistant to failure — even under high-burnup conditions.

Results of the BIGR program, as documented in this report, demonstrate the continued value of the cooperative efforts of the Kurchatov Institute, the IRSN, and the NRC. This collaborative program further allows a comparison of conclusions from other data sources (e.g., France, Japan, and the U.S.). By comparing these results, studying the employed techniques, and creating a common language necessary for the mutual understanding these events, it will be possible to establish more appropriate regulatory limits for reactivity-initiated accidents.



Vladimir G. Asmolov, Director
Research and Development
Russian Research Centre -
"Kurchatov Institute"



Michel Schwarz, Director
Major Accident
Prevention Division
Institut de Radioprotection
et de Sûreté Nucléaire



Carl J. Paperiello, Director
Office of Nuclear
Regulatory Research
U.S. Nuclear Regulatory
Commission

TABLE OF CONTENTS

Page

ABSTRACT iii

FOREWORD v

TABLE OF CONTENTS vii

LIST OF APPENDICES ix

ACKNOWLEDGEMENTS xi

EXECUTIVE SUMMARY 1.1

GUIDE TO THE DATA BASE 2.1

COMMENTS TO APPENDIX A 2.1

COMMENTS TO APPENDIX B 2.1

COMMENTS TO APPENDIX C 2.2

COMMENTS TO APPENDIX D 2.2

COMMENTS TO APPENDIX E 2.2

APPENDIX A Reference Characteristics of VVER-440 and VVER-1000 Commercial Fuel Elements before the Base Irradiation A-1

APPENDIX B Fuel Cycle Parameters and Post-Irradiation Characteristics of Commercial Fuel Rods B-1

APPENDIX C Characteristics of Refabricated Fuel Rods before the BIGR Tests C-1

APPENDIX D Characteristics of the BIGR Power Pulses D-1

APPENDIX E Characteristics of Refabricated Fuel Rods after the BIGR Tests E-1

LIST OF APPENDICES

		Page
Appendix A	**Reference Characteristics of VVER-440 and VVER-1000 Commercial Fuel Elements before the Base Irradiation**	**A-1**
Appendix B	**Fuel Cycle Parameters and Post-Irradiation Characteristics of Commercial Fuel Rods**	**B-1**
Appendix C	**Characteristics of Refabricated Fuel Rods before the BIGR Tests**	**C-1**
Appendix C-1	*Individual Characteristics of Fuel Rod # RT1 before the BIGR Test*	*C-7*
Appendix C-2	*Individual Characteristics of Fuel Rod # RT2 before the BIGR Test*	*C-15*
Appendix C-3	*Individual Characteristics of Fuel Rod # RT3 before the BIGR Test*	*C-23*
Appendix C-4	*Individual Characteristics of Fuel Rod # RT4 before the BIGR Test*	*C-31*
Appendix C-5	*Individual Characteristics of Fuel Rod # RT5 before the BIGR Test*	*C-39*
Appendix C-6	*Individual Characteristics of Fuel Rod # RT6 before the BIGR Test*	*C-47*
Appendix C-7	*Individual Characteristics of Fuel Rod # RT7 before the BIGR Test*	*C-55*
Appendix C-8	*Individual Characteristics of Fuel Rod # RT8 before the BIGR Test*	*C-63*
Appendix C-9	*Individual Characteristics of Fuel Rod # RT9 before the BIGR Test*	*C-71*
Appendix C-10	*Individual Characteristics of Fuel Rod # RT10 before the BIGR Test*	*C-79*
Appendix C-11	*Individual Characteristics of Fuel Rod # RT11 before the BIGR Test*	*C-87*
Appendix C-12	*Individual Characteristics of Fuel Rod # RT12 before the BIGR Test*	*C-95*
Appendix D	**Characteristics of the BIGR Power Pulses**	**D-1**
Appendix E	**Characteristics of Refabricated Fuel Rods after the BIGR Tests**	**E-1**
Appendix E-1	*Individual Characteristics of Fuel Rod # RT1 after the BIGR Test*	*E-1*
Appendix E-2	*Individual Characteristics of Fuel Rod # RT2 after the BIGR Test*	*E-15*
Appendix E-3	*Individual Characteristics of Fuel Rod # RT3 after the BIGR Test*	*E-29*
Appendix E-4	*Individual Characteristics of Fuel Rod # RT4 after the BIGR Test*	*E-43*
Appendix E-5	*Individual Characteristics of Fuel Rod # RT5 after the BIGR Test*	*E-59*
Appendix E-6	*Individual Characteristics of Fuel Rod # RT6 after the BIGR Test*	*E-75*
Appendix E-7	*Individual Characteristics of Fuel Rod # RT7 after the BIGR Test*	*E-91*

Appendix E-8 *Individual Characteristics of Fuel Rod # RT8 after the BIGR Test* *E-105*

Appendix E-9 *Individual Characteristics of Fuel Rod # RT9 after the BIGR Test* *E-121*

Appendix E-10 *Individual Characteristics of Fuel Rod # RT10 after the BIGR Test* *E-141*

Appendix E-11 *Individual Characteristics of Fuel Rod # RT11 after the BIGR Test* *E-157*

Appendix E-12 *Individual Characteristics of Fuel Rod # RT12 after the BIGR Test* *E-173*

Appendix E-13 *Azimuthal Distribution of Cladding Thickness for Fuel Rods ## RT7–12* *E-187*

ACKNOWLEDGEMENTS

The authors are deeply grateful the support and assistance of the following specialists in the Russian Federation:

- V. Sazhnov (Russian Federal Nuclear Centre "All-Russian Research Institute of Experimental Physics:): the performance of the BIGR tests with VVER refabricated fuel rods;
- A. Bortash, A. Zvyageen, V. Malofeev, A. Avvakumov, E. Kaplar (Nuclear Safety Institute and Institute of Nuclear Reactors of Russian Research Centre "Kurchatov Institute"): neutronic calculations and energy deposition determination;
- G. Maslov, V. Ilyin (Russian Federal Nuclear Centre "All-Russian Research Institute of Experimental Physics"): experimental measurements and computer calculations of neutronic parameters during the BIGR tests;
- A. Shestopalov (Nuclear Safety Institute of Russian Research Centre "Kurchatov Institute"): FRAP-T6/VVER calculations of thermal mechanical parameters of high burnup fuel rods under the BIGR test conditions;
- E. Zvir, L. Stupina, A. Svyatkin (State Research Centre "Research Institute of Atomic Reactors"): pre-test and post-test examinations of refabricated fuel rods including metallographic studies and computer processing of obtained data;
- A. Chetvyarikov (State Research Centre "Research Institute of Atomic Reactors"): the management by radio chemical measurements of the fuel isotopic composition;
- A. Konobeev, G. Abyshov (Nuclear Safety Institute of Russian Research Centre "Kurchatov Institute"): the computer processing of some experimental data.

Without the efforts of these individuals, and their willingness to share results of several special investigations, this report would not have been possible.

1. EXECUTIVE SUMMARY

Taking into account that the BIGR[a] tests were performed under reactivity-initiated-accident (RIA) conditions to widen the VVER[b] RIA high burnup fuel data base obtained earlier due to the pulse graphite reactor (IGR[c]) tests, it was decided to keep approximately the same format of the test data organization, which was developed during the preparation of the IGR/RIA data base [1]. In accordance with this approach, the Volume 2 of the BIGR report contains several types of test data listed in Fig. 1. As it can be observed from this Figure, the high burnup fuel rods tested in the BIGR reactor were refabricated from the VVER-440 and VVER-1000 fuel elements irradiated at the NovoVoronezh and Kola nuclear power plants (NV[d] NPP and Kola[e] NPP). To follow the evolution of the cladding and fuel changes from the beginning of fuel cycles at the NPP to RIA accident conditions at the burnup 50, 60 MW d/kg U, special measurements of fuel rod parameters were performed and presented in several Appendices of this volume of the report. The contents of each Appendix are given in Chapter 2 of this volume.

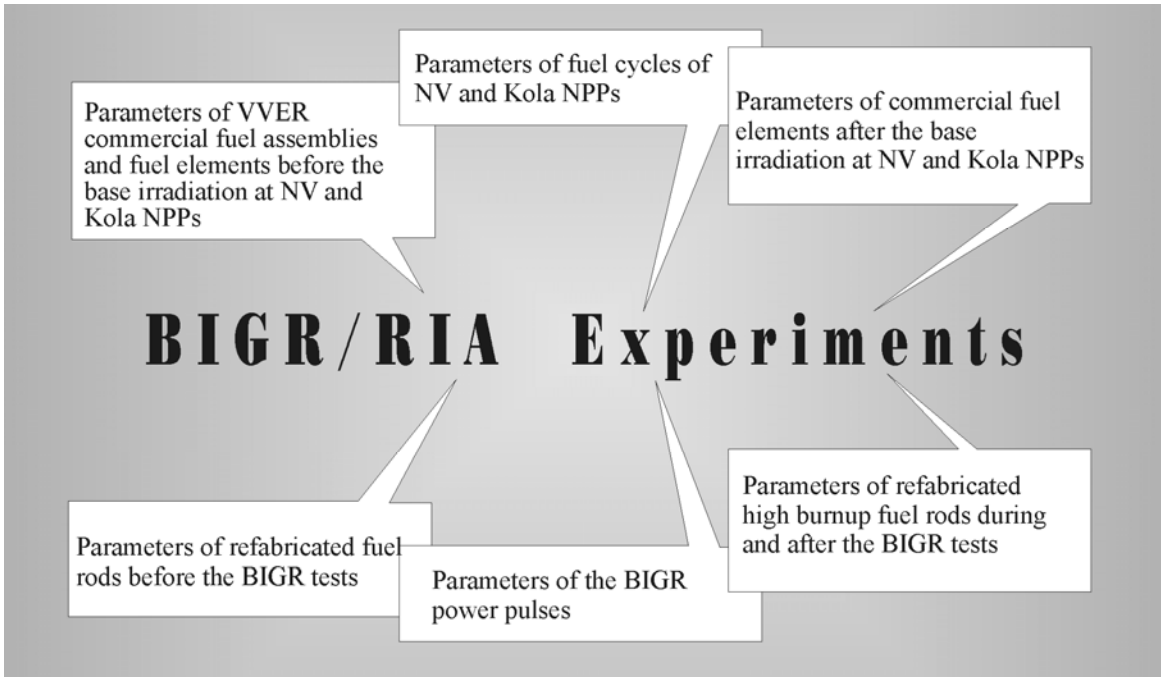


Fig. 1. Arrangement of the BIGR/RIA test results

[a] BIGR – Bystry Impulsny Graphitovy Reactor (Fast Pulse Graphite Reactor)

[b] VVER – Vodo-Vodyanoy Energetichesky Reactor (Russian type of Pressurized Water Reactor)

[c] IGR – Impulsny Graphitovy Reactor (Pulse Graphite Reactor)

[d] NV – Novovoronezhskay (Nuclear Power Plant)

[e] Kola – Kolskay (Nuclear Power Plant)

REFERENCES

[1] Yegorova L., Asmolov V., Abyshov G., Malofeev V., Avvakumov A., Kaplar E., Lioutov K., Shestopalov A., Bortash A., Maiorov L., Mikitiouk K., Polvanov V., Smirnov V., Goryachev A., Prokhorov V., and Vurim A. "Data Base on the Behavior of High Burnup Fuel Rods with Zr-1%Nb Cladding and UO_2 Fuel (VVER Type) under Reactivity Accident Conditions", RRC "Kurchatov Institute" report NSI RRC 2179, Vol.1-3, 1999 (also USNRC report NUREG/IA-0156 and IPSN report IPSN 99/08–2).

2. GUIDE TO THE DATA BASE

The BIGR/RIA data base is subdivided into five subject sets of data presented in the following Appendices:

Appendix A	Reference Characteristics of VVER-440 and VVER-1000 Commercial Fuel Elements before the Base Irradiation
Appendix B	Fuel Cycle Parameters and Post-Irradiation Characteristics of Commercial Fuel Rods
Appendix C	Characteristics of Refabricated Fuel Rods before the BIGR Tests
Appendix D	Characteristics of the BIGR Power Pulses
Appendix E	Characteristics of Refabricated Fuel Rods after the BIGR Tests

The subsections of this Chapter contain some important comments, which may simplify the work with this data base.

2.1. Comments to Appendix A

In this Appendix reference parameters of three fuel assemblies of the VVER-440 and VVER-1000 types are presented. The most part of these parameters was determined with using the standard documentation of the manufacturer. As for differences in characteristics of these assemblies at the beginning of the base irradiation, the following parameters may be pointed out:

- the initial fill gas pressure in VVER-440 fuel elements (Helium, 0.5–0.7 MPa)[a] is lesser significantly than that in VVER-1000 fuel elements (Helium, 1.9–2.6 MPa)[a];
- each of these three fuel assemblies had fuel elements with a central hole, but of a different diameter fuel pellet (1.2, 1.6–1.7, 2.4 mm);
- two types of fuel pellets were used in these fuel assemblies:
  - simple cylindrical pellets;
  - cylindrical pellets with chamfers.

2.2. Comments to Appendix B

This Appendix contains two types of the data:

1. The data characterizing fuel cycles of six fuel elements, which were used for the manufacturing of twelve refabricated fuel rods tested in the BIGR reactor.
2. The data characterizing parameters of these six fuel elements in accordance with the post-irradiation-examination (PIE) results.

The first type of the data allowed to perform neutronic calculations of base irradiation histories for these fuel elements. Due to these calculations, radial and axial distributions of the isotopic composition of high burnup fuel was determined in the each fuel element.

The second type of the data characterizes the microstructure of fuel and cladding for six fuel elements, the fission gas release (FGR) at the end of irradiation, fuel burnup, hydrogen content in the irradiated cladding and geometrical sizes of high burnup fuel and irradiated cladding. The analysis of these data allowed to reveal the following important features:

- four fuel elements of the VVER-1000 type had approximately the similar maximum burnup (47.8–50.12 MW d/kg U), geometrical parameters of fuel and cladding, cladding hydrogen content ($5 \cdot 10^{-3}$ % by volume), rim layer thickness (0.05–0.07 mm) and residual value of fuel/cladding gap (0.017–0.032 mm);
- two fuel elements of the VVER-440 type had the similar maximum burnup also (61.6 and 61.7 MW d/kg U). Unfortunately, it was impossible to compare the most part of other characteristics for these fuel elements because the PIE data of one of these elements were very limited;
- nevertheless, the comparison of parameters of fuel elements on two levels of the maximum fuel burnup (47.8–50.12 and 61.6–61.7 MW d/kg U correspondently) allowed to reveal that:

[a] This parameter is presented at the room temperature

- the rim layer thickness was increased from 50–70 μm at 50 MW d/kg U up to 150–200 μm at 62 MW d/kg U burnup;
- a radial fuel/cladding gap was not apparent at 62 MW d/kg U burnup;
- the hydrogen content in the irradiated cladding was somewhat increased at 62 MW d/kg U burnup. This fact correlates with the data presented in Table C.1 of Appendix C to characterize the cladding oxidation after the base irradiation. These data showed that at 50 MW d/kg U burnup, the irradiated cladding was covered with the 3–5 μm zirconium dioxide layer on the outer surface only. At 62 MW d/kg U burnup, the oxidation of the cladding internal surface was observed. The thickness of inner ZrO_2 layer was 8–10 μm although the outer oxide layer remained 3–5 μm.

2.3. Comments to Appendix C

This Appendix is devoted to the presentation of measured and calculated parameters of twelve refabricated fuel rods before the BIGR tests. The individual characterization of each fuel rod is contained in Appendices C-1 – C-12. Besides, the reference and average representative values of parameters are listed in Tables C.1–C.3 of Appendix C. Design schemes of refabricated fuel rods supplement this data base.

Individual characteristics of fuel rods presented in Appendices C-1 – C-12 include the following graphical and tabular data:

- radial distribution of isotopic nuclear concentrations in four radial fuel layers;
- axial distributions of the cladding average outer diameter, fuel mass, gas flow area, burnup, intensity of Cs and Eu isotopes and results of the eddy current examination.

General differences between initial parameters of these fuel rods were as follows:

- eight fuel rods had burnup in the range 46.9–48.6 MW d/kg U and four fuel rods had the burnup in the range 59.8–60.5 MW d/kg U;
- ten fuel rods had the initial fill gas pressure in the range 2.0–2.1 MPa and two fuel rods had the initial fill gas pressure 0.1 MPa;
- the fuel stack in one fuel rod (#RT3) was damaged at the refabrication. The obtained fuel configuration (along the axis) is presented in the data base.

2.4. Comments to Appendix D

This Appendix consists of the following data characterizing the BIGR pulse conditions:

- the BIGR power history at the test of each fuel rod;
- pulse half-width for the BIGR tests of twelve fuel rods.

The BIGR power histories presented in this Appendix have the status of the as-measured parameter. This data base was developed in accordance with the neutron detector recording. The procedure of these experimental data transformation into the input data for the computer codes is described in the Volume 1 of the report.

2.5. Comments to Appendix E

This appendix consists of twelve subappendices with the following types of data:

- appearance of the fuel rod and photographs of fuel and cladding microstructure obtained in the PIE procedures;
- time dependent energy characteristics of the fuel rod during the BIGR test (power, number of fissions, energy deposition, fuel enthalpy). It should be noted that two independent procedures were used to determine neutronic parameters of the fuel rod versus time and the fuel enthalpy versus time. In the first case, these two procedures were developed in the Russian Research Centre “Kurchatov Institute” (RRC KI) and Russian Federal Nuclear Centre “All-Russian Research Institute of Experimental Physics” (VNIIEF) (see volume 1 of the report).

In the second case, two different codes (FRAP-T6/VVER and RAPTA-5) were used in the RRC KI and A.A. Bochvar All-Russian Research Institute of Inorganic Materials (VNIINM) to calculate the fuel enthalpy (see volume 1 of the report). Taking into account that results of neutronic calculations performed in accordance with RRC KI and VNIIEF procedures are very similar, the tabular data contain the average values only. The RRC KI and

VNIINM data characterizing the fuel enthalpy are similar in general. But to compare definite differences in these data, results of both calculations are presented in the report:

- to illustrate the specific character of the energy deposition radial distribution in the high burnup fuel, the tabular and graphical data were incorporated into the data base. In addition to these data, the transformation of the fuel enthalpy radial profile as a function of time is presented also in accordance with the FRAP-T6/VVER and RAPTA-5 calculations;
- the interpretation of the fuel rod thermal mechanical behavior during the BIGR test is presented in accordance with results of FRAP-T6/VVER and RAPTA-5 calculations;
- PIE results characterizing the cladding and fuel strain, cladding oxidation and FGR are listed in the graphical and tabular forms. Appendix A–13 contains the data base characterizing the azimuthal distribution of cladding thickness in fuel rods ## RT7–12 obtained duel to the processing of cross-section images;
- the last position of each subappendix contains the major results of the BIGR test in accordance with the calculated and experimental data.

To overcome the difficulties with terminology used in this Appendix, a special glossary is presented in Table 2.1.

Table 2.1. The glossary of neutronics and energy parameters presented in Appendix E

Term	Meaning of term
1. Relative reactor power vs. time (per-unit)	The reactor power in the place of the VVER fuel rod installation determined in accordance with the procedure presented in Volume 1 of the report
2. Cumulative number of fissions in the fuel rod vs. time (fiss.)	A total number of fissions occurred within the whole fuel mass by the i-time
3. Power of fuel rod vs. time (kW)	Power generated in the total mass of fuel due to the whole set of fissile isotopes by the i-time
4. Energy deposition in the fuel rod vs. time (cal/g fuel)	Energy generated in the whole fuel mass by i-time and normalized for the fuel mass
5. Number of fissions vs. radial fuel layer (fiss.)	A total number of fissions occurred in the undamaged part of a given radial layer of the fuel column within 0–∞ s
6. Power vs. radial fuel layer (kW)	The maximum power noted during the BIGR test in the radial fuel layer
7. Energy deposition vs. radial fuel layer (cal/g fuel)	Total energy deposition generated in a given radial layer normalized for the fuel mass within time interval 0–∞ s
8. Energy deposition vs. radial fuel layer (per-unit)	Energy deposition of a given radial layer of the fuel column normalized for energy deposition in the 4^{th} radial layer
9. Fuel enthalpy vs. time (cal/g fuel)	Radially averaged fuel enthalpy versus time for any cross-section (the axial peak power factor is 1)

APPENDIX A

REFERENCE CHARACTERISTICS OF VVER-440 AND VVER-1000 COMMERCIAL FUEL ELEMENTS BEFORE THE BASE IRRADIATION

Table A.1. Reference characteristics of VVER commercial fuel element before the irradiation

Characteristic	Unit	Value		
Fuel assembly type	–	VVER-440	VVER-1000	VVER-440
Commercial number of fuel assembly	–	14422222	ED4108	23635228
1. UO_2 fuel				
1.1. Isotopic composition				
U^{235}	% by weight	4.37*	4.40	3.60
U^{238}	% by weight	95.57	95.54	–
U^{234}	% by weight	0.03	0.03	–
U^{236}	% by weight	0.03*	0.03	–
1.2. Enrichment	%	4.37*	4.40	3.60
1.3. Oxygen-to-metal ratio	per-unit	2.001–2.002*	2.000–2.015	–
1.4. Density	g/cm^3	10.5–10.7*	10.5–10.8	10.4–10.8
1.5. Grain size	μm	6.6*	4–8	–
1.6. Pellet shape	–	without chamfers	without chamfers	with chamfers
1.7. Pellet outer diameter	mm	7.54–7.58*	$7.57_{-0.04}$	$7.60_{-0.07}$
1.8. Diameter of central hole	mm	1.6–1.7*	2.4±0.05	$1.20^{+0.8}$
1.9. Pellet height	mm	8–14	9–14	11±3
1.10. Fuel mass	g	1087±22	1469±22	1041±21
2. Zr-1%Nb cladding				
2.1. Composition:				
Zr	% by weight	98.67–98.87	98.67–98.87	98.67–98.87
Nb	% by weight	0.9–1.1	0.9–1.1	0.9–1.1
O_2	% by weight	< 0.1	< 0.1	< 0.1
N, C, Si, Al, Mo, Ni, Fe	% by weight	< 0.13	< 0.13	< 0.13
2.2. Outer diameter	mm	$9.1^{+0.1}_{-0.05}$	$9.13^{+0.06}_{-0.05}$	$9.1^{+0.1}_{-0.05}$
2.3. Inner diameter	mm	$7.72^{+0.08}$	$7.72^{+0.08}$	$7.72^{+0.08}$
3. Fuel rod				
3.1. Design	–	See Fig. A.1	See Fig. A.2	See Fig. A.3
3.2. Upper plenum length	m	$85^{+8.0}_{-9.0}$	$239^{+21.0}_{-4.0}$	–
3.3. Fuel stack length	mm	2420^{+10}_{-10}	3530^{+4}_{-12}	2320^{+10}_{-10}
3.4. Gas pressure**	MPa	0.5–0.7	1.9–2.6	0.5–0.7
3.5. Gas composition	–	He	He	He
3.6. Internal void volume	cm^3	13.7	14.5	38.3
3.7. Pitch***	mm	12.2	12.75	12.2
3.8. Hydraulic diameter	mm	8.93	10.5	8.93

* These values were measured during the fabrication. Other values were determined from specifications of fuel rods

** At the room temperature

*** The distance between the centers of 2 adjacent rods in the VVER hexagonal geometry

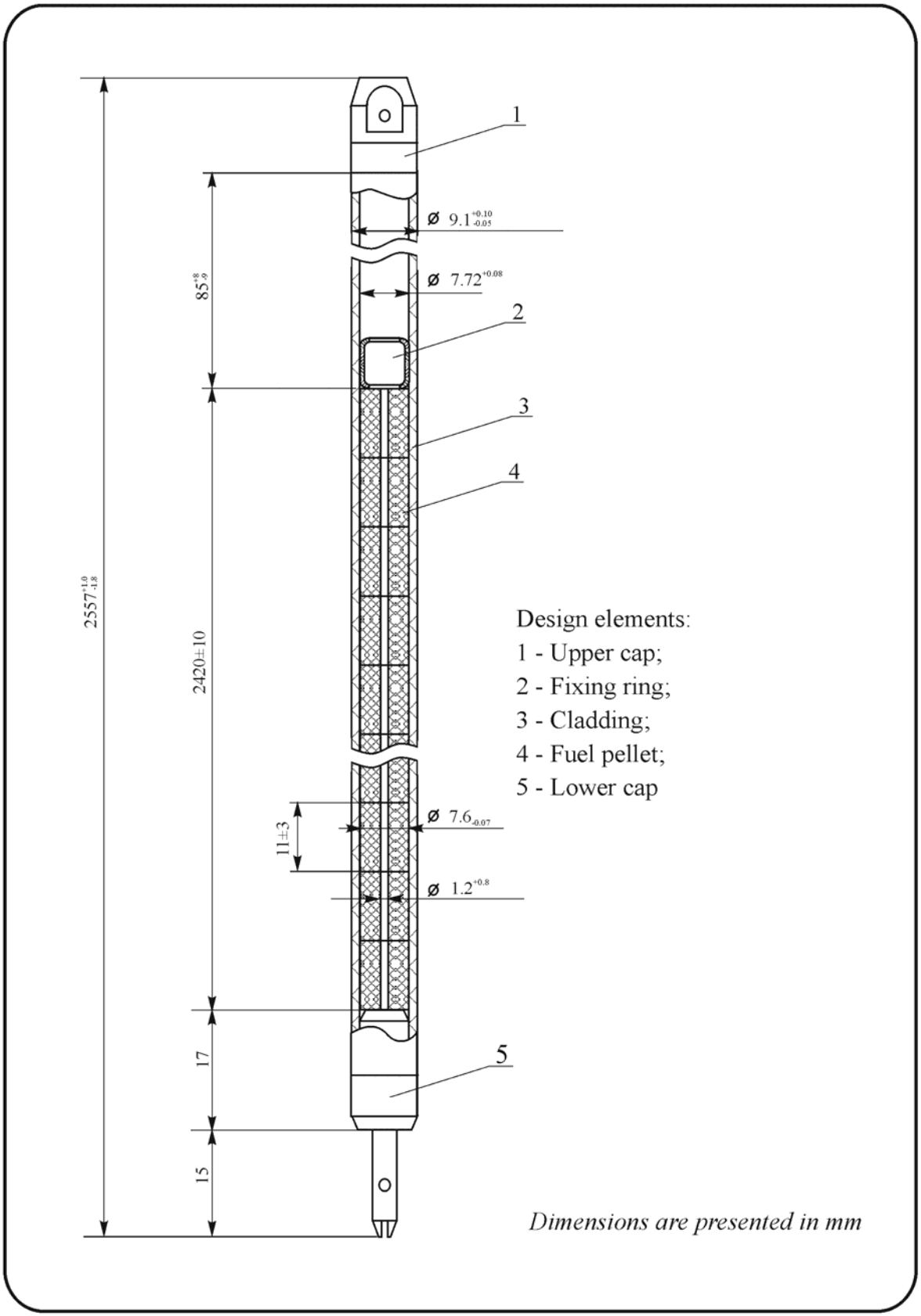


Fig. A.1. Design scheme of VVER-440 commercial fuel rod from the fuel assembly #14422222

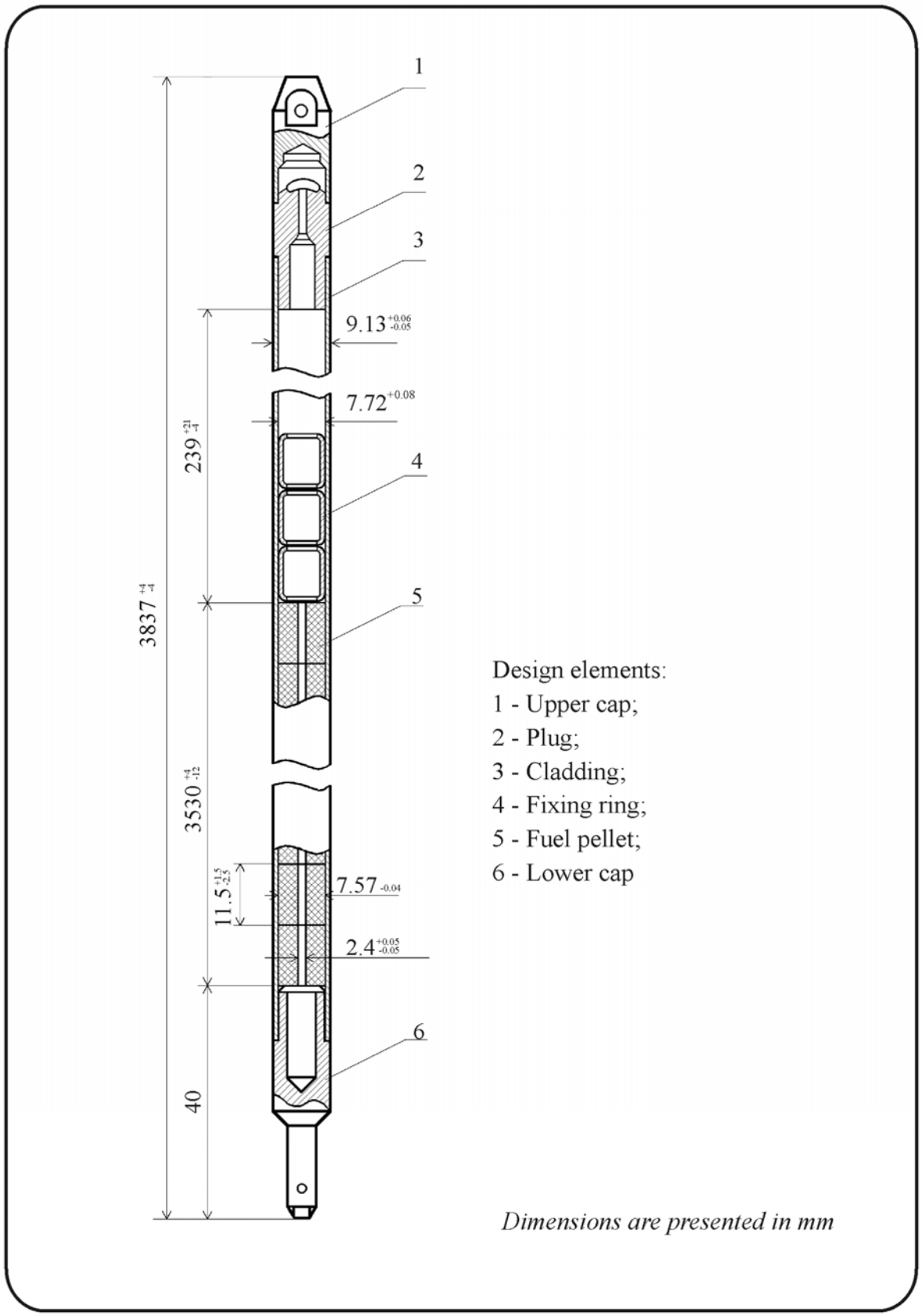


Fig. A.2. Design scheme of VVER-1000 commercial fuel rod from the fuel assembly #ED4108

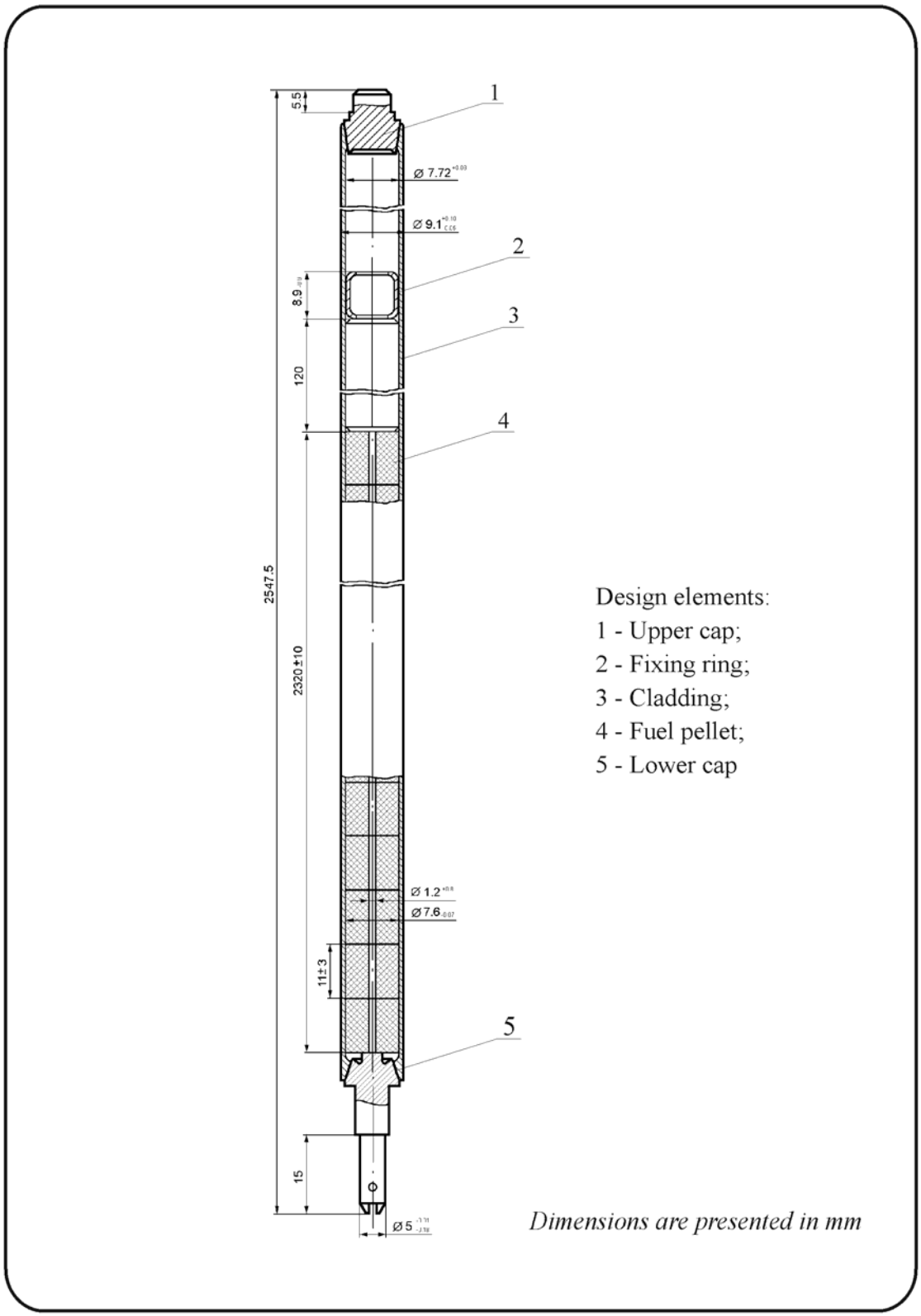


Fig. A.3. Design scheme of VVER-440 commercial fuel rod from the fuel assembly #23635228

APPENDIX B

FUEL CYCLE PARAMETERS AND POST-IRRADIATION CHARACTERISTICS OF COMMERCIAL FUEL RODS

Table B.1. Base irradiation history of fuel assembly #14422222

Characteristic	Unit	Value
1. Number of fuel assembly	–	14422222
2. Operation place	–	3rd unit of Kola NPP
3. Number of cycles	–	5
4. Operation periods	ef.day	245.6; 336.0; 298.5; 379.7; 305.5[a]
5. Irradiation beginning	–	24.09.86
6. Irradiation end	–	15.10.91
7. Reactor thermal power	MW	1375
8. Fuel assembly location in the reactor for each fuel cycle	–	See Fig. B.1.
9. The arrangement of fuel rods in the fuel assembly	–	See Fig. B.2
10. Boric acid concentration for each fuel cycle	g/kg	5.95; 6.84; 6.71; 7.38; 5.26
11. Inlet coolant temperature	C	268
12. Outlet coolant temperature	C	298
13. Coolant pressure	MPa	12.8
14. Mass flow rate	kg/m^2s	4000
15. Power history[b]	–	see Table B.6

Table B.2. Base irradiation history of fuel assembly #ED4108

Characteristic	Unit	Value
1. Number of fuel assembly	–	ED4108
2. Operation place	–	5th unit of NovoVoronezh NPP
3. Number of cycles	–	3
4. Operation periods	ef.day	301.7; 261.7; 317.8[a]
5. Irradiation beginning	–	05.06.86
6. Irradiation end	–	11.07.90
7. Reactor thermal power	MW	3000
8. Fuel assembly location in the reactor for each fuel cycle	–	See Fig. B.3
9. The arrangement of fuel rods in the fuel assembly	–	See Fig. B.4
10. Boric acid concentration for each fuel cycle	g/kg	6.33; 6.33; 7.15
11. Inlet coolant temperature	C	287
12. Outlet coolant temperature	C	317
13. Coolant pressure	MPa	15.7
14. Mass flow rate	kg/m^2s	5000
15. Power history	–	see Table B.5

[a] It is the list of durations for each fuel cycle (ef.day)

[b] see comments to Table B.3

Table B.3. Base irradiation history of fuel assembly #23635228

Characteristic	Unit	Value
1. Number of fuel assembly	–	23635228
2. Operation place	–	4th unit of NovoVoronezh NPP
3. Number of cycles	–	5
4. Operation periods	ef.day	98.7; 325.1; 372.1; 350.7; 368.1[a]
5. Irradiation beginning	–	17.01.90
6. Irradiation end	–	15.02.97
7. Reactor thermal power	MW	–[bb]
8. Fuel assembly location in the reactor for each fuel cycle	–	See Fig. B.5
9. The arrangement of fuel rods in the fuel assembly	–	See Fig. B.6
10. Boric acid concentration for each fuel cycle	g/kg	–[b]
11. Inlet coolant temperature	C	–[b]
12. Outlet coolant temperature	C	–[b]
13. Coolant pressure	MPa	–[b]
14. Mass flow rate	kg/m^2s	–[b]
15. Power history [c]	–	–[b]

[a] It is the list of durations for each fuel cycle (ef.day)

[b] The data were not open to this research

[c] The VVER-440 reactor contains two types of fuel assemblies, operating assemblies and follower (control) assemblies. Assembly #228, from which refabricated rod #RT7 was taken, is the follower type. Therefore, the design of the appropriate fuel elements differs from the design of the operating fuel element (#222), from which other refrabricated rods were taken. The follower assemblies are the part of the reactor control system. In the general case, the follower assemblies are not in the core with their full length. Their positions can change during the operation of the unit. Therefore, the characterization of the power history for such an assembly is a very difficult task and the linear heat rating for refrabricated rod #RT7 is not presented in appropriate Table.

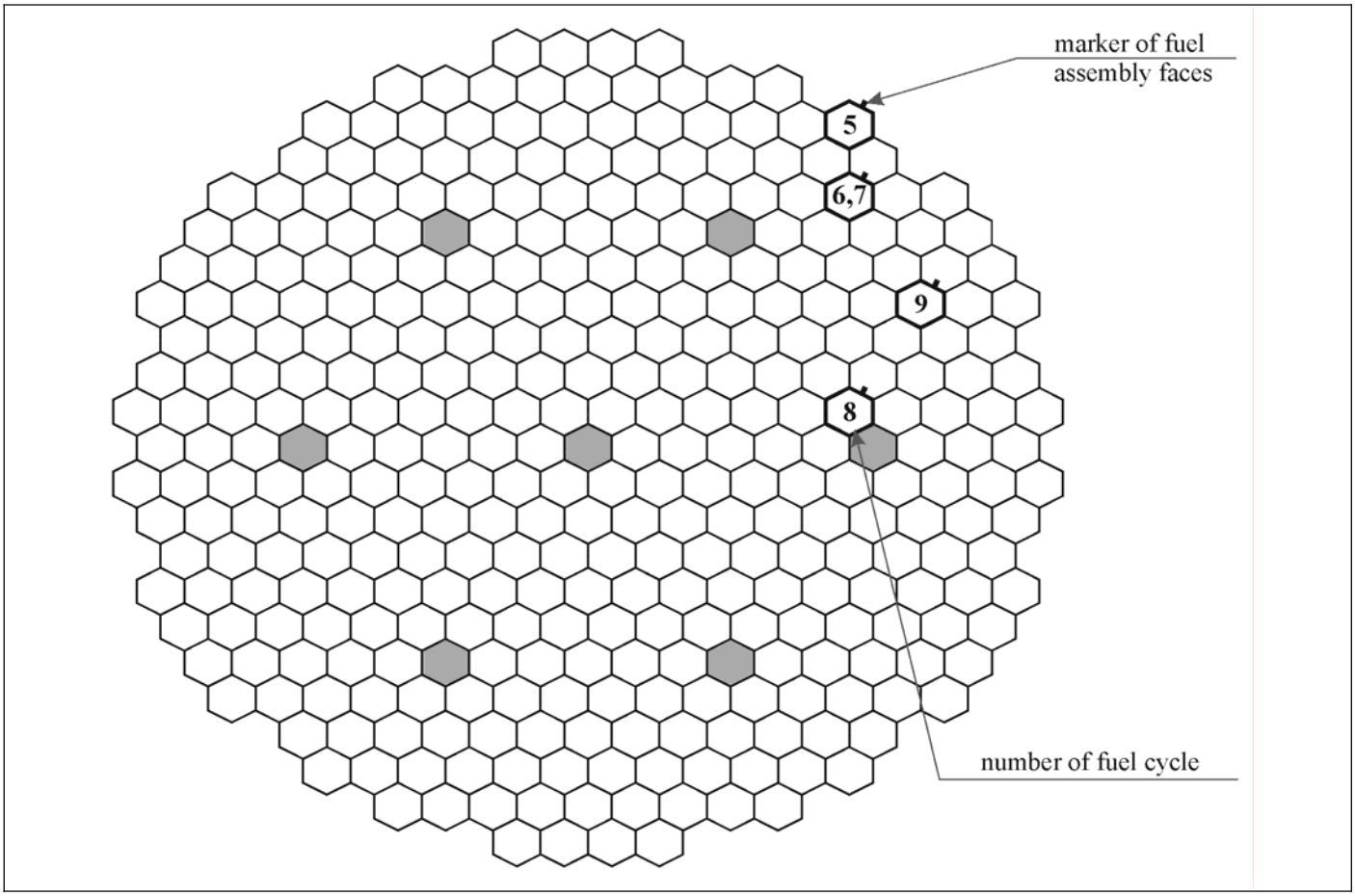


Fig. B.1. Arrangement of fuel assembly #14422222 (222) in the reactor core

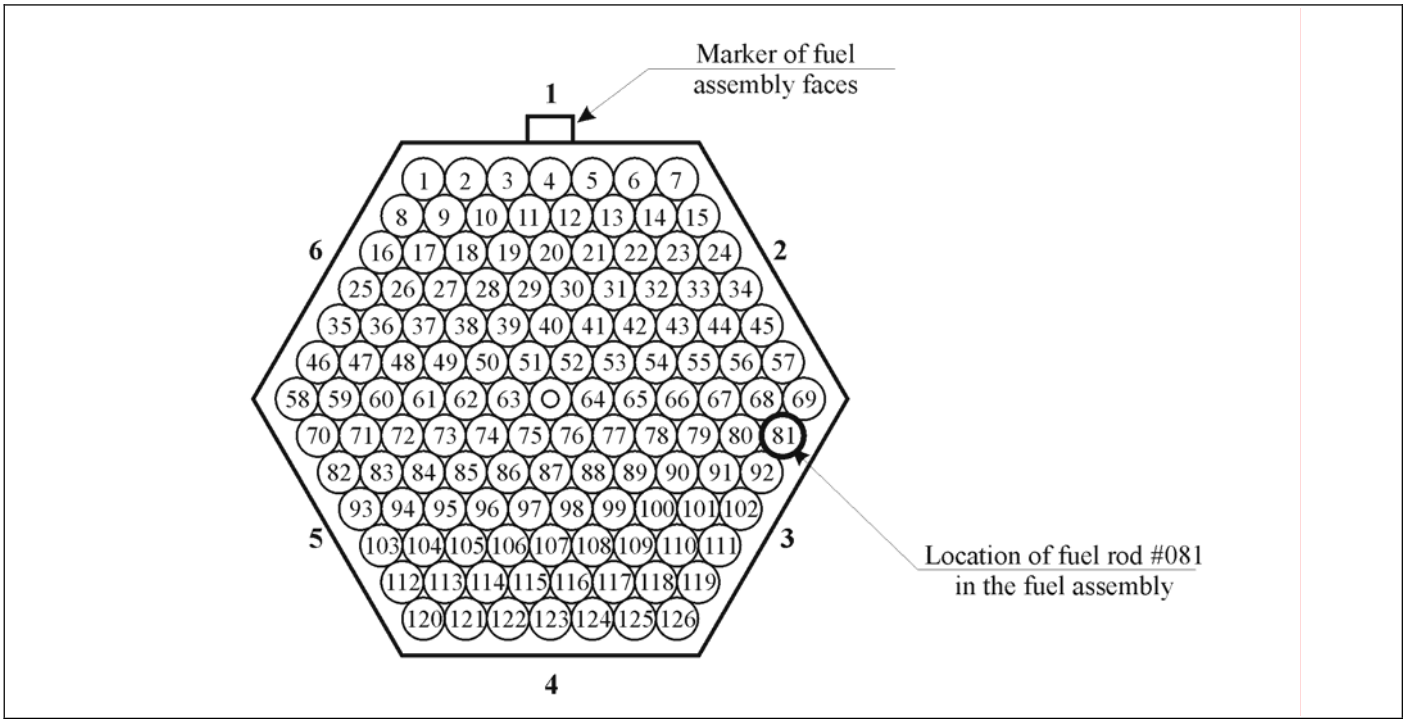


Fig. B.2. Arrangement of fuel rods in the fuel assembly #222

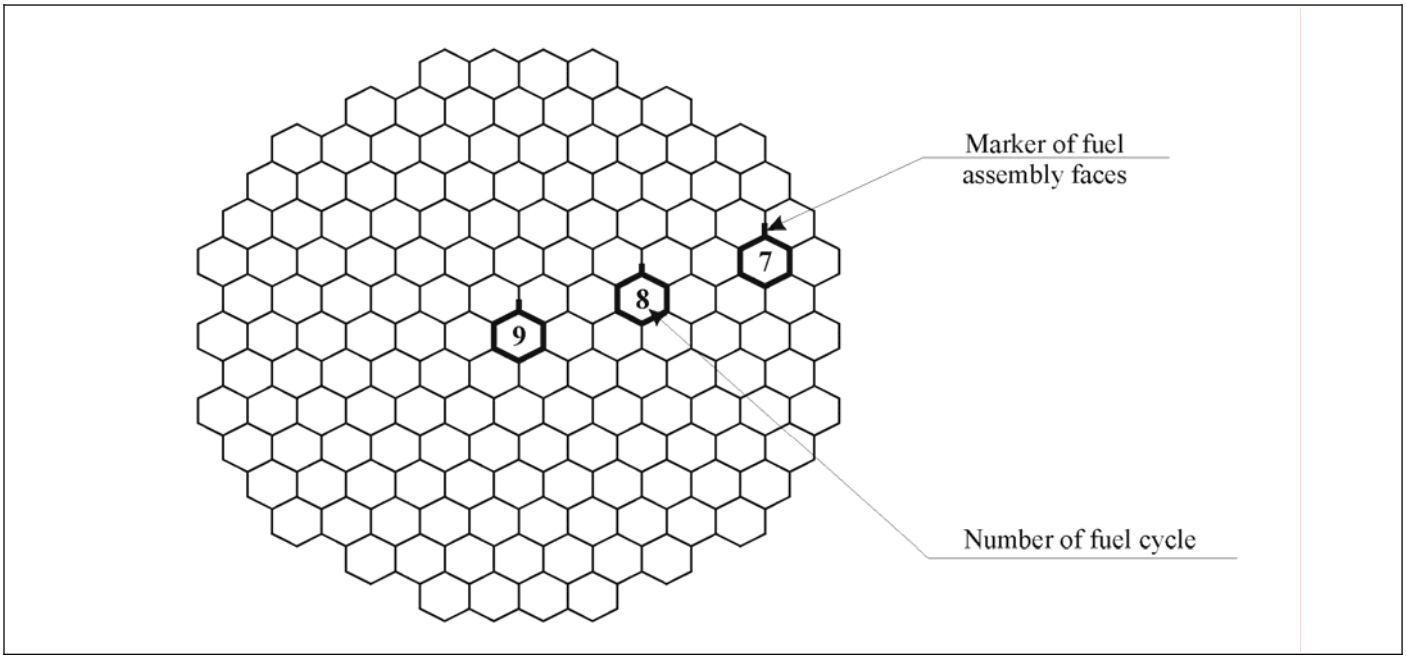


Fig. B.3. Arrangement of fuel assembly #ED4108 (108) in the reactor core

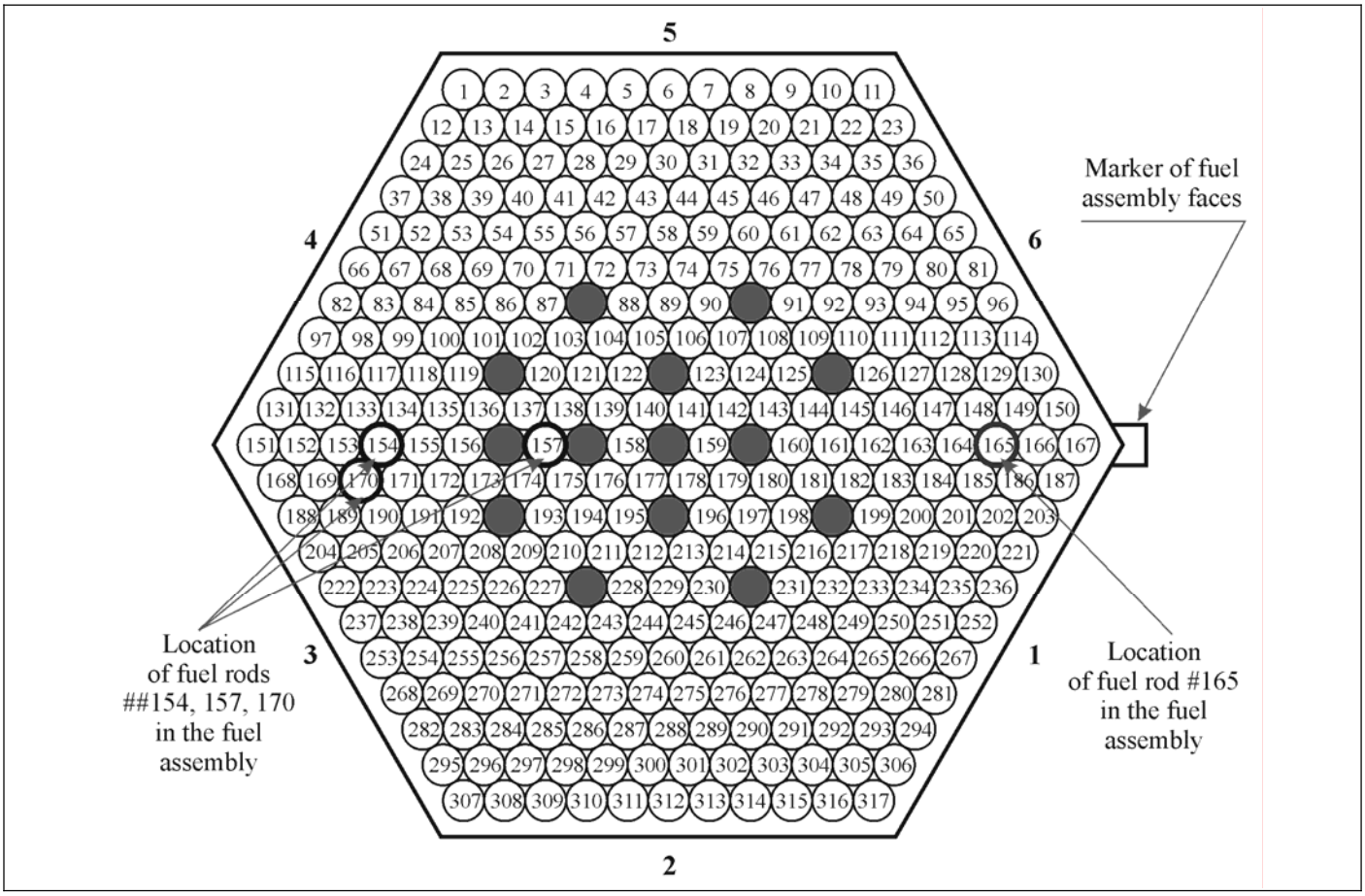


Fig. B.4. Arrangement of fuel rods in the fuel assembly #ED4108 (108)

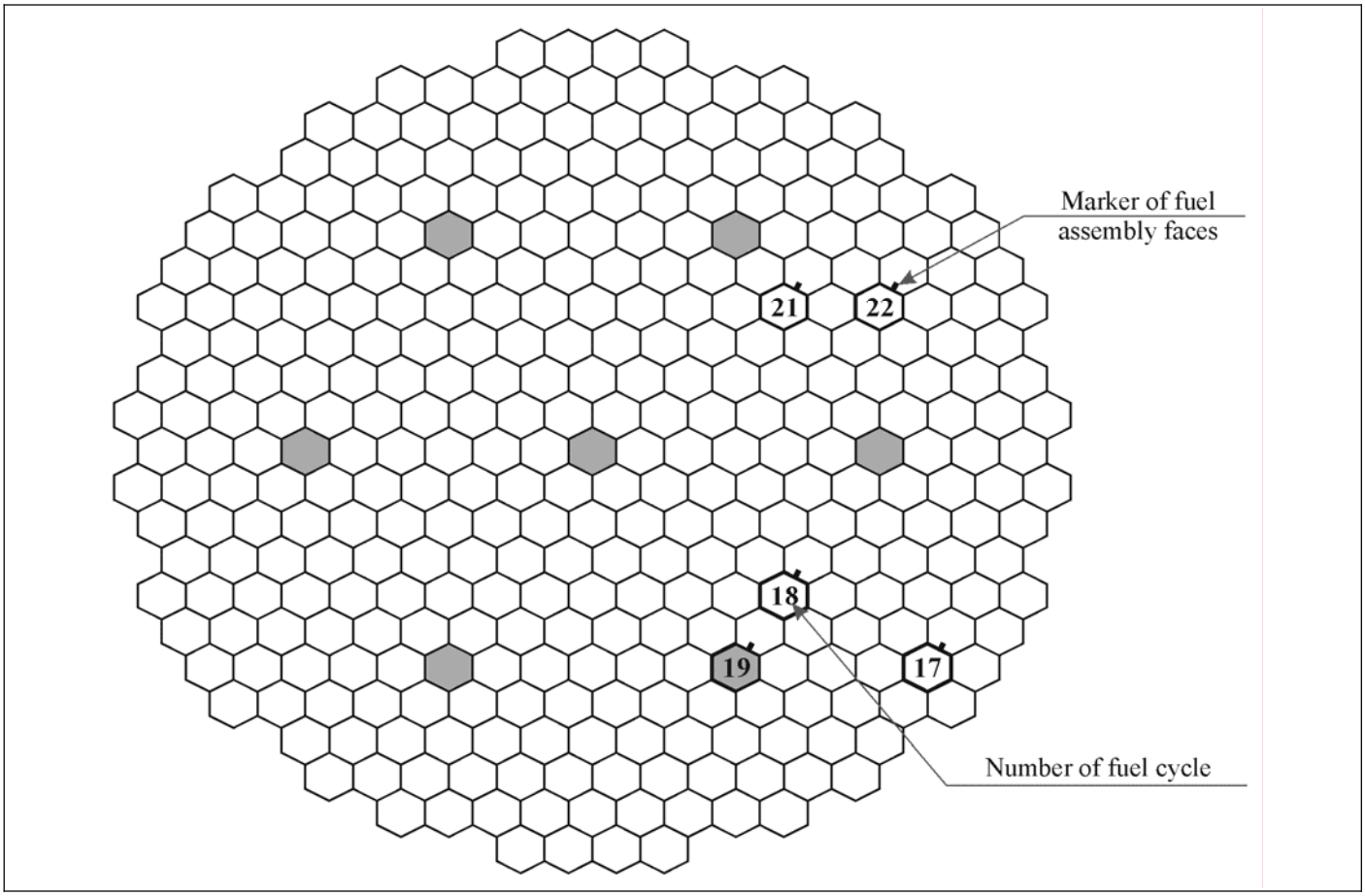


Fig. B.5. Arrangement of fuel assembly #23635228 (228) in the reactor core

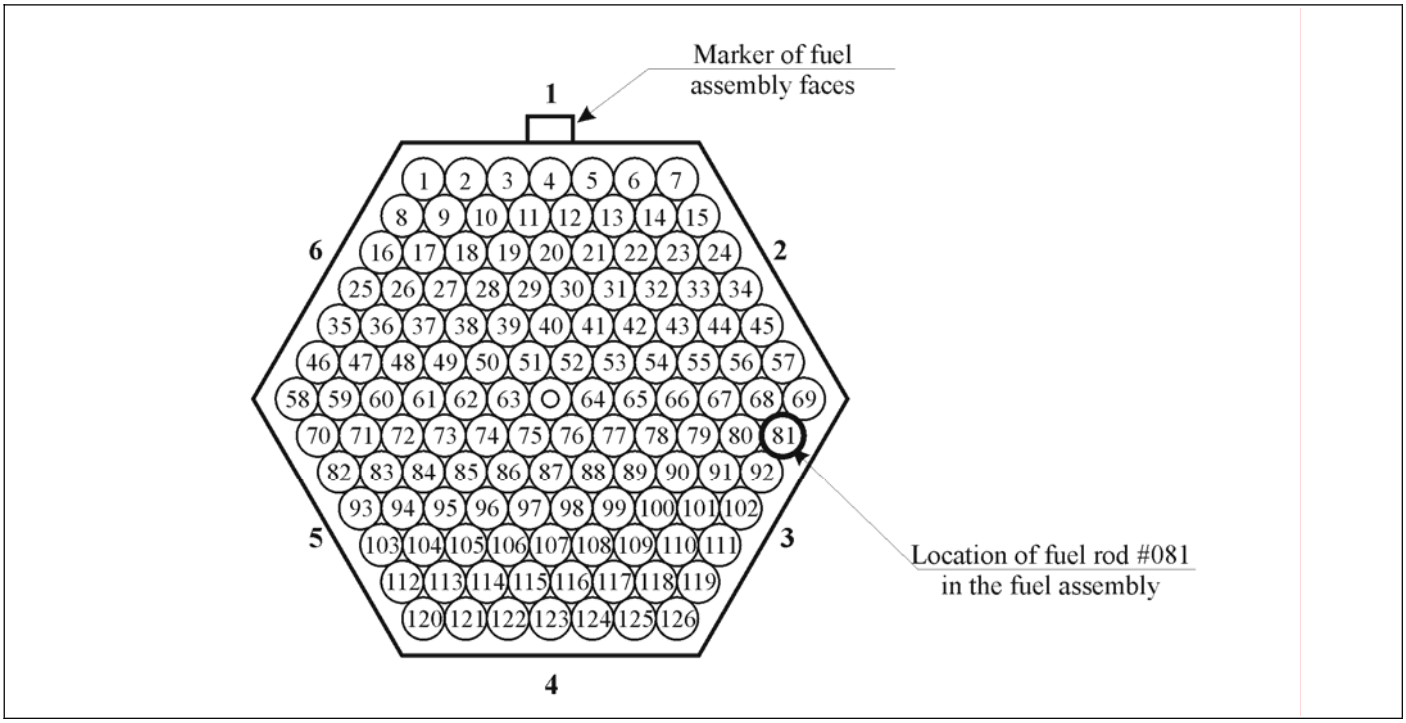


Fig. B.6. Arrangement of fuel rods in the fuel assembly #228

Table B.4. Characteristics of commercial fuel rods used for the refabrication after the base irradiation (in accordance with PIE results)

Characteristic	Unit	Value					
Fuel rod type	–	VVER-440	VVER-1000	VVER-1000	VVER-1000	VVER-1000	VVER-440
Number of fuel assembly	–	222	108	108	108	108	228
Number of fuel rod (see Fig. B.2, Fig. B.4, Fig. B.6)	–	081	154	157	165	170	081
Commercial number of fuel rod	–	18801/75	E023269	E023261	E023267	E023404	–
Fuel rod							
Gas pressure	MPa	1.26	2.64	2.93	2.86	2.87	1.08
He content in the gas composition	% by volume	67.72	95.65	92.58	94.69	96.61	86.05
Kr and Xe content	% by volume	28.84	4.01	6.94	4.62	3.25	13.73
FGR	% by volume	2.82	2.41	4.46	2.85	2.08	1.15
Radial fuel/cladding gap*	mm	0	0.032	0.017	0.025	–	–
Internal void volume	cm^3	10.4	35.4	33.3	32.7	33.4	10.1
Fuel							
Average burnup	MW d/kg U	52.35	43.54	44.49	44.01	44.5	55.4
Maximum burnup	MW d/kg U	61.58	49.01	50.12	49.62	47.8	61.7
Fuel outer diameter	mm	7.61	7.62	7.66	7.57	7.66	7.68
Fuel inner diameter	mm	1.70	2.50	2.50	2.46	2.50	1.65
Density*	g/cm^3	10.1–10.3	10.3–10.5	10.3–10.5	10.3–10.5	10.3–10.5	–
Grain size*	μm	3	3–8	3–8	3–8	3–8	–
Rim layer thickness	mm	0.15–0.20	0.05–0.07	0.05–0.07	0.05–0.07	0.05–0.07	–
ZrO_2 outer thickness*	μm	3–5	3–5	3–5	3–5	3–5	3–5
ZrO_2 inner thickness*	μm	10	0	0	0	0	8–10
Cladding							
Average diameter along upper plenum	mm	9.137	9.14	9.14	9.14	9.154	9.101
Average diameter along fuel stack	mm	9.07	9.08	9.08	9.07	9.083	9.045
Average thickness	mm	0.73	0.70	0.69	0.72	0.69	–
H_2 content	% by weight	$6–8 \cdot 10^{-3}$	$5 \cdot 10^{-3}$	$5 \cdot 10^{-3}$	$5 \cdot 10^{-3}$	$5 \cdot 10^{-3}$	–
ZrO_2 outer thickness	μm	3–5	3–5	3–5	3–5	3–5	3–5
ZrO_2 inner thickness	μm	0–10	0	0	0	0	0–10

* This parameter characterizes that part of the fuel element, which was used for the refabrication

Table B.5. The calculated linear heat rating of VVER-1000 fuel elements during the base irradiation at elevations used for the manufacture of refabricated fuel rods

Number of fuel element*	Elevation (mm)	Number of refabricated fuel rod	Linear heat rating (kW/m)					
			7th cycle		8th cycle		9th cycle	
			B**	E***	B	E	B	E
154	2180	RT6	26.0	23.7	23.3	17.7	18.0	15.0
157	2410	RT5	24.0	22.0	25.3	19.0	18.7	15.7
165	1120	RT1	27.0	26.0	23.3	19.0	18.3	15.0
165	1350	RT2	27.0	25.3	24.0	18.7	18.3	14.3
165	2410	RT3	24.7	24.0	23.7	18.7	18.7	15.0
170	2180	RT10	27.0	24.2	23.3	17.7	18.3	14.7
170	2410	RT11	25.7	24.3	23.7	17.7	18.0	14.7
170	2650	RT12	25.0	24.0	23.7	18.0	18.0	15.3

* Numbers are presented in accordance with Fig. B.4
** The Beginning (B) of cycle
*** The End (E) of cycle

Table B.6. The calculated linear heat rating of VVER-440 (FA #222) fuel elements during the base irradiation at elevations used for the manufacture of refabricated fuel rods

Num-ber of fuel ele-ment*	Eleva-tion (mm)	Number of refabricated fuel rod	Linear heat rating (kW/m)									
			5th cycle		6th cycle		7th cycle		8th cycle		9th cycle	
			B**	E***	B	E	B	E	B	E	B	E
81	860	RT4	15.0	13.3	20.0	16.0	17.7	15.0	15.3	13.3	12.0	10.7
81	970	RT8	15.0	13.3	20.0	16.3	18.0	15.0	15.7	13.3	12.0	10.7
81	1210	RT9	15.7	13.3	19.3	16.7	17.0	15.0	15.0	13.7	11.3	11.0

* Numbers are presented in accordance with Fig. B.4
** The Beginning (B) of cycle
*** The End (E) of cycle

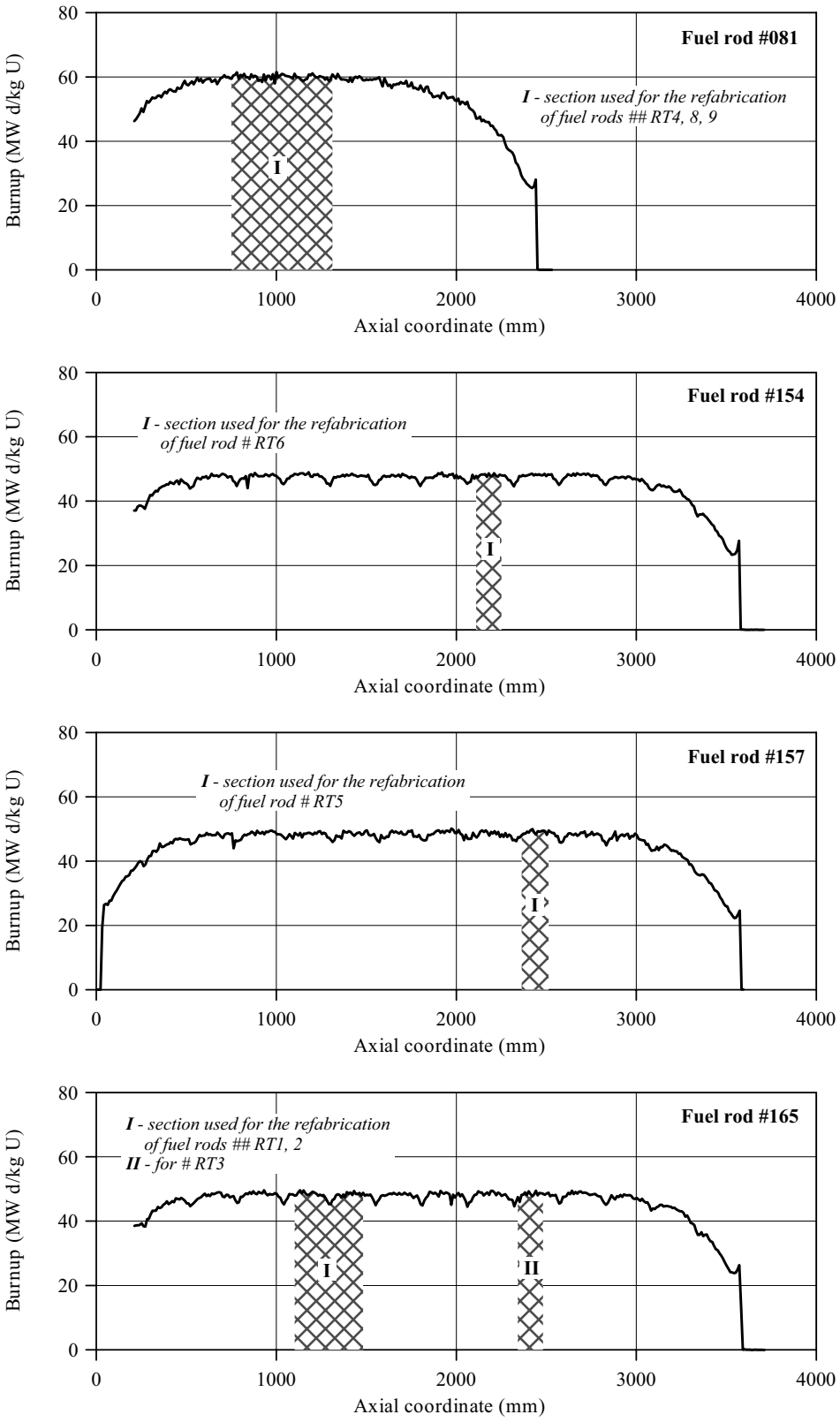


Fig. B.7. Axial distribution of fuel burnup in fuel rods ## 081, 154, 157, 165 of fuel assemblies ##222, 108

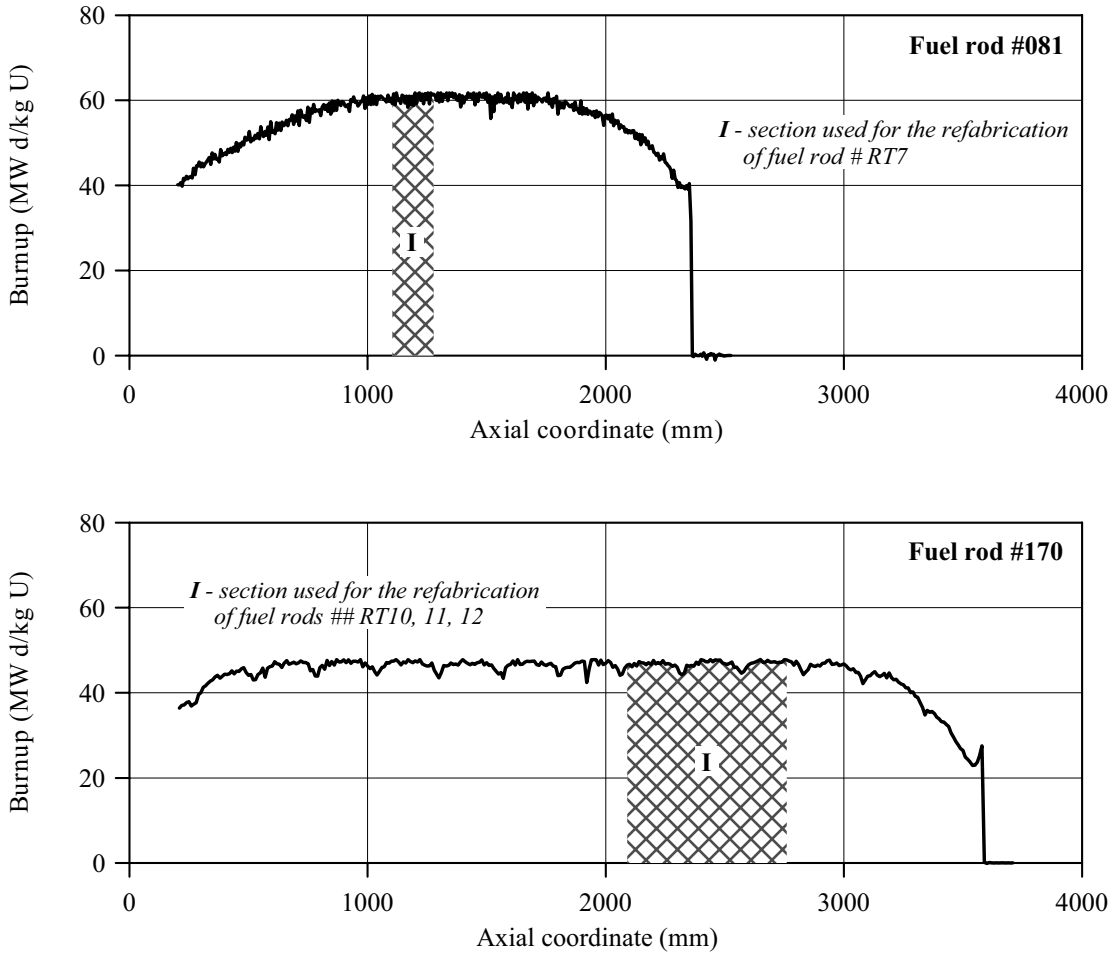


Fig. B.8. Axial distribution of fuel burnup in fuel rods ## 081, 170 of fuel assemblies ##228, 108

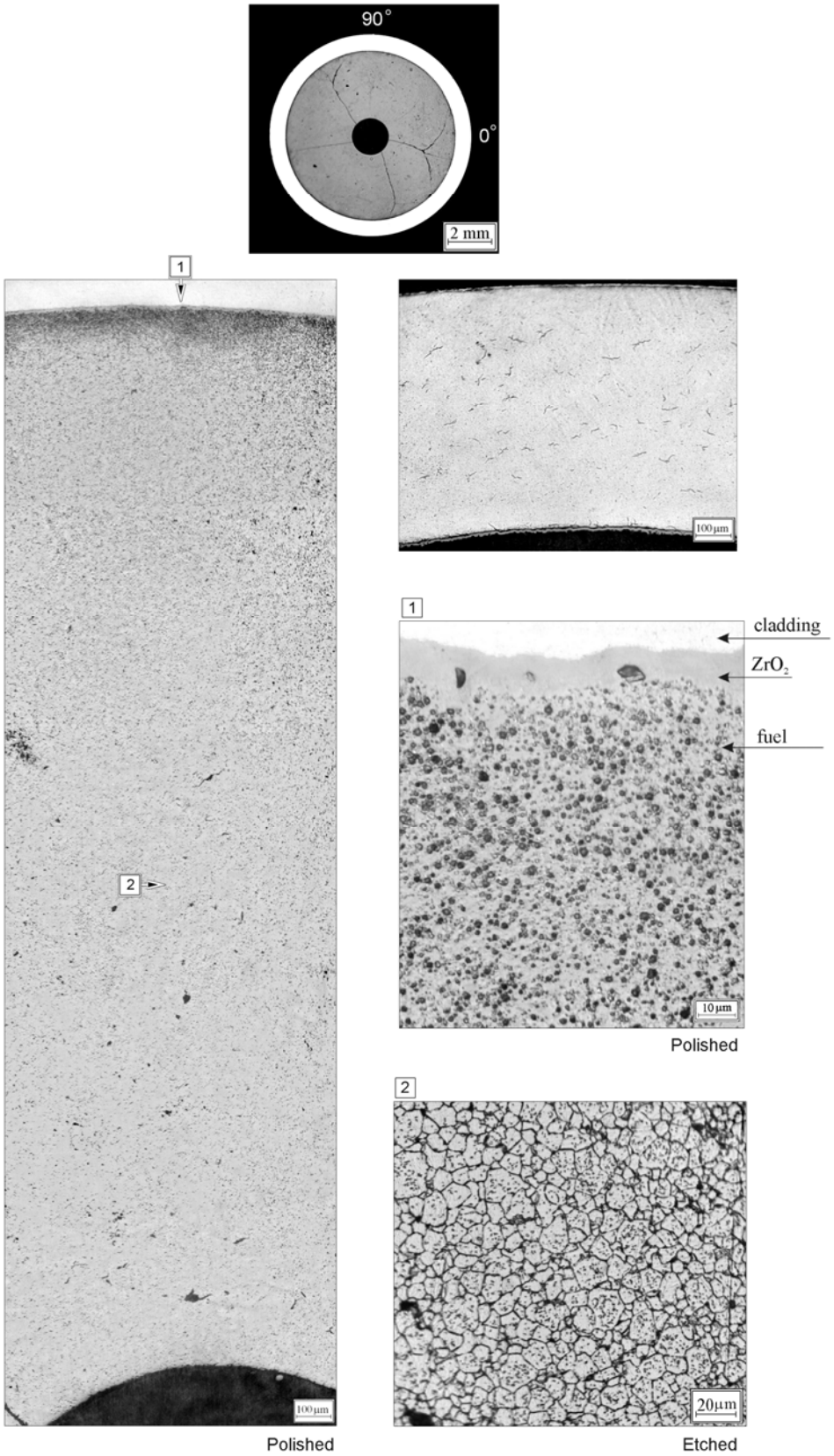


Fig. B.9. Macro- and microstructures of fuel and cladding in commercial fuel rod #081 (VVER-440, fuel assembly #222) at 1110 mm elevation after the base irradiation

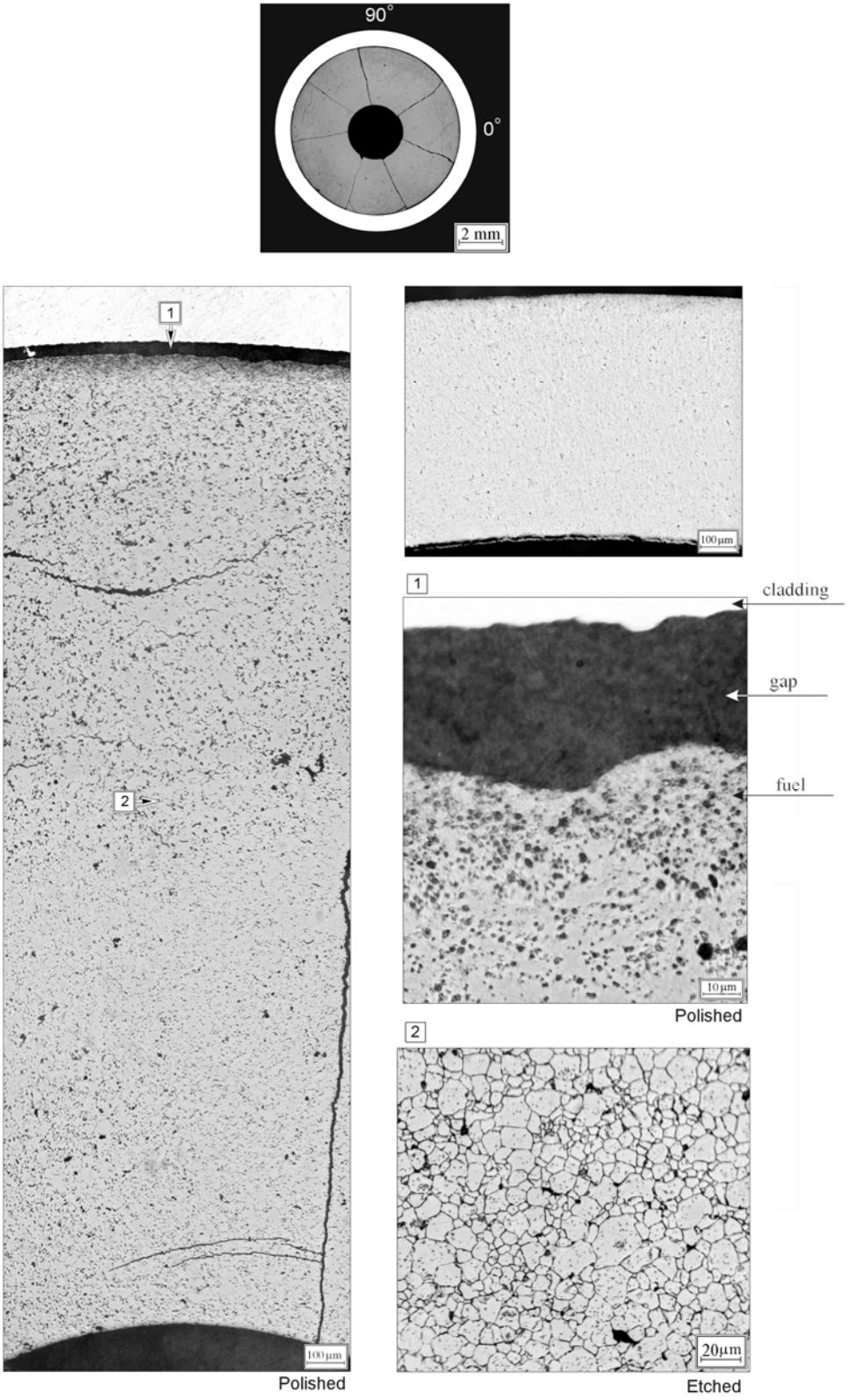


Fig. B.10. Macro- and microstructures of fuel and cladding in commercial fuel rod #154 (VVER-1000, fuel assembly #108) at 2080 mm elevation after the base irradiation

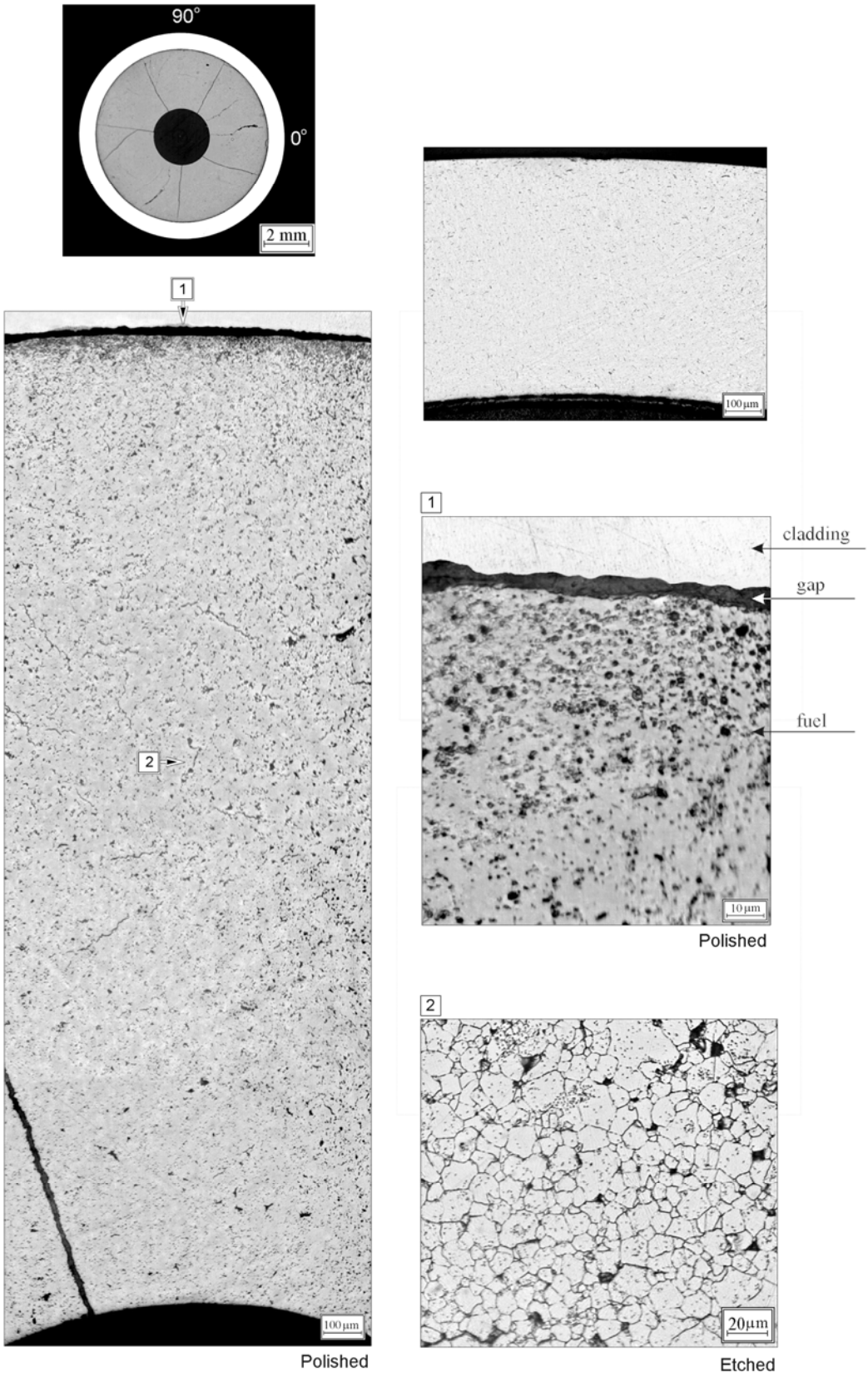


Fig. B.11. Macro- and microstructures of fuel and cladding in commercial fuel rod #157 (VVER-1000, fuel assembly #108) at 2340 mm elevation after the base irradiation

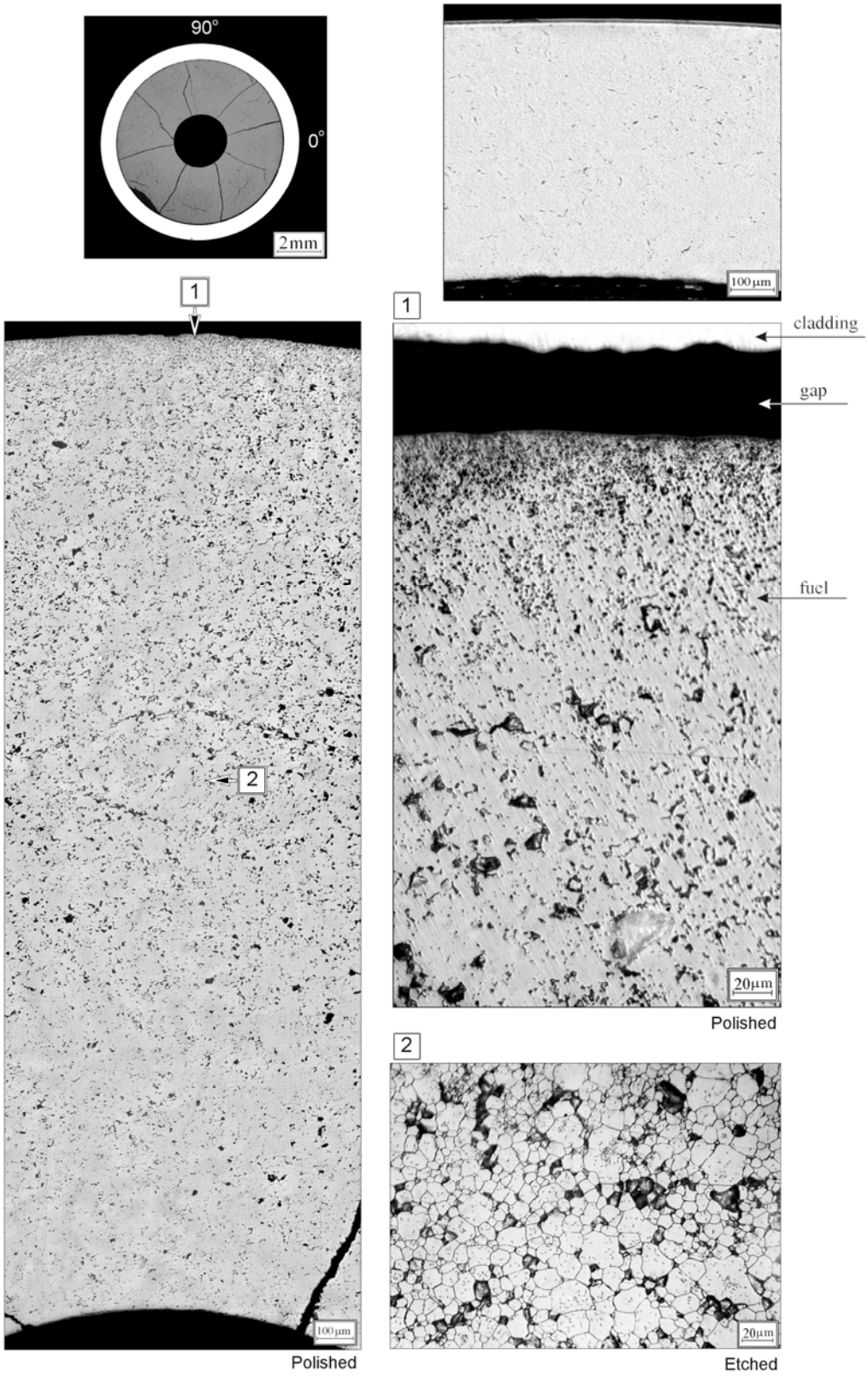


Fig. B.12. Macro- and microstructures of fuel and cladding in commercial fuel rod #165 (VVER-1000, fuel assembly #108) at 1495 mm elevation after the base irradiation

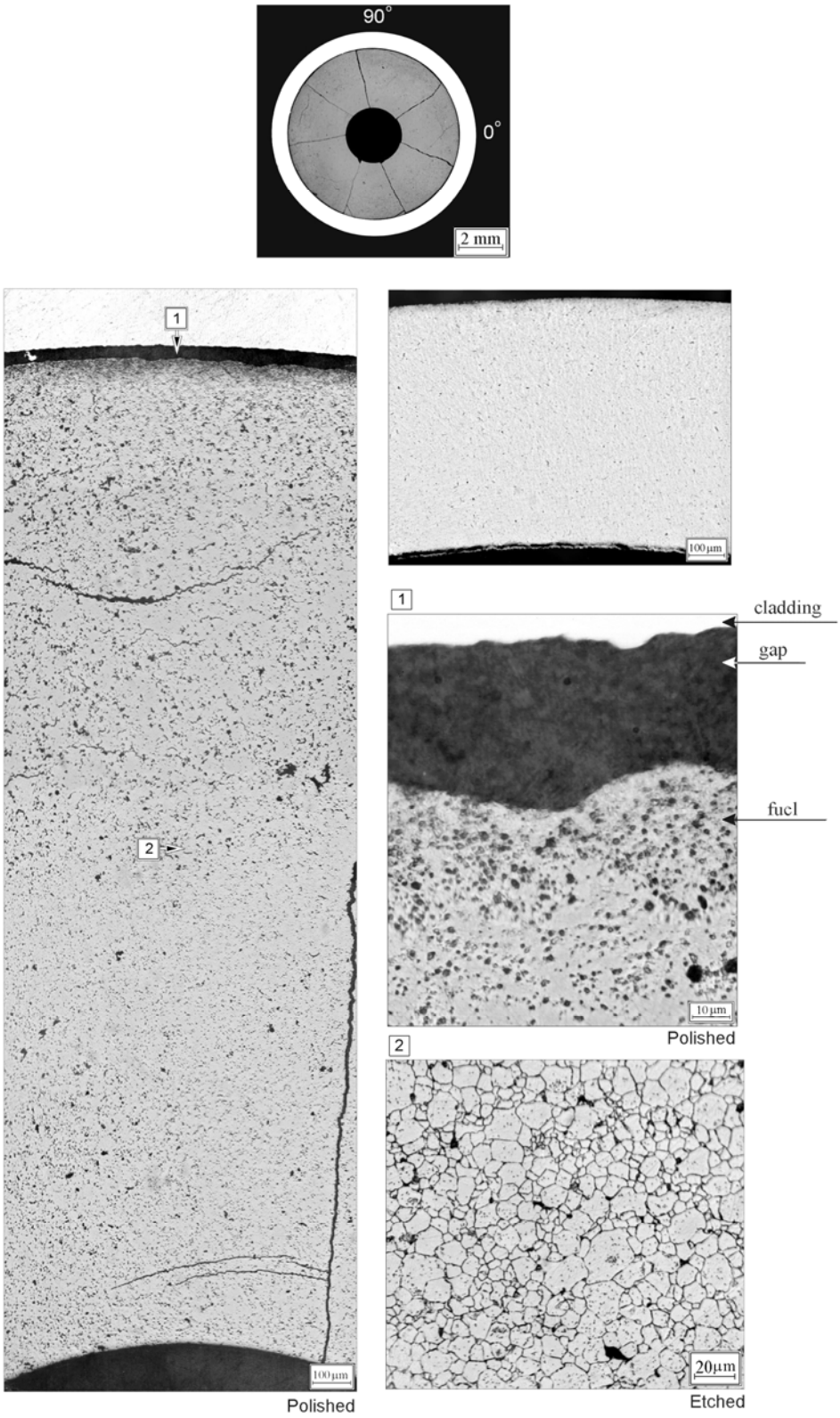


Fig. B.13. Macro- and microstructures of fuel and cladding in commercial fuel rod #170 (VVER-1000, fuel assembly #108) at 2270 mm elevation after the base irradiation

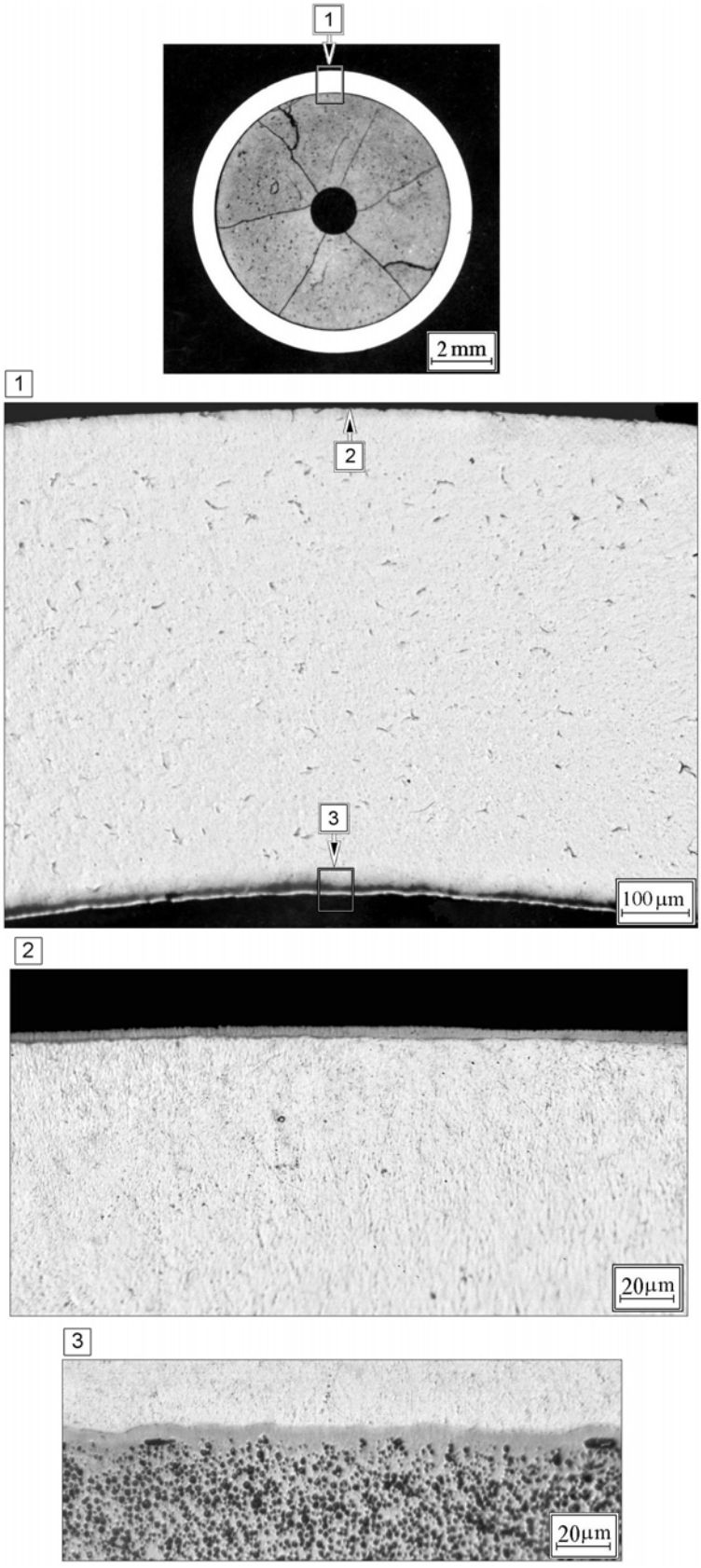


Fig. B.14. Macro- and microstructures of fuel and cladding in commercial fuel rod #081 (VVER-440, fuel assembly #228) at 1300 mm elevation after the base irradiation

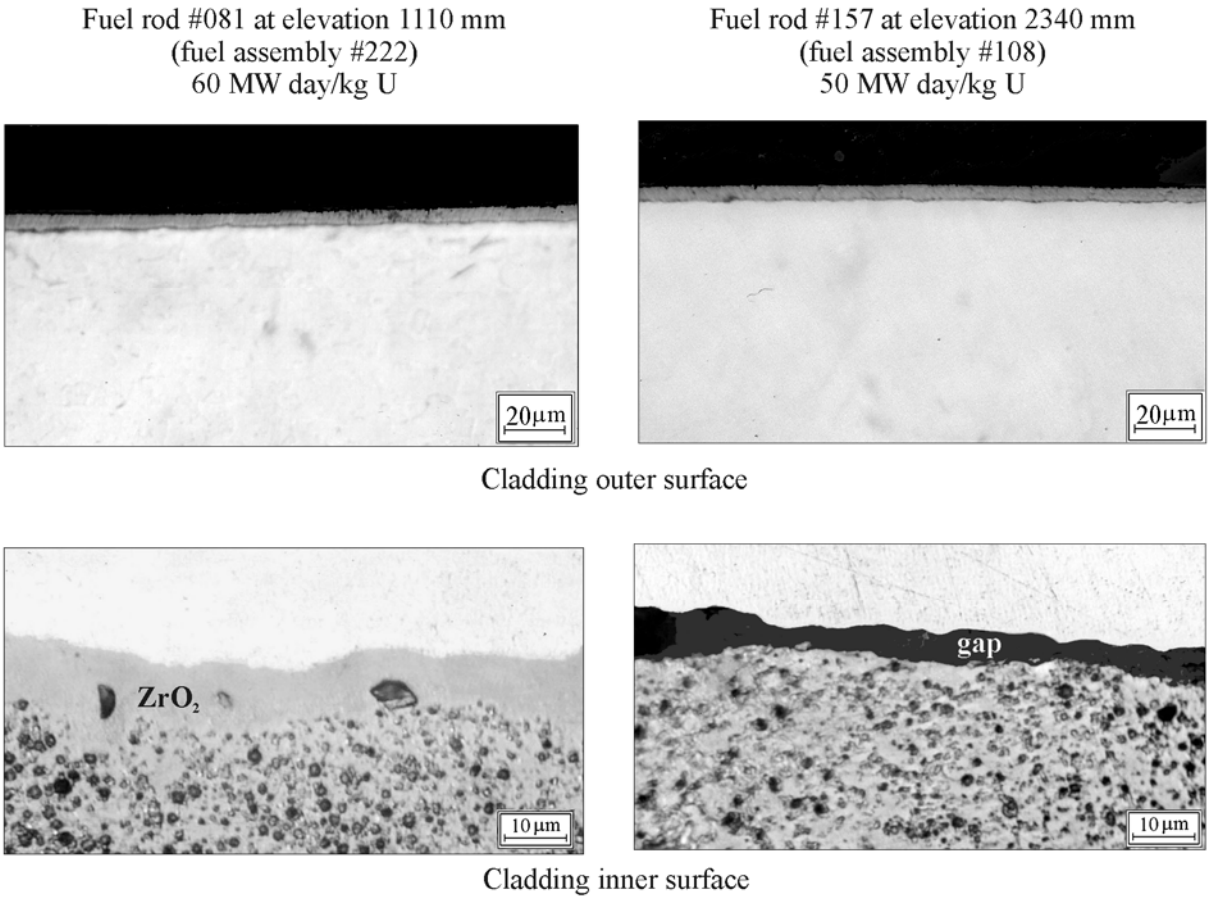


Fig. B.15. Comparative data characterizing the cladding oxidation and fuel/cladding gap at burnup 50 and 60 MW d/kg U

APPENDIX C

CHARACTERISTICS OF REFABRICATED FUEL RODS BEFORE THE BIGR TESTS

Table C.1. Characteristics of fuel rods before BIGR tests: Reference data[*]

Characteristic	Unit	Value		
Commercial fuel rod type	–	VVER-440	VVER-1000	VVER-440
Number of fuel assembly	–	222	4108	228
Number of commercial fuel rod	–	081	154, 157, 165, 170	081
Number of refabricated fuel rod	–	RT 4, 8, 9	RT 1, 2, 3, 5, 6, 10, 11, 12	RT 7
1. Fuel				
1.1. Outer diameter	mm	7.61	7.57–7.66	7.68
1.2. Inner diameter	mm	1.7	2.46–2.5	1.65
1.3. Density	g/cm^3	10.1–10.3	10.3–10.5	–
1.4. Grain size	μm	3	3–8	–
2. Cladding				
2.1. Outer diameter	mm	9.07–9.09	9.06–9.08	9.06
2.2. Thickness	mm	0.73	0.69–0.72	0.69
2.3. ZrO_2 outer thickness	μm	3–5	3–5	3–5
2.4. ZrO_2 inner thickness	μm	10	0	8–10
2.5. Hydrogen content	% by weight	$6–8 \cdot 10^{-3}$	$5 \cdot 10^{-3}$	–
3. Refabricated fuel rod				
3.1. Design	–	RT4 see Fig. C.1 RT8, 9 see Fig. C.2	see Fig. C.1	see Fig. C.1
3.2. Gas composition	–	He	He	He

Table C.2. Individual parameters of refabricated fuel rods ## RT1–6 before BIGR tests[**]

Parameter	Number of fuel rod					
	RT1	RT2	RT3	RT4	RT5	RT6
Number of mother fuel rods	165	165	165	081	157	154
Coordinates of mother fuel rod section used for refabrication[***] (mm)	1093 1246	1331 1482	2340 2489	745 900	2360 2513	2103 2254
Pellet stack coordinate[***] (mm)	24 177	25.4 176.4	23.6 172.6	22 177	24 177	23 174
Coordinates of undamaged section of pellet stack[****] (mm)	24 177	25.4 176.4	65.5 110.5	22 177	24 177	23 165
Undamaged section length (mm)	153	151	45	155	153	142
Average burnup (MW d/kg U)	48.3	48.0	47.5	60.1	48.6	47.8
Total fuel mass (g)	63.5	62.1	60.4	69.5	63.1	61.9
Mass of undamaged fuel section (g)	63.5	62.1	18.36	69.5	63.1	58.4
L_1[*****] (mm)	4.6	6.0	4.2	2.6	4.6	3.6
L_2[*****] (mm)	153	151	149	155	153	151
L_3[*****] (mm)	4.5	3.1	3.4	2.5	2.5	2.5
L_4[*****] (mm)	302	300	296.5	300	300	297
Total gas volume (cm^3)	6.13	6.12	6.08	5.54	6.07	6.03
Cladding outer diameter (mm)	9.06	9.06	9.06	9.08	9.06	9.07
Fuel-cladding radial gap (mm)	0.025	0.025	0.025	0.000	0.017	0.032
Central hole diameter (mm)	2.46	2.46	2.46	1.65	2.50	2.50
Internal gas pressure (MPa)	2.1	2.1	2.1	2.1	2.1	2.1

[*] Characteristics were developed in accordance with data of Table B.4.
[**] Parameters were determined using pre-test examination results
[***] From lower cap of fuel rod
[****] Taking into account the risk of fuel damage at the refabrication procedure, special measurements were performed to estimate the coordinates of that part of fuel stack, which was identified as "undamaged" after the refabrication. The coordinates of undamaged part was determined from lower cap of fuel rod
[*****] See Fig. C.1

Table C.3. Individual parameters of refabricated fuel rods ## RT7–12 before BIGR tests [*]

Parameter	Number of fuel rod					
	RT7	RT8	RT9	RT10	RT11	RT12
Number of mother fuel rods	081	081	081	170	170	170
Coordinates of mother fuel rod section used for refabrication [**] (mm)	1100 1278	931 1109	1133 1311	2090 2268	2343 2522	2590 2769
Pellet stack coordinate [**] (mm)	23 176.1	7 157	8 157	21.4 173.4	23 175	21.3 173.9
Coordinates of undamaged section of pellet stack [***] (mm)	23 176.1	7 157	8 157	21.4 173.4	23 175	21.3 173.9
Fuel stack length (mm)	153.1	150	149	152	152	152.6
Average burnup (MW d/kg U)	60.5	60.0	59.8	46.9	47.2	47.3
Total fuel mass (g)	66.8	66.2	66.2	62.6	62.9	63.0
L_1 [****] (mm)	3.6	0.0	0.0	2.0	3.6	1.9
L_2 [****] (mm)	153.1	150.0	149.0	152.0	152.0	152.6
L_3 [****] (mm)	2.4	9.1	10.1	5.1	3.5	5.6
L_4 [****] (mm)	299	299	299	299	299	300
Total gas volume (cm^3)	5.75	5.93	5.88	6.10	6.23	6.11
Cladding outer diameter (mm)	9.062	9.09	9.07	9.072	9.08	9.066
Fuel-cladding radial gap (mm)	0.003	0.003	0.001	0.023	0.018	0.012
Central hole diameter (mm)	1.65	1.65	1.65	2.50	2.50	2.50
Internal gas pressure (MPa)	2.0	2.0	0.1	2.0	2.0	0.1

[*] Parameters were determined using pre-test examination results
[**] From lower cap of fuel rod
[***] Taking into account the risk of fuel damage at the refabrication procedure, special measurements were performed to estimate the coordinates of that part of fuel stack, which was identified as “undamaged” after the refabrication. The coordinates of undamaged part was determined from lower cap of fuel rod
[****] See Figs. C.1, C.2

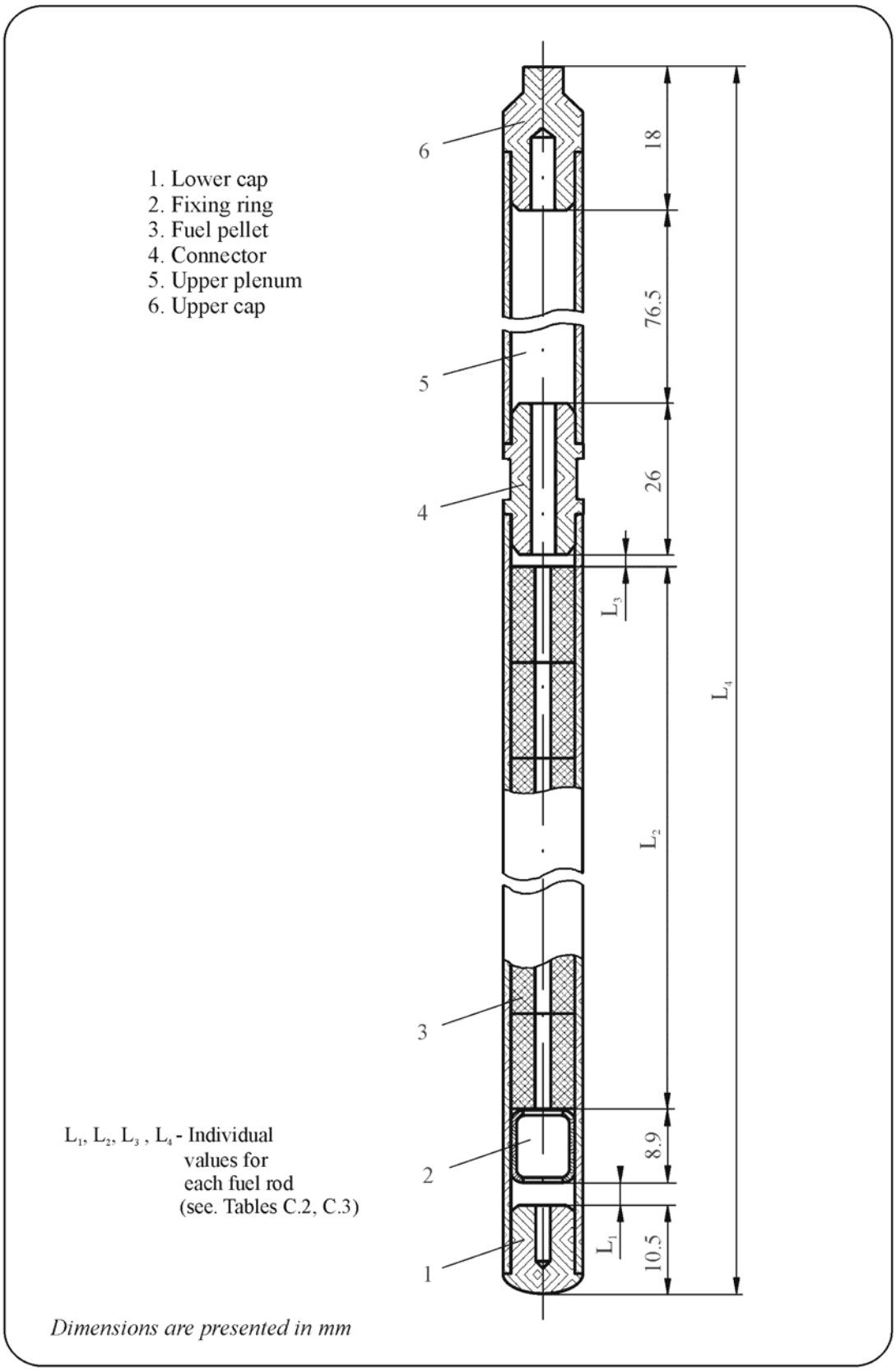


Fig. C.1. Design scheme of refabricated fuel rods ## RT 1–7, 10, 12

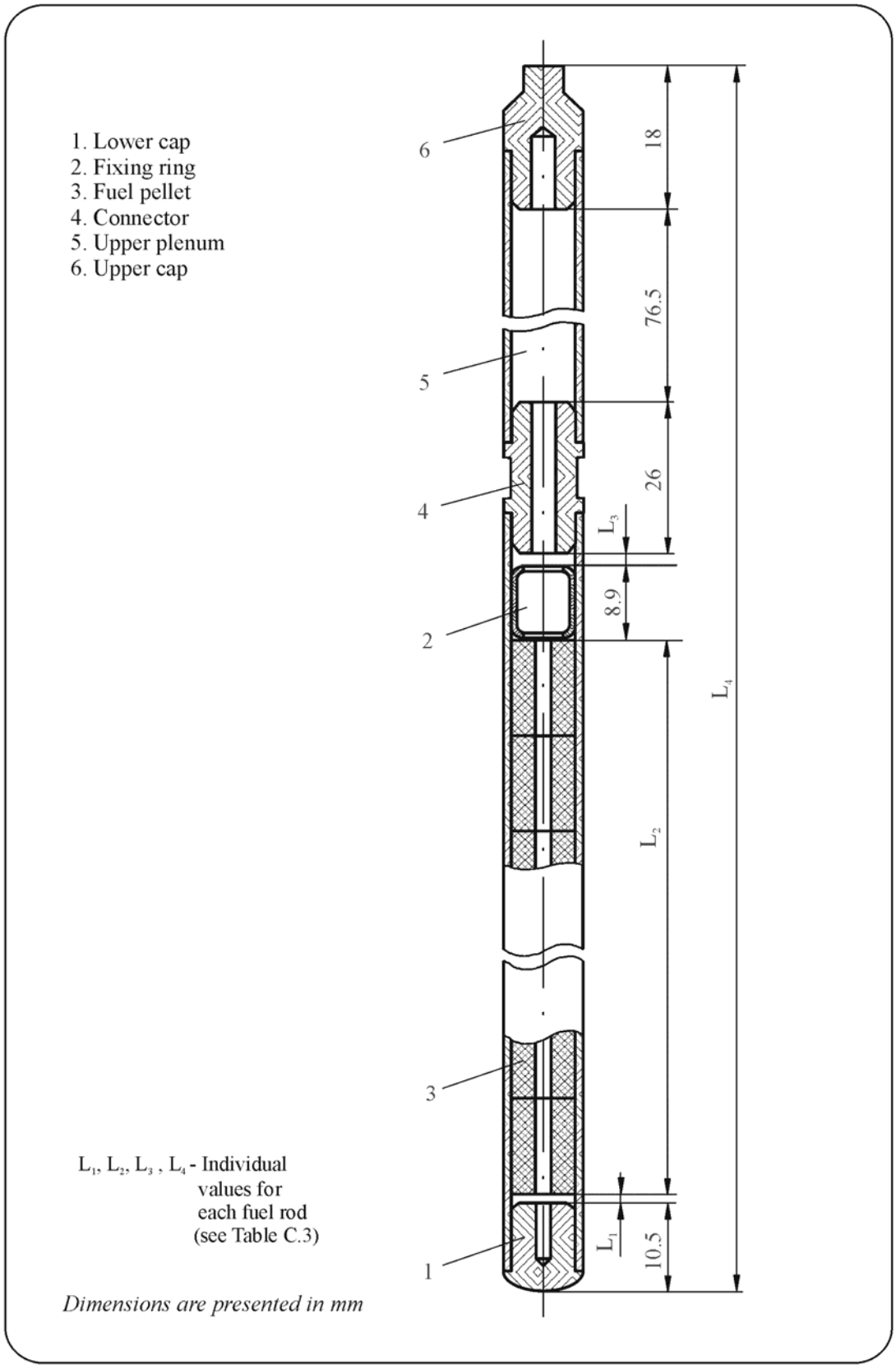


Fig. C.2. Design scheme of refabricated fuel rods ## RT8, 9

Appendix C-1

Individual Characteristics of Fuel Rod # RT1 before the BIGR Test

RT1

Table C-1.1. Radial distribution of isotope nuclear concentrations for fuel rod #RT1 (values averaged of over the fuel stack length)*

Isotope	Isotopic concentrations (kg/t U) in four fuel radial layers			
	1.23-2.82 mm	2.82-3.44 mm	3.44-3.71 mm	3.71-3.795 mm
U^{234}	0.233	0.229	0.226	0.222
U^{235}	7.714	7.414	7.140	6.952
U^{236}	6.401	6.413	6.425	6.440
U^{238}	928.8	925.1	913.6	882.2
Pu^{238}	0.361	0.381	0.412	0.468
Pu^{239}	4.952	5.516	7.463	12.68
Pu^{240}	2.581	2.740	3.537	5.775
Pu^{241}	1.037	1.217	1.738	3.134
Pu^{242}	0.751	0.905	1.332	2.480
Np^{237}	0.606	0.625	0.644	0.657
Am^{241}	0.382	0.443	0.627	1.132
Oxygen	134.5	134.5	134.5	134.5
Other fission products	47.16	50.05	58.19	79.88

* Measured averaged concentrations and calculated relative radial distributions of isotopes (TRIFOB code) were used to develop these data

Table C-1.2. Initial individual characteristics of fuel rod # RT1*

Axial coordinate (from lower cap) (mm)	Cladding average outer diameter (mm)	Fuel mass ** (g)	Linear fuel mass** (g/cm)	Gas flow area[3]** (mm^2)	Burnup** (MW d/kg U)
25[1]	-	1.47	4.18	4.800	48.05
30	9.065	2.08	4.17	4.806	47.98
35	9.066	2.07	4.14	5.101	47.95
40	9.065	2.08	4.17	4.806	47.98
45	9.063	2.13	4.25	4.800	47.94
50	9.067	2.12	4.25	4.800	47.75
55	9.063	2.13	4.26	4.800	47.56
60	9.064	2.08	4.17	4.806	47.51
65	9.063	2.07	4.14	5.101	47.70
70	9.067	2.07	4.13	5.199	48.14
75	9.066	2.02	4.03	6.183	48.72
80	9.064	2.06	4.12	5.298	49.20
85	9.065	2.03	4.07	5.790	49.17
90	9.063	2.06	4.12	5.298	48.59
95	9.061	2.08	4.17	4.806	48.34
100	9.061	2.04	4.07	5.790	48.83
105	9.065	2.00	3.99	6.576	49.17
110	9.063	2.03	4.05	5.986	48.77
115	9.065	2.10	4.20	4.800	48.17
120	9.063	2.10	4.20	4.800	47.82
125	9.059	2.11	4.22	4.800	47.71
130	9.061	2.12	4.24	4.800	47.75
135	9.059	2.11	4.23	4.800	47.90
140	9.061	2.11	4.21	4.800	48.13
145	9.059	2.09	4.17	4.806	48.40
150	9.059	2.09	4.17	4.806	48.68
155	9.059	2.07	4.14	5.101	48.79
160	9.058	2.08	4.16	4.904	48.68
165	9.059	2.06	4.12	5.298	48.49
170	9.062	2.05	4.10	5.495	48.32
175[2]	9.066	1.83	4.05	5.986	48.16

* All parameters were determined using results of pre-test examinations

** Average values at the length interval equal to the axial coordinate ±2.5 mm

[1] Bottom end coordinate of fuel stack is 24 mm; [2] Top end coordinate of fuel stack is 177 mm

[3] Gas flow area beyond the fuel stack (mm^2):

Bottom: 0.0-3.0mm – 0.00; 3.0-10.5mm – 12.56; 10.5-15.1mm – 45.82; 15.1-24.0mm – 24.97

Top: 177.0-181.5mm – 45.82; 181.5-207.5mm – 28.26; 207.5-284mm – 45.82; 284-293mm – 28.26; 293-302mm – 0.00

RT1

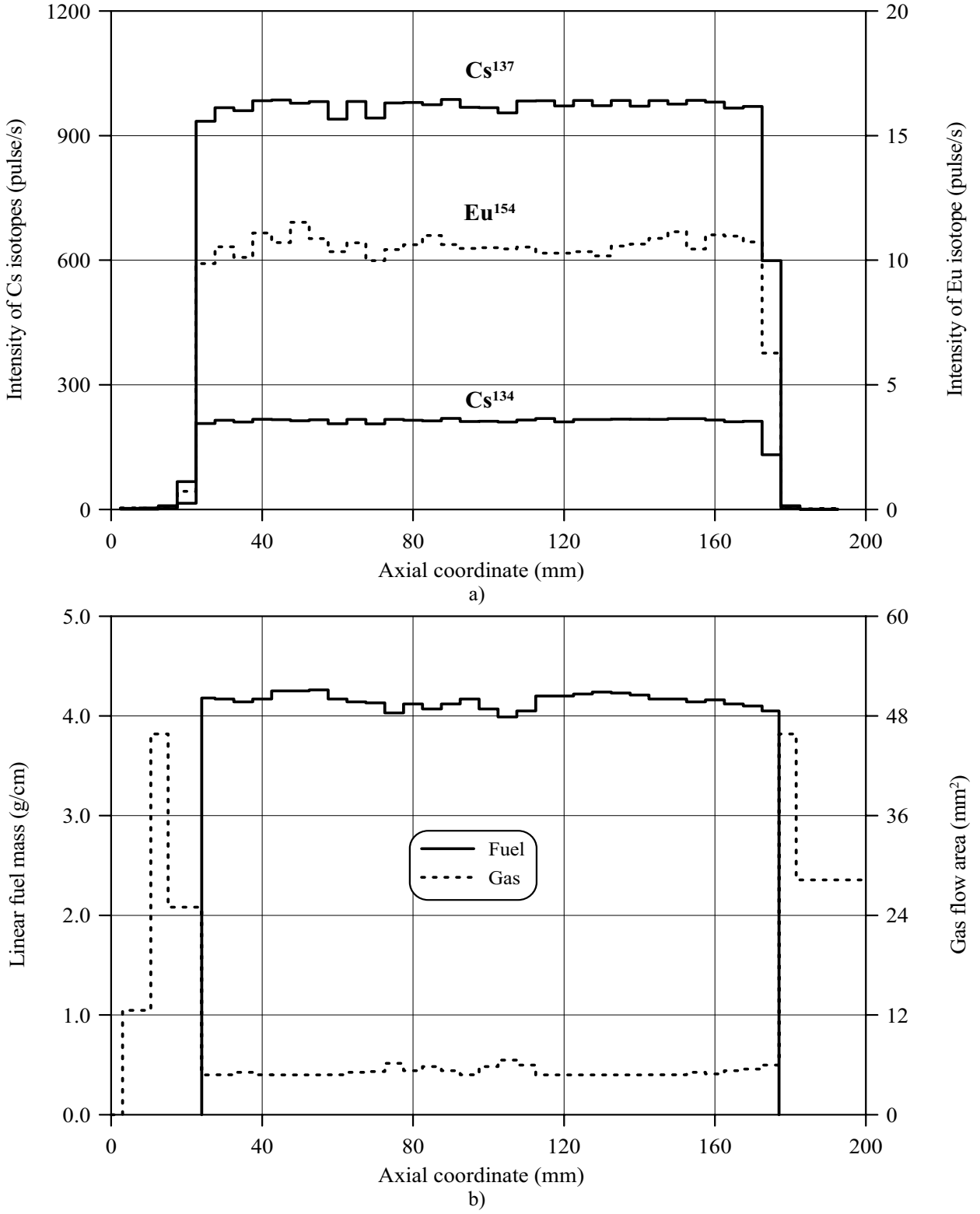
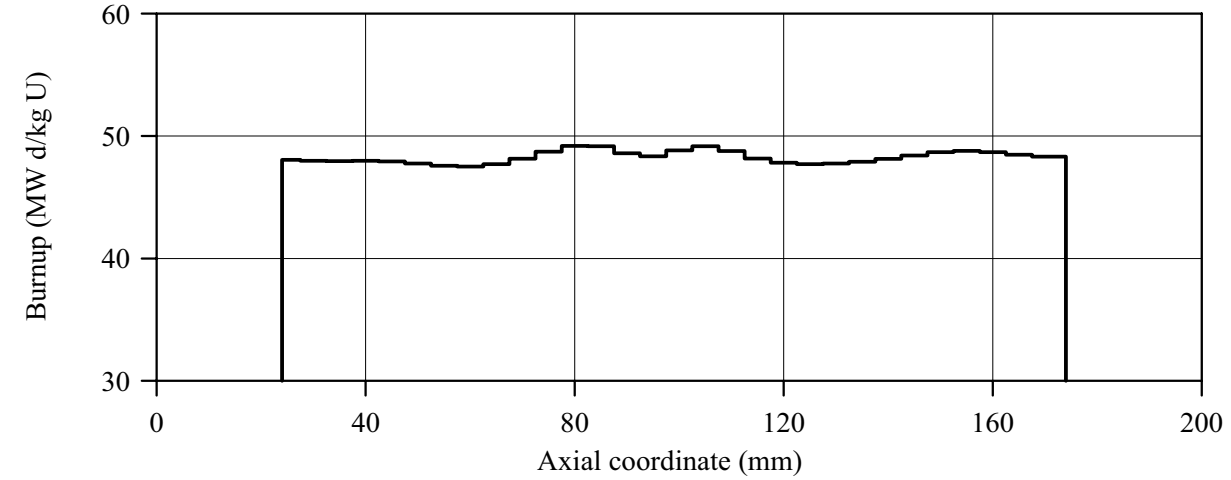
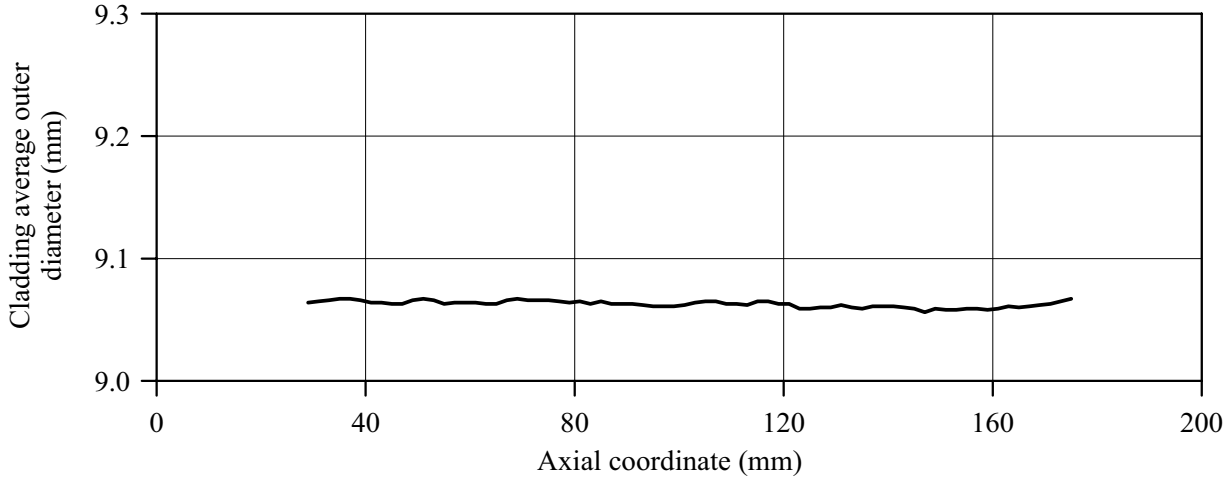


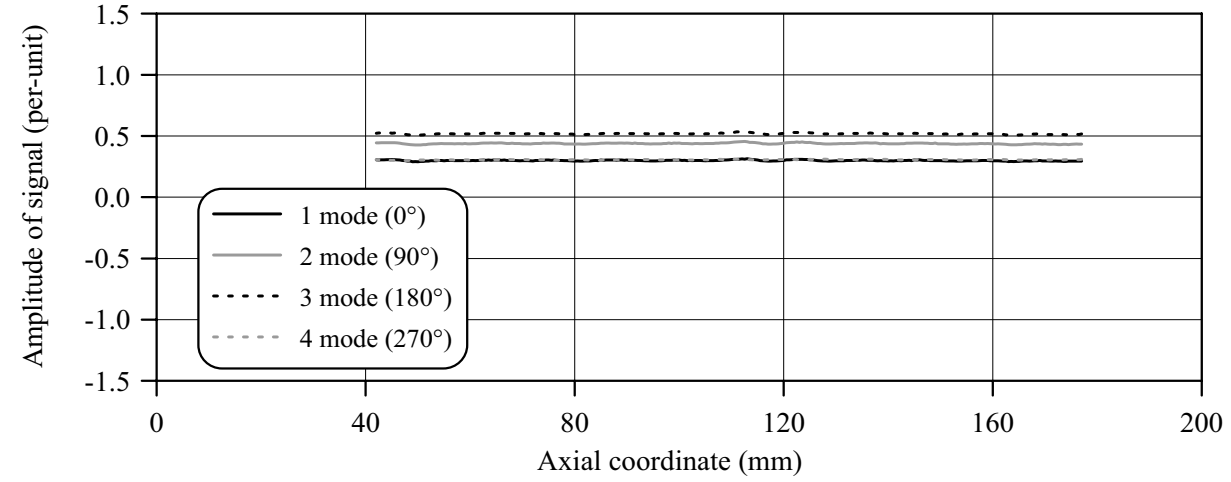
Fig.C-1.1. (a) Results of γ-scanning, (b) Axial fuel mass distribution and axial gas flow area distribution for fuel rod # RT1



a)



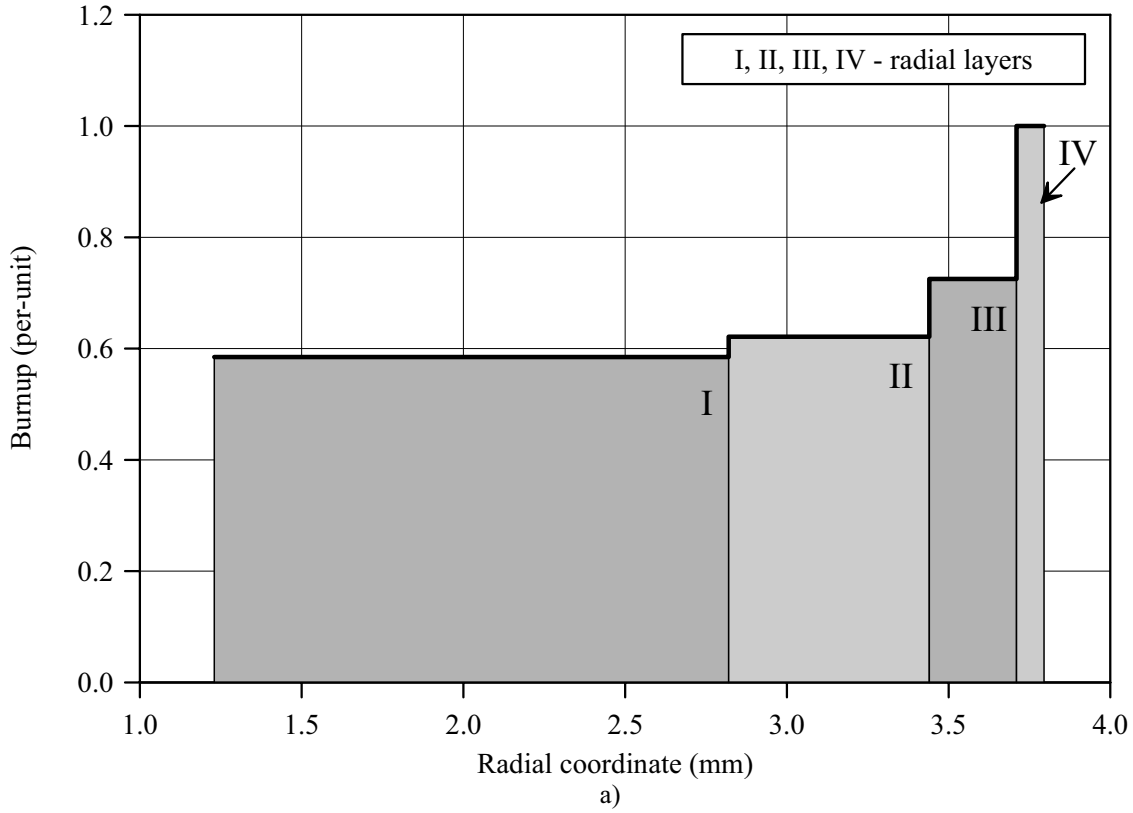
b)



c)

Fig.C-1.2. (a) Axial burnup distribution and (b) results of profilometry and (c) eddy-current examination of fuel rod # RT1

RT1



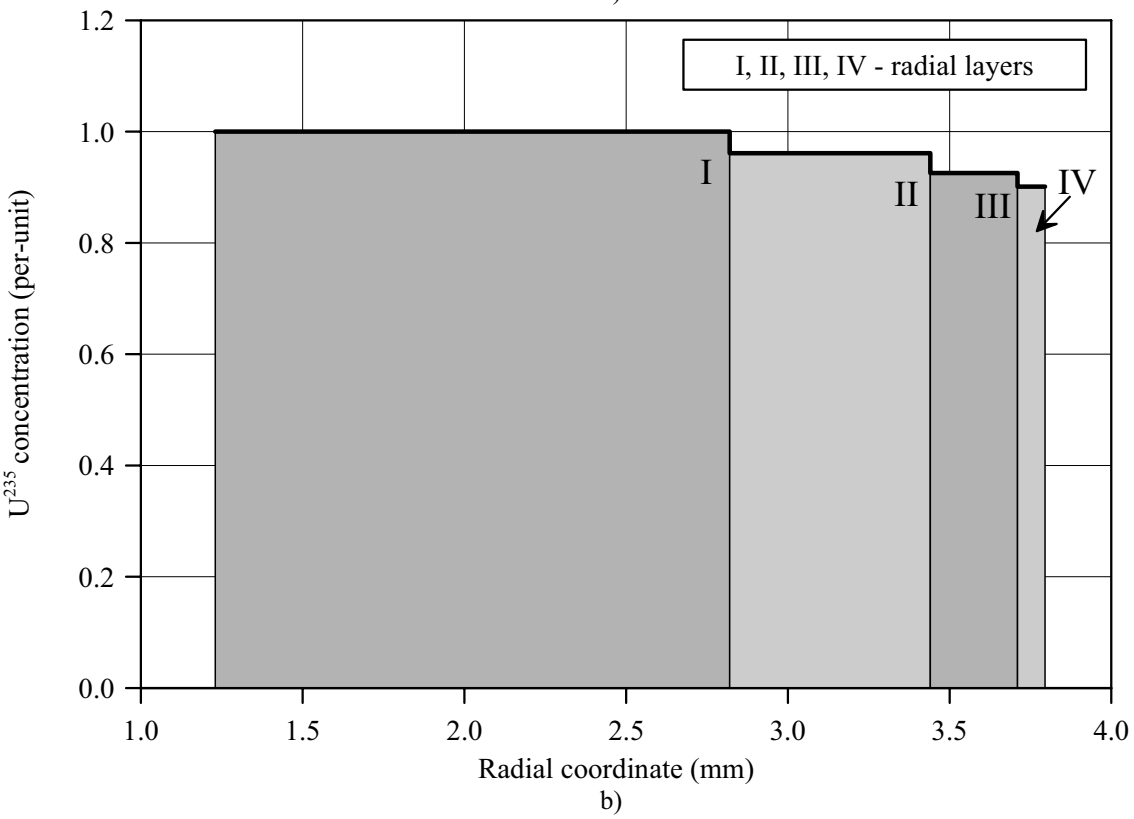


Fig.C-1.3. (a) Burnup radial distribution and (b) U^{235} radial distribution for fuel rod # RT1 (calculated values)

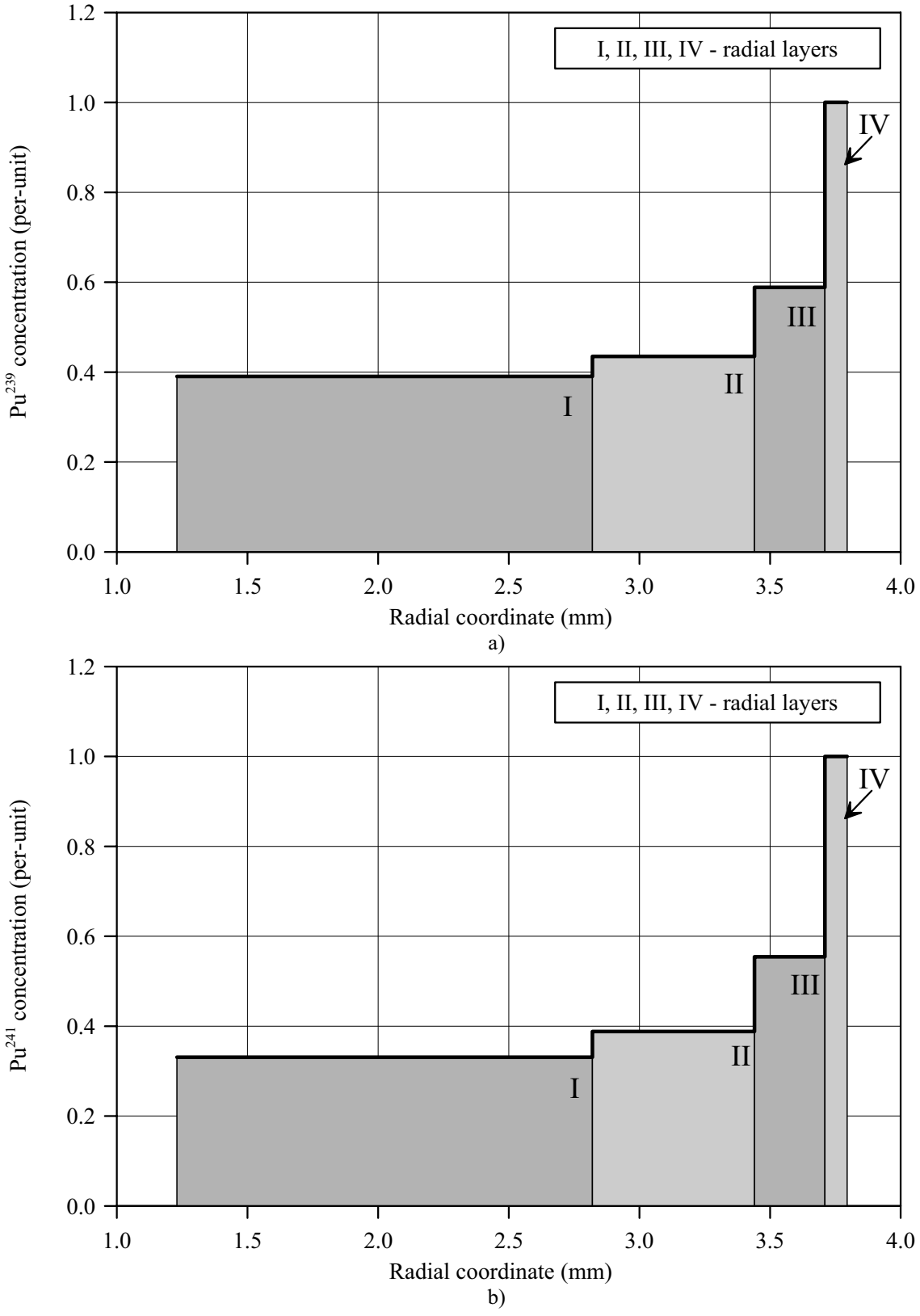


Fig.C-1.4. Radial distribution of (a) Pu^{239} and (b) Pu^{241} for fuel rod # RT1 (calculated values)

Appendix C-2

Individual Characteristics of Fuel Rod # RT2 before the BIGR Test

RT2

Table C-2.1. Radial distribution of isotope nuclear concentrations for fuel rod #RT2 (values averaged of over the fuel stack length)*

Isotope	Isotopic concentrations (kg/t U) in four fuel radial layers			
	1.23-2.82 mm	2.82-3.44 mm	3.44-3.71 mm	3.71-3.795 mm
U^{234}	0.233	0.229	0.226	0.222
U^{235}	7.796	7.493	7.216	7.026
U^{236}	6.451	6.463	6.475	6.490
U^{238}	928.7	925.0	913.5	882.1
Pu^{238}	0.352	0.371	0.401	0.456
Pu^{239}	4.766	5.310	7.184	12.20
Pu^{240}	2.466	2.618	3.380	5.519
Pu^{241}	0.997	1.170	1.671	3.014
Pu^{242}	0.712	0.859	1.263	2.352
Np^{237}	0.606	0.625	0.644	0.657
Am^{241}	0.366	0.424	0.601	1.084
Oxygen	134.5	134.5	134.5	134.5
Other fission products	47.48	50.42	58.72	80.81

* Measured averaged concentrations and calculated relative radial distributions of isotopes (TRIFOB code) were used to develop these data

Table C-2.2. Initial individual characteristics of fuel rod # RT2*

Axial coordinate (from lower cap) (mm)	Cladding average outer diameter (mm)	Fuel mass ** (g)	Linear fuel mass** (g/cm)	Gas flow area[3]** (mm^2)	Burnup** (MW d/kg U)
25[1]	-	0.85	4.07	5.410	47.65
30	-	2.04	4.08	5.310	47.82
35	9.067	2.03	4.06	5.509	47.97
40	9.067	2.02	4.05	5.608	48.03
45	9.064	2.04	4.08	5.310	47.81
50	9.066	2.05	4.10	5.112	47.23
55	9.063	2.09	4.19	4.800	46.90
60	9.064	2.09	4.18	4.800	47.41
65	9.063	2.10	4.20	4.800	47.93
70	9.065	2.05	4.11	5.013	47.53
75	9.066	2.12	4.23	4.800	47.11
80	9.063	2.10	4.20	4.800	47.76
85	9.063	2.06	4.13	4.814	48.63
90	9.063	2.04	4.08	5.310	48.58
95	9.063	2.01	4.02	5.906	48.21
100	9.063	2.06	4.13	4.814	48.36
105	9.062	2.04	4.08	5.310	48.53
110	9.062	2.06	4.12	4.913	48.09
115	9.061	2.04	4.09	5.211	47.73
120	9.063	2.07	4.15	4.800	48.29
125	9.061	2.06	4.11	5.013	48.96
130	9.063	2.01	4.03	5.807	48.74
135	9.060	2.06	4.12	4.913	48.13
140	9.060	2.06	4.12	4.913	47.93
145	9.058	2.08	4.16	4.800	48.12
150	9.058	2.07	4.13	4.814	48.40
155	9.059	2.09	4.19	4.800	48.43
160	9.058	2.08	4.16	4.800	47.99
165	9.061	2.03	4.06	5.509	47.61
170	9.062	2.00	3.99	6.204	47.86
175[2]	-	1.58	4.06	5.509	48.39

* All parameters were determined using results of pre-test examinations

** Average values at the length interval equal to the axial coordinate ±2.5 mm

[1] Bottom end coordinate of fuel stack is 25.4 mm; [2] Top end coordinate of fuel stack is 176.4 mm

[3] Gas flow area beyond the fuel stack (mm^2):

Bottom: 0.0-3.0mm – 0.00; 3.0-10.5mm – 12.56; 10.5-16.5mm – 45.82; 15.1-25.4mm – 24.97

Top: 176.4-179.5mm – 45.82; 179.5-205.5mm – 28.26; 205.5-282mm – 45.82; 282-291mm – 28.26; 291-300mm – 0.00

RT2

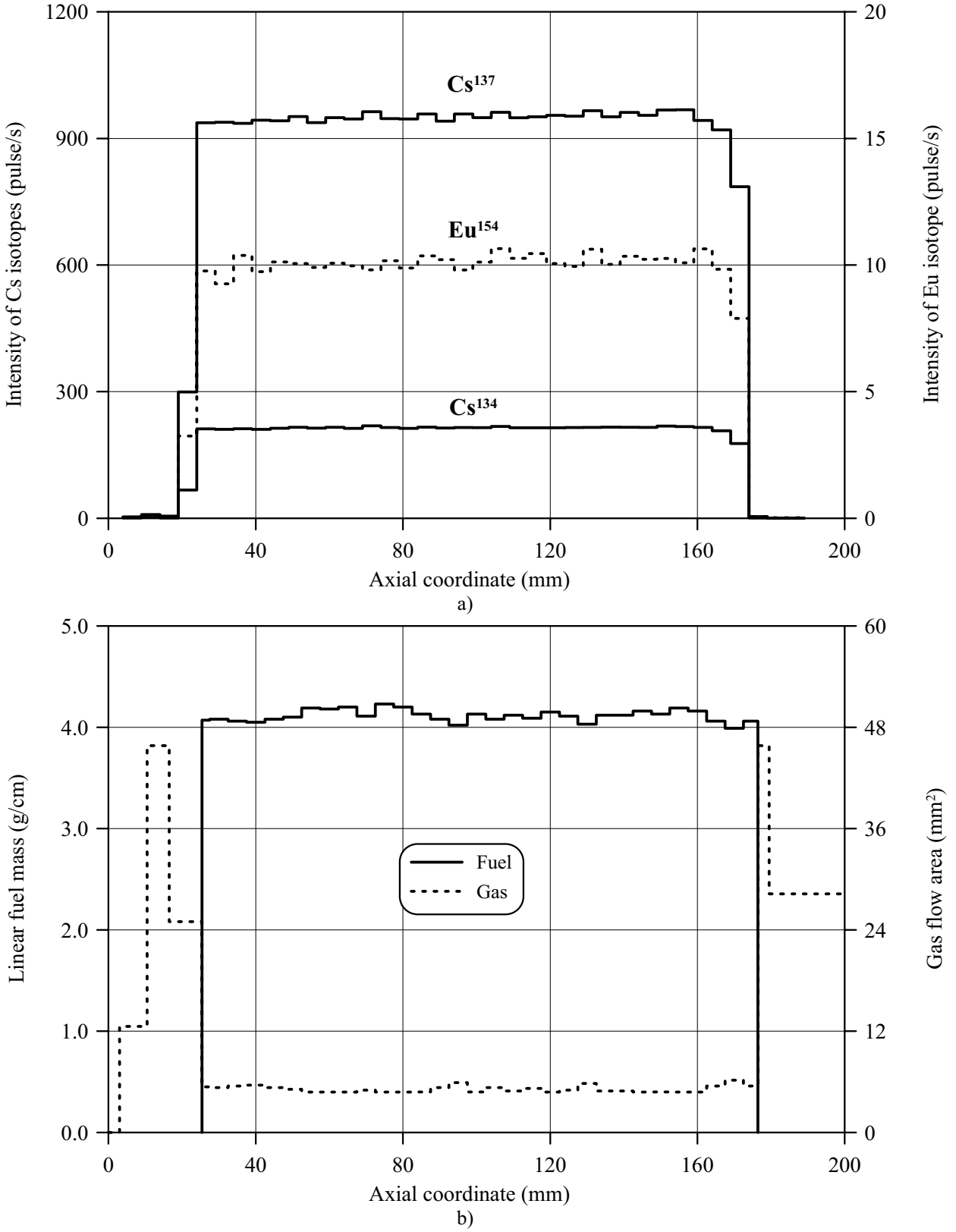


Fig.C-2.1. (a) Results of γ-scanning, (b) Axial fuel mass distribution and axial gas flow area distribution for fuel rod # RT2

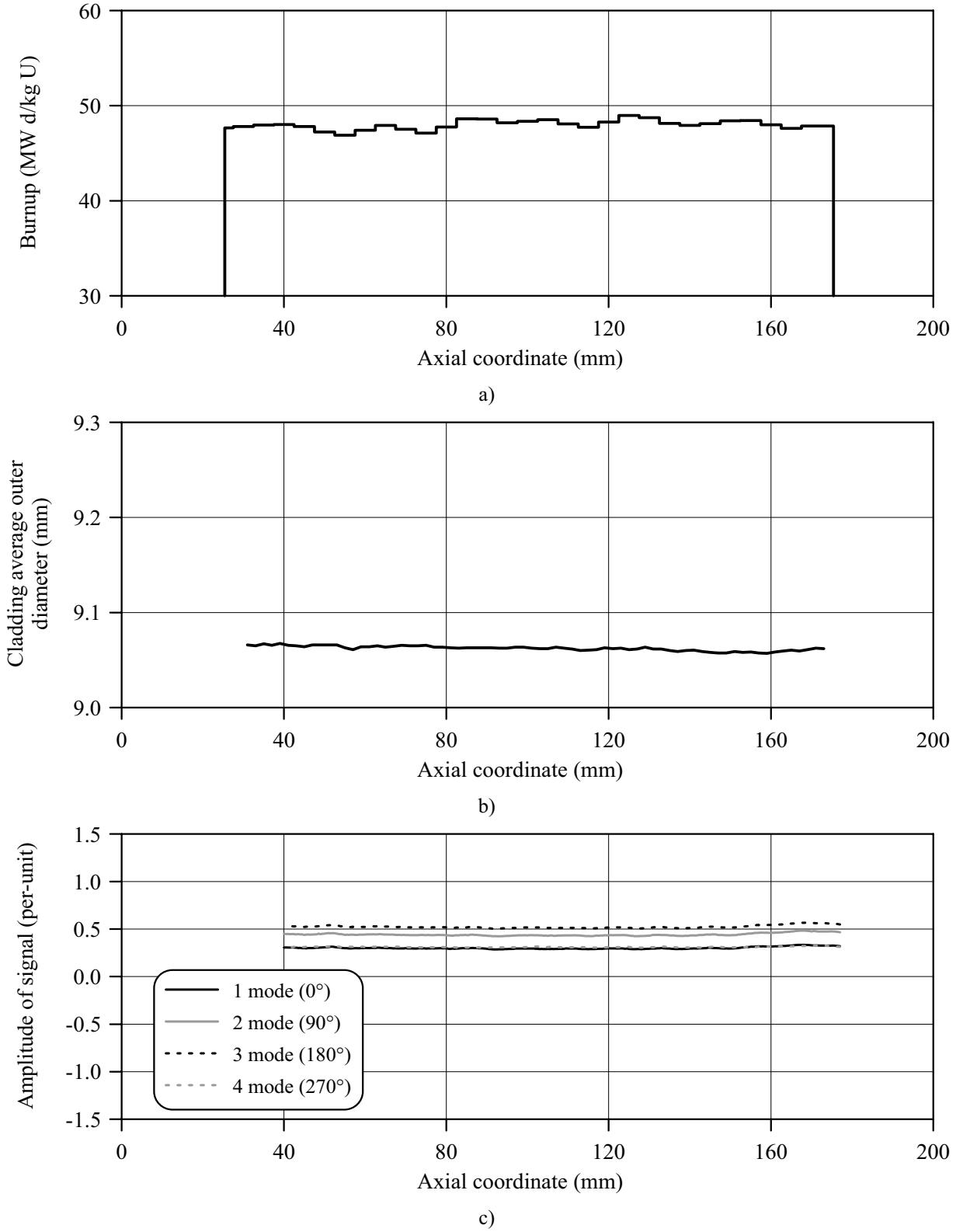


Fig.C-2.2. (a) Axial burnup distribution and (b) results of profilometry and (c) eddy-current examination of fuel rod # RT2

RT2

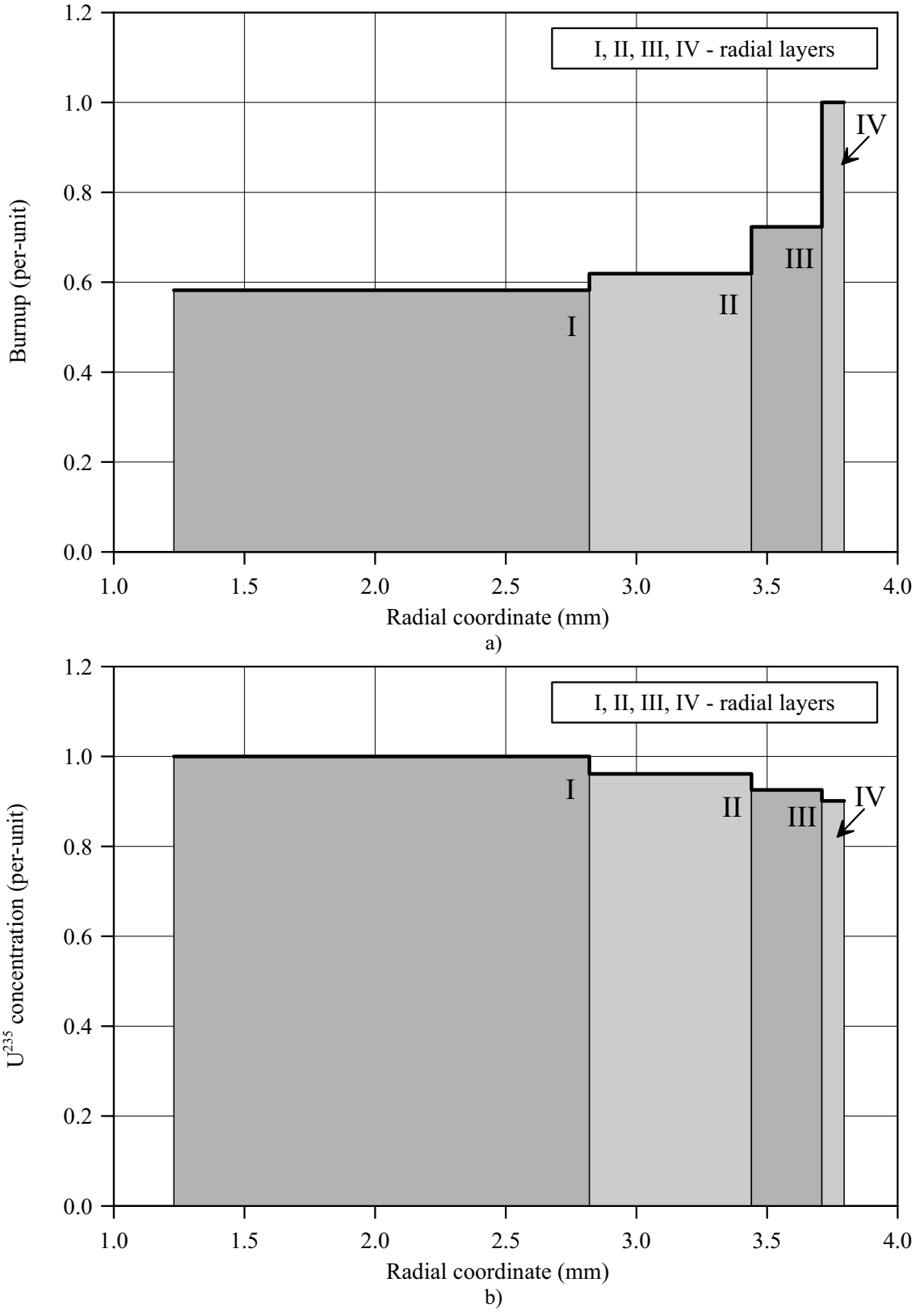


Fig.C-2.3. (a) Burnup radial distribution and (b) U^{235} radial distribution for fuel rod # RT2 (calculated values)

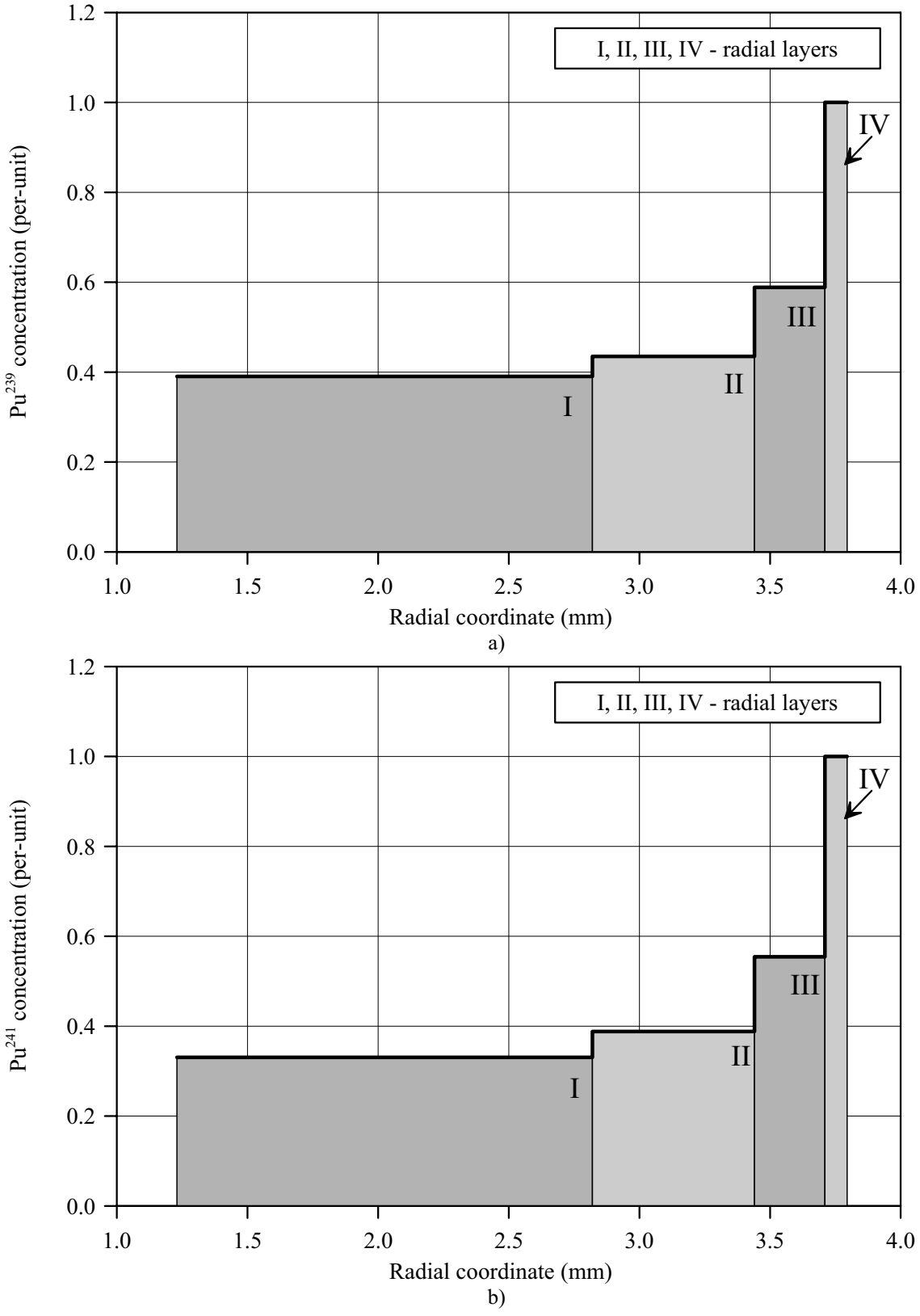


Fig.C-2.4. Radial distribution of (a) Pu^{239} and (b) Pu^{241} for fuel rod # RT2 (calculated values)

Appendix C-3

Individual Characteristics of Fuel Rod # RT3 before the BIGR Test

RT3

Table C-3.1. Radial distribution of isotope nuclear concentrations for fuel rod #RT3 (values averaged of over the fuel stack length)*

Isotope	Isotopic concentrations (kg/t U) in four fuel radial layers			
	1.23-2.82 mm	2.82-3.44 mm	3.44-3.71 mm	3.71-3.795 mm
U^{234}	0.202	0.199	0.196	0.193
U^{235}	7.828	7.537	7.269	7.085
U^{236}	6.220	6.233	6.247	6.262
U^{238}	929.1	925.4	913.7	882.1
Pu^{238}	0.380	0.401	0.433	0.491
Pu^{239}	5.029	5.601	7.576	12.85
Pu^{240}	2.565	2.722	3.511	5.718
Pu^{241}	1.053	1.236	1.765	3.180
Pu^{242}	0.728	0.878	1.290	2.397
Np^{237}	0.620	0.640	0.659	0.672
Am^{241}	0.393	0.455	0.643	1.158
Oxygen	134.5	134.5	134.5	134.5
Other fission products	46.83	49.69	58.00	79.91

* Measured averaged concentrations and calculated relative radial distributions of isotopes (TRIFOB code) were used to develop these data

Table C-3.2. Initial individual characteristics of fuel rod # RT3*

Axial coordinate (from lower cap) (mm)	Cladding average outer diameter (mm)	Fuel mass ** (g)	Linear fuel mass** (g/cm)	Gas flow area[3]** (mm^2)	Burnup** (MW d/kg U)
25[1]	-	1.58	3.97	5.704	44.35
30	-	2.01	4.03	5.098	44.41
35	9.061	2.05	4.09	4.800	44.59
40	9.063	2.02	4.04	4.997	45.19
45	9.063	2.01	4.01	5.300	46.06
50	9.061	2.00	3.99	5.502	47.09
55	9.062	1.90	3.81	7.321	47.14
60	9.062	1.76	3.51	10.352	46.10
65	9.057	1.87	3.73	8.129	45.83
70	9.060	2.03	4.06	4.795	47.06
75	9.066	2.02	4.04	4.997	48.09
80	9.062	2.05	4.10	4.800	48.08
85	9.059	2.02	4.03	5.098	48.06
90	9.063	2.01	4.02	5.199	48.54
95	9.059	2.04	4.08	4.800	48.64
100	9.064	2.09	4.18	4.800	48.09
105	9.062	2.08	4.16	4.800	47.97
110	9.070	2.02	4.05	4.896	48.65
115	9.061	1.93	3.86	6.816	49.05
120	9.056	1.93	3.86	6.816	48.60
125	9.058	2.05	4.10	4.800	47.94
130	9.054	2.10	4.19	4.800	47.57
135	9.059	2.11	4.21	4.800	47.51
140	9.056	2.11	4.21	4.800	47.75
145	9.052	2.05	4.11	4.800	48.36
150	9.053	2.02	4.04	4.997	49.08
155	9.050	2.08	4.16	4.800	49.09
160	9.049	2.13	4.25	4.800	48.25
165	9.048	2.09	4.19	4.800	47.75
170	9.049	2.07	4.14	4.800	48.14
175[2]	9.054	0.04	4.11	4.800	48.51

* All parameters were determined using results of pre-test examinations

** Average values at the length interval equal to the axial coordinate ±2.5 mm

[1] Bottom end coordinate of fuel stack is 23.6 mm; [2] Top end coordinate of fuel stack is 172.6 mm

[3] Gas flow area beyond the fuel stack (mm^2):

Bottom: 0.0-3.0mm – 0.00; 3.0-10.5mm – 12.56; 10.5-14.7mm – 45.82; 14.7-23.6mm – 24.97

Top: 172.6-176mm – 45.82; 176-202mm – 28.26; 202-278.5mm – 45.82; 278.5-287.5mm – 28.26; 287.5-296.5mm – 0.00

RT3

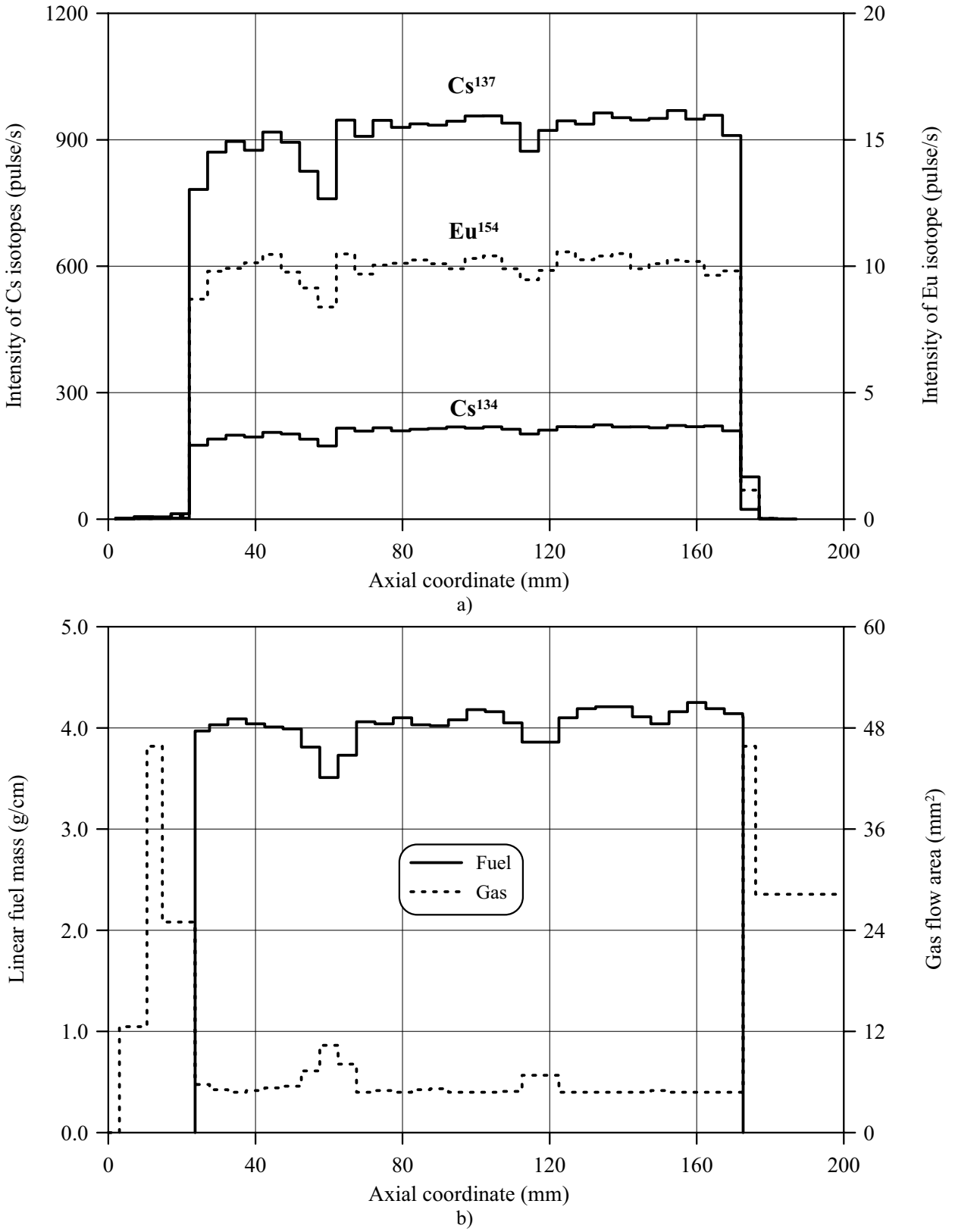


Fig.C-3.1. (a) Results of γ-scanning, (b) Axial fuel mass distribution and axial gas flow area distribution for fuel rod # RT3

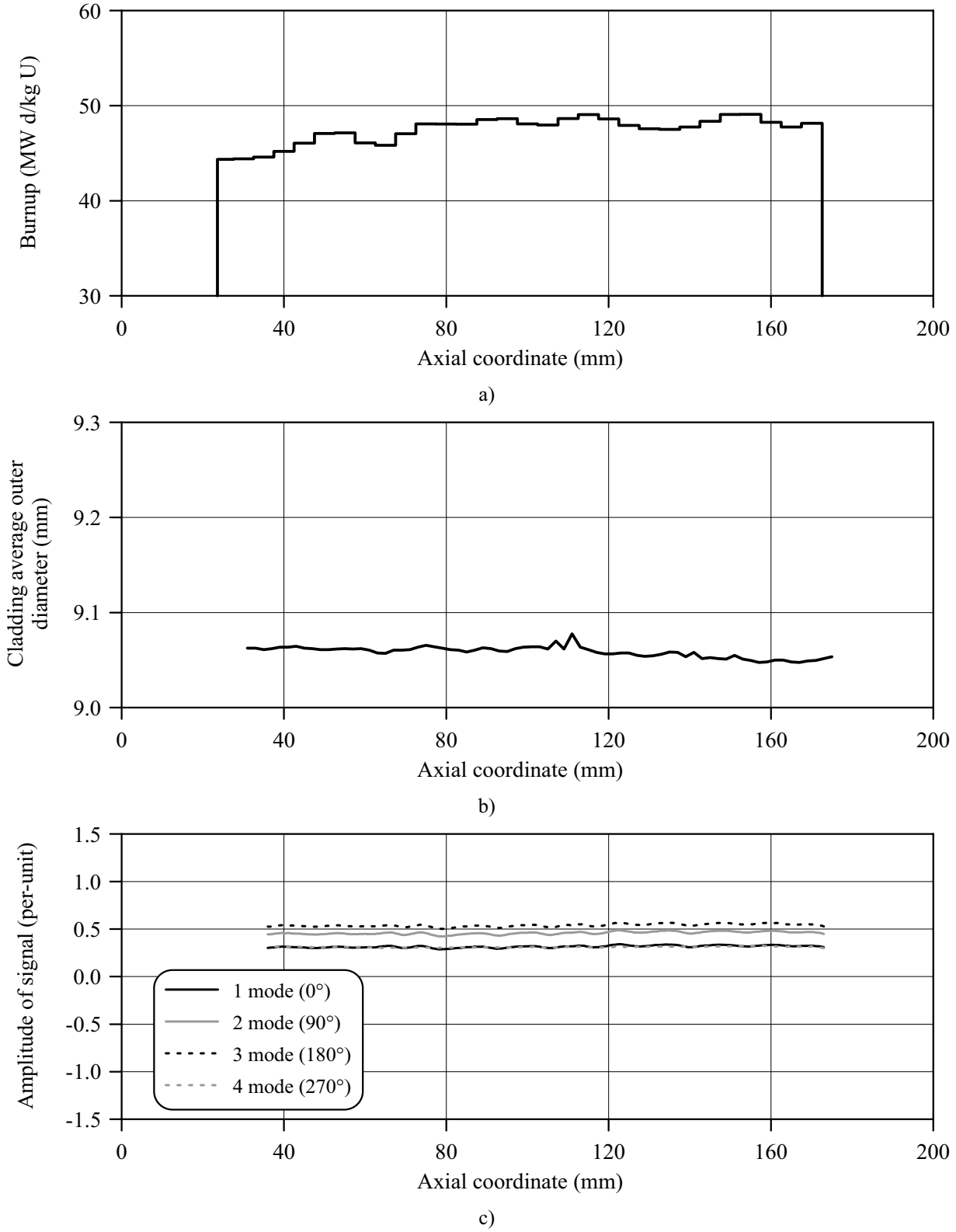


Fig.C-3.2. (a) Axial burnup distribution and (b) results of profilometry and (c) eddy-current examination of fuel rod # RT3

RT3

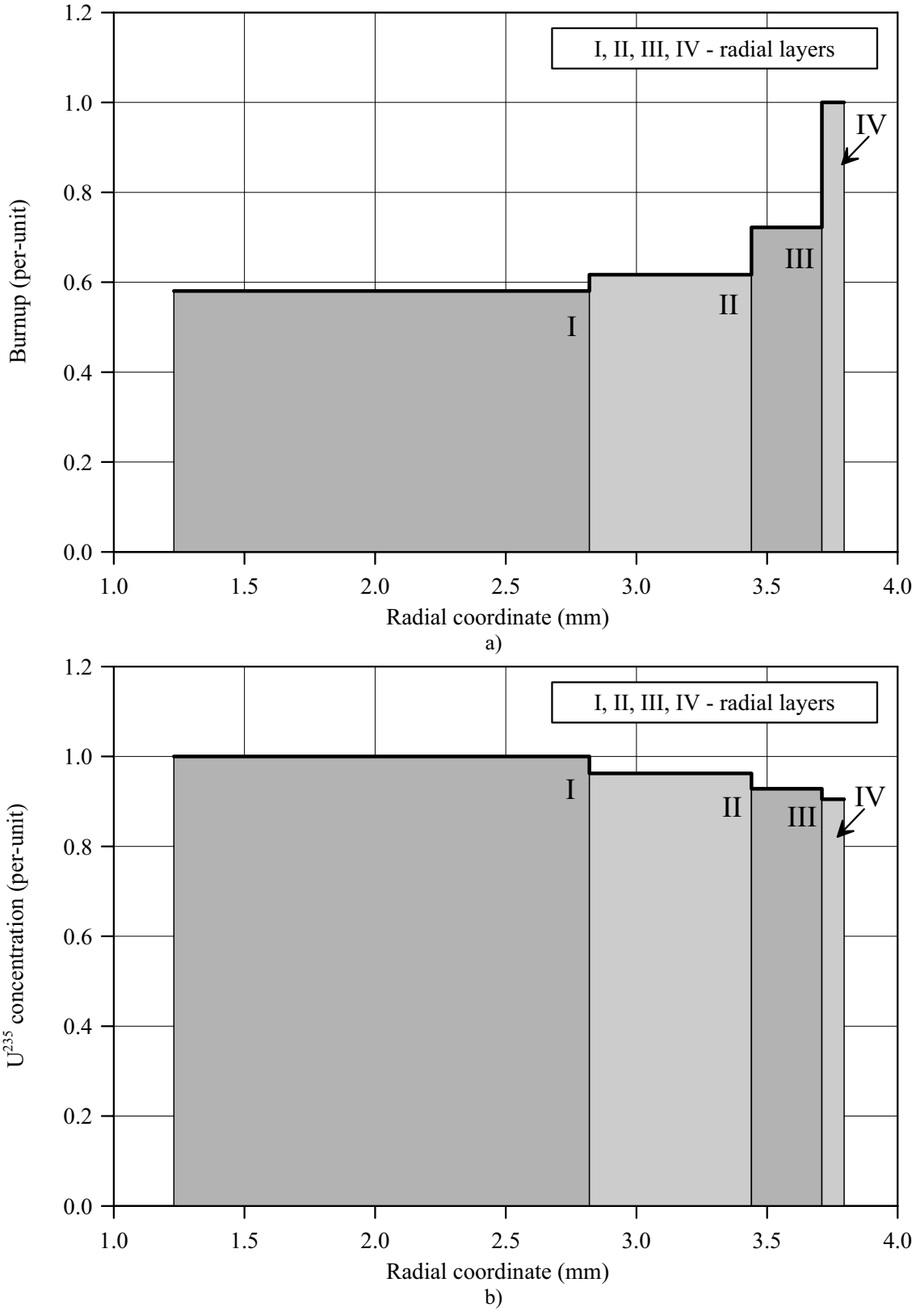


Fig.C-3.3. (a) Burnup radial distribution and (b) U^{235} radial distribution for fuel rod # RT3 (calculated values)

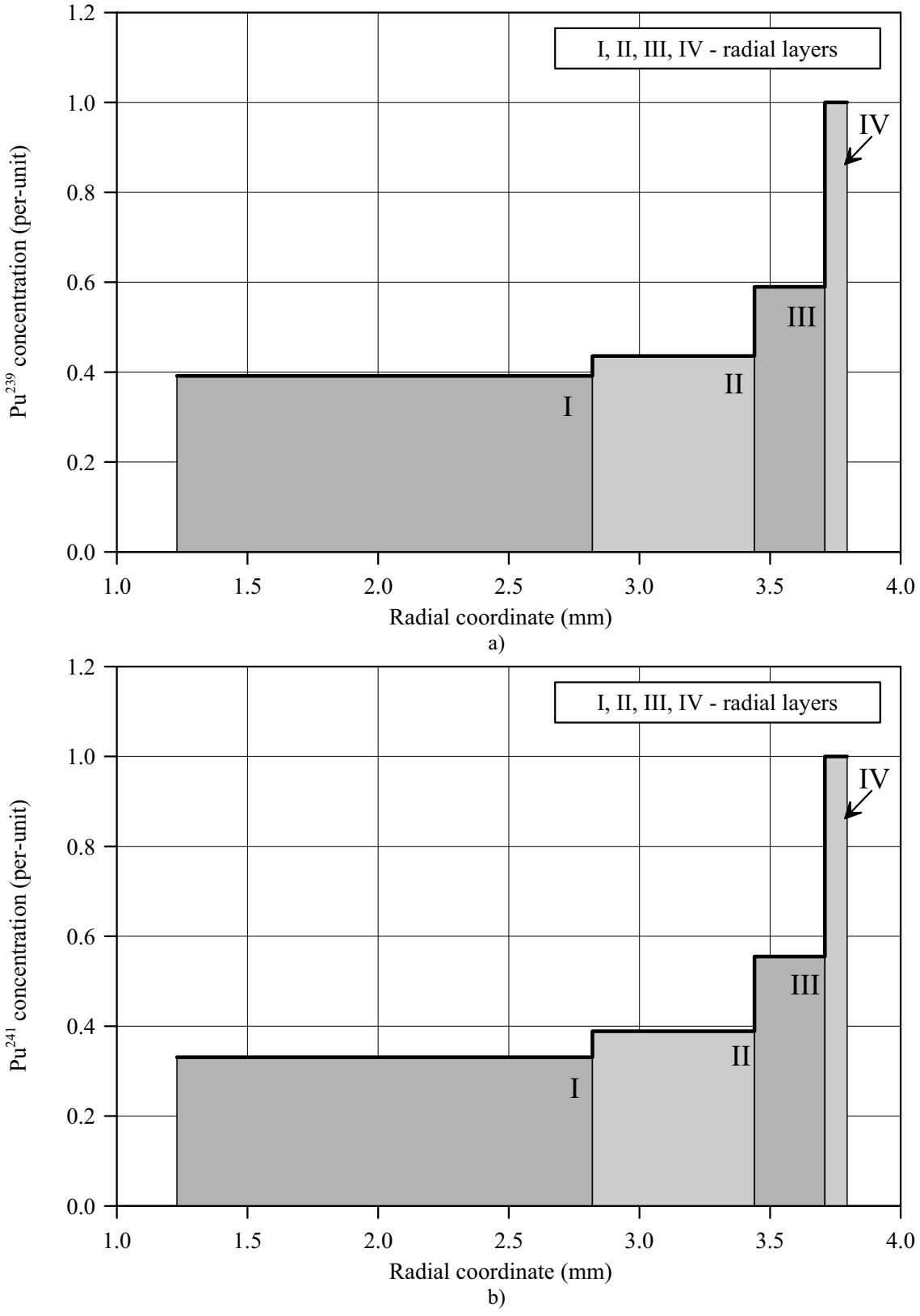


Fig.C-3.4. Radial distribution of (a) Pu^{239} and (b) Pu^{241} for fuel rod # RT3 (calculated values)

Appendix C-4

Individual Characteristics of Fuel Rod # RT4 before the BIGR Test

RT4

Table C-4.1. Radial distribution of isotope nuclear concentrations for fuel rod #RT4 (values averaged of over the fuel stack length)*

Isotope	Isotopic concentrations (kg/t U) in four fuel radial layers			
	0.825-2.77 mm	2.77-3.45 mm	3.45-3.75 mm	3.75-3.84 mm
U^{234}	0.220	0.219	0.220	0.227
U^{235}	4.900	4.626	4.403	4.255
U^{236}	6.668	6.642	6.620	6.610
U^{238}	922.3	917.6	904.3	865.5
Pu^{238}	0.531	0.574	0.648	0.822
Pu^{239}	4.923	5.421	7.106	11.97
Pu^{240}	2.757	2.839	3.487	5.564
Pu^{241}	1.064	1.244	1.728	3.116
Pu^{242}	0.985	1.196	1.720	3.217
Np^{237}	0.773	0.803	0.828	0.846
Am^{241}	0.903	1.054	1.463	2.639
Oxygen	134.5	134.5	134.5	134.5
Other fission products	55.69	59.58	69.70	98.70

* Measured averaged concentrations and calculated relative radial distributions of isotopes (TRIFOB code) were used to develop these data

Table C-4.2. Initial individual characteristics of fuel rod # RT4*

Axial coordinate (from lower cap) (mm)	Cladding average outer diameter (mm)	Fuel mass ** (g)	Linear fuel mass** (g/cm)	Gas flow area[3]** (mm^2)	Burnup** (MW d/kg U)
25[1]	9.066	2.48	4.50	2.270	58.72
30	9.069	2.25	4.49	2.339	59.36
35	9.078	2.27	4.53	2.270	60.53
40	9.073	2.27	4.54	2.270	60.51
45	9.087	2.24	4.48	2.437	60.03
50	9.075	2.22	4.45	2.731	59.74
55	9.087	2.22	4.43	2.927	60.13
60	9.092	2.22	4.43	2.927	60.72
65	9.085	2.24	4.48	2.437	60.41
70	9.077	2.24	4.48	2.437	59.48
75	9.078	2.22	4.45	2.731	59.27
80	9.073	2.22	4.43	2.927	59.74
85	9.077	2.25	4.50	2.270	59.88
90	9.082	2.29	4.57	2.270	59.75
95	9.077	2.28	4.56	2.270	60.14
100	9.083	2.27	4.55	2.270	60.81
105	9.075	2.27	4.54	2.270	60.73
110	9.076	2.27	4.54	2.270	60.15
115	9.067	2.25	4.50	2.270	60.18
120	9.077	2.23	4.46	2.633	60.58
125	9.066	2.24	4.48	2.437	60.18
130	9.082	2.26	4.53	2.270	59.41
135	9.086	2.25	4.50	2.270	59.80
140	9.093	2.23	4.47	2.535	61.00
145	9.080	2.26	4.52	2.270	61.34
150	9.076	2.28	4.56	2.270	60.76
155	9.085	2.26	4.52	2.270	60.42
160	9.085	2.22	4.44	2.829	60.44
165	9.083	2.22	4.44	2.829	60.17
170	9.080	2.25	4.49	2.339	59.57
175[2]	9.086	1.98	4.40	3.221	59.10

* All parameters were determined using results of pre-test examinations

** Average values at the length interval equal to the axial coordinate ±2.5 mm

[1] Bottom end coordinate of fuel stack is 22 mm; [2] Top end coordinate of fuel stack is 177 mm

[3] Gas flow area beyond the fuel stack (mm^2):

Bottom: 0.0-3.0mm – 0.00; 3.0-10.5mm – 12.56; 10.5-13.1mm – 46.35; 13.1-22.0mm – 25.36

Top: 177-179.5mm – 46.35; 179.5-205.5mm – 28.26; 205.5-282mm – 46.35; 282-291mm – 28.26; 291-300mm – 0.00

RT4

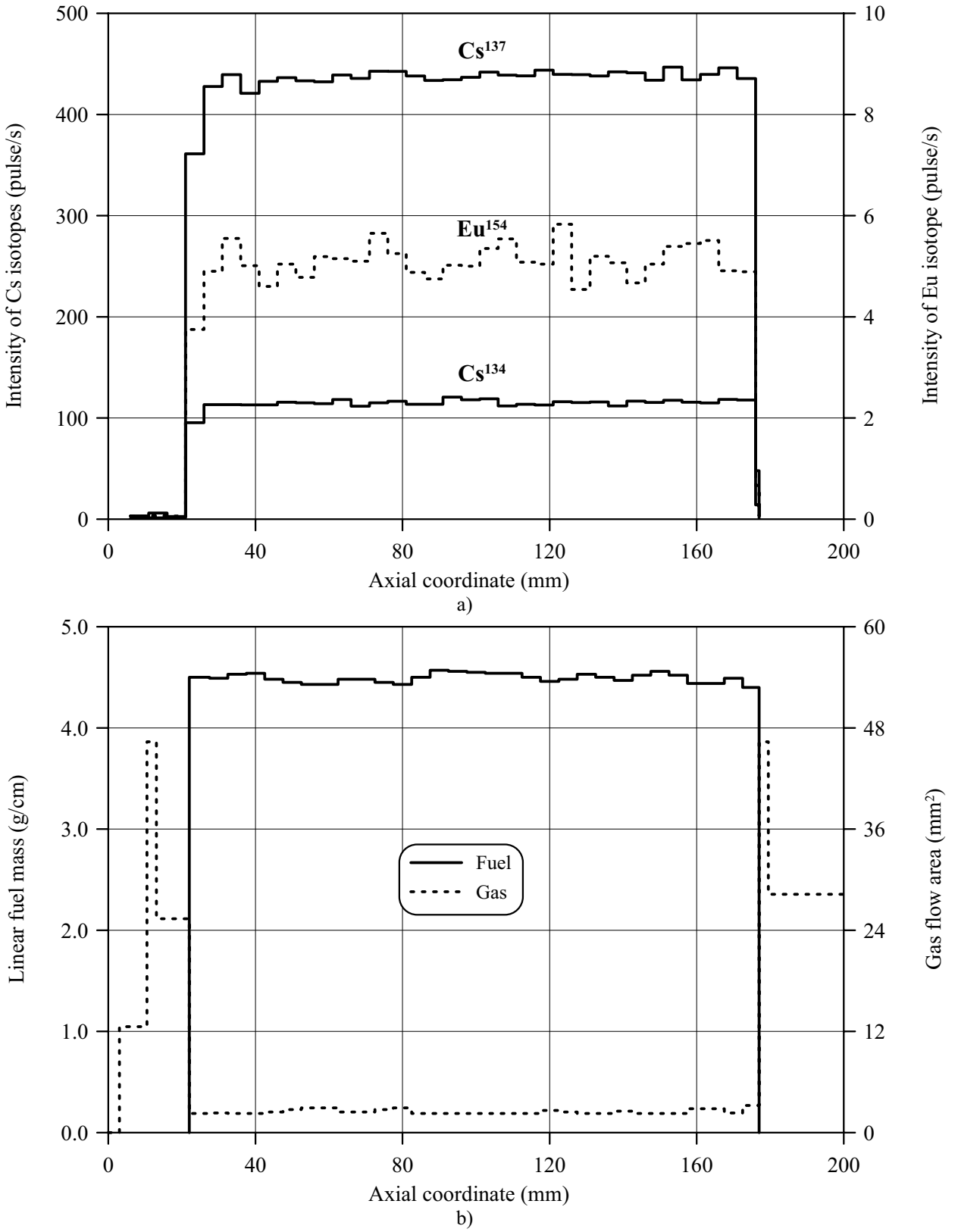


Fig.C-4.1. (a) Results of γ-scanning, (b) Axial fuel mass distribution and axial gas flow area distribution for fuel rod # RT4

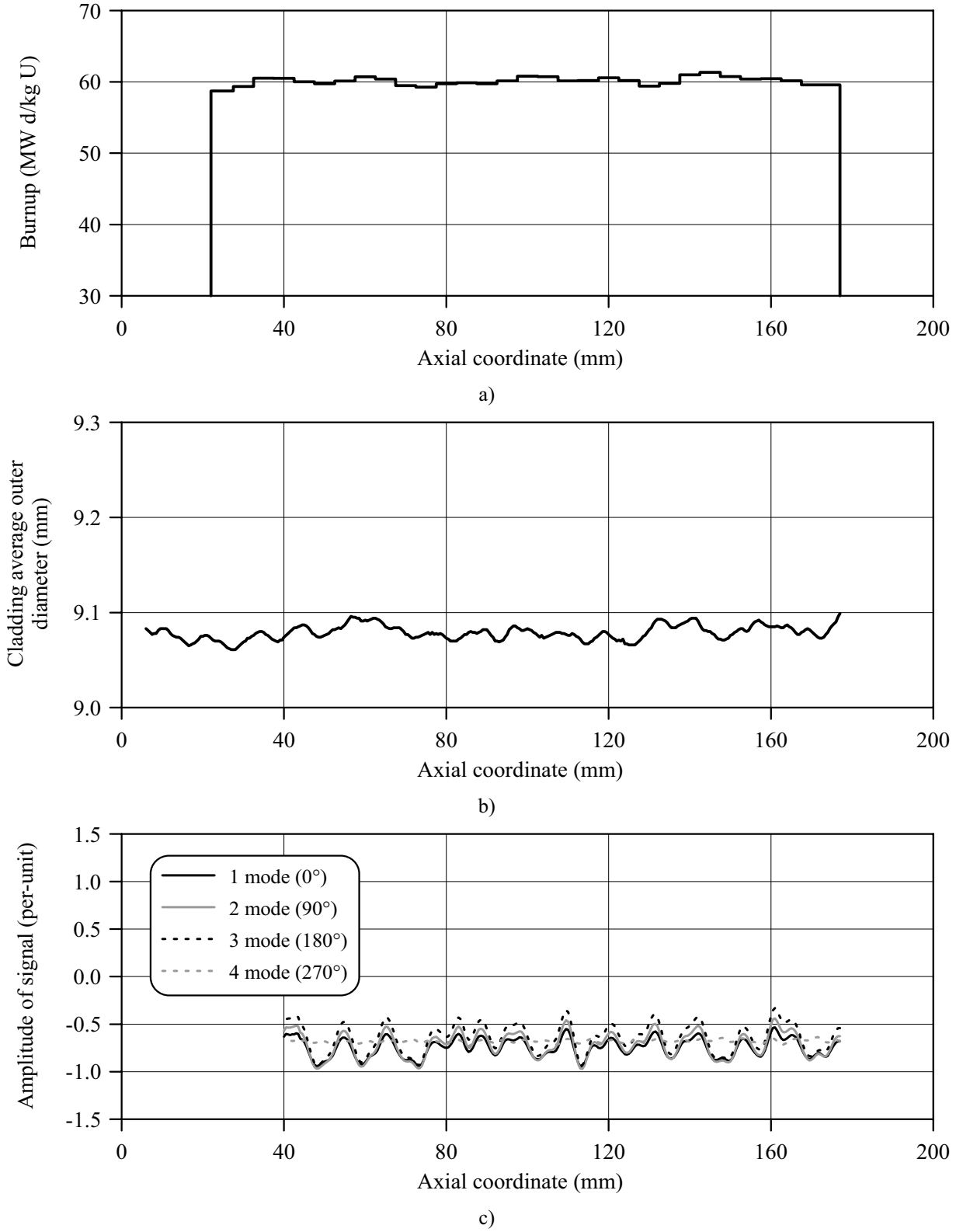


Fig.C-4.2. (a) Axial burnup distribution and (b) results of profilometry and (c) eddy-current examination of fuel rod # RT4

RT4

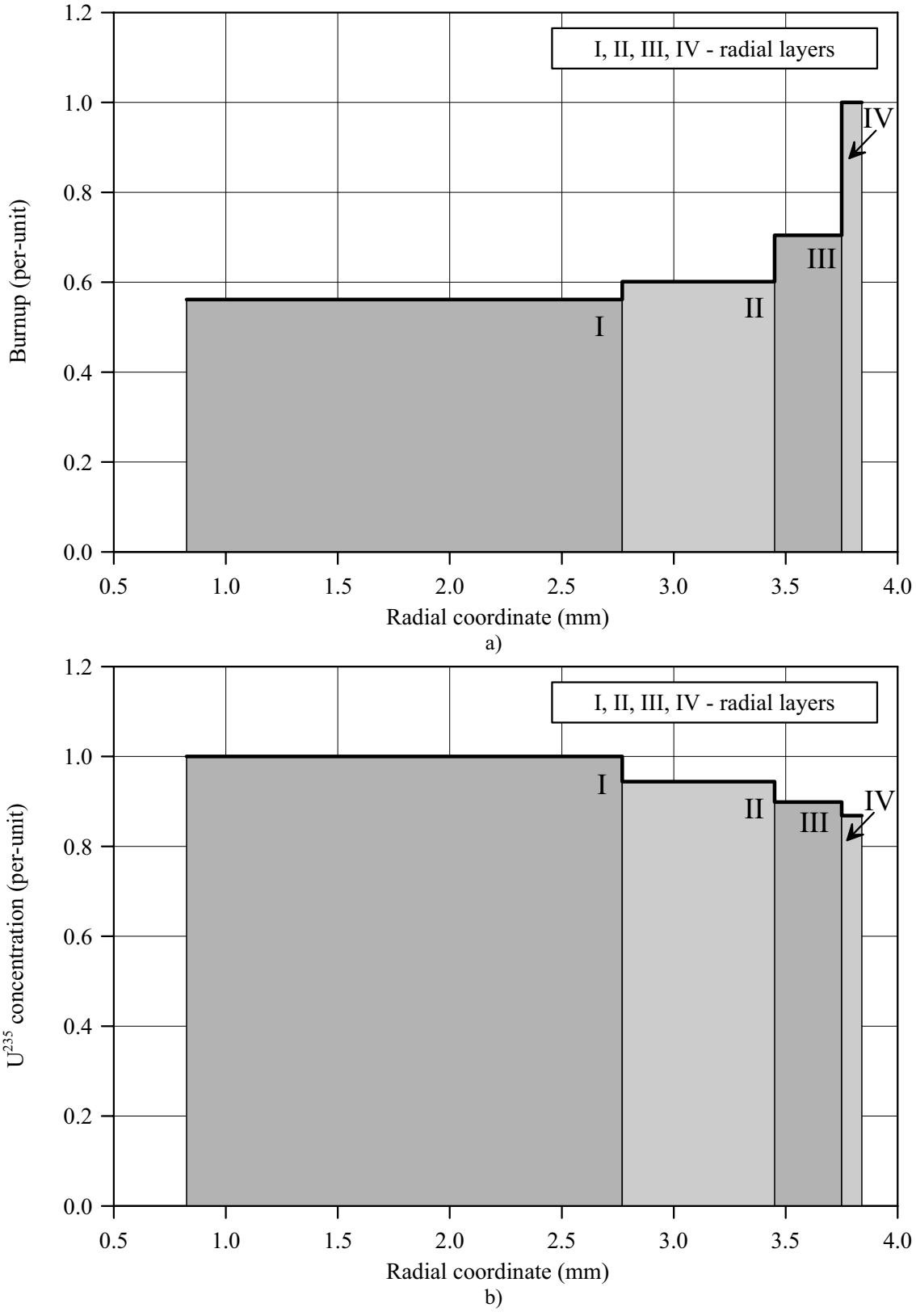


Fig.C-4.3. (a) Burnup radial distribution and (b) U^{235} radial distribution for fuel rod # RT4 (calculated values)

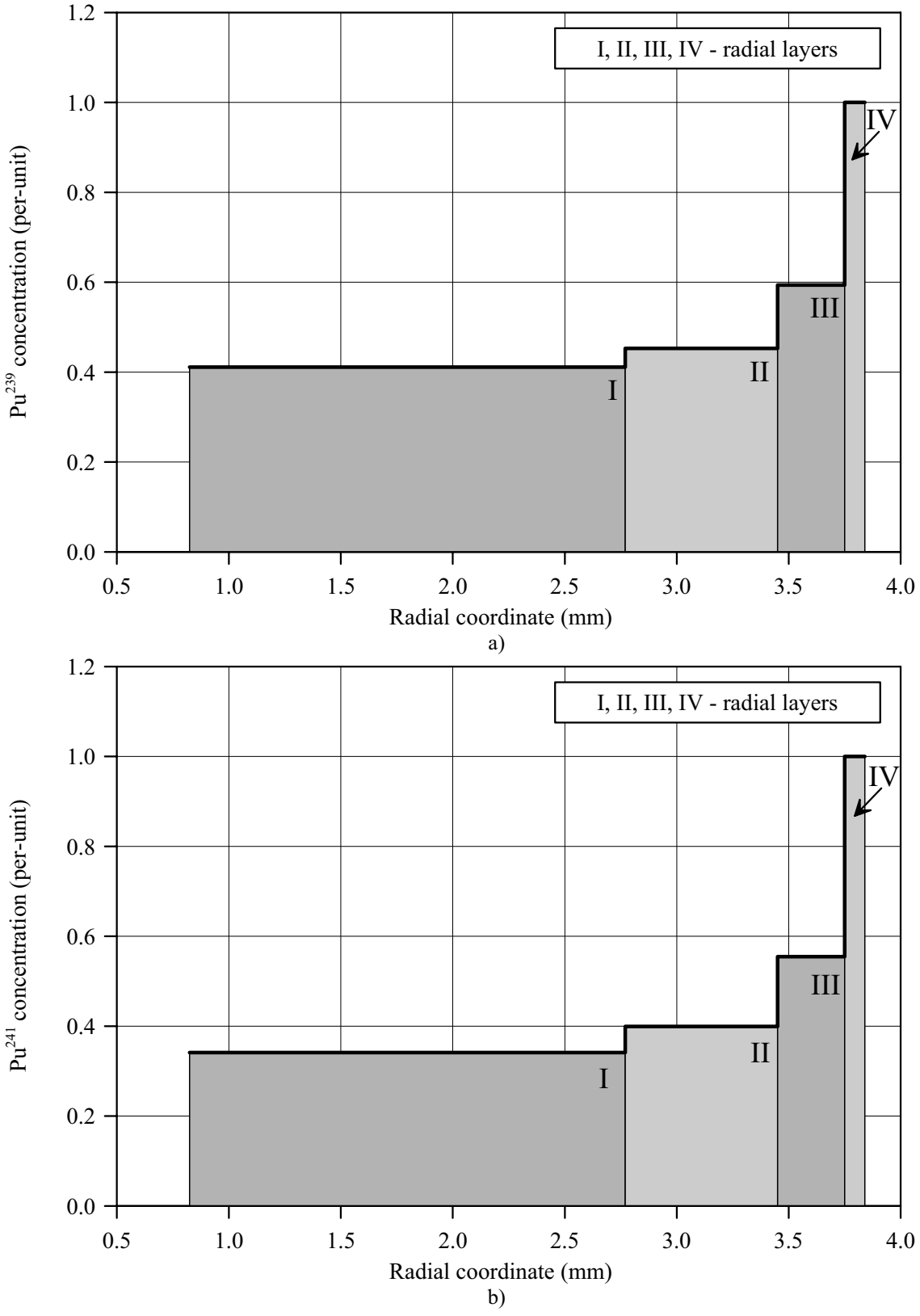


Fig.C-4.4. Radial distribution of (a) Pu^{239} and (b) Pu^{241} for fuel rod # RT4 (calculated values)

Appendix C-5

Individual Characteristics of Fuel Rod # RT5 before the BIGR Test

RT5

Table C-5.1. Radial distribution of isotope nuclear concentrations for fuel rod #RT5 (values averaged of over the fuel stack length)*

Isotope	Isotopic concentrations (kg/t U) in four fuel radial layers			
	1.25-2.84 mm	2.84-3.47 mm	3.47-3.74 mm	3.74-3.808 mm
U^{234}	0.293	0.289	0.284	0.280
U^{235}	8.104	7.783	7.488	7.286
U^{236}	6.275	6.281	6.288	6.298
U^{238}	925.6	921.8	909.3	876.0
Pu^{238}	0.406	0.428	0.463	0.526
Pu^{239}	5.032	5.598	7.550	12.74
Pu^{240}	2.661	2.807	3.592	5.795
Pu^{241}	0.999	1.170	1.664	2.980
Pu^{242}	0.804	0.969	1.421	2.630
Np^{237}	0.659	0.679	0.698	0.712
Am^{241}	0.514	0.595	0.839	1.503
Oxygen	134.5	134.5	134.5	134.5
Other fission products	49.77	52.91	61.98	85.83

* Measured averaged concentrations and calculated relative radial distributions of isotopes (TRIFOB code) were used to develop these data

Table C-5.2. Initial individual characteristics of fuel rod # RT5*

Axial coordinate (from lower cap) (mm)	Cladding average outer diameter (mm)	Fuel mass ** (g)	Linear fuel mass** (g/cm)	Gas flow area[3]** (mm^2)	Burnup** (MW d/kg U)
25[1]	9.059	1.42	4.05	5.898	47.81
30	9.059	2.04	4.09	5.503	49.16
35	9.060	2.09	4.18	4.910	48.76
40	9.056	2.11	4.23	4.910	48.28
45	9.056	2.09	4.18	4.910	48.85
50	9.055	2.05	4.10	5.404	49.27
55	9.055	2.03	4.06	5.799	48.80
60	9.054	2.02	4.05	5.898	48.48
65	9.056	2.04	4.08	5.602	48.88
70	9.056	2.05	4.09	5.503	48.98
75	9.056	2.05	4.10	5.404	48.27
80	9.061	2.06	4.12	5.206	47.80
85	9.059	2.05	4.10	5.404	48.26
90	9.060	2.07	4.13	5.107	49.02
95	9.059	2.08	4.17	4.910	49.47
100	9.061	2.09	4.19	4.910	49.48
105	9.062	2.08	4.16	4.910	49.14
110	9.062	2.07	4.13	5.107	48.98
115	9.063	2.04	4.08	5.602	49.25
120	9.063	2.01	4.02	6.195	49.53
125	9.064	2.03	4.07	5.701	49.45
130	9.057	2.03	4.06	5.799	49.05
135	9.057	2.05	4.10	5.404	48.44
140	9.051	2.07	4.14	5.008	47.83
145	9.056	2.06	4.12	5.206	47.39
150	9.055	2.06	4.12	5.206	47.26
155	9.053	2.07	4.14	5.008	47.46
160	9.054	2.09	4.18	4.910	47.88
165	9.053	2.06	4.12	5.206	48.38
170	9.058	2.04	4.08	5.602	48.88
175[2]	9.037	1.85	4.10	5.404	49.33

* All parameters were determined using results of pre-test examinations

** Average values at the length interval equal to the axial coordinate ±2.5 mm

[1] Bottom end coordinate of fuel stack is 24 mm; [2] Top end coordinate of fuel stack is 177 mm

[3] Gas flow area beyond the fuel stack (mm^2):

Bottom: 0.0-3.0mm – 0.00; 3.0-10.5mm – 12.56; 10.5-15.1mm – 45.94; 15.1-24.0mm – 25.06

Top: 177.0-179.5mm – 45.94; 179.5-205.5mm – 28.26; 205.5-282.0mm – 45.94; 282-291mm – 28.26; 291-300mm – 0.00

RT5

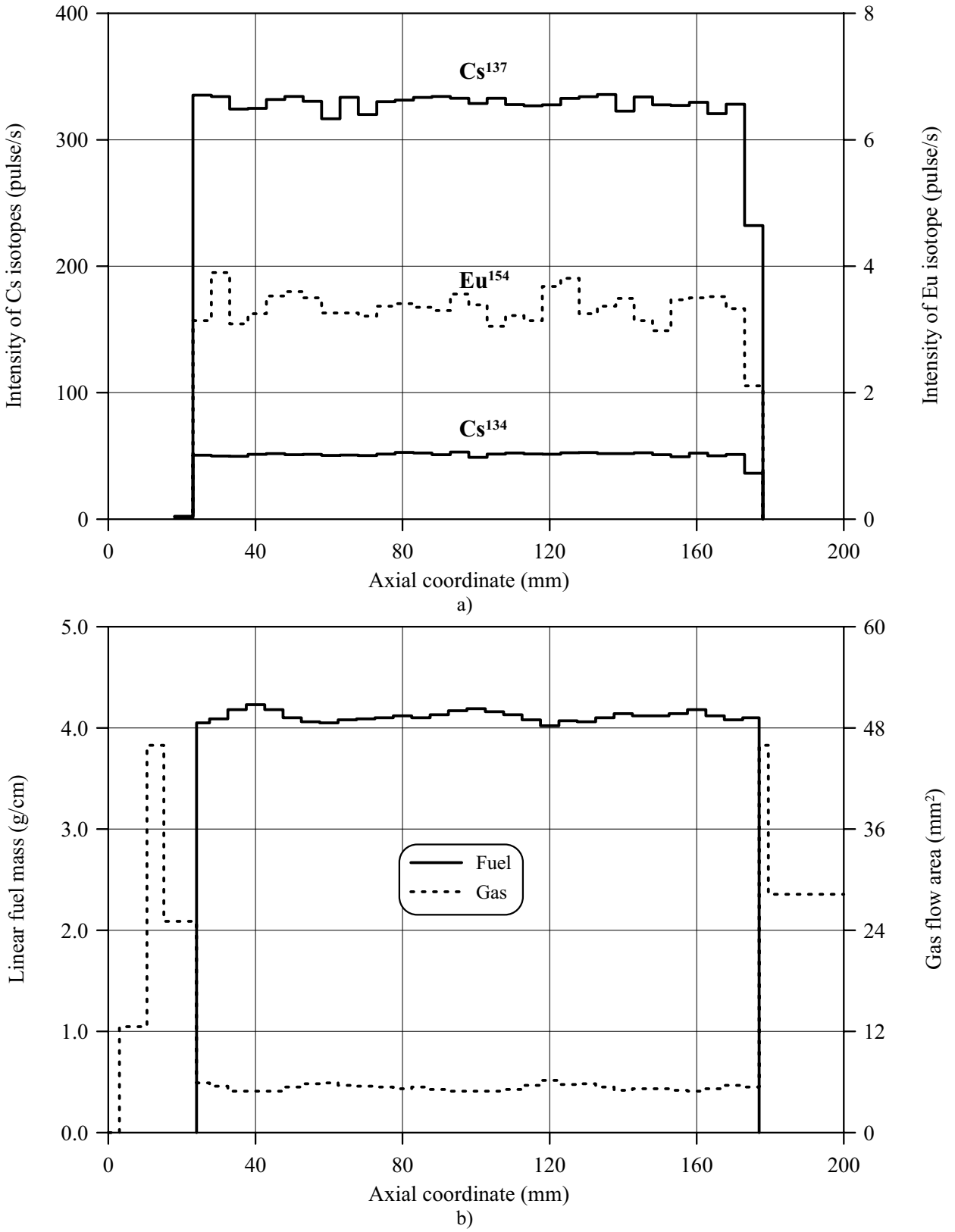


Fig.C-5.1. (a) Results of γ-scanning, (b) Axial fuel mass distribution and axial gas flow area distribution for fuel rod # RT5

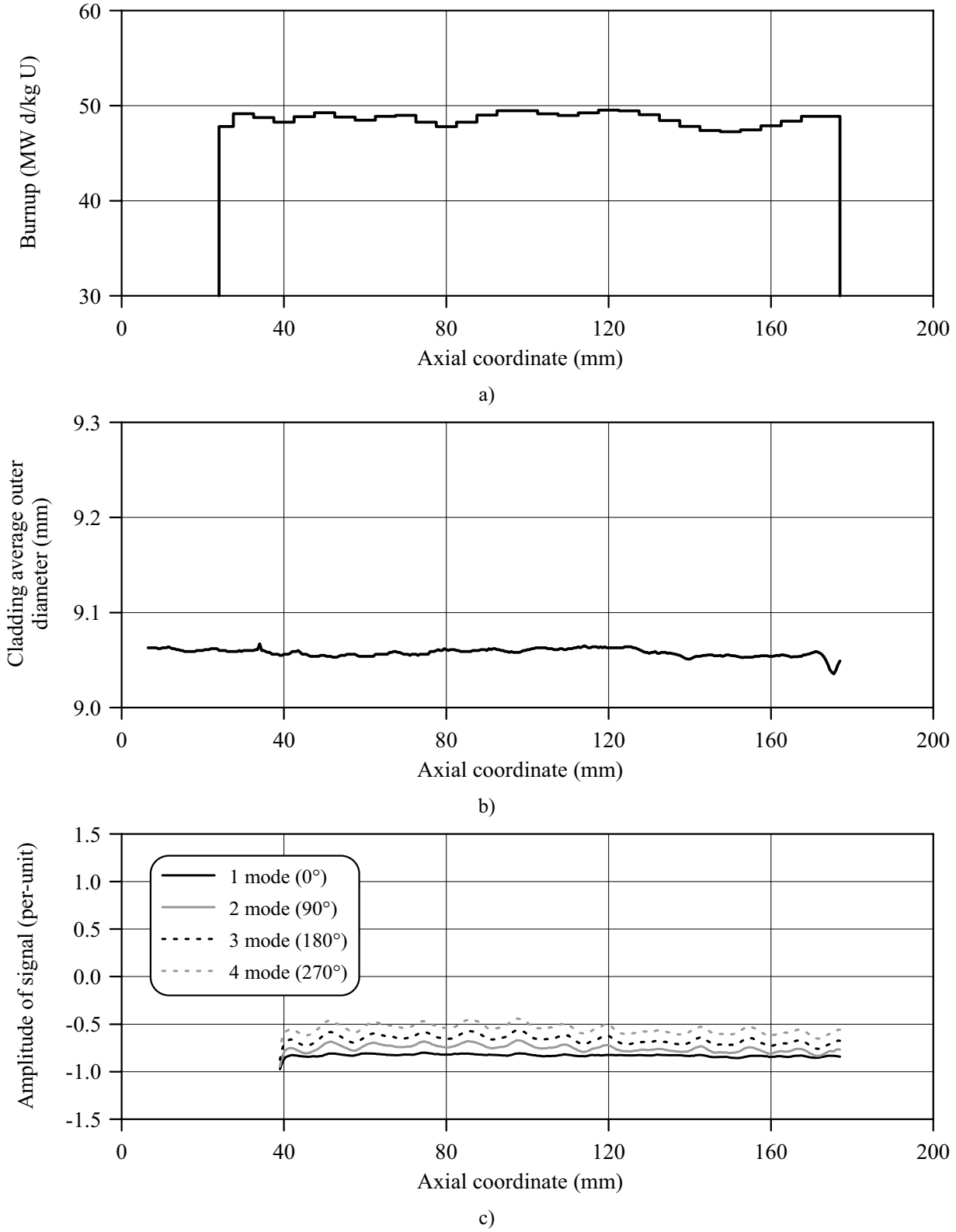
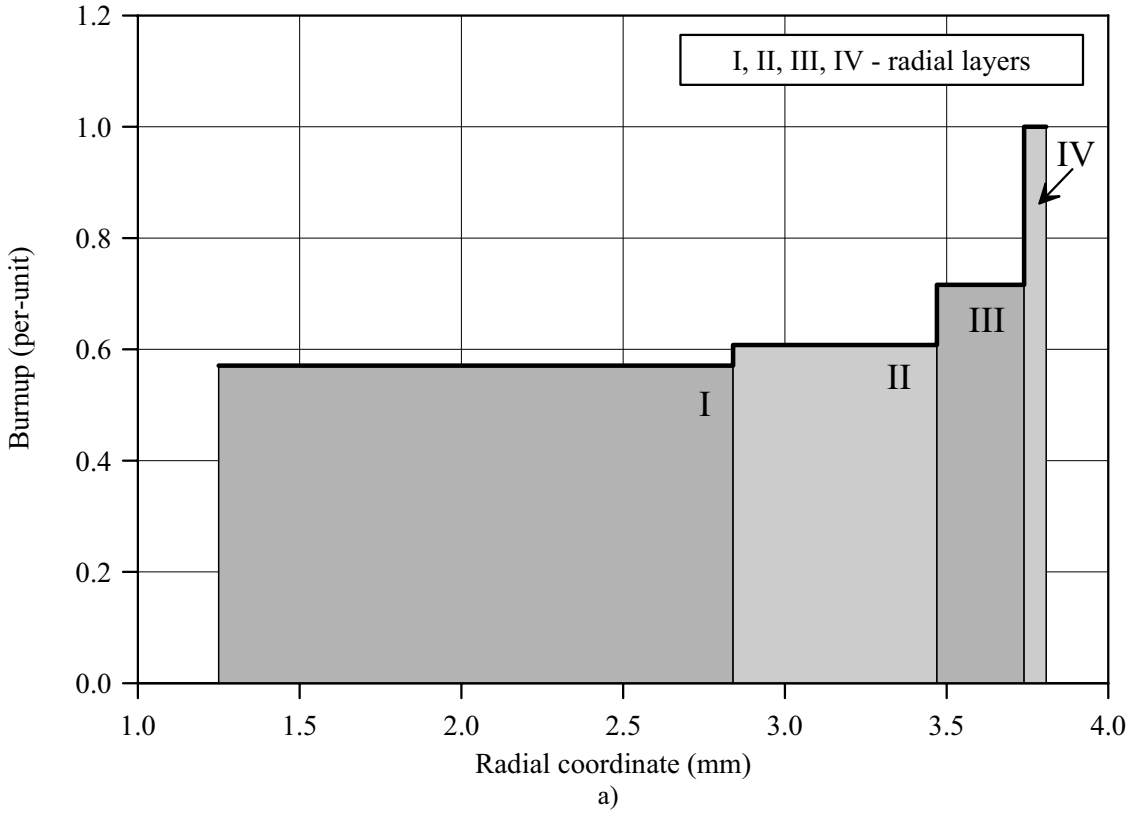


Fig.C-5.2. (a) Axial burnup distribution and (b) results of profilometry and (c) eddy-current examination of fuel rod # RT5

RT5



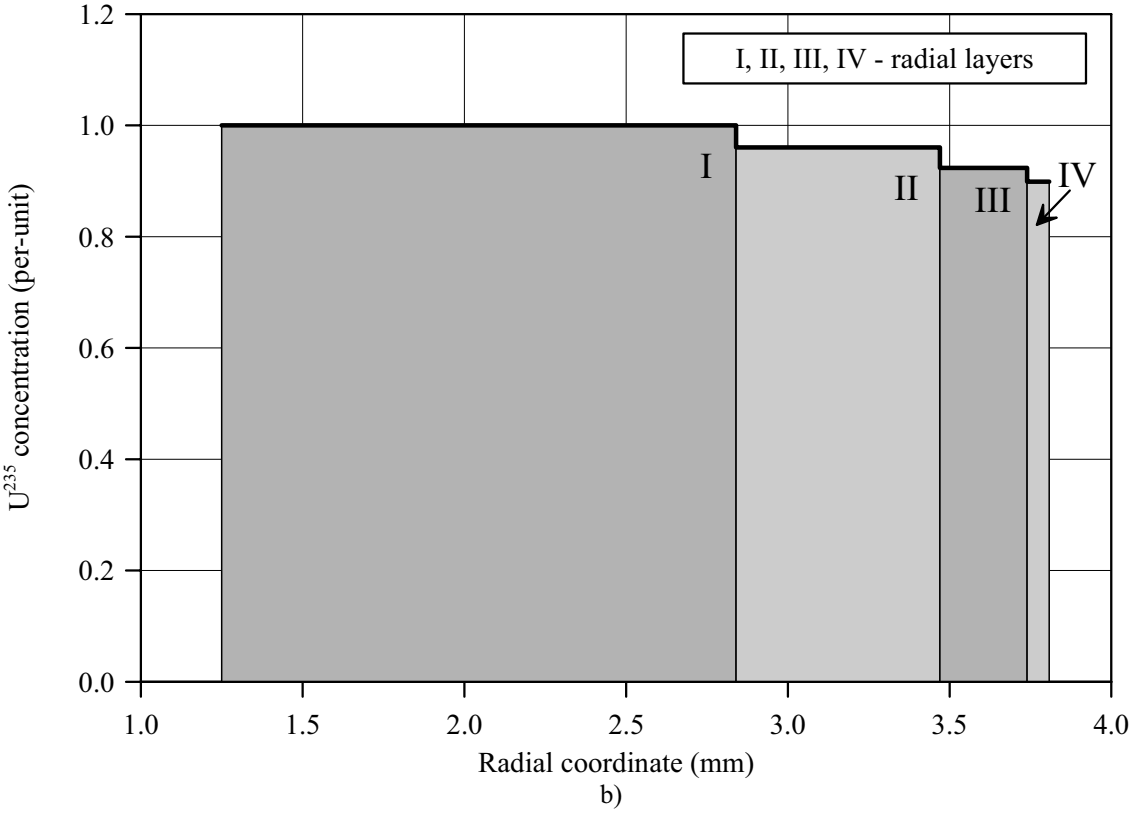


Fig.C-5.3. (a) Burnup radial distribution and (b) U^{235} radial distribution for fuel rod # RT5 (calculated values)

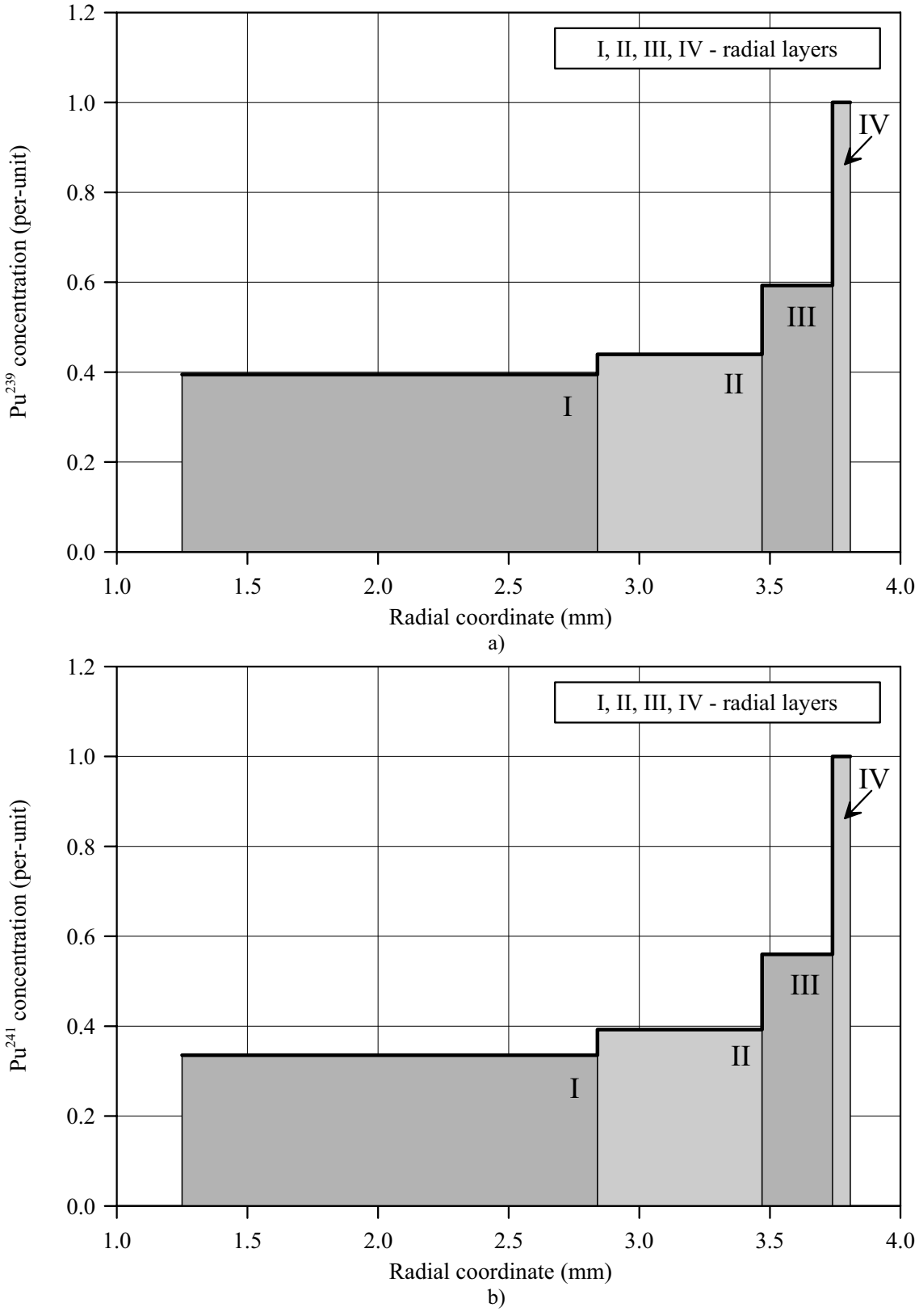


Fig.C-5.4. Radial distribution of (a) Pu^{239} and (b) Pu^{241} for fuel rod # RT5 (calculated values)

Appendix C-6

Individual Characteristics of Fuel Rod # RT6 before the BIGR Test

RT6

Table C-6.1. Radial distribution of isotope nuclear concentrations for fuel rod #RT6 (values averaged of over the fuel stack length)*

Isotope	Isotopic concentrations (kg/t U) in four fuel radial layers			
	1.25-2.82 mm	2.82-3.44 mm	3.44-3.71 mm	3.71-3.795 mm
U^{234}	0.273	0.269	0.265	0.261
U^{235}	8.512	8.188	7.891	7.687
U^{236}	6.251	6.263	6.275	6.290
U^{238}	928.4	924.6	912.9	881.2
Pu^{238}	0.370	0.390	0.421	0.479
Pu^{239}	4.856	5.410	7.320	12.43
Pu^{240}	2.485	2.636	3.400	5.540
Pu^{241}	0.908	1.067	1.523	2.746
Pu^{242}	0.681	0.821	1.207	2.245
Np^{237}	0.618	0.637	0.656	0.669
Am^{241}	0.480	0.556	0.787	1.419
Oxygen	134.5	134.5	134.5	134.5
Other fission products	47.25	50.28	58.81	81.35

* Measured averaged concentrations and calculated relative radial distributions of isotopes (TRIFOB code) were used to develop these data

Table C-6.2. Initial individual characteristics of fuel rod # RT6*

Axial coordinate (from lower cap) (mm)	Cladding average outer diameter (mm)	Fuel mass ** (g)	Linear fuel mass** (g/cm)	Gas flow area[3]** (mm^2)	Burnup** (MW d/kg U)
25[1]	9.072	1.82	4.04	6.139	48.06
30	9.068	2.05	4.10	5.548	47.99
35	9.062	2.05	4.11	5.449	48.09
40	9.061	2.05	4.09	5.646	48.33
45	9.060	2.04	4.09	5.646	48.37
50	9.060	2.01	4.02	6.336	48.19
55	9.061	2.04	4.07	5.843	48.15
60	9.065	2.06	4.13	5.252	48.33
65	9.070	2.05	4.09	5.646	48.31
70	9.072	2.08	4.15	5.055	48.06
75	9.073	2.05	4.09	5.646	48.05
80	9.075	2.04	4.09	5.646	48.38
85	9.075	2.05	4.09	5.646	48.56
90	9.071	2.11	4.21	4.910	48.43
95	9.069	2.05	4.11	5.449	48.24
100	9.069	2.03	4.07	5.843	48.14
105	9.068	2.03	4.07	5.843	48.08
110	9.068	2.02	4.03	6.237	48.02
115	9.066	2.05	4.09	5.646	47.89
120	9.069	2.05	4.11	5.449	47.77
125	9.071	2.05	4.09	5.646	47.85
130	9.073	2.04	4.08	5.745	48.08
135	9.073	2.07	4.15	5.055	48.06
140	9.075	2.10	4.19	4.910	47.77
145	9.077	2.08	4.17	4.910	47.70
150	9.080	2.07	4.14	5.154	47.85
155	9.075	2.08	4.16	4.957	47.57
160	9.075	2.09	4.17	4.910	46.78
165	9.076	2.03	4.06	5.942	46.16
170	9.078	1.96	3.92	7.321	45.95
175[2]	-	0.58	3.88	7.715	45.71

* All parameters were determined using results of pre-test examinations

** Average values at the length interval equal to the axial coordinate ±2.5 mm

[1] Bottom end coordinate of fuel stack is 23 mm; [2] Top end coordinate of fuel stack is 174 mm

[3] Gas flow area beyond the fuel stack (mm^2):

Bottom: 0.0-3.0mm – 0.00; 3.0-10.5mm – 12.56; 10.5-14.1mm – 45.94; 14.1-23.0mm – 25.06

Top: 174.0-176.5mm – 45.94; 176.5-202.5mm – 28.26; 202.5-279mm – 45.94; 279-288mm – 28.26; 288-297mm – 0.00

RT6

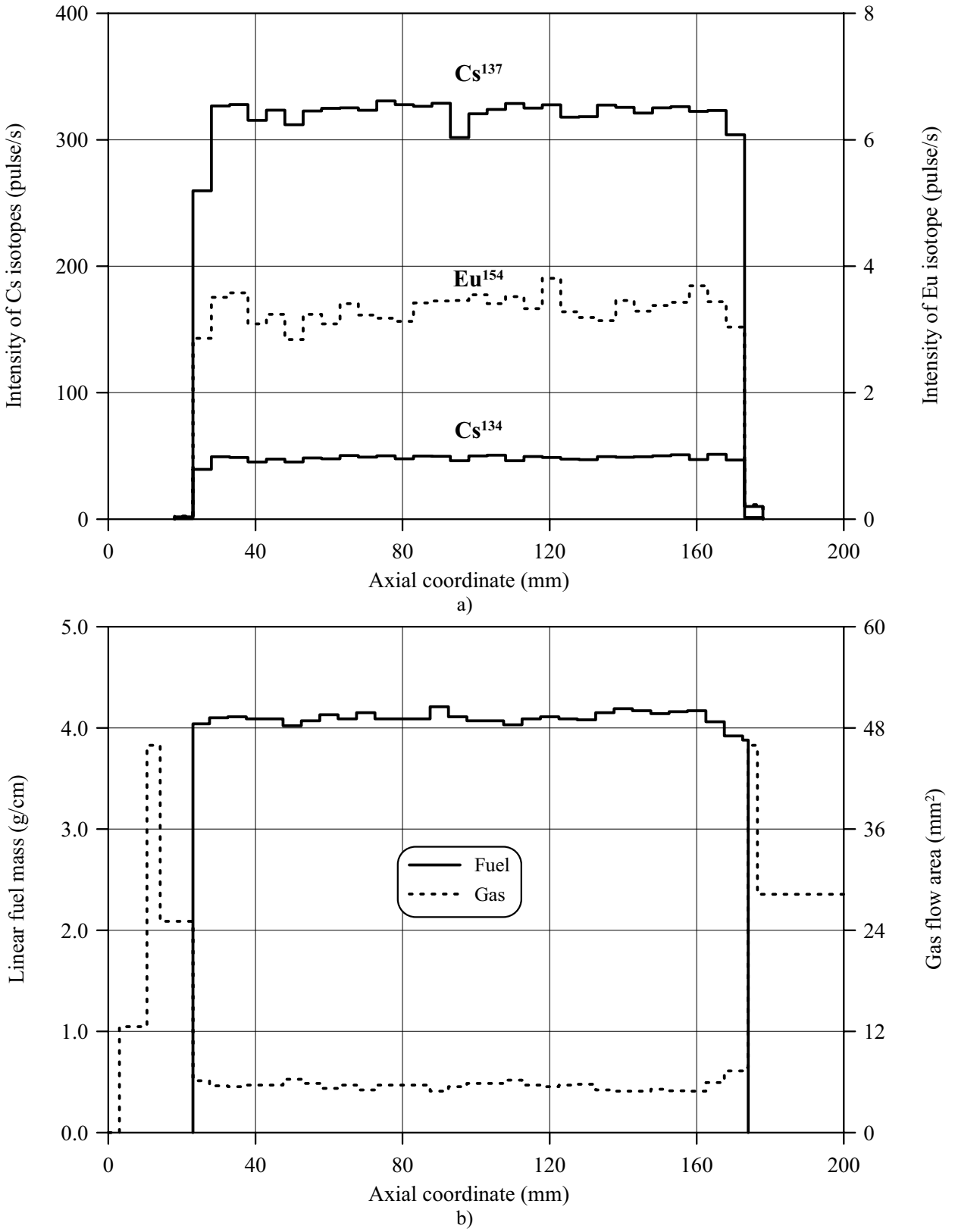


Fig.C-6.1. (a) Results of γ-scanning, (b) Axial fuel mass distribution and axial gas flow area distribution for fuel rod # RT6

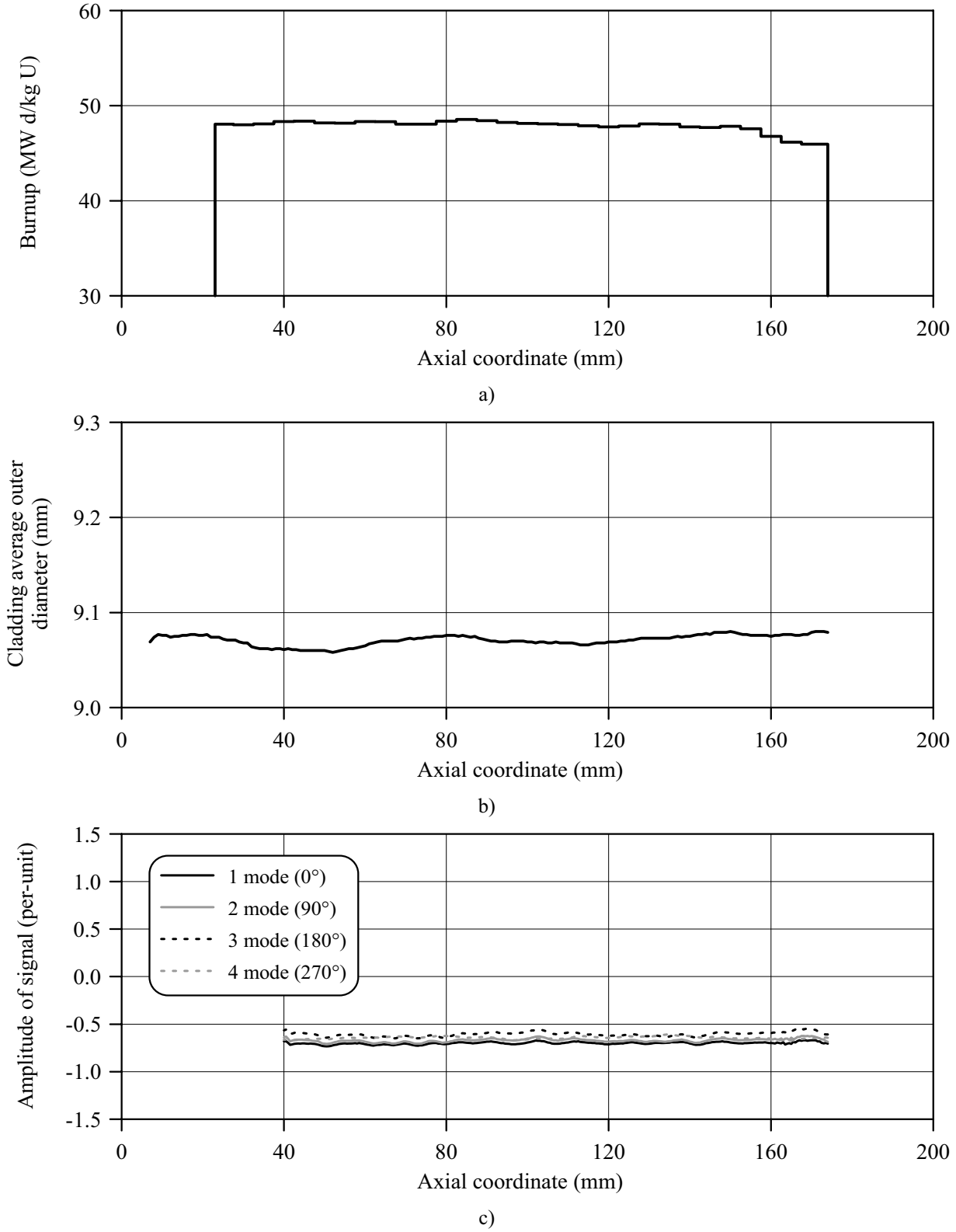


Fig.C-6.2. (a) Axial burnup distribution and (b) results of profilometry and (c) eddy-current examination of fuel rod # RT6

RT6

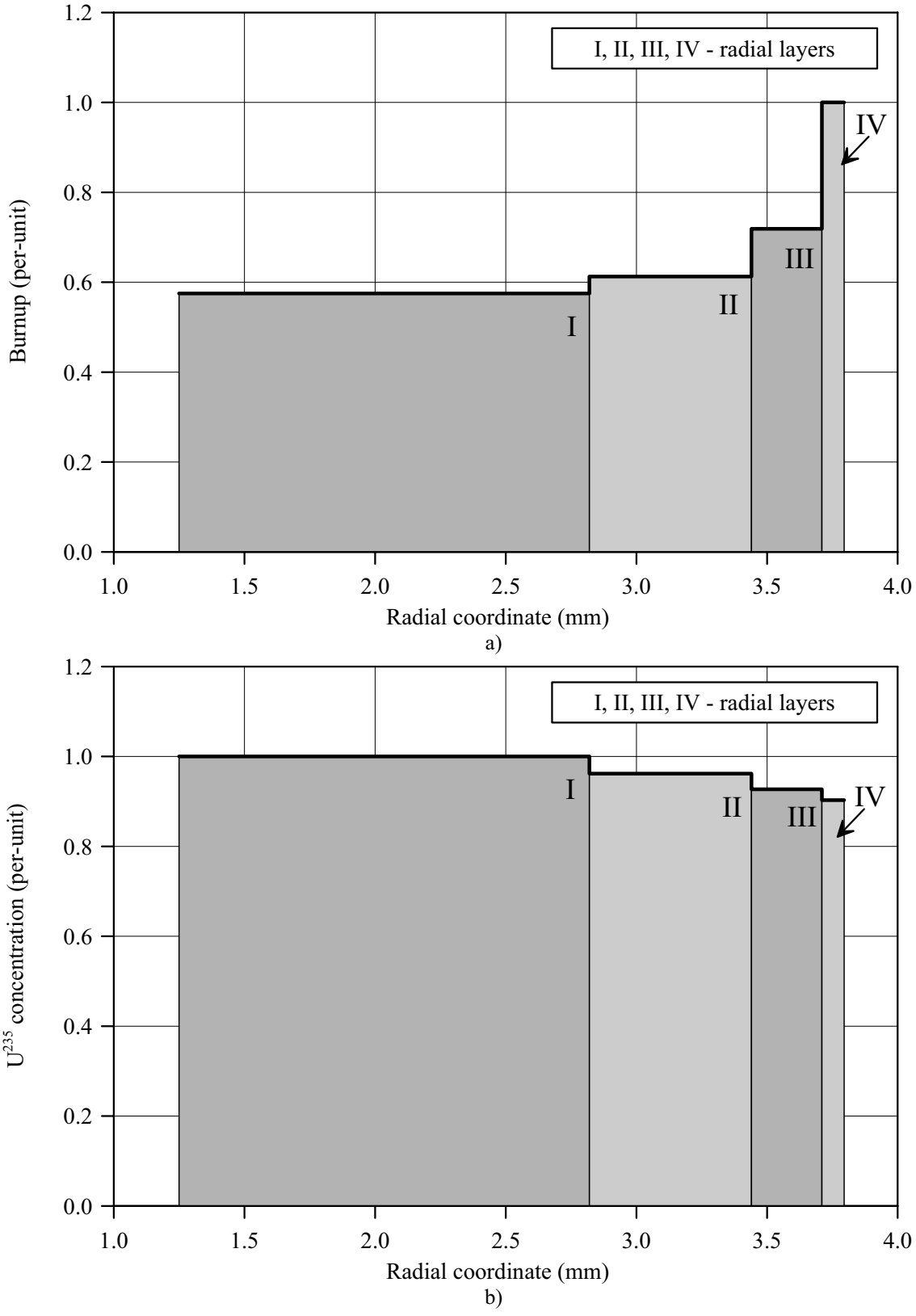


Fig.C-6.3. (a) Burnup radial distribution and (b) U^{235} radial distribution for fuel rod # RT6 (calculated values)

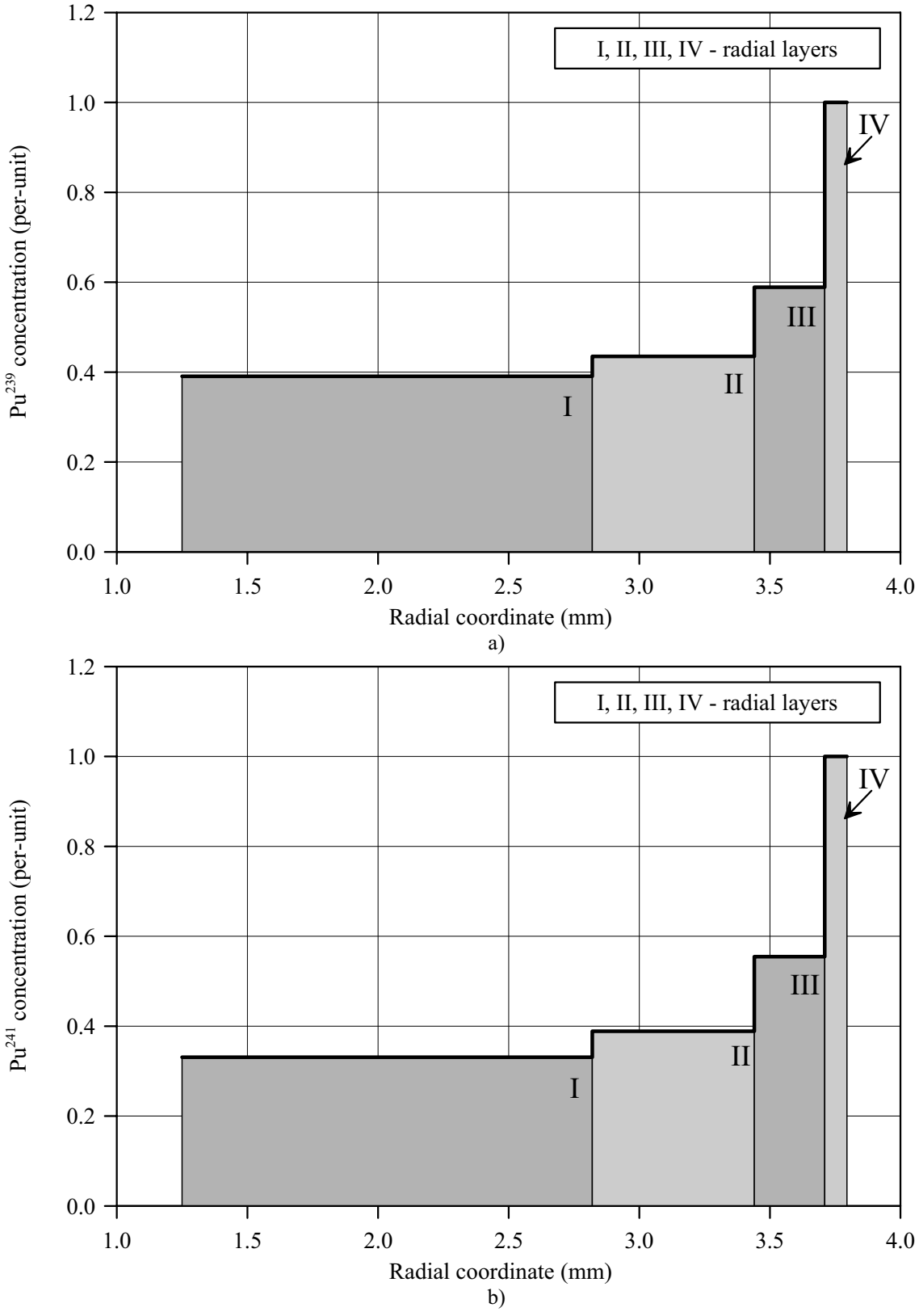


Fig.C-6.4. Radial distribution of (a) Pu^{239} and (b) Pu^{241} for fuel rod # RT6 (calculated values)

Appendix C-7

Individual Characteristics of Fuel Rod # RT7 before the BIGR Test

RT7

Table C-7.1. Radial distribution of isotope nuclear concentrations for fuel rod #RT7 (values averaged of over the fuel stack length)*

Isotope	Isotopic concentrations (kg/t U) in four fuel radial layers			
	0.825-2.777 mm	2.777-3.454 mm	3.454-3.747 mm	3.747-3.840 mm
U^{234}	0.190	0.189	0.190	0.197
U^{235}	2.435	2.297	2.185	2.111
U^{236}	5.767	5.743	5.721	5.712
U^{238}	923.5	918.8	905.4	866.0
Pu^{238}	0.378	0.408	0.461	0.586
Pu^{239}	4.744	5.223	6.840	11.50
Pu^{240}	2.978	3.063	3.755	5.978
Pu^{241}	1.324	1.545	2.144	3.859
Pu^{242}	1.335	1.619	2.328	4.349
Np^{237}	0.000	0.000	0.000	0.000
Am^{241}	0.162	0.188	0.261	0.470
Oxygen	134.5	134.5	134.5	134.5
Other fission products	57.00	60.68	70.43	98.62

* Measured averaged concentrations and calculated relative radial distributions of isotopes (TRIFOB code) were used to develop these data

Table C-7.2. Initial individual characteristics of fuel rod # RT7*

Axial coordinate (from lower cap) (mm)	Cladding average outer diameter (mm)	Fuel mass ** (g)	Linear fuel mass** (g/cm)	Gas flow area[3]** (mm^2)	Burnup** (MW d/kg U)
25[1]	9.063	2.03	4.51	2.14	58.94
30	9.054	2.17	4.34	3.80	59.75
35	9.064	2.14	4.28	4.39	61.75
40	9.059	2.16	4.33	3.90	60.24
45	9.059	2.18	4.36	3.61	60.34
50	9.052	2.19	4.39	3.31	59.58
55	9.064	2.16	4.32	4.00	59.87
60	9.066	2.17	4.34	3.80	61.50
65	9.063	2.12	4.25	4.68	60.79
70	9.062	2.17	4.34	3.80	59.33
75	9.056	2.19	4.37	3.51	60.91
80	9.059	2.19	4.38	3.41	59.23
85	9.051	2.20	4.40	3.21	59.31
90	9.062	2.20	4.40	3.21	60.73
95	9.051	2.21	4.41	3.12	59.03
100	9.057	2.21	4.41	3.12	60.93
105	9.056	2.22	4.44	2.82	59.04
110	9.070	2.20	4.41	3.12	60.63
115	9.073	2.20	4.39	3.31	60.96
120	9.063	2.16	4.32	4.00	59.31
125	9.064	2.18	4.36	3.61	61.62
130	9.063	2.16	4.31	4.10	61.89
135	9.071	2.17	4.35	3.70	60.11
140	9.057	2.19	4.38	3.41	61.07
145	9.075	2.17	4.34	3.80	60.52
150	9.063	2.17	4.34	3.80	59.56
155	9.072	2.15	4.30	4.19	61.62
160	9.064	2.18	4.36	3.61	60.18
165	9.069	2.22	4.44	2.82	61.60
170	9.069	2.19	4.39	3.31	60.14
175[2]	9.056	1.55	4.29	4.29	59.81

* All parameters were determined using results of pre-test examinations

** Average values at the length interval equal to the axial coordinate ±2.5 mm

[1] Bottom end coordinate of fuel stack is 23 mm; [2] Top end coordinate of fuel stack is 176.1 mm

[3] Gas flow area beyond the fuel stack (mm^2):

Bottom: 0.0-3.0mm – 0.00; 3.0-10.5mm – 12.56; 10.5-14.1mm – 46.37; 14.1-23.0mm – 25.38

Top: 176.1-178.5mm – 46.37; 178.5-204.5mm – 28.26; 204.5-281mm – 47.27; 281-290mm – 28.26; 290-299mm – 0.00

RT7

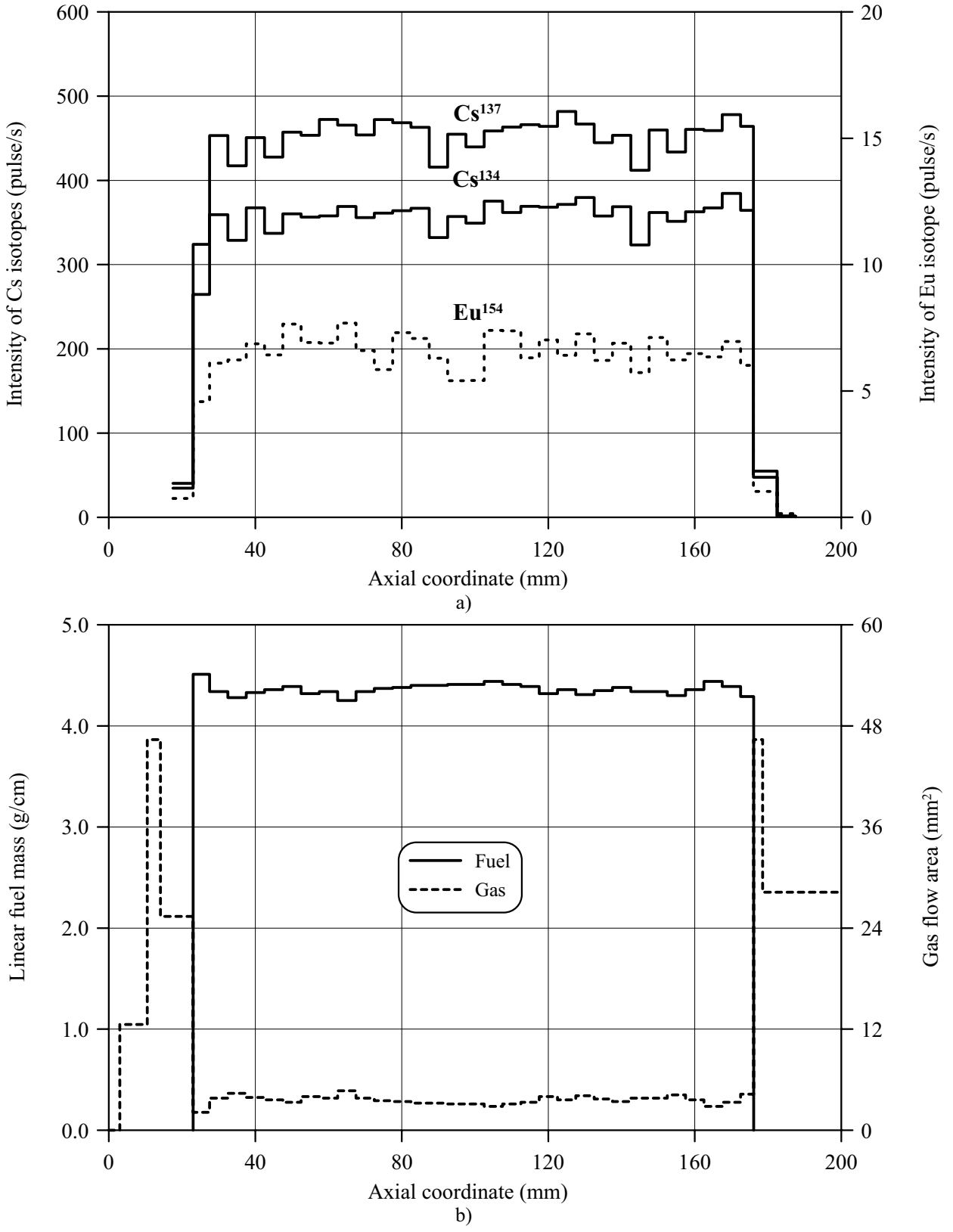


Fig.C-7.1. (a) Results of γ-scanning, (b) Axial fuel mass distribution and axial gas flow area distribution for fuel rod # RT7

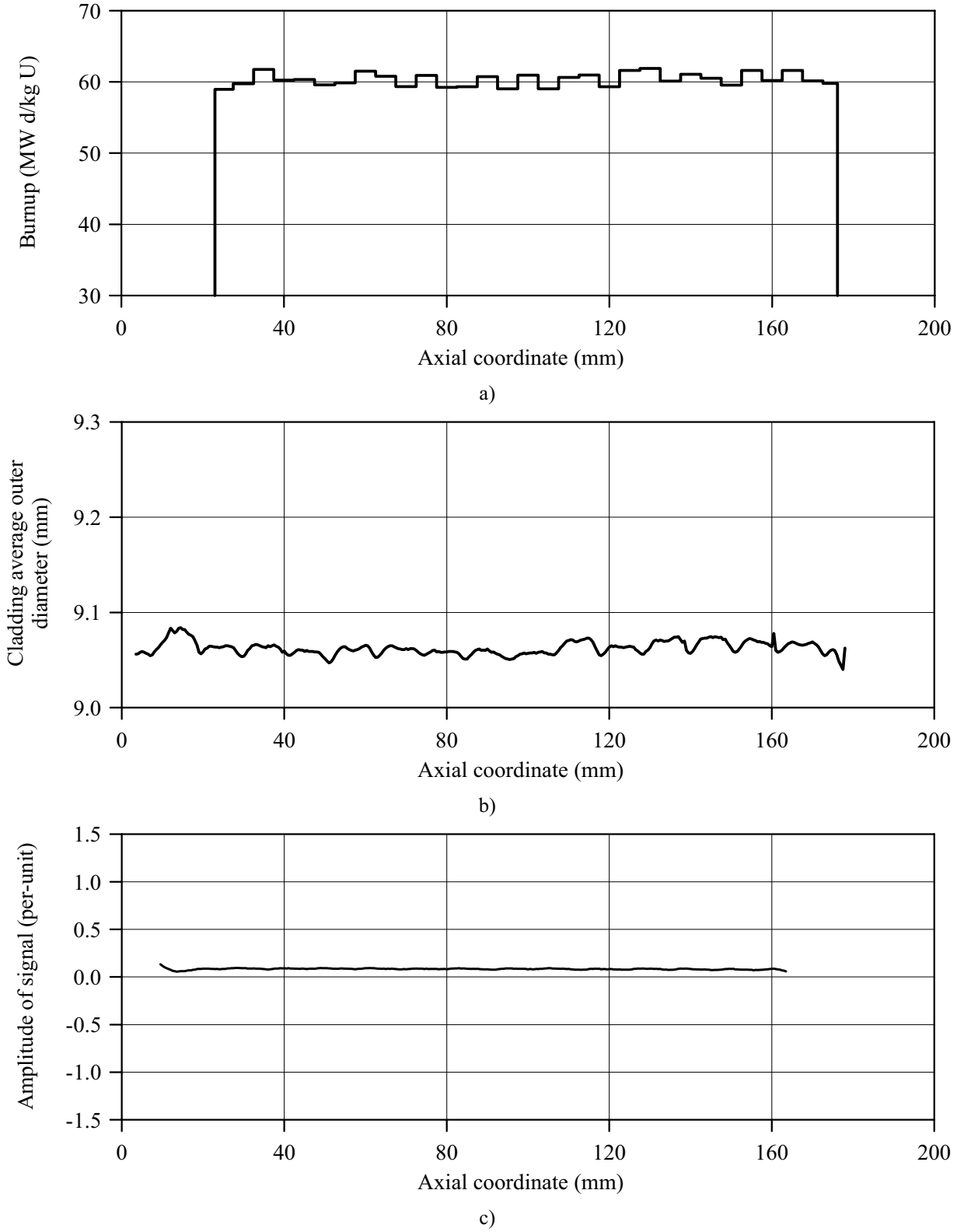
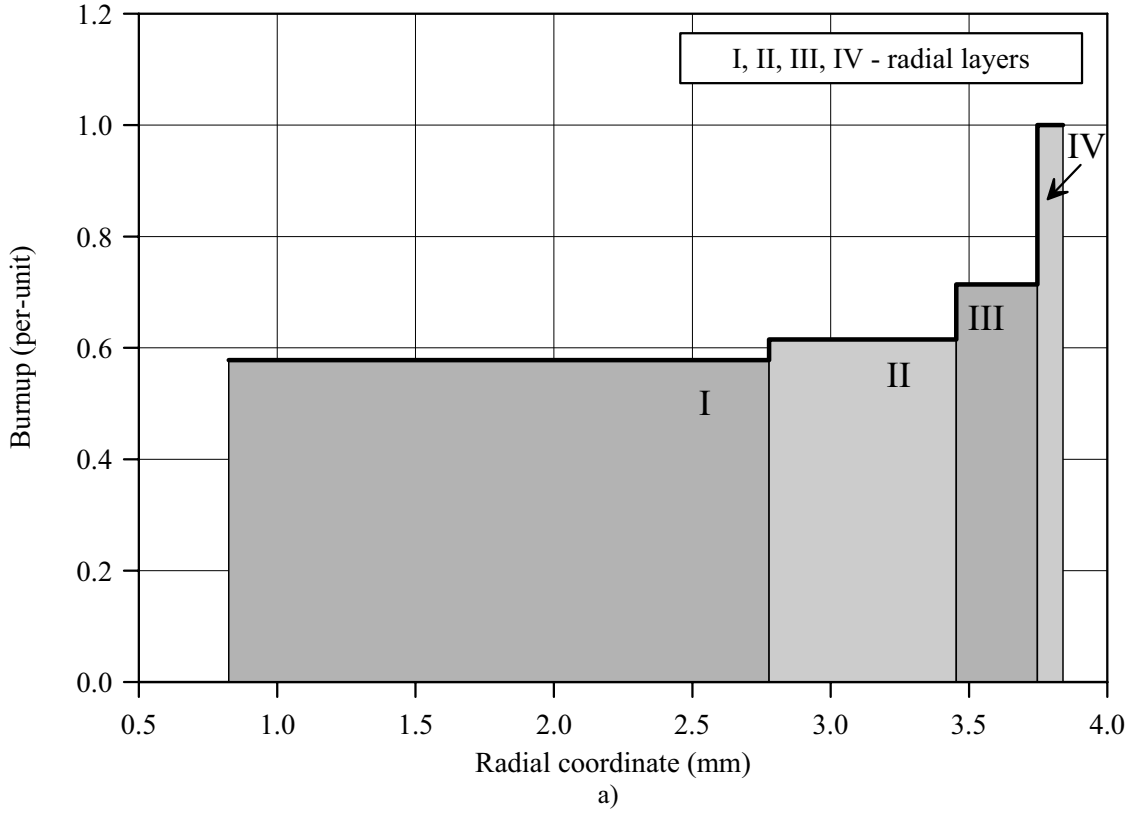


Fig.C-7.2. (a) Axial burnup distribution and (b) results of profilometry and (c) eddy-current examination of fuel rod # RT7

RT7



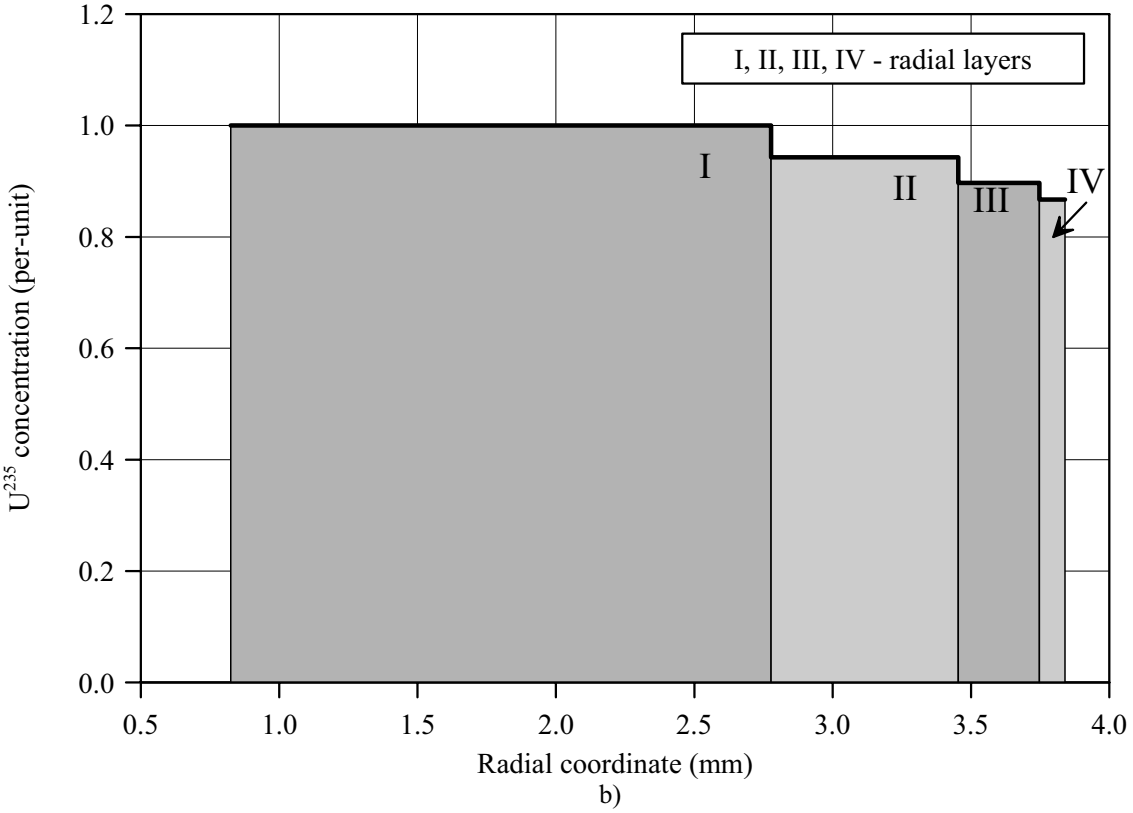
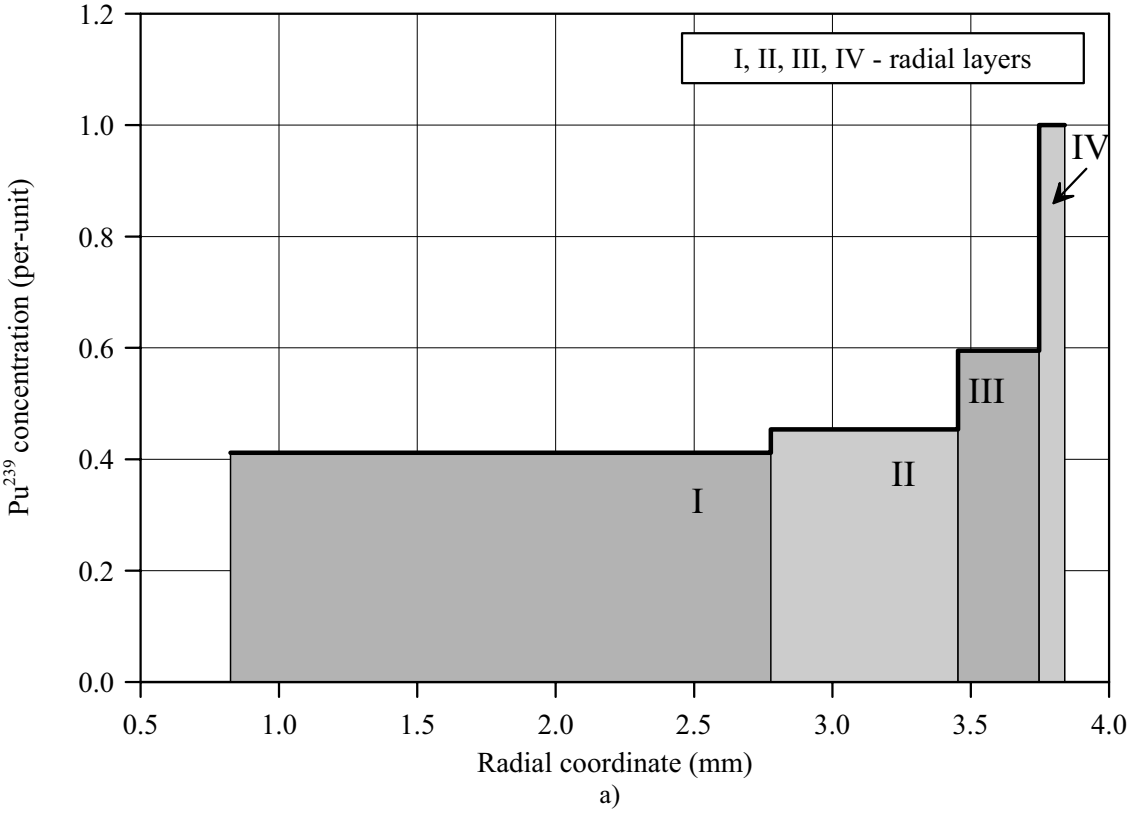
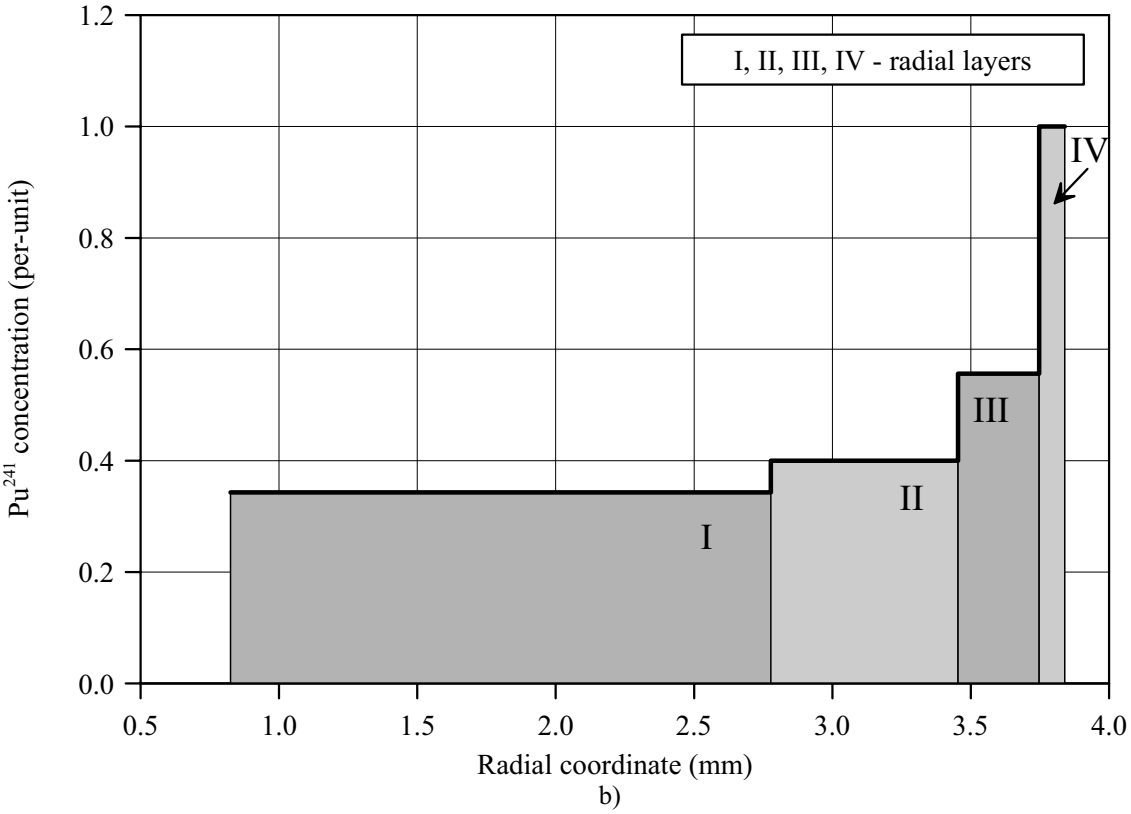


Fig.C-7.3. (a) Burnup radial distribution and (b) U^{235} radial distribution for fuel rod # RT7 (calculated values)



a)



b)

Fig.C-7.4. Radial distribution of (a) Pu^{239} and (b) Pu^{241} for fuel rod # RT7 (calculated values)

Appendix C-8

Individual Characteristics of Fuel Rod # RT8 before the BIGR Test

RT8

Table C-8.1. Radial distribution of isotope nuclear concentrations for fuel rod #RT8 (values averaged of over the fuel stack length)*

Isotope	Isotopic concentrations (kg/t U) in four fuel radial layers			
	0.825-2.777 mm	2.777-3.454 mm	3.454-3.747 mm	3.747-3.840 mm
U^{234}	0.220	0.219	0.220	0.227
U^{235}	4.898	4.625	4.403	4.255
U^{236}	6.668	6.642	6.620	6.611
U^{238}	922.3	917.7	904.4	865.6
Pu^{238}	0.523	0.565	0.638	0.810
Pu^{239}	4.920	5.419	7.104	11.97
Pu^{240}	2.755	2.838	3.487	5.565
Pu^{241}	0.967	1.131	1.571	2.833
Pu^{242}	0.985	1.196	1.720	3.217
Np^{237}	1.406	1.460	1.507	1.538
Am^{241}	0.052	0.060	0.084	0.151
Oxygen	134.5	134.5	134.5	134.5
Other fission products	55.63	59.53	69.78	99.19

* Measured averaged concentrations and calculated relative radial distributions of isotopes (TRIFOB code) were used to develop these data

Table C-8.2. Initial individual characteristics of fuel rod # RT8*

Axial coordinate (from lower cap) (mm)	Cladding average outer diameter (mm)	Fuel mass ** (g)	Linear fuel mass** (g/cm)	Gas flow area[3]** (mm^2)	Burnup** (MW d/kg U)
10[1]	9.087	0.16	3.23	15.22	60.37
15	9.087	1.68	3.35	14.06	60.50
20	9.081	2.25	4.49	3.10	59.88
25	9.083	2.26	4.52	2.81	59.16
30	9.073	2.25	4.50	3.00	59.80
35	9.083	2.24	4.48	3.20	60.92
40	9.082	2.28	4.56	2.43	60.06
45	9.085	2.30	4.59	2.14	58.18
50	9.080	2.29	4.57	2.33	58.69
55	9.092	2.26	4.52	2.81	60.98
60	9.097	2.23	4.45	3.48	61.60
65	9.104	2.22	4.44	3.58	60.40
70	9.085	2.25	4.51	2.91	59.78
75	9.095	2.25	4.50	3.00	60.21
80	9.093	2.24	4.47	3.29	60.72
85	9.105	2.23	4.46	3.39	60.94
90	9.089	2.23	4.46	3.39	60.96
95	9.080	2.23	4.46	3.39	60.86
100	9.083	2.24	4.47	3.29	60.67
105	9.078	2.24	4.48	3.20	60.46
110	9.087	2.24	4.48	3.20	60.32
115	9.084	2.24	4.48	3.20	60.26
120	9.086	2.24	4.48	3.20	60.21
125	9.073	2.24	4.49	3.10	60.17
130	9.085	2.25	4.49	3.10	60.12
135	9.084	2.26	4.51	2.91	59.99
140	9.096	2.26	4.52	2.81	59.65
145	9.088	2.26	4.52	2.81	59.39
150	9.094	2.26	4.52	2.81	59.79
155	9.091	2.13	4.25	5.41	60.69
160[2]	9.091	1.51	3.36	13.97	61.03

* All parameters were determined using results of pre-test examinations

** Average values at the length interval equal to the axial coordinate ±2.5 mm

[1] Bottom end coordinate of fuel stack is 10.5 mm; [2] Top end coordinate of fuel stack is 160.5 mm

[3] Gas flow area beyond the fuel stack (mm^2):

Bottom: 0.0-3.0mm – 0.00; 3.0-10.5mm – 12.56

Bepx: 160.5-169.4mm – 25.36; 169.4-178.5mm – 46.35; 178.5-204.5mm – 28.26; 204.5-281mm – 47.27; 281-290mm – 28.26; 290-299mm – 0

RT8

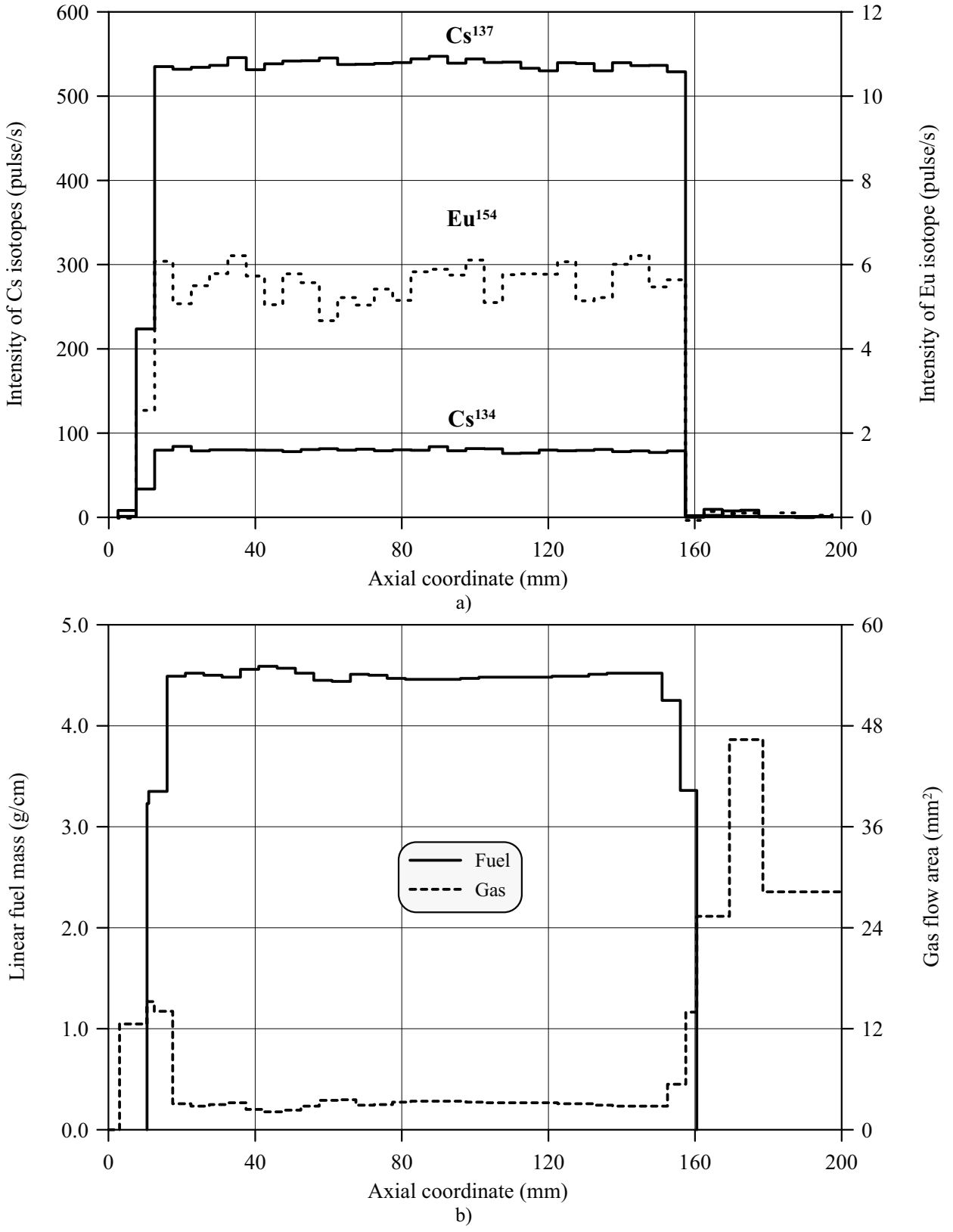


Fig.C-8.1. (a) Results of γ-scanning, (b) Axial fuel mass distribution and axial gas flow area distribution for fuel rod # RT8

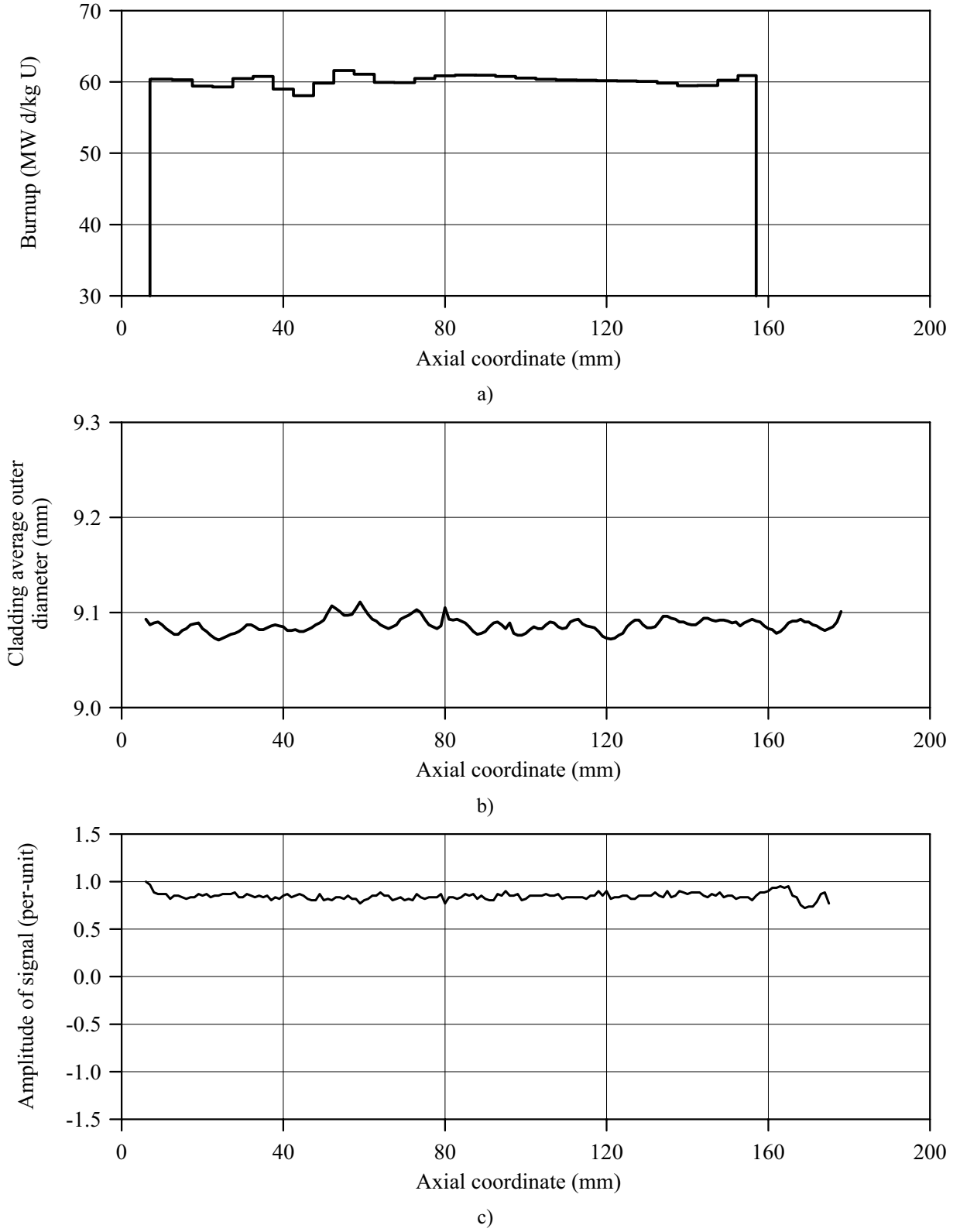


Fig.C-8.2. (a) Axial burnup distribution and (b) results of profilometry and (c) eddy-current examination of fuel rod # RT8

RT8

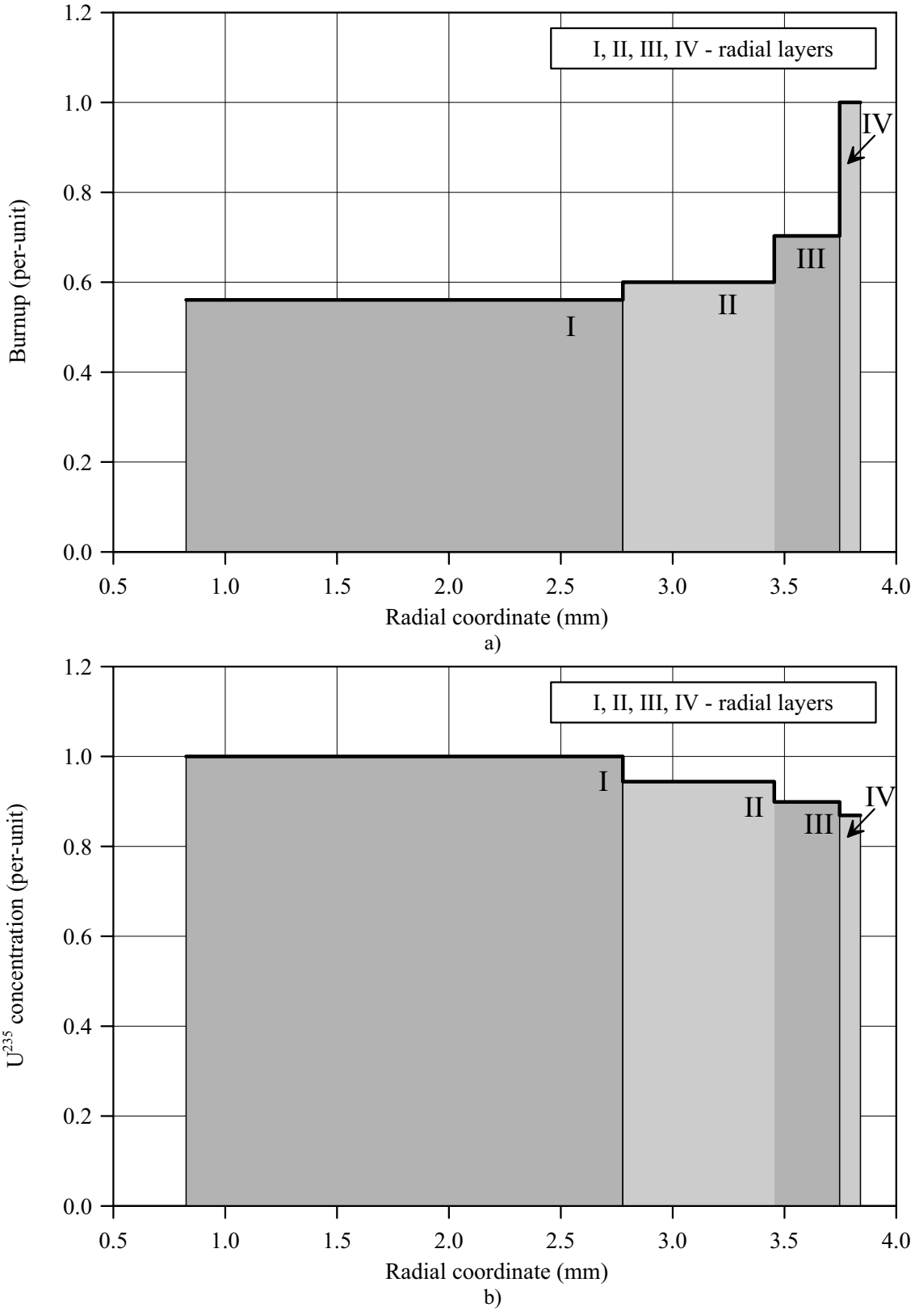
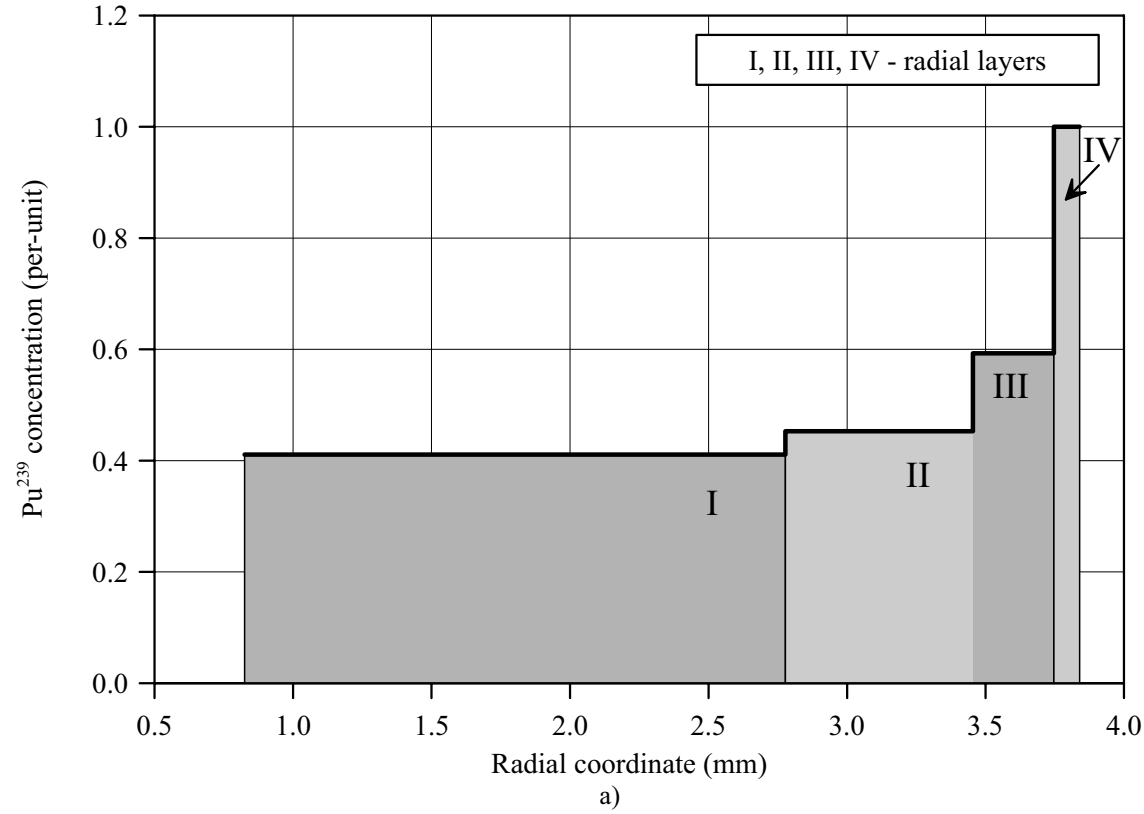
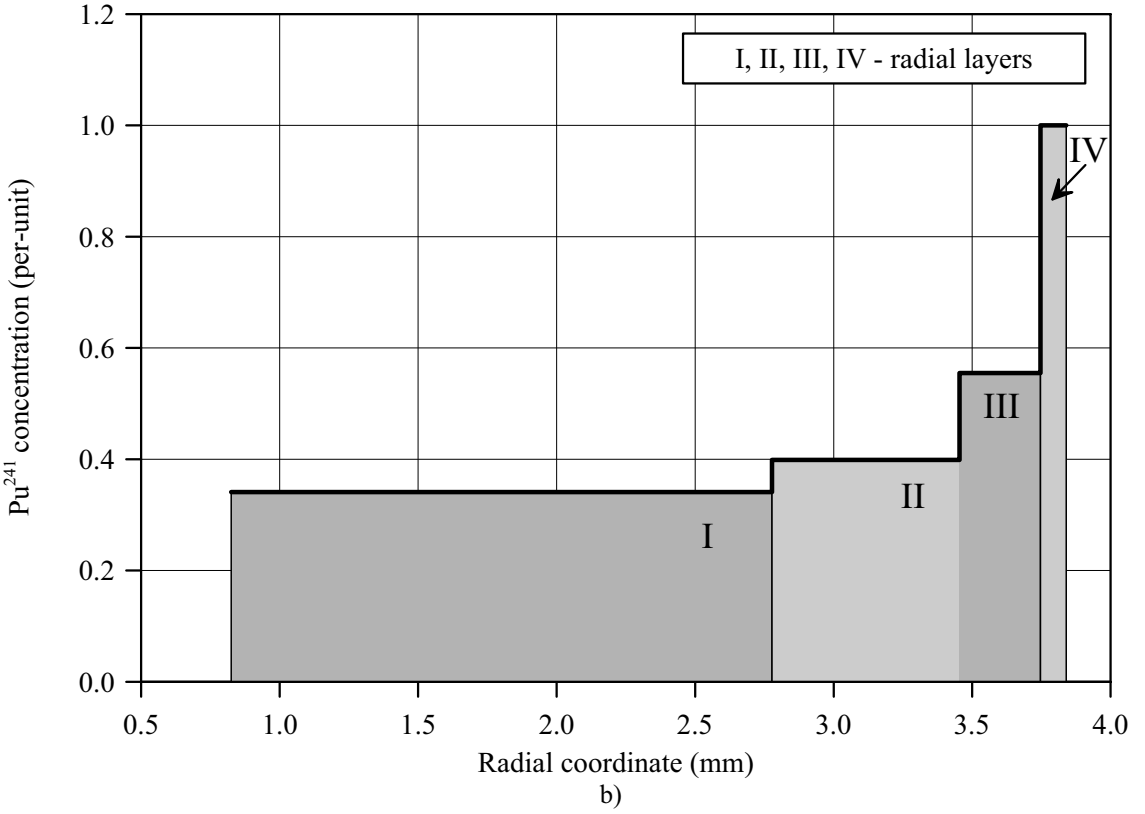


Fig.C-8.3. (a) Burnup radial distribution and (b) U^{235} radial distribution for fuel rod # RT8 (calculated values)



a)



b)

Fig.C-8.4. Radial distribution of (a) Pu^{239} and (b) Pu^{241} for fuel rod # RT8 (calculated values)

Appendix C-9

Individual Characteristics of Fuel Rod # RT9 before the BIGR Test

RT9

Table C-9.1. Radial distribution of isotope nuclear concentrations for fuel rod #RT9 (values averaged of over the fuel stack length)*

Isotope	Isotopic concentrations (kg/t U) in four fuel radial layers			
	0.825-2.777 mm	2.777-3.454 mm	3.454-3.747 mm	3.747-3.840 mm
U^{234}	0.220	0.219	0.220	0.227
U^{235}	4.898	4.625	4.403	4.255
U^{236}	6.668	6.642	6.620	6.611
U^{238}	922.3	917.7	904.4	865.6
Pu^{238}	0.523	0.565	0.638	0.810
Pu^{239}	4.920	5.419	7.104	11.97
Pu^{240}	2.755	2.838	3.487	5.565
Pu^{241}	0.967	1.131	1.571	2.833
Pu^{242}	0.985	1.196	1.720	3.217
Np^{237}	1.406	1.460	1.507	1.538
Am^{241}	0.052	0.060	0.084	0.151
Oxygen	134.5	134.5	134.5	134.5
Other fission products	55.63	59.53	69.78	99.19

* Measured averaged concentrations and calculated relative radial distributions of isotopes (TRIFOB code) were used to develop these data

Table C-9.2. Initial individual characteristics of fuel rod # RT9*

Axial coordinate (from lower cap) (mm)	Cladding average outer diameter (mm)	Fuel mass ** (g)	Linear fuel mass** (g/cm)	Gas flow area[3]** (mm^2)	Burnup** (MW d/kg U)
10[1]	9.068	1.88	4.20	5.62	58.98
15	9.072	2.28	4.56	2.14	59.33
20	9.073	2.25	4.51	2.62	59.75
25	9.062	2.23	4.46	3.11	59.99
30	9.070	2.21	4.42	3.49	60.03
35	9.051	2.20	4.41	3.59	60.10
40	9.059	2.20	4.41	3.59	60.24
45	9.063	2.21	4.43	3.40	60.19
50	9.071	2.22	4.45	3.20	59.92
55	9.068	2.23	4.45	3.20	59.75
60	9.073	2.22	4.44	3.30	59.79
65	9.073	2.22	4.44	3.30	59.93
70	9.075	2.21	4.42	3.49	60.15
75	9.076	2.20	4.39	3.78	60.57
80	9.068	2.19	4.37	3.98	61.05
85	9.076	2.19	4.38	3.88	61.06
90	9.078	2.20	4.39	3.78	60.64
95	9.073	2.20	4.41	3.59	60.52
100	9.073	2.21	4.43	3.40	60.77
105	9.072	2.22	4.45	3.20	60.59
110	9.073	2.24	4.47	3.01	59.82
115	9.080	2.25	4.50	2.72	59.27
120	9.068	2.25	4.50	2.72	59.22
125	9.069	2.24	4.48	2.91	59.14
130	9.066	2.24	4.48	2.91	58.87
135	9.067	2.25	4.50	2.72	58.73
140	9.066	2.26	4.52	2.52	58.87
145	9.069	2.27	4.54	2.33	59.15
150	9.068	2.27	4.54	2.33	59.47
155	9.063	1.90	4.27	4.95	59.78
160[2]	9.072	1.94	4.29	4.75	60.05

* All parameters were determined using results of pre-test examinations

** Average values at the length interval equal to the axial coordinate ±2.5 mm

[1] Bottom end coordinate of fuel stack is 10.5 mm; [2] Top end coordinate of fuel stack is 159.5 mm

[3] Gas flow area beyond the fuel stack (mm^2):

Bottom: 0.0-3.0mm – 0.00; 3.0-10.5mm – 12.56

Top:159.5-159.4mm–25.34;159.4-178.5mm–46.35;178.5-204.5mm–28.26;204.5-281mm–47.27;281-290mm–28.26;290-299mm–0

RT9

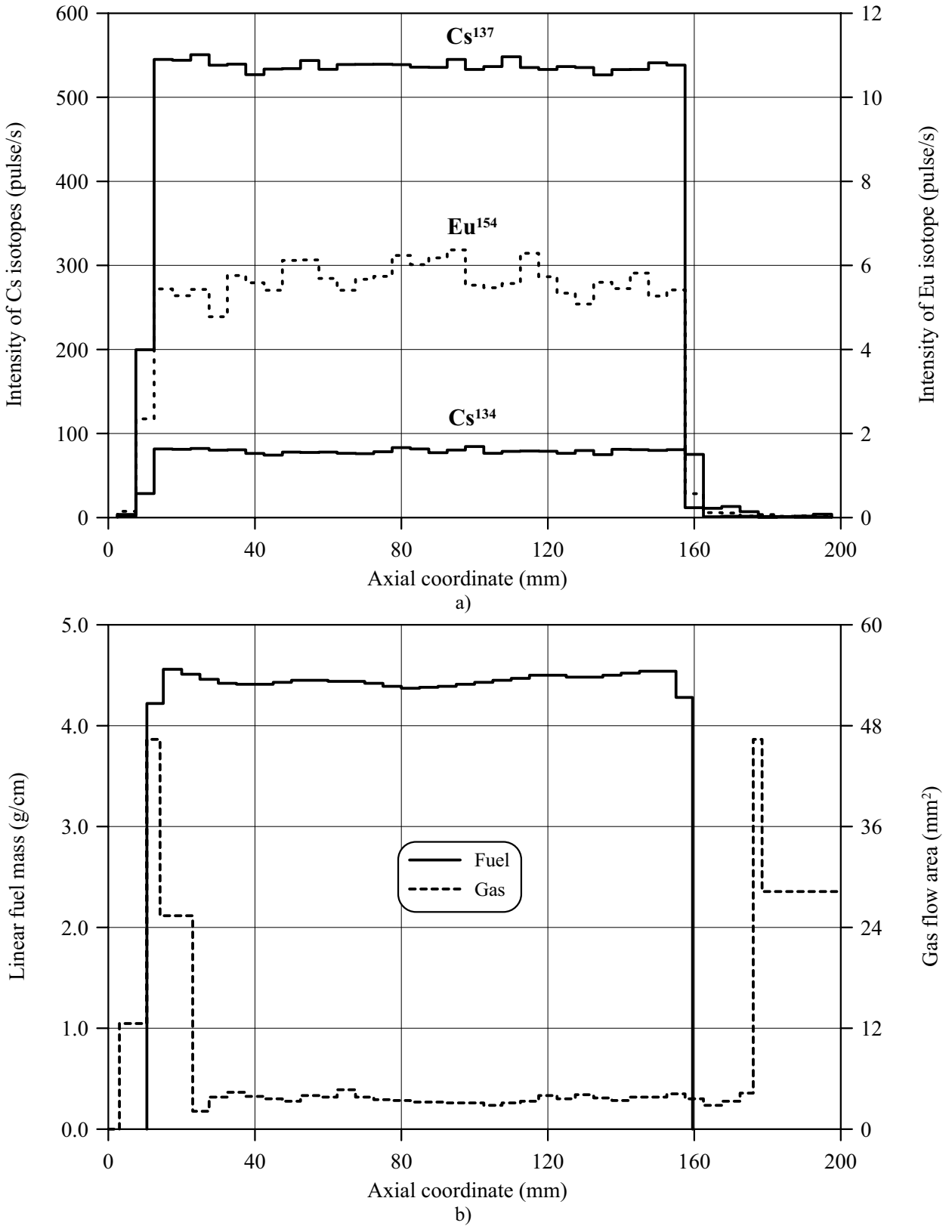


Fig.C-9.1. (a) Results of γ-scanning, (b) Axial fuel mass distribution and axial gas flow area distribution for fuel rod # RT9

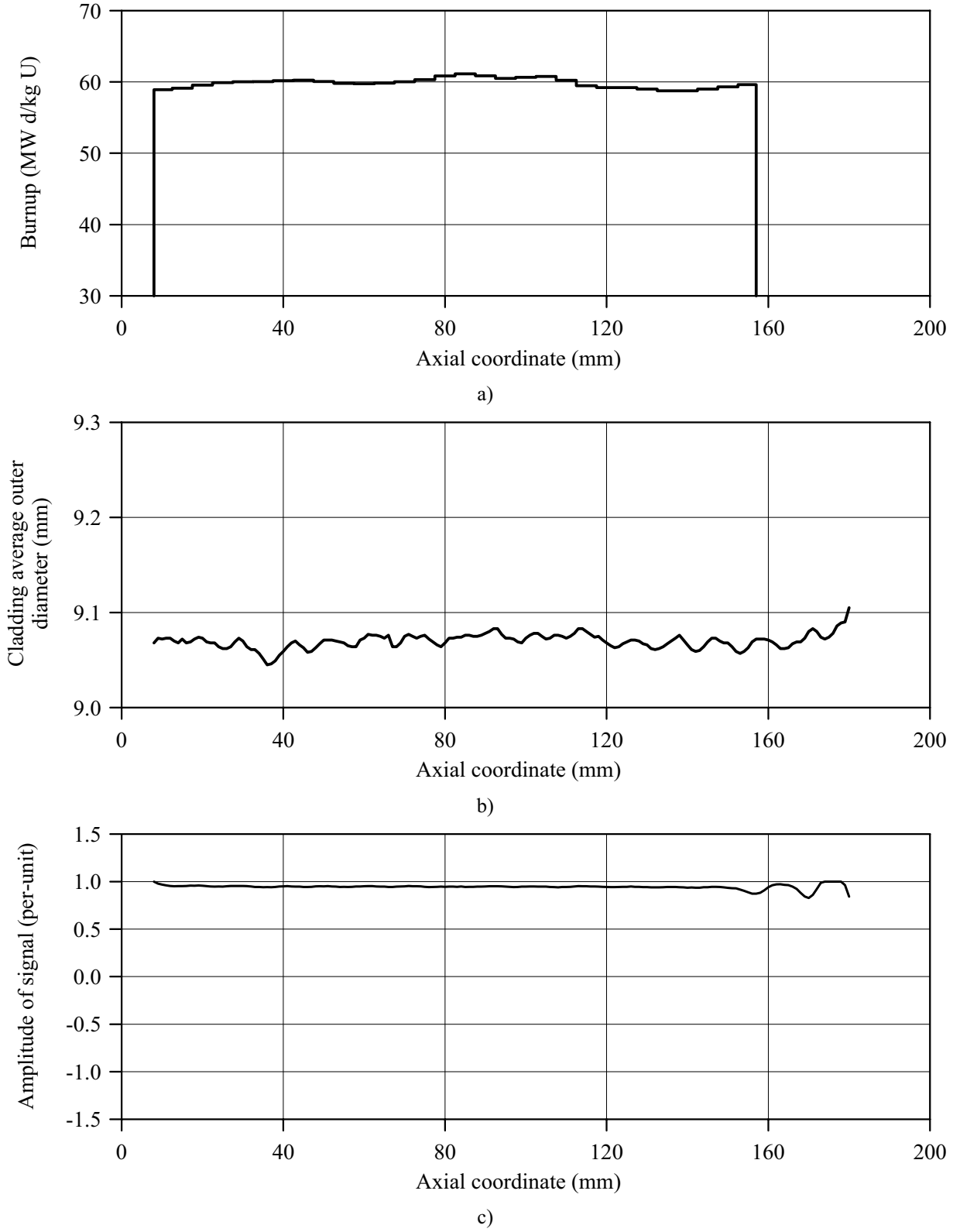


Fig.C-9.2. (a) Axial burnup distribution and (b) results of profilometry and (c) eddy-current examination of fuel rod # RT9

RT9

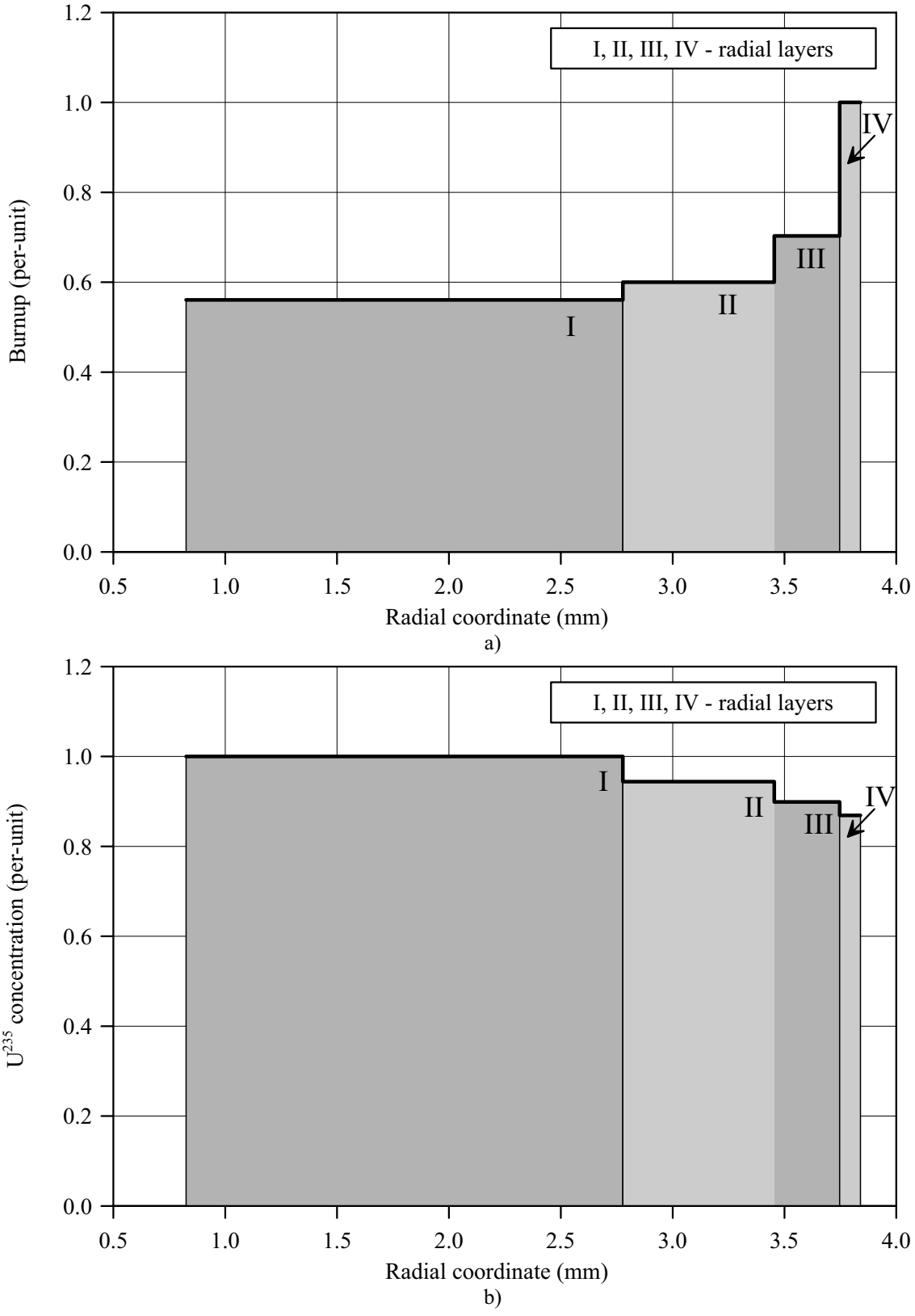
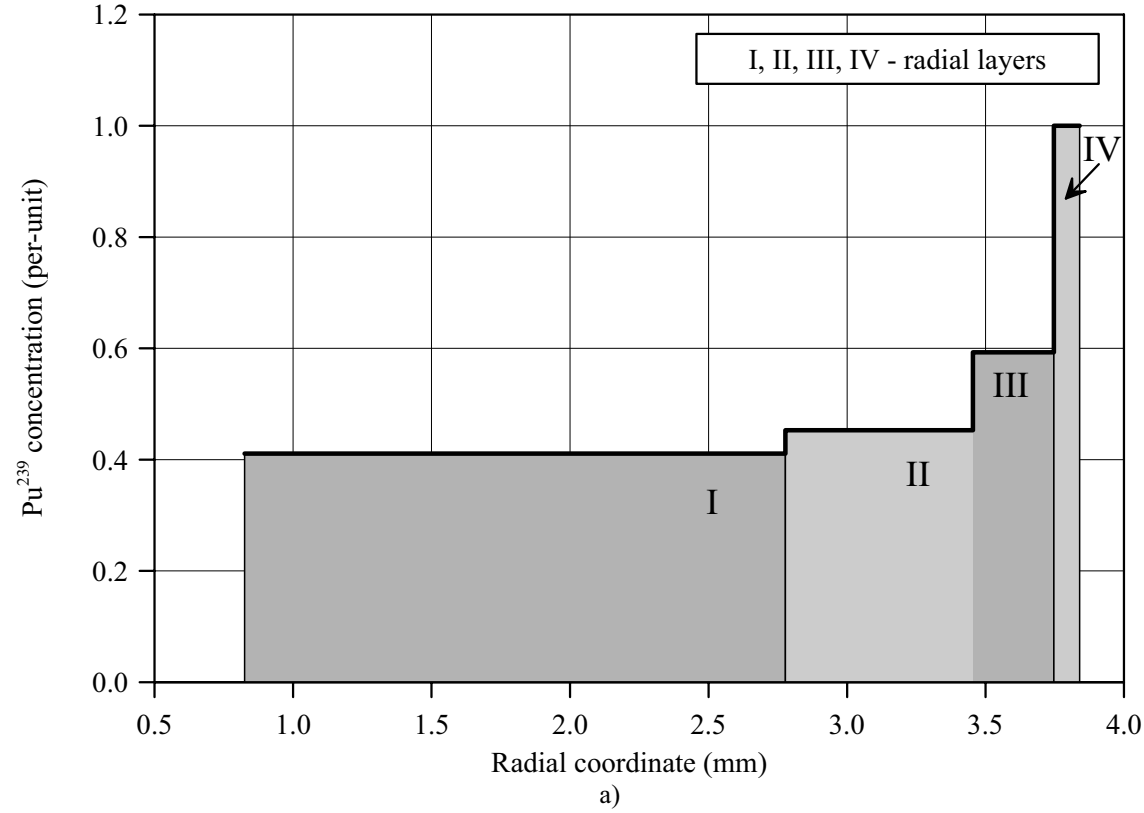
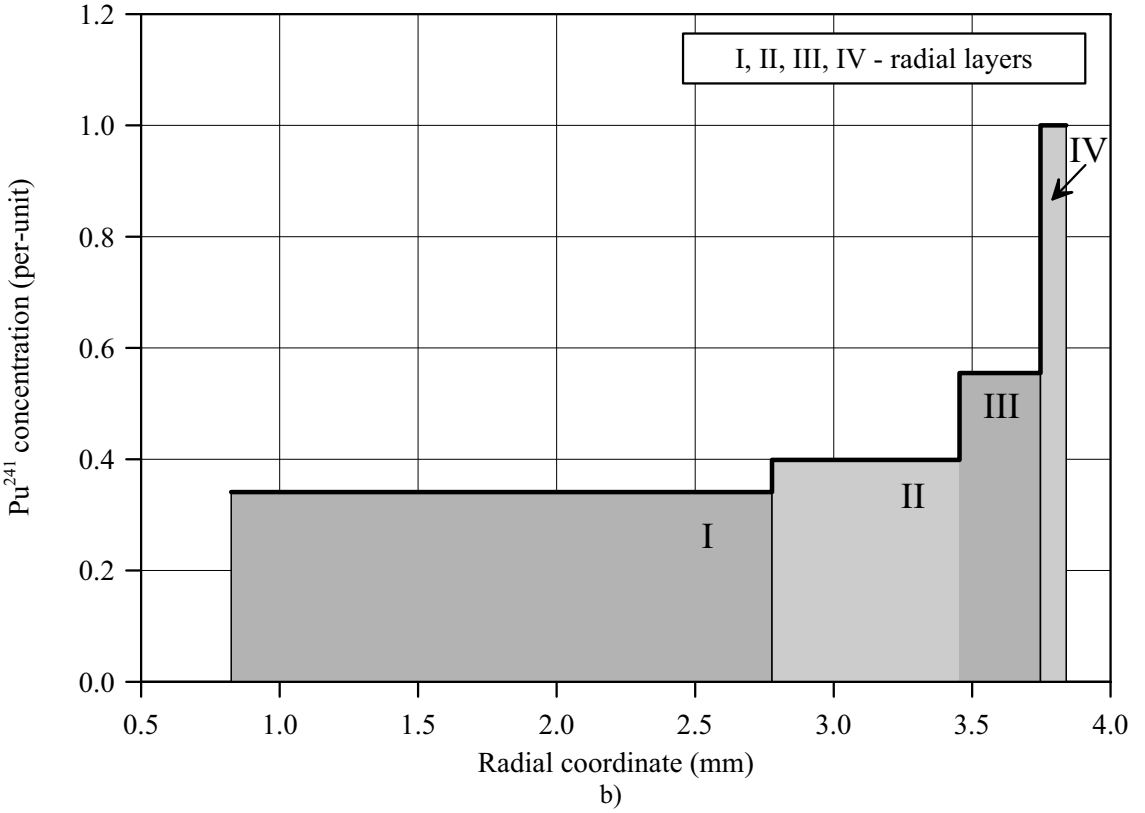


Fig.C-9.3. (a) Burnup radial distribution and (b) U^{235} radial distribution for fuel rod # RT9 (calculated values)



a)



b)

Fig.C-9.4. Radial distribution of (a) Pu^{239} and (b) Pu^{241} for fuel rod # RT9 (calculated values)

Appendix C-10

Individual Characteristics

of Fuel Rod # RT10 before the BIGR Test

RT10

Table C-10.1. Radial distribution of isotope nuclear concentrations for fuel rod #RT10 (values averaged of over the fuel stack length)*

Isotope	Isotopic concentrations (kg/t U) in four fuel radial layers			
	1.250-2.834 mm	2.834-3.452 mm	3.452-3.722 mm	3.722-3.808 mm
U^{234}	0.212	0.209	0.206	0.203
U^{235}	8.058	7.767	7.500	7.316
U^{236}	6.746	6.765	6.783	6.802
U^{238}	928.2	924.7	913.3	882.7
Pu^{238}	0.266	0.281	0.303	0.343
Pu^{239}	4.835	5.389	7.299	12.42
Pu^{240}	2.546	2.711	3.509	5.742
Pu^{241}	0.867	1.020	1.459	2.635
Pu^{242}	0.719	0.868	1.277	2.375
Np^{237}	1.290	1.331	1.371	1.399
Am^{241}	0.990	1.149	1.625	2.932
Oxygen	134.5	134.5	134.5	134.5
Other fission products	46.19	48.79	56.35	76.27

* Measured averaged concentrations and calculated relative radial distributions of isotopes (TRIFOB code) were used to develop these data

Table C-10.2. Initial individual characteristics of fuel rod # RT10*

Axial coordinate (from lower cap) (mm)	Cladding average outer diameter (mm)	Fuel mass ** (g)	Linear fuel mass** (g/cm)	Gas flow area[3]** (mm^2)	Burnup** (MW d/kg U)
20[1]	9.076	0.45	4.11	5.68	46.87
25	9.075	2.07	4.13	5.49	46.93
30	9.073	2.09	4.18	5.00	46.60
35	9.073	2.10	4.19	4.91	46.31
40	9.074	2.09	4.18	5.00	46.65
45	9.074	2.07	4.15	5.29	47.25
50	9.075	2.06	4.12	5.58	47.36
55	9.073	2.05	4.10	5.78	47.10
60	9.073	2.06	4.11	5.68	47.02
65	9.076	2.07	4.15	5.29	47.06
70	9.075	2.07	4.15	5.29	46.85
75	9.075	2.07	4.14	5.39	46.60
80	9.073	2.07	4.13	5.49	46.77
85	9.071	2.06	4.12	5.58	47.08
90	9.080	2.08	4.15	5.29	46.91
95	9.072	2.08	4.16	5.20	46.61
100	9.072	2.07	4.13	5.49	46.97
105	9.068	2.06	4.11	5.68	47.56
110	9.066	2.04	4.08	5.97	47.44
115	9.071	2.04	4.08	5.97	46.91
120	9.071	2.05	4.10	5.78	46.84
125	9.070	2.06	4.11	5.68	47.08
130	9.069	2.06	4.13	5.49	47.02
135	9.071	2.07	4.13	5.49	46.84
140	9.069	2.06	4.11	5.68	47.13
145	9.069	2.05	4.11	5.68	47.54
150	9.069	2.05	4.10	5.78	47.36
155	9.068	2.05	4.11	5.68	46.82
160	9.071	2.03	4.06	6.17	46.65
165	9.068	1.99	3.99	6.85	46.83
170	9.070	2.01	4.02	6.55	46.91
175[2]	9.069	0.37	4.11	5.68	46.89

* All parameters were determined using results of pre-test examinations

** Average values at the length interval equal to the axial coordinate ±2.5 mm

[1] Bottom end coordinate of fuel stack is 21.4 mm; [2] Top end coordinate of fuel stack is 173.4 mm

[3] Gas flow area beyond the fuel stack (mm^2):

Bottom: 0.0-3.0mm – 0.00; 3.0-10.5mm – 12.56; 10.5-12.5mm – 46.08; 12.5-23.0mm – 25.17

Top: 173.4-178.5mm – 46.08; 178.5-204.5mm – 28.26; 204.5-281mm – 47.27; 281-290mm – 28.26; 290-299mm – 0.00

RT10

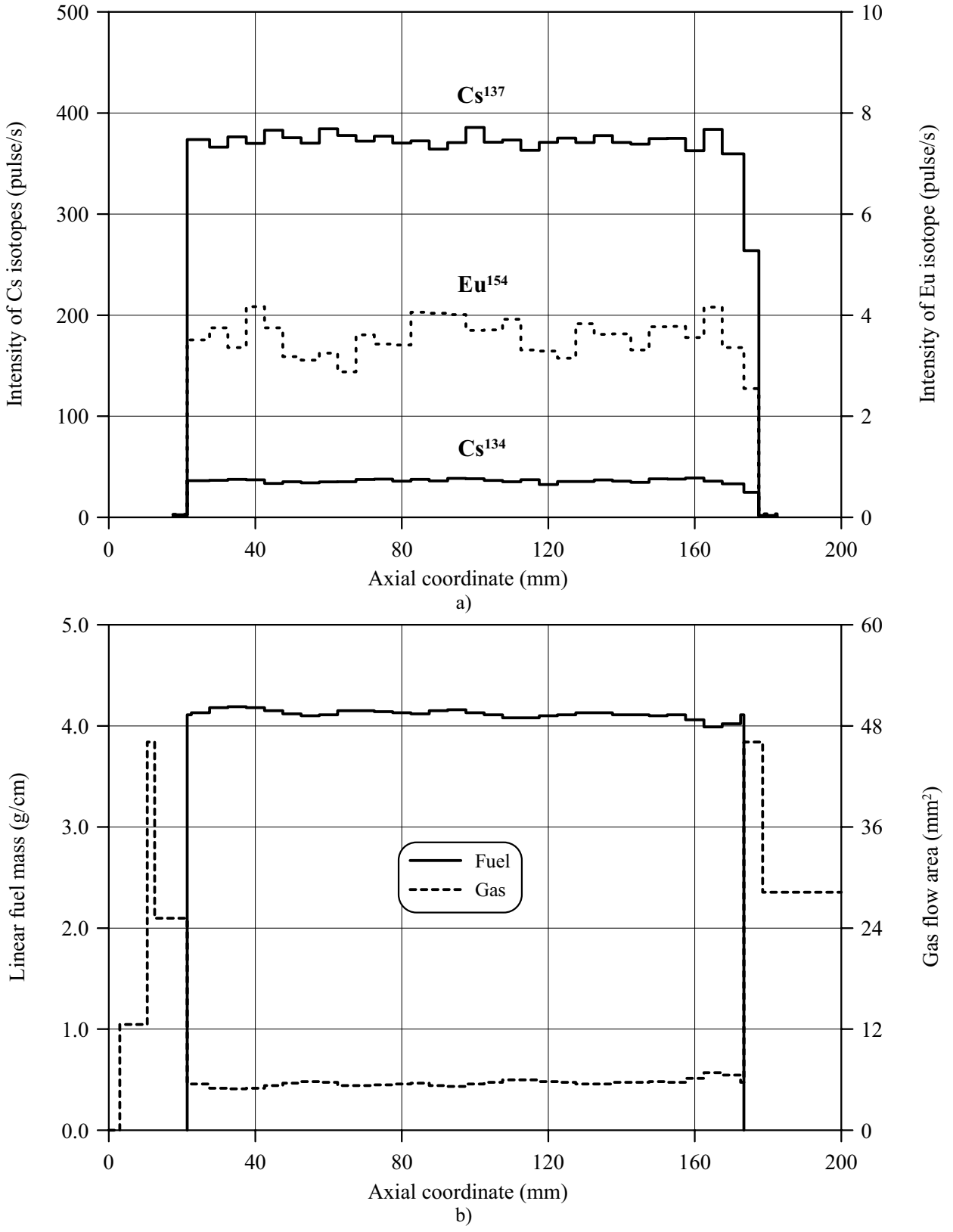


Fig.C-10.1. (a) Results of γ-scanning, (b) Axial fuel mass distribution and axial gas flow area distribution for fuel rod # RT10

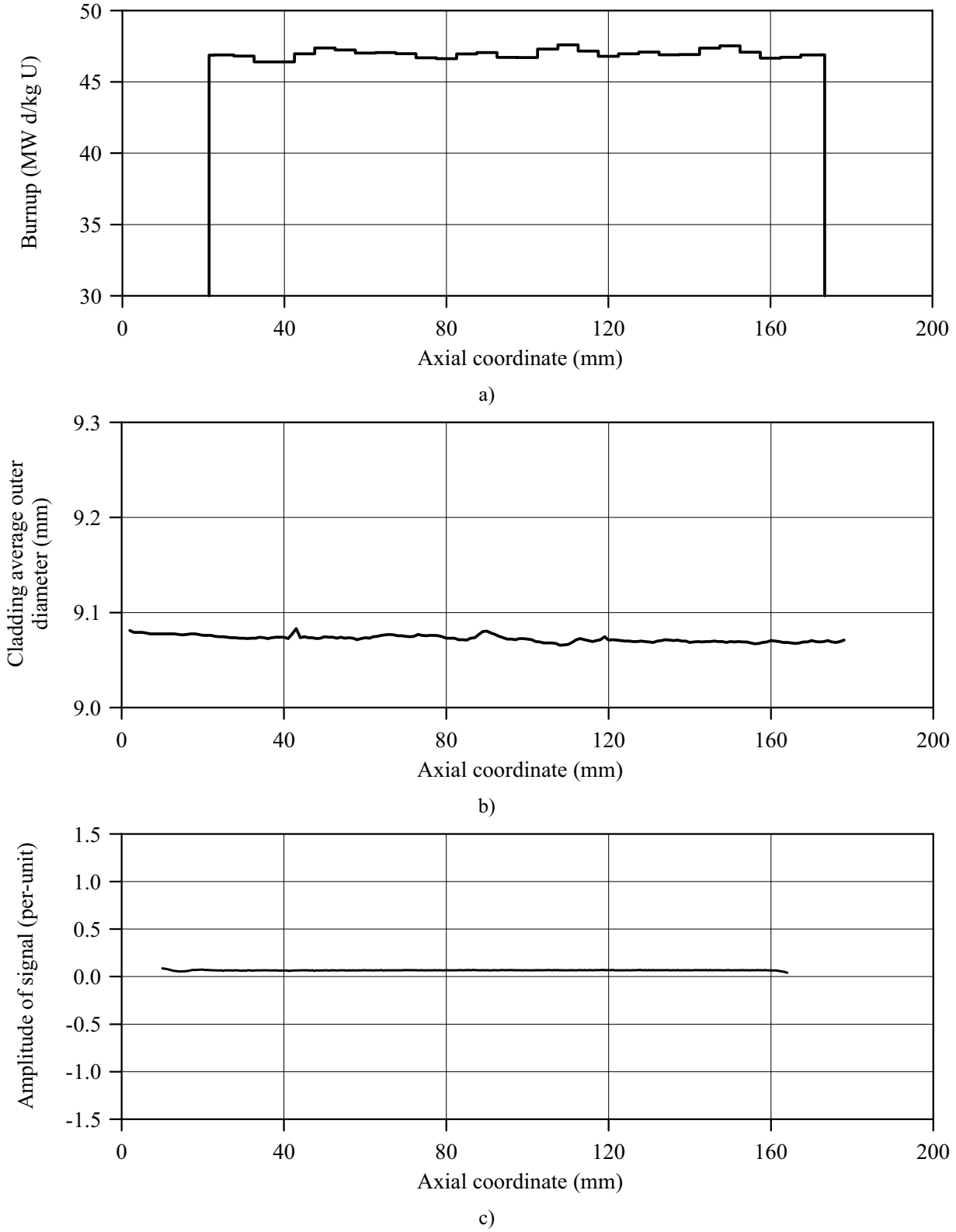


Fig.C-10.2. (a) Axial burnup distribution and (b) results of profilometry and (c) eddy-current examination of fuel rod # RT10

RT10

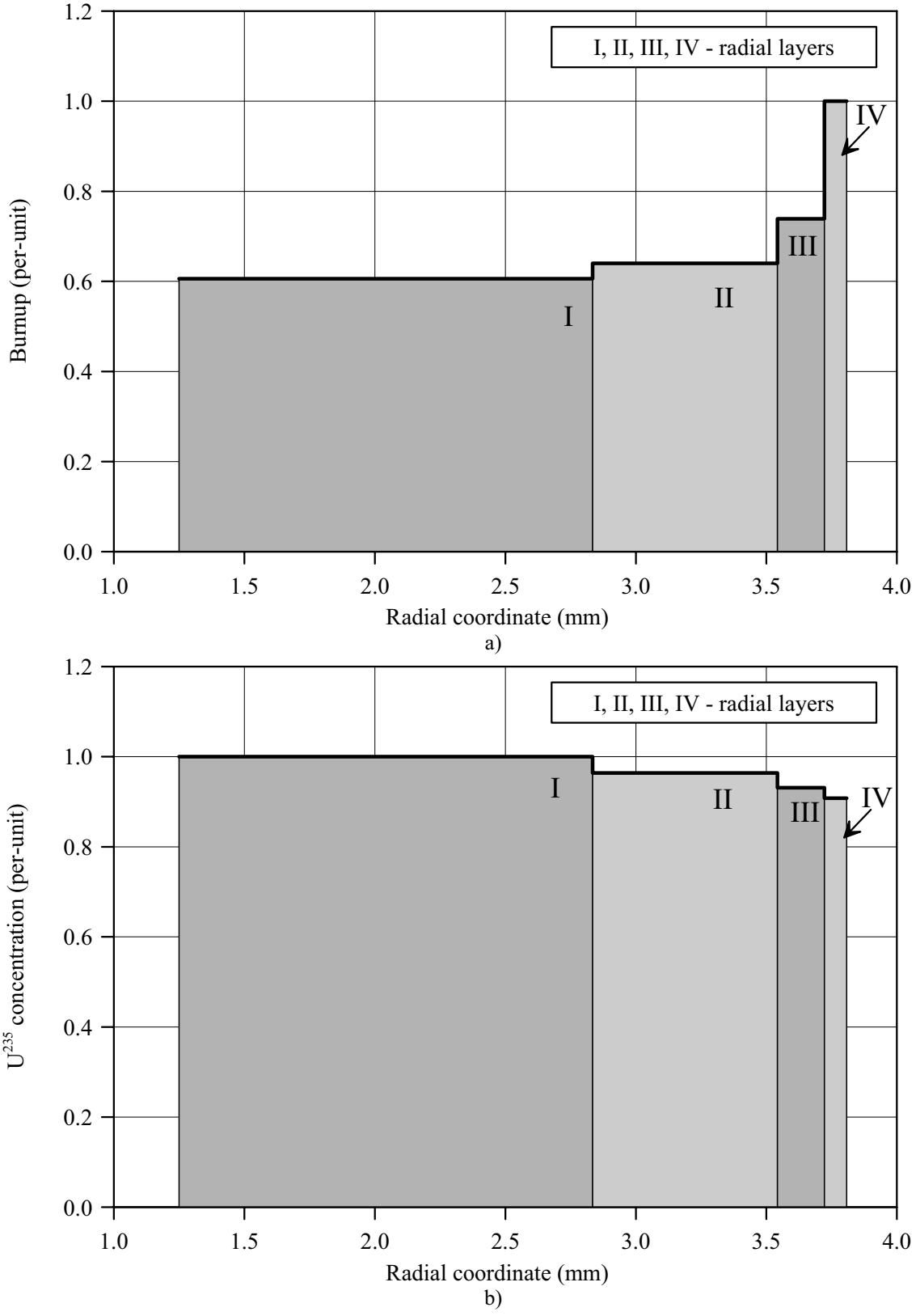


Fig.C-10.3. (a) Burnup radial distribution and (b) U^{235} radial distribution for fuel rod # RT10 (calculated values)

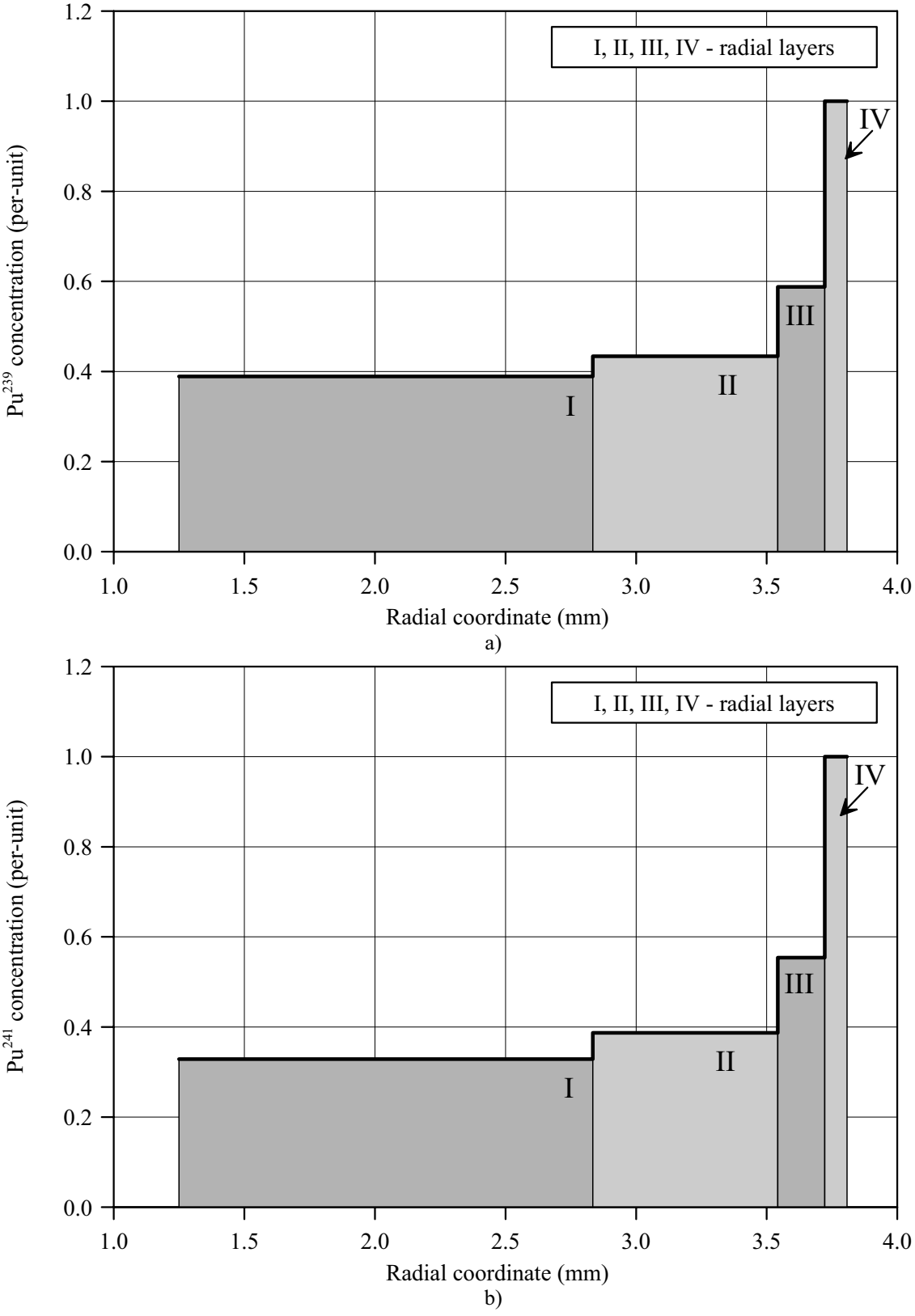


Fig.C-10.4. Radial distribution of (a) Pu^{239} and (b) Pu^{241} for fuel rod # RT10 (calculated values)

Appendix C-11

Individual Characteristics

of Fuel Rod # RT11 before the BIGR Test

RT11

Table C-11.1. Radial distribution of isotope nuclear concentrations for fuel rod #RT11 (values averaged of over the fuel stack length)*

Isotope	Isotopic concentrations (kg/t U) in four fuel radial layers			
	1.250-2.834 mm	2.834-3.452 mm	3.452-3.722 mm	3.722-3.808 mm
U^{234}	0.212	0.209	0.206	0.203
U^{235}	8.058	7.767	7.500	7.316
U^{236}	6.746	6.765	6.783	6.802
U^{238}	928.2	924.7	913.3	882.7
Pu^{238}	0.266	0.281	0.303	0.343
Pu^{239}	4.835	5.389	7.299	12.42
Pu^{240}	2.546	2.711	3.509	5.742
Pu^{241}	0.851	1.001	1.432	2.587
Pu^{242}	0.719	0.868	1.277	2.375
Np^{237}	1.290	1.331	1.371	1.399
Am^{241}	0.990	1.149	1.625	2.932
Oxygen	134.5	134.5	134.5	134.5
Other fission products	46.11	48.69	56.22	76.05

* Measured averaged concentrations and calculated relative radial distributions of isotopes (TRIFOB code) were used to develop these data

Table C-11.2. Initial individual characteristics of fuel rod # RT11*

Axial coordinate (from lower cap) (mm)	Cladding average outer diameter (mm)	Fuel mass ** (g)	Linear fuel mass** (g/cm)	Gas flow area[3]** (mm^2)	Burnup** (MW d/kg U)
25[1]	9.095	1.76	3.91	8.59	46.49
30	9.088	2.02	4.03	7.46	46.30
35	9.087	2.10	4.19	5.95	46.26
40	9.089	2.15	4.30	4.91	46.41
45	9.087	2.15	4.30	4.91	46.39
50	9.089	2.15	4.29	5.00	46.22
55	9.088	2.14	4.27	5.19	46.44
60	9.083	2.13	4.26	5.28	47.02
65	9.083	2.13	4.26	5.28	47.16
70	9.083	2.11	4.22	5.66	46.77
75	9.082	2.11	4.21	5.76	46.81
80	9.081	2.11	4.21	5.76	47.48
85	9.083	2.09	4.18	6.04	47.93
90	9.083	2.08	4.16	6.23	47.81
95	9.082	2.07	4.15	6.32	47.56
100	9.085	2.08	4.15	6.32	47.40
105	9.082	2.09	4.18	6.04	47.28
110	9.085	2.11	4.21	5.76	47.23
115	9.082	2.10	4.20	5.85	47.42
120	9.081	2.08	4.17	6.13	47.76
125	9.085	2.06	4.13	6.51	47.76
130	9.081	2.07	4.14	6.42	47.42
135	9.085	2.07	4.13	6.51	47.32
140	9.080	2.07	4.14	6.42	47.62
145	9.082	2.07	4.14	6.42	47.81
150	9.080	2.06	4.12	6.61	47.72
155	9.080	2.07	4.13	6.51	47.68
160	9.082	2.07	4.14	6.42	47.76
165	9.080	2.10	4.21	5.76	47.64
170	9.083	1.82	3.64	11.14	47.27
175[2]	9.082	0.71	2.84	18.70	46.92

* All parameters were determined using results of pre-test examinations

** Average values at the length interval equal to the axial coordinate ±2.5 mm

[1] Bottom end coordinate of fuel stack is 23 mm; [2] Top end coordinate of fuel stack is 175 mm

[3] Gas flow area beyond the fuel stack (mm^2):

Bottom: 0.0-3.0mm – 0.00; 3.0-10.5mm – 12.56; 10.5-14.1mm – 45.96; 14.1-23.0mm – 25.08

Top: 176.1-178.5mm – 45.96; 178.5-204.5mm – 28.26; 204.5-281mm – 47.27; 281-290mm – 28.26; 290-299mm – 0.00

RT11

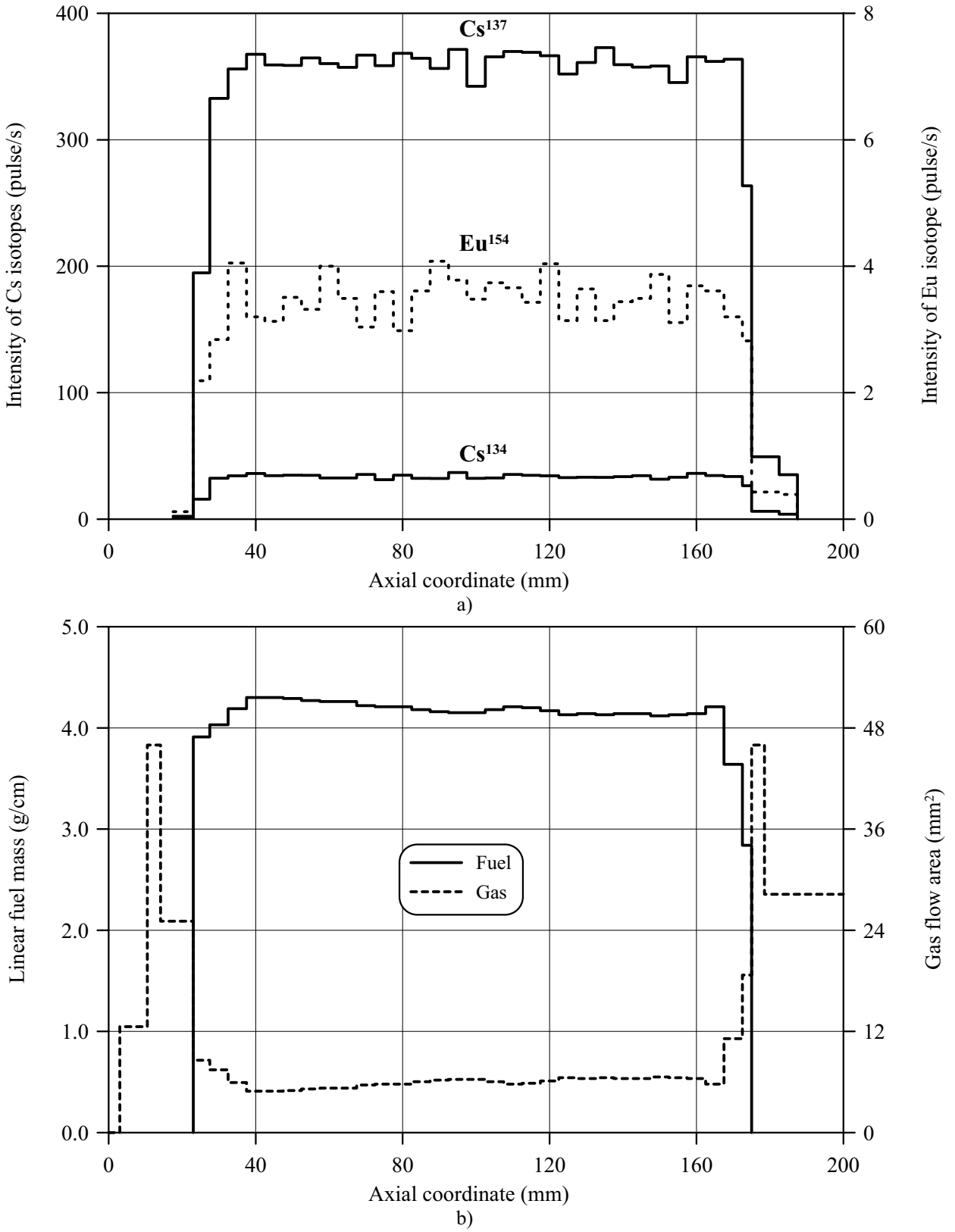


Fig.C-11.1. (a) Results of γ-scanning, (b) Axial fuel mass distribution and axial gas flow area distribution for fuel rod # RT11

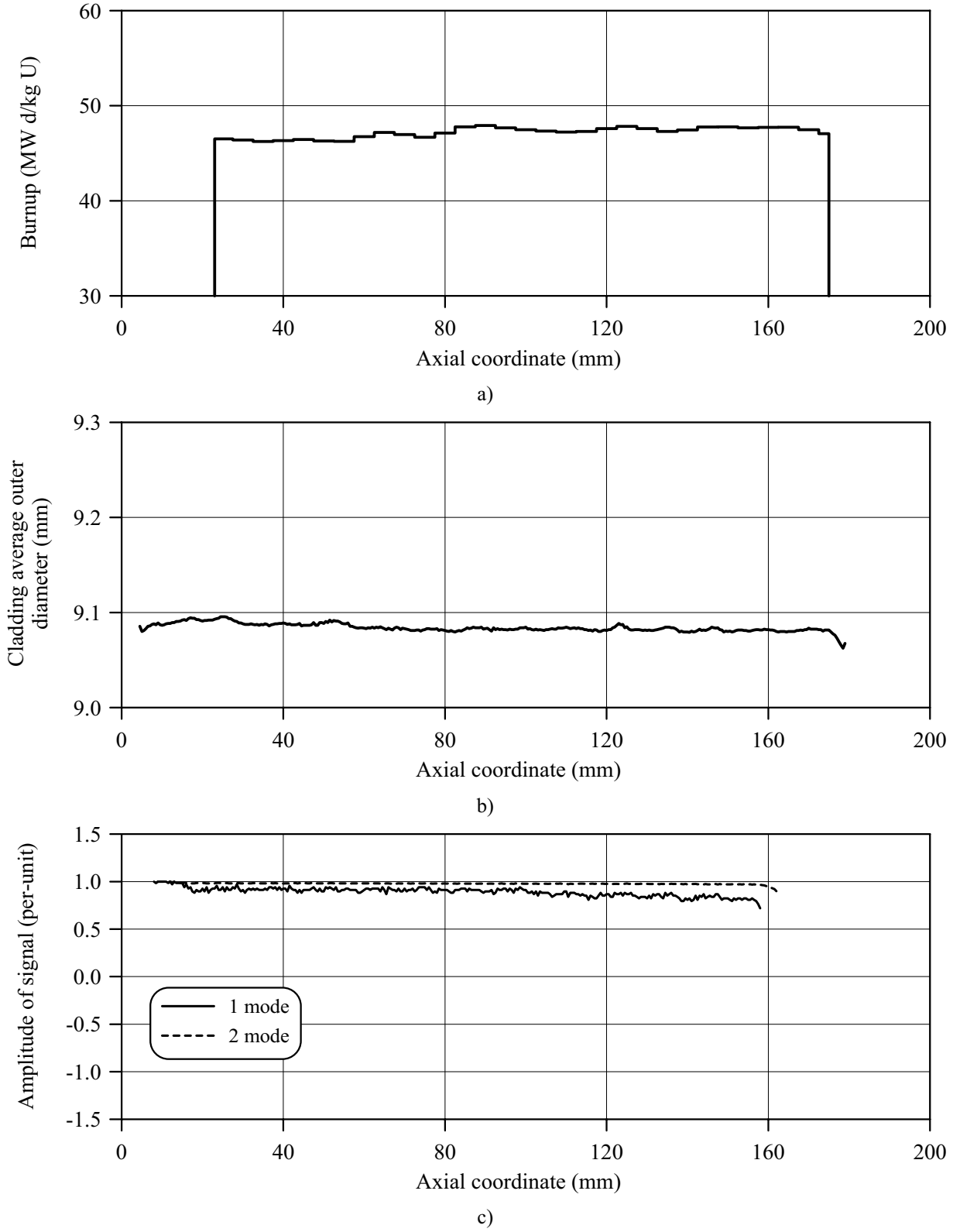


Fig.C-11.2. (a) Axial burnup distribution and (b) results of profilometry and (c) eddy-current examination of fuel rod # RT11

RT11

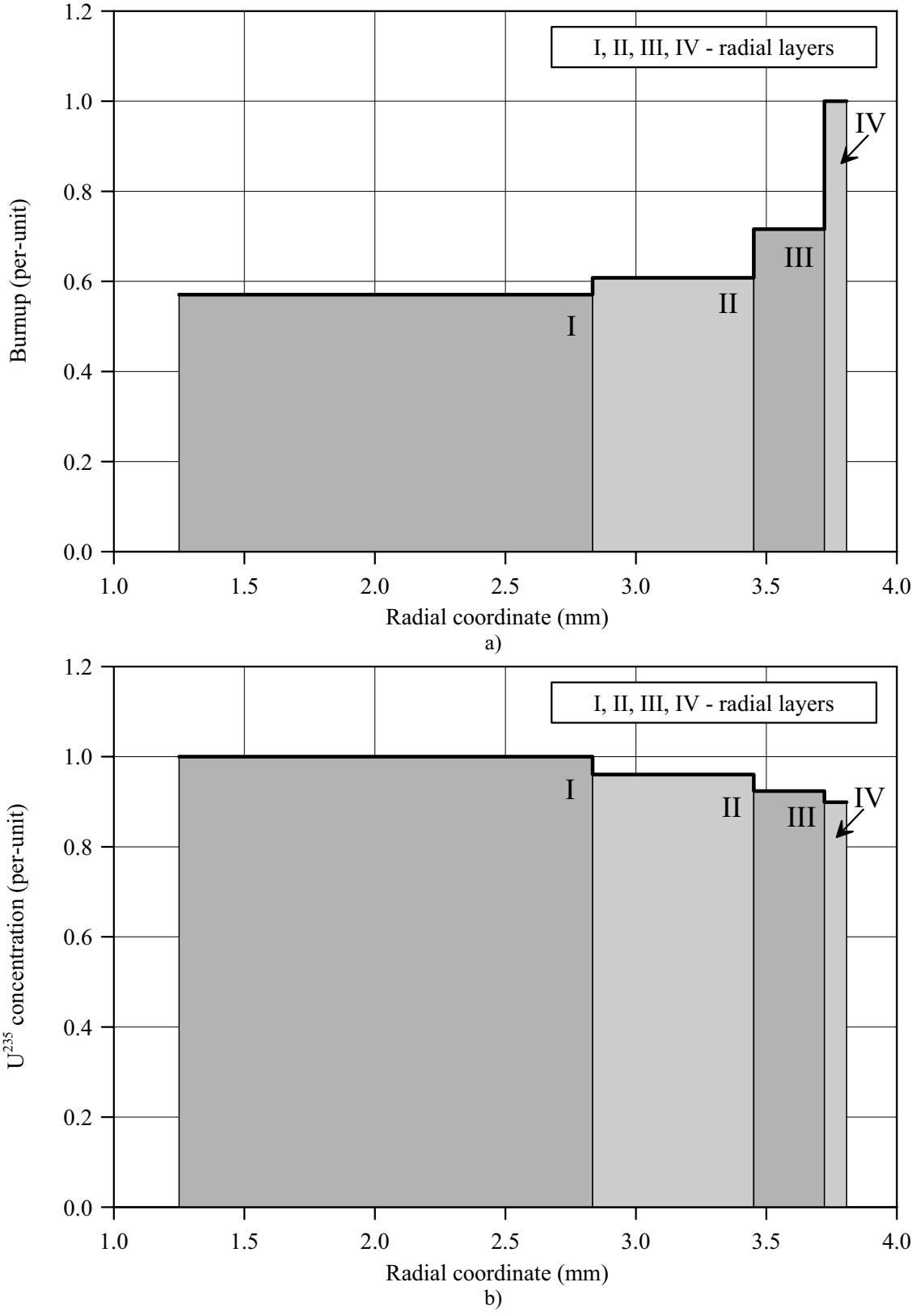
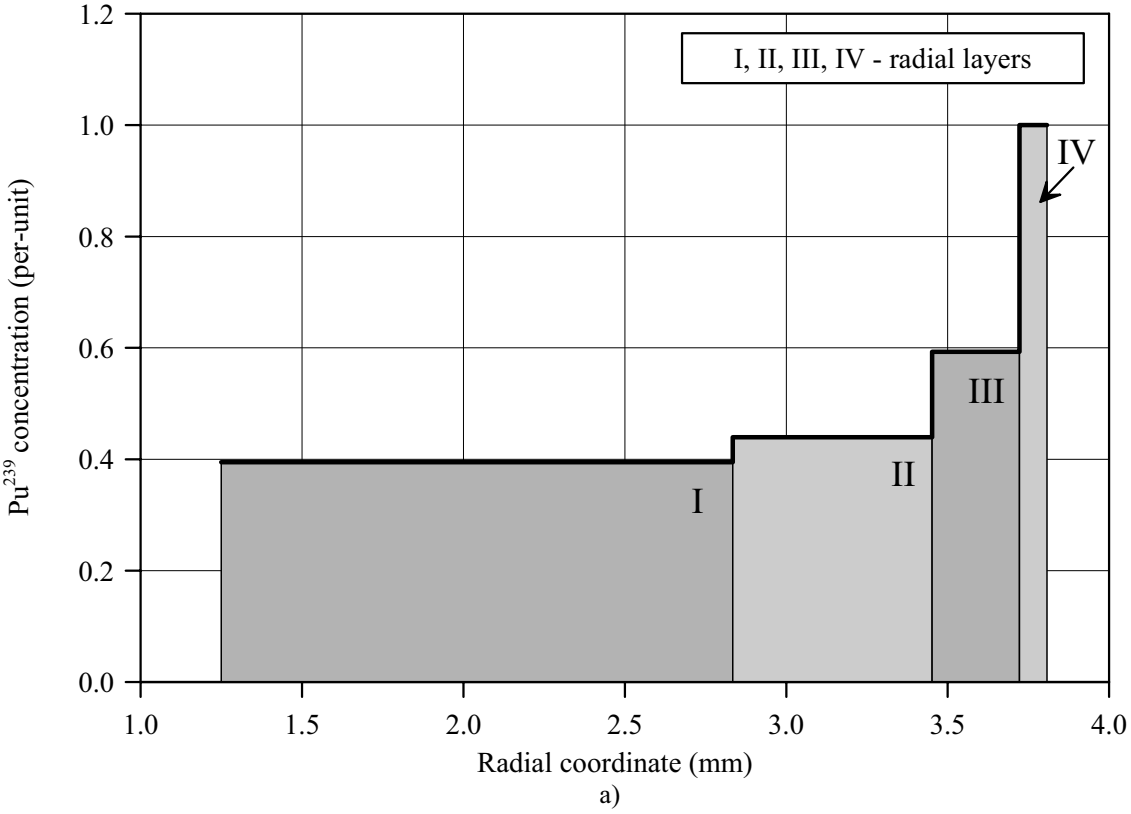
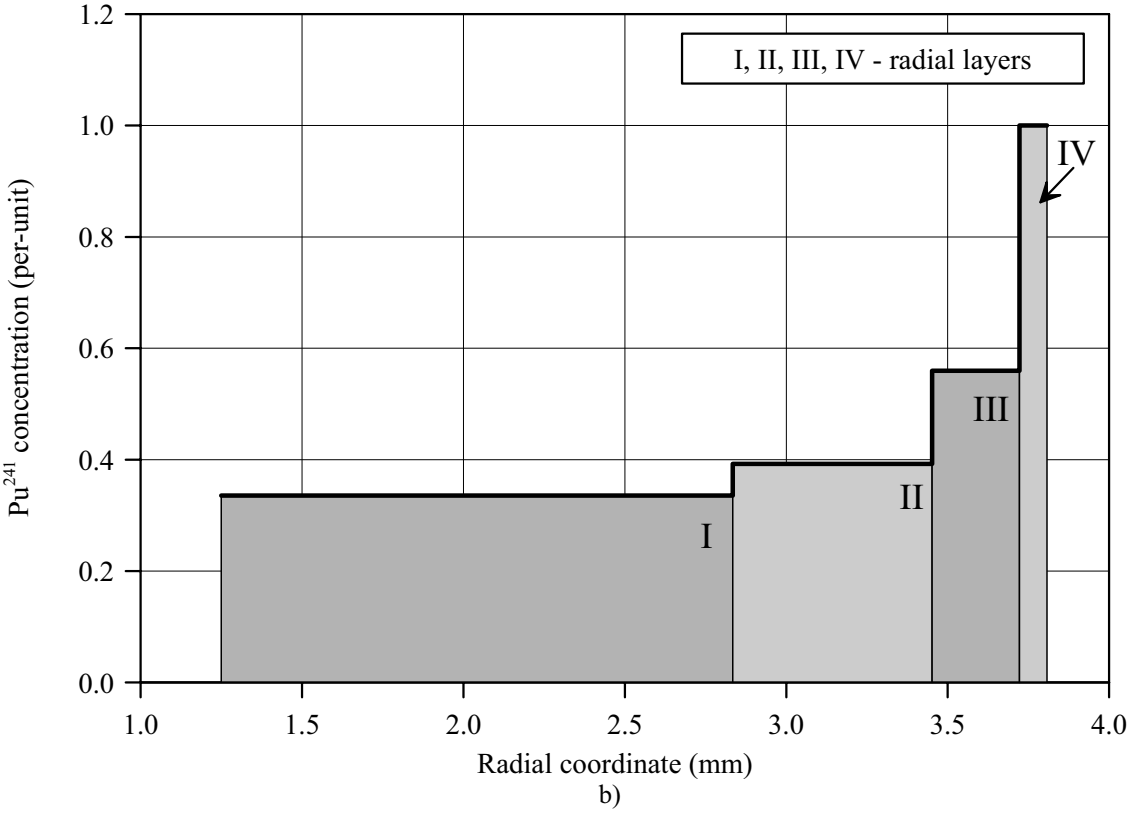


Fig.C-11.3. (a) Burnup radial distribution and (b) U^{235} radial distribution for fuel rod # RT11 (calculated values)



a)



b)

Fig.C-11.4. Radial distribution of (a) Pu^{239} and (b) Pu^{241} for fuel rod # RT11 (calculated values)

Appendix C-12

Individual Characteristics

of Fuel Rod # RT12 before the BIGR Test

RT12

Table C-12.1. Radial distribution of isotope nuclear concentrations for fuel rod #RT12 (values averaged of over the fuel stack length)*

Isotope	Isotopic concentrations (kg/t U) in four fuel radial layers			
	1.250-2.834 mm	2.834-3.452 mm	3.452-3.722 mm	3.722-3.808 mm
U^{234}	0.212	0.209	0.206	0.203
U^{235}	8.058	7.767	7.500	7.316
U^{236}	6.746	6.765	6.783	6.802
U^{238}	928.2	924.7	913.3	882.7
Pu^{238}	0.266	0.281	0.303	0.343
Pu^{239}	4.835	5.389	7.299	12.42
Pu^{240}	2.546	2.711	3.509	5.742
Pu^{241}	0.867	1.020	1.459	2.635
Pu^{242}	0.719	0.868	1.277	2.375
Np^{237}	1.290	1.331	1.371	1.399
Am^{241}	0.990	1.149	1.625	2.932
Oxygen	134.5	134.5	134.5	134.5
Other fission products	46.19	48.79	56.35	76.27

* Measured averaged concentrations and calculated relative radial distributions of isotopes (TRIFOB code) were used to develop these data

Table C-12.2. Initial individual characteristics of fuel rod # RT12*

Axial coordinate (from lower cap) (mm)	Cladding average outer diameter (mm)	Fuel mass ** (g)	Linear fuel mass** (g/cm)	Gas flow area[3]** (mm^2)	Burnup** (MW d/kg U)
20[1]	9.073	0.50	4.14	5.39	47.30
25	9.070	2.07	4.14	5.39	47.23
30	9.072	2.07	4.14	5.39	47.32
35	9.073	2.07	4.15	5.29	47.39
40	9.069	2.07	4.13	5.49	47.49
45	9.072	2.06	4.13	5.49	47.63
50	9.070	2.06	4.12	5.58	47.78
55	9.073	2.06	4.13	5.49	47.87
60	9.071	2.07	4.15	5.29	47.74
65	9.070	2.08	4.17	5.10	47.40
70	9.067	2.09	4.18	5.00	47.16
75	9.066	2.09	4.17	5.10	47.18
80	9.063	2.08	4.17	5.10	47.20
85	9.062	2.08	4.16	5.20	47.09
90	9.065	2.07	4.15	5.29	47.07
95	9.063	2.07	4.14	5.39	47.23
100	9.066	2.07	4.13	5.49	47.37
105	9.064	2.06	4.12	5.58	47.35
110	9.069	2.06	4.12	5.58	47.24
115	9.064	2.06	4.12	5.58	47.16
120	9.065	2.06	4.12	5.58	47.26
125	9.064	2.06	4.11	5.68	47.53
130	9.066	2.05	4.10	5.78	47.64
135	9.067	2.06	4.11	5.68	47.42
140	9.062	2.06	4.12	5.58	47.13
145	9.062	2.06	4.12	5.58	47.02
150	9.058	2.05	4.11	5.68	47.20
155	9.059	2.04	4.08	5.97	47.62
160	9.063	2.03	4.06	6.17	47.87
165	9.059	2.03	4.06	6.17	47.74
170	9.063	2.06	4.11	5.68	47.51
175[2]	9.066	0.59	4.19	4.91	47.39

* All parameters were determined using results of pre-test examinations

** Average values at the length interval equal to the axial coordinate ±2.5 mm

[1] Bottom end coordinate of fuel stack is 21.3 mm; [2] Top end coordinate of fuel stack is 173.9 mm

[3] Gas flow area beyond the fuel stack (mm^2):

Bottom: 0.0-3.0mm – 0.00; 3.0-10.5mm – 12.56; 10.5-12.4mm – 45.82; 12.4-21.3mm – 24.97

Top: 173.9-180.0mm – 45.82; 180.0-206.0mm – 28.26; 206.0-282mm – 47.27; 282-291mm – 28.26; 291-300mm – 0.00

RT12

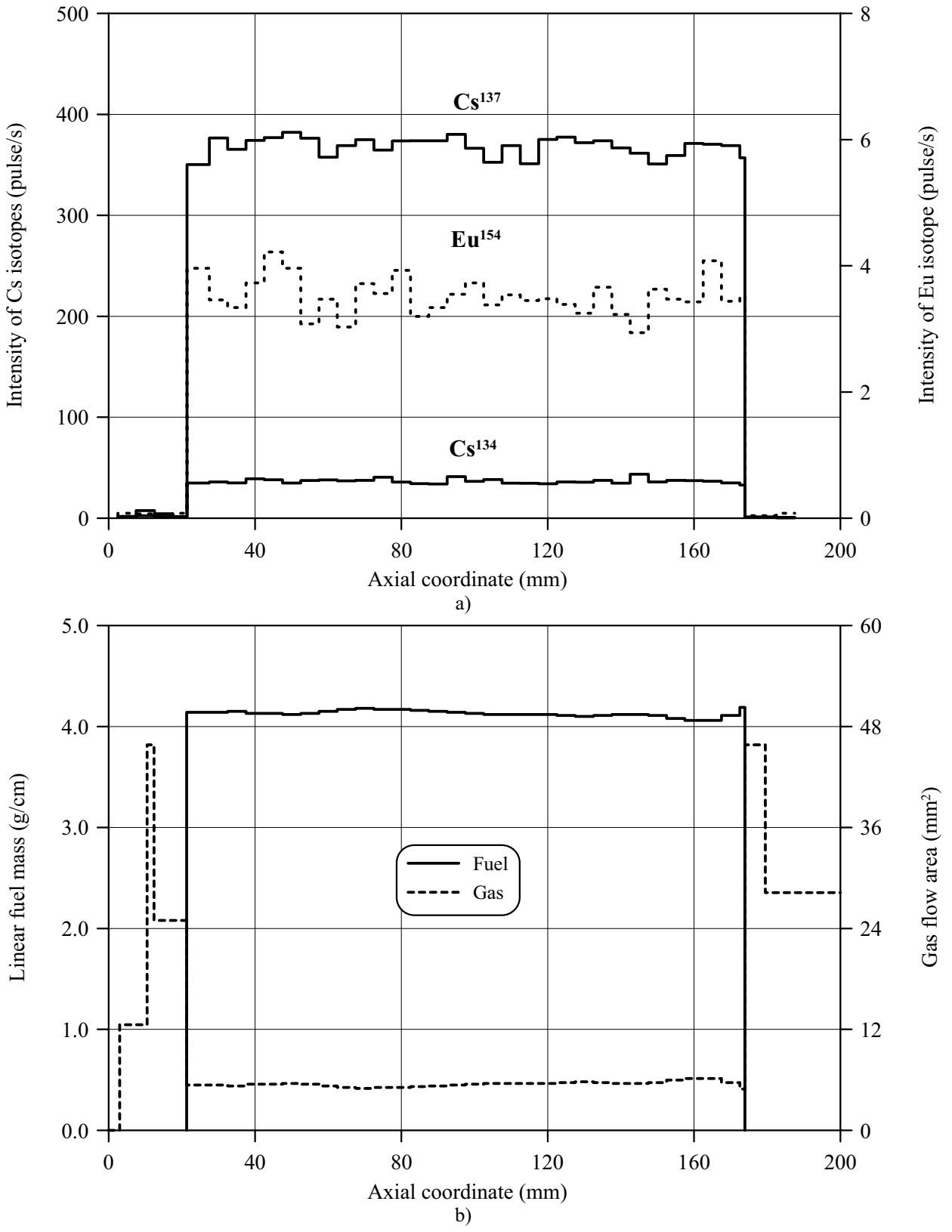


Fig.C-12.1. (a) Results of γ-scanning, (b) Axial fuel mass distribution and axial gas flow area distribution for fuel rod # RT12

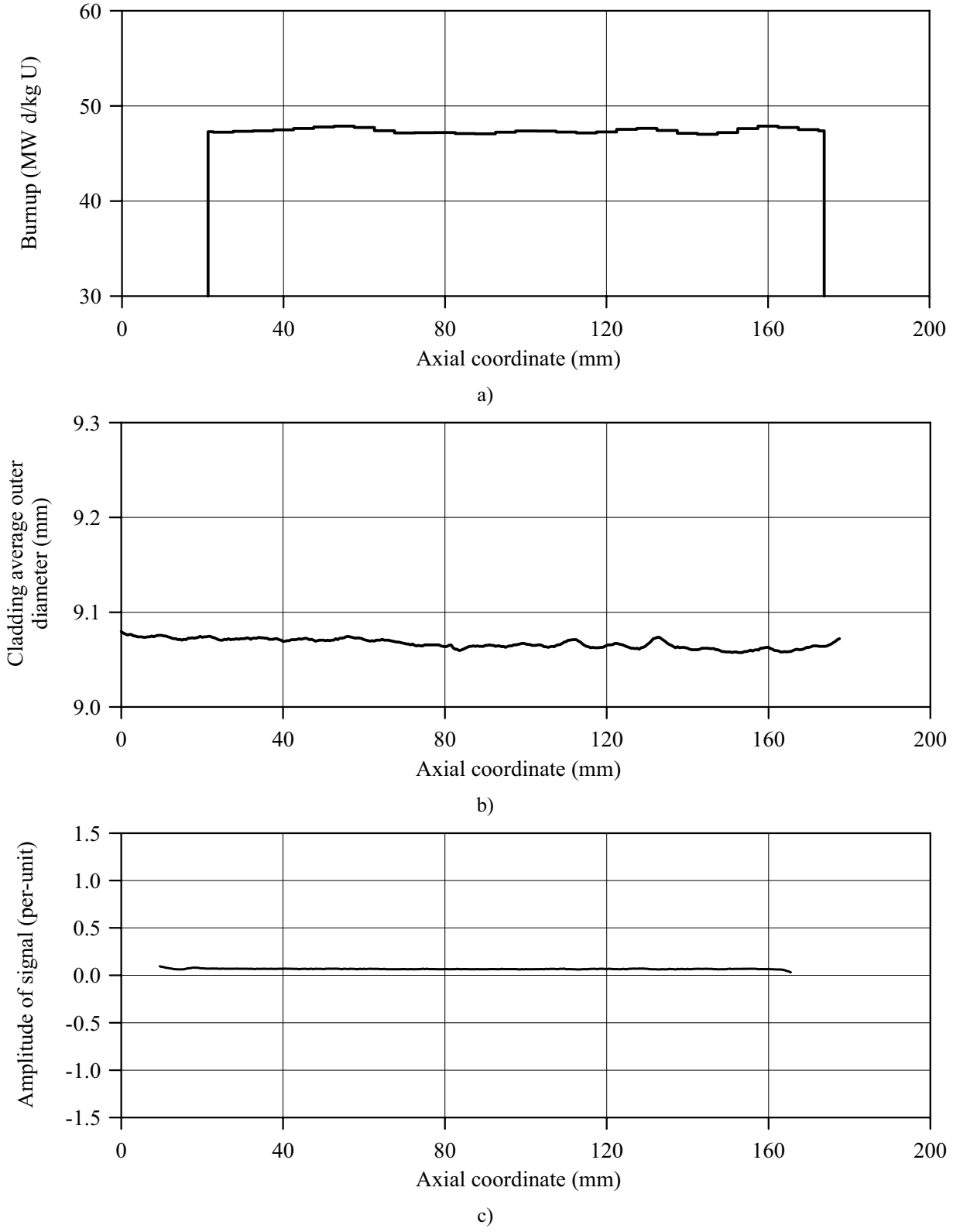


Fig.C-12.2. (a) Axial burnup distribution and (b) results of profilometry and (c) eddy-current examination of fuel rod # RT12

RT12

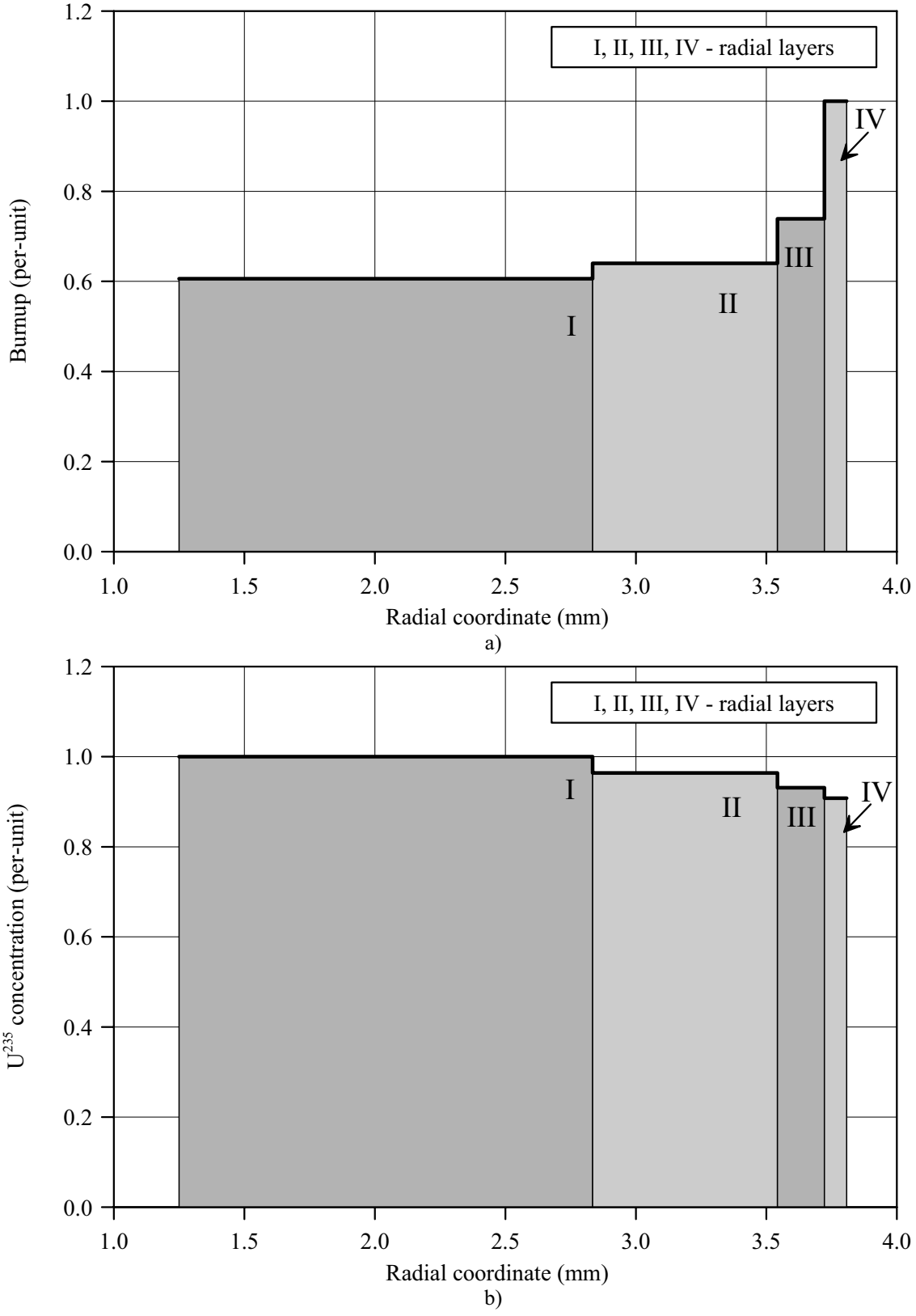
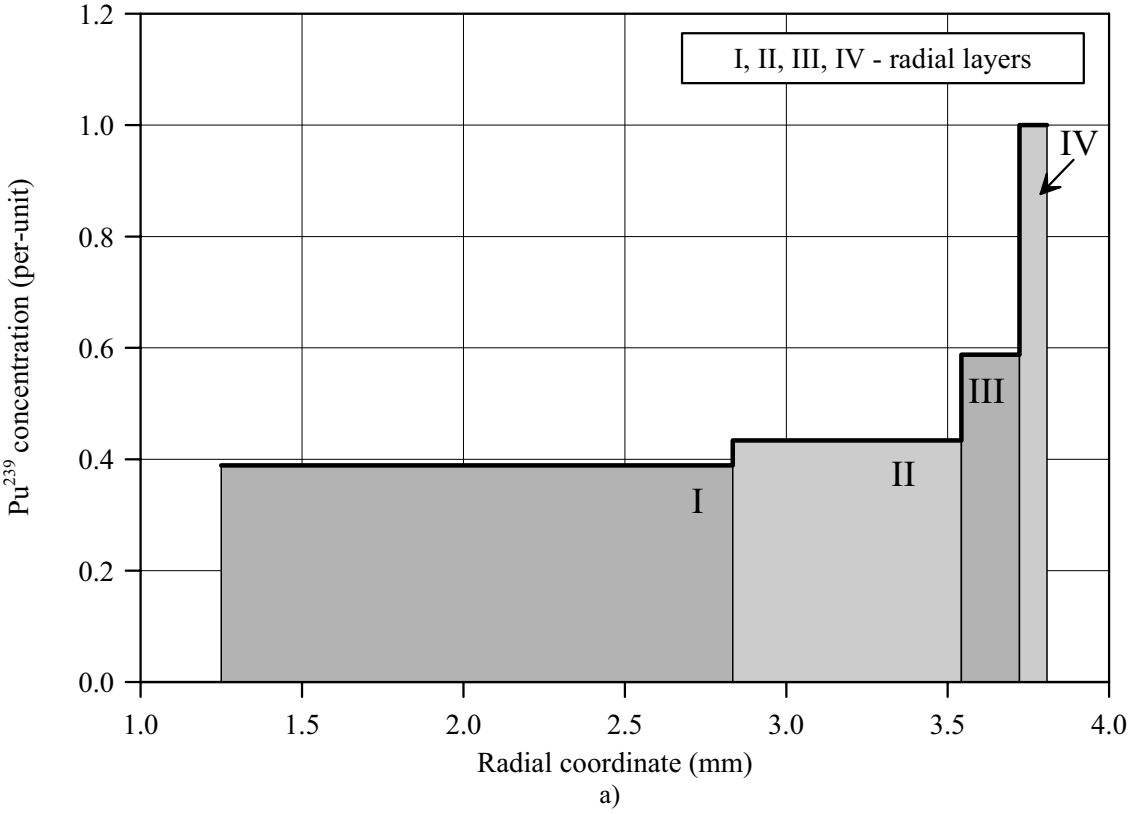
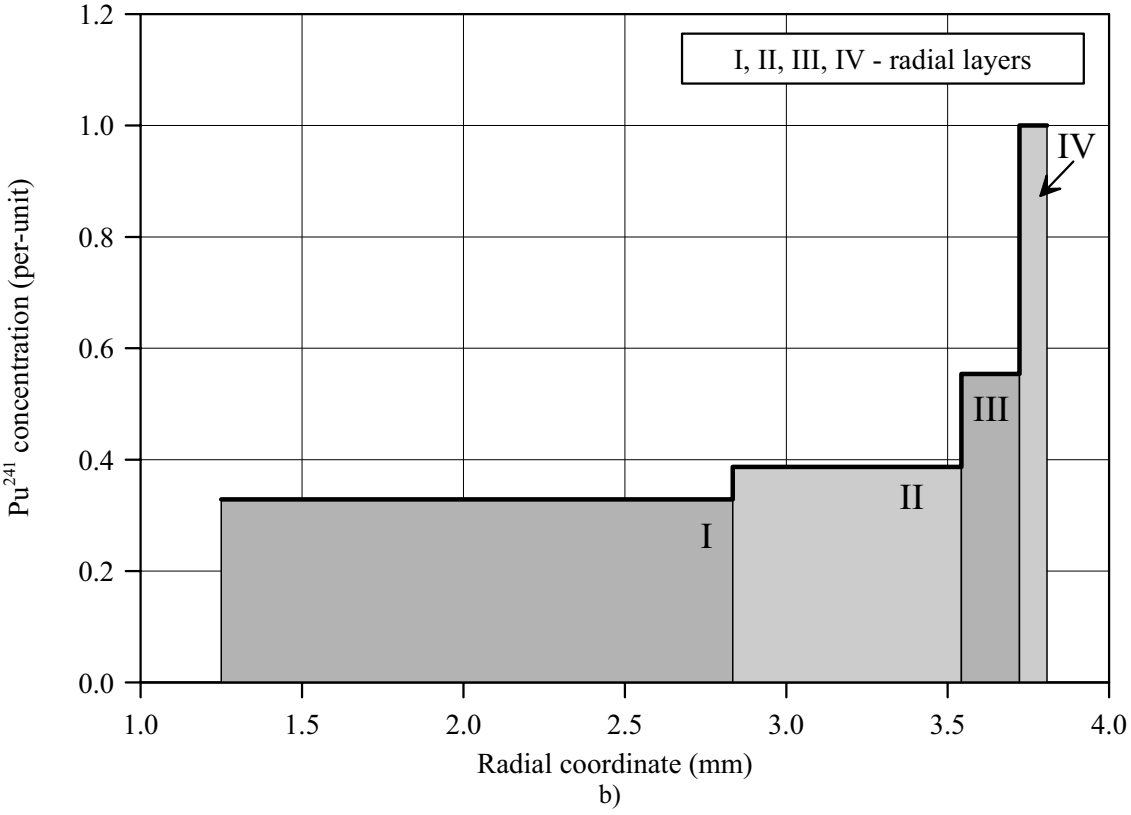


Fig.C-12.3. (a) Burnup radial distribution and (b) U^{235} radial distribution for fuel rod # RT12 (calculated values)



a)



b)

Fig.C-12.4. Radial distribution of (a) Pu^{239} and (b) Pu^{241} for fuel rod # RT12 (calculated values)

APPENDIX D

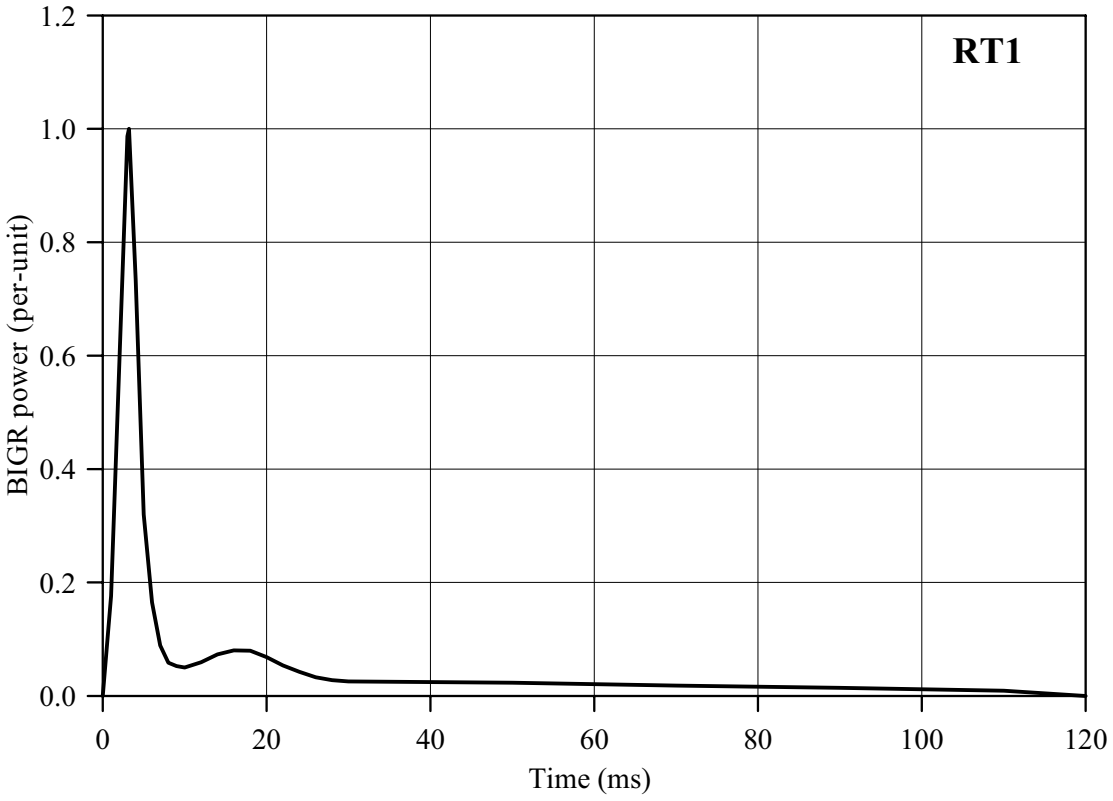
CHARACTERISTICS OF THE BIGR POWER PULSES

Table D.1. Reference data characterizing BIGR tests of refabricated fuel rods ## RT 1–12

Number of fuel rods	Number of BIGR test	Date of BIGR test	Pulse half width (ms)
RT1	833	06.11.97	2.6
RT2	834	10.11.97	3.1
RT3	832	04.11.97	2.5
RT4	846	13.11.97	2.5
RT5	847	16.11.97	2.5
RT6	845	11.11.97	2.6
RT7	881	30.06.2000	2.6
RT8	889	17.11.2000	2.6
RT9	887	11.11.2000	2.7
RT10	880	27.06.2000	2.6
RT11	888	14.11.2000	2.6
RT12	882	05.07.2000	2.8

Table D.2. BIGR power for fuel rods ## RT1–12 in accordance with the Neutron detector recording

Time (s)	Reactor power (V)											
	Number of fuel rod											
	RT1	RT2	RT3	RT4	RT5	RT6	RT7	RT8	RT9	RT10	RT11	RT12
0.000	0.000	0.000	0.000	0.000	0.000	0.000	0.001	0.000	0.000	0.000	0.000	0.000
0.001	0.810	1.598	0.946	0.917	0.931	0.788	0.004	0.003	0.003	0.009	0.003	0.003
0.002	2.636	3.254	2.966	2.894	2.891	2.840	0.017	0.012	0.013	0.041	0.012	0.012
0.003	4.545	3.384	4.800	4.800	4.900	4.500	0.076	0.055	0.057	0.185	0.053	0.049
0.004	3.367	2.232	3.269	3.110	3.200	3.051	0.314	0.238	0.240	0.620	0.229	0.195
0.005	1.467	1.109	1.406	1.277	1.318	1.269	0.837	0.706	0.688	1.003	0.689	0.603
0.006	0.759	0.562	0.710	0.682	0.715	0.684	0.939	0.990	0.998	0.684	0.993	0.997
0.007	0.409	0.356	0.387	0.364	0.379	0.374	0.520	0.619	0.670	0.318	0.632	0.764
0.008	0.270	0.267	0.268	0.253	0.264	0.261	0.234	0.282	0.319	0.150	0.289	0.389
0.009	0.241	0.238	0.236	0.216	0.221	0.218	0.119	0.136	0.155	0.086	0.138	0.192
0.010	0.230	0.230	0.229	0.213	0.220	0.213	0.075	0.081	0.092	0.062	0.082	0.109
0.012	0.273	0.237	0.256	0.255	0.260	0.247	0.054	0.054	0.059	0.052	0.054	0.063
0.014	0.337	0.250	0.316	0.321	0.321	0.300	0.056	0.054	0.061	0.057	0.054	0.059
0.016	0.370	0.242	0.345	0.360	0.363	0.338	0.066	0.064	0.072	0.065	0.064	0.064
0.018	0.366	0.219	0.332	0.352	0.357	0.329	0.075	0.074	0.083	0.070	0.074	0.070
0.020	0.315	0.188	0.275	0.310	0.300	0.275	0.076	0.078	0.086	0.067	0.079	0.070
0.022	0.247	0.156	0.219	0.284	0.241	0.220	0.069	0.074	0.081	0.059	0.074	0.064
0.024	0.194	0.131	0.173	0.250	0.191	0.174	0.059	0.062	0.070	0.050	0.062	0.056
0.026	0.151	0.115	0.139	0.201	0.146	0.140	0.049	0.050	0.058	0.042	0.050	0.047
0.028	0.127	0.107	0.117	0.154	0.118	0.118	0.040	0.040	0.047	0.035	0.040	0.040
0.030	0.117	0.104	0.110	0.123	0.109	0.106	0.034	0.034	0.039	0.031	0.034	0.035
0.050	0.107	0.104	0.112	0.091	0.091	0.091	0.028	0.027	0.030	0.026	0.028	0.031
0.070	0.085	0.084	0.090	0.082	0.079	0.079	0.025	0.024	0.027	0.022	0.025	0.025
0.090	0.066	0.069	0.071	0.061	0.056	0.056	0.018	0.021	0.023	0.015	0.022	0.018
0.110	0.042	0.038	0.038	0.039	0.034	0.035	0.005	0.012	0.013	0.003	0.013	0.008
0.120	0.000	0.000	0.000	0.000	0.000	0.000	0.000	0.000	0.000	0.000	0.000	0.000



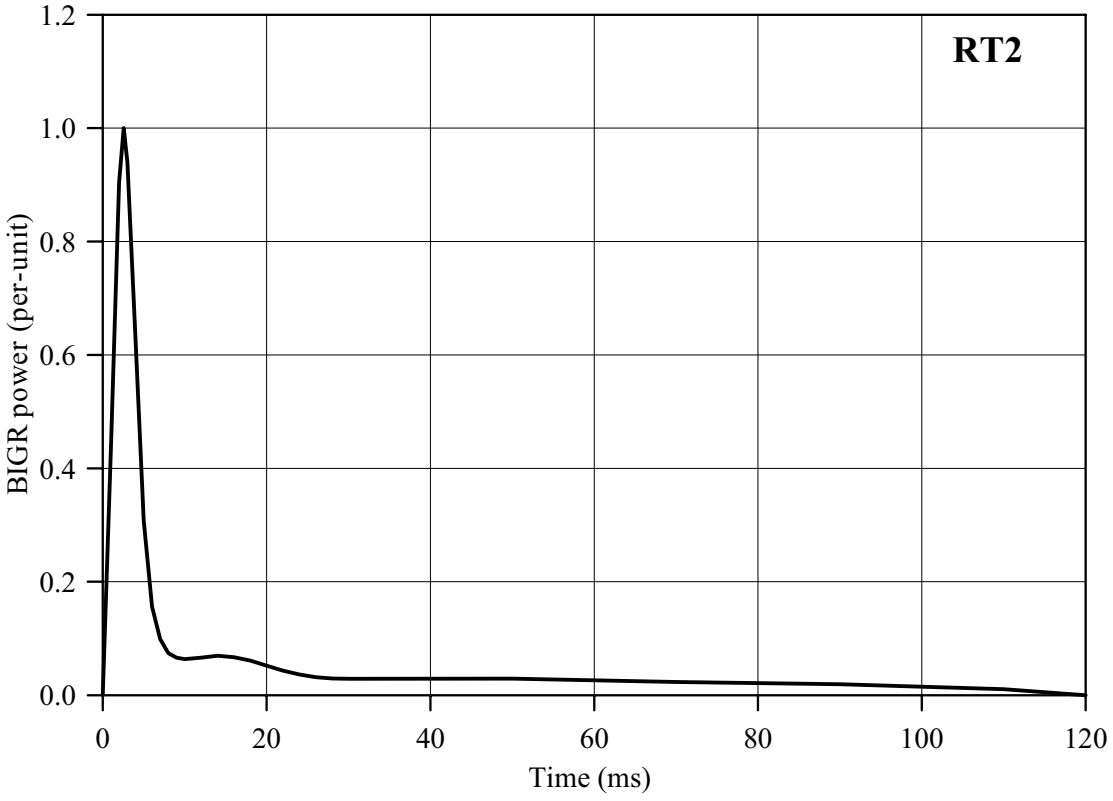
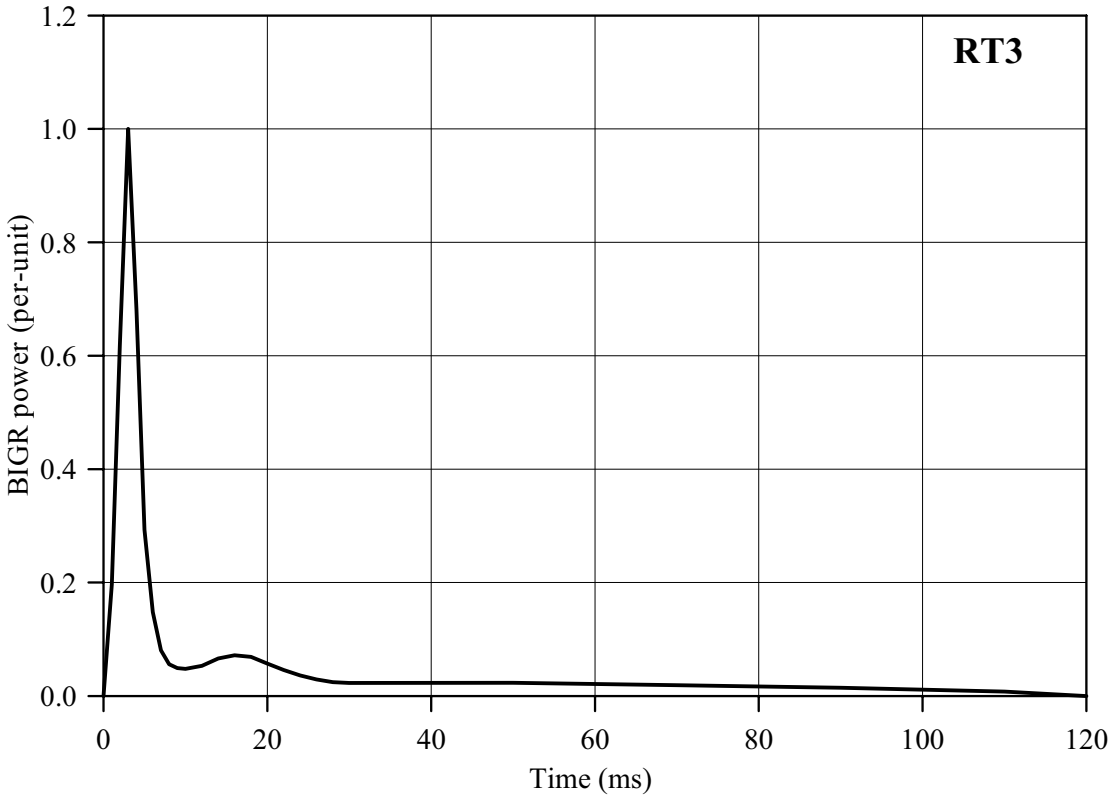


Fig. D.1. BIGR power for fuel rods # RT1 and # RT2



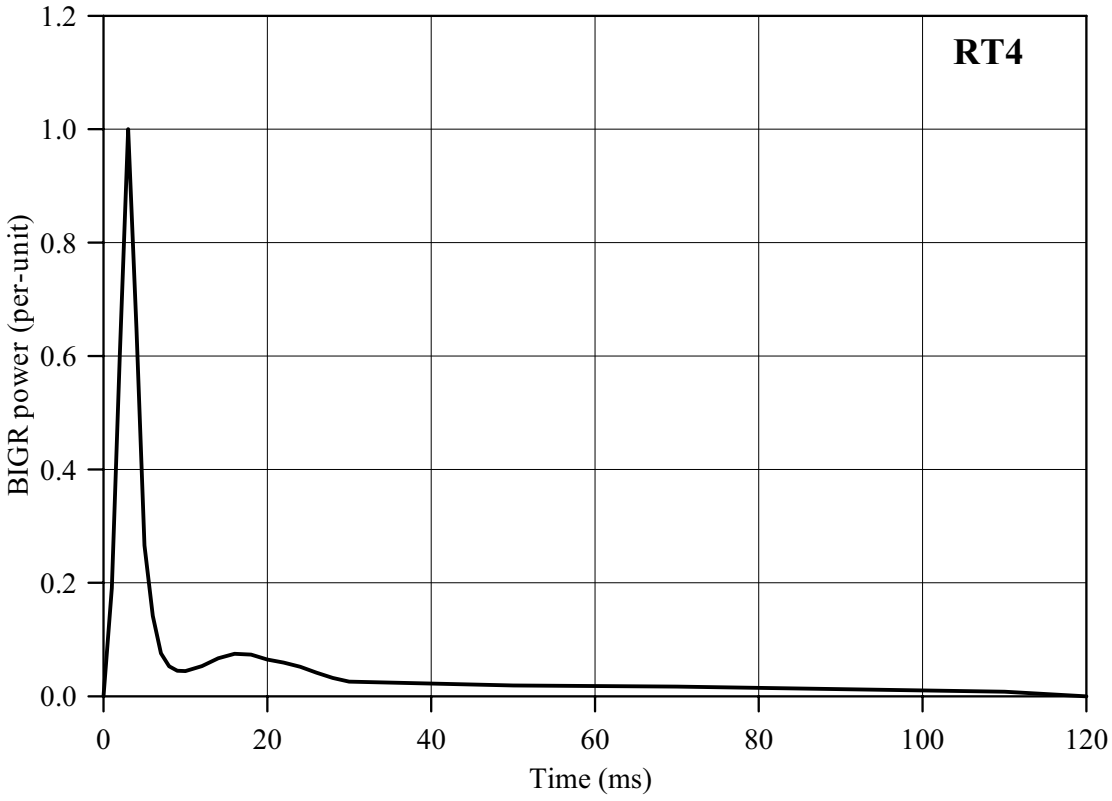
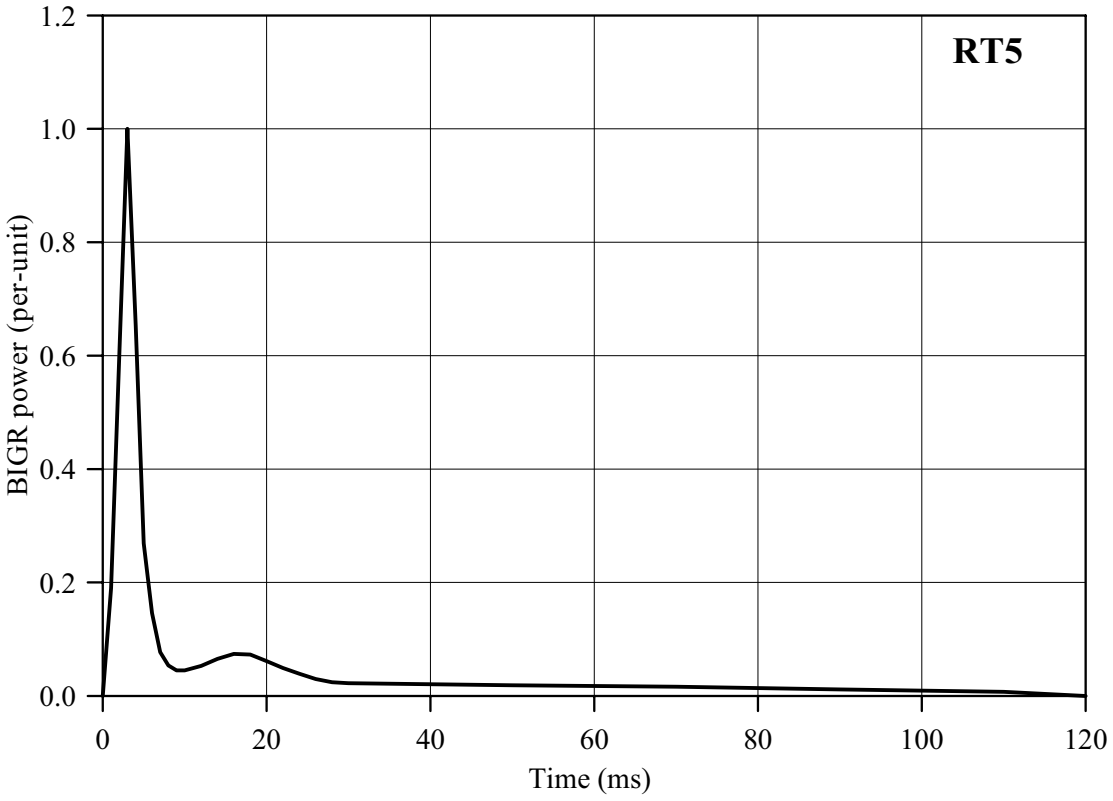


Fig. D.2. BIGR power for fuel rods # RT3 and # RT4



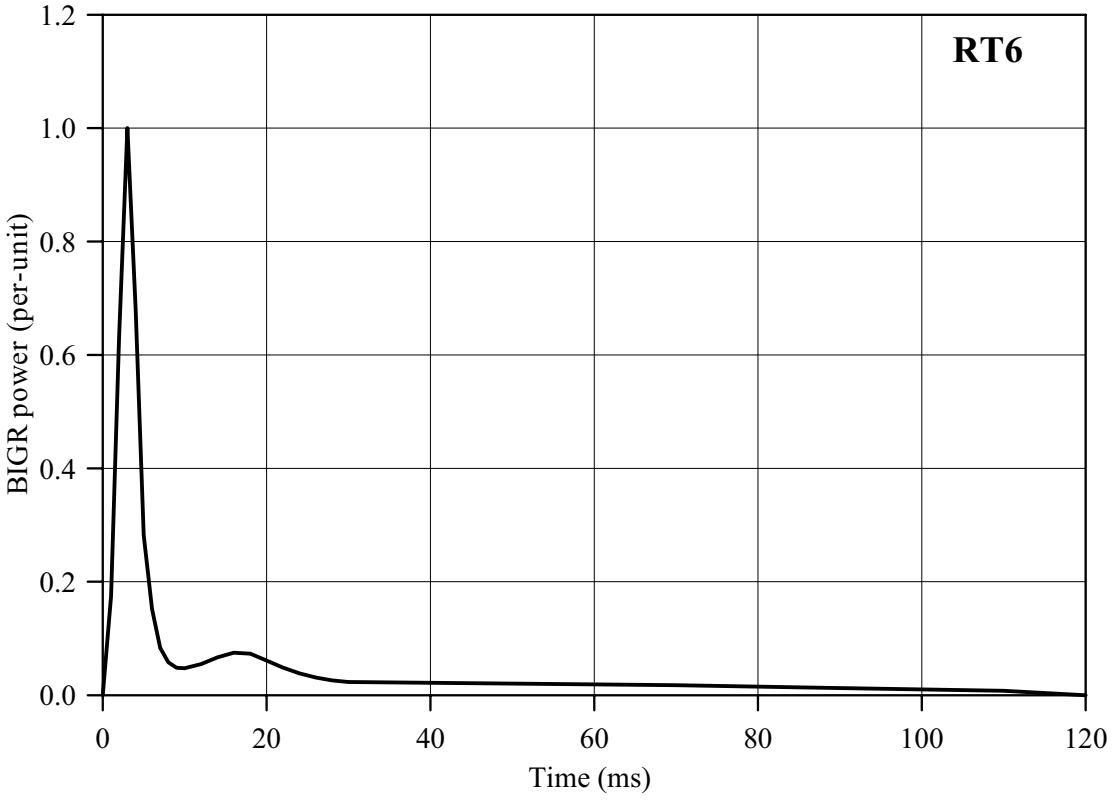
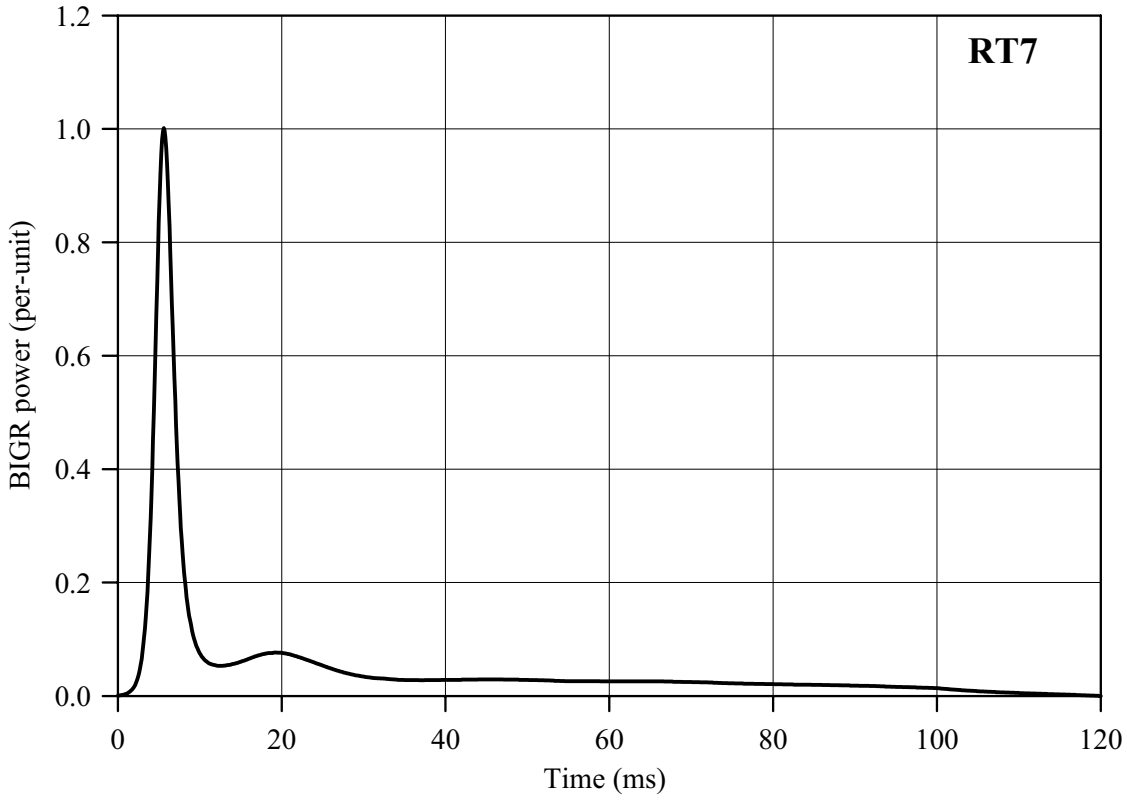


Fig. D.3. BIGR power for fuel rods # RT5 and # RT6



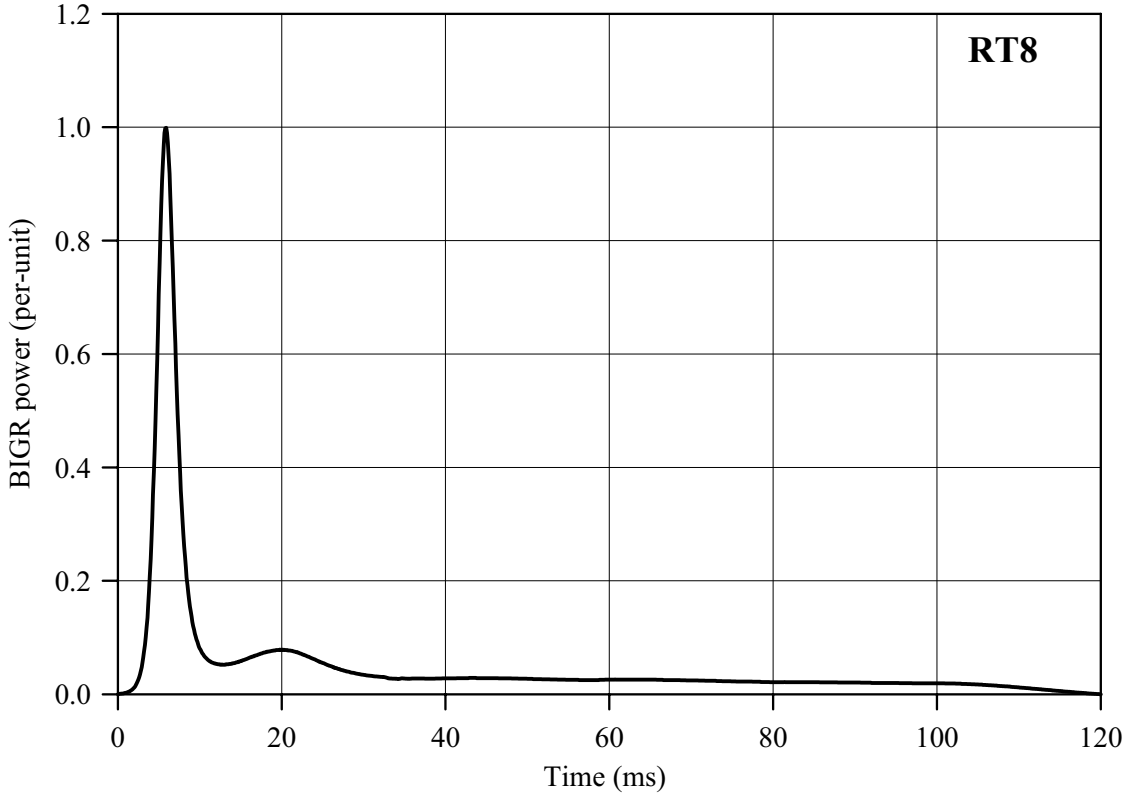
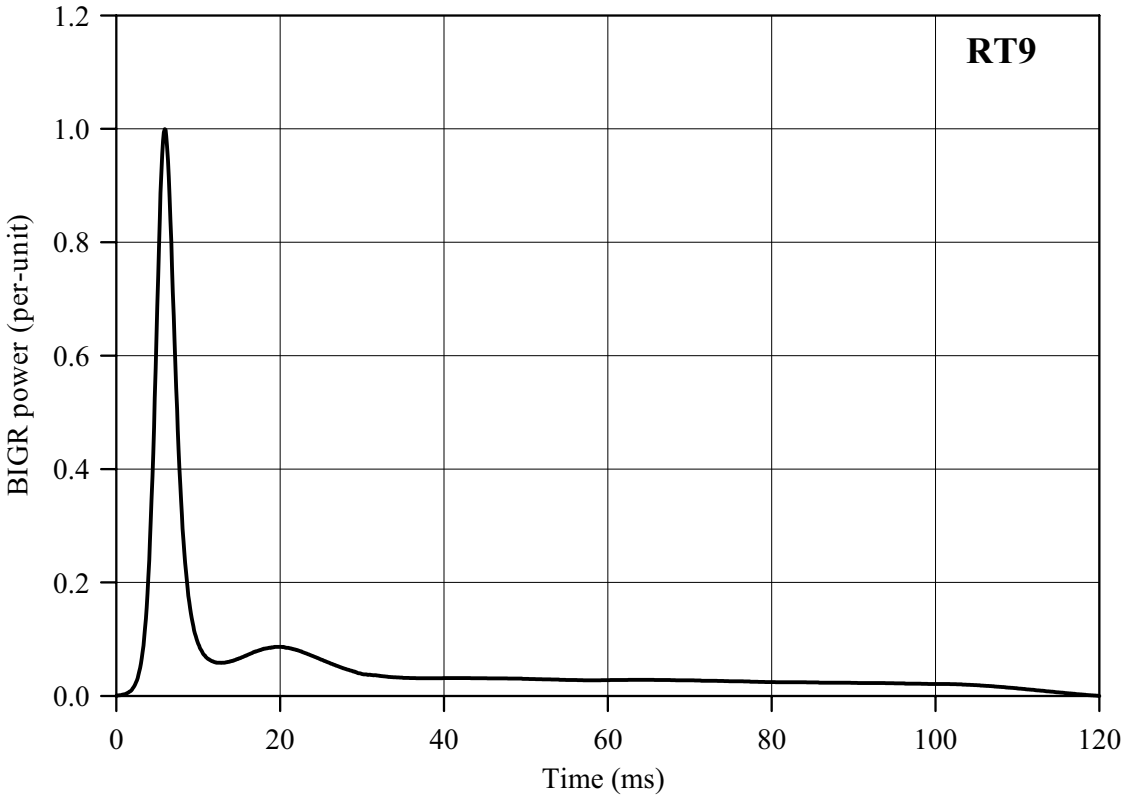


Fig. D.4. BIGR power for fuel rods # RT7 and # RT8



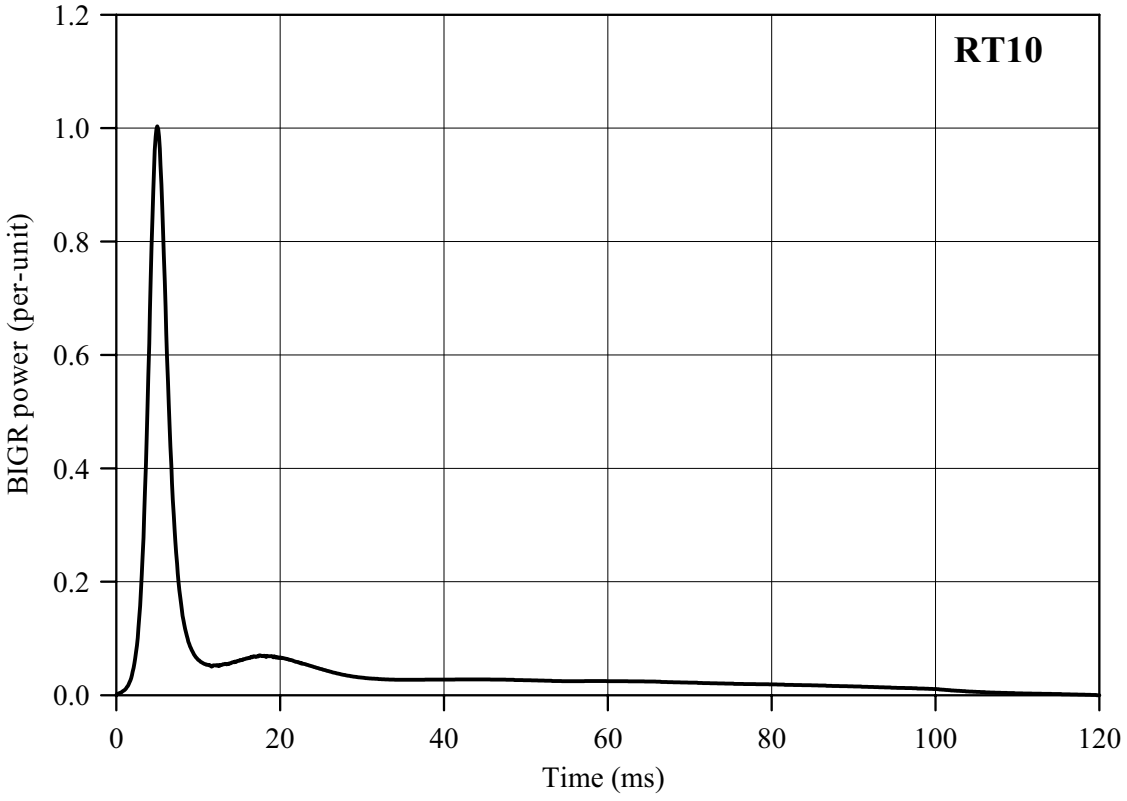
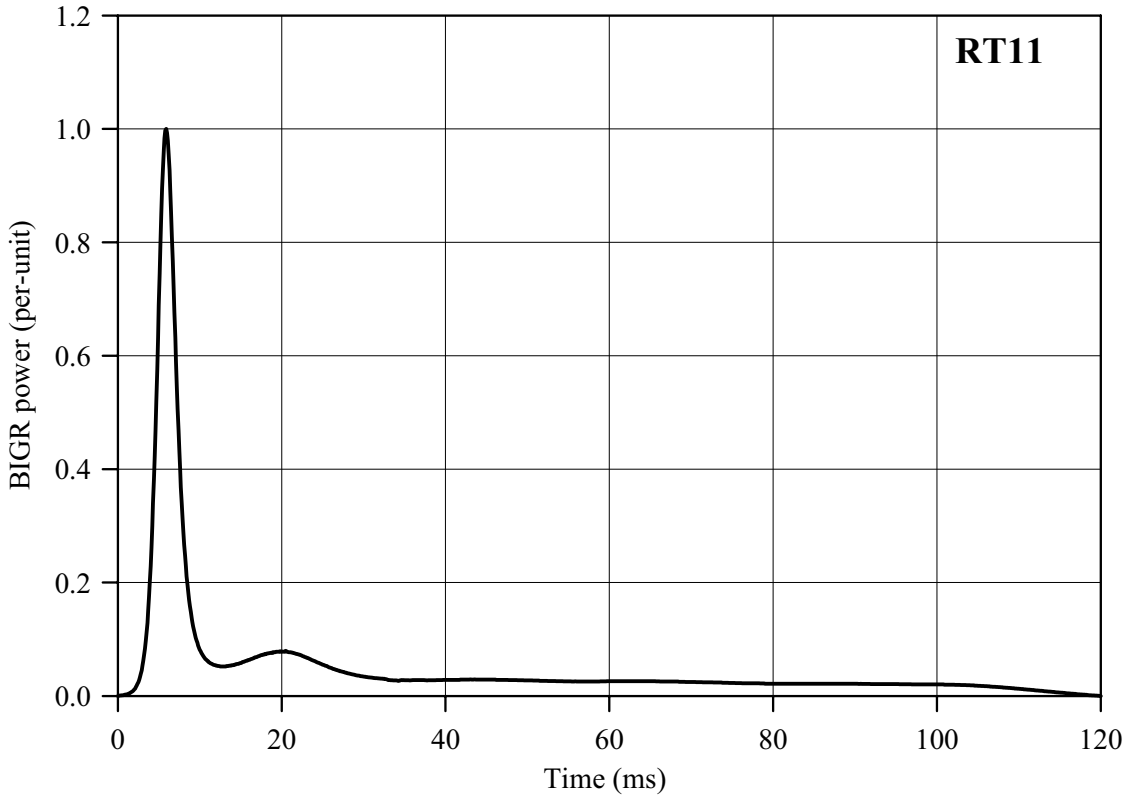


Fig. D.5. BIGR power for fuel rods # RT9 and # RT10



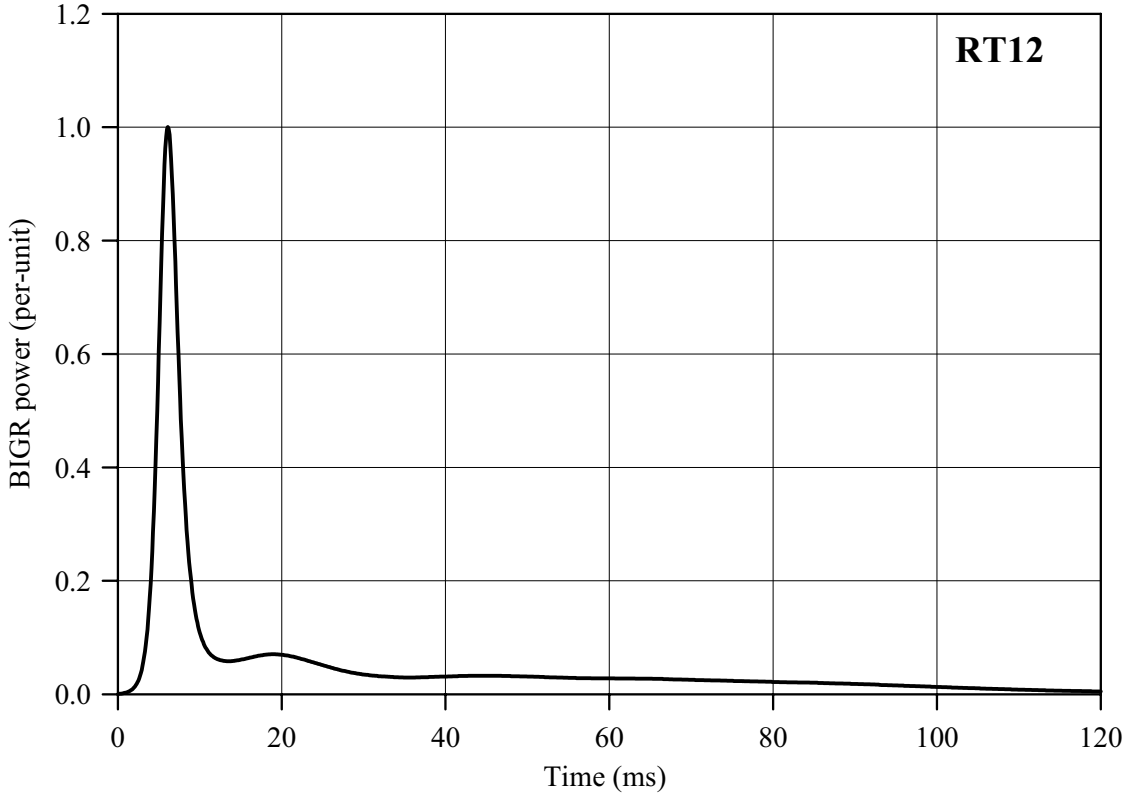


Fig. D.6. BIGR power for fuel rods # RT11 and # RT12

APPENDIX E

CHARACTERISTICS OF REFABRICATED FUEL RODS AFTER THE BIGR TESTS

Appendix E–1

Individual Characteristics of Fuel Rod # RT1 after the BIGR Test

RT1

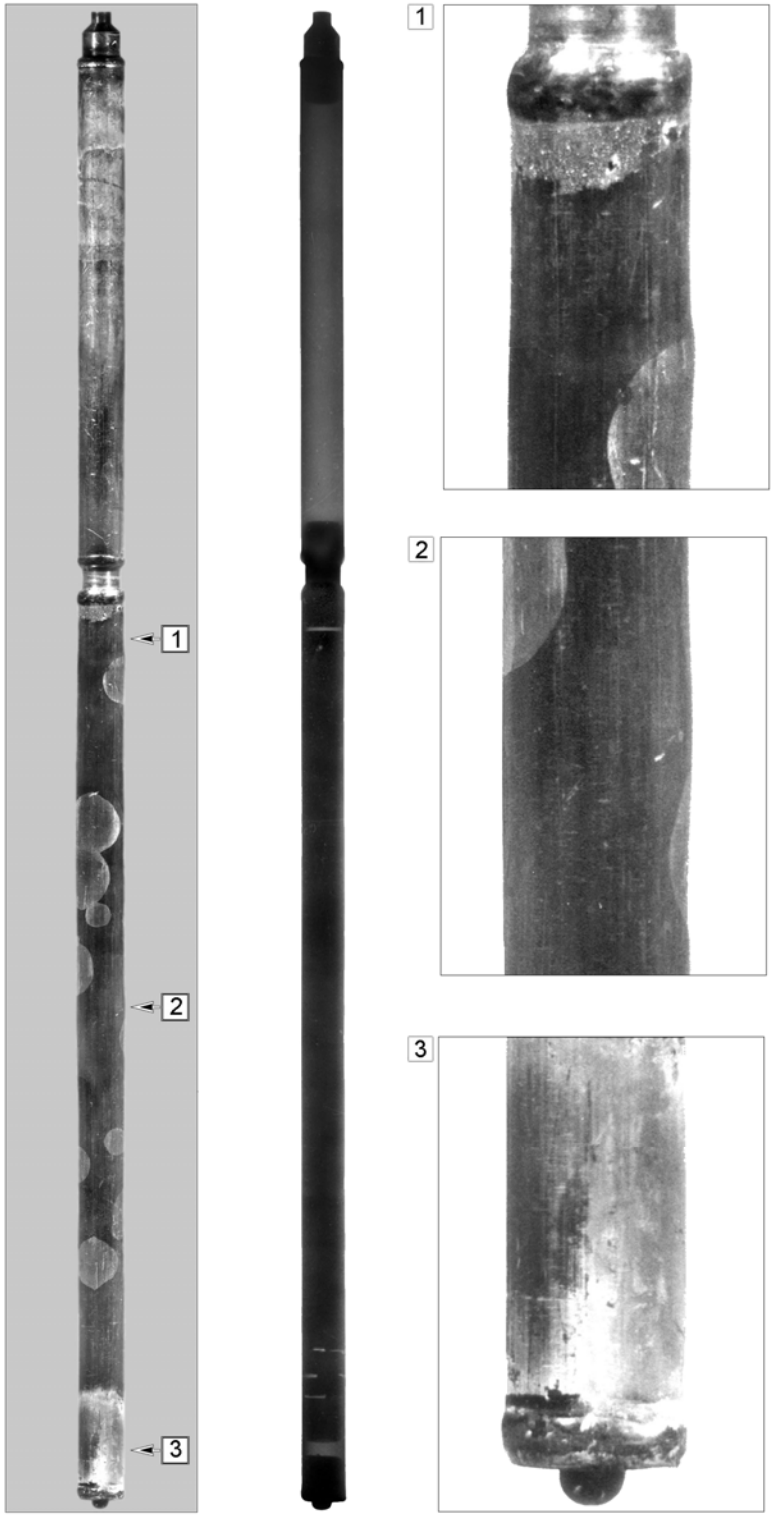


Fig.E-1.1. Appearance of unfailed fuel rod # RT1 after the BIGR test (photographs and X-ray photograph)

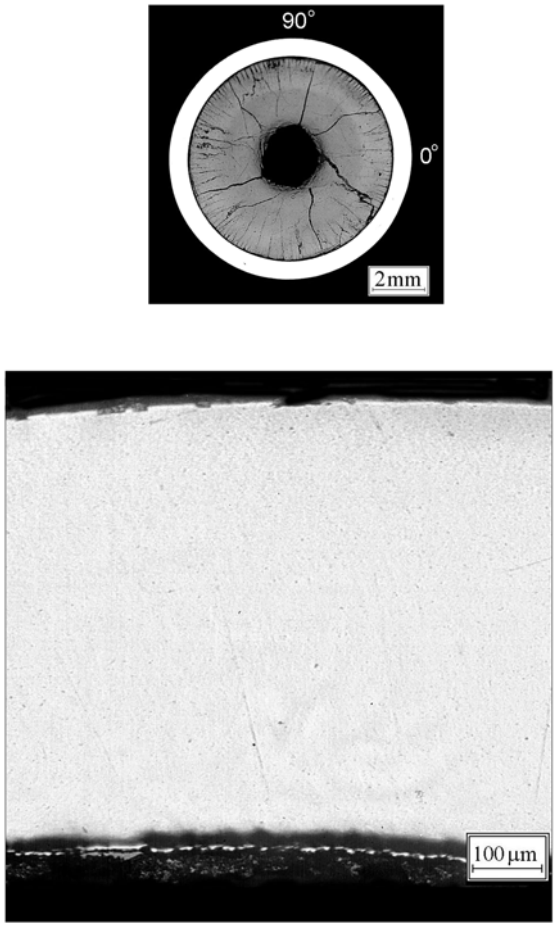


Fig.E-1.2. Cross-section and cladding microstructure of fuel rod # RT1 at 113 mm elevation (from low cap)

RT1

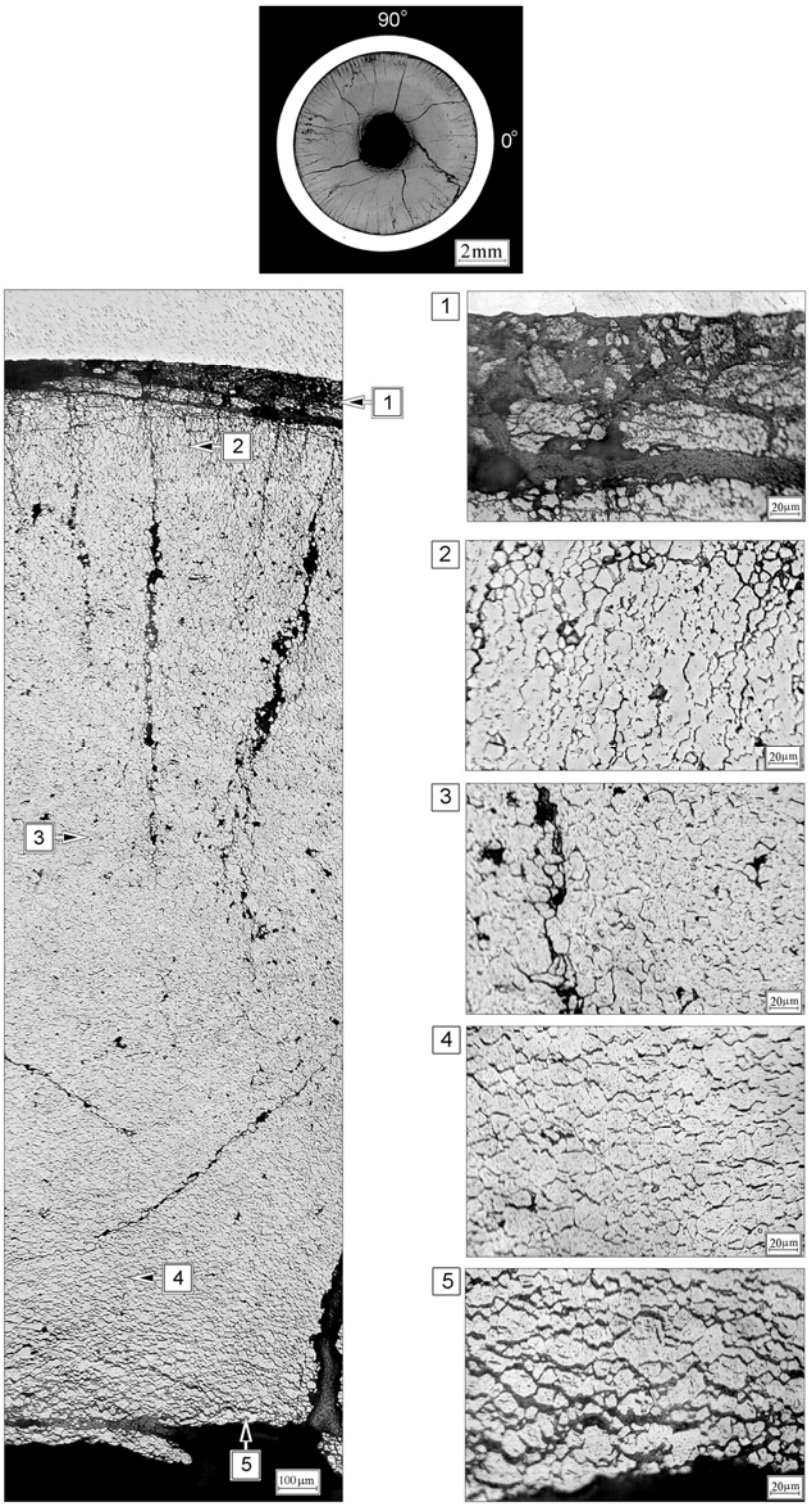


Fig.E-1.3. Cross-section and fuel microstructure of fuel rod # RT1 at 113 mm elevation (from low cap)

Table E-1.1. Time dependent energy characteristics of fuel rod # RT1

Time (s)	Relative reactor power (current/ maximum value) (per-unit)	Cumulative number of fissions in fuel rod (fiss) x10^{-14}	Power of fuel rod[1)2)] (kW)	Energy deposition		Fuel enthalpy[3)]	
				(cal/g fuel)	(J/g fuel)	FRAP-T6	RAPTA-5
0.000	0.00E+00	0.000	0.000	0.000	0.000	0.000	0.000
0.001	1.76E-01	0.240	1260	2.507	10.49	3.010	2.386
0.002	5.73E-01	1.166	4095	12.13	50.79	13.201	12.045
0.003	9.88E-01	3.301	7069	34.44	144.2	35.610	34.383
0.004	7.32E-01	5.690	5233	59.33	248.4	60.455	59.119
0.005	3.19E-01	7.017	2281	73.16	306.3	74.106	72.559
0.006	1.65E-01	7.630	1181	79.57	333.1	80.313	78.541
0.007	8.90E-02	7.949	636.8	82.88	347.0	83.360	81.459
0.008	5.88E-02	8.138	420.7	84.84	355.2	85.045	83.077
0.009	5.24E-02	8.284	374.5	86.33	361.4	86.262	84.264
0.010	5.00E-02	8.416	357.7	87.72	367.3	87.385	85.379
0.012	5.93E-02	8.691	424.0	90.65	379.5	89.796	87.862
0.014	7.33E-02	9.037	524.4	94.22	394.5	92.851	90.944
0.016	8.05E-02	9.446	575.8	98.50	412.4	96.592	94.697
0.018	7.95E-02	9.869	568.9	102.9	430.8	100.483	98.676
0.020	6.85E-02	10.26	490.0	107.0	447.9	104.037	102.320
0.022	5.38E-02	10.58	384.7	110.3	461.9	106.885	105.220
0.024	4.21E-02	10.83	301.4	112.9	472.9	109.026	107.410
0.026	3.29E-02	11.03	235.3	115.0	481.4	110.633	109.200
0.028	2.76E-02	11.18	197.8	116.6	488.1	111.865	110.410
0.030	2.55E-02	11.32	182.3	118.0	494.2	112.927	111.370
0.050	2.33E-02	12.59	166.4	131.3	549.7	122.572	121.330
0.070	1.84E-02	13.68	131.8	142.7	597.5	130.730	129.710
0.090	1.43E-02	14.54	102.6	151.6	634.7	136.829	135.920
0.110	9.12E-03	15.17	65.43	158.2	662.5	141.113	140.300
0.130	3.38E-03	15.48	24.39	161.4	675.7	142.614	141.550
0.150	1.29E-03	15.59	9.439	162.6	680.7	142.832	141.070
0.200	3.45E-04	15.68	2.730	163.6	684.8	141.257	138.770
1.000	3.11E-05	15.81	0.341	165.4	692.3	121.068	117.990
10.00	3.60E-06	16.04	0.050	169.5	709.7	29.703	27.267
100.0	7.01E-08	16.15	0.008	172.5	722.4	5.033	4.508
1000	2.74E-13	16.16	1.73E-04	174.0	728.5	0.000	0.000

[1)] Average values determined in accordance with results of RRC KI and VNIIEF calculations

[2)] Maximum power value is 7152.5 kW (t=0.0032 s)

[3)] Average radial value

RT1

Table E-1.2. Radial energy characteristics of fuel rod # RT1*

Parameters	Coordinates of fuel radial layers (mm)			
	1 layer (1.23-2.82)	2 layer (2.82-3.44)	3 layer (3.44-3.71)	4 layer (3.71-3.795)
Number of fissions $x10^{-14}$ (fiss)	7.266	4.700	2.829	1.364
Fission density $x10^{-13}$ (fiss/g fuel)	2.292	2.431	2.997	4.417
Power** (kW)	3173	2086	1264	629.7
Energy deposition (cal/g fuel)	156.6	166.5	205.1	303.3
Energy deposition (J/g fuel)	655.8	697.3	858.9	1270
Energy deposition*** (per-unit)	0.517	0.550	0.677	1.000

* Average values were determined in accordance with results of RRC KI and VNIIEF calculations

** The power for the entire length of each layer at time 0.0032 s

*** Energy deposition in current layer/energy deposition in 4^{th} layer

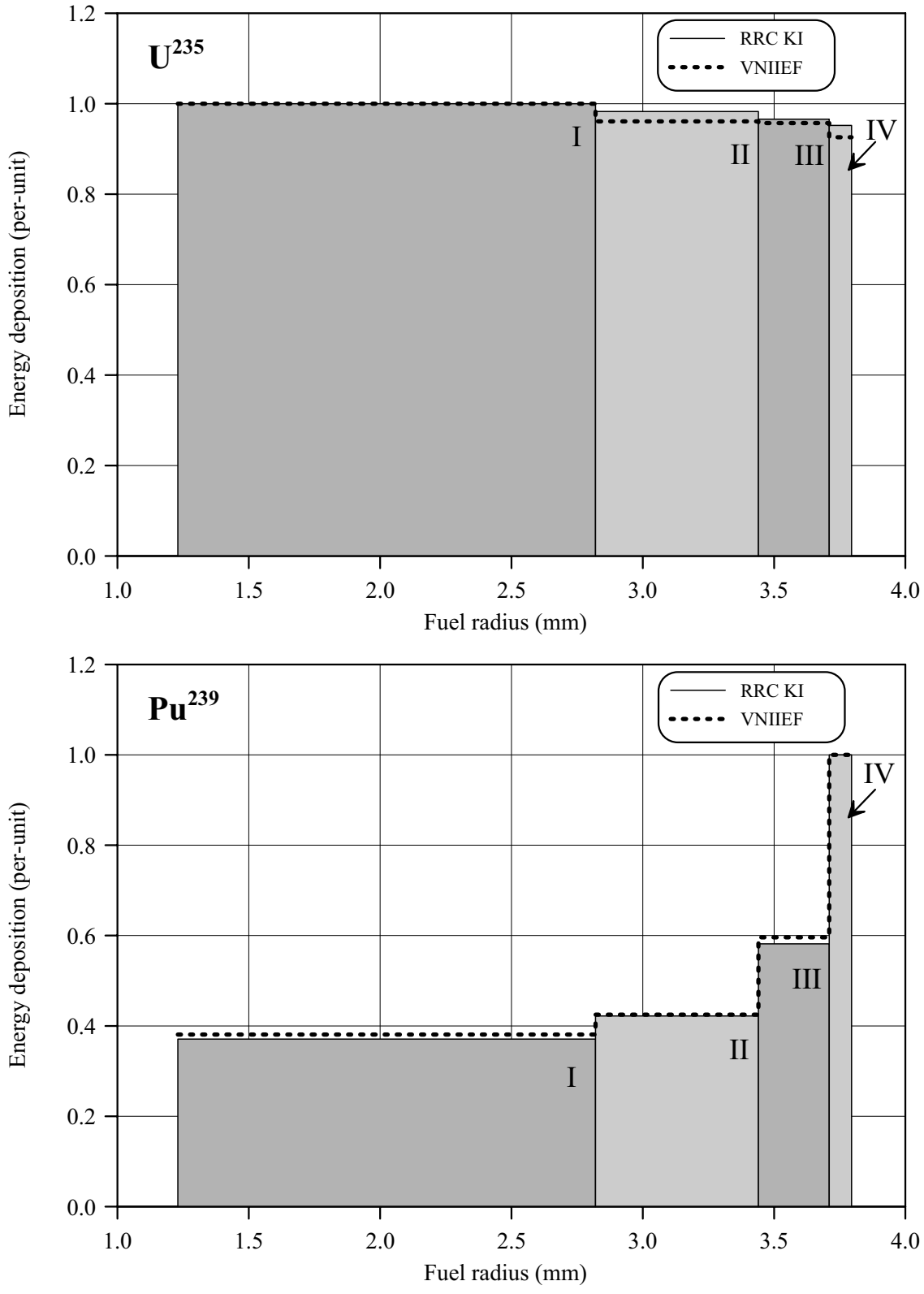
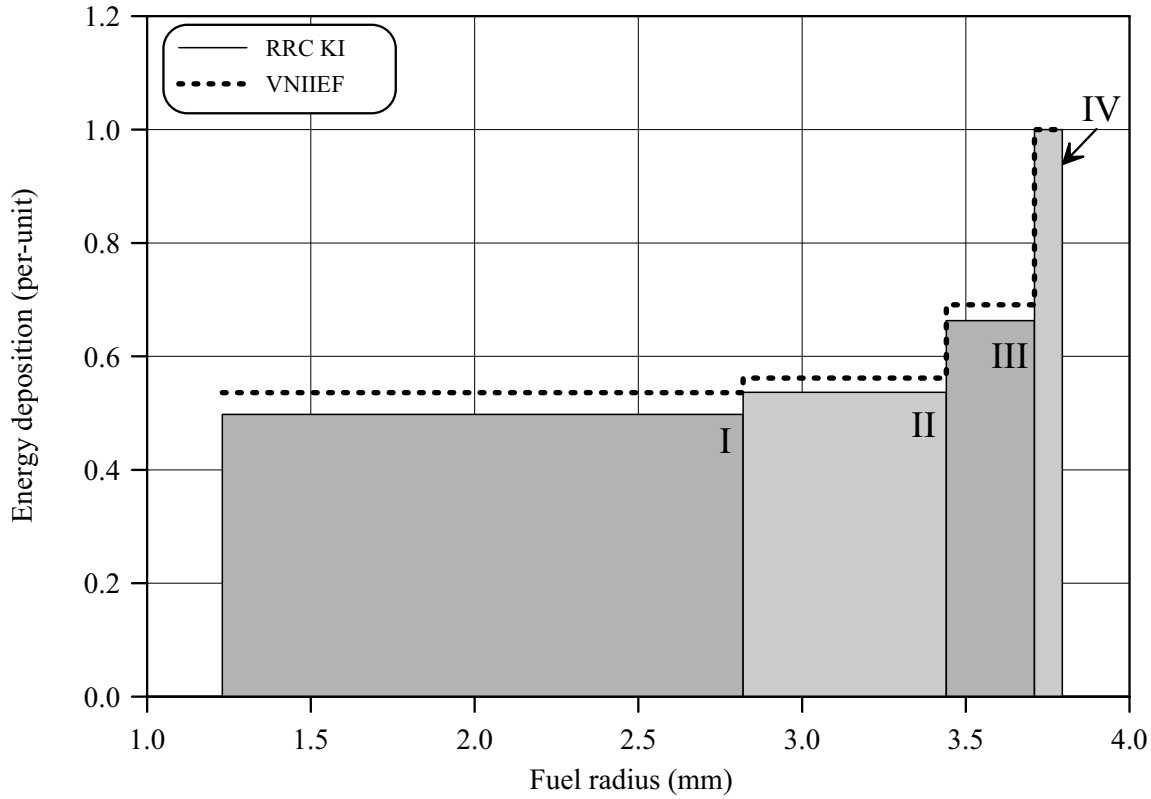


Fig.E-1.4. U^{235} and Pu^{239} radial distribution of energy deposition for fuel rod # RT1

RT1



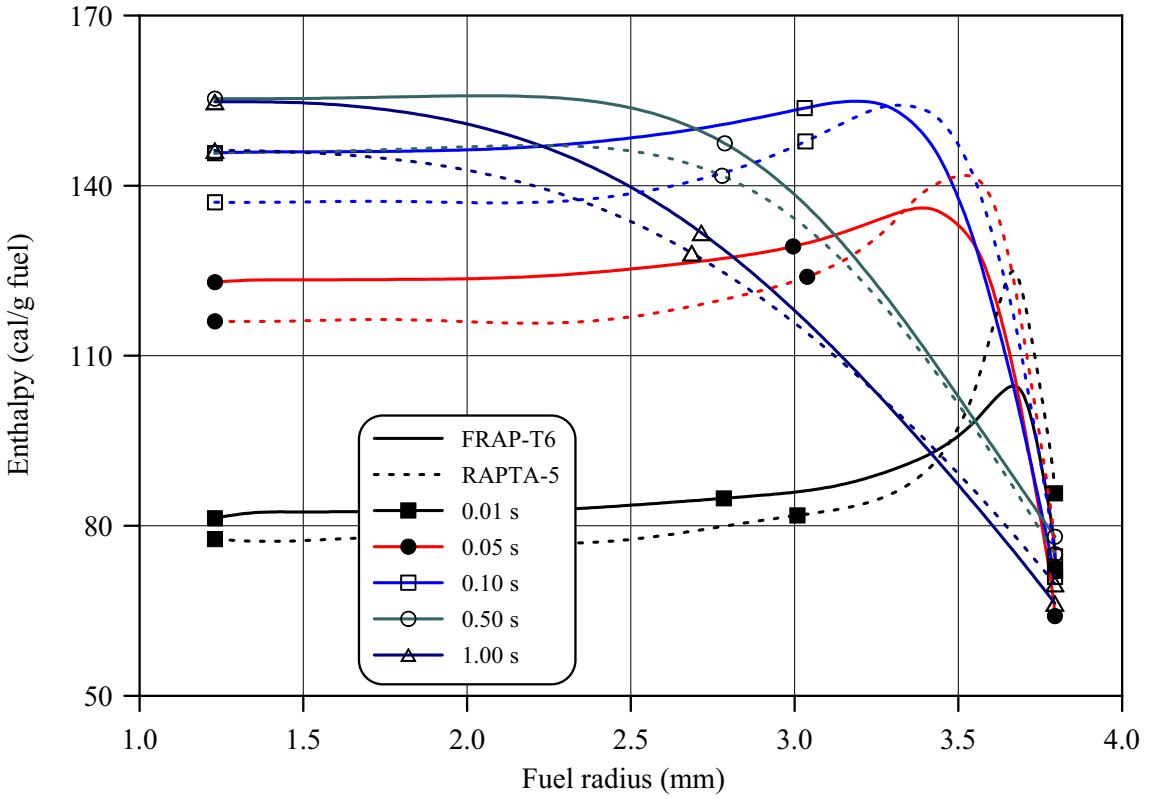


Fig.E-1.5. Radial distribution of energy deposition and fuel enthalpy for fuel rod # RT1

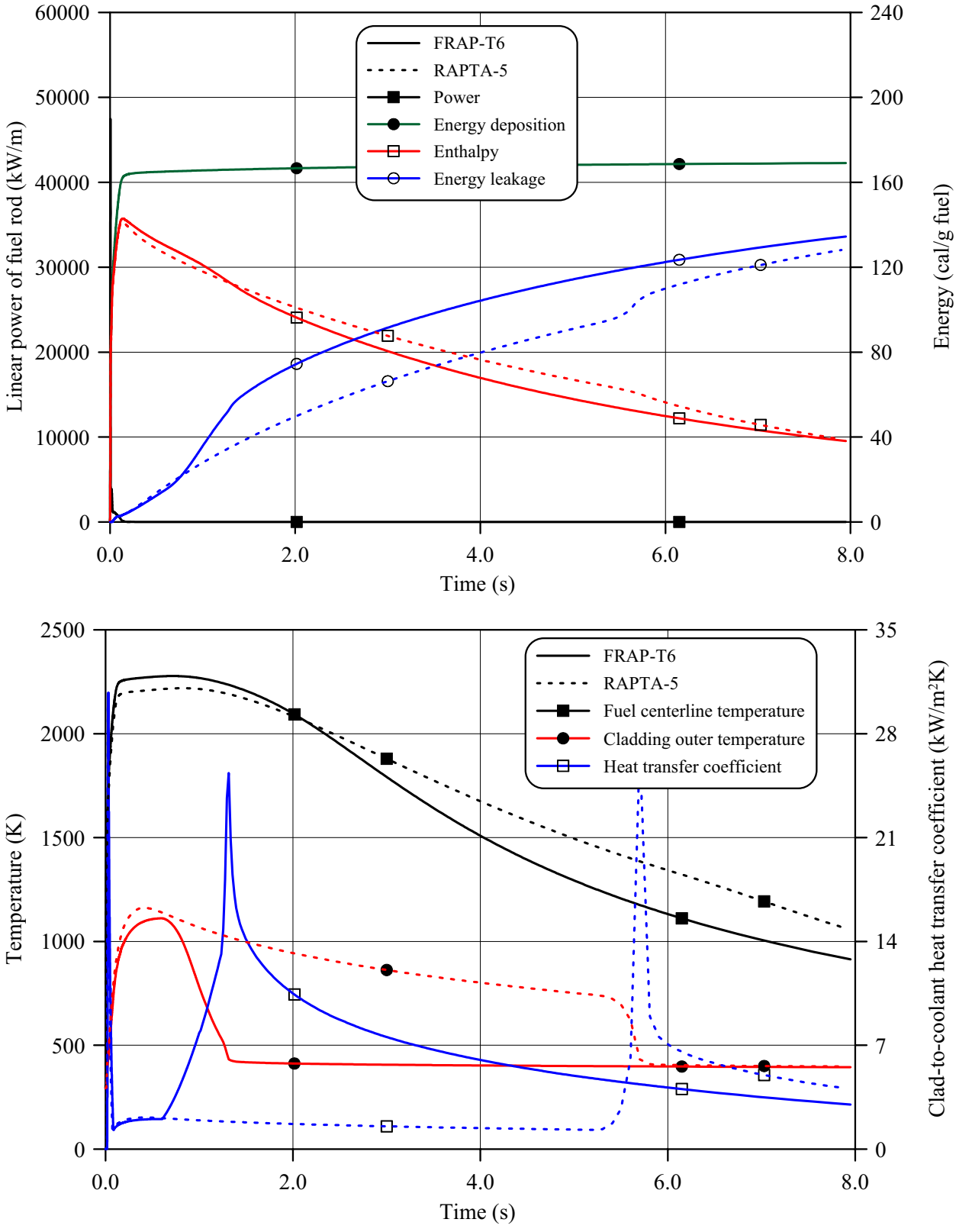


Fig.E-1.6. Thermal history of fuel rod # RT1 during the BIGR test in accordance with FRAP-T6/VVER and RAPTA-5 calculations

RT1

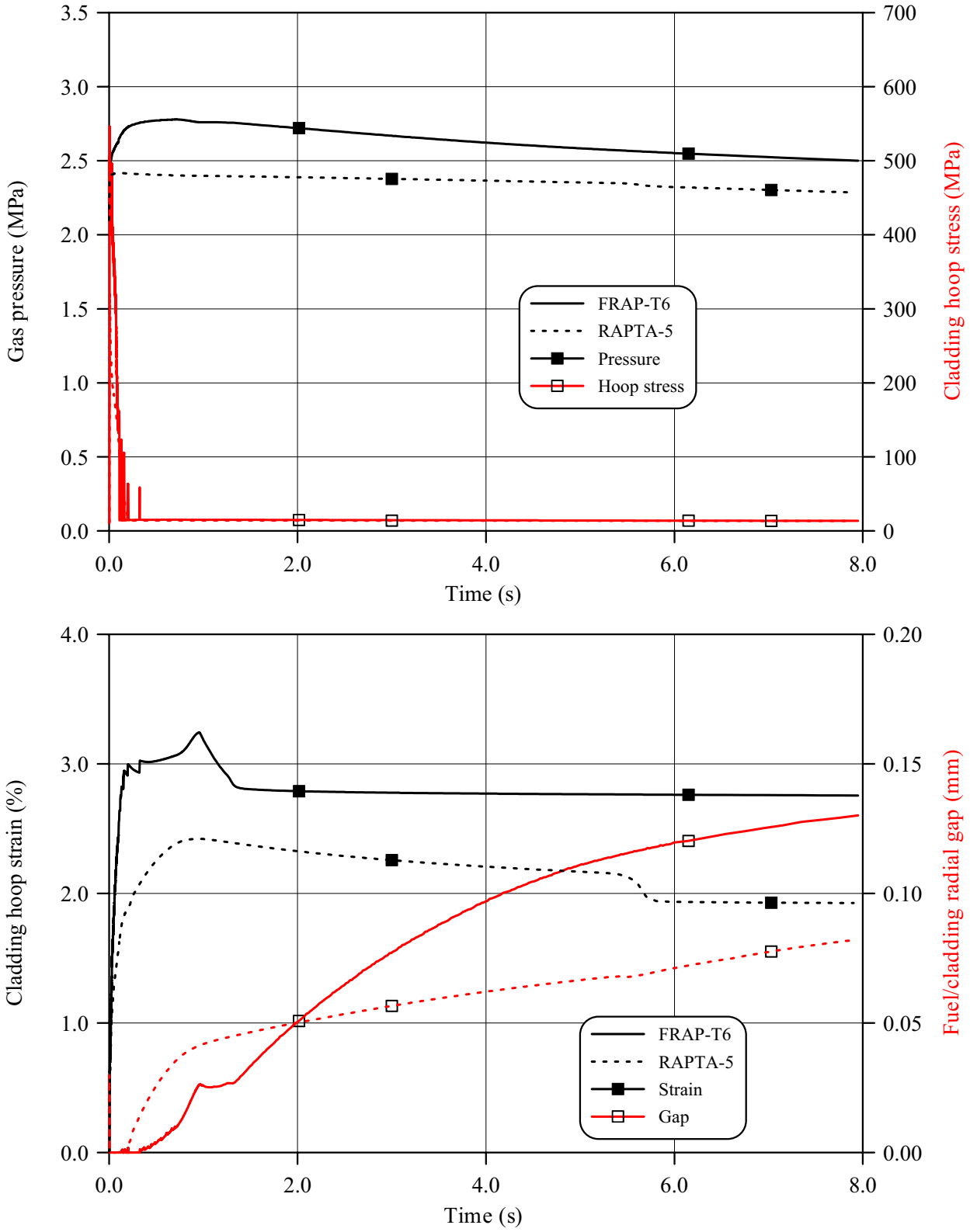


Fig.E-1.7. Mechanical behavior of fuel rod # RT1 during the BIGR test in accordance with FRAP-T6/VVER and RAPTA-5 calculations

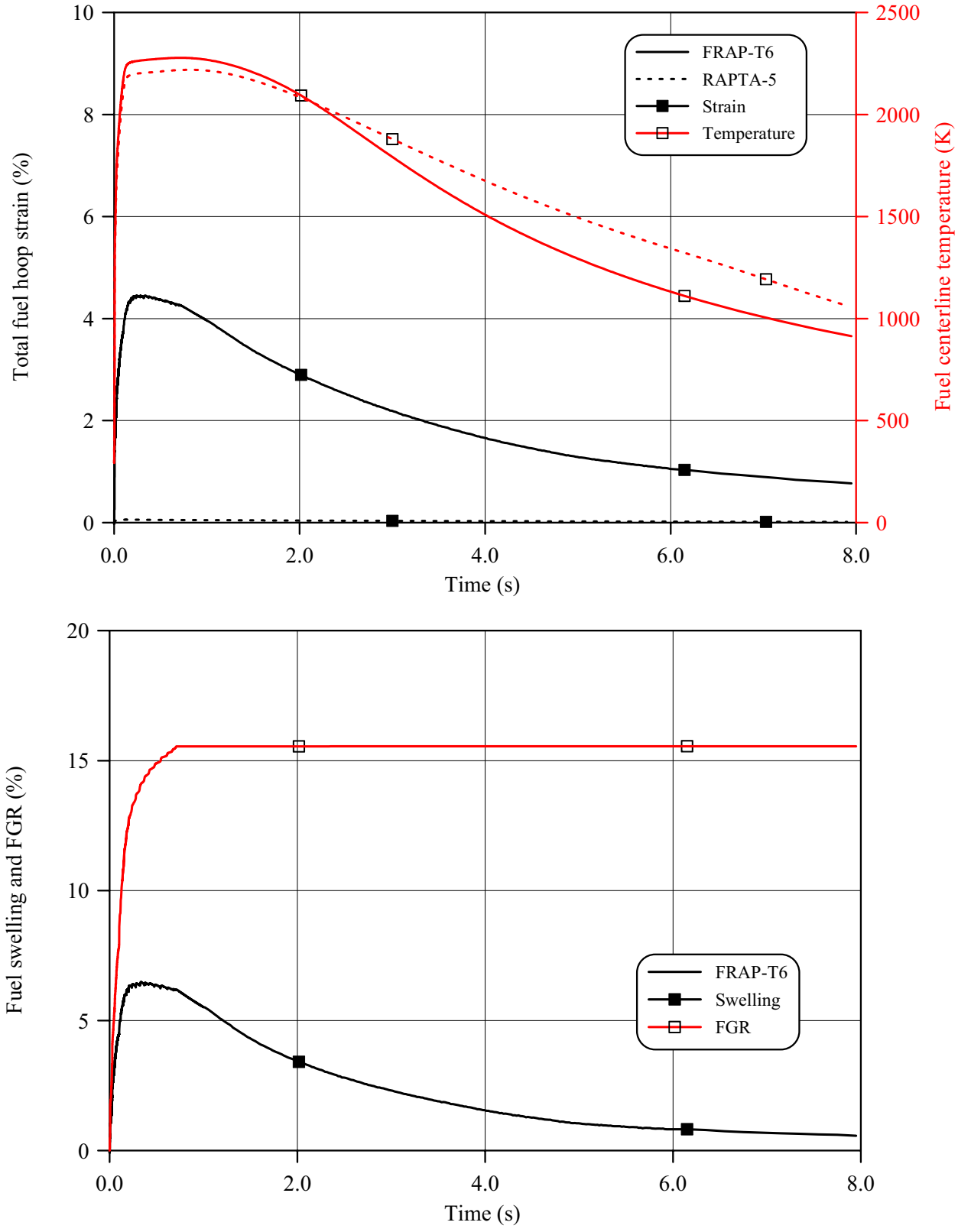


Fig.E-1.8. Fuel behavior during the BIGR test of fuel rod # RT1 in accordance with FRAP-T6/VVER and RAPTA-5 calculations

RT1

Table E-1.3. Axial distribution of cladding average outer diameter in fuel rod # RT1*

Axial coordinate (mm)	Cladding diameter (mm)	Axial coordinate (mm)	Cladding diameter (mm)	Axial coordinate (mm)	Cladding diameter (mm)	Axial coordinate (mm)	Cladding diameter (mm)
30	9.200	68	9.238	106	9.248	144	9.336
32	9.197	70	9.250	108	9.265	146	9.293
34	9.213	72	9.252	110	9.248	148	9.228
36	9.226	74	9.263	112	9.220	150	9.237
38	9.239	76	9.264	114	9.198	152	9.294
40	9.235	78	9.249	116	9.245	154	9.354
42	9.214	80	9.257	118	9.304	156	9.360
44	9.203	82	9.266	120	9.344	158	9.303
46	9.220	84	9.283	122	9.308	160	9.246
48	9.227	86	9.310	124	9.244	162	9.277
50	9.235	88	9.321	126	9.221	164	9.349
52	9.226	90	9.309	128	9.268	166	9.426
54	9.184	92	9.315	130	9.310	168	9.338
56	9.160	94	9.321	132	9.325	170	9.181
58	9.168	96	9.352	134	9.312	172	9.097
60	9.185	98	9.358	136	9.289	174	9.065
62	9.211	100	9.299	138	9.306	176	9.075
64	9.236	102	9.219	140	9.340	178	9.073
66	9.235	104	9.217	142	9.346	180	9.315

* Measured value determined on the basis of profilometry data (16 azimuthal directions)

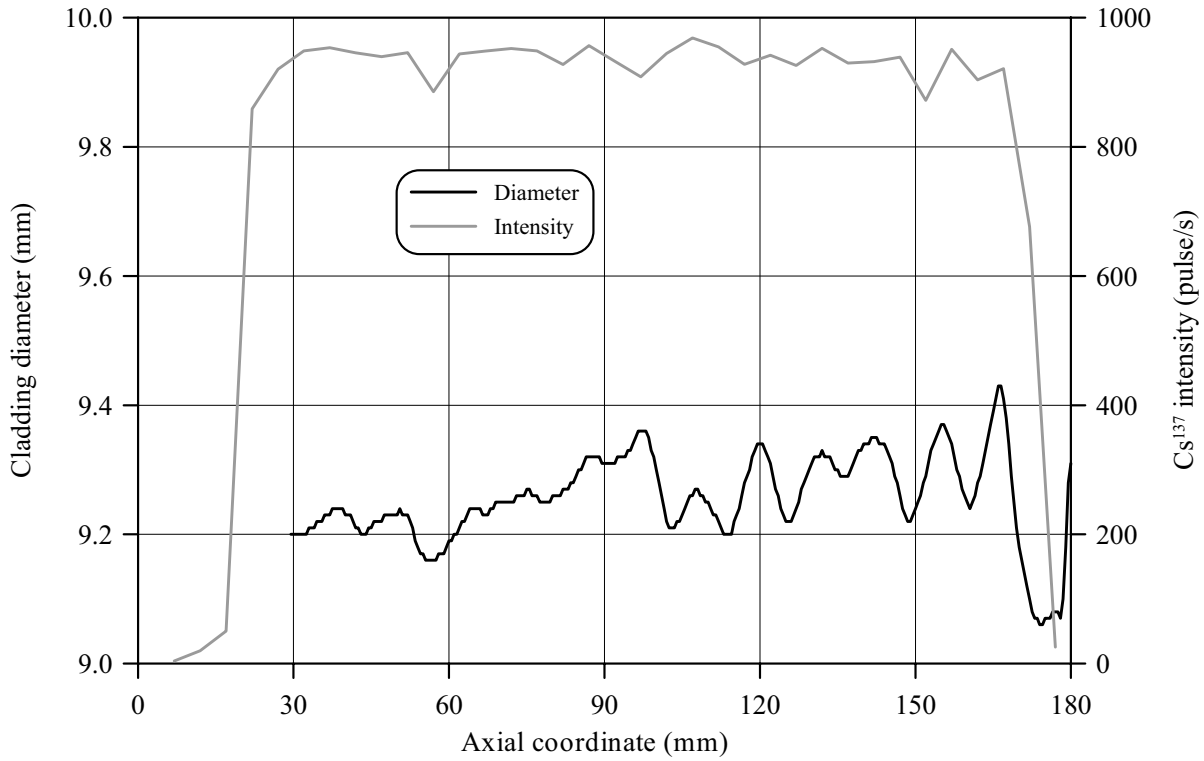


Fig.E-1.9. Cladding measured average diameter and γ-scanning results for fuel rod # RT1

Table E-1.4. The PIE results for fuel rod # RT1

	Parameter	Value
1.	Cladding outer diameter (mm):	
1.1.	Maximum diameter of the bidimensional data sample in "fuel rod length - azimuthal angle" coordinates (mm)	9.50
1.2.	Averaged azimuthal diameter and maximum diameter along the length selected from the sample of averaged azimuthal diameter (mm)	9.43
1.3.	Averaged diameter of the bidimensional data sample in "fuel rod length - azimuthal angle" coordinates (mm)	9.26
2.	Cladding maximum residual hoop strain (%)	4.06
3.	Fuel pellet conditional diameter (mm) in cross-section*:	
	at 113 mm elevation	7.64
4.	ZrO_2 outer thickness (μm) in cross-section:	
	at 113 mm elevation	3–5
5.	ZrO_2 inner thickness (μm) in cross-section:	
	at 113 mm elevation	0
6.	Parameters characterizing FGR:	
6.1.	Gas composition (% by volume):	
	He	86.08
	N_2	0.70
	O_2	0.13
	Ar	0.014
	CO_2	0.011
	Kr	1.19
	Xe	11.88
6.2.	Free gas volume (cm^3)	6.5
6.3.	Gas volume under normal conditions (cm^3)	142.3
6.4.	Gas pressure under normal conditions (MPa)	2.19
6.5.	FGR (%)	22.8

* Reference value determined by the processing of fuel cross-section photographs

RT1

Table E-1.5. Organized BIGR test results for fuel rod # RT1

Parameter		Unit	Value		
			Measured	Calculated	
				FRAP-T6	RAPTA-5
1.	Fuel burnup	MW d/kg U	48.3	48.3	48.3
2.	Initial gas pressure	MPa	2.1	2.1	2.1
3.	Energy deposition	cal/g fuel	174.0	174.0	174.0
4.	Peak fuel enthalpy*	cal/g fuel	-	142.9	141.6
5.	Fuel maximum temperature	K	-	2313	2327
6.	Maximum temperature of cladding outer surface	K	-	1111	1162
7.	Cladding burst	Failed, Unfailed	Unfailed	Unfailed	Unfailed
8.	Cladding residual hoop strain**	%	2.20	2.66	1.86
9.	Kr volume content in gas composition after the BIGR test	%	1.19	1.67	-
10.	Xe volume content in gas composition after the BIGR test	%	11.88	10.00	-

* Average value of peak fuel enthalpy is 142.2 cal/g fuel

** Average value along the fuel stack length

Appendix E–2

Individual Characteristics of Fuel Rod # RT2

after the BIGR Test

RT2

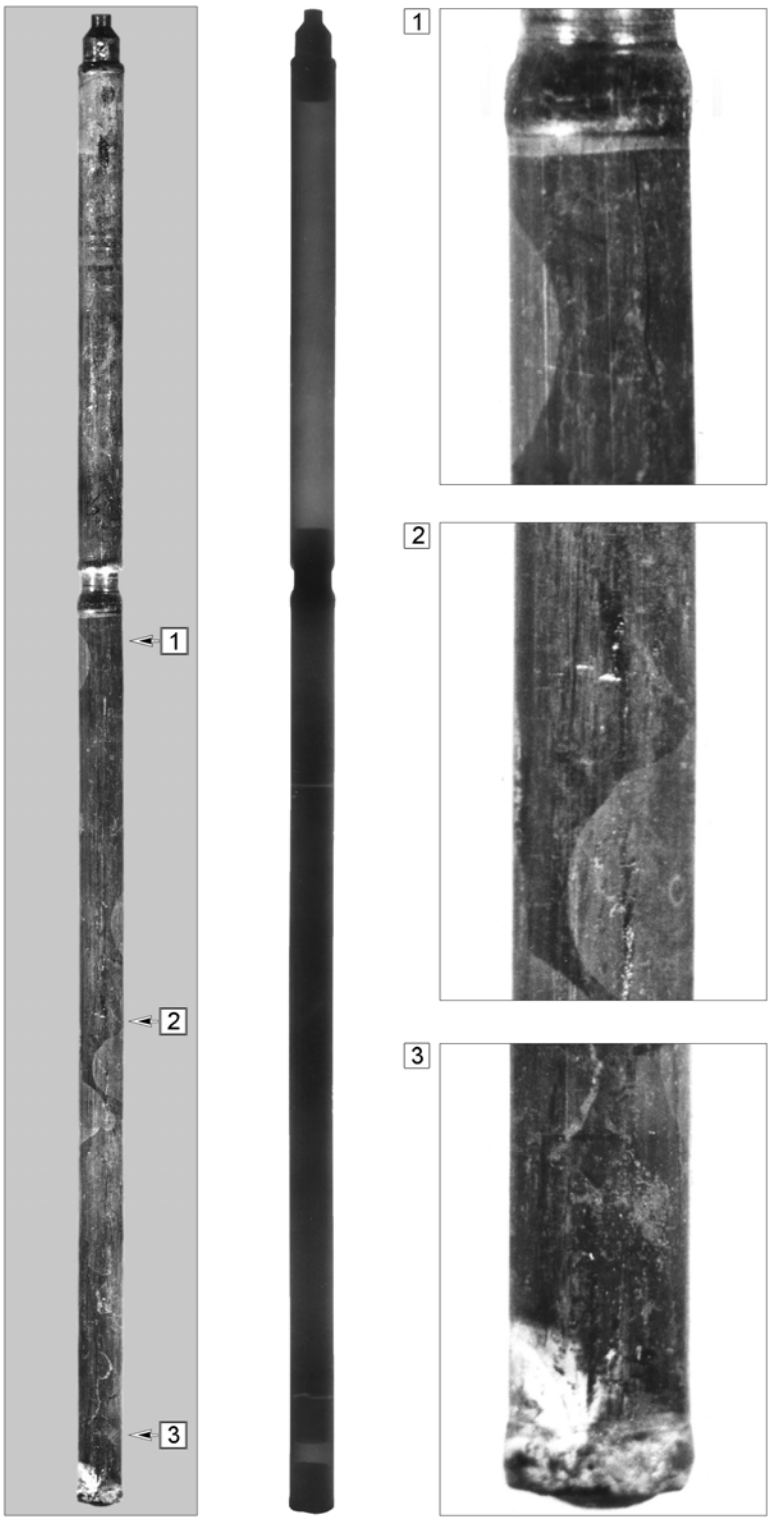


Fig.E-2.1. Appearance of unfailed fuel rod # RT2 after the BIGR test (photographs and X-ray photograph)

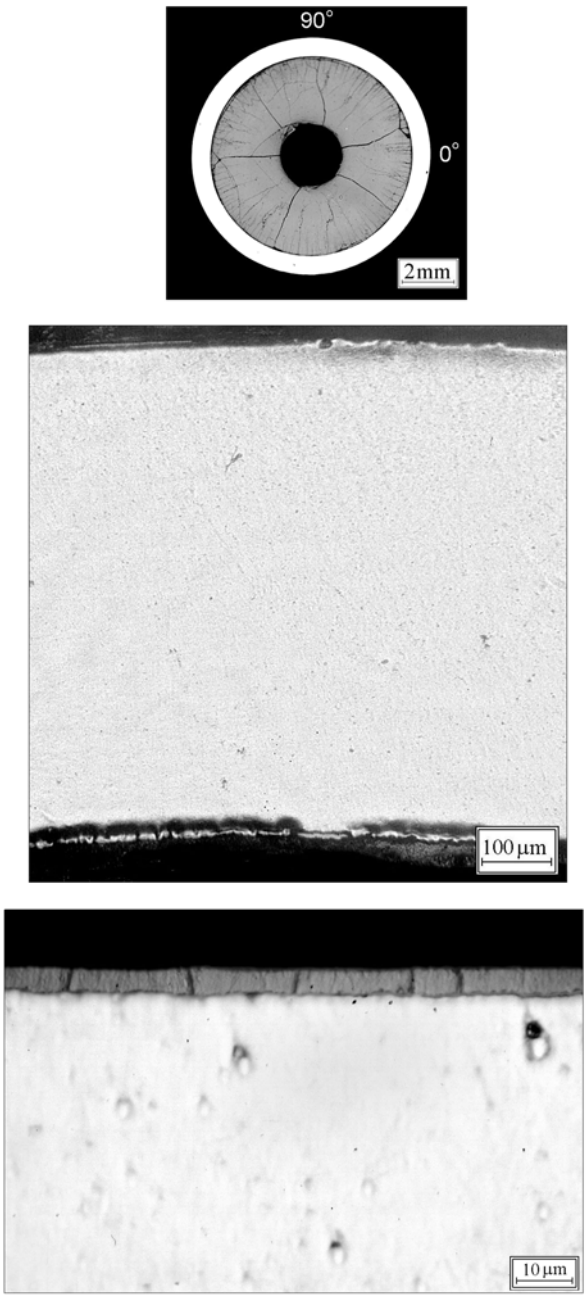


Fig.E-2.2. Cross-section and cladding microstructure of fuel rod # RT2 at 99 mm elevation (from low cap)

RT2

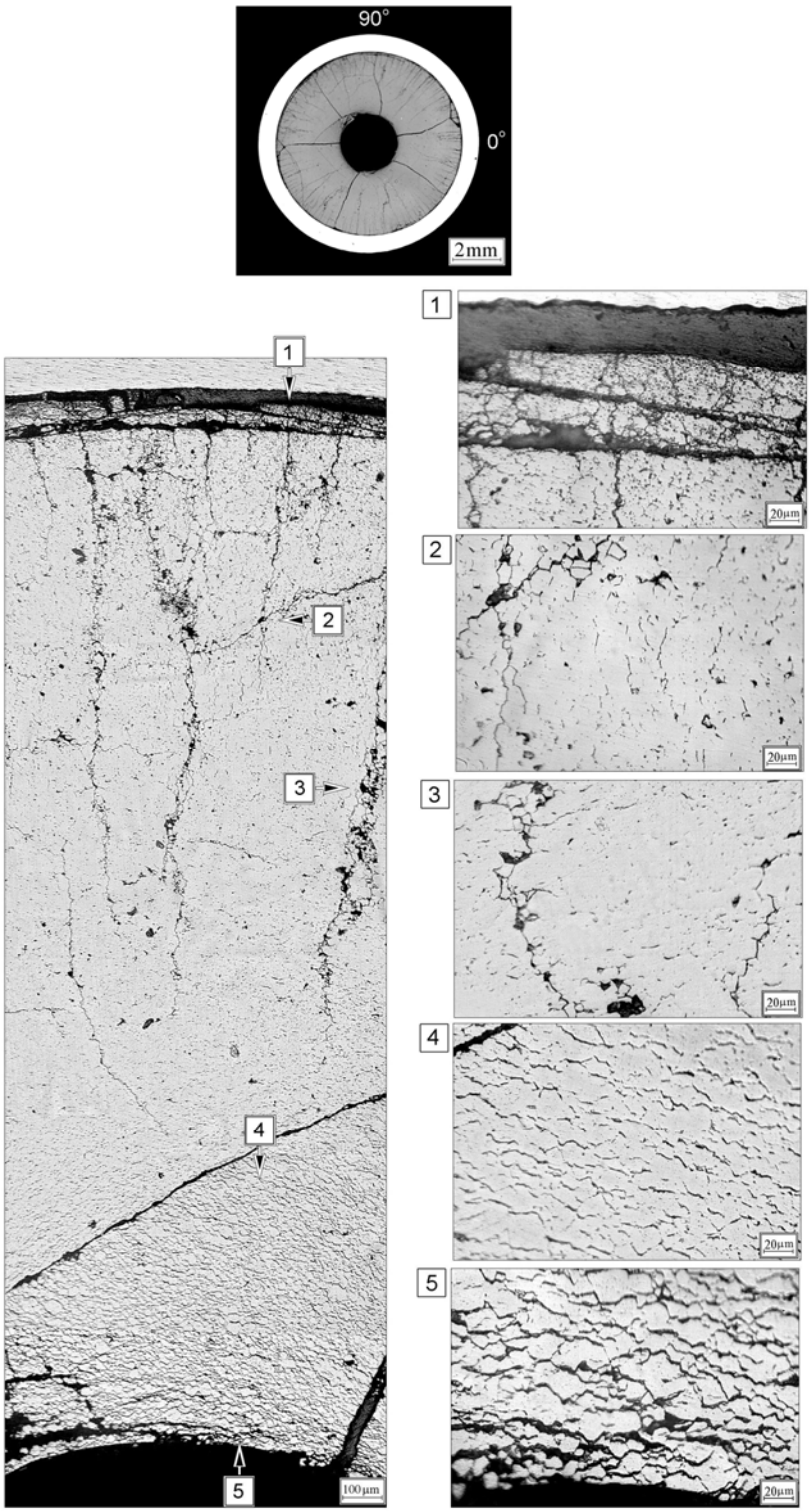


Fig.E-2.3. Cross-section and fuel microstructure of fuel rod # RT2 at 99 mm elevation (from low cap)

Table E-2.1. Time dependent energy characteristics of fuel rod # RT2

Time (s)	Relative reactor power (current/ maximum value) (per-unit)	Cumulative number of fissions in fuel rod (fiss) x10^{-14}	Power of fuel rod[1)2)] (kW)	Energy deposition		Fuel enthalpy[3)]	
				(cal/g fuel)	(J/g fuel)	FRAP-T6	RAPTA-5
0.000	7.10E-02	0.000	0.000	0.000	0.000	0.000	0.000
0.001	4.44E-01	0.516	2415	5.397	22.59	5.829	5.110
0.002	9.04E-01	1.777	4917	18.76	78.52	19.119	18.520
0.003	9.40E-01	3.576	5115	37.83	158.4	37.673	37.576
0.004	6.20E-01	5.042	3374	53.34	223.3	52.772	52.916
0.005	3.08E-01	5.890	1673	62.41	261.3	61.506	61.691
0.006	1.56E-01	6.302	846.7	66.68	279.2	65.486	65.655
0.007	9.88E-02	6.530	537.4	69.11	289.3	67.641	67.796
0.008	7.42E-02	6.685	403.6	70.79	296.4	69.046	69.202
0.009	6.61E-02	6.812	359.4	72.14	302.0	70.151	70.318
0.010	6.38E-02	6.938	347.0	73.41	307.3	71.177	71.364
0.012	6.59E-02	7.176	358.7	75.94	317.9	73.233	73.405
0.014	6.95E-02	7.431	378.0	78.64	329.3	75.489	75.808
0.016	6.71E-02	7.688	365.4	81.37	340.6	77.764	78.147
0.018	6.08E-02	7.926	330.8	83.91	351.3	79.884	80.304
0.020	5.21E-02	8.138	283.6	86.14	360.6	81.698	82.379
0.022	4.33E-02	8.309	235.8	88.02	368.5	83.194	83.861
0.024	3.65E-02	8.460	198.7	89.58	375.0	84.396	85.038
0.026	3.20E-02	8.590	174.5	90.92	380.7	85.397	86.178
0.028	2.96E-02	8.699	161.1	92.13	385.7	86.280	87.089
0.030	2.88E-02	8.809	156.8	93.27	390.5	87.109	87.794
0.050	2.90E-02	9.936	157.8	105.2	440.4	95.999	97.218
0.070	2.33E-02	10.90	126.9	115.4	483.3	103.409	104.960
0.090	1.92E-02	11.70	104.8	123.8	518.4	109.210	111.040
0.110	1.06E-02	12.27	57.66	129.9	544.0	113.001	115.210
0.130	3.90E-03	12.51	21.44	132.6	555.1	114.296	116.180
0.150	1.49E-03	12.61	8.302	133.6	559.2	114.072	115.740
0.200	4.00E-04	12.68	2.414	134.4	562.6	112.792	113.770
1.000	3.59E-05	12.79	0.300	135.9	568.8	96.970	96.035
10.00	4.15E-06	12.98	0.044	139.3	583.1	20.562	17.632
100.0	8.08E-08	13.07	0.007	141.8	593.8	4.773	4.276
1000	3.16E-13	13.08	1.59E-04	143.0	598.8	0.000	0.000

[1)] Average values determined in accordance with results of RRC KI and VNIIEF calculations

[2)] Maximum power value is 5440.5 kW (t=0.0026 s)

[3)] Average radial value

RT2

Table E-2.2. Radial energy characteristics of fuel rod # RT2*

Parameters	Coordinates of fuel radial layers (mm)			
	1 layer (1.23-2.82)	2 layer (2.82-3.44)	3 layer (3.44-3.71)	4 layer (3.71-3.795)
Number of fissions $x10^{-14}$ (fiss)	5.879	3.819	2.269	1.103
Fission density $x10^{-13}$ (fiss/g fuel)	1.878	2.008	2.444	3.629
Power** (kW)	2426	1585	955.5	474.6
Energy deposition (cal/g fuel)	128.6	137.3	167.4	252.3
Energy deposition (J/g fuel)	538.6	574.9	700.8	1056
Energy deposition*** (per-unit)	0.510	0.544	0.663	1.000

* Average values were determined in accordance with results of RRC KI and VNIIEF calculations

** The power for the entire length of each layer at time 0.0026 s

*** Energy deposition in current layer/energy deposition in 4^{th} layer

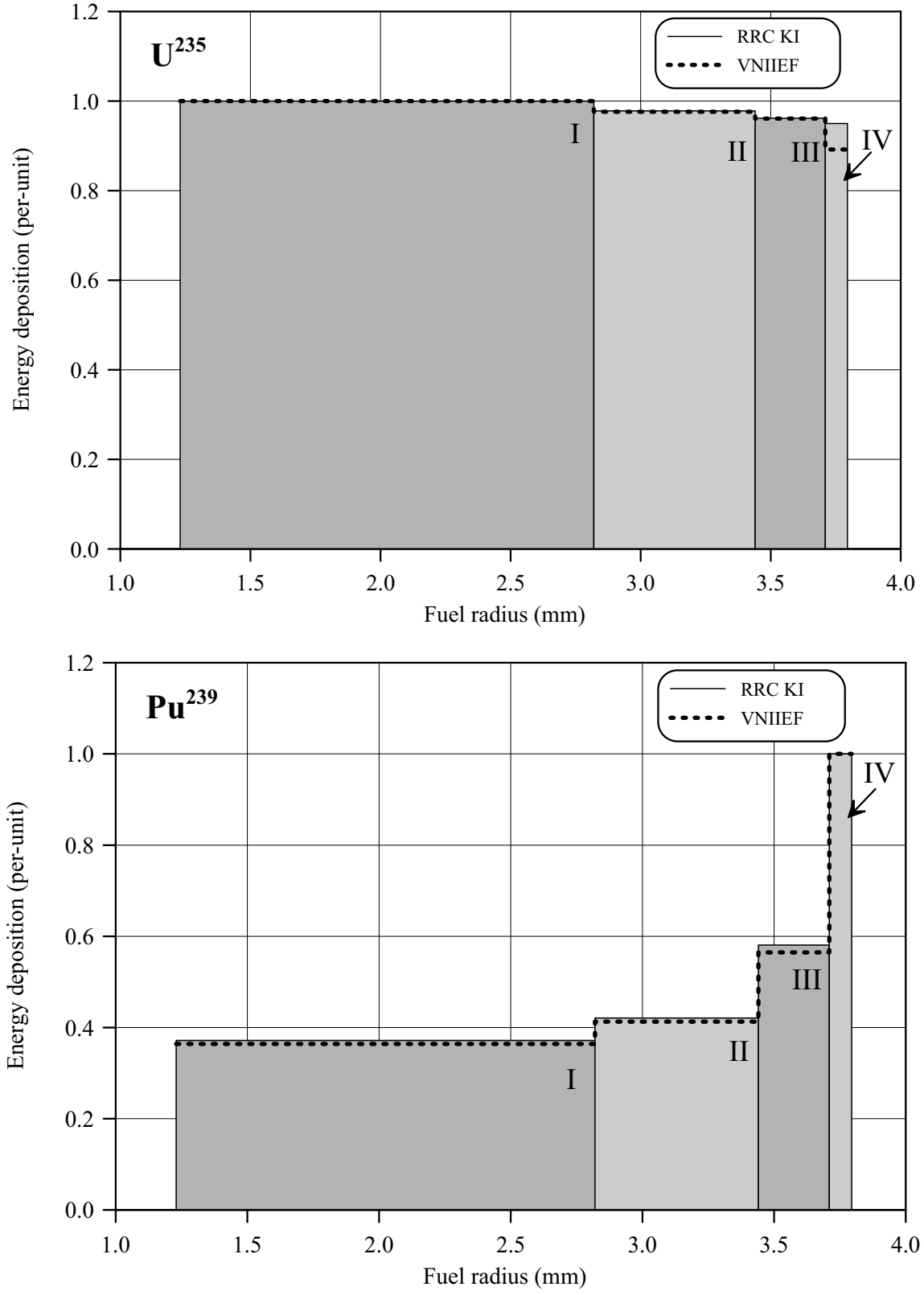


Fig.E-2.4. U^{235} and Pu^{239} radial distribution of energy deposition for fuel rod # RT2

RT2

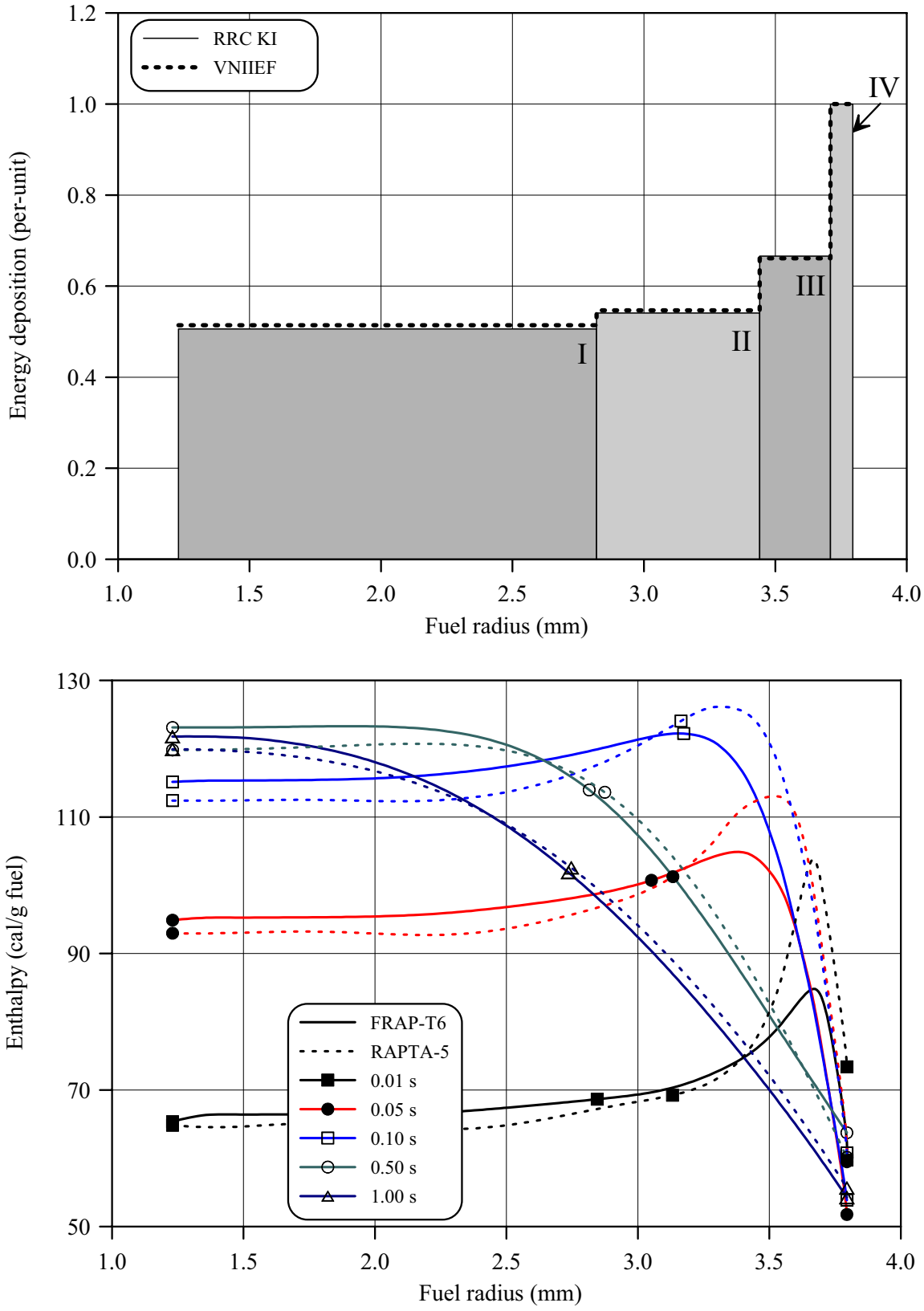


Fig.E-2.5. Radial distribution of energy deposition and fuel enthalpy for fuel rod # RT2

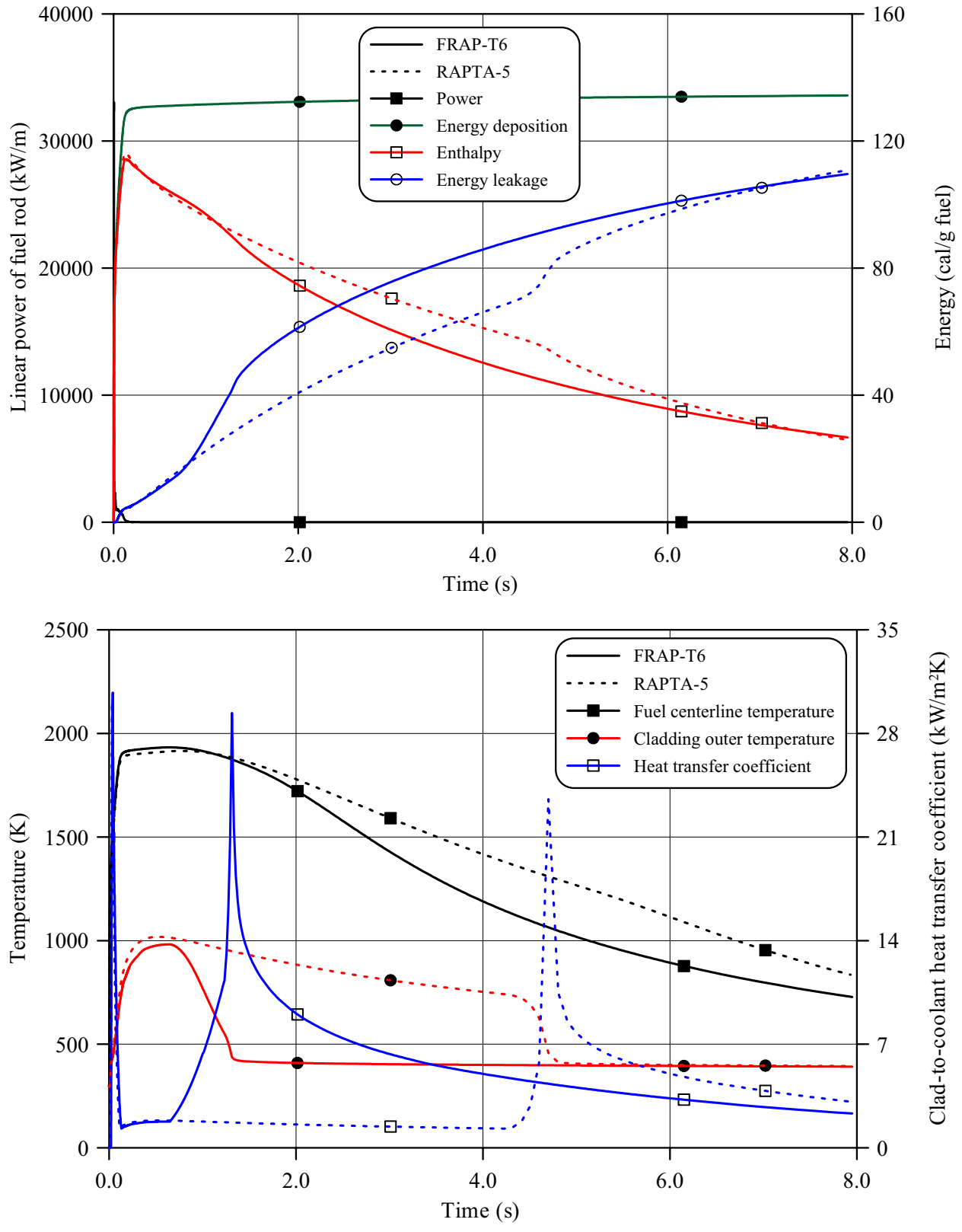


Fig.E-2.6. Thermal history of fuel rod # RT2 during the BIGR test in accordance with FRAP-T6/VVER and RAPTA-5 calculations

RT2

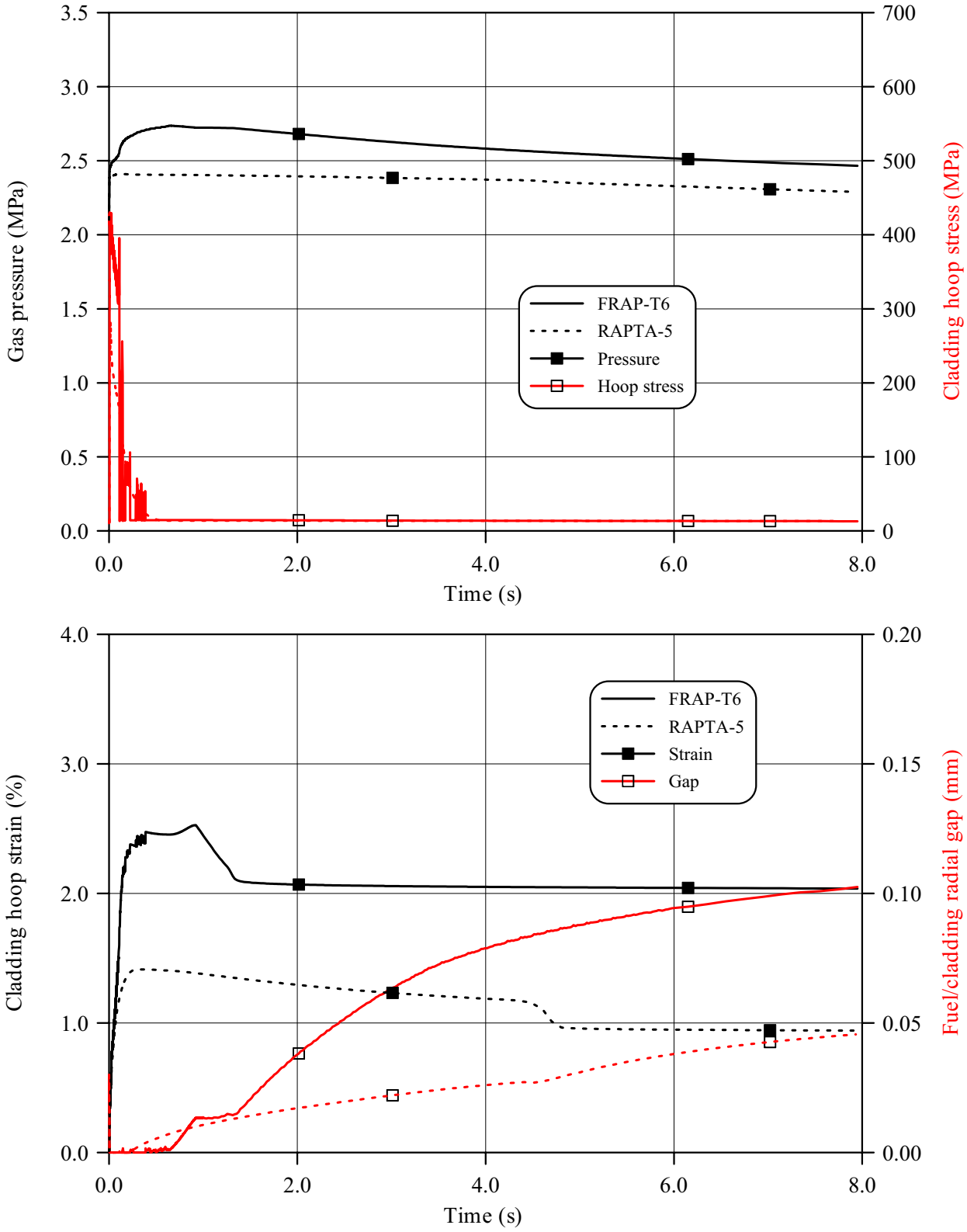


Fig.E-2.7. Mechanical behavior of fuel rod # RT2 during the BIGR test in accordance with FRAP-T6/VVER and RAPTA-5 calculations

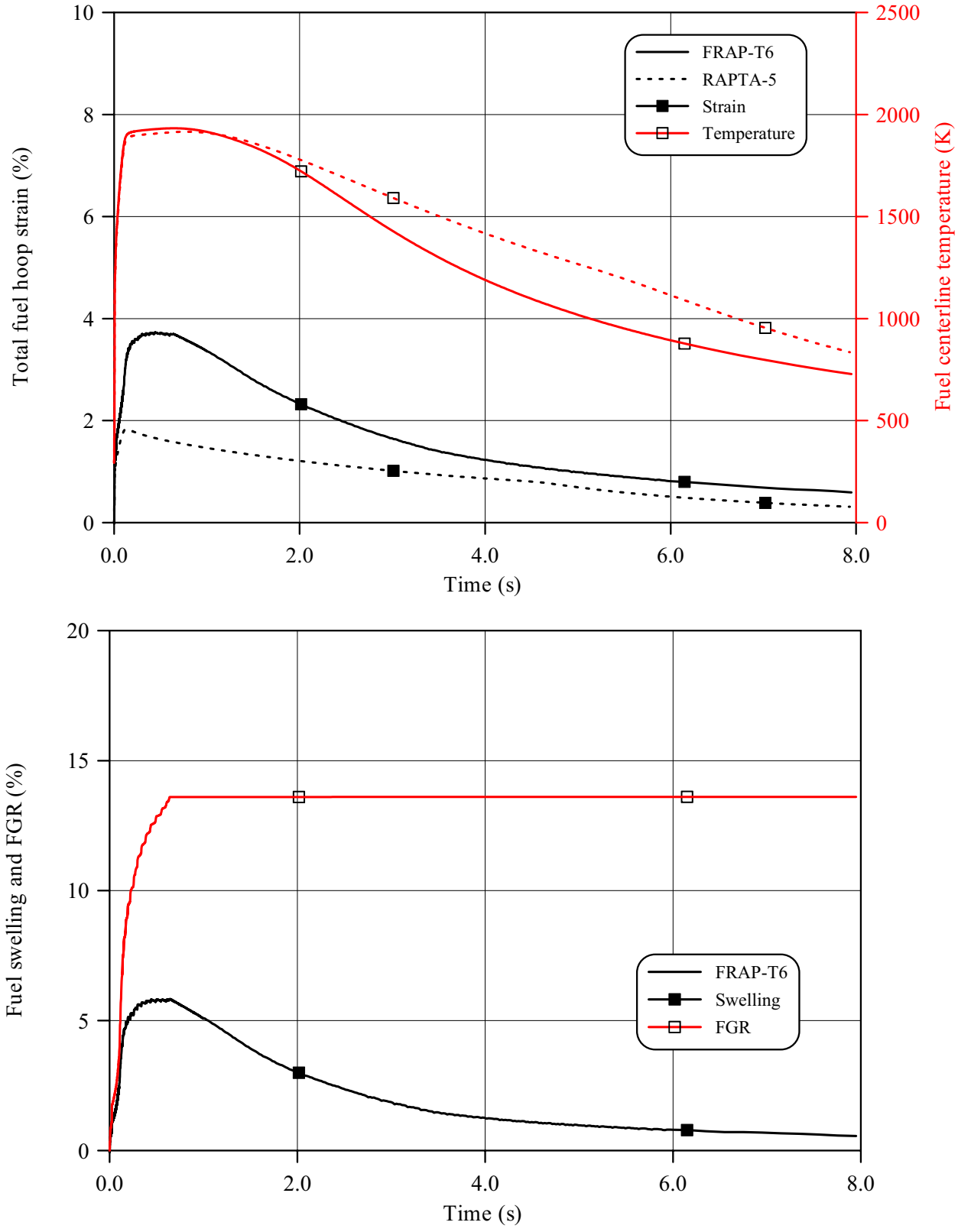


Fig.E-2.8. Fuel behavior during the BIGR test of fuel rod # RT2 in accordance with FRAP-T6/VVER and RAPTA-5 calculations

RT2

Table E-2.3. Axial distribution of cladding average outer diameter in fuel rod # RT2*

Axial coordinate (mm)	Cladding diameter (mm)	Axial coordinate (mm)	Cladding diameter (mm)	Axial coordinate (mm)	Cladding diameter (mm)	Axial coordinate (mm)	Cladding diameter (mm)
30	9.102	68	9.112	106	9.116	144	9.124
32	9.103	70	9.114	108	9.123	146	9.129
34	9.105	72	9.112	110	9.125	148	9.130
36	9.108	74	9.114	112	9.128	150	9.128
38	9.098	76	9.111	114	9.129	152	9.133
40	9.112	78	9.112	116	9.129	154	9.134
42	9.111	80	9.116	118	9.118	156	9.134
44	9.110	82	9.119	120	9.132	158	9.135
46	9.113	84	9.111	122	9.137	160	9.128
48	9.108	86	9.126	124	9.140	162	9.119
50	9.108	88	9.125	126	9.137	164	9.112
52	9.109	90	9.124	128	9.136	166	9.098
54	9.108	92	9.127	130	9.129	168	9.072
56	9.112	94	9.126	132	9.135	170	9.067
58	9.120	96	9.121	134	9.139	172	9.065
60	9.118	98	9.124	136	9.138	174	9.042
62	9.111	100	9.127	138	9.132	176	9.141
64	9.119	102	9.129	140	9.131	178	9.433
66	9.120	104	9.127	142	9.124	180	8.937

* Measured value determined on the basis of profilometry data (16 azimuthal directions)

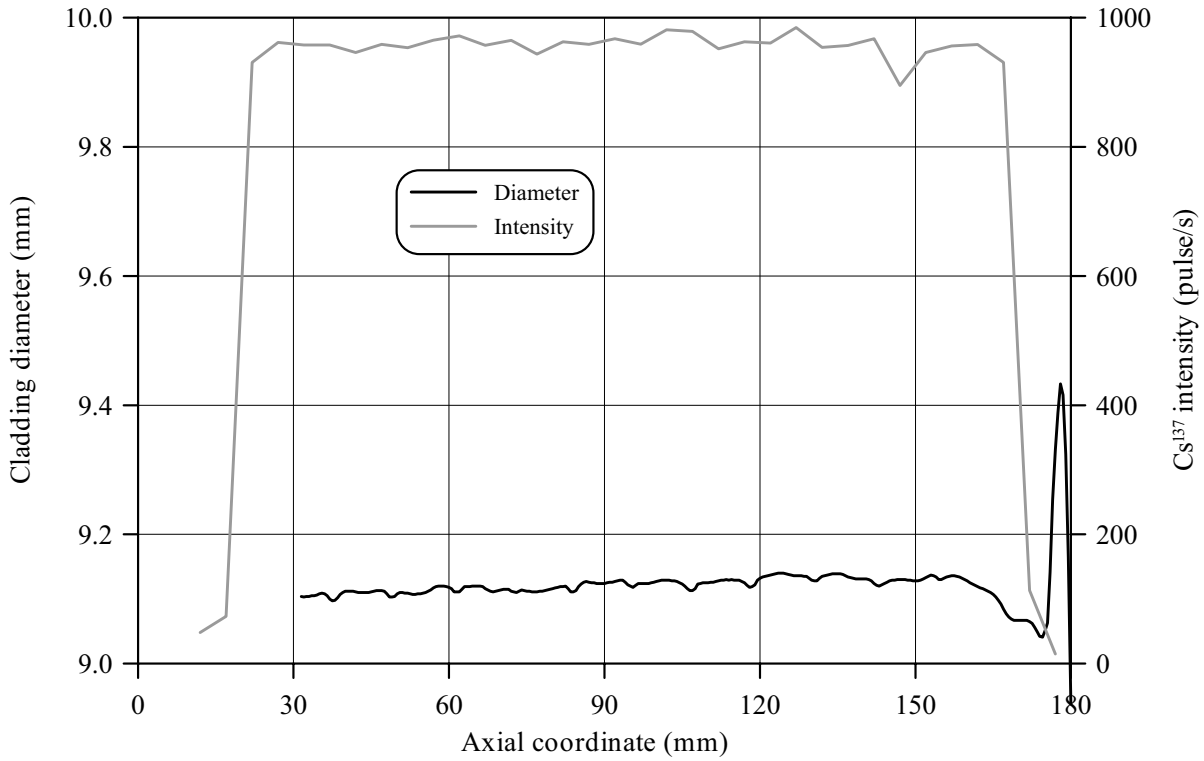


Fig.E-2.9. Cladding measured average diameter and γ-scanning results for fuel rod # RT2

Table E-2.4. The PIE results for fuel rod # RT2

	Parameter	Value
1.	Cladding outer diameter (mm):	
1.1.	Maximum diameter of the bidimensional data sample in "fuel rod length - azimuthal angle" coordinates (mm)	9.15
1.2.	Averaged azimuthal diameter and maximum diameter along the length selected from the sample of averaged azimuthal diameter (mm)	9.14
1.3.	Averaged diameter of the bidimensional data sample in "fuel rod length - azimuthal angle" coordinates (mm)	9.12
2.	Cladding maximum residual hoop strain (%)	0.85
3.	Fuel pellet conditional diameter (mm) in cross-section*:	
	at 99 mm elevation	7.64
4.	ZrO_2 outer thickness (μm) in cross-section:	
	at 99 mm elevation	3-5
5.	ZrO_2 inner thickness (μm) in cross-section:	
	at 99 mm elevation	0
6.	Parameters characterizing FGR:	
6.1.	Gas composition (% by volume):	
	He	86.08
	N_2	4.05
	O_2	0.12
	Ar	0.018
	CO_2	0.010
	Kr	0.90
	Xe	8.97
6.2.	Free gas volume (cm^3)	6.2
6.3.	Gas volume under normal conditions (cm^3)	137.5
6.4.	Gas pressure under normal conditions (MPa)	2.22
6.5.	FGR (%)	16.1

* Reference value determined by the processing of fuel cross-section photographs

RT2

Table E-2.5. Organized BIGR test results for fuel rod # RT2

	Parameter	Unit	Value		
			Measured	Calculated	
				FRAP-T6	RAPTA-5
1.	Fuel burnup	MW d/kg U	48.0	48.0	48.0
2.	Initial gas pressure	MPa	2.1	2.1	2.1
3.	Energy deposition	cal/g fuel	143.0	143.0	143.0
4.	Peak fuel enthalpy*	cal/g fuel	-	114.3	116.2
5.	Fuel maximum temperature	K	-	1963	2011
6.	Maximum temperature of cladding outer surface	K	-	982	1019
7.	Cladding burst	Failed, Unfailed	Unfailed	Unfailed	Unfailed
8.	Cladding residual hoop strain**	%	0.63	1.94	0.88
9.	Kr volume content in gas composition after the BIGR test	%	0.90	1.50	-
10.	Xe volume content in gas composition after the BIGR test	%	8.97	9.01	-

* Average value of peak fuel enthalpy is 115.2 cal/g fuel

** Average value along the fuel stack length

Appendix E–3

Individual Characteristics of Fuel Rod # RT3

after the BIGR Test

RT3

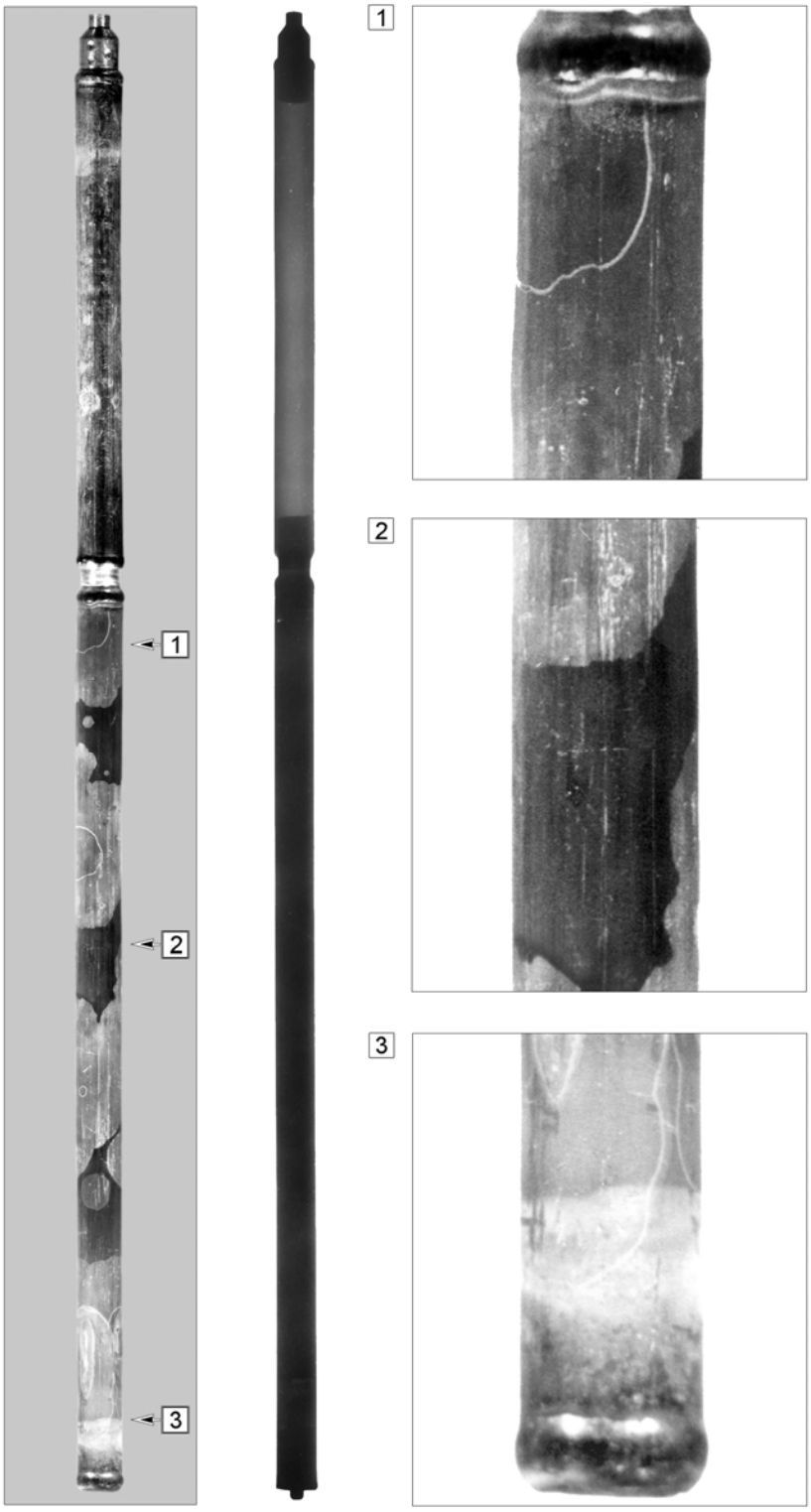


Fig.E-3.1. Appearance of unfailed fuel rod # RT3 after the BIGR test (photographs and X-ray photograph)

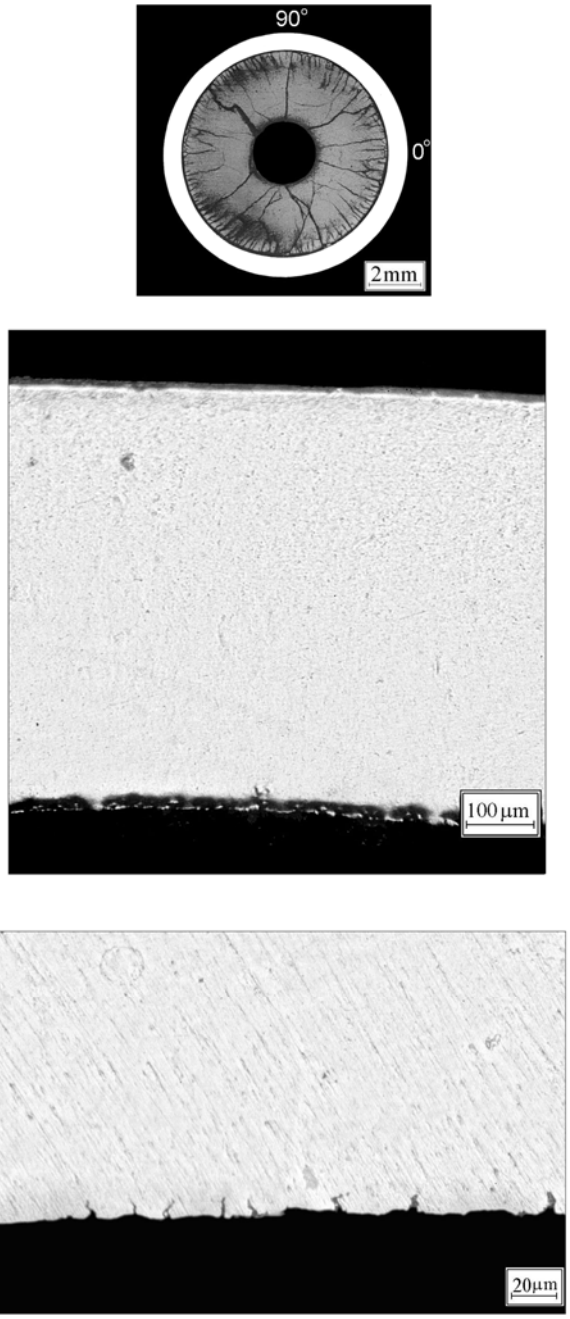


Fig.E-3.2. Cross-section and cladding microstructure of fuel rod # RT3 at 113 mm elevation (from low cap)

RT3

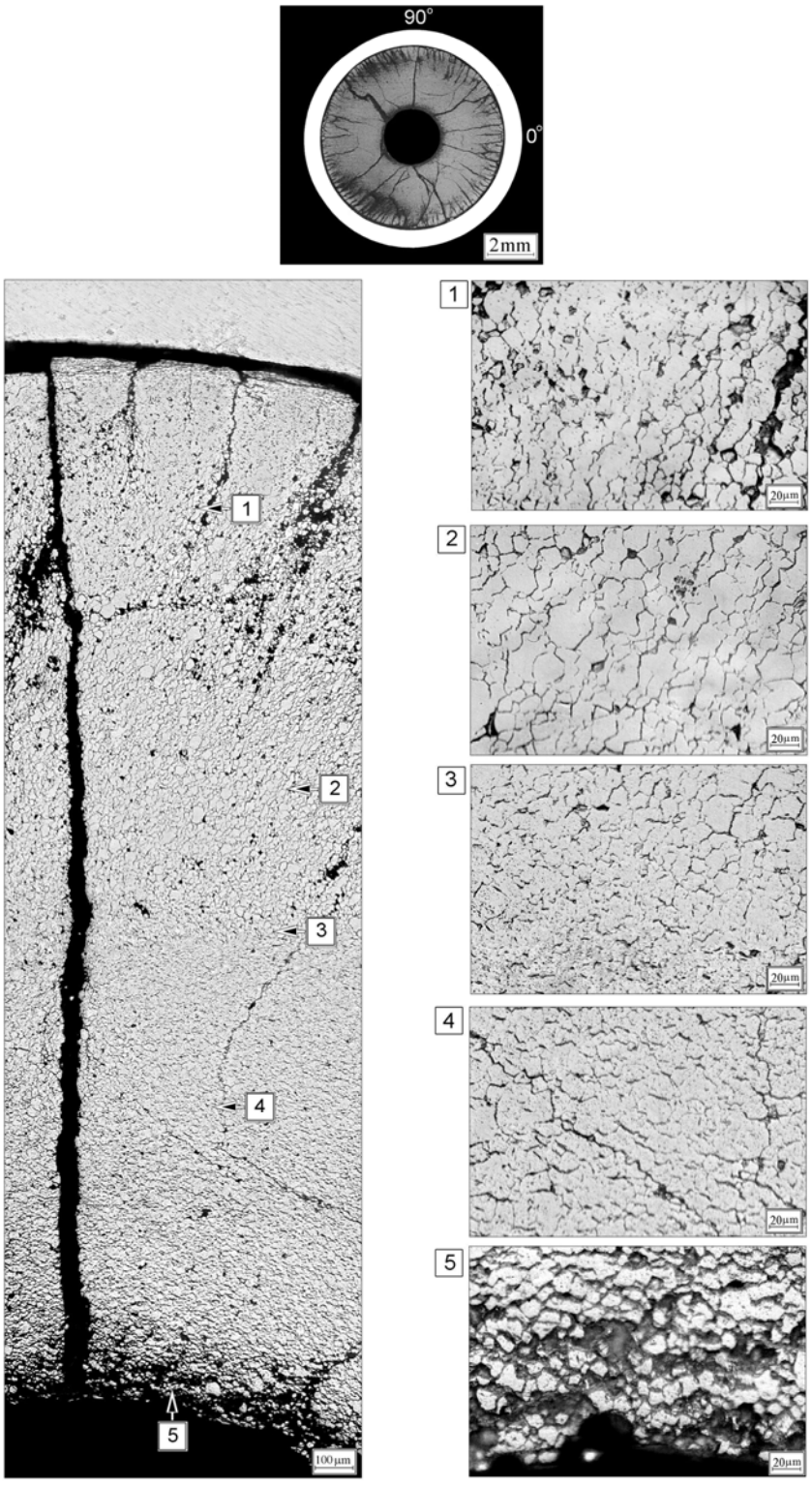


Fig.E-3.3. Cross-section and fuel microstructure of fuel rod # RT3 at 113 mm elevation (from low cap)

Table E-3.1. Time dependent energy characteristics of fuel rod # RT3

Time (s)	Relative reactor power (current/ maximum value) (per-unit)	Cumulative number of fissions in fuel rod (fiss) x10^{-14}	Power of fuel rod[1)2)] (kW)	Energy deposition		Fuel enthalpy[3)]	
				(cal/g fuel)	(J/g fuel)	FRAP-T6	RAPTA-5
0.000	2.09E-02	0.000	0.000	0.000	0.000	0.000	0.000
0.001	1.97E-01	0.080	408.2	2.791	11.68	3.323	2.662
0.002	6.18E-01	0.376	1283	13.35	55.89	14.463	13.272
0.003	1.00E+00	1.028	2076	36.58	153.1	37.846	36.544
0.004	6.81E-01	1.702	1413	60.68	254.1	61.942	60.481
0.005	2.93E-01	2.065	608.2	73.47	307.6	74.603	72.889
0.006	1.48E-01	2.228	307.8	79.25	331.8	80.187	78.245
0.007	8.06E-02	2.310	167.3	82.23	344.3	82.916	80.850
0.008	5.58E-02	2.361	115.7	84.04	351.8	84.446	82.319
0.009	4.91E-02	2.401	102.0	85.45	357.7	85.585	83.429
0.010	4.78E-02	2.440	99.15	86.76	363.2	86.639	84.475
0.012	5.33E-02	2.514	110.7	89.50	374.7	88.872	86.778
0.014	6.59E-02	2.606	136.7	92.76	388.4	91.647	89.527
0.016	7.19E-02	2.715	149.2	96.53	404.1	94.924	92.891
0.018	6.92E-02	2.820	143.6	100.4	420.4	98.329	96.463
0.020	5.73E-02	2.915	119.0	103.9	434.9	101.320	99.371
0.022	4.57E-02	2.995	94.94	106.7	446.7	103.683	101.860
0.024	3.61E-02	3.062	74.92	108.9	456.1	105.485	103.670
0.026	2.90E-02	3.112	60.31	110.7	463.5	106.859	105.120
0.028	2.43E-02	3.148	50.46	112.1	469.4	107.931	106.030
0.030	2.29E-02	3.186	47.61	113.4	474.7	108.843	106.940
0.050	2.33E-02	3.558	48.44	126.5	529.7	118.563	116.950
0.070	1.88E-02	3.877	39.07	138.0	577.8	126.855	125.630
0.090	1.47E-02	4.139	30.65	147.2	616.4	133.304	132.350
0.110	7.95E-03	4.313	16.57	153.5	642.7	137.205	136.340
0.130	2.98E-03	4.394	6.240	156.3	654.5	138.624	137.210
0.150	1.13E-03	4.418	2.415	157.3	658.8	138.338	136.620
0.200	3.05E-04	4.440	0.701	158.2	662.4	136.674	134.300
1.000	2.77E-05	4.477	0.089	159.8	669.2	116.316	113.690
10.00	3.16E-06	4.537	0.013	163.6	685.1	23.629	24.851
100.0	6.15E-08	4.567	0.002	166.5	696.9	4.865	4.419
1000	2.40E-13	4.568	4.46E-05	167.9	702.8	0.000	0.000

[1)] Average values determined in accordance with results of RRC KI and VNIIEF calculations

[2)] Maximum power value is 2075.5 кВт (t=0.003 c)

[3)] Average radial value

RT3

Table E-3.2. Radial energy characteristics of fuel rod # RT3*

Parameters**	Coordinates of fuel radial layers (mm)			
	1 layer (1.23-2.82)	2 layer (2.82-3.44)	3 layer (3.44-3.71)	4 layer (3.71-3.795)
Number of fissions $x10^{-14}$ (fiss)	4.417	2.893	1.730	0.848
Fission density $x10^{-13}$ (fiss/g fuel)	2.192	2.357	2.896	4.358
Power*** (kW)	920.8	605.2	366.6	182.5
Energy deposition (cal/g fuel)	149.8	161.5	198.7	299.2
Energy deposition (J/g fuel)	627.4	676.0	832.0	1253
Energy deposition**** (per-unit)	0.501	0.540	0.664	1.000

* Average values were determined in accordance with results of RRC KI and VNIIEF calculations

** All parameters were determined for the undamaged section of a fuel stack (see Table C.2)

*** The power for the entire length of each layer at time 0.003 s

**** Energy deposition in current layer/energy deposition in 4^{th} layer

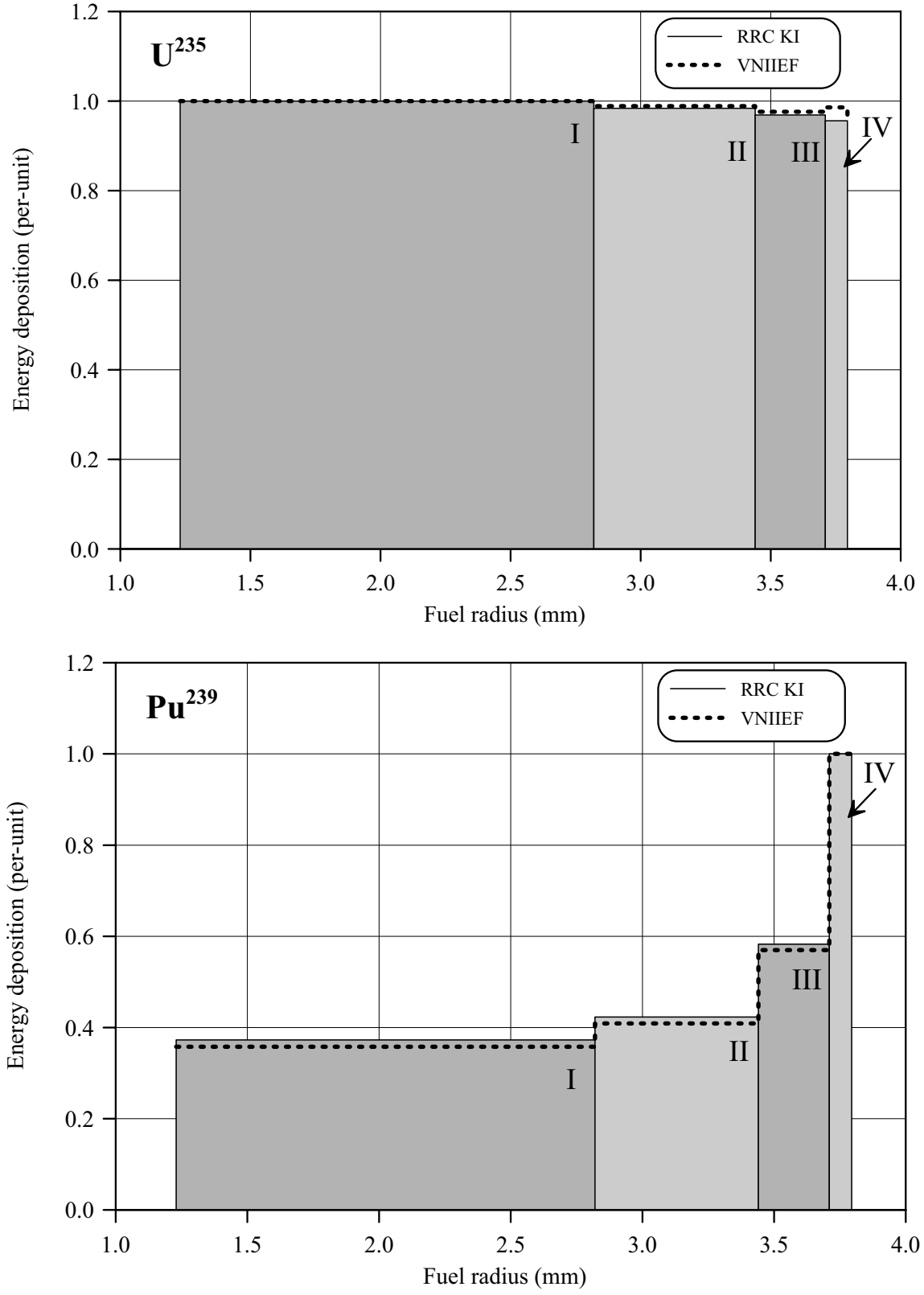
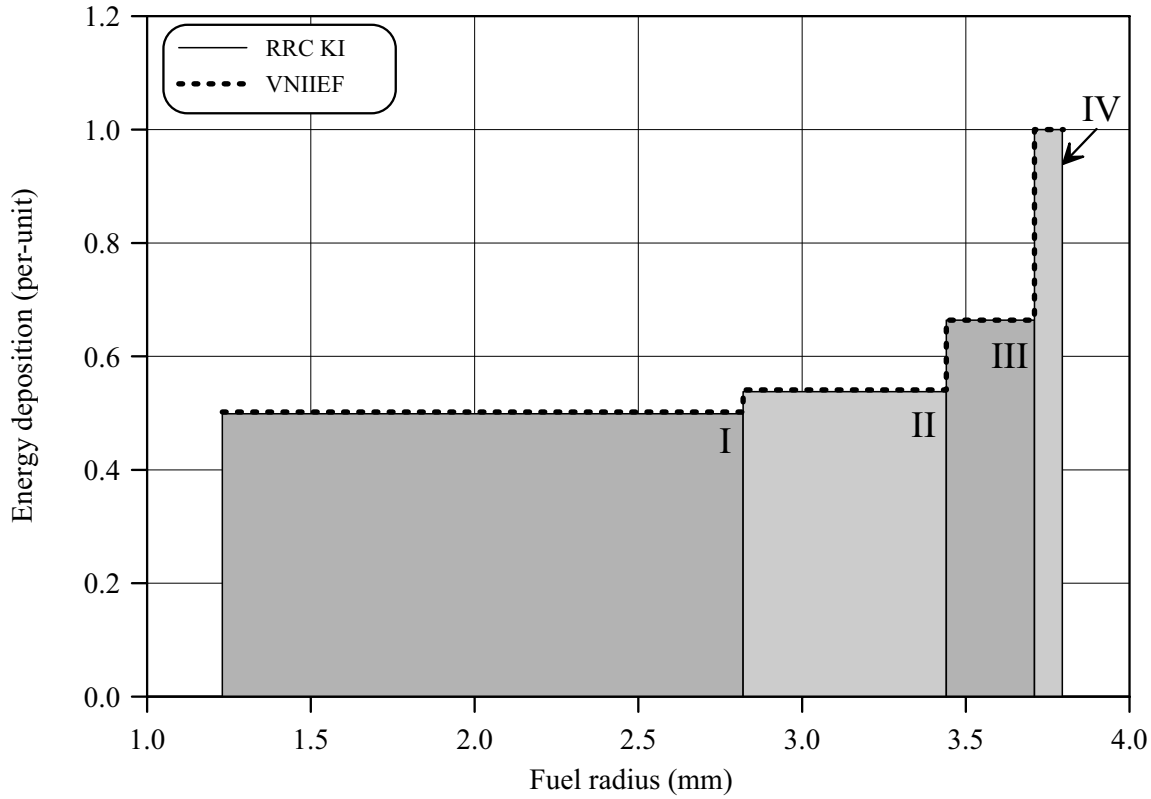


Fig.E-3.4. U^{235} and Pu^{239} radial distribution of energy deposition for fuel rod # RT3

RT3



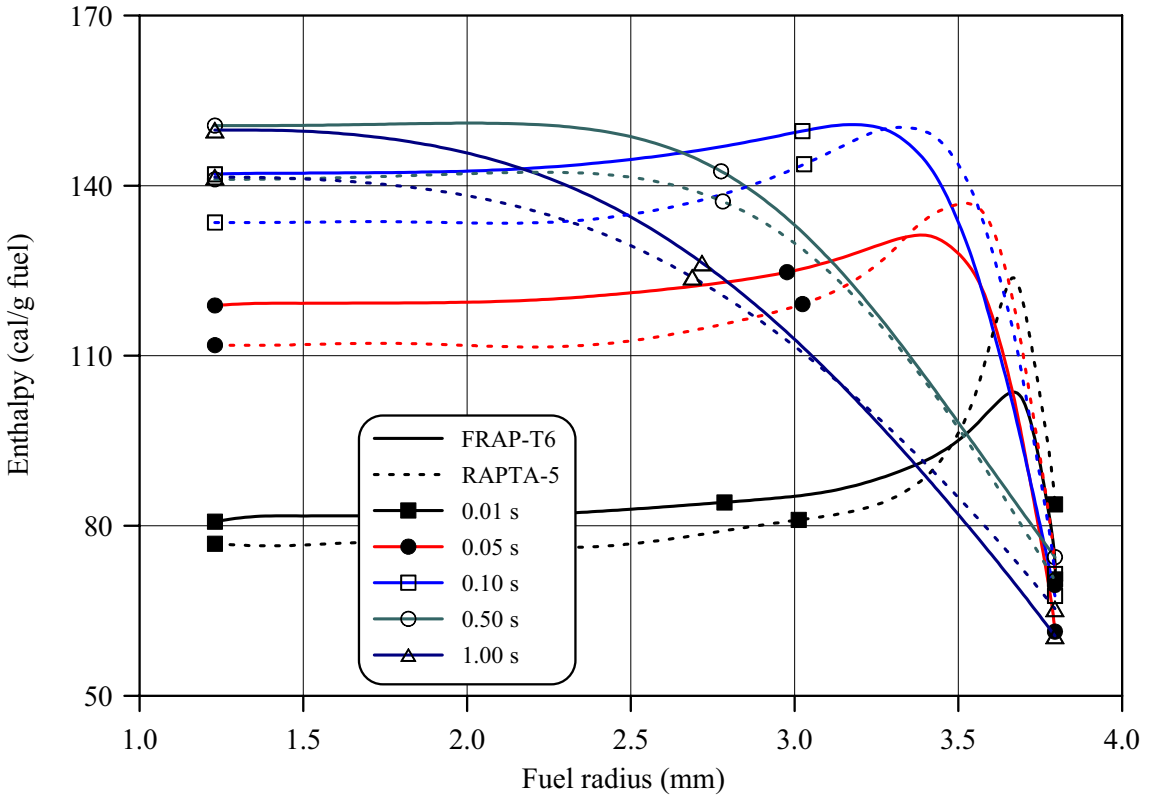


Fig.E-3.5. Radial distribution of energy deposition and fuel enthalpy for fuel rod # RT3

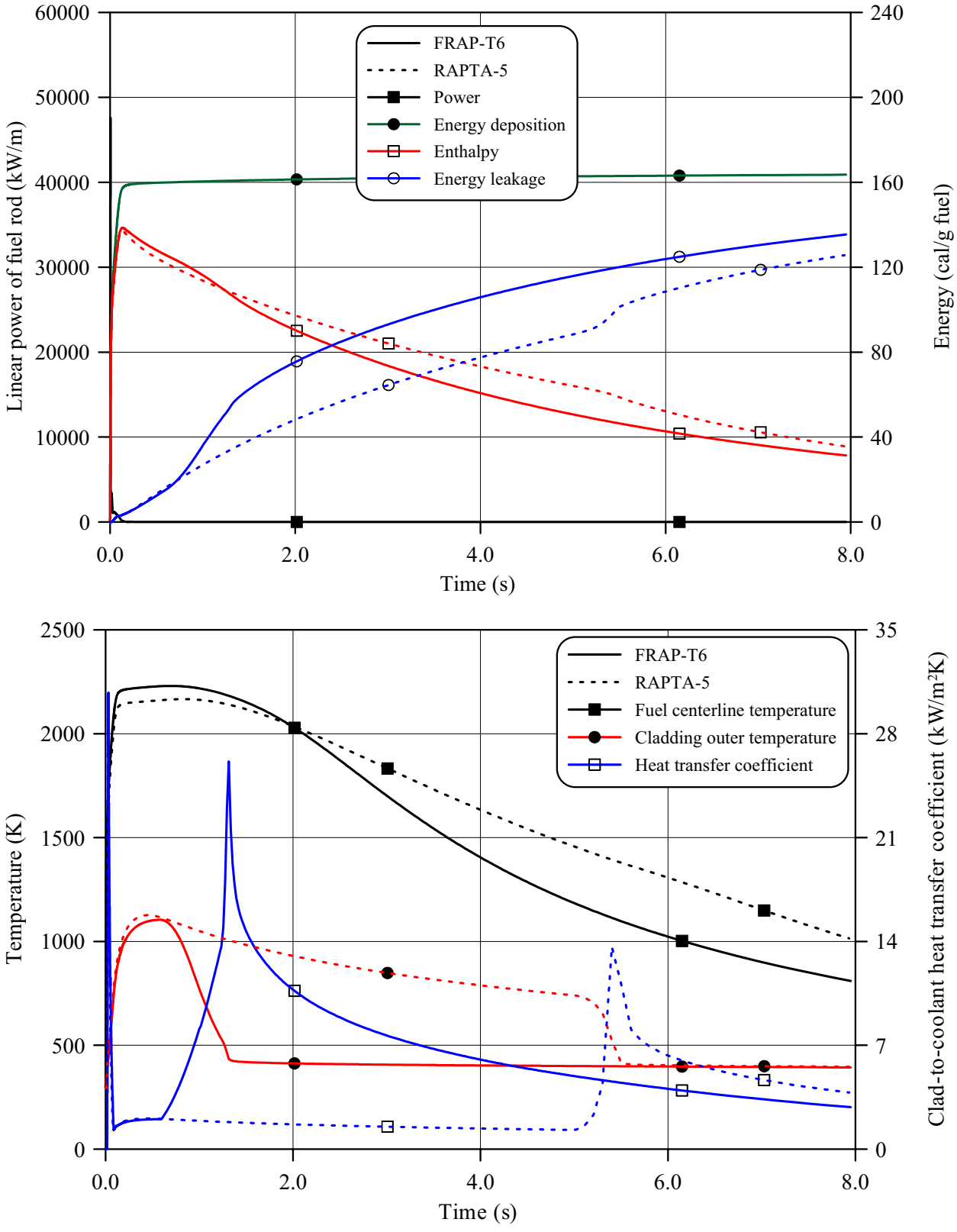


Fig.E-3.6. Thermal history of fuel rod # RT3 during the BIGR test in accordance with FRAP-T6/VVER and RAPTA-5 calculations

RT3

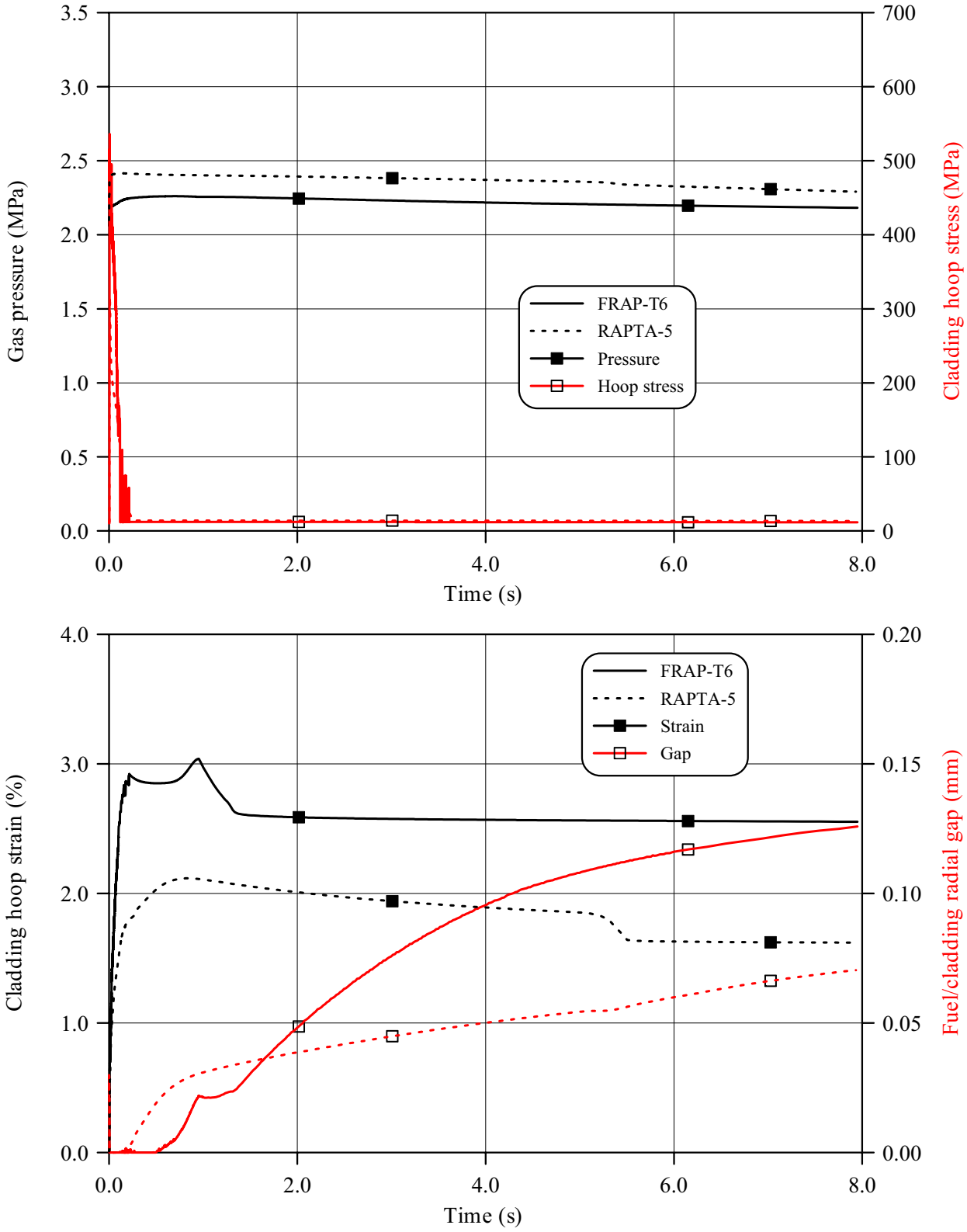


Fig.E-3.7. Mechanical behavior of fuel rod # RT3 during the BIGR test in accordance with FRAP-T6/VVER and RAPTA-5 calculations

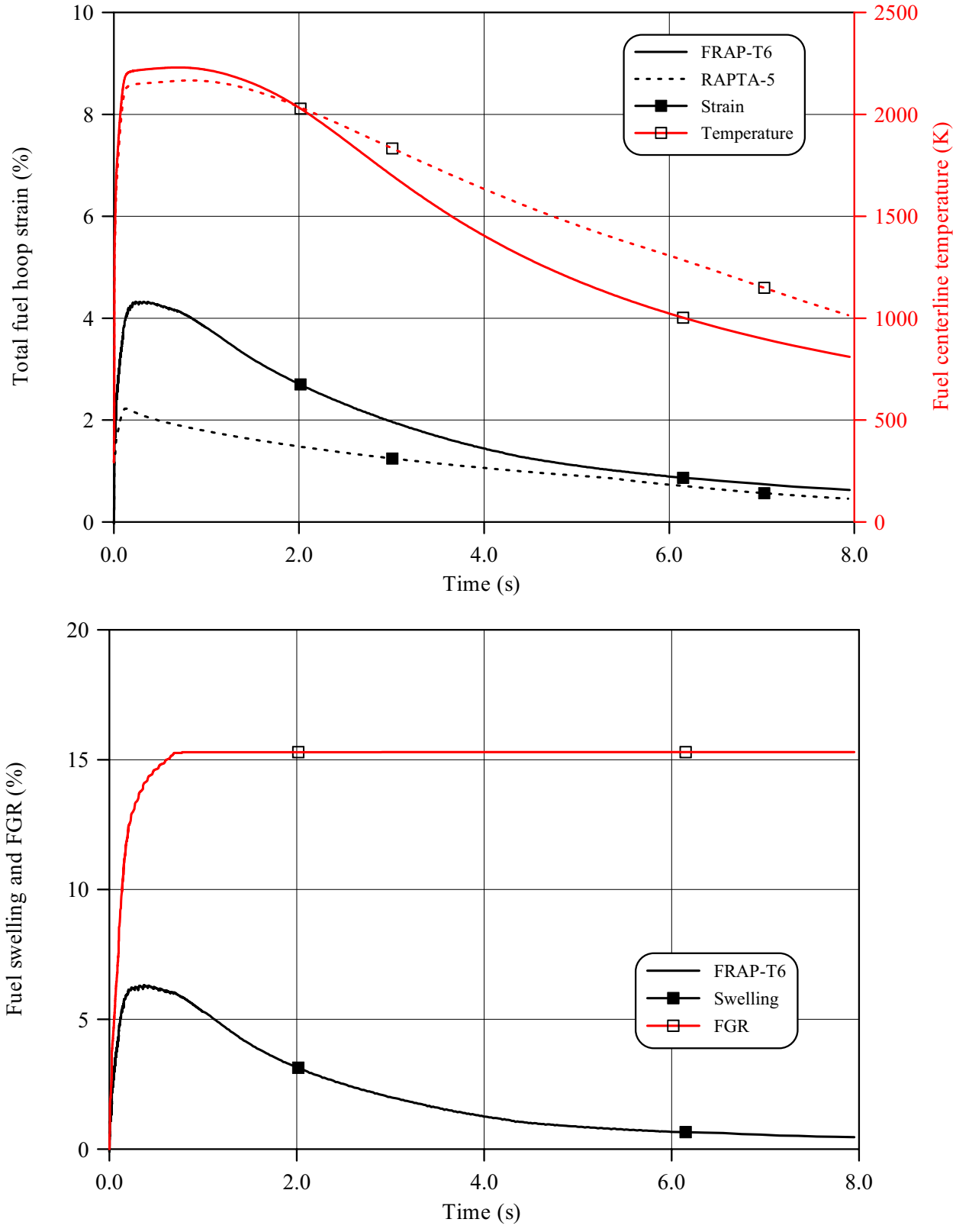


Fig.E-3.8. Fuel behavior during the BIGR test of fuel rod # RT3 in accordance with FRAP-T6/VVER and RAPTA-5 calculations

RT3

Table E-3.3. Axial distribution of cladding average outer diameter in fuel rod # RT3*

Axial coordinate (mm)	Cladding diameter (mm)	Axial coordinate (mm)	Cladding diameter (mm)	Axial coordinate (mm)	Cladding diameter (mm)	Axial coordinate (mm)	Cladding diameter (mm)
36	9.208	74	9.251	112	9.293	150	9.314
38	9.231	76	9.265	114	9.286	152	9.307
40	9.245	78	9.286	116	9.267	154	9.300
42	9.242	80	9.302	118	9.235	156	9.308
44	9.242	82	9.296	120	9.245	158	9.340
46	9.205	84	9.271	122	9.260	160	9.365
48	9.150	86	9.261	124	9.259	162	9.372
50	9.131	88	9.271	126	9.252	164	9.323
52	9.092	90	9.298	128	9.227	166	9.225
54	9.064	92	9.300	130	9.226	168	9.129
56	9.059	94	9.270	132	9.269	170	9.070
58	9.058	96	9.237	134	9.316	172	9.052
60	9.059	98	9.255	136	9.328	174	9.051
62	9.073	100	9.278	138	9.292	176	9.045
64	9.137	102	9.308	140	9.252	178	9.409
66	9.198	104	9.303	142	9.241	180	8.521
68	9.251	106	9.278	144	9.272		
70	9.260	108	9.270	146	9.298		
72	9.253	110	9.281	148	9.314		

* Measured value determined on the basis of profilometry data (16 azimuthal directions)

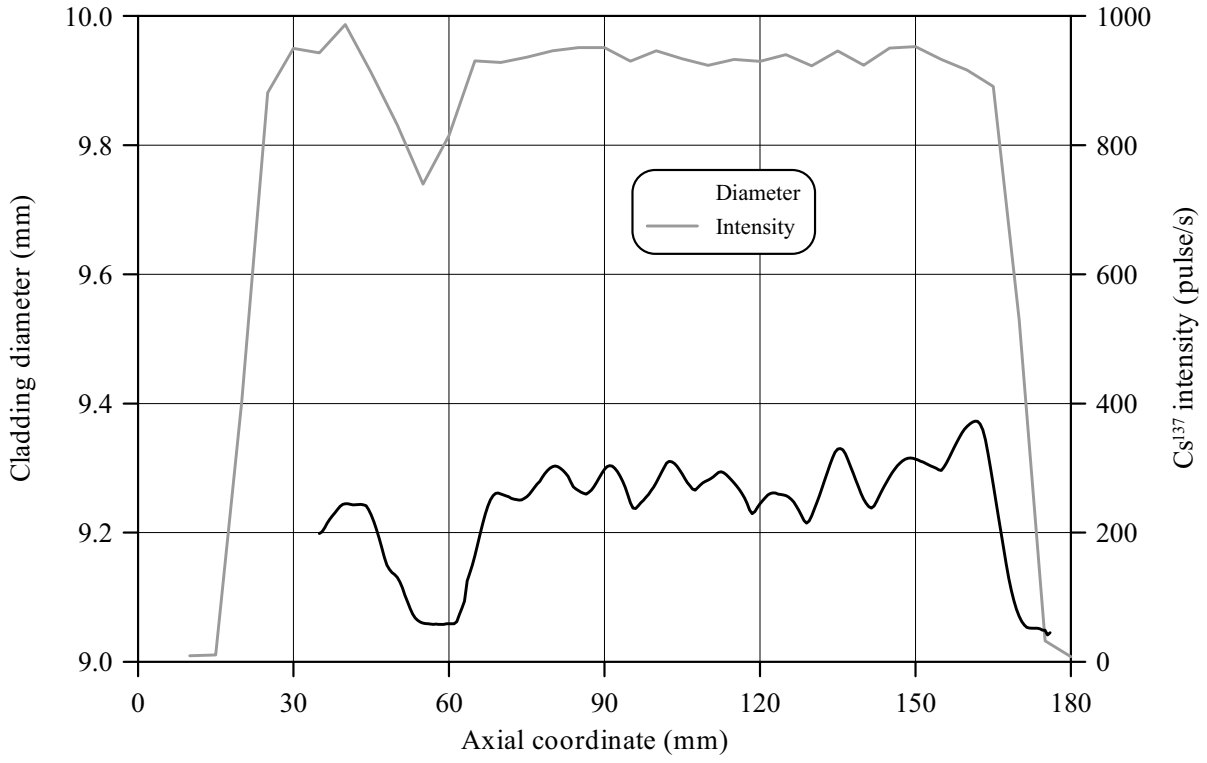


Fig.E-3.9. Cladding measured average diameter and γ-scanning results for fuel rod # RT3

Table E-3.4. The PIE results for fuel rod # RT3

	Parameter	Value
1.	Cladding outer diameter (mm):	
1.1.	Maximum diameter of the bidimensional data sample in "fuel rod length - azimuthal angle" coordinates (mm)	9.47
1.2.	Averaged azimuthal diameter and maximum diameter along the length selected from the sample of averaged azimuthal diameter (mm)	9.37
1.3.	Averaged diameter of the bidimensional data sample in "fuel rod length - azimuthal angle" coordinates (mm)	9.24
2.	Cladding maximum residual hoop strain (%)	3.40
3.	Fuel pellet conditional diameter (mm) in cross-section*:	
	at 113 mm elevation	7.71
4.	ZrO_2 outer thickness (μm) in cross-section:	
	at 113 mm elevation	3–5
5.	ZrO_2 inner thickness (μm) in cross-section:	
	at 113 mm elevation	0
6.	Parameters characterizing FGR:	
6.1.	Gas composition (% by volume):	
	He	84.76
	N_2	0.91
	O_2	0.17
	Ar	0.015
	CO_2	0.010
	Kr	1.28
	Xe	12.85
6.2.	Free gas volume (cm^3)	6.1
6.3.	Gas volume under normal conditions (cm^3)	143.5
6.4.	Gas pressure under normal conditions (MPa)	2.35
6.5.	FGR (%)	21.30

* Reference value determined by the processing of fuel cross-section photographs

RT3

Table E-3.5. Organized BIGR test results for fuel rod # RT3

Parameter		Unit	Value		
			Measured	Calculated	
				FRAP-T6	RAPTA-5
1.	Fuel burnup	MW d/kg U	47.5	47.5	47.5
2.	Initial gas pressure	MPa	2.1	2.1	2.1
3.	Energy deposition	cal/g fuel	167.9	167.9	167.9
4.	Peak fuel enthalpy*	cal/g fuel	-	138.6	137.2
5.	Fuel maximum temperature	K	-	2266	2279
6.	Maximum temperature of cladding outer surface	K	-	1104	1127
7.	Cladding burst	Failed, Unfailed	Unfailed	Unfailed	Unfailed
8.	Cladding residual hoop strain**	%	2.00	2.46	1.55
9.	Kr volume content in gas composition after the BIGR test	%	1.28	0.56	-
10.	Xe volume content in gas composition after the BIGR test	%	12.85	3.37	-

* Average value of peak fuel enthalpy is 137.9 cal/g fuel

** Average value along the fuel stack length

Appendix E–4

Individual Characteristics of Fuel Rod # RT4

after the BIGR Test

RT4

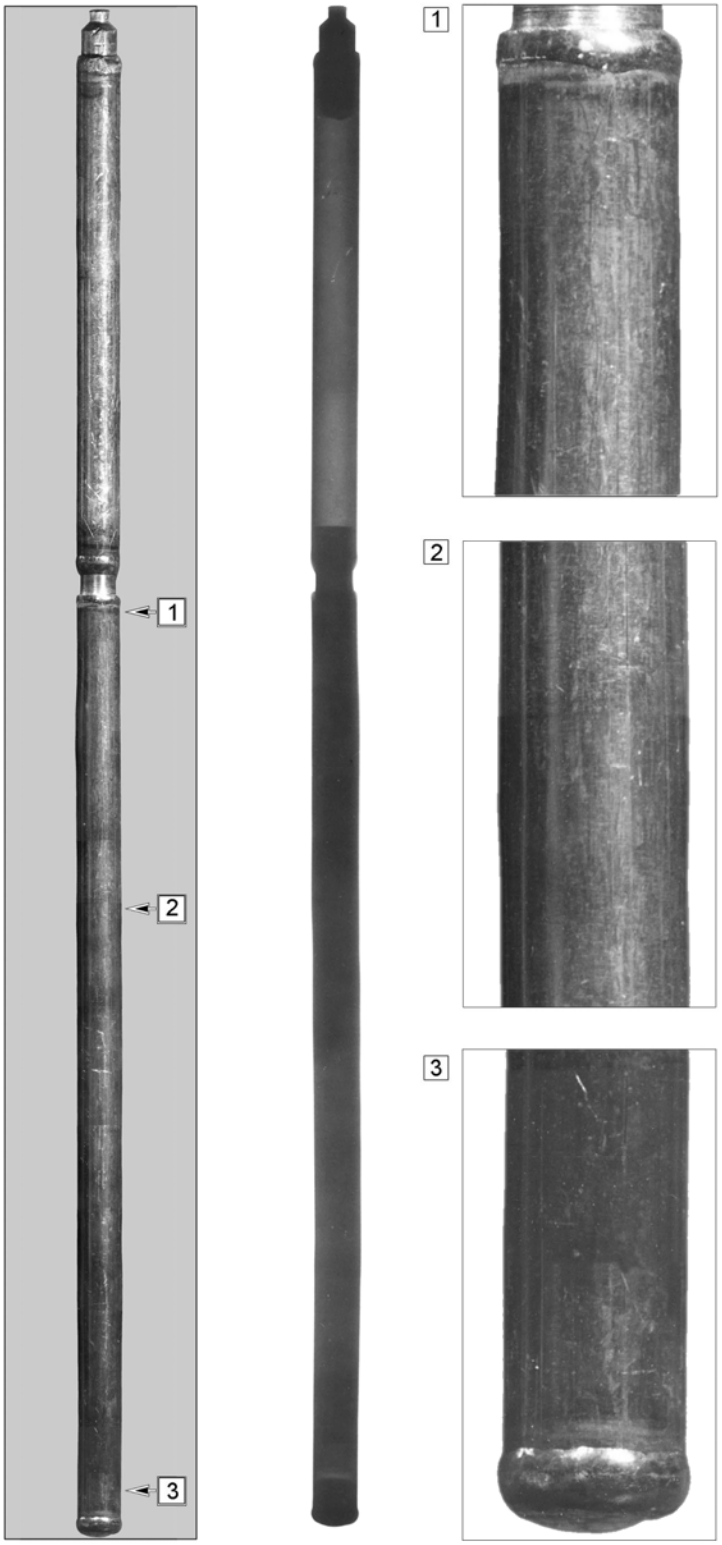


Fig.E-4.1. Appearance of unfailed fuel rod # RT4 after the BIGR test (photographs and X-ray photograph)

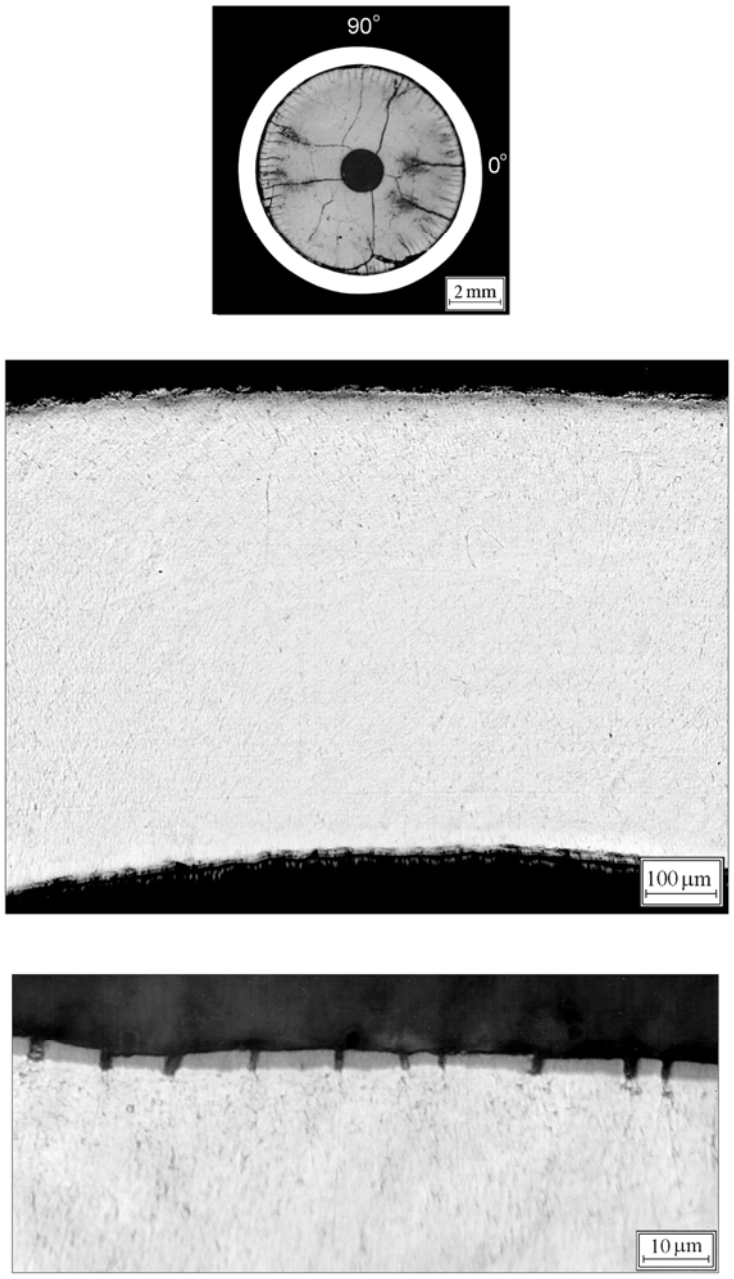


Fig.E-4.2. Cross-section and cladding microstructure of fuel rod # RT4 at 108 mm elevation (from low cap)

RT4

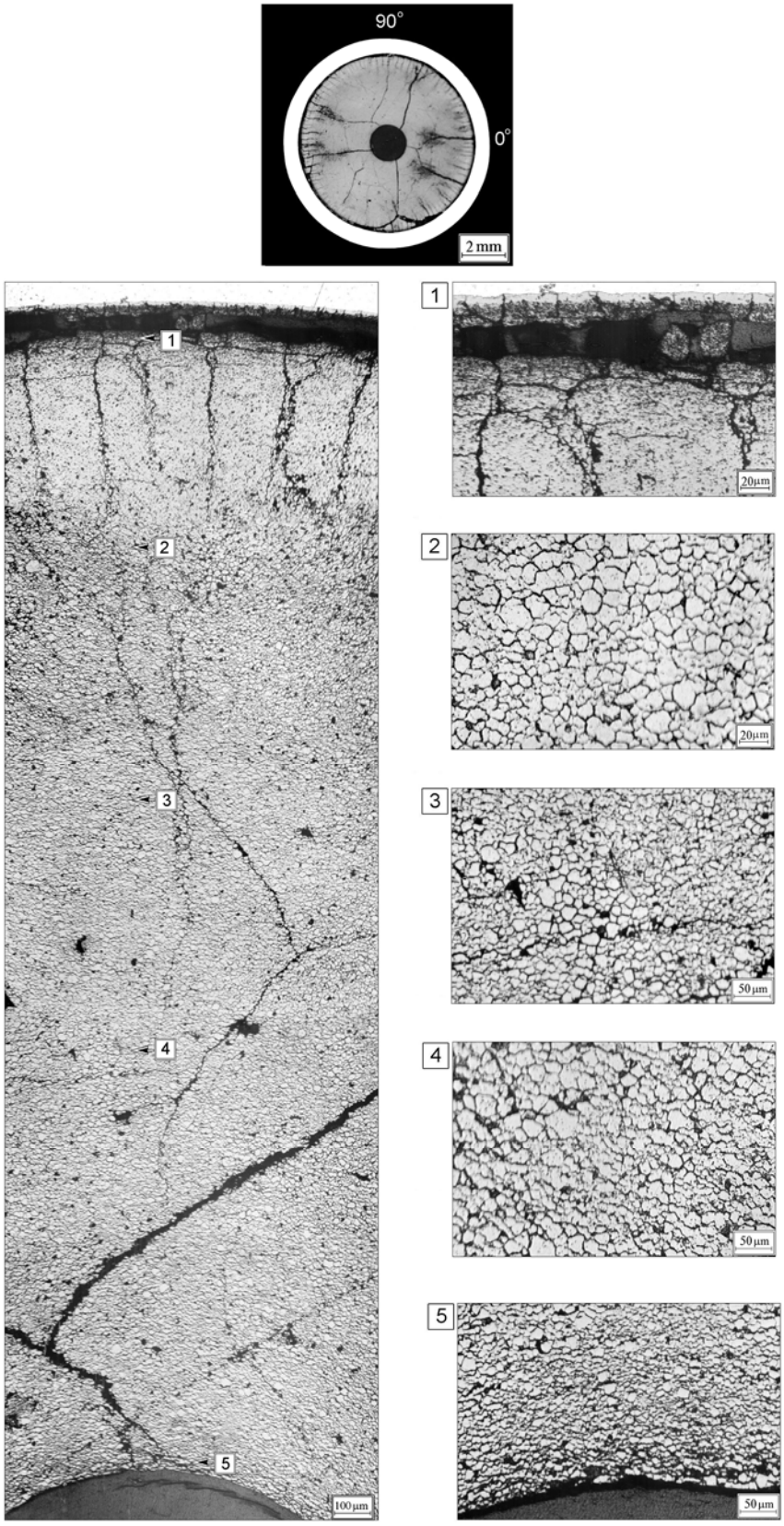


Fig.E-4.3. Cross-section and fuel microstructure of fuel rod # RT4 at 108 mm elevation (from low cap)

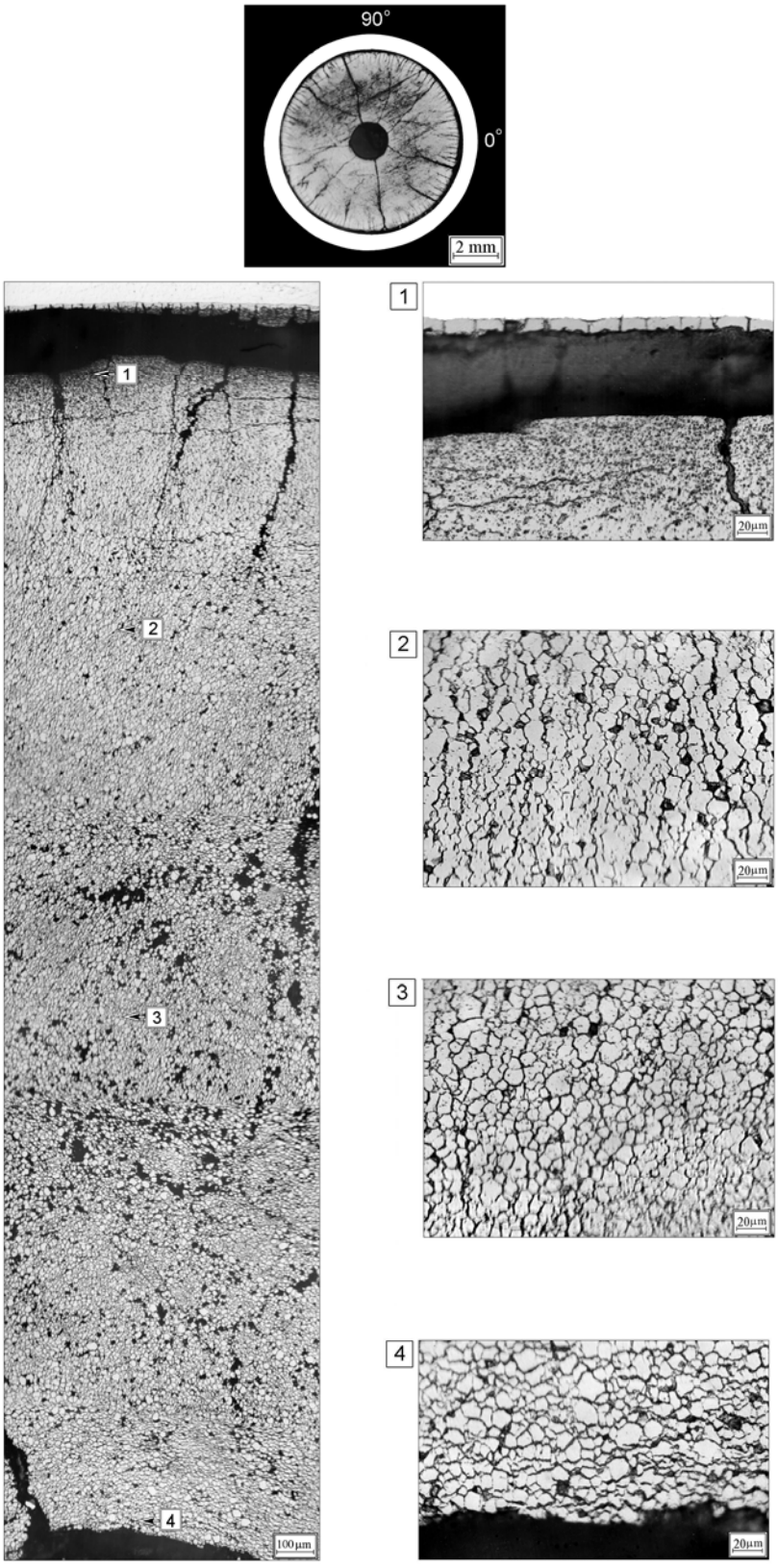


Fig.E-4.4. Cross-section and fuel microstructure of fuel rod # RT4 after the BIGR test at 117 mm elevation (from low cap)

RT4

Table E-4.1. Time dependent energy characteristics of fuel rod # RT4

Time (s)	Relative reactor power (current/ maximum value) (per-unit)	Cumulative number of fissions in fuel rod (fiss) x10^{-14}	Power of fuel rod[1)2)] (kW)	Energy deposition		Fuel enthalpy[3)]	
				(cal/g fuel)	(J/g fuel)	FRAP-T6	RAPTA-5
0.000	1.88E-02	0.000	0.000	0.000	0.000	0.000	0.000
0.001	1.91E-01	0.257	1297	2.477	10.37	3.138	2.366
0.002	6.03E-01	1.247	4085	12.07	50.51	13.615	11.950
0.003	1.00E+00	3.438	6778	33.38	139.8	35.372	33.202
0.004	6.48E-01	5.663	4393	54.98	230.2	56.687	54.522
0.005	2.66E-01	6.805	1804	66.06	276.6	67.189	65.110
0.006	1.42E-01	7.321	961.5	71.06	297.5	71.731	69.656
0.007	7.58E-02	7.575	513.9	73.49	307.7	73.952	71.890
0.008	5.27E-02	7.756	357.1	75.28	315.2	75.188	73.149
0.009	4.50E-02	7.878	304.8	76.50	320.3	76.058	74.091
0.010	4.44E-02	8.001	300.7	77.61	324.9	76.919	74.963
0.012	5.31E-02	8.252	359.8	80.07	335.2	78.844	76.956
0.014	6.69E-02	8.567	453.3	83.11	348.0	81.379	79.559
0.016	7.50E-02	8.938	508.6	86.75	363.2	84.510	82.711
0.018	7.34E-02	9.332	497.6	90.55	379.1	87.719	86.298
0.020	6.46E-02	9.694	438.0	94.09	393.9	90.803	89.384
0.022	5.92E-02	10.02	401.4	97.21	407.0	93.371	92.225
0.024	5.21E-02	10.31	353.2	100.0	418.9	95.776	94.529
0.026	4.18E-02	10.56	283.4	102.4	428.8	97.670	96.723
0.028	3.21E-02	10.75	217.4	104.3	436.6	99.134	98.213
0.030	2.57E-02	10.90	174.0	105.7	442.7	100.164	99.336
0.050	1.89E-02	12.02	128.4	116.6	488.0	108.491	107.080
0.070	1.71E-02	12.98	116.4	126.0	527.3	114.982	114.030
0.090	1.27E-02	13.76	86.32	133.5	558.9	120.271	119.230
0.110	8.10E-03	14.32	55.07	138.9	581.7	124.073	122.830
0.130	3.02E-03	14.59	20.66	141.6	592.8	125.177	123.870
0.150	1.15E-03	14.69	7.992	142.6	596.9	125.119	123.500
0.200	3.10E-04	14.77	2.316	143.4	600.3	123.882	121.670
1.000	2.83E-05	14.88	0.295	144.9	606.6	104.923	104.430
10.00	3.21E-06	15.09	0.042	148.4	621.2	32.490	25.516
100.0	6.25E-08	15.20	0.006	151.0	632.2	5.621	4.506
1000	2.45E-13	15.20	1.49E-04	152.3	637.5	0.000	0.000

[1)] Average values determined in accordance with results of RRC KI and VNIIEF calculations

[2)] Maximum power value is 6778 кВт (t=0.003 c)

[3)] Average radial value

Table E-4.2. Radial energy characteristics of fuel rod # RT4*

Parameters	Coordinates of fuel radial layers (mm)			
	1 layer (0.825-2.77)	2 layer (2.77-3.45)	3 layer (3.45-3.75)	4 layer (3.75-3.84)
Number of fissions $x10^{-14}$ (fiss)	6.702	4.402	2.759	1.333
Fission density $x10^{-13}$ (fiss/g fuel)	1.960	2.134	2.629	4.165
Power** (kW)	2990	1948	1238	600.5
Energy deposition (cal/g fuel)	146.0	155.1	191.7	288.5
Energy deposition (J/g fuel)	611.4	649.3	802.5	1208
Energy deposition*** (per-unit)	0.506	0.538	0.664	1.000

* Average values were determined in accordance with results of RRC KI and VNIIEF calculations

** The power for the entire length of each layer at time 0.003 s

*** Energy deposition in current layer/energy deposition in 4^{th} layer

RT4

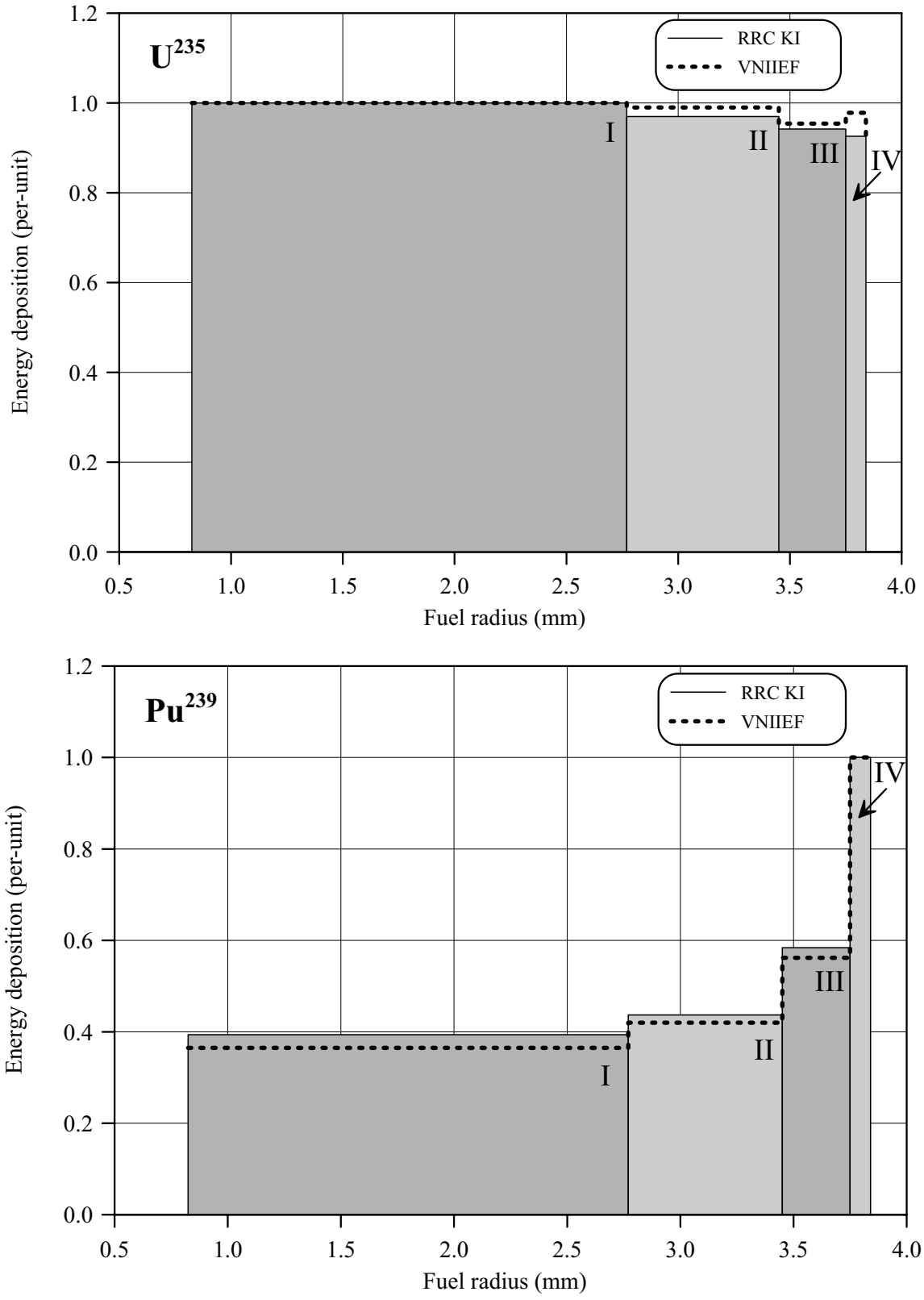
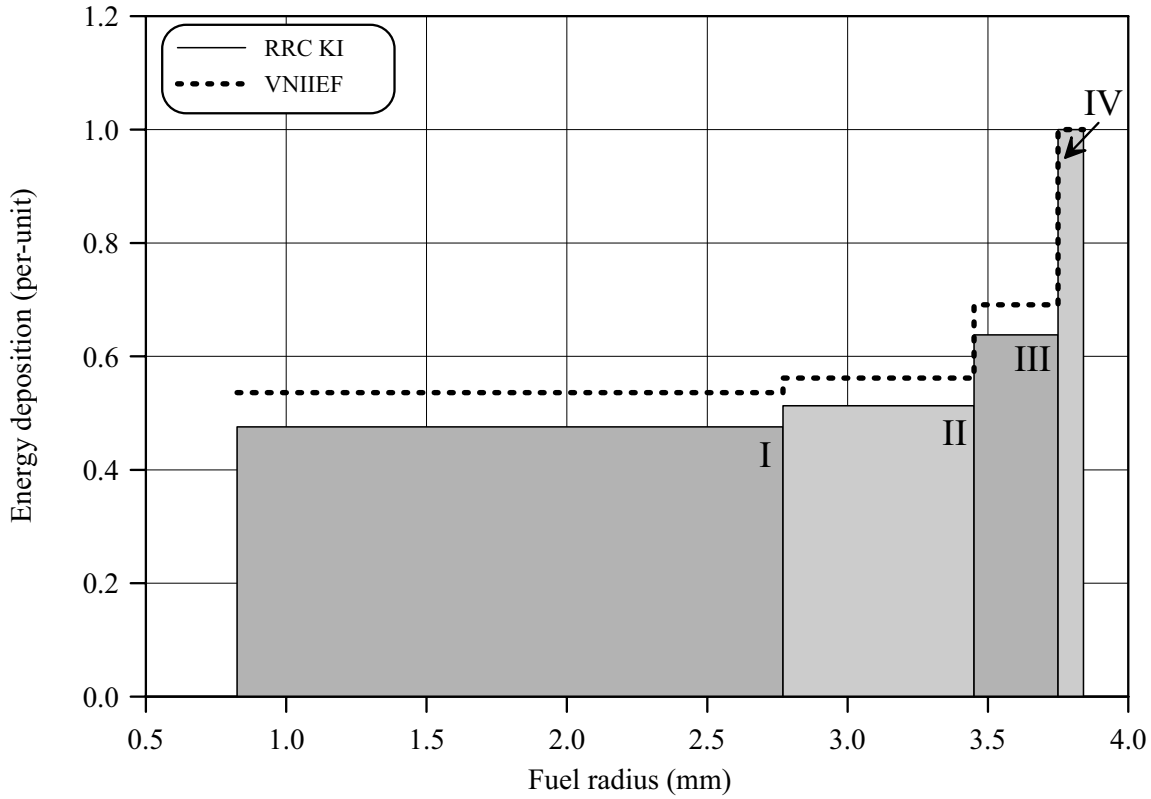


Fig.E-4.5. U^{235} and Pu^{239} radial distribution of energy deposition for fuel rod # RT4



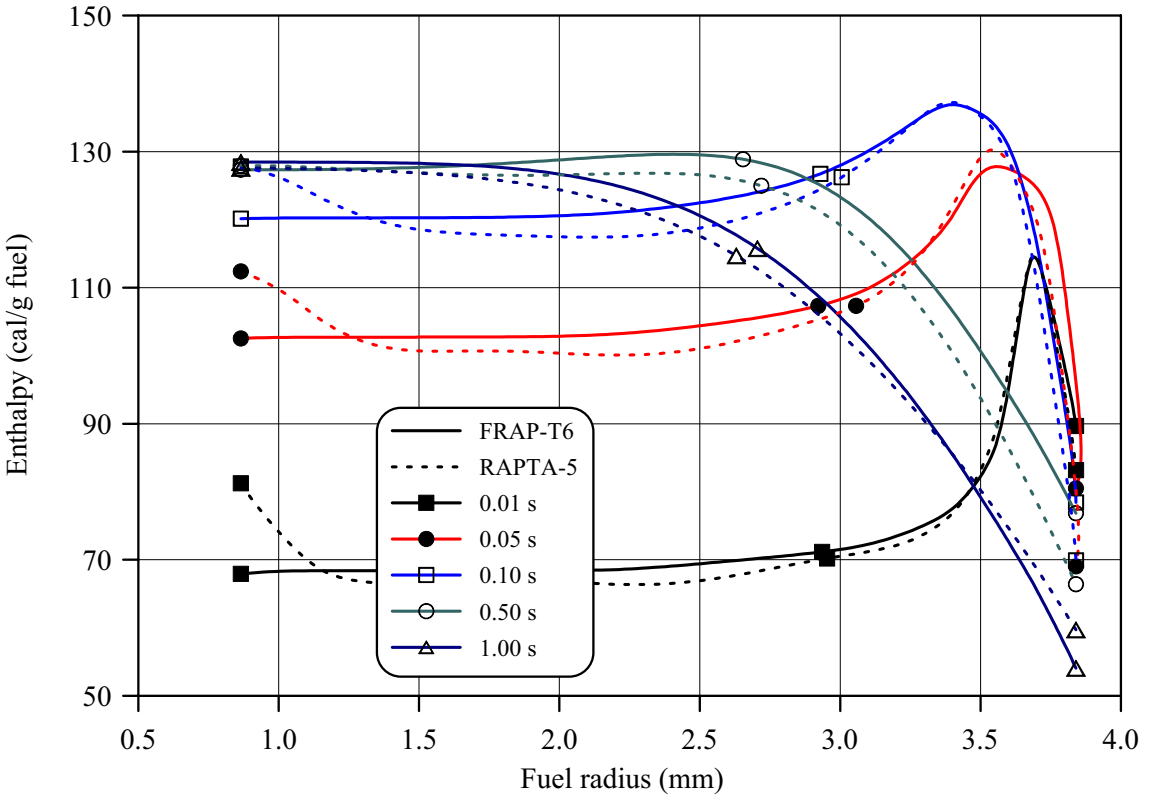


Fig.E-4.6. Radial distribution of energy deposition and fuel enthalpy for fuel rod # RT4

RT4

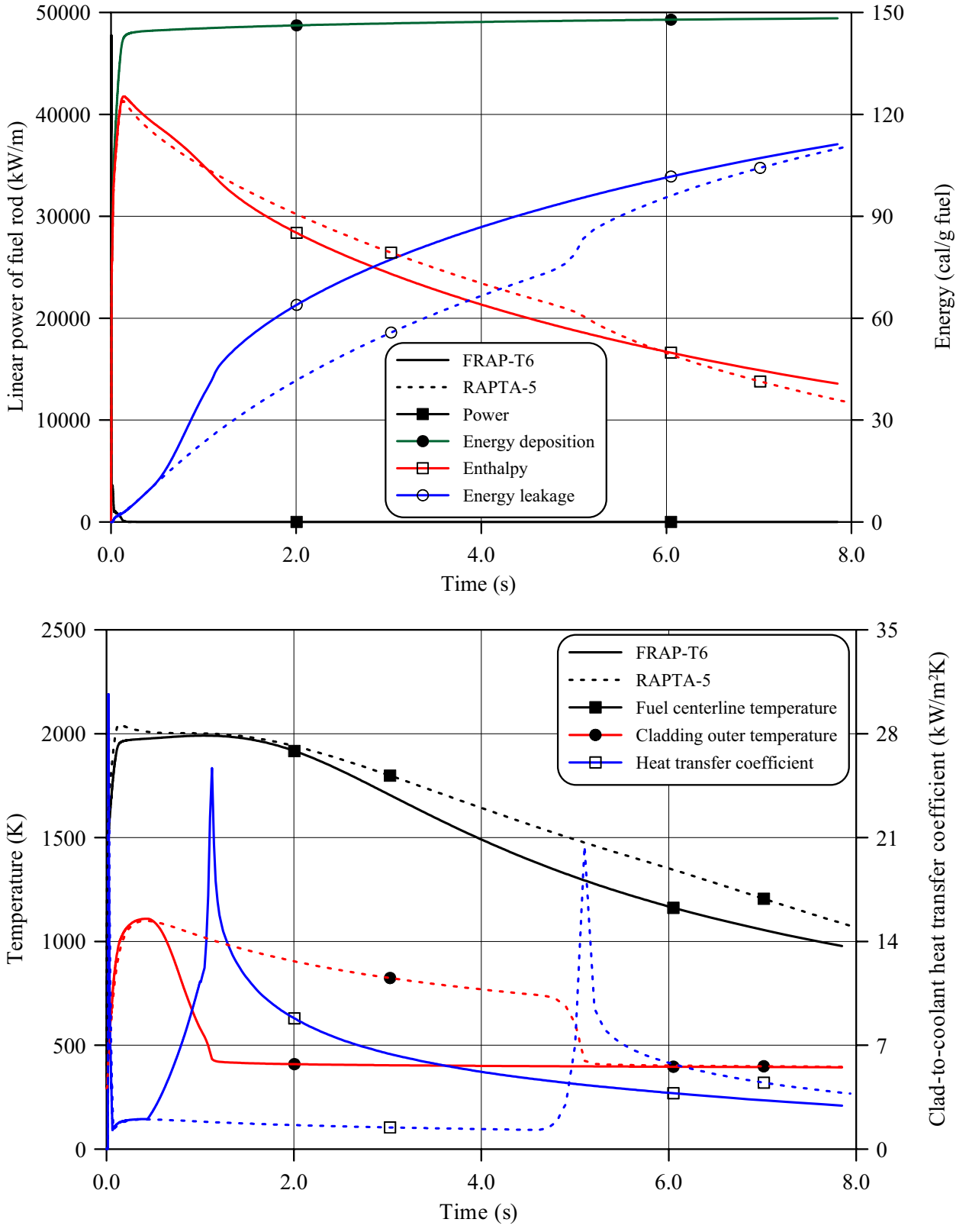


Fig.E-4.7. Thermal history of fuel rod # RT4 during the BIGR test in accordance with FRAP-T6/VVER and RAPTA-5 calculations

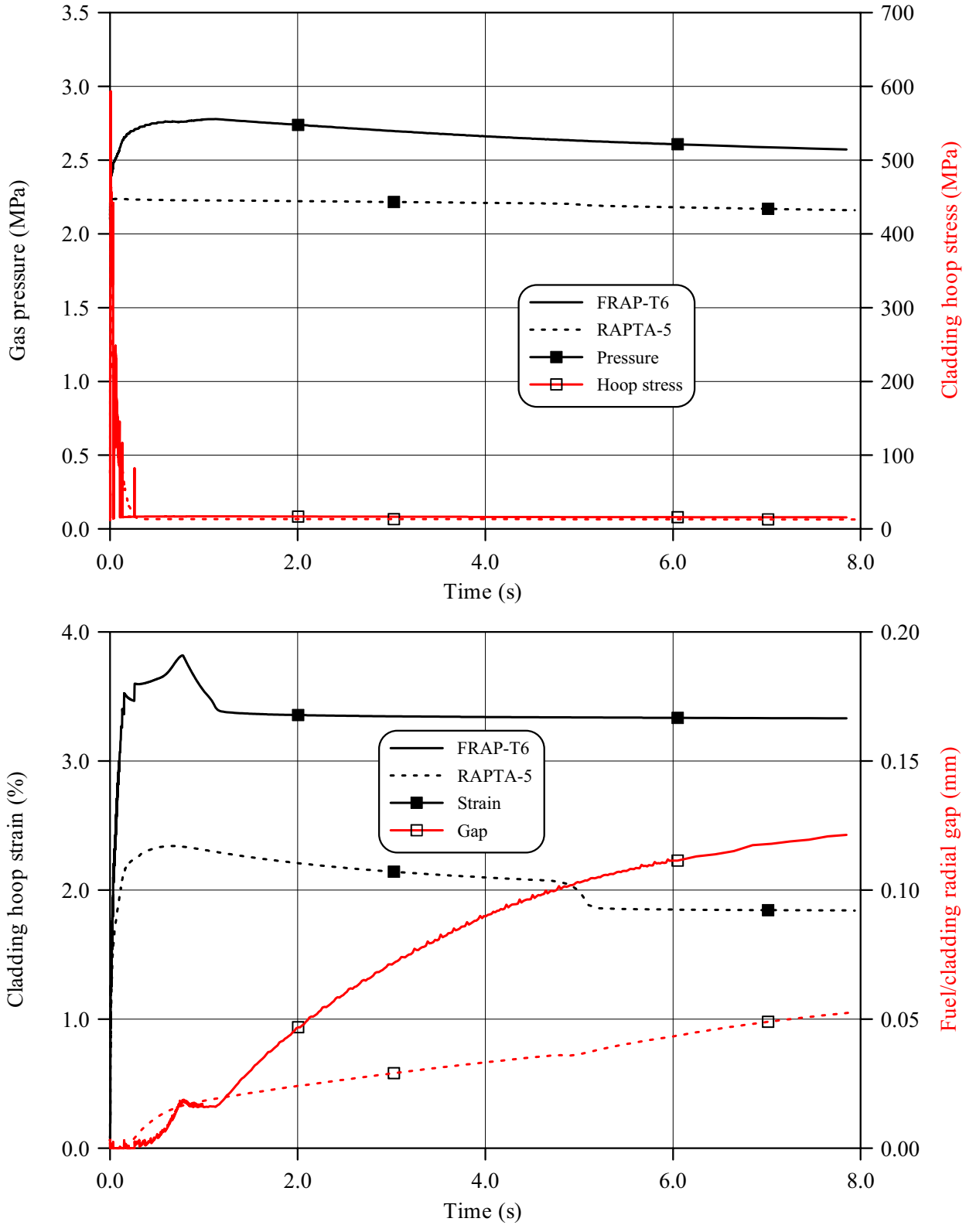


Fig.E-4.8. Mechanical behavior of fuel rod # RT4 during the BIGR test in accordance with FRAP-T6/VVER and RAPTA-5 calculations

RT4

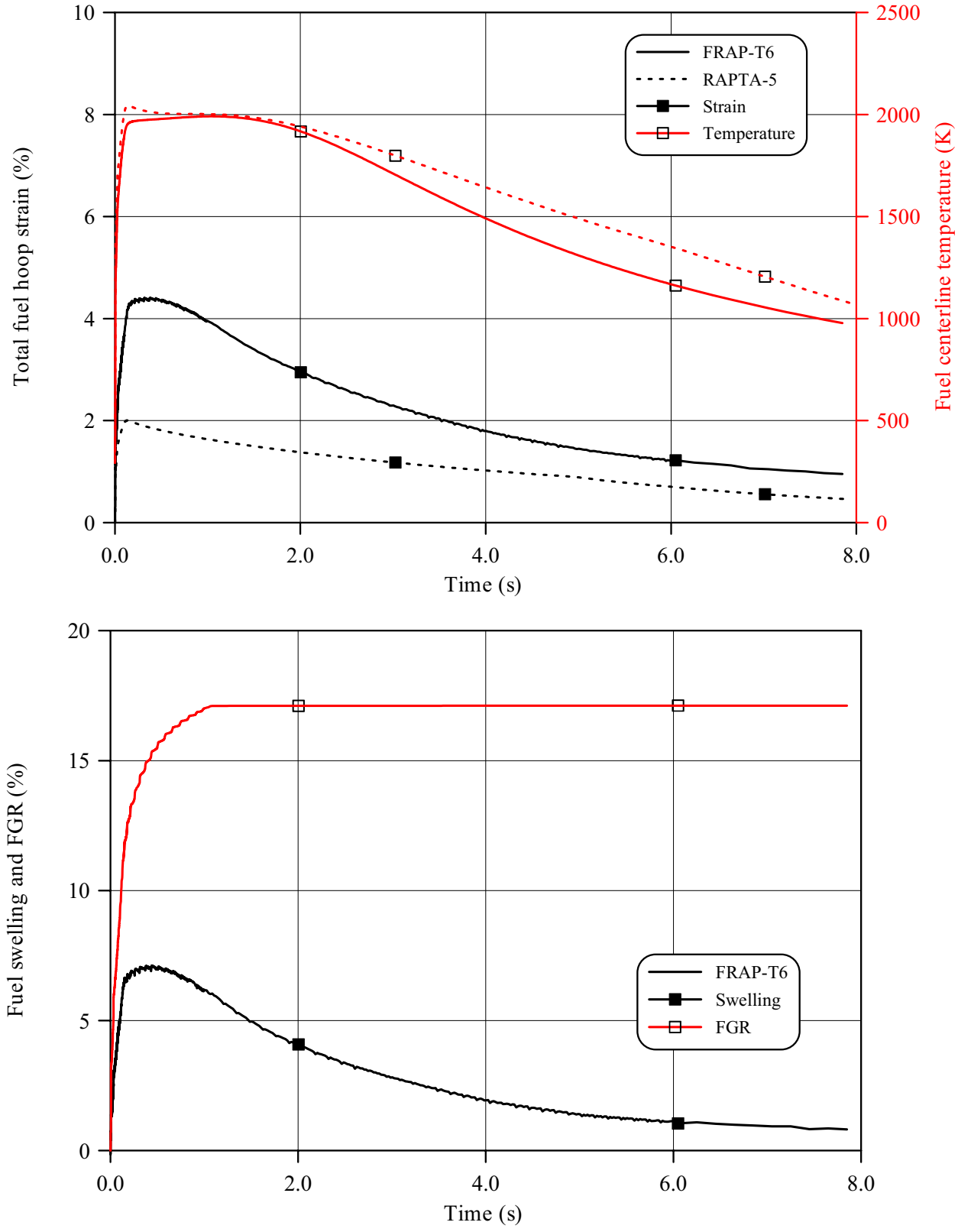


Fig.E-4.9. Fuel behavior during the BIGR test of fuel rod # RT4 in accordance with FRAP-T6/VVER and RAPTA-5 calculations

Table E-4.3. Axial distribution of cladding average outer diameter in fuel rod # RT4*

Axial coordinate (mm)	Cladding diameter (mm)	Axial coordinate (mm)	Cladding diameter (mm)	Axial coordinate (mm)	Cladding diameter (mm)	Axial coordinate (mm)	Cladding diameter (mm)
6	9.101	50	9.452	94	9.573	138	9.408
8	9.107	52	9.428	96	9.562	140	9.417
10	9.106	54	9.423	98	9.546	142	9.412
12	9.100	56	9.435	100	9.550	144	9.422
14	9.090	58	9.446	102	9.542	146	9.455
16	9.123	60	9.448	104	9.510	148	9.488
18	9.187	62	9.447	106	9.459	150	9.521
20	9.199	64	9.438	108	9.416	152	9.521
22	9.208	66	9.446	110	9.406	154	9.493
24	9.212	68	9.459	112	9.424	156	9.481
26	9.226	70	9.452	114	9.460	158	9.450
28	9.257	72	9.441	116	9.502	160	9.395
30	9.284	74	9.432	118	9.523	162	9.332
32	9.314	76	9.427	120	9.510	164	9.259
34	9.344	78	9.440	122	9.486	166	9.163
36	9.374	80	9.456	124	9.456	168	9.098
38	9.409	82	9.477	126	9.429	170	9.091
40	9.440	84	9.489	128	9.412	172	9.088
42	9.465	86	9.494	130	9.394	174	9.098
44	9.494	88	9.521	132	9.382	176	9.100
46	9.503	90	9.556	134	9.381	178	9.121
48	9.482	92	9.568	136	9.392	180	9.317

* Measured value determined on the basis of profilometry data (16 azimuthal directions)

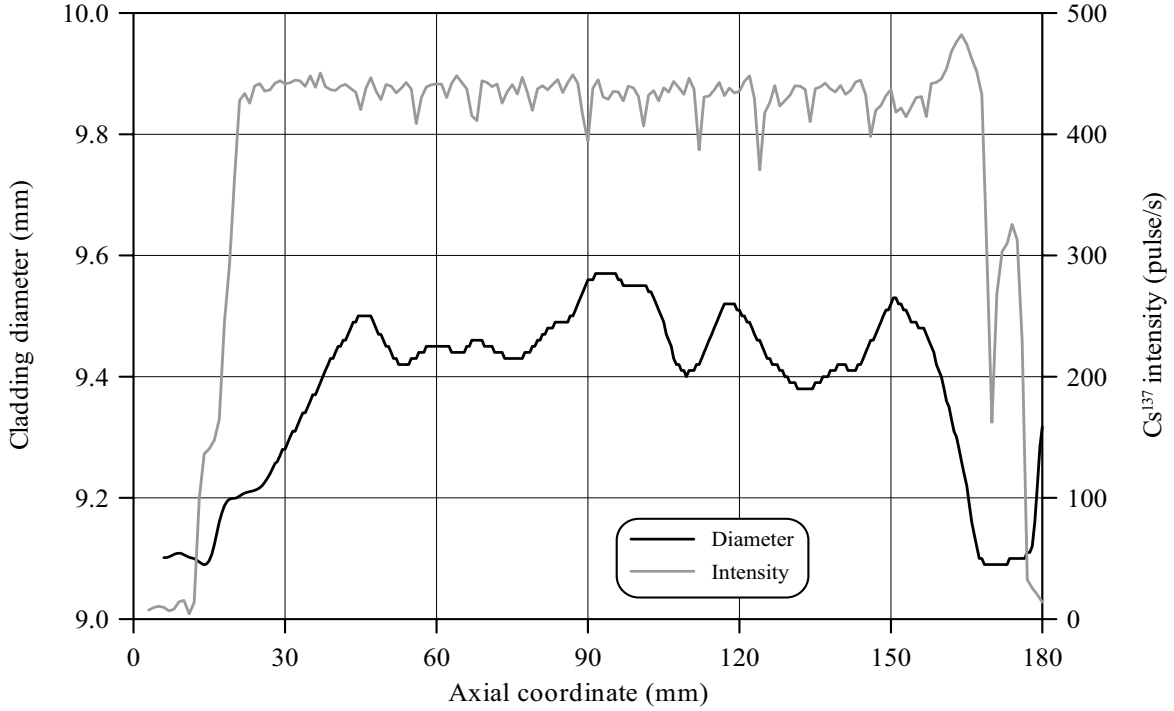


Fig.E-4.10. Cladding measured average diameter and γ-scanning results for fuel rod # RT4

RT4

Table E-4.4. The PIE results for fuel rod # RT4

Parameter		Value
1.	Cladding outer diameter (mm):	
1.1.	Maximum diameter of the bidimensional data sample in "fuel rod length - azimuthal angle" coordinates (mm)	9.65
1.2.	Averaged azimuthal diameter and maximum diameter along the length selected from the sample of averaged azimuthal diameter (mm)	9.58
1.3.	Averaged diameter of the bidimensional data sample in "fuel rod length - azimuthal angle" coordinates (mm)	9.41
2.	Cladding maximum residual hoop strain (%)	5.50
3.	Fuel pellet conditional diameter (mm) in cross-section*:	
	at 108 mm elevation	7.98
	at 117 mm elevation	7.88
4.	ZrO_2 outer thickness (μm) in cross-section:	
	at 108 mm elevation	3-5
	at 117 mm elevation	3-5
5.	ZrO_2 inner thickness (μm) in cross-section:	
	at 108 mm elevation	6
	at 117 mm elevation	8
6.	Parameters characterizing FGR:	
6.1.	Gas composition (% by volume):	
	He	-
	N_2	-
	O_2	-
	Ar	-
	CO_2	-
	Kr	-
	Xe	-
6.2.	Free gas volume (cm^3)	-
6.3.	Gas volume under normal conditions (cm^3)	-
6.4.	Gas pressure under normal conditions (MPa)	-

* Reference value determined by the processing of fuel cross-section photographs

Table E-4.5. Organized BIGR test results for fuel rod # RT4

Parameter		Unit	Value		
			Measured	Calculated	
				FRAP-T6	RAPTA-5
1.	Fuel burnup	MW d/kg U	60.1	60.1	60.1
2.	Initial gas pressure	MPa	2.1	2.1	2.1
3.	Energy deposition	cal/g fuel	152.3	152.3	152.3
4.	Peak fuel enthalpy*	cal/g fuel	-	125.3	123.9
5.	Fuel maximum temperature	K	-	2099	2126
6.	Maximum temperature of cladding outer surface	K	-	1110	1099
7.	Cladding burst	Failed, Unfailed	Unfailed	Unfailed	Unfailed
8.	Cladding residual hoop strain**	%	3.70	3.23	1.77
9.	Kr volume content in gas composition after the BIGR test	%	-	2.81	-
10.	Xe volume content in gas composition after the BIGR test	%	-	16.82	-

* Average value of peak fuel enthalpy is 124.6 cal/g fuel

** Average value along the fuel stack length

Appendix E–5

Individual Characteristics of Fuel Rod # RT5

after the BIGR Test

RT5

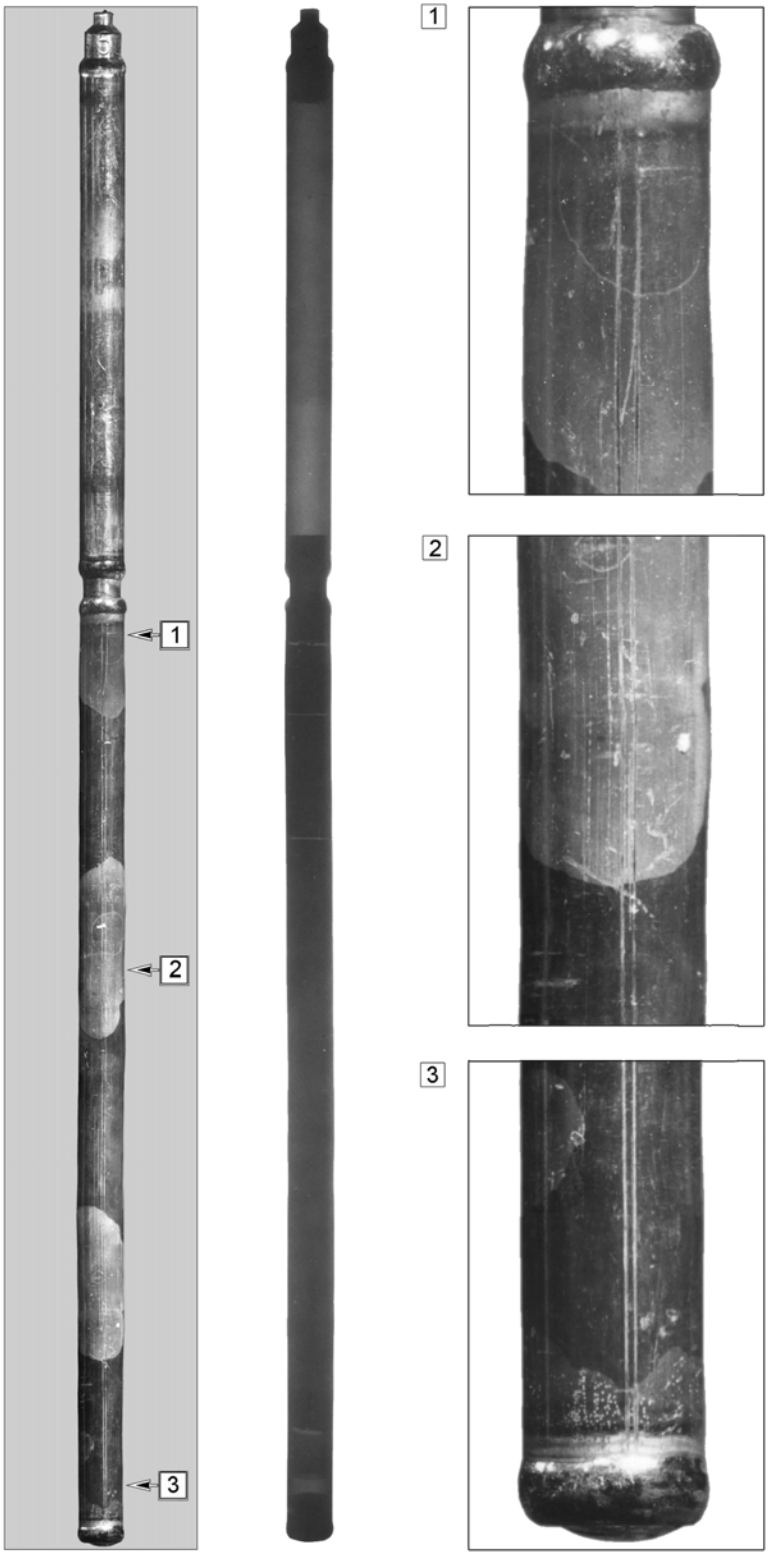


Fig.E-5.1. Appearance of unfailed fuel rod # RT5 after the BIGR test (photographs and X-ray photograph)

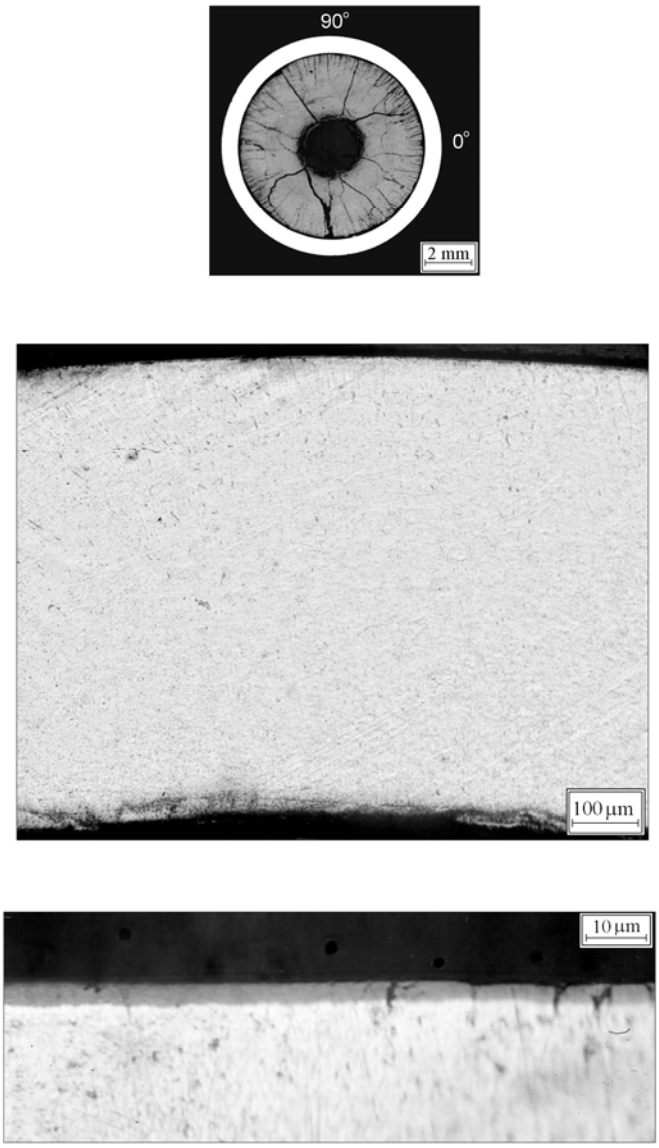


Fig.E-5.2. Cross-section and cladding microstructure of fuel rod # RT5 at 105 mm elevation (from low cap)

RT5

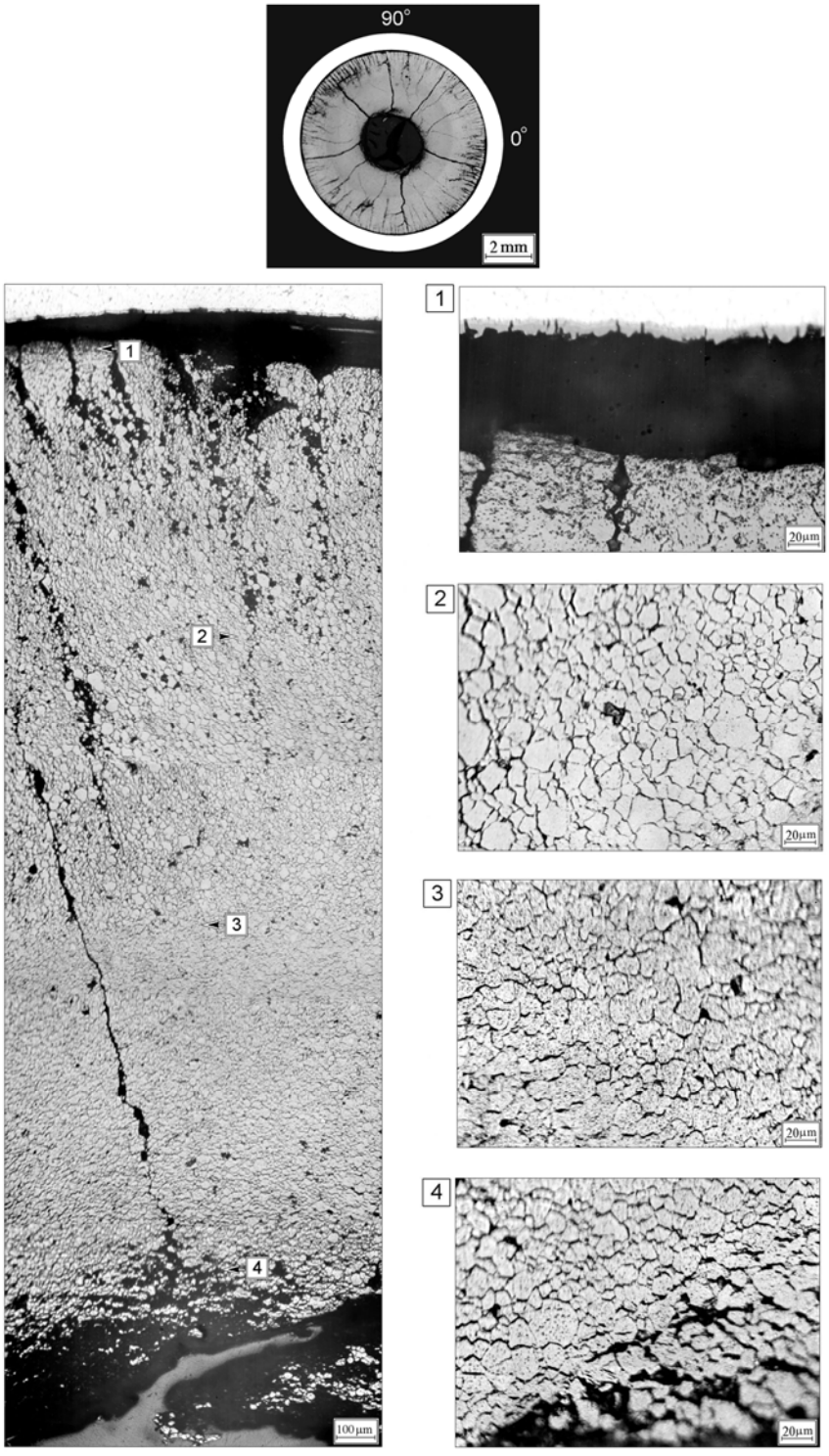


Fig.E-5.3. Cross-section and fuel microstructure of fuel rod # RT5 at 105 mm elevation (from low cap)

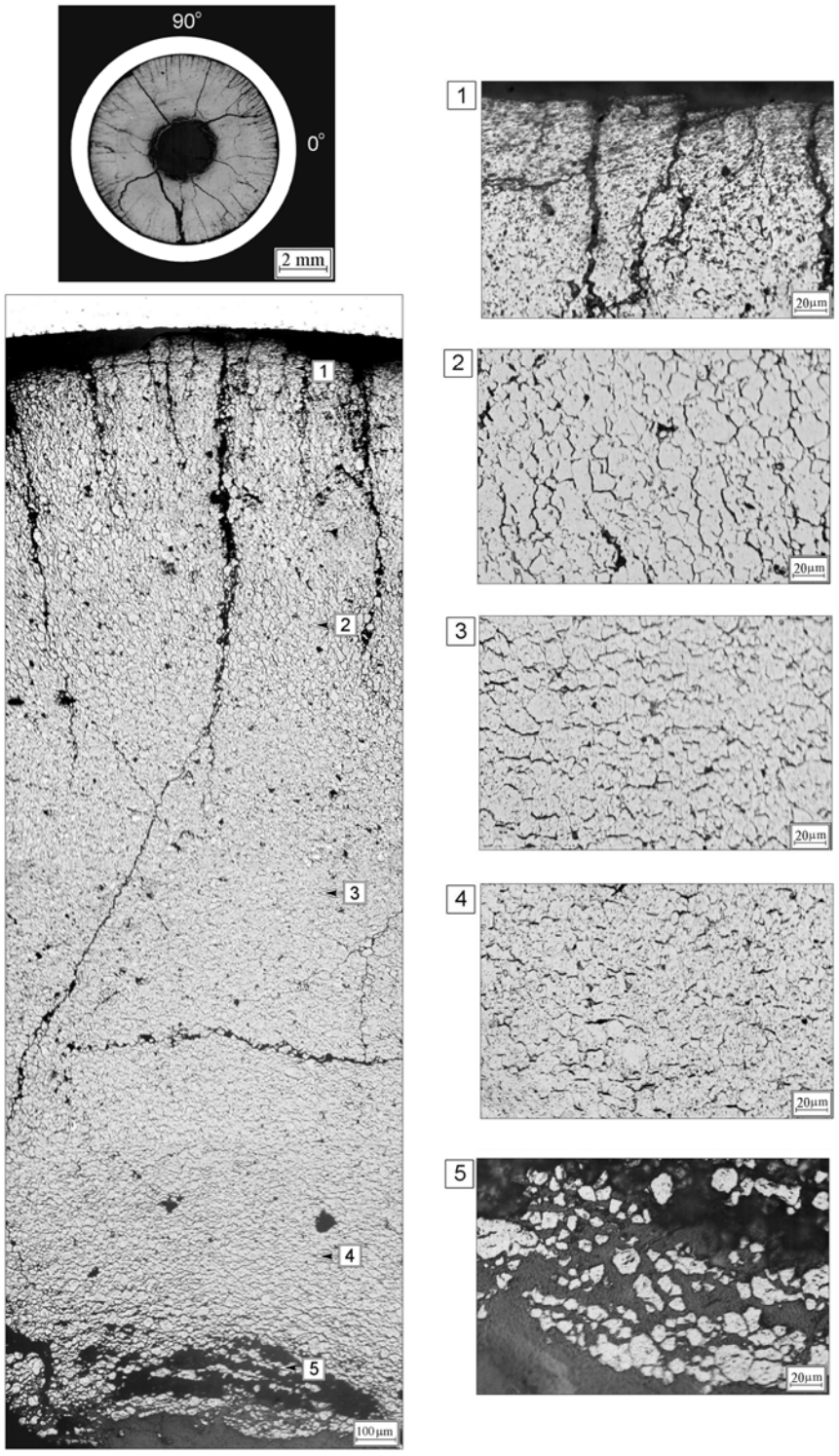


Fig.E-5.4. Cross-section and fuel microstructure of fuel rod # RT5 after the BIGR test at 122 mm elevation (from low cap)

RT5

Table E-5.1. Time dependent energy characteristics of fuel rod # RT5

Time (s)	Relative reactor power (current/ maximum value) (per-unit)	Cumulative number of fissions in fuel rod (fiss) x10^{-14}	Power of fuel rod[1)2)] (kW)	Energy deposition		Fuel enthalpy[3)]	
				(cal/g fuel)	(J/g fuel)	FRAP-T6	RAPTA-5
0.000	1.74E-02	0.000	0.000	0.000	0.000	0.000	0.000
0.001	1.90E-01	0.287	1455	3.009	12.60	3.560	2.884
0.002	5.90E-01	1.377	4520	14.46	60.52	15.511	14.376
0.003	1.00E+00	3.803	7661	39.97	167.3	41.007	39.902
0.004	6.53E-01	6.297	5005	66.17	277.0	66.919	65.870
0.005	2.69E-01	7.583	2061	79.70	333.7	80.280	78.956
0.006	1.46E-01	8.172	1121	85.91	359.7	86.224	84.688
0.007	7.73E-02	8.482	591.8	89.17	373.3	89.159	87.538
0.008	5.38E-02	8.673	411.8	91.14	381.6	90.806	89.143
0.009	4.52E-02	8.816	346.1	92.64	387.9	92.001	90.323
0.010	4.49E-02	8.948	344.0	94.03	393.7	93.086	91.409
0.012	5.30E-02	9.231	406.1	97.02	406.2	95.520	93.875
0.014	6.55E-02	9.583	501.5	100.7	421.5	98.613	96.972
0.016	7.41E-02	9.995	567.8	105.0	439.6	102.367	100.780
0.018	7.28E-02	10.42	557.8	109.5	458.6	106.351	104.820
0.020	6.12E-02	10.82	468.9	113.8	476.3	109.976	108.800
0.022	4.91E-02	11.15	376.0	117.2	490.5	112.797	111.730
0.024	3.90E-02	11.40	298.9	119.9	501.8	115.005	113.980
0.026	2.98E-02	11.60	228.6	122.0	510.7	116.645	115.540
0.028	2.41E-02	11.76	185.0	123.6	517.5	117.847	116.750
0.030	2.22E-02	11.90	170.4	125.0	523.4	118.850	117.940
0.050	1.85E-02	13.14	142.0	138.1	578.3	128.238	127.630
0.070	1.62E-02	14.18	124.2	149.1	624.2	135.808	135.660
0.090	1.15E-02	14.99	88.35	157.6	660.0	141.600	141.310
0.110	6.98E-03	15.54	53.63	163.5	684.4	145.075	144.810
0.130	2.60E-03	15.81	20.14	166.2	695.9	146.269	145.590
0.150	9.92E-04	15.91	7.801	167.2	700.2	146.280	144.940
0.200	2.67E-04	15.98	2.270	168.1	703.9	144.671	142.520
1.000	2.44E-05	16.09	0.294	169.7	710.5	123.856	121.150
10.00	2.76E-06	16.29	0.043	173.6	726.8	31.755	28.725
100.0	5.38E-08	16.39	0.007	176.5	739.0	5.054	4.463
1000	2.11E-13	16.39	1.52E-04	178.0	745.3	0.000	0.000

[1)] Average values determined in accordance with results of RRC KI and VNIIEF calculations

[2)] Maximum power value is 7660.5 kW (t=0.003 s)

[3)] Average radial value

Table E-5.2. Radial energy characteristics of fuel rod # RT5*

Parameters	Coordinates of fuel radial layers (mm)			
	1 layer (1.25-2.84)	2 layer (2.84-3.47)	3 layer (3.47-3.74)	4 layer (3.74-3.808)
Number of fissions $x10^{-14}$ (fiss)	7.363	4.783	2.872	1.381
Fission density $x10^{-13}$ (fiss/g fuel)	2.341	2.493	3.068	4.513
Power** (kW)	3414	2238	1346	662.4
Energy deposition (cal/g fuel)	156.4	166.0	203.8	299.2
Energy deposition (J/g fuel)	654.8	695.0	853.2	1253
Energy deposition*** (per-unit)	0.523	0.555	0.681	1.000

* Average values were determined in accordance with results of RRC KI and VNIIEF calculations

** The power for the entire length of each layer at time 0.003 s

*** Energy deposition in current layer/energy deposition in 4^{th} layer

RT5

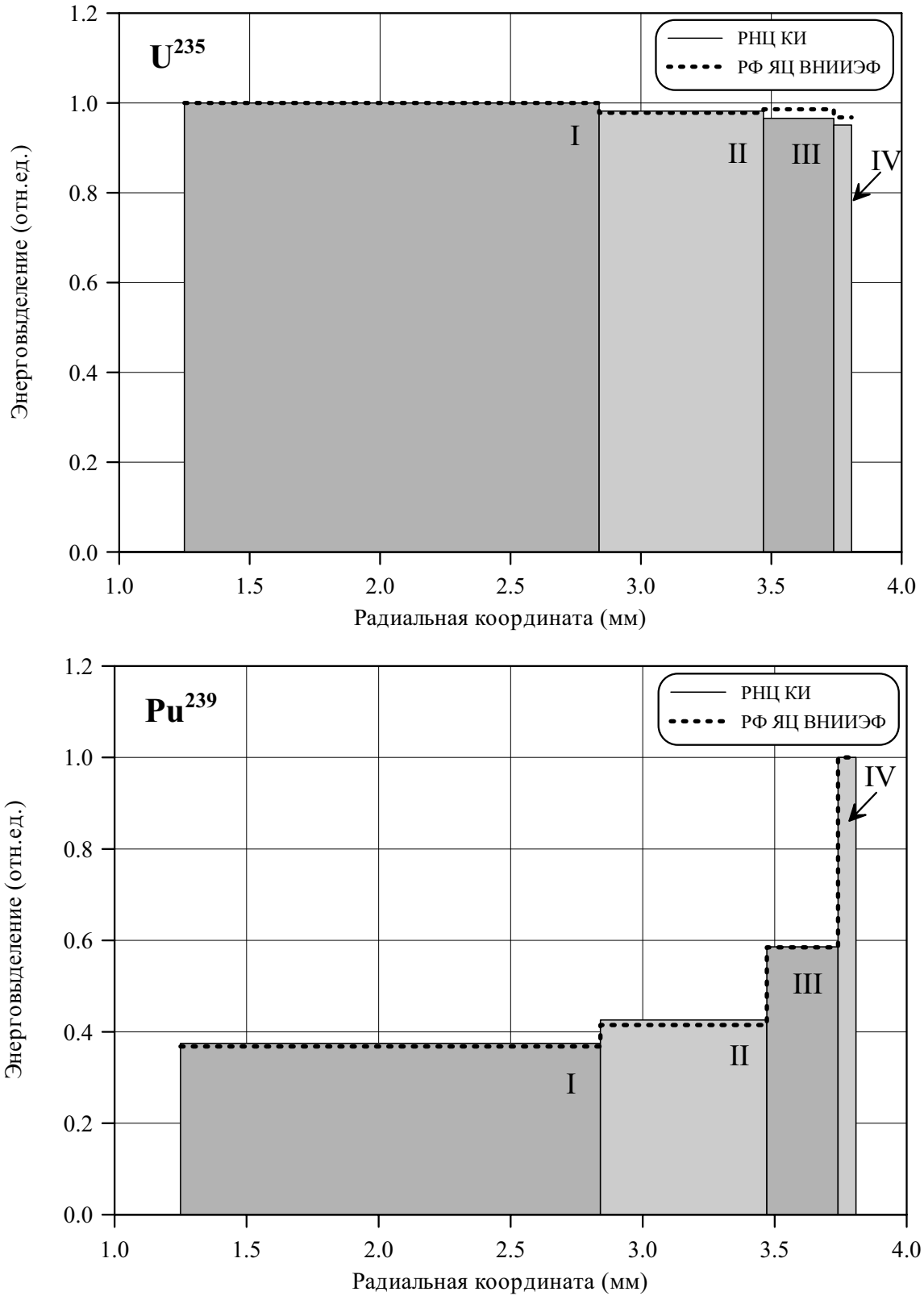


Fig.E-5.5. U^{235} and Pu^{239} radial distribution of energy deposition for fuel rod # RT5

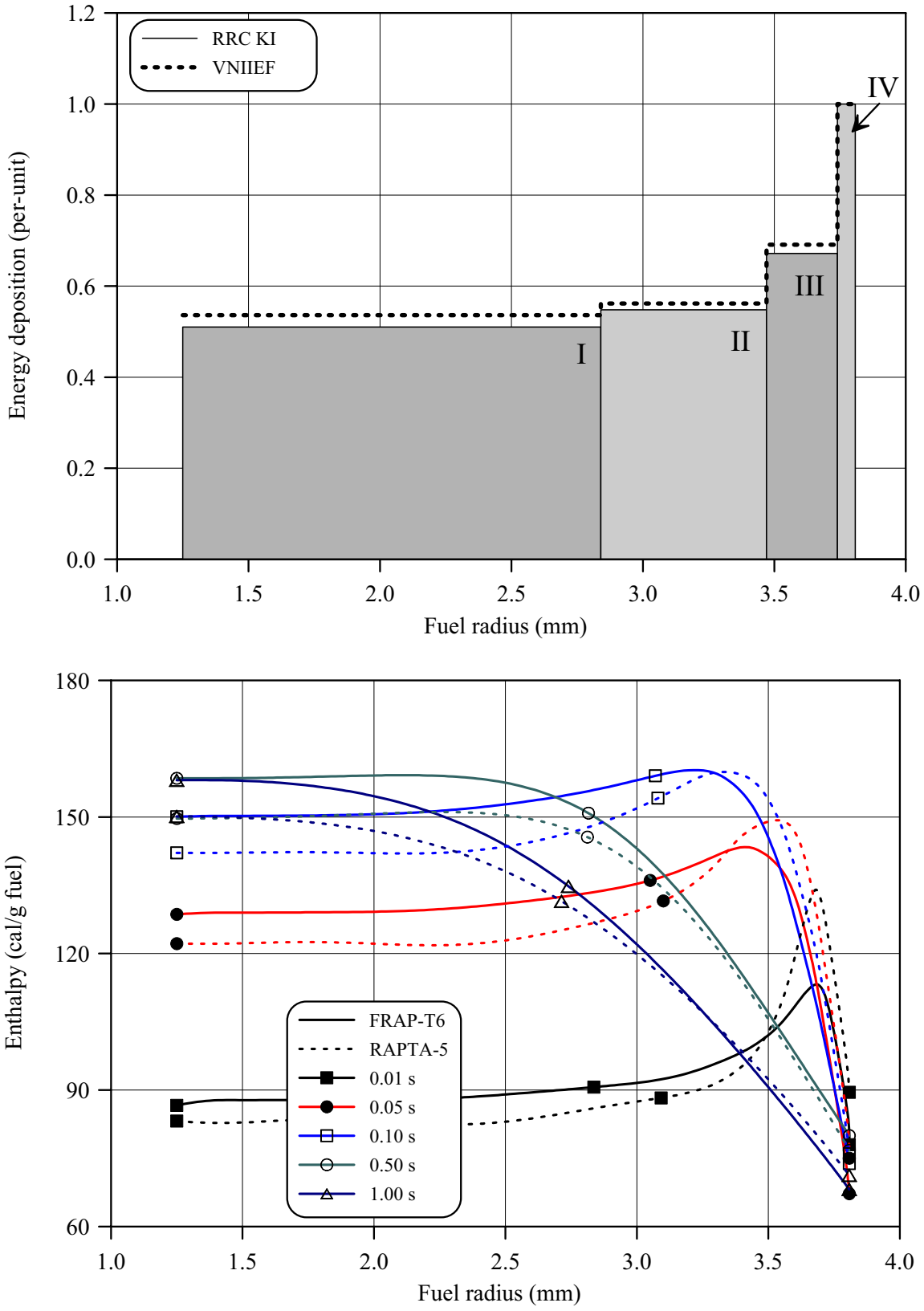


Fig.E-5.6. Radial distribution of energy deposition and fuel enthalpy for fuel rod # RT5

RT5

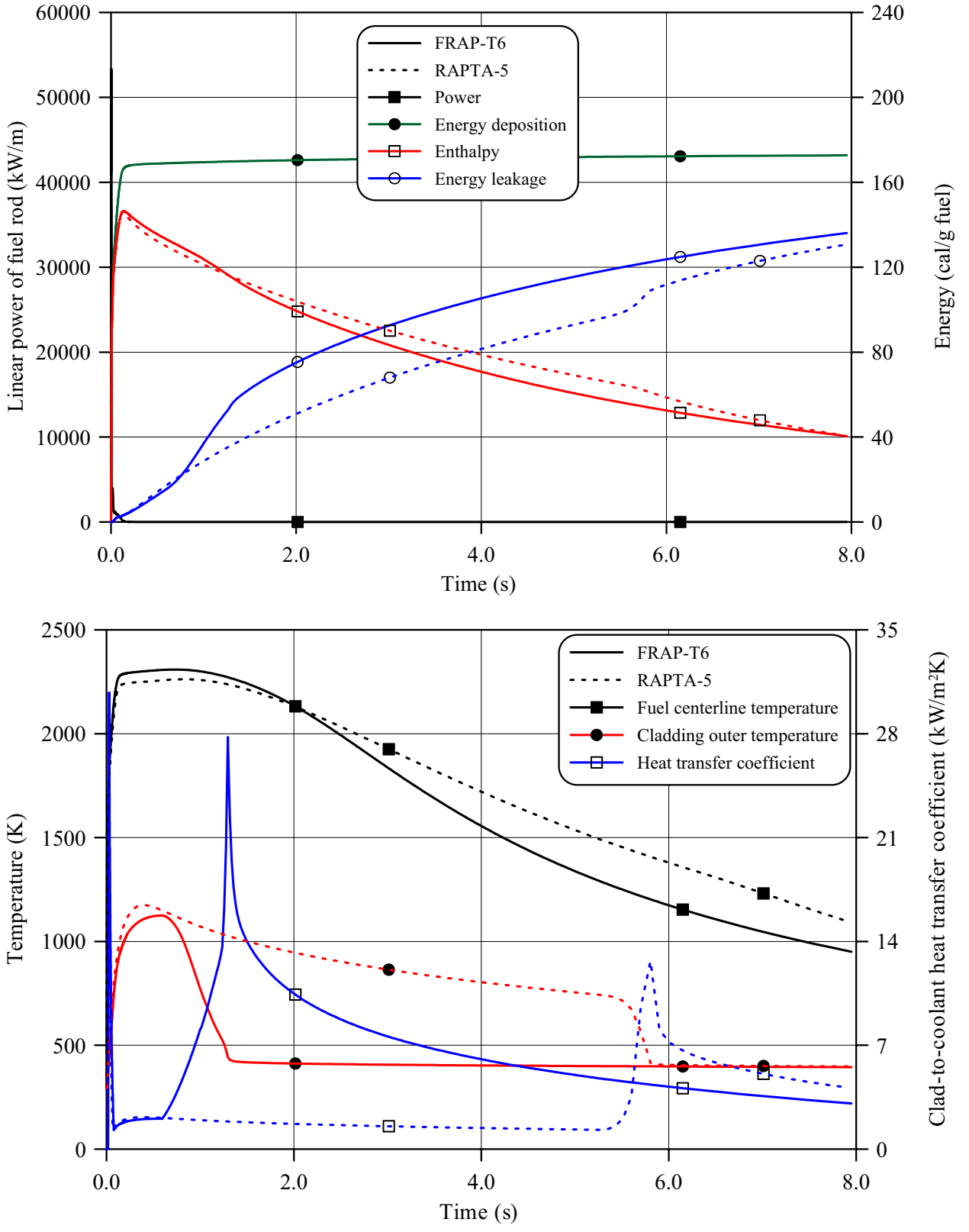


Fig.E-5.7. Thermal history of fuel rod # RT5 during the BIGR test in accordance with FRAP-T6/VVER and RAPTA-5 calculations

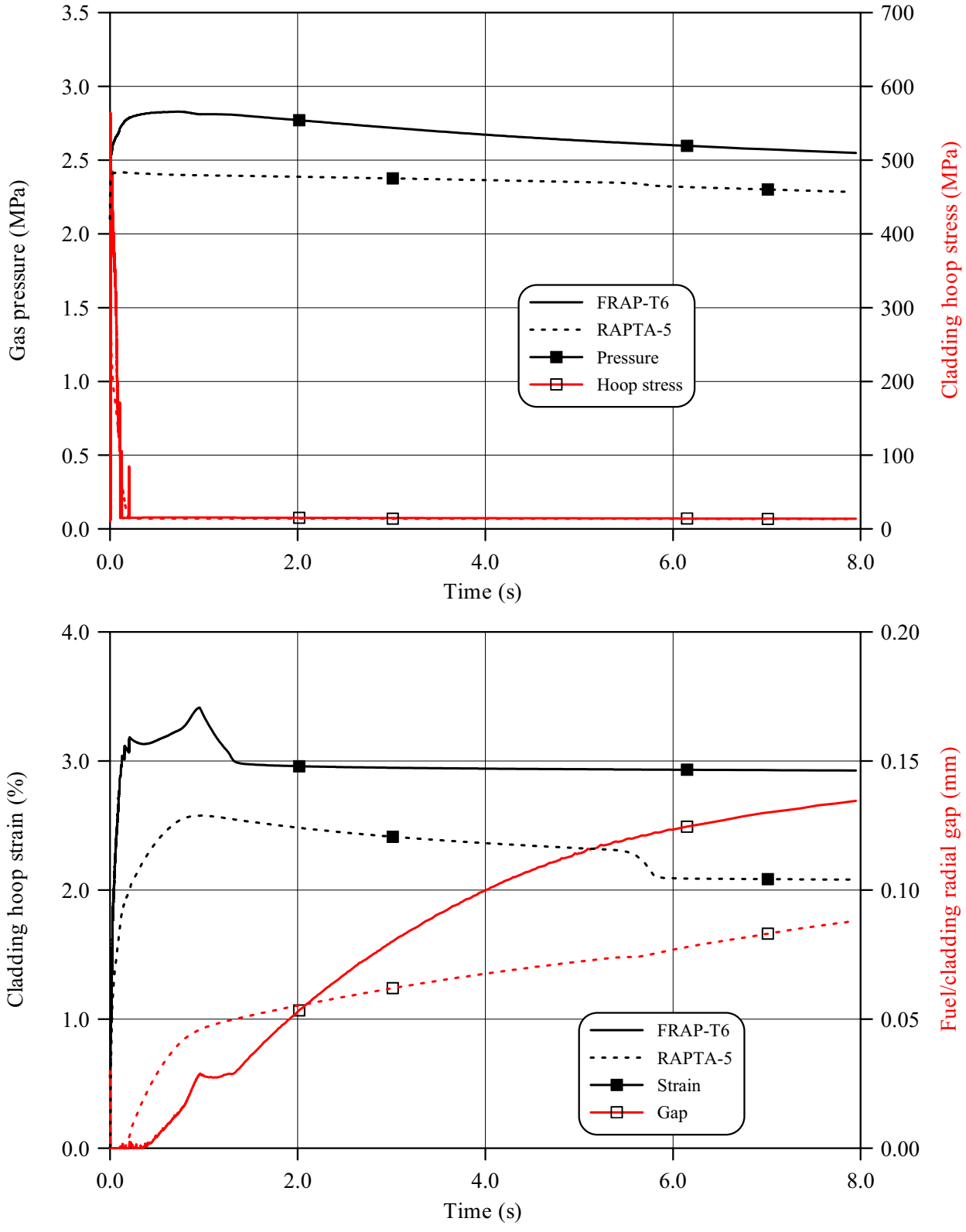


Fig.E-5.8. Mechanical behavior of fuel rod # RT5 during the BIGR test in accordance with FRAP-T6/VVER and RAPTA-5 calculations

RT5

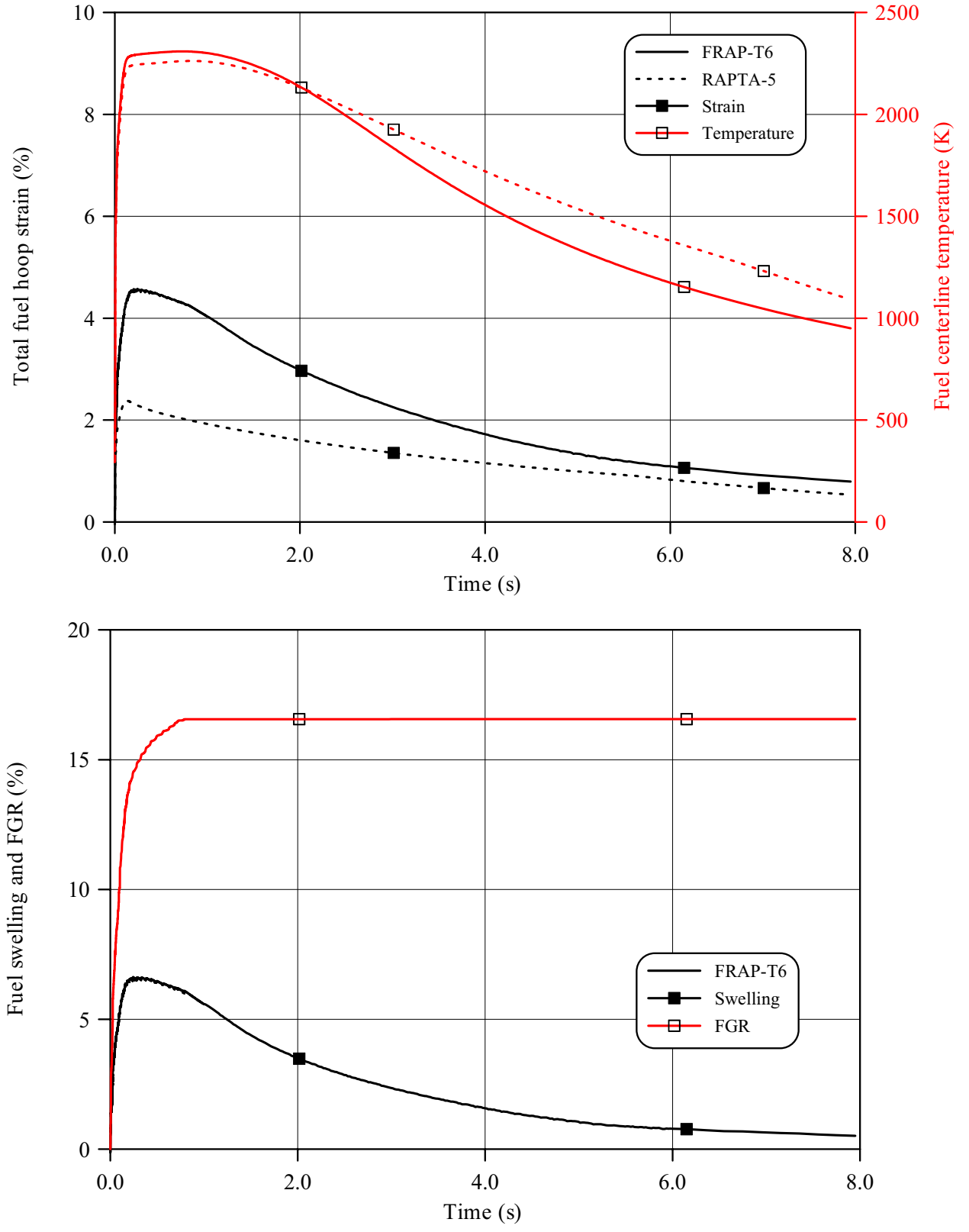


Fig.E-5.9. Fuel behavior during the BIGR test of fuel rod # RT5 in accordance with FRAP-T6/VVER and RAPTA-5 calculations

Table E-5.3. Axial distribution of cladding average outer diameter in fuel rod # RT5*

Axial coordinate (mm)	Cladding diameter (mm)	Axial coordinate (mm)	Cladding diameter (mm)	Axial coordinate (mm)	Cladding diameter (mm)	Axial coordinate (mm)	Cladding diameter (mm)
6	9.064	50	9.415	94	9.273	138	9.287
8	9.066	52	9.387	96	9.259	140	9.287
10	9.068	54	9.376	98	9.255	142	9.269
12	9.065	56	9.404	100	9.259	144	9.247
14	9.063	58	9.406	102	9.310	146	9.227
16	9.060	60	9.377	104	9.356	148	9.249
18	9.068	62	9.323	106	9.376	150	9.293
20	9.123	64	9.278	108	9.353	152	9.311
22	9.176	66	9.247	110	9.314	154	9.307
24	9.209	68	9.277	112	9.272	156	9.287
26	9.227	70	9.328	114	9.273	158	9.266
28	9.229	72	9.392	116	9.279	160	9.285
30	9.231	74	9.402	118	9.281	162	9.330
32	9.276	76	9.370	120	9.274	164	9.345
34	9.330	78	9.368	122	9.255	166	9.322
36	9.385	80	9.400	124	9.263	168	9.269
38	9.401	82	9.386	126	9.287	170	9.178
40	9.389	84	9.335	128	9.290	172	9.074
42	9.376	86	9.291	130	9.288	174	9.043
44	9.402	88	9.256	132	9.273	176	9.053
46	9.428	90	9.256	134	9.250	178	9.231
48	9.434	92	9.276	136	9.264	180	9.337

* Measured value determined on the basis of profilometry data (16 azimuthal directions)

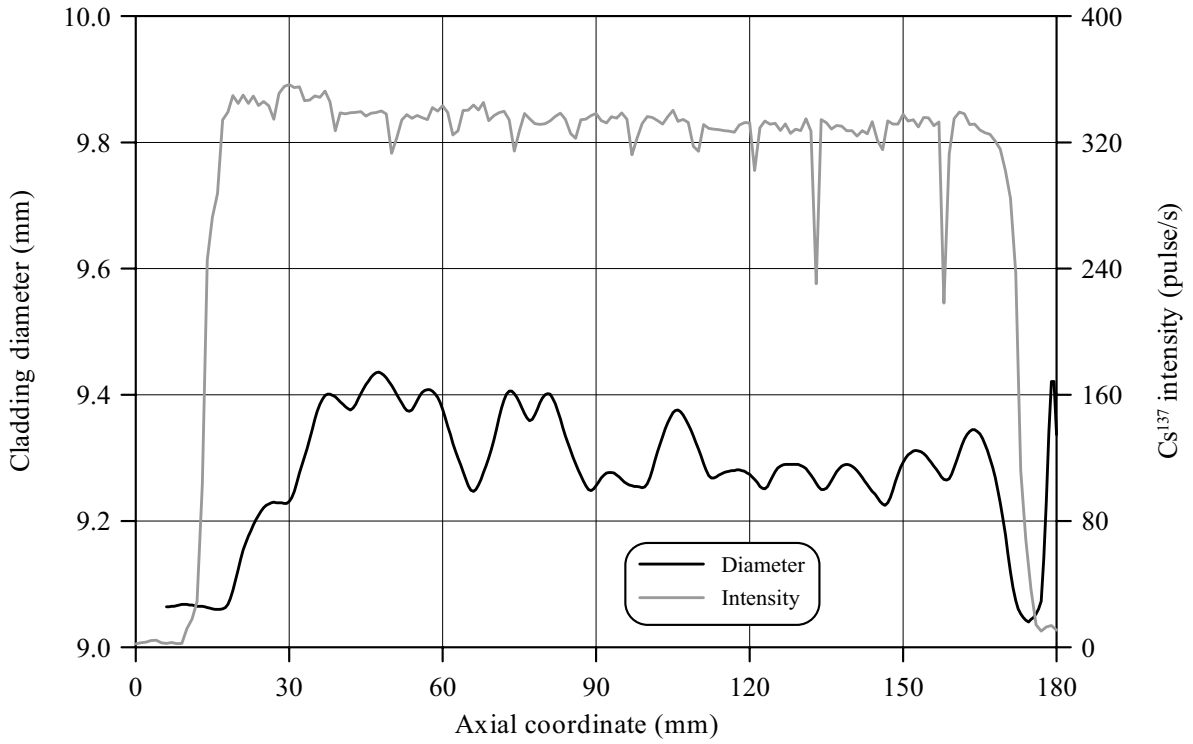


Fig.E-5.10. Cladding measured average diameter and γ-scanning results for fuel rod # RT5

RT5

Table E-5.4. The PIE results for fuel rod # RT5

	Parameter		Value
1.	Cladding outer diameter (mm):		
1.1.	Maximum diameter of the bidimensional data sample in "fuel rod length - azimuthal angle" coordinates (mm)		9.49
1.2.	Averaged azimuthal diameter and maximum diameter along the length selected from the sample of averaged azimuthal diameter (mm)		9.44
1.3.	Averaged diameter of the bidimensional data sample in "fuel rod length - azimuthal angle" coordinates (mm)		9.30
2.	Cladding maximum residual hoop strain (%)		4.20
3.	Fuel pellet conditional diameter (mm) in cross-section*:		
		at 105 mm elevation	7.72
		at 122 mm elevation	7.76
4.	ZrO_2 outer thickness (μm) in cross-section:		
		at 105 mm elevation	3-5
		at 122 mm elevation	3-5
5.	ZrO_2 inner thickness (μm) in cross-section:		
		at 105 mm elevation	7
6.	Parameters characterizing FGR:		
6.1.	Gas composition (% by volume):		
		He	81.16
		N_2	0.52
		O_2	0.033
		Ar	0.017
		CO_2	0.01
		Kr	1.52
		Xe	16.75
6.2.	Free gas volume (cm^3)		6.2
6.3.	Gas volume under normal conditions (cm^3)		138.7
6.4.	Gas pressure under normal conditions (MPa)		2.24
6.5.	FGR (%)		26.00

* Reference value determined by the processing of fuel cross-section photographs

Table E-5.5. Organized BIGR test results for fuel rod # RT5

Parameter		Unit	Value		
			Measured	Calculated	
				FRAP-T6	RAPTA-5
1.	Fuel burnup	MW d/kg U	48.6	48.6	48.6
2.	Initial gas pressure	MPa	2.1	2.1	2.1
3.	Energy deposition	cal/g fuel	178.0	178.0	178.0
4.	Peak fuel enthalpy*	cal/g fuel	-	146.4	145.6
5.	Fuel maximum temperature	K	-	2353	2379
6.	Maximum temperature of cladding outer surface	K	-	1125	1175
7.	Cladding burst	Failed, Unfailed	Unfailed	Unfailed	Unfailed
8.	Cladding residual hoop strain**	%	2.70	2.83	2.01
9.	Kr volume content in gas composition after the BIGR test	%	1.52	1.87	-
10.	Xe volume content in gas composition after the BIGR test	%	16.75	11.18	-

* Average value of peak fuel enthalpy is 146.0 cal/g fuel

** Average value along the fuel stack length

Appendix E–6

Individual Characteristics of Fuel Rod # RT6

after the BIGR Test

RT6

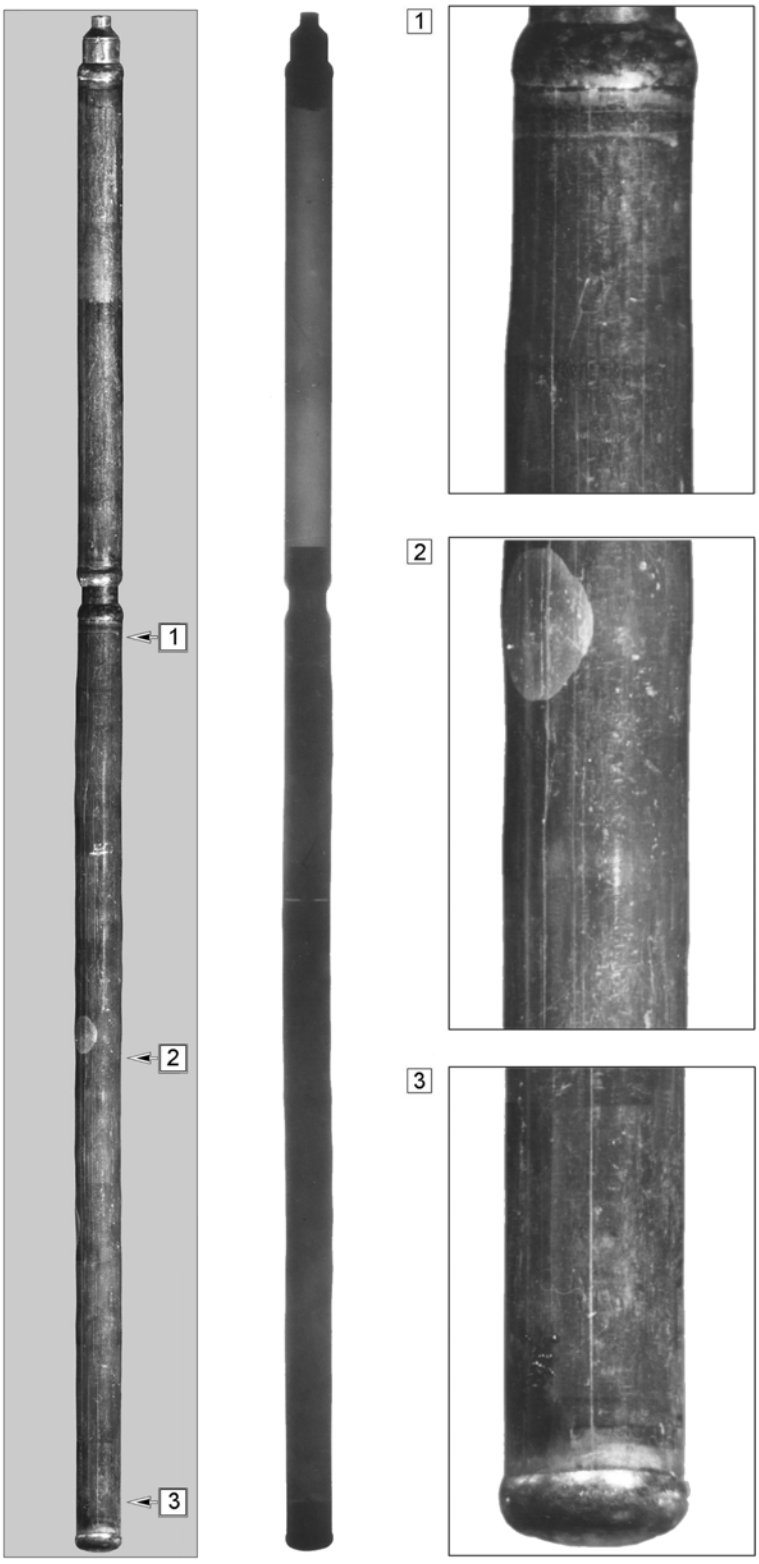


Fig.E-6.1. Appearance of unfailed fuel rod # RT6 after the BIGR test (photographs and X-ray photograph)

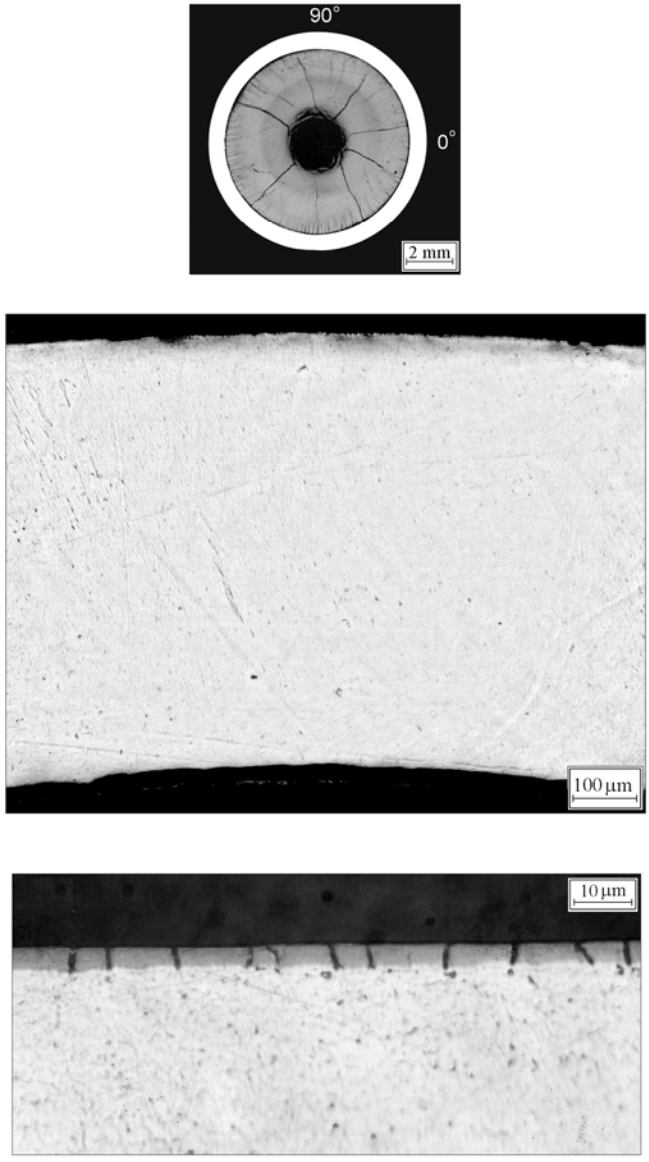


Fig.E-6.2. Cross-section and cladding microstructure of fuel rod # RT6 at 114 mm elevation (from low cap)

RT6

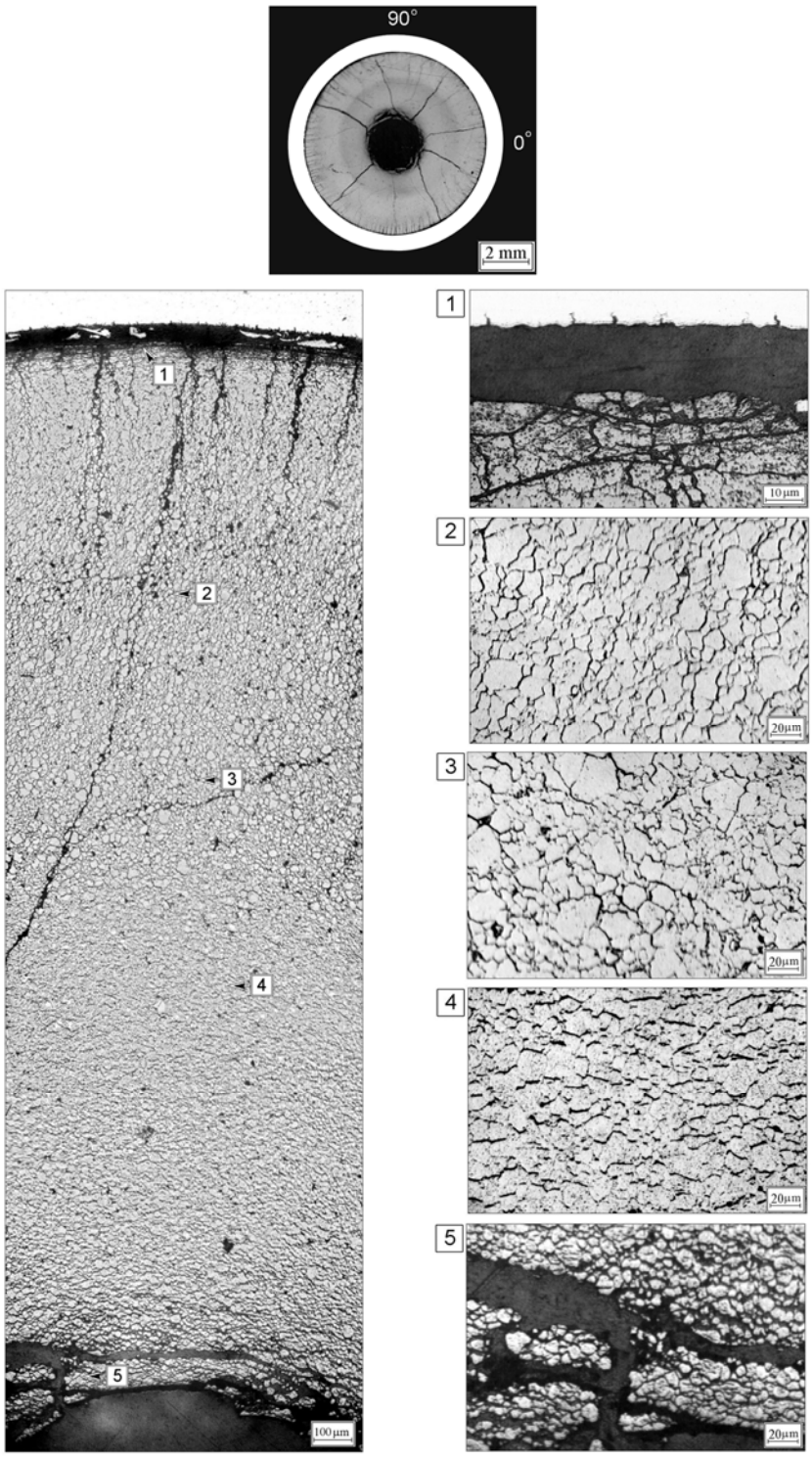


Fig.E-6.3. Cross-section and fuel microstructure of fuel rod # RT6 at 114 mm elevation (from low cap)

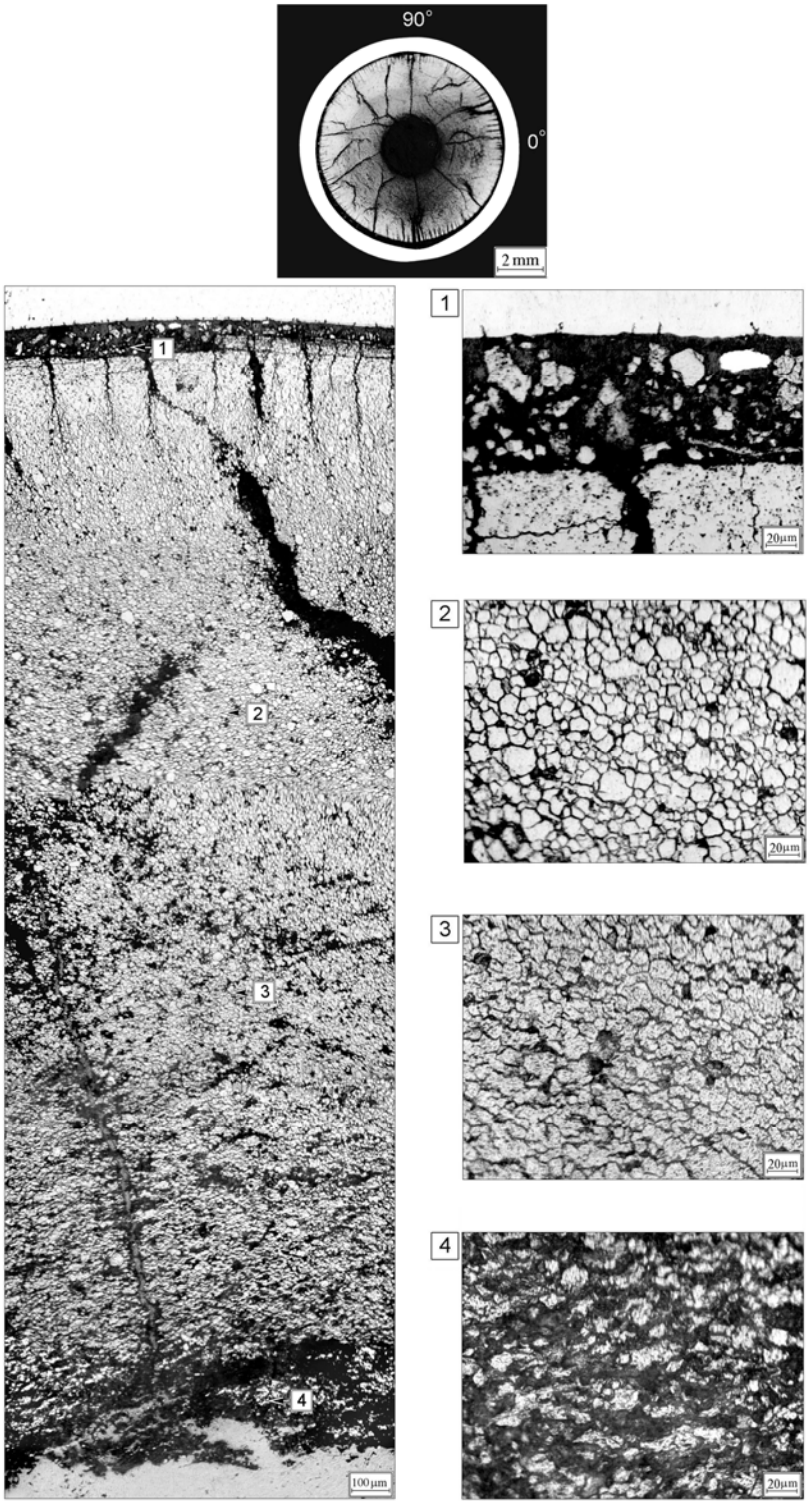


Fig.E-6.4. Cross-section and fuel microstructure of fuel rod # RT6 after the BIGR test at 132 mm elevation (from low cap)

RT6

Table E-6.1. Time dependent energy characteristics of fuel rod # RT6

Time (s)	Relative reactor power (current/ maximum value) (per-unit)	Cumulative number of fissions in fuel rod (fiss) x10^{-14}	Power of fuel rod[1)2)] (kW)	Energy deposition		Fuel enthalpy[3)]	
				(cal/g fuel)	(J/g fuel)	FRAP-T6	RAPTA-5
0.000	5.55E-03	0.000	0.000	0.000	0.000	0.000	0.000
0.001	1.75E-01	0.192	1286	2.184	9.142	3.244	2.139
0.002	6.31E-01	1.266	4633	14.20	59.45	13.059	14.203
0.003	1.00E+00	3.620	7340	40.77	170.7	44.285	40.783
0.004	6.78E-01	6.040	4979	68.03	284.8	66.083	67.795
0.005	2.82E-01	7.294	2069	82.17	344.0	83.034	81.459
0.006	1.52E-01	7.878	1118	88.69	371.3	88.089	87.484
0.007	8.32E-02	8.183	610.4	92.17	385.9	91.939	90.526
0.008	5.79E-02	8.372	425.3	94.30	394.8	93.381	92.280
0.009	4.84E-02	8.519	355.1	95.92	401.6	94.956	93.567
0.010	4.74E-02	8.644	347.7	97.37	407.7	95.869	94.721
0.012	5.49E-02	8.923	403.3	100.5	420.8	98.352	97.226
0.014	6.67E-02	9.262	489.5	104.3	436.6	101.475	100.620
0.016	7.50E-02	9.661	550.3	108.8	455.6	105.267	104.490
0.018	7.30E-02	10.08	535.8	113.4	474.9	109.262	108.870
0.020	6.10E-02	10.44	447.7	117.7	492.7	112.878	112.560
0.022	4.89E-02	10.75	358.8	121.1	506.9	115.719	115.520
0.024	3.86E-02	10.99	283.7	123.8	518.2	117.902	117.770
0.026	3.11E-02	11.18	228.0	125.9	527.2	119.573	119.360
0.028	2.62E-02	11.33	192.7	127.7	534.5	120.880	120.620
0.030	2.35E-02	11.47	172.5	129.2	540.8	121.980	121.860
0.050	2.02E-02	12.73	148.7	143.4	600.5	132.238	132.490
0.070	1.76E-02	13.80	129.4	155.5	650.9	140.860	141.510
0.090	1.24E-02	14.62	91.47	164.7	689.6	147.338	147.820
0.110	7.71E-03	15.19	56.77	171.1	716.5	151.832	151.750
0.130	2.88E-03	15.46	21.30	174.2	729.2	152.508	152.670
0.150	1.10E-03	15.56	8.248	175.3	734.0	152.417	152.040
0.200	2.93E-04	15.64	2.397	176.3	738.1	151.207	149.570
1.000	2.63E-05	15.75	0.302	178.0	745.3	131.264	127.660
10.00	3.06E-06	15.96	0.044	182.3	763.0	38.467	32.063
100.0	5.95E-08	16.06	0.007	185.4	776.1	5.210	4.530
1000	2.32E-13	16.07	1.57E-04	186.9	782.7	0.000	0.000

[1)] Average values determined in accordance with results of RRC KI and VNIIEF calculations

[2)] Maximum power value is 7340 kW (t=0.003 s)

[3)] Average radial value

Table E-6.2. Radial energy characteristics of fuel rod # RT6*

Parameters**	Coordinates of fuel radial layers (mm)			
	1 layer (1.25-2.82)	2 layer (2.82-3.44)	3 layer (3.44-3.71)	4 layer (3.71-3.795)
Number of fissions $x10^{-14}$ (fiss)	7.469	4.829	2.876	1.404
Fission density $x10^{-13}$ (fiss/g fuel)	2.469	2.618	3.195	4.766
Power*** (kW)	3281	2145	1285	629.6
Energy deposition (cal/g fuel)	163.6	173.5	212.5	311.5
Energy deposition (J/g fuel)	684.9	726.4	889.6	1304
Energy deposition**** (per-unit)	0.526	0.557	0.683	1.000

* Average values were determined in accordance with results of RRC KI and VNIIEF calculations

** All parameters were determined for the undamaged section of a fuel stack (see Table C.2)

*** The power for the entire length of each layer at time 0.003 s

**** Energy deposition in current layer/energy deposition in 4^{th} layer

RT6

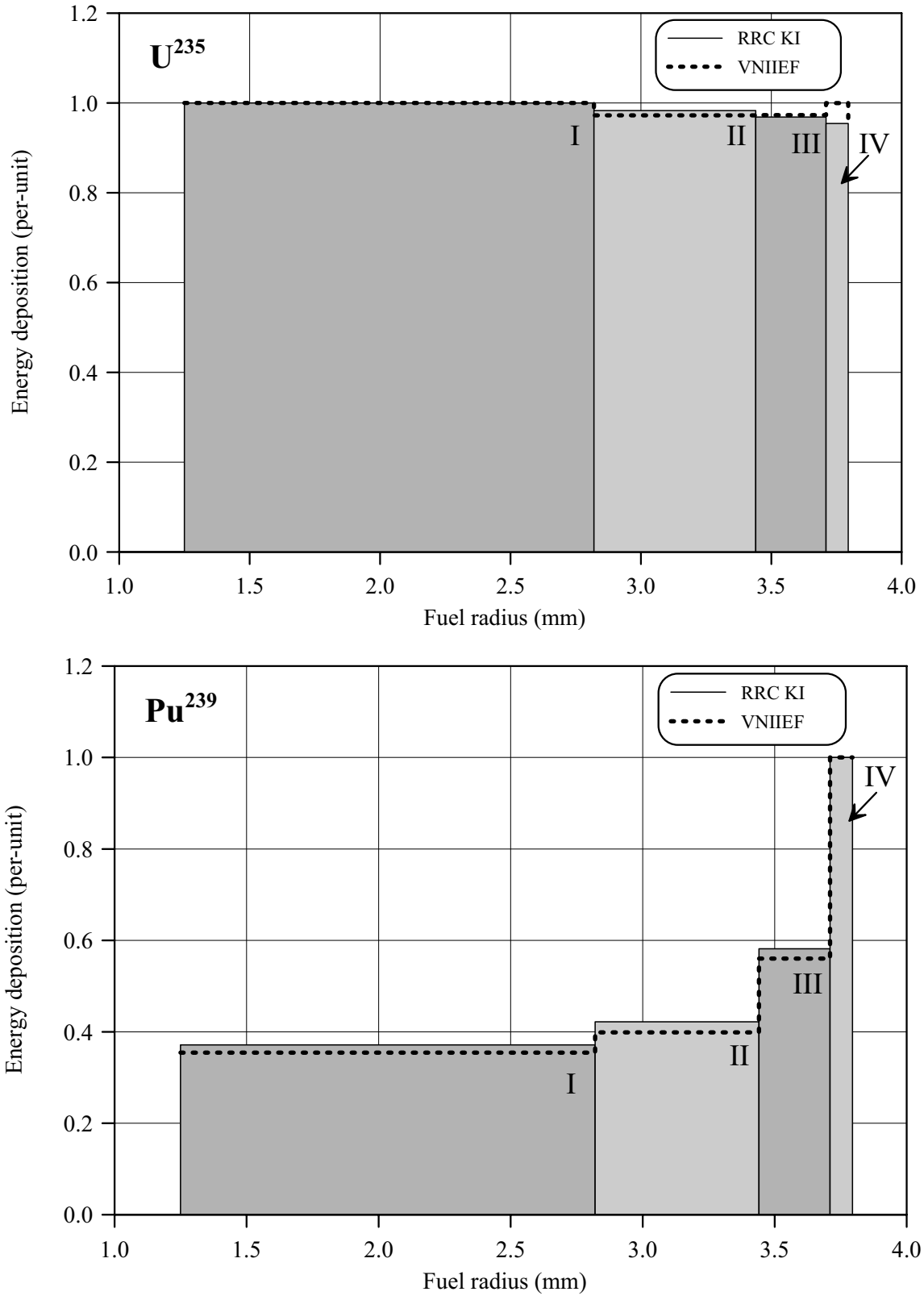


Fig.E-6.5. U^{235} and Pu^{239} radial distribution of energy deposition for fuel rod # RT6

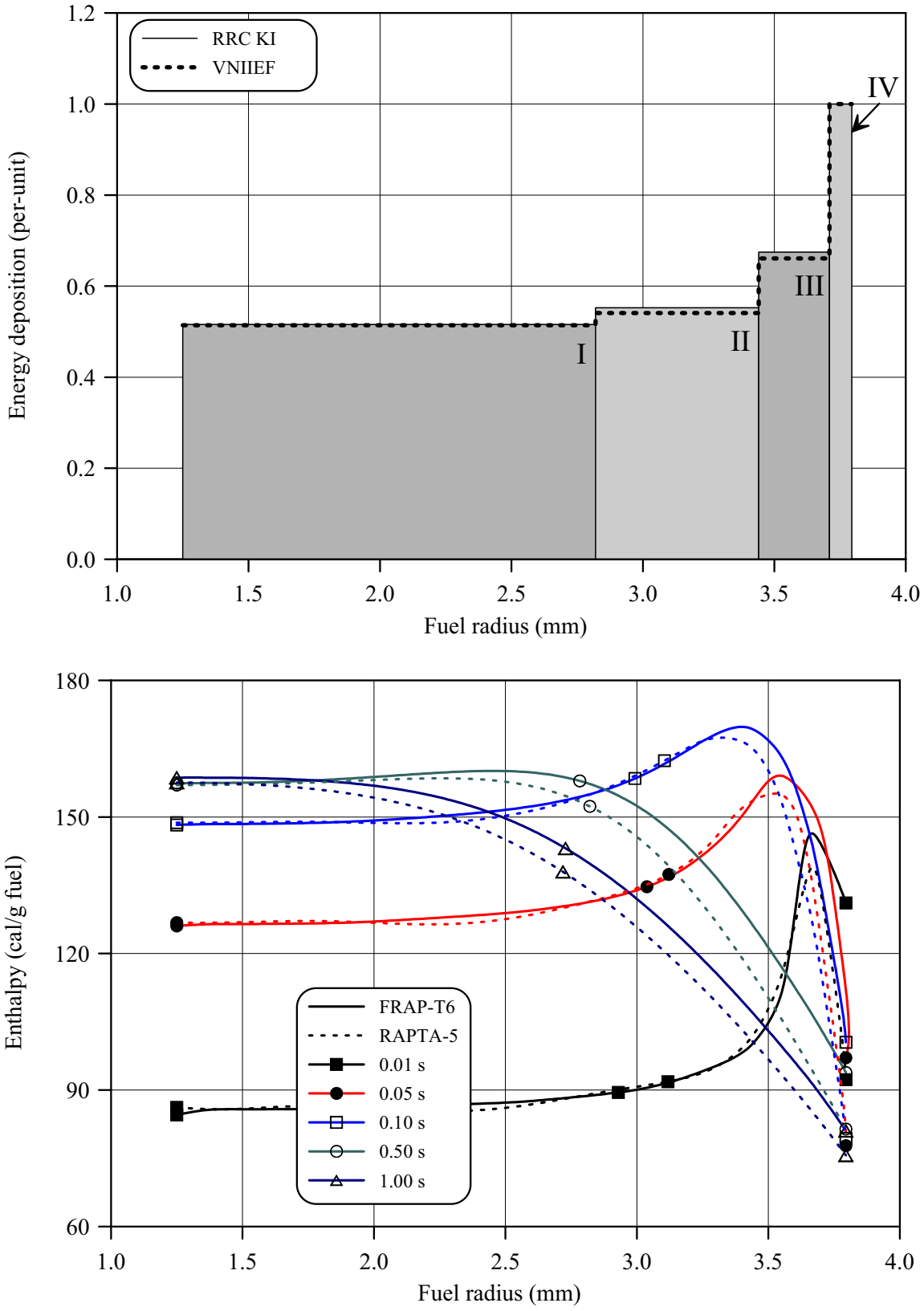


Fig.E-6.6. Radial distribution of energy deposition and fuel enthalpy for fuel rod # RT6

RT6

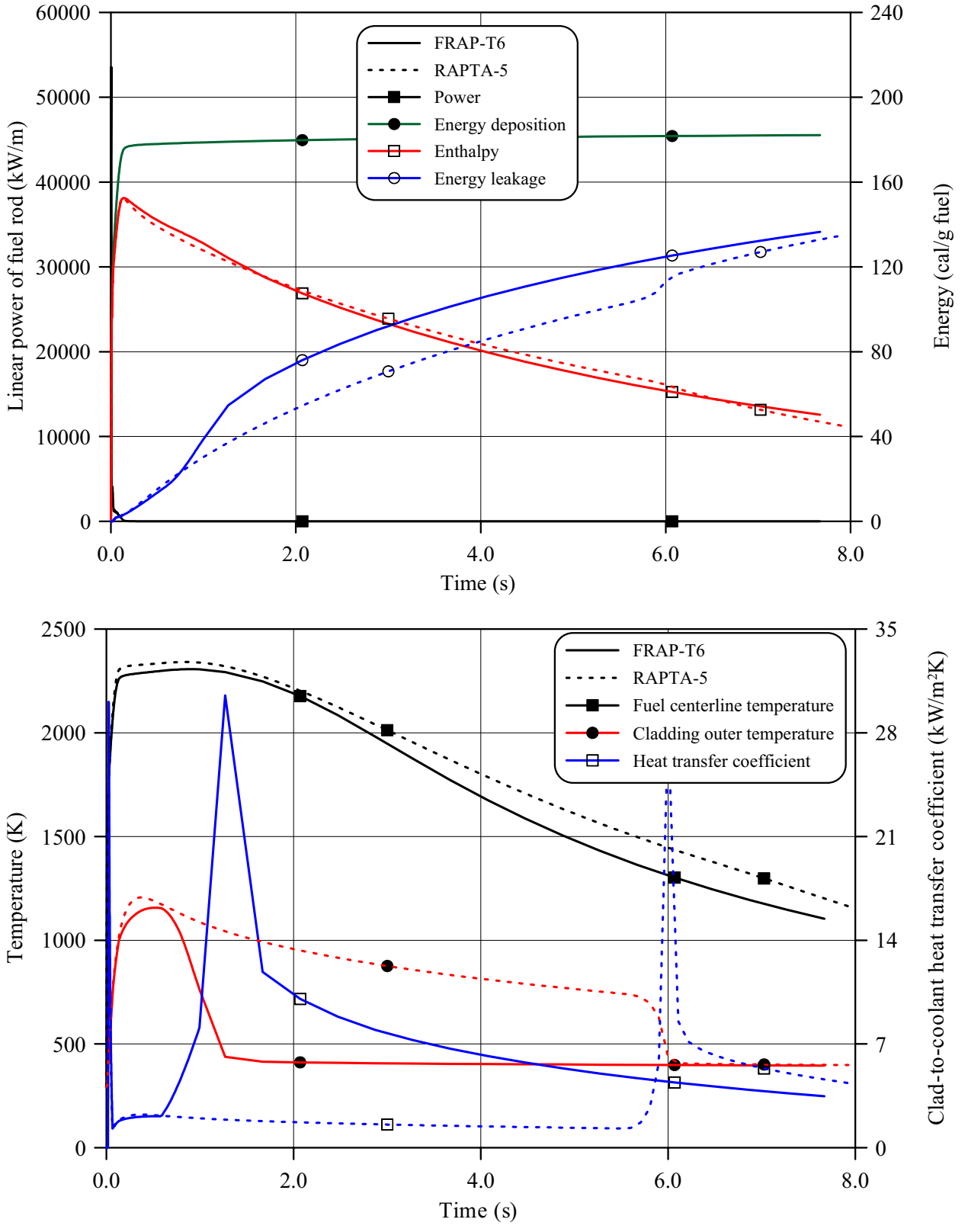


Fig.E-6.7. Thermal history of fuel rod # RT6 during the BIGR test in accordance with FRAP-T6/VVER and RAPTA-5 calculations

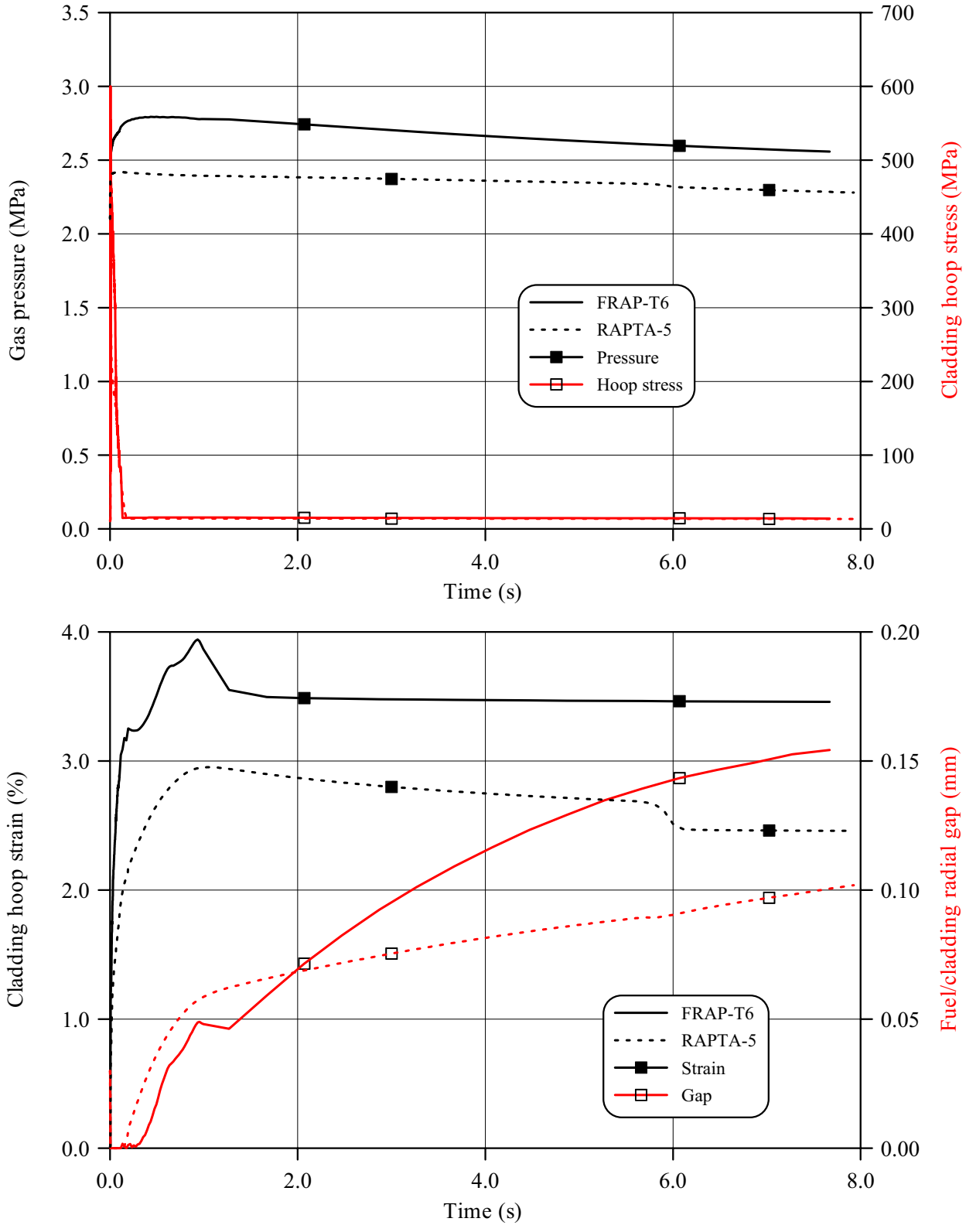


Fig.E-6.8. Mechanical behavior of fuel rod # RT6 during the BIGR test in accordance with FRAP-T6/VVER and RAPTA-5 calculations

RT6

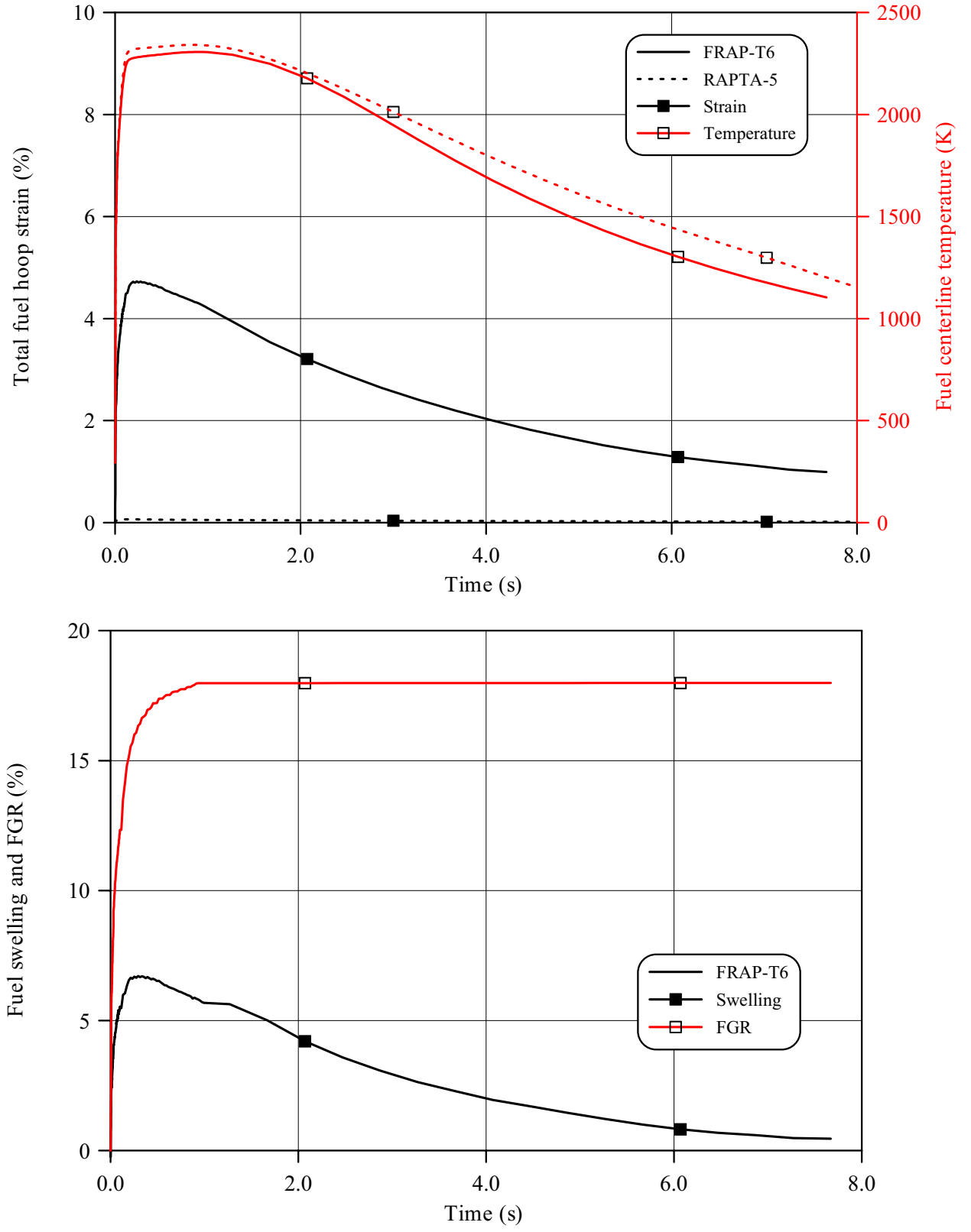


Fig.E-6.9. Fuel behavior during the BIGR test of fuel rod # RT6 in accordance with FRAP-T6/VVER and RAPTA-5 calculations

Table E-6.3. Axial distribution of cladding average outer diameter in fuel rod # RT6*

Axial coordinate (mm)	Cladding diameter (mm)	Axial coordinate (mm)	Cladding diameter (mm)	Axial coordinate (mm)	Cladding diameter (mm)	Axial coordinate (mm)	Cladding diameter (mm)
6	9.073	50	9.327	94	9.316	138	9.428
8	9.074	52	9.377	96	9.417	140	9.460
10	9.072	54	9.322	98	9.488	142	9.473
12	9.071	56	9.234	100	9.420	144	9.459
14	9.072	58	9.214	102	9.344	146	9.405
16	9.071	60	9.277	104	9.337	148	9.355
18	9.073	62	9.385	106	9.388	150	9.392
20	9.108	64	9.428	108	9.456	152	9.500
22	9.156	66	9.357	110	9.461	154	9.555
24	9.195	68	9.284	112	9.362	156	9.511
26	9.233	70	9.291	114	9.286	158	9.437
28	9.267	72	9.360	116	9.314	160	9.387
30	9.301	74	9.461	118	9.384	162	9.397
32	9.307	76	9.447	120	9.429	164	9.418
34	9.300	78	9.324	122	9.429	166	9.372
36	9.323	80	9.279	124	9.363	168	9.216
38	9.357	82	9.317	126	9.343	170	9.109
40	9.393	84	9.391	128	9.411	172	9.070
42	9.358	86	9.486	130	9.522	174	9.066
44	9.266	88	9.427	132	9.597	176	9.063
46	9.229	90	9.306	134	9.554	178	9.122
48	9.265	92	9.272	136	9.454	180	9.222

* Measured value determined on the basis of profilometry data (16 azimuthal directions)

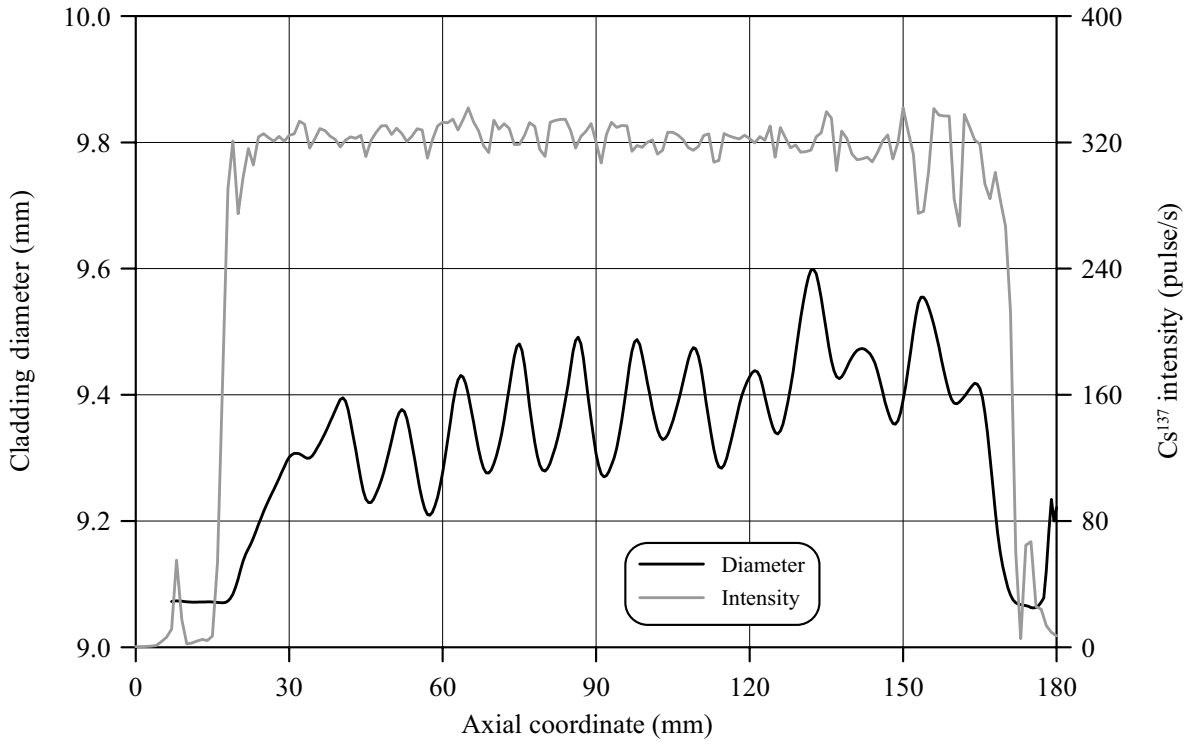


Fig.E-6.10. Cladding measured average diameter and γ-scanning results for fuel rod # RT6

RT6

Table E-6.4. The PIE results for fuel rod # RT6

Parameter		Value
1.	Cladding outer diameter (mm):	
1.1.	Maximum diameter of the bidimensional data sample in "fuel rod length - azimuthal angle" coordinates (mm)	9.76
1.2.	Averaged azimuthal diameter and maximum diameter along the length selected from the sample of averaged azimuthal diameter (mm)	9.61
1.3.	Averaged diameter of the bidimensional data sample in "fuel rod length - azimuthal angle" coordinates (mm)	9.36
2.	Cladding maximum residual hoop strain (%)	6.00
3.	Fuel pellet conditional diameter (mm) in cross-section*:	
	at 114 mm elevation	7.84
	at 132 mm elevation	7.92
4.	ZrO_2 outer thickness (μm) in cross-section:	
	at 114 mm elevation	3-5
	at 132 mm elevation	3-5
5.	ZrO_2 inner thickness (μm) in cross-section:	
	at 114 mm elevation	0
	at 132 mm elevation	0
6.	Parameters characterizing FGR:	
6.1.	Gas composition (% by volume):	
	He	81.53
	N_2	1.11
	O_2	0.09
	Ar	0.021
	CO_2	0.015
	Kr	1.53
	Xe	15.69
6.2.	Free gas volume (cm^3)	6.2
6.3.	Gas volume under normal conditions (cm^3)	141.8
6.4.	Gas pressure under normal conditions (MPa)	2.29
6.5.	FGR (%)	26.50

* Reference value determined by the processing of fuel cross-section photographs

Table E-6.5. Organized BIGR test results for fuel rod # RT6

Parameter		Unit	Value		
			Measured	Calculated	
				FRAP-T6	RAPTA-5
1.	Fuel burnup	MW d/kg U	47.84	47.84	47.84
2.	Initial gas pressure	MPa	2.1	2.1	2.1
3.	Energy deposition	cal/g fuel	186.9	186.9	186.9
4.	Peak fuel enthalpy*	cal/g fuel	-	152.5	152.7
5.	Fuel maximum temperature	K	-	2421	2459
6.	Maximum temperature of cladding outer surface	K	-	1157	1207
7.	Cladding burst	Failed, Unfailed	Unfailed	Unfailed	Unfailed
8.	Cladding residual hoop strain**	%	3.20	3.36	2.39
9.	Kr volume content in gas composition after the BIGR test	%	1.53	1.89	-
10.	Xe volume content in gas composition after the BIGR test	%	15.69	11.30	-

* Average value of peak fuel enthalpy is 152.6 cal/g fuel

** Average value along the fuel stack length

Appendix E–7

Individual Characteristics of Fuel Rod # RT7

after the BIGR Test

RT7

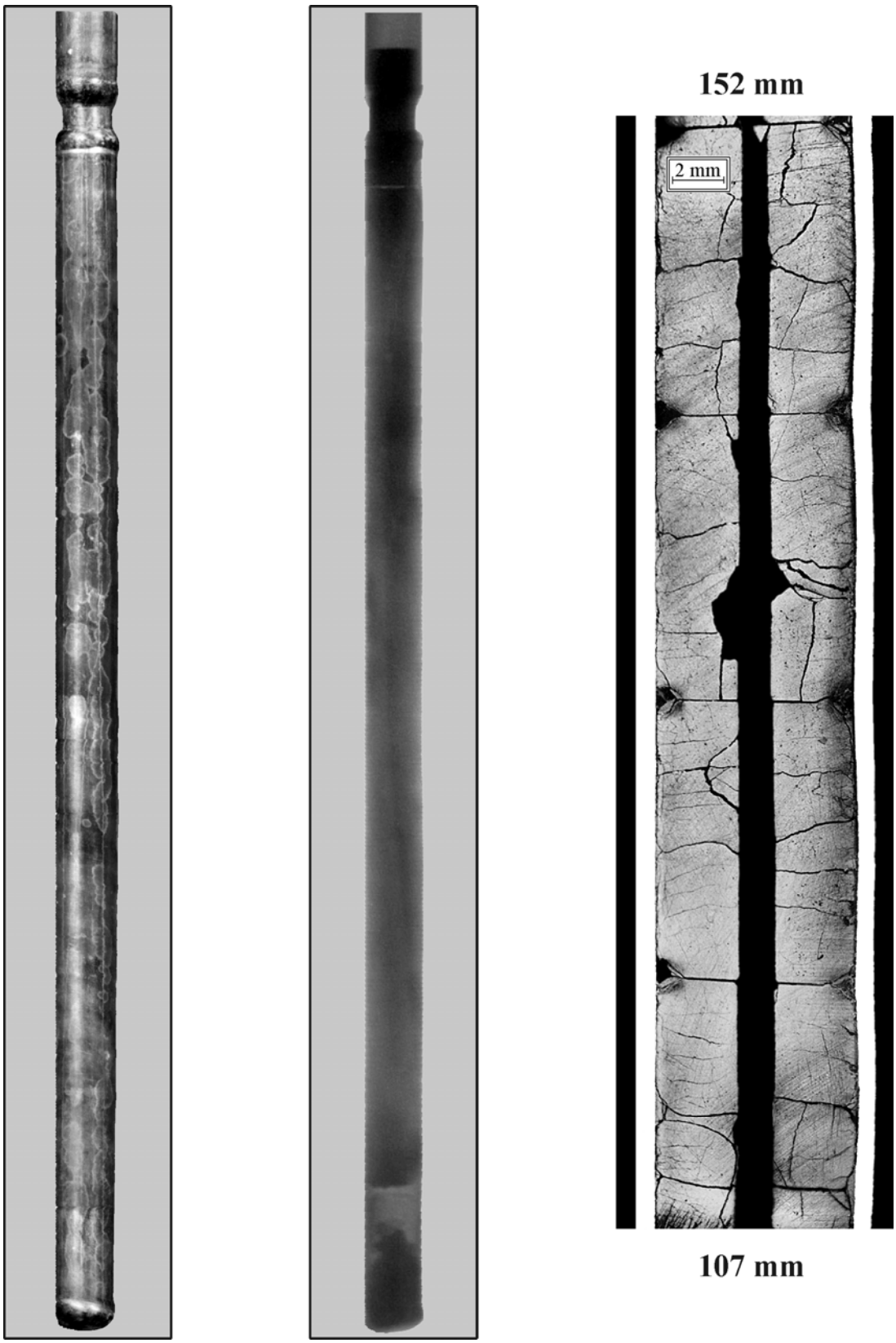


Fig.E-7.1. Appearance of unfailed fuel rod # RT7 after the BIGR test (photographs and X-ray photograph) and longitudinal metallographic specimen image

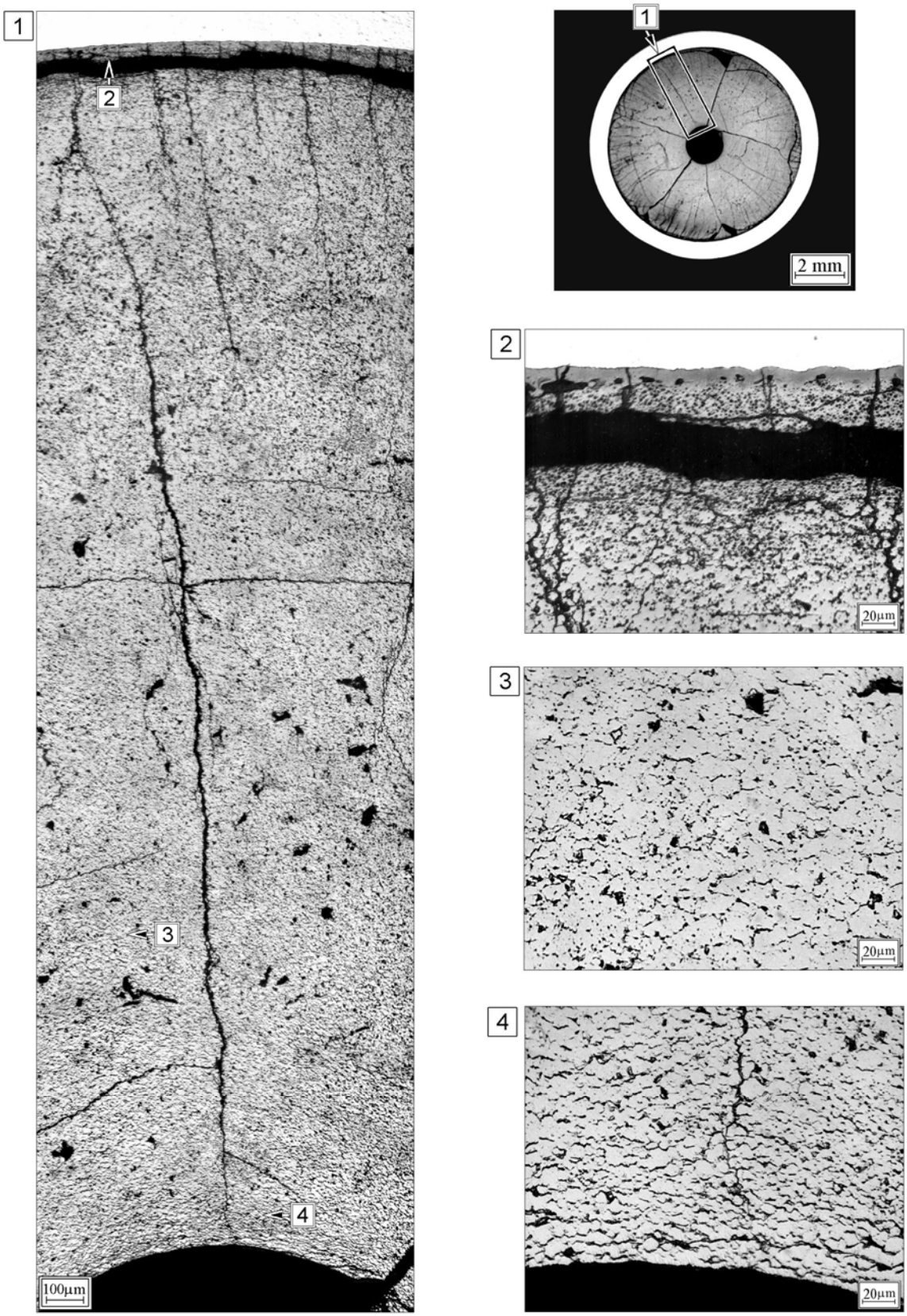


Fig.E-7.2. Cross-section and cladding microstructure of fuel rod # RT7 at 107 mm elevation (from low cap)

RT7

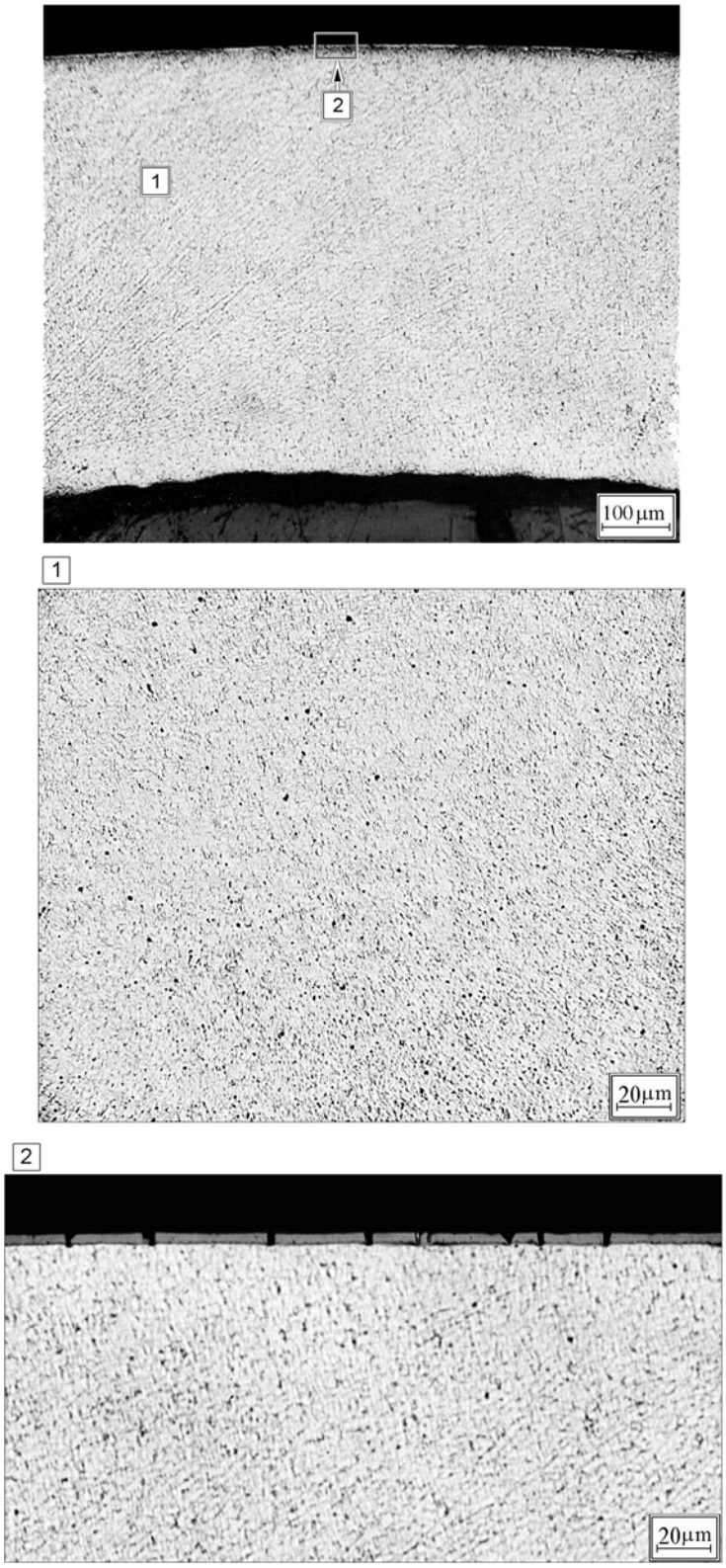


Fig.E-7.3. Cladding microstructure of fuel rod # RT7 at 107 mm elevation (from low cap)

Table E-7.1. Time dependent energy characteristics of fuel rod # RT7

Time (s)	Relative reactor power (current/ maximum value) (per-unit)	Cumulative number of fissions in fuel rod (fiss) x10^{-14}	Power of fuel rod[1)2)] (kW)	Energy deposition		Fuel enthalpy[3)]	
				(cal/g fuel)	(J/g fuel)	FRAP-T6	RAPTA-5
0.000	0.00E+00	0.000	0.000	0.000	0.000	0.000	0.000
0.001	3.77E-03	0.045	25.09	0.046	0.194	0.671	0.004
0.002	1.65E-02	0.248	109.7	0.255	1.067	0.671	0.013
0.003	7.63E-02	1.153	508.5	1.187	4.968	0.671	0.031
0.004	3.14E-01	5.134	2090	5.268	22.06	0.671	0.130
0.005	8.37E-01	18.27	5577	18.73	78.42	0.844	0.542
0.006	9.39E-01	40.46	6260	41.56	174.0	2.954	2.713
0.007	5.20E-01	57.56	3462	59.10	247.4	11.084	10.941
0.008	2.34E-01	65.86	1560	67.63	283.1	30.369	30.902
0.009	1.19E-01	69.64	796.4	71.61	299.8	51.815	53.058
0.010	7.54E-02	71.86	502.5	73.84	309.2	64.176	65.721
0.012	5.38E-02	74.73	358.3	76.74	321.3	72.209	73.965
0.014	5.62E-02	77.15	374.7	79.31	332.1	74.823	76.698
0.016	6.56E-02	79.97	437.0	82.20	344.1	76.831	78.858
0.018	7.47E-02	83.30	497.7	85.56	358.2	79.111	81.308
0.020	7.60E-02	86.80	506.6	89.18	373.4	81.899	84.282
0.022	6.89E-02	90.20	459.1	92.67	388.0	85.046	87.624
0.024	5.89E-02	93.23	393.0	95.72	400.8	88.160	90.927
0.026	4.85E-02	95.64	323.6	98.28	411.5	90.906	93.838
0.028	3.99E-02	97.71	266.2	100.4	420.4	93.182	96.258
0.030	3.41E-02	99.42	227.6	102.1	427.5	94.995	98.186
0.050	2.83E-02	113.0	189.0	116.0	485.8	106.142	110.175
0.070	2.46E-02	125.1	163.7	128.4	537.7	116.336	120.734
0.090	1.83E-02	134.5	121.9	138.5	579.7	124.433	129.209
0.110	9.39E-03	141.3	62.72	145.1	607.3	129.425	134.525
0.130	3.68E-03	143.7	24.68	147.9	619.4	131.404	136.246
0.150	1.69E-03	145.3	11.46	149.1	624.3	131.628	136.222
0.200	4.93E-04	146.3	3.441	150.3	629.1	130.640	134.603
1.000	7.30E-05	148.5	0.594	152.9	640.2	115.626	116.979
10.00	8.50E-06	153.4	0.079	159.5	667.8	46.313	33.119
100.0	1.72E-07	155.7	0.003	163.7	685.4	7.031	5.041
1000	6.74E-13	155.7	1.43E-04	165.2	691.7	0.000	0.000

[1)] Average values determined in accordance with results of RRC KI and VNIIEF calculations

[2)] Maximum power value is 6663 kW (t=0.00555 s)

[3)] Average radial value

RT7

Table E-7.2. Radial energy characteristics of fuel rod # RT7*

Parameters	Coordinates of fuel radial layers (mm)			
	1 layer (0.825-2.777)	2 layer (2.777-3.454)	3 layer (3.454-3.747)	4 layer (3.747-3.840)
Number of fissions $x10^{-14}$ (fiss)	6.673	4.455	2.879	1.590
Fission density $x10^{-13}$ (fiss/g fuel)	1.999	2.224	2.873	4.745
Power** (kW)	2847	1903	1231	681.5
Energy deposition (cal/g fuel)	141.2	157.3	203.4	336.6
Energy deposition (J/g fuel)	591.2	658.5	851.8	1409
Energy deposition*** (per-unit)	0.420	0.467	0.604	1.000

* Average values were determined in accordance with results of RRC KI and VNIIEF calculations

** The power for the entire length of each layer at time 0.00555 s

*** Energy deposition in current layer/energy deposition in 4^{th} layer

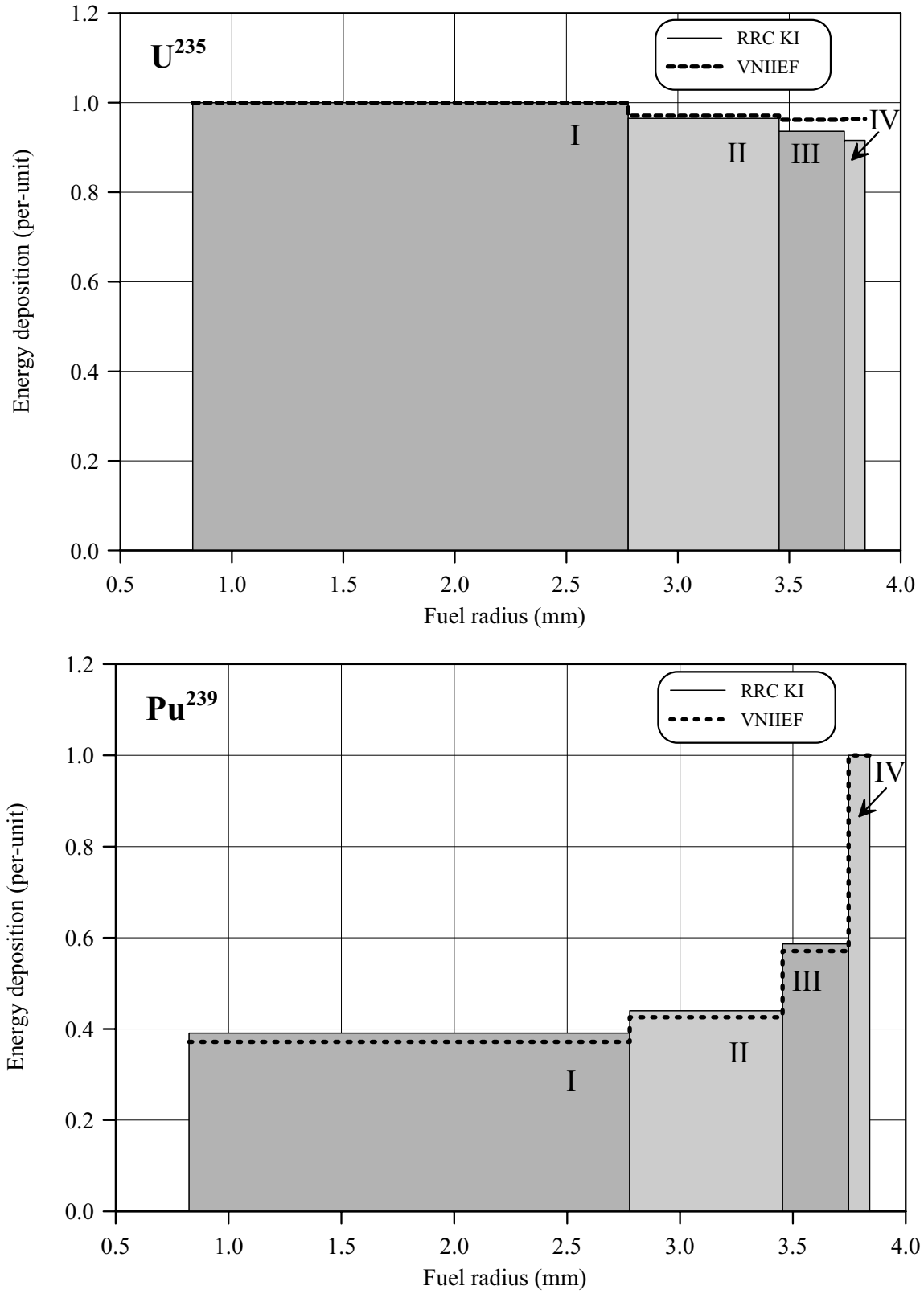
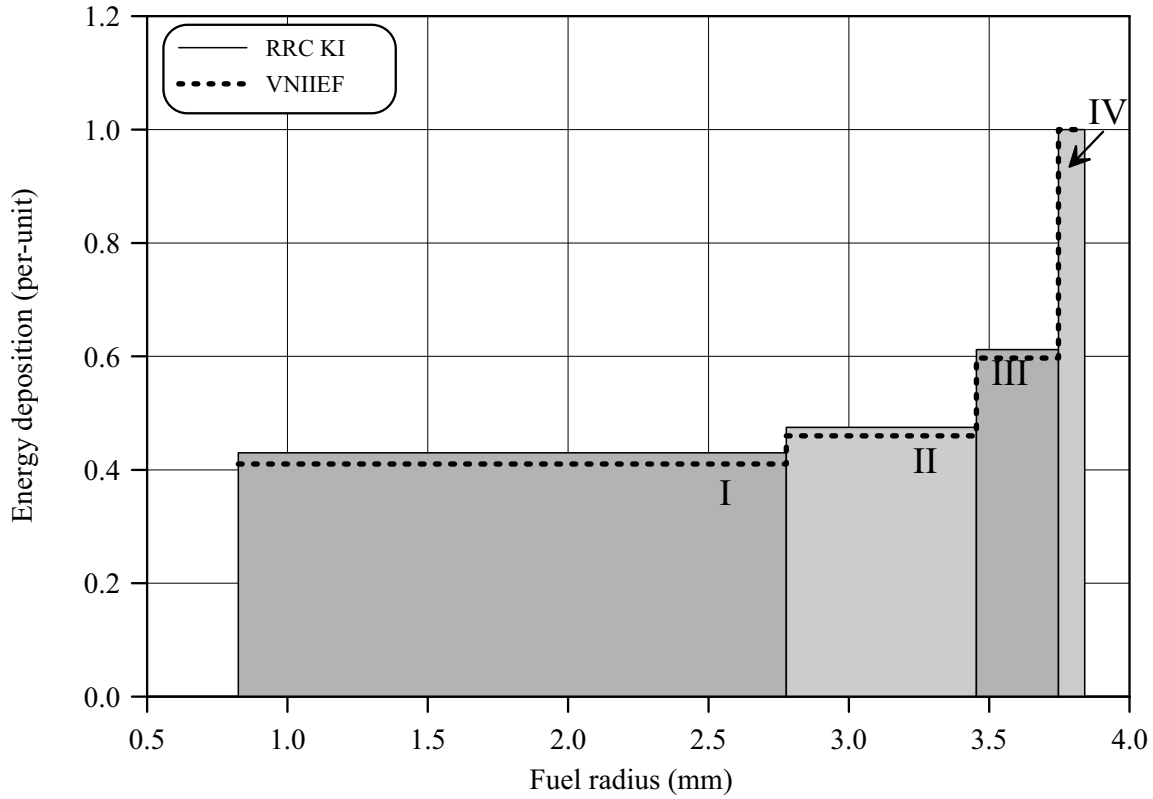


Fig.E-7.4. U^{235} and Pu^{239} radial distribution of energy deposition for fuel rod # RT7

RT7



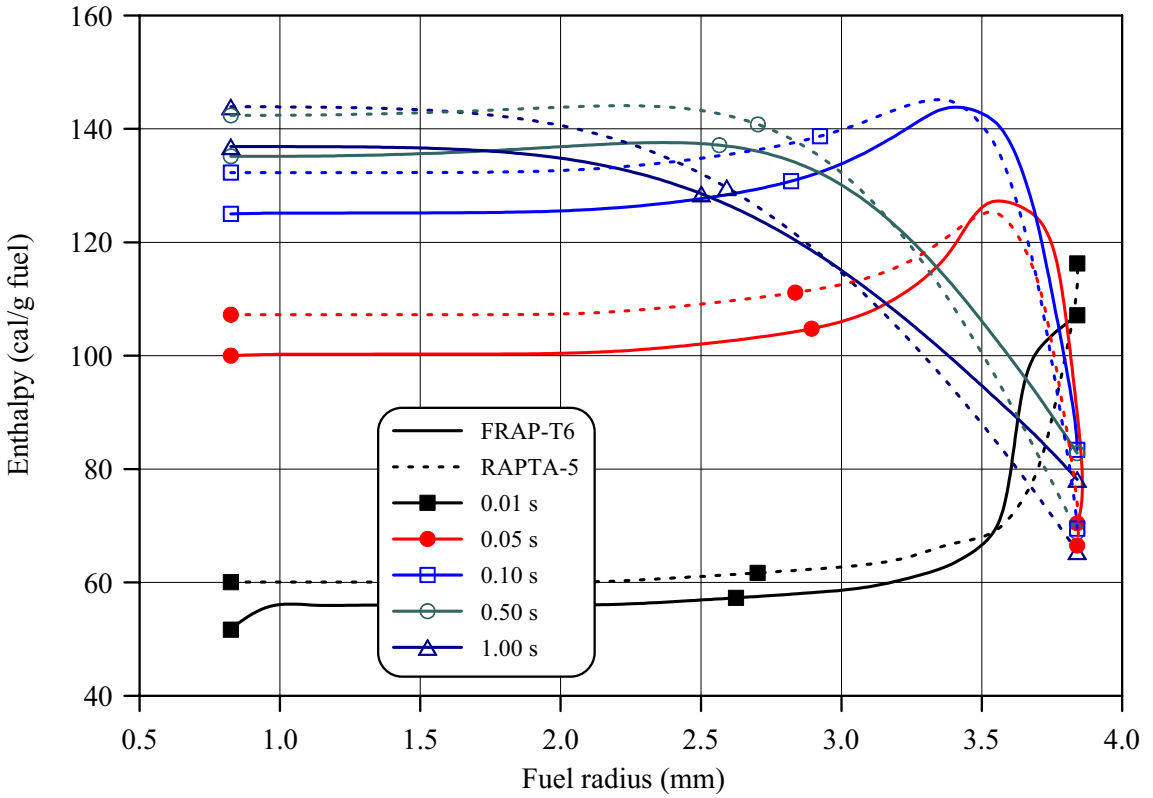


Fig.E-7.5. Radial distribution of energy deposition and fuel enthalpy for fuel rod # RT7

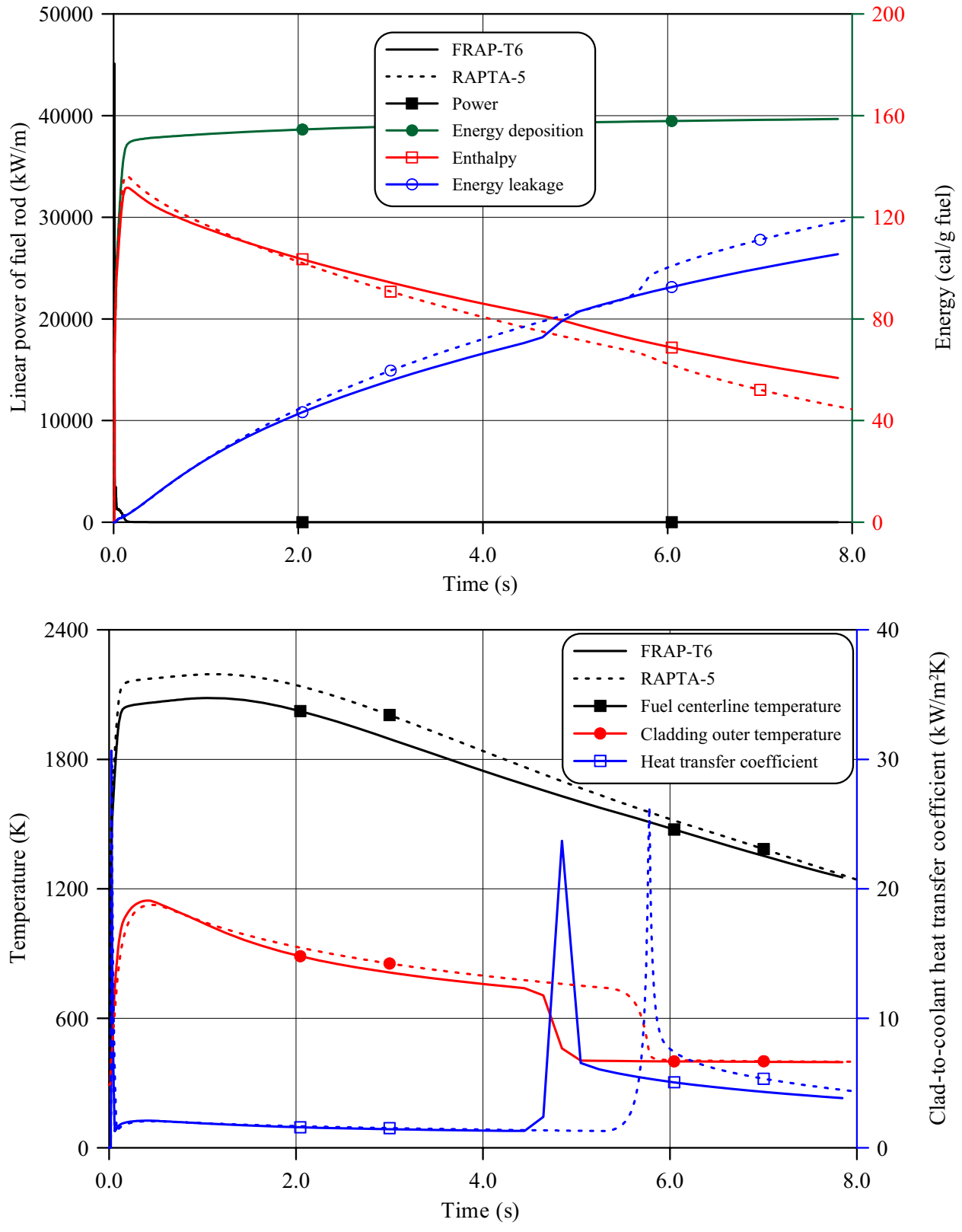


Fig.E-7.6. Thermal history of fuel rod # RT7 during the BIGR test in accordance with FRAP-T6/VVER and RAPTA-5 calculations

RT7

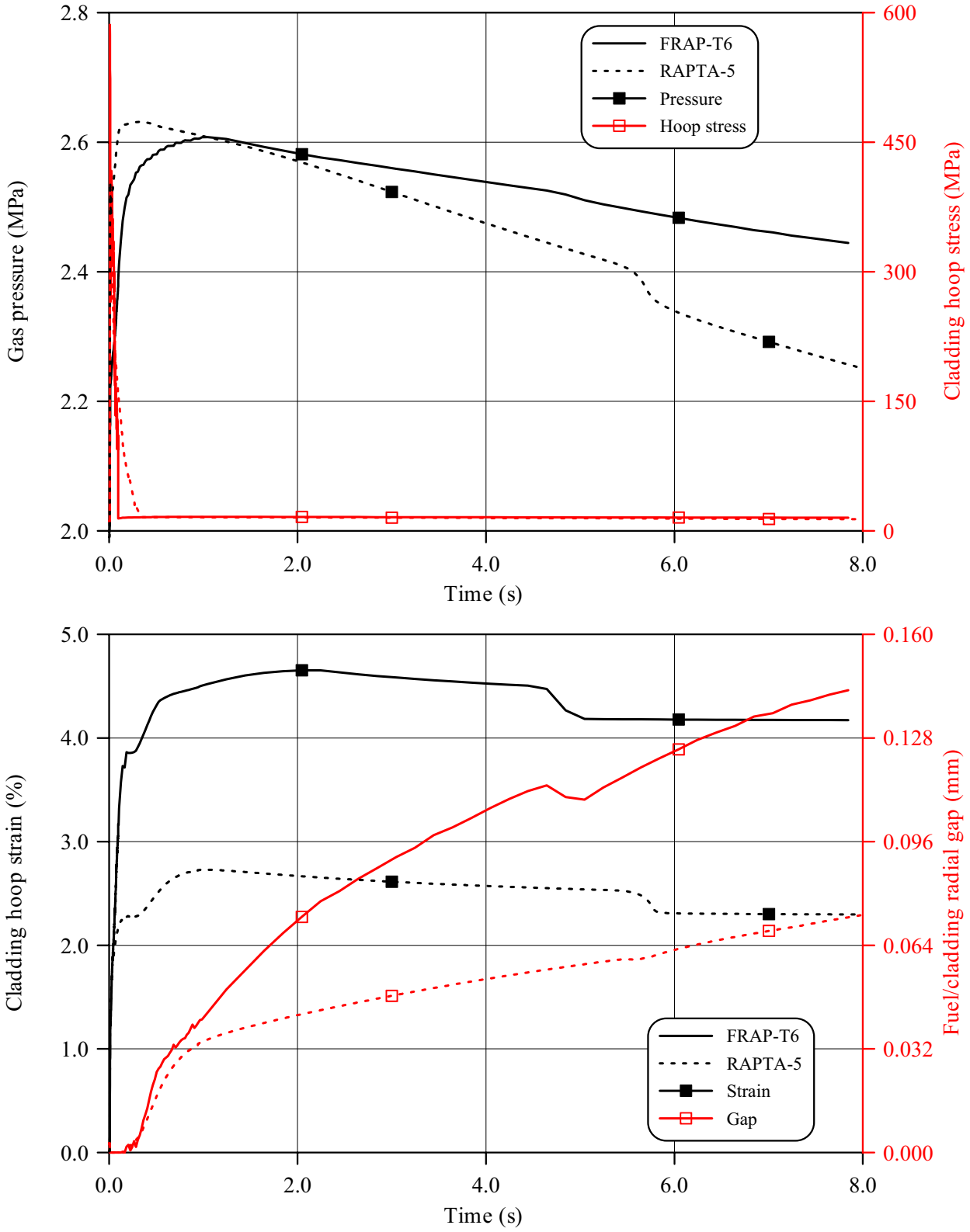


Fig.E-7.7. Mechanical behavior of fuel rod # RT7 during the BIGR test in accordance with FRAP-T6/VVER and RAPTA-5 calculations

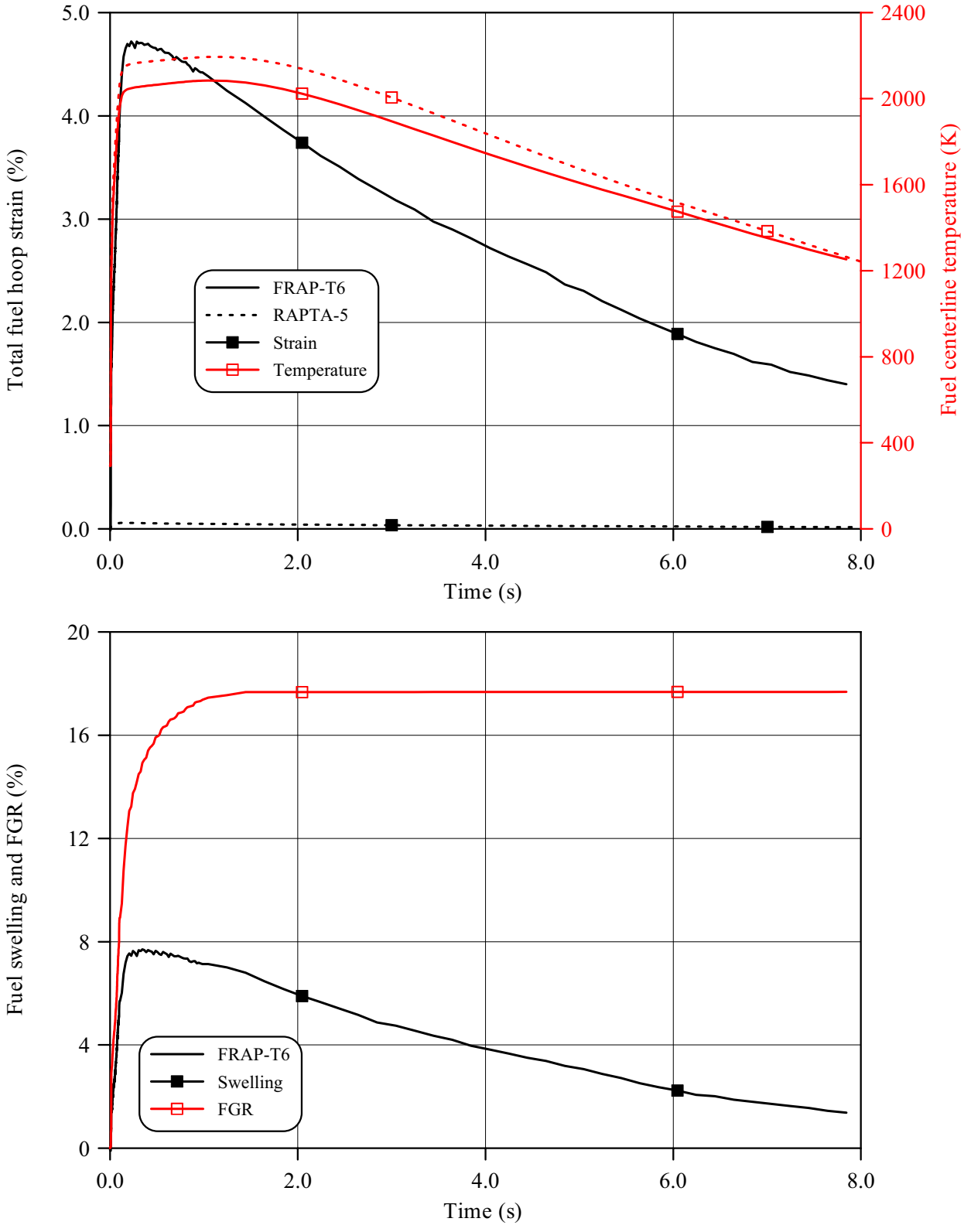


Fig.E-7.8. Fuel behavior during the BIGR test of fuel rod # RT7 in accordance with FRAP-T6/VVER and RAPTA-5 calculations

RT7

Table E-7.3. Axial distribution of cladding average outer diameter in fuel rod # RT7*

Axial coordinate (mm)	Cladding diameter (mm)	Axial coordinate (mm)	Cladding diameter (mm)	Axial coordinate (mm)	Cladding diameter (mm)	Axial coordinate (mm)	Cladding diameter (mm)
26	9.180	64	9.250	102	9.330	140	9.130
28	9.150	66	9.320	104	9.270	142	9.180
30	9.160	68	9.370	106	9.230	144	9.220
32	9.220	70	9.330	108	9.270	146	9.240
34	9.260	72	9.280	110	9.310	148	9.210
36	9.280	74	9.300	112	9.310	150	9.160
38	9.250	76	9.350	114	9.310	152	9.180
40	9.220	78	9.380	116	9.230	154	9.250
42	9.260	80	9.370	118	9.230	156	9.290
44	9.290	82	9.310	120	9.240	158	9.310
46	9.270	84	9.260	122	9.270	160	9.290
48	9.260	86	9.290	124	9.270	162	9.270
50	9.180	88	9.320	126	9.200	164	9.290
52	9.210	90	9.350	128	9.140	166	9.310
54	9.280	92	9.310	130	9.160	168	9.310
56	9.340	94	9.240	132	9.190	170	9.290
58	9.310	96	9.240	134	9.230	172	9.190
60	9.270	98	9.300	136	9.220	174	9.100
62	9.220	100	9.340	138	9.170	176	9.100

* Measured value determined on the basis of profilometry data (16 azimuthal directions)

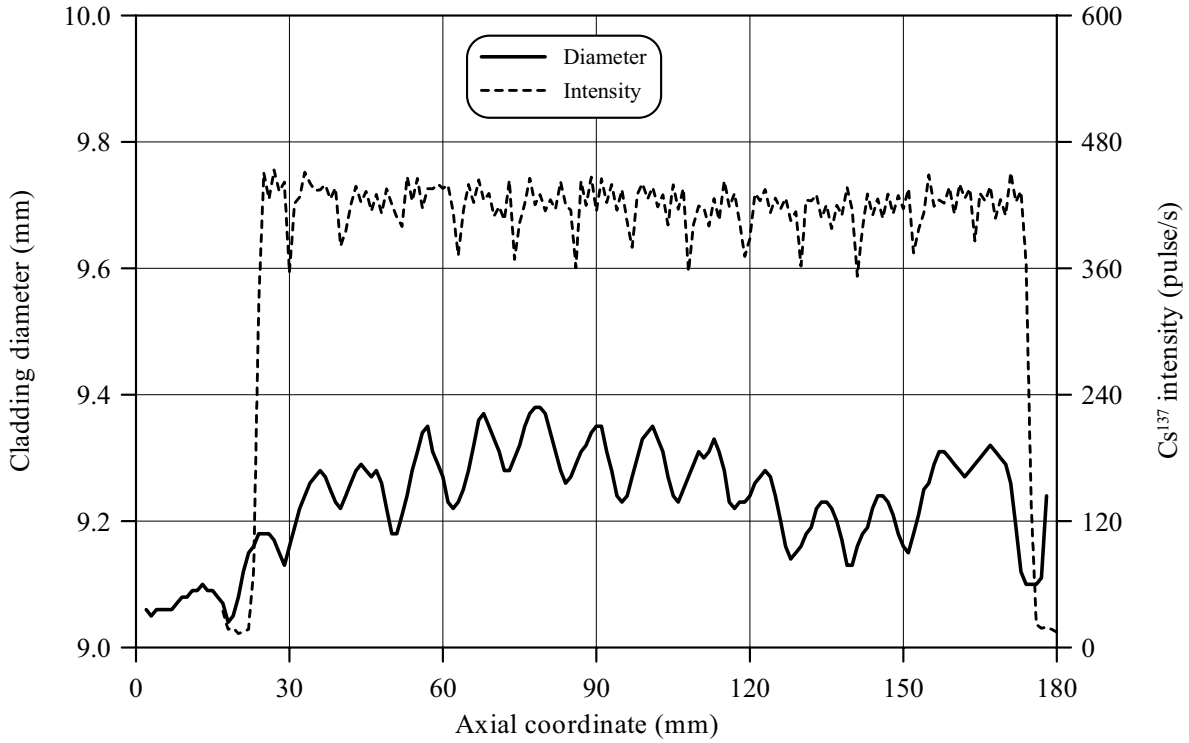


Fig.E-7.9. Cladding measured average diameter and γ-scanning results for fuel rod # RT7

Table E-7.4. The PIE results for fuel rod # RT7

	Parameter	Value
1.	Cladding outer diameter (mm):	
1.1.	Maximum diameter of the bidimensional data sample in "fuel rod length - azimuthal angle" coordinates (mm)	9.38
1.2.	Averaged azimuthal diameter and maximum diameter along the length selected from the sample of averaged azimuthal diameter (mm)	9.38
1.3.	Averaged diameter of the bidimensional data sample in "fuel rod length - azimuthal angle" coordinates (mm)	9.25
2.	Cladding maximum residual hoop strain (%)	3.50
3.	Fuel pellet conditional diameter (mm) in cross-section*:	
	at 107 mm elevation	7.74
4.	ZrO_2 outer thickness (μm) in cross-section:	
	at 107 mm elevation	3-5
5.	ZrO_2 inner thickness (μm) in cross-section:	
	at 107 mm elevation	9
6.	Parameters characterizing FGR:	
6.1.	Gas composition (% by volume):	
	He	76.83
	N_2	1.92
	O_2	0.05
	Ar	0.014
	CO_2	0.080
	Kr	1.82
	Xe	19.29
6.2.	Free gas volume (cm^3)	5.9
6.3.	Gas volume under normal conditions (cm^3)	158.9
6.4.	Gas pressure under normal conditions (MPa)	2.7
6.5.	FGR (%)	26.8

* Reference value determined by the processing of fuel cross-section photographs

RT7

Table E-7.5. Organized BIGR test results for fuel rod # RT7

Parameter		Unit	Value		
			Measured	Calculated	
				FRAP-T6	RAPTA-5
1.	Fuel burnup	MW d/kg U	60.3	60.3	60.3
2.	Initial gas pressure	MPa	2.0	2.0	2.0
3.	Energy deposition	cal/g fuel	165.2	165.2	165.2
4.	Peak fuel enthalpy*	cal/g fuel	-	131.7	136.4
5.	Fuel maximum temperature	K	-	2183	2251
6.	Maximum temperature of cladding outer surface	K	-	1146	1126
7.	Cladding burst	Failed, Unfailed	Unfailed	Unfailed	Unfailed
8.	Cladding residual hoop strain				
	- average**	%	2.07	3.68	2.73
	- maximum	%	3.50	3.68	2.73
9.	Kr volume content in gas composition after the BIGR test	%	1.82	2.99	-
10.	Xe volume content in gas composition after the BIGR test	%	19.29	17.93	-

* Average value of peak fuel enthalpy 134.0 cal/g fuel

** Average value along the fuel stack length

Appendix E–8

Individual Characteristics of Fuel Rod # RT8

after the BIGR Test

RT8

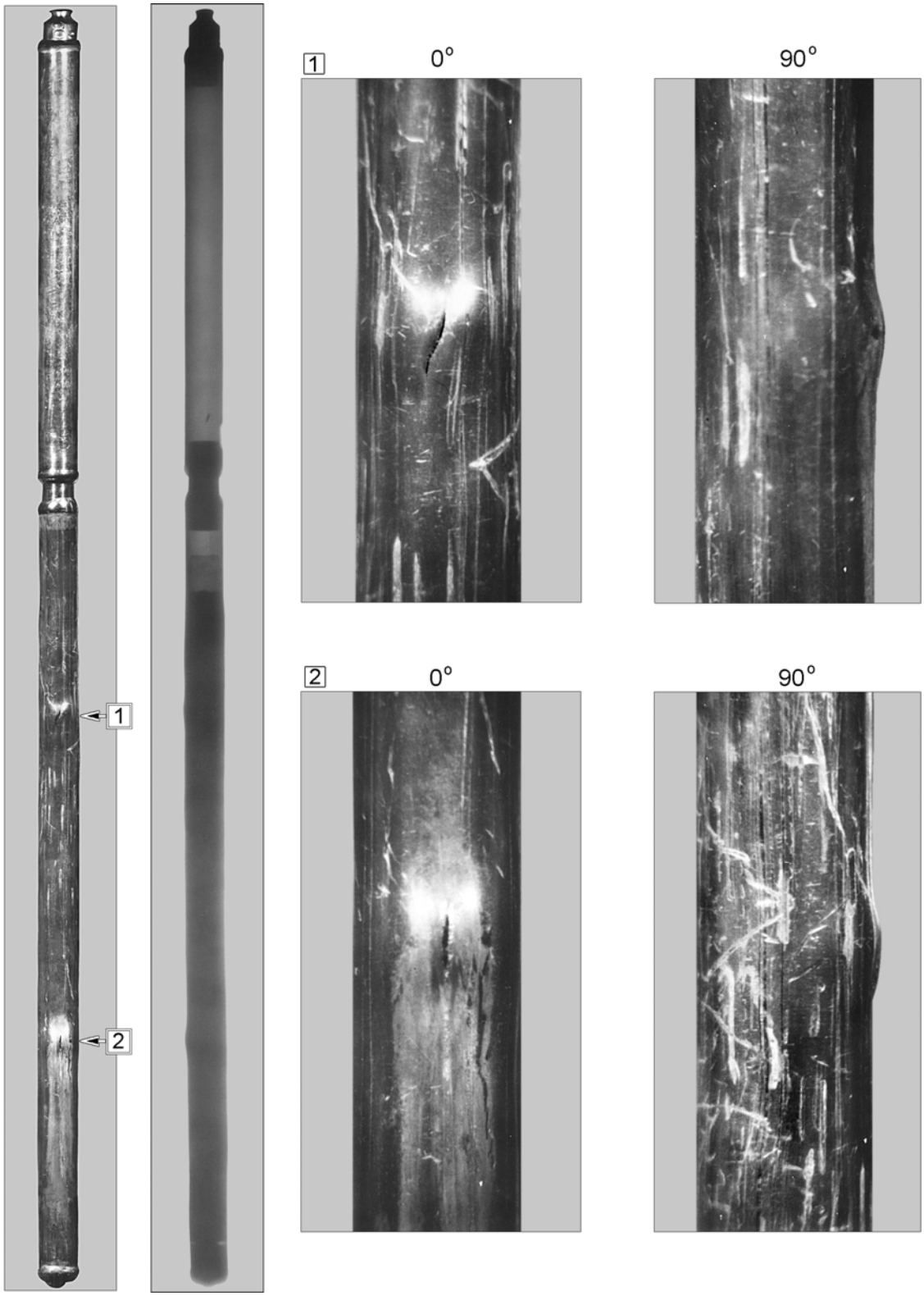


Fig.E-8.1. Appearance of failed fuel rod # RT8 after the BIGR test (photographs and X-ray photograph)

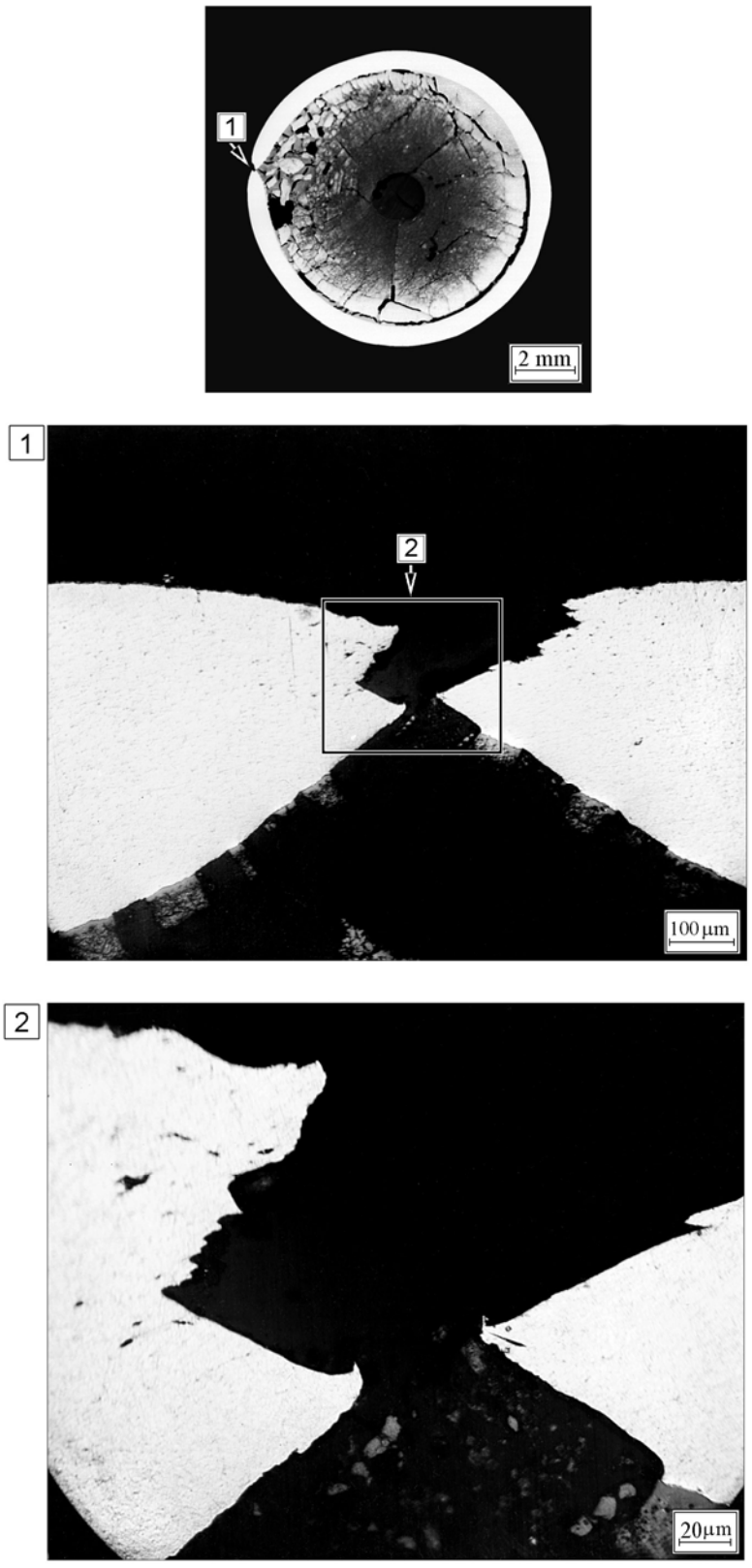


Fig.E-8.2. Cross-section and cladding microstructure in the burst area of fuel rod # RT8 at 53 mm elevation (from low cap)

RT8

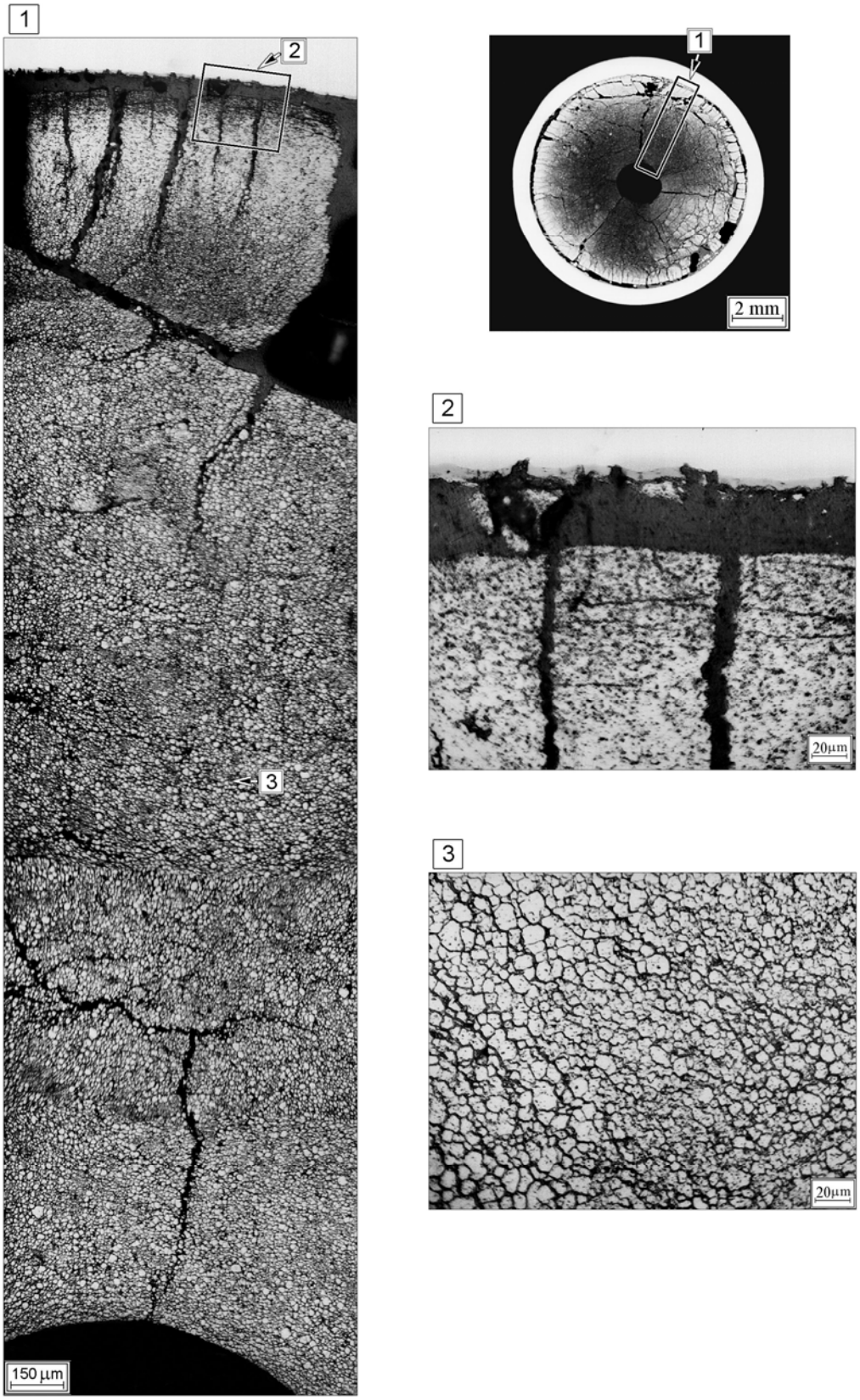


Fig.E-8.3. Cross-section and fuel microstructure of fuel rod # RT8 at 97 mm elevation (from low cap)

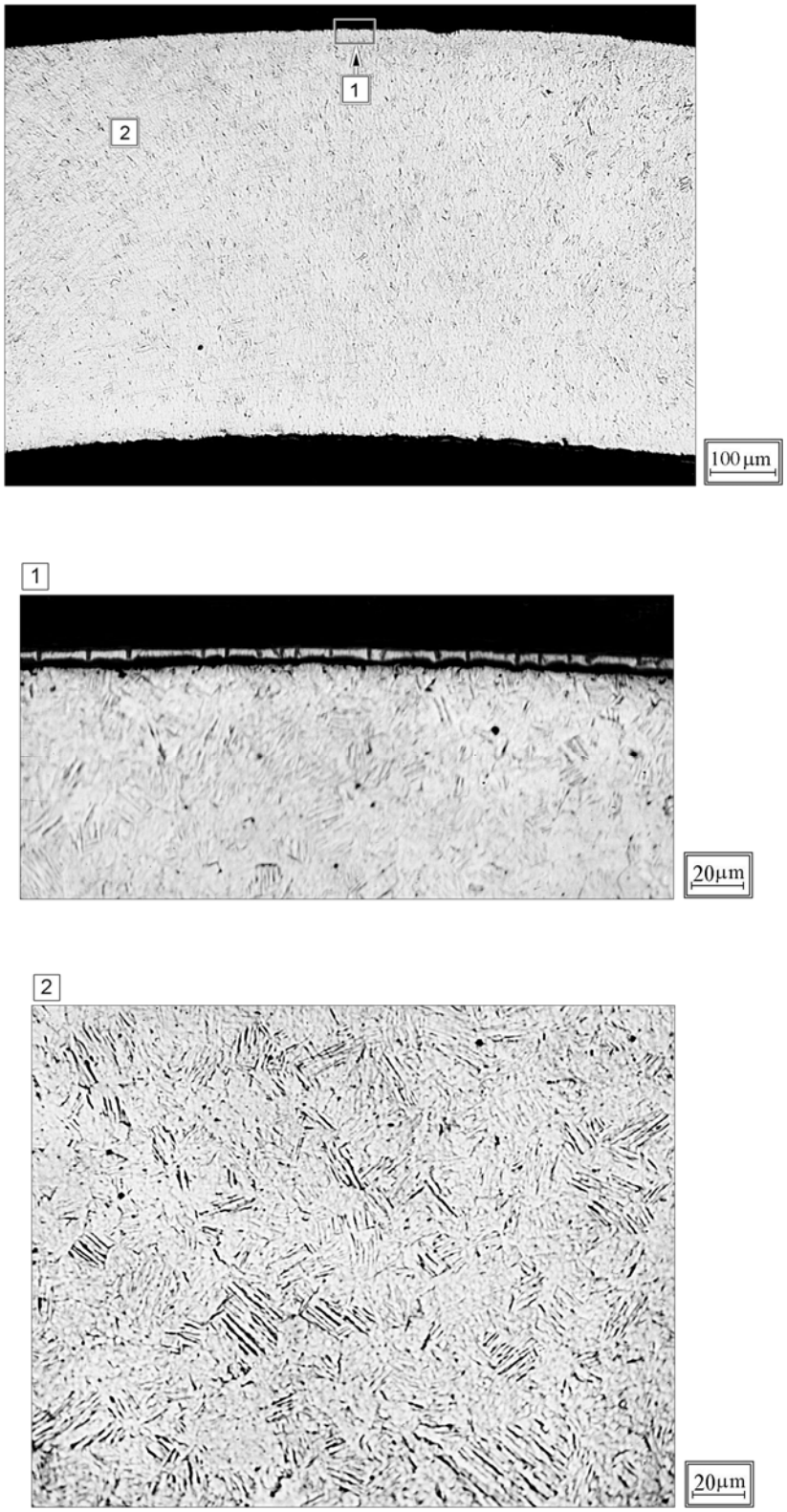


Fig.E-8.4. Cladding microstructure of fuel rod # RT8 at 97 mm elevation (from low cap)

RT8

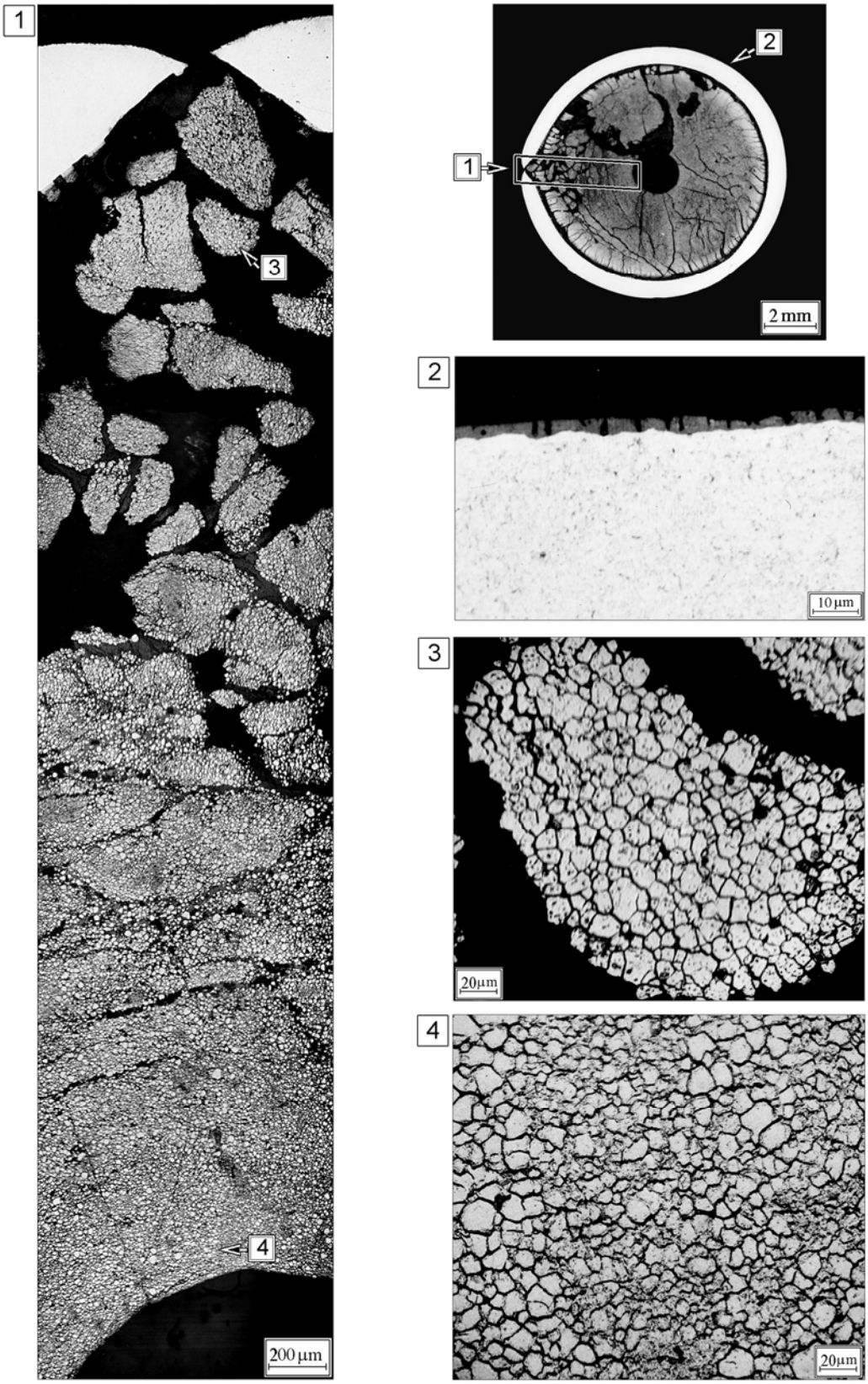


Fig.E-8.5. Cross-section and cladding microstructure of fuel rod # RT8 at 133 mm elevation (from low cap)

Table E-8.1. Time dependent energy characteristics of fuel rod # RT8

Time (s)	Relative reactor power (current/ maximum value) (per-unit)	Cumulative number of fissions in fuel rod (fiss) x10^{-14}	Power of fuel rod[1)2)] (kW)	Energy deposition		Fuel enthalpy[3)]	
				(cal/g fuel)	(J/g fuel)	FRAP-T6	RAPTA-5
0.000	0.00E+00	0.000	0.000	0.000	0.000	0.000	0.000
0.001	2.74E-03	0.037	21.08	0.038	0.161	0.671	0.039
0.002	1.20E-02	0.206	92.68	0.213	0.890	0.671	0.204
0.003	5.50E-02	0.970	423.4	1.001	4.191	1.276	1.074
0.004	2.39E-01	4.391	1836	4.530	18.97	4.939	4.676
0.005	7.06E-01	16.47	5432	17.01	71.21	17.598	17.715
0.006	9.90E-01	40.90	7613	42.26	176.9	42.949	43.901
0.007	6.19E-01	63.22	4758	65.26	273.2	65.896	67.516
0.008	2.82E-01	74.86	2171	77.26	323.5	77.575	79.466
0.009	1.36E-01	80.15	1046	82.74	346.4	82.629	84.594
0.010	8.10E-02	82.97	623.4	85.62	358.5	85.108	87.175
0.012	5.36E-02	86.35	412.1	89.11	373.1	87.862	90.099
0.014	5.43E-02	89.18	417.8	92.05	385.4	90.164	92.594
0.016	6.39E-02	92.32	492.1	95.30	399.0	92.864	95.506
0.018	7.43E-02	96.12	572.0	99.15	415.1	96.196	99.043
0.020	7.80E-02	100.2	600.6	103.4	432.9	99.972	103.046
0.022	7.36E-02	104.3	566.3	107.7	450.8	103.748	107.029
0.024	6.17E-02	108.2	474.9	111.4	466.4	107.027	110.502
0.026	4.96E-02	111.2	381.7	114.5	479.3	109.629	113.275
0.028	4.02E-02	113.3	309.2	117.0	489.6	111.646	115.445
0.030	3.42E-02	115.4	263.2	119.1	498.4	113.264	117.197
0.050	2.72E-02	130.6	209.4	134.9	564.7	125.680	130.399
0.070	2.44E-02	144.6	187.7	149.1	624.3	137.020	142.329
0.090	2.06E-02	156.1	158.5	161.3	675.4	147.055	152.391
0.110	1.57E-02	166.2	120.7	171.8	719.1	155.898	160.736
0.130	7.95E-03	173.0	61.39	178.4	746.9	160.853	165.400
0.150	3.05E-03	175.7	23.65	181.2	758.8	162.225	166.440
0.200	6.92E-04	177.3	5.511	183.3	767.3	161.502	164.962
1.000	7.64E-05	180.3	0.717	186.7	781.8	151.533	147.195
10.00	8.86E-06	186.3	0.095	194.7	815.4	76.383	55.533
100.0	1.79E-07	189.4	0.004	199.9	836.7	8.643	5.231
1000	7.01E-13	189.5	1.70E-04	201.7	844.3	0.000	0.000

[1)] Average values determined in accordance with results of RRC KI and VNIIEF calculations

[2)] Maximum power value is 7693 kW (t=0.00588 s)

[3)] Average radial value

RT8

Table E-8.2. Radial energy characteristics of fuel rod # RT8*

Parameters	Coordinates of fuel radial layers (mm)			
	1 layer (0.825-2.777)	2 layer (2.777-3.454)	3 layer (3.454-3.747)	4 layer (3.747-3.840)
Number of fissions $x10^{-14}$ (fiss)	8.381	5.429	3.366	1.780
Fission density $x10^{-13}$ (fiss/g fuel)	2.533	2.734	3.389	5.360
Power** (kW)	3396	2202	1369	726.3
Energy deposition (cal/g fuel)	178.1	192.5	239.1	379.1
Energy deposition (J/g fuel)	745.6	805.8	1000.9	1587
Energy deposition*** (per-unit)	0.470	0.508	0.631	1.000

* Average values were determined in accordance with results of RRC KI and VNIIEF calculations

** The power for the entire length of each layer at time 0.00588 s

*** Energy deposition in current layer/energy deposition in 4^{th} layer

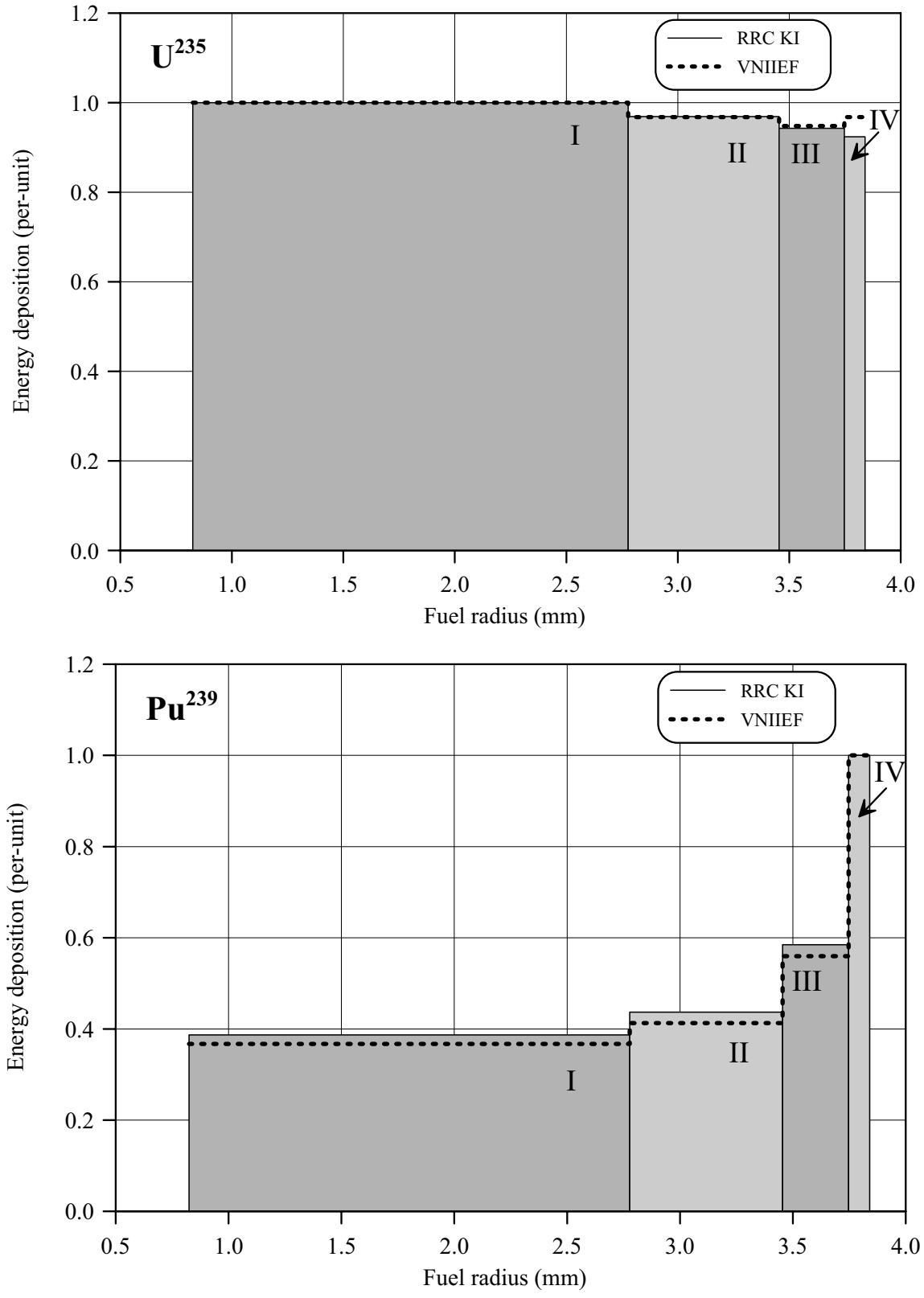
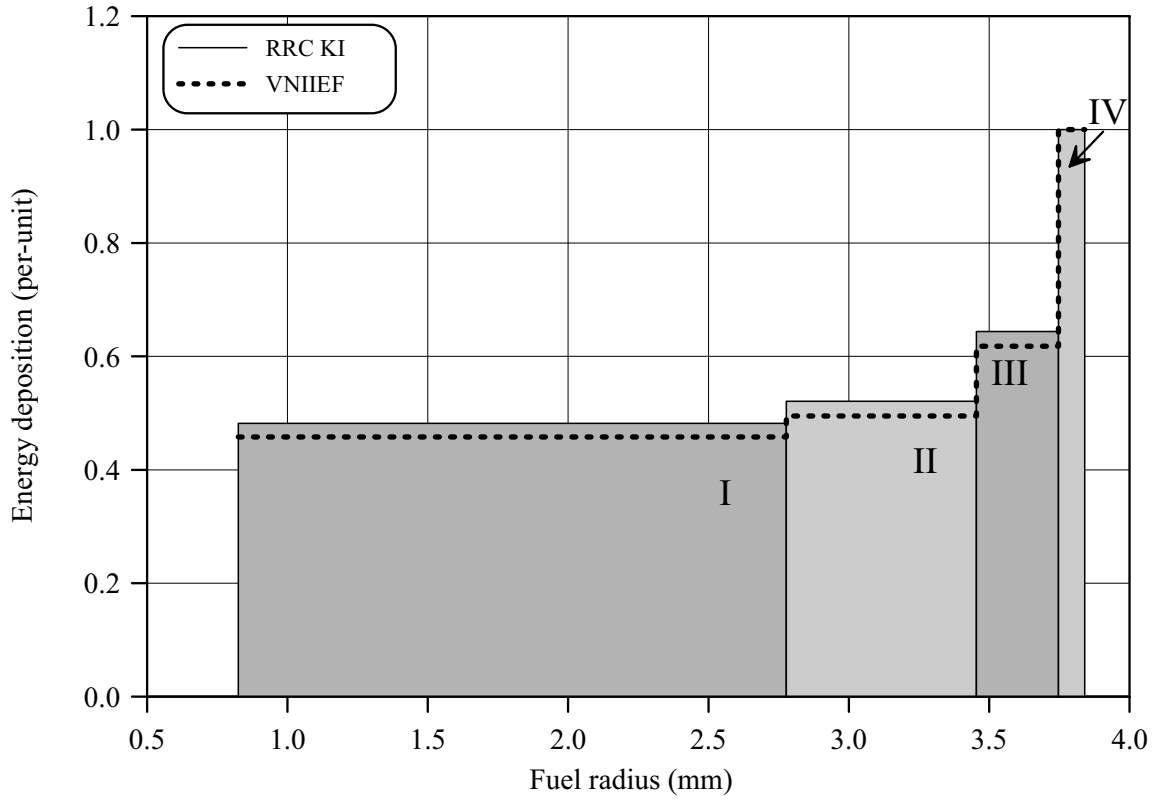


Fig.E-8.6. U^{235} and Pu^{239} radial distribution of energy deposition for fuel rod # RT8

RT8



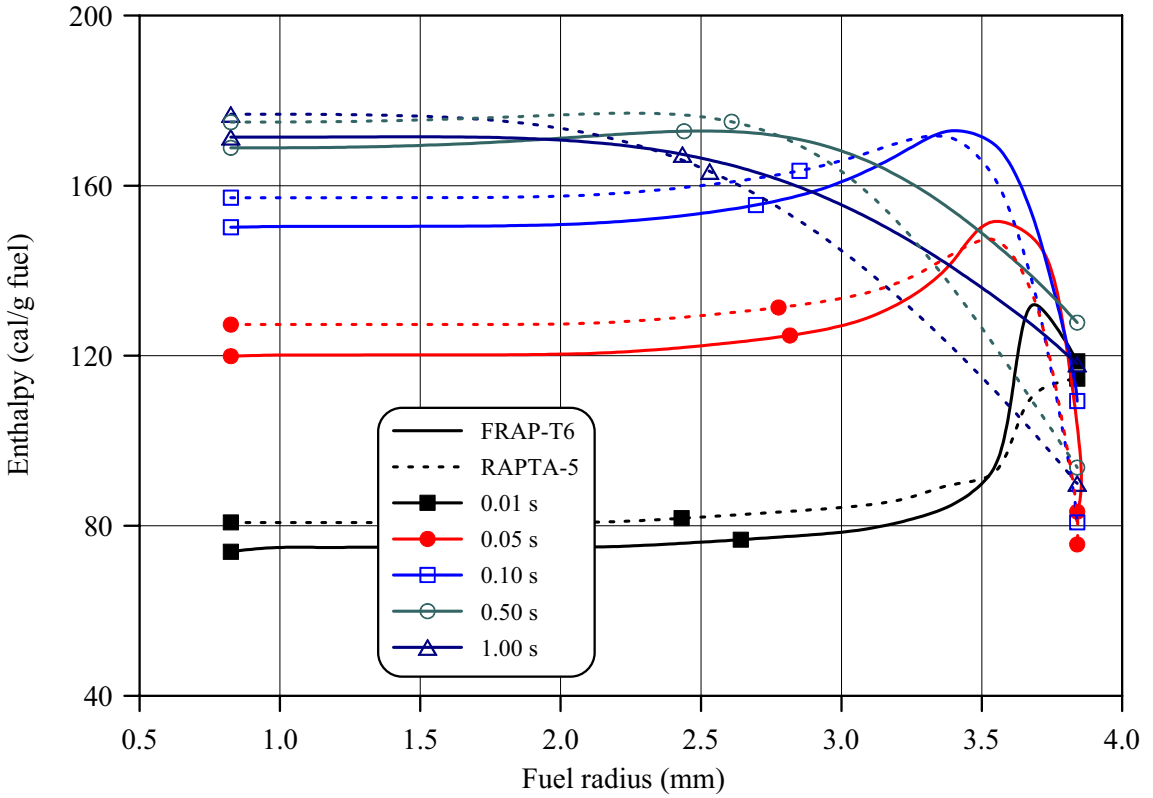


Fig.E-8.7. Radial distribution of energy deposition and fuel enthalpy for fuel rod # RT8

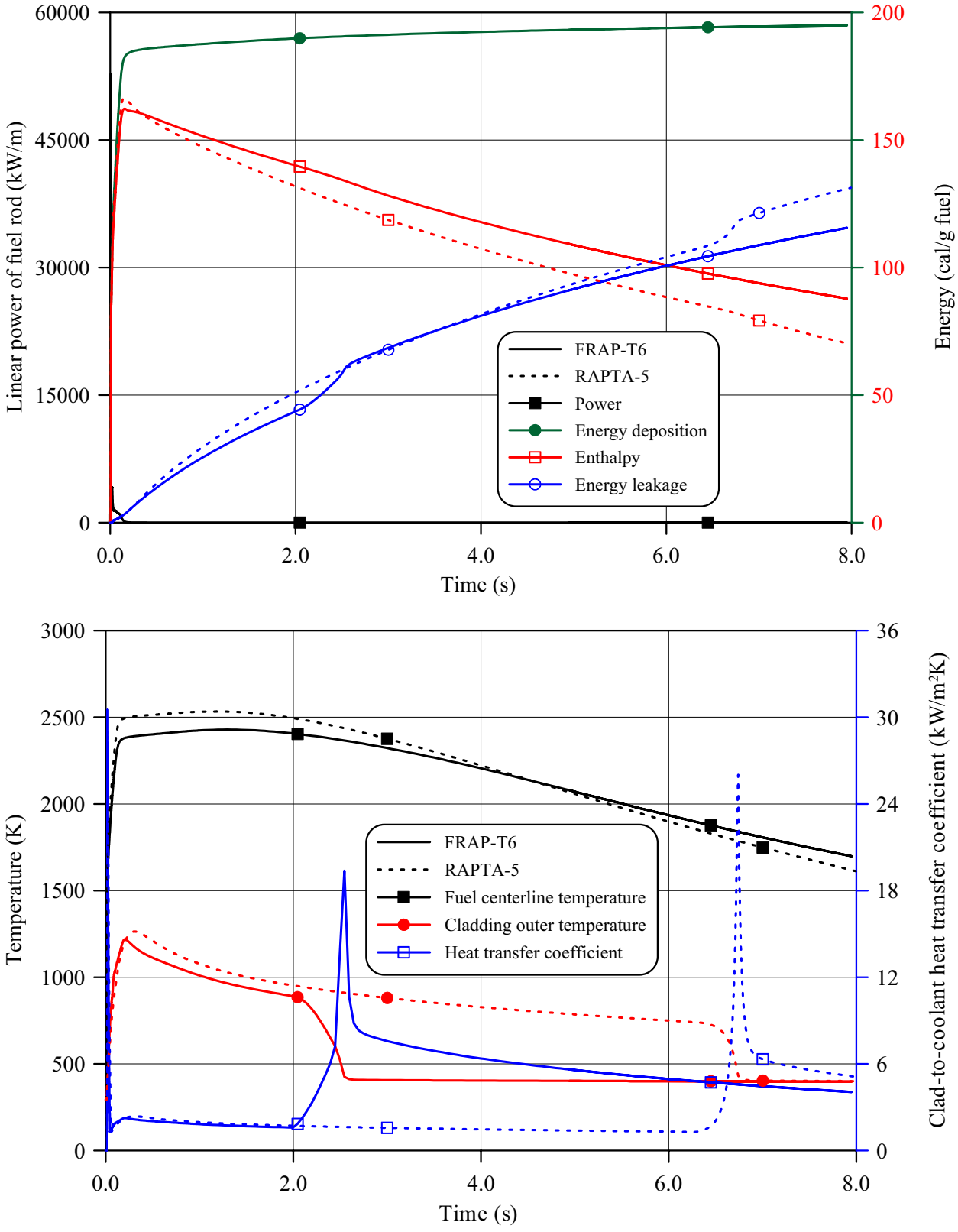


Fig.E-8.8. Thermal history of fuel rod # RT8 during the BIGR test in accordance with FRAP-T6/VVER and RAPTA-5 calculations

RT8

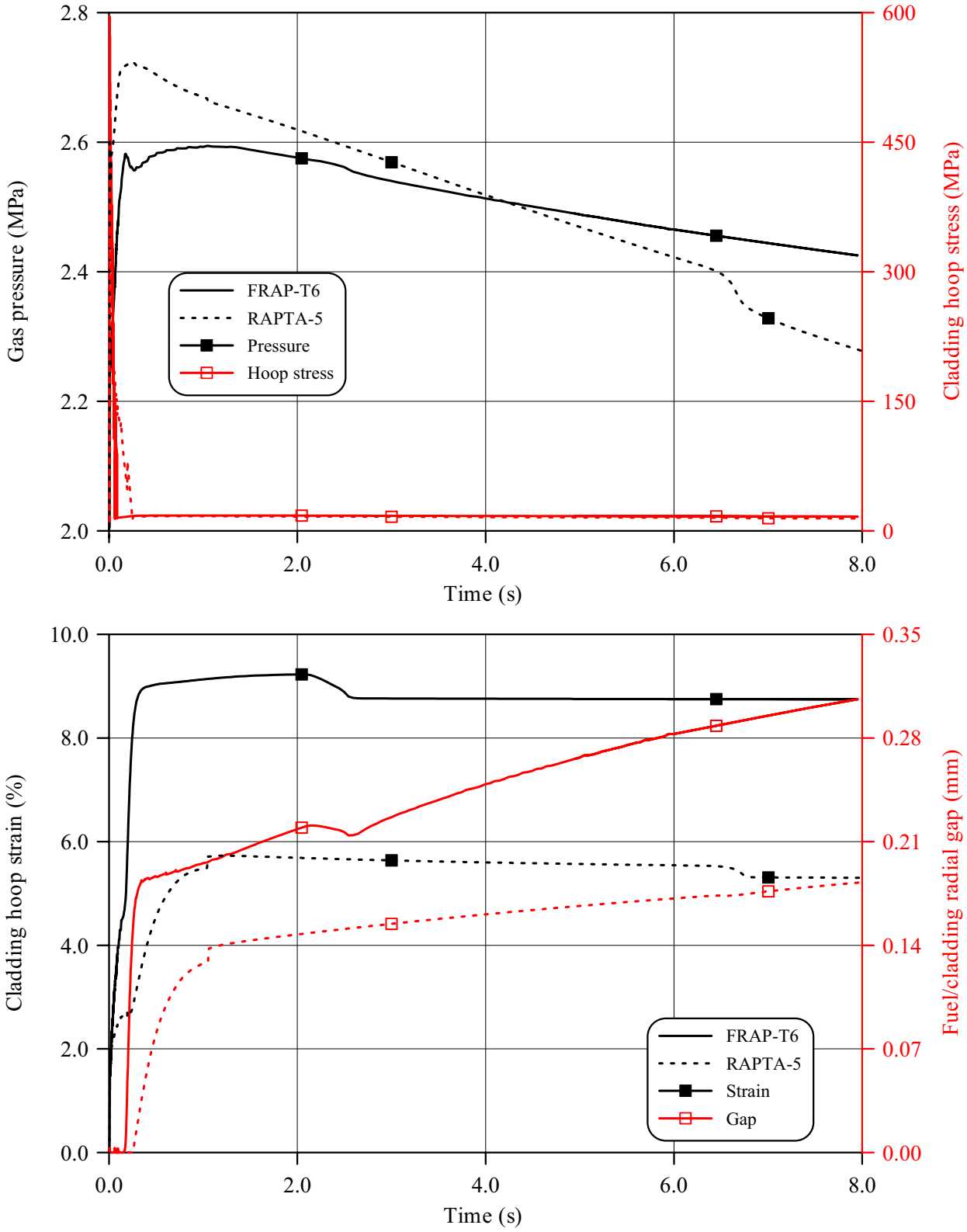


Fig.E-8.9. Mechanical behavior of fuel rod # RT8 during the BIGR test in accordance with FRAP-T6/VVER and RAPTA-5 calculations

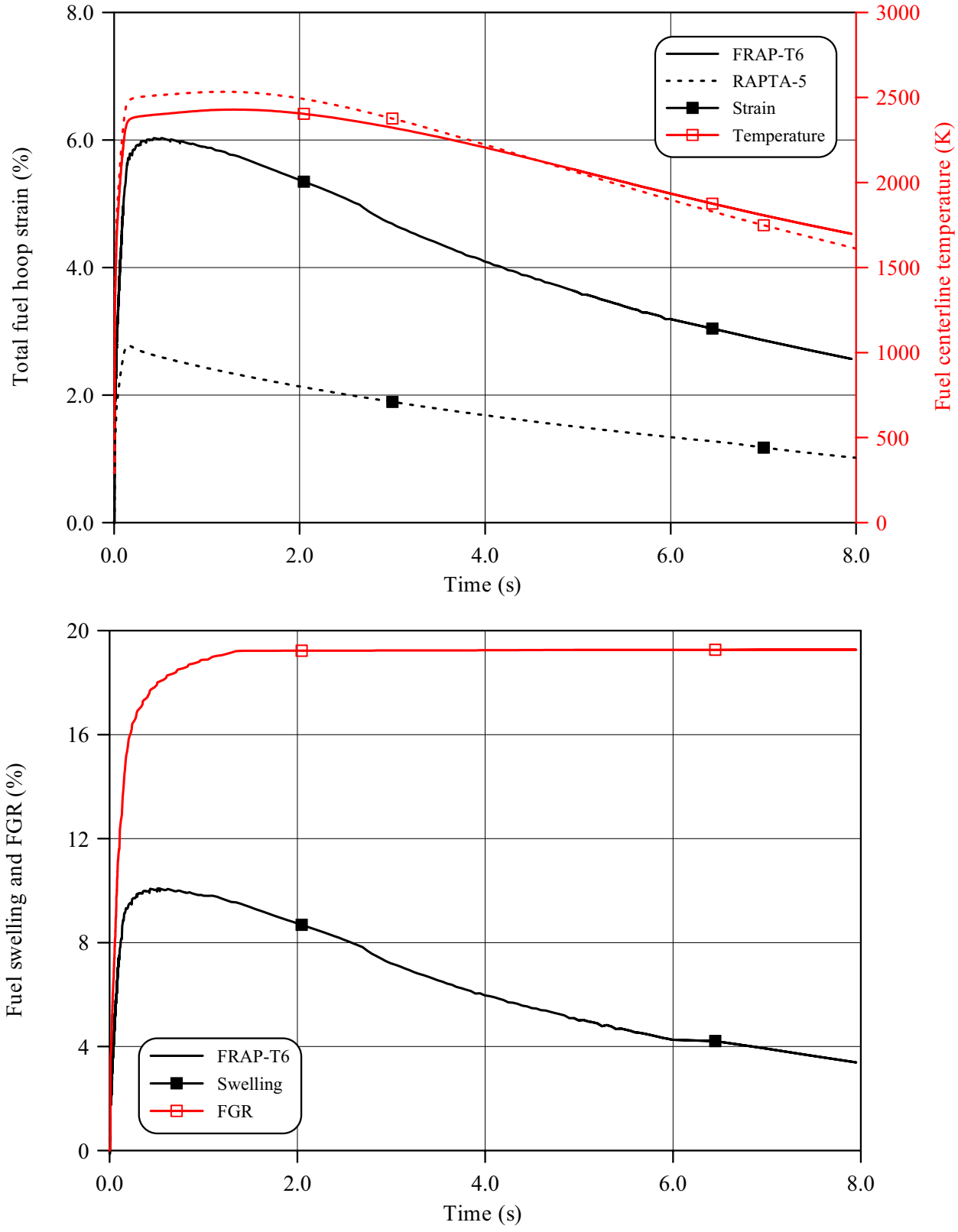


Fig.E-8.10. Fuel behavior during the BIGR test of fuel rod # RT8 in accordance with FRAP-T6/VVER and RAPTA-5 calculations

RT8

Table E-8.3. Axial distribution of cladding average outer diameter in fuel rod # RT8*

Axial coordinate (mm)	Cladding diameter (mm)	Axial coordinate (mm)	Cladding diameter (mm)	Axial coordinate (mm)	Cladding diameter (mm)	Axial coordinate (mm)	Cladding diameter (mm)
7	9.128	45	9.663	83	9.695	121	9.703
9	9.223	47	9.694	85	9.713	123	9.655
11	9.290	49	9.783	87	9.714	125	9.626
13	9.326	51	9.914	89	9.723	127	9.649
15	9.296	53	10.058	91	9.702	129	9.734
17	9.257	55	10.085	93	9.701	131	9.824
19	9.247	57	9.938	95	9.733	133	9.801
21	9.277	59	9.795	97	9.731	135	9.680
23	9.343	61	9.745	99	9.688	137	9.670
25	9.409	63	9.716	101	9.620	139	9.694
27	9.496	65	9.701	103	9.642	141	9.715
29	9.584	67	9.680	105	9.733	143	9.703
31	9.626	69	9.664	107	9.783	145	9.650
33	9.645	71	9.681	109	9.751	147	9.613
35	9.634	73	9.733	111	9.663	149	9.602
37	9.619	75	9.745	113	9.608	151	9.567
39	9.651	77	9.728	115	9.615	153	9.521
41	9.676	79	9.681	117	9.670	155	9.442
43	9.673	81	9.659	119	9.705	157	9.261

* Measured value determined on the basis of profilometry data (16 azimuthal directions)

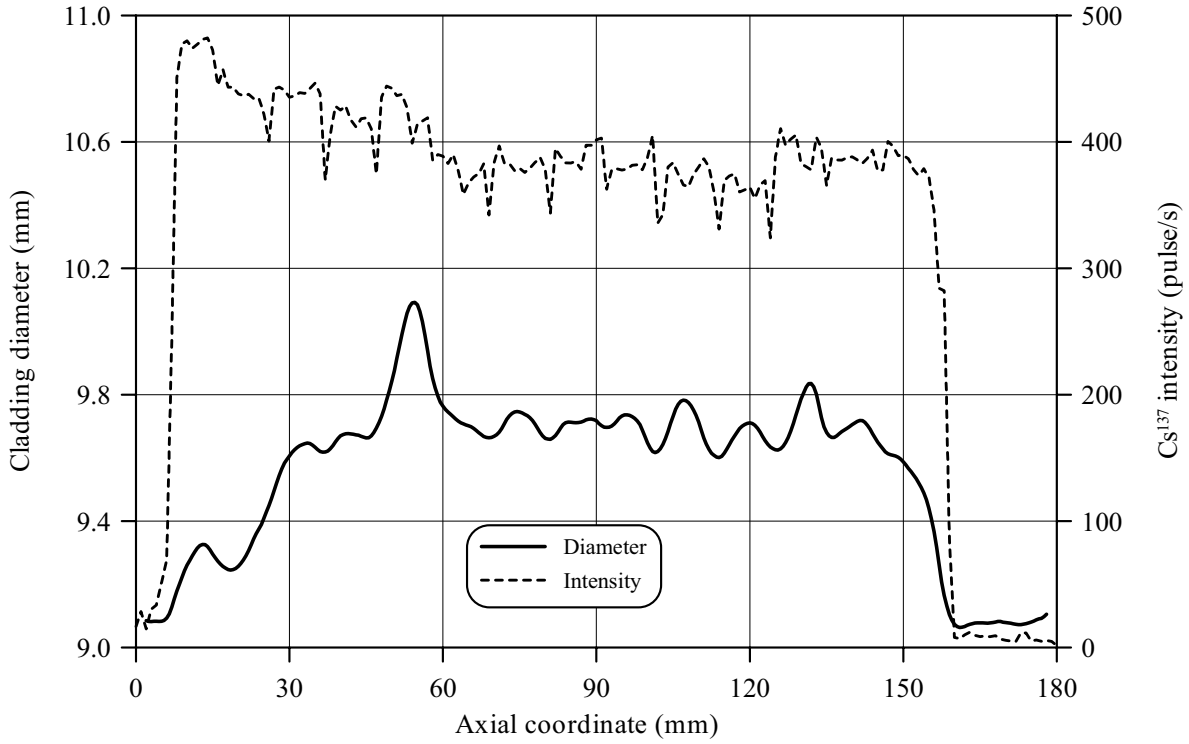


Fig.E-8.11. Cladding measured average diameter and γ-scanning results for fuel rod # RT8

Table E-8.4. The PIE results for fuel rod # RT8

	Parameter	Value
1.	Cladding outer diameter (mm):	
1.1.	Maximum diameter of the bidimensional data sample in "fuel rod length - azimuthal angle" coordinates (mm)	10.35
1.2.	Averaged azimuthal diameter and maximum diameter along the length selected from the sample of averaged azimuthal diameter (mm)	10.09
1.3.	Averaged diameter of the bidimensional data sample in "fuel rod length - azimuthal angle" coordinates (mm)	9.60
2.	Cladding residual hoop strain (%):	
2.1.	Maximum hoop strain	11.10
2.2.	Hoop strain at rupture	11.1, 8.3
3.	Fuel pellet conditional diameter (mm) in cross-section*:	
	at 53 mm elevation	8.33
	at 97 mm elevation	8.28
	at 133 mm elevation	8.22
4.	ZrO_2 outer thickness (μm) in cross-section:	
	at 53, 97, 133 mm elevations	5-7
5.	ZrO_2 inner thickness (μm) in cross-section:	
	at 97 mm elevation	4
6.	Parameters characterizing FGR:	
6.1.	Gas composition (% by volume):	
	He	-
	N_2	-
	O_2	-
	Ar	-
	CO_2	-
	Kr	-
	Xe	-
6.2.	Free gas volume (cm^3)	-
6.3.	Gas volume under normal conditions (cm^3)	-
6.4.	Gas pressure under normal conditions (MPa)	-

* Reference value determined by the processing of fuel cross-section photographs

RT8

Table E-8.5. Organized BIGR test results for fuel rod # RT8

Parameter		Unit	Value		
			Measured	Calculated	
				FRAP-T6	RAPTA-5
1.	Fuel burnup	MW d/kg U	60.2	60.2	60.2
2.	Initial gas pressure	MPa	2.0	2.0	2.0
3.	Energy deposition	cal/g fuel	201.7	201.7	201.7
4.	Peak fuel enthalpy*	cal/g fuel	-	162.3	166.4
5.	Fuel maximum temperature	K	-	2514	2580
6.	Maximum temperature of cladding outer surface	K	-	1219	1264
7.	Cladding burst	Failed, Unfailed	Failed	-**	-**
8.	Cladding residual hoop strain				
	- average***	%	6.08	8.64	5.73
	- maximum	%	11.10	8.64	5.73

* Average value of peak fuel enthalpy 164.3 cal/g fuel

** This parameter was not calculated

*** Average value along the fuel stack length

Appendix E–9

Individual Characteristics of Fuel Rod # RT9

after the BIGR Test

RT9

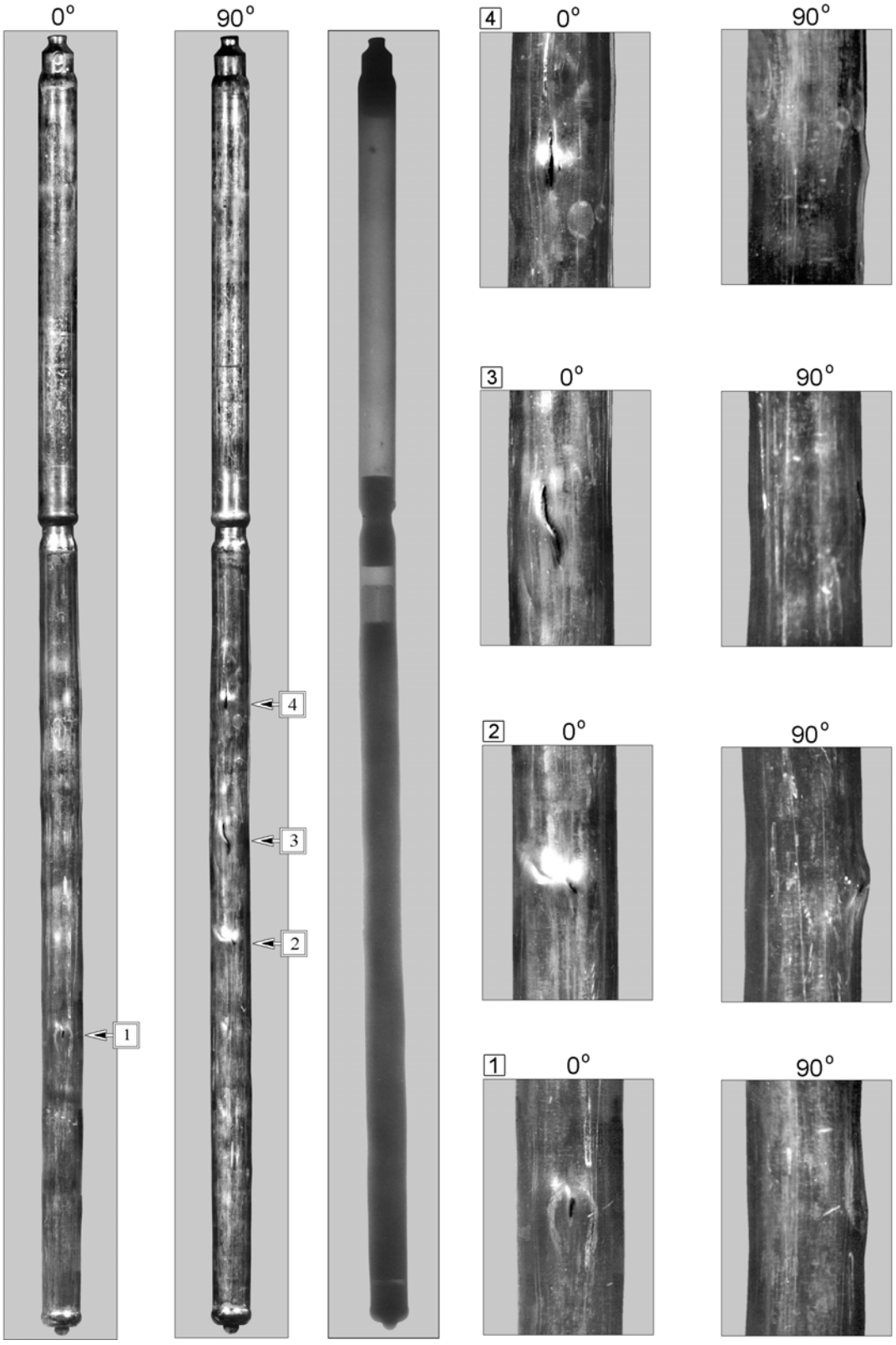


Fig.E-9.1. Appearance of failed fuel rod # RT9 after the BIGR test (photographs and X-ray photograph)

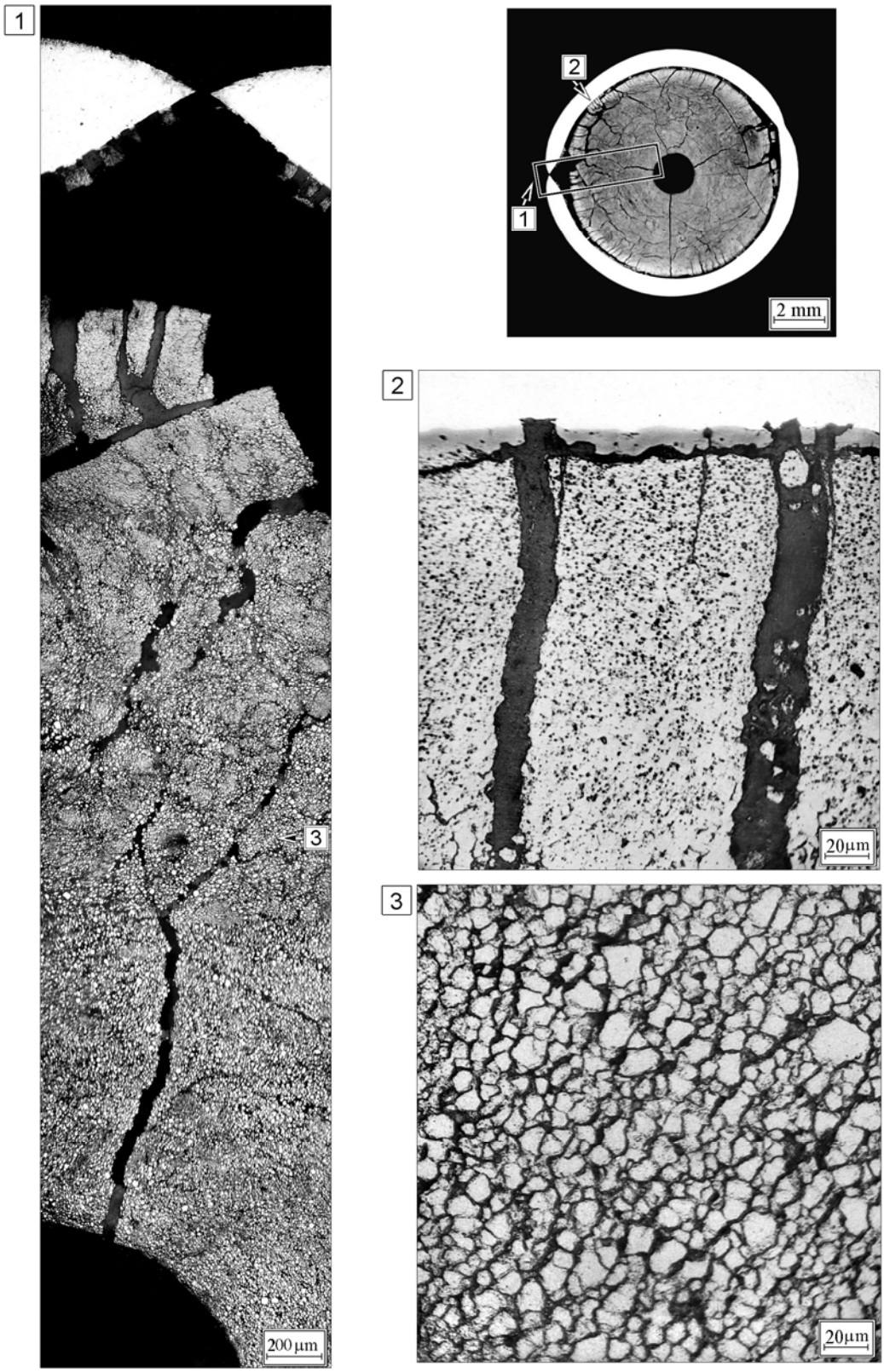


Fig.E-9.2. Cross-section and microstructure of fuel and cladding of fuel rod # RT9 at 69 mm elevation (from low cap)

RT9

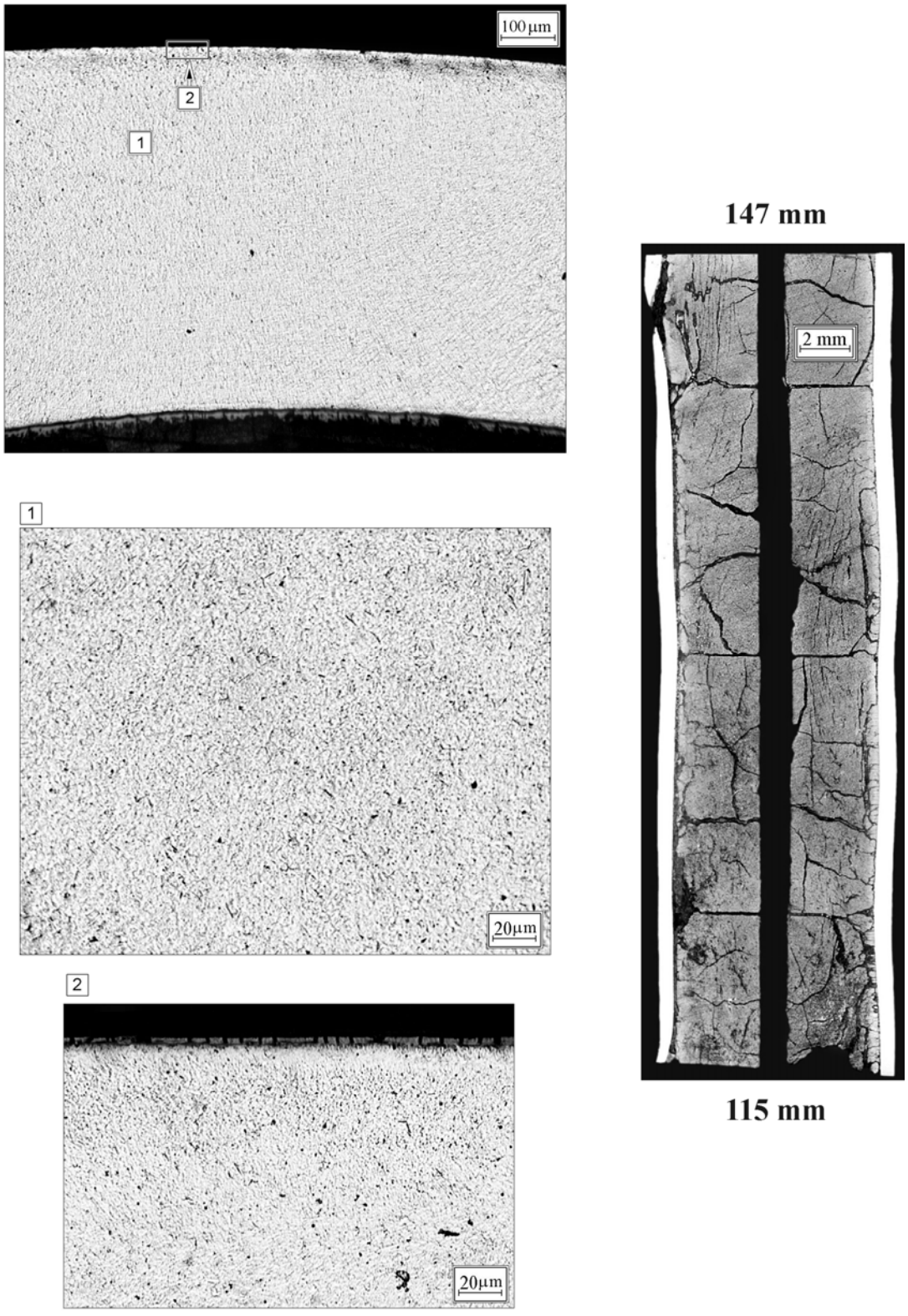


Fig.E-9.3. Cladding microstructure at 69 mm elevation (from low cap) and longitudinal metallographic specimen image of fuel rod # RT9

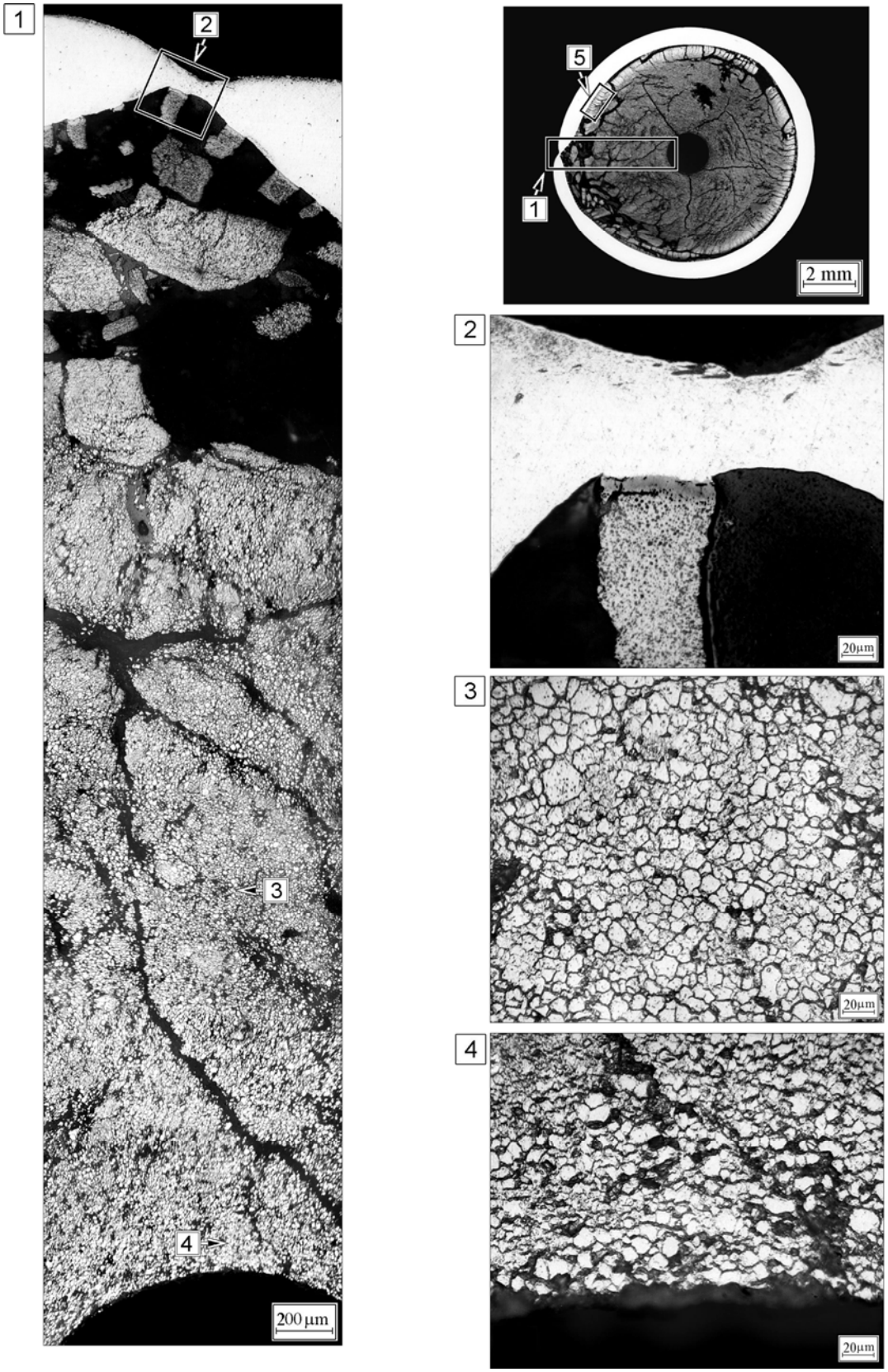
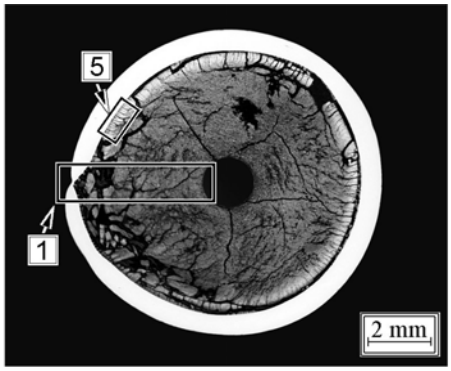
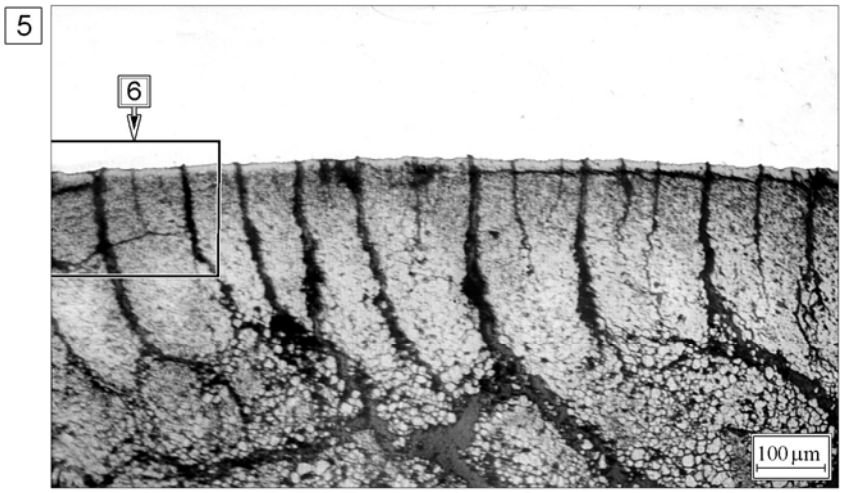


Fig.E-9.4. Cross-section and microstructure of fuel and cladding of fuel rod # RT9 at 88 mm elevation (from low cap)

RT9





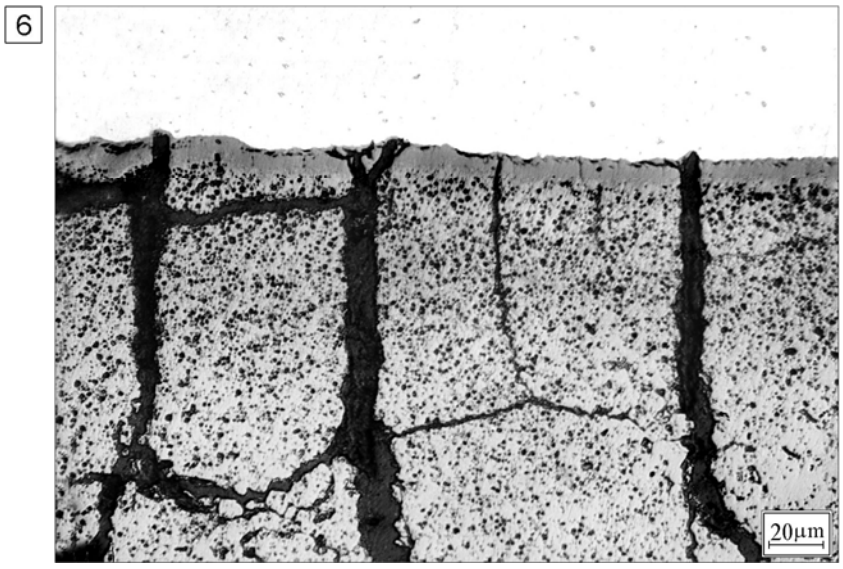


Fig.E-9.5. Microstructure of fuel and cladding in their interaction area for fuel rod # RT9 at 88 mm elevation (from low cap)

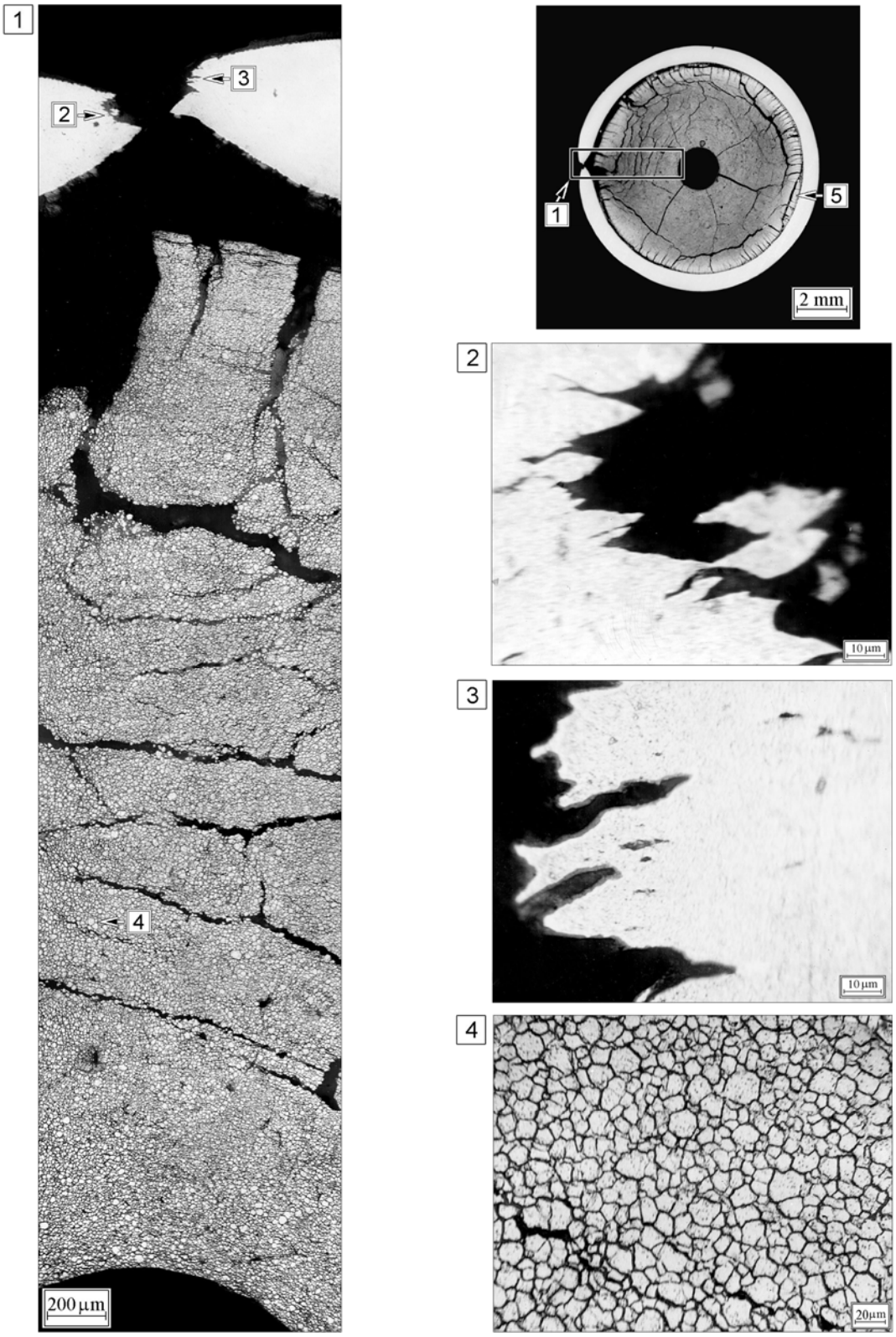


Fig.E-9.6. Cross-section and microstructure of fuel and cladding of fuel rod # RT9 at 110 mm elevation (from low cap)

RT9

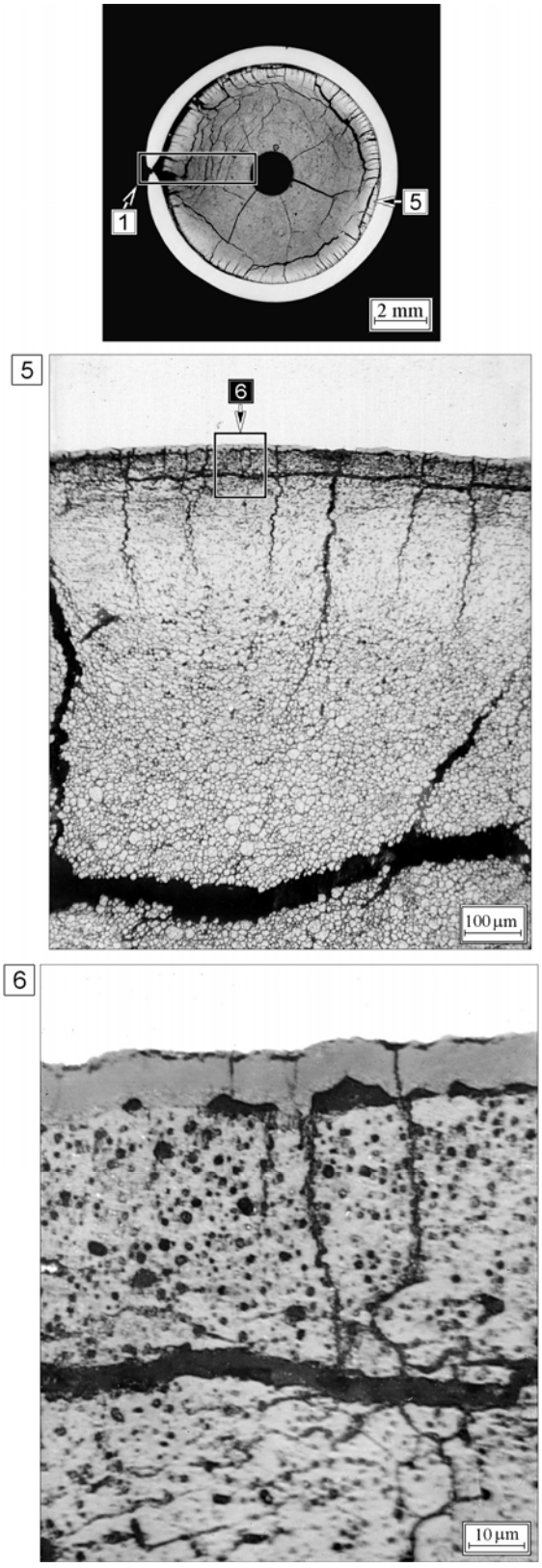


Fig.E-9.7. Microstructure of fuel and cladding in their interaction area for fuel rod # RT9 at 110 mm elevation (from low cap)

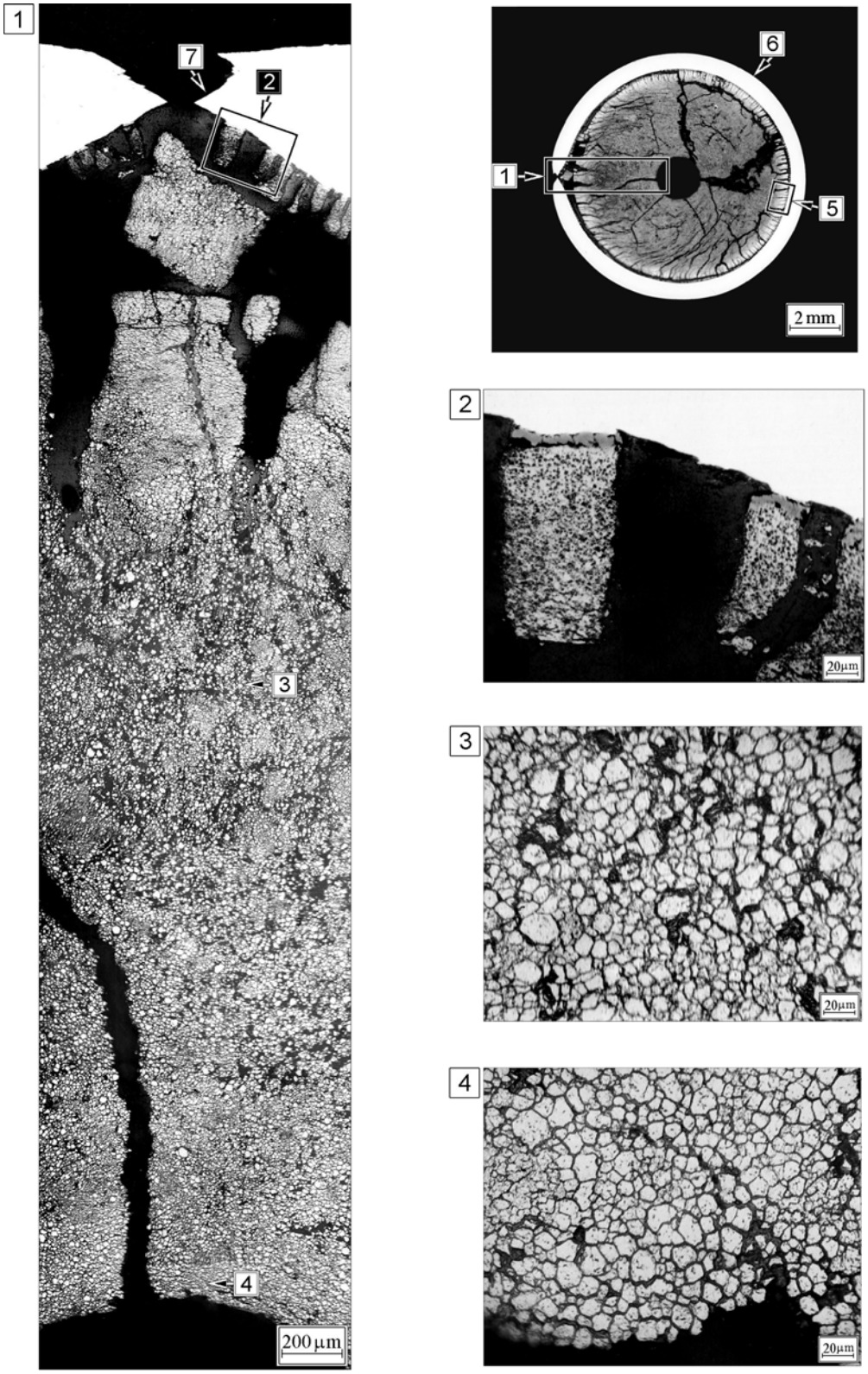


Fig.E-9.8. Cross-section and microstructure of fuel and cladding of fuel rod # RT9 at 144 mm elevation (from low cap)

RT9

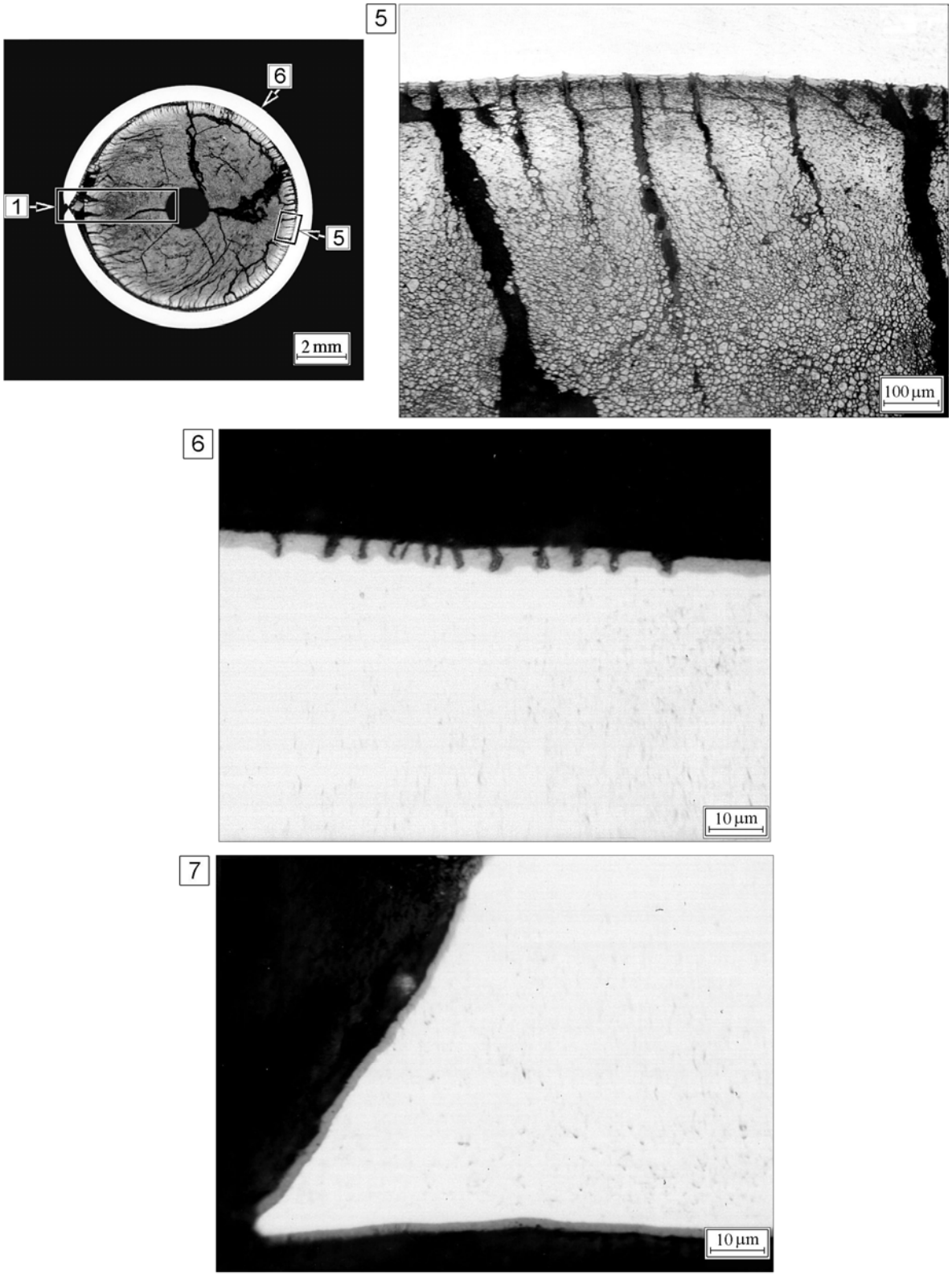


Fig.E-9.9. Fuel and cladding microstructures in their interaction area, cladding microstructure in the burst area at 144 mm elevation (from low cap) for fuel rod # RT9

Table E-9.1. Time dependent energy characteristics of fuel rod # RT9

Time (s)	Relative reactor power (current/ maximum value) (per-unit)	Cumulative number of fissions in fuel rod (fiss) x10^{-14}	Power of fuel rod[1)2)] (kW)	Energy deposition		Fuel enthalpy[3)]	
				(cal/g fuel)	(J/g fuel)	FRAP-T6	RAPTA-5
0.000	0.00E+00	0.000	0.000	0.000	0.000	0.000	0.000
0.001	3.10E-03	0.040	22.09	0.041	0.173	0.671	0.044
0.002	1.31E-02	0.211	93.19	0.218	0.911	0.671	0.213
0.003	5.73E-02	0.961	408.0	0.990	4.143	1.257	1.037
0.004	2.40E-01	4.153	1705	4.283	17.93	4.653	4.408
0.005	6.88E-01	15.16	4895	15.62	65.38	16.101	16.216
0.006	9.98E-01	37.52	7104	38.64	161.8	39.125	40.065
0.007	6.70E-01	59.06	4767	60.82	254.7	61.314	62.915
0.008	3.19E-01	70.98	2269	73.10	306.0	73.501	75.284
0.009	1.55E-01	76.58	1103	78.87	330.2	79.094	80.938
0.010	9.19E-02	79.51	654.8	81.91	342.9	81.940	83.814
0.012	5.93E-02	82.98	422.2	85.52	358.1	85.168	86.986
0.014	6.09E-02	85.98	433.6	88.56	370.8	87.826	89.659
0.016	7.20E-02	89.32	513.0	91.96	385.0	90.861	92.773
0.018	8.32E-02	93.20	592.4	95.97	401.8	94.503	96.536
0.020	8.64E-02	97.43	615.1	100.4	420.1	98.522	100.700
0.022	8.11E-02	101.7	577.3	104.7	438.2	102.487	104.809
0.024	7.01E-02	105.6	499.5	108.6	454.7	106.028	108.464
0.026	5.82E-02	108.7	414.5	111.9	468.4	108.974	111.515
0.028	4.75E-02	111.1	338.1	114.6	479.7	111.362	113.964
0.030	3.86E-02	113.6	275.4	116.8	489.0	113.405	115.907
0.050	3.01E-02	129.2	214.8	133.3	558.2	127.090	129.994
0.070	2.74E-02	143.4	195.0	147.8	618.7	135.847	142.414
0.090	2.31E-02	156.1	164.4	160.6	672.3	145.515	153.144
0.110	1.78E-02	166.3	127.1	171.3	717.2	154.950	161.897
0.130	8.36E-03	173.1	59.70	178.1	745.7	160.310	166.618
0.150	3.09E-03	175.2	22.14	180.7	756.5	161.988	167.474
0.200	7.25E-04	177.3	5.351	182.8	765.1	162.116	165.632
1.000	8.18E-05	180.2	0.712	186.1	779.1	145.296	142.784
10.00	9.48E-06	186.5	0.094	194.1	812.4	77.015	42.662
100.0	1.91E-07	189.1	0.004	199.1	833.6	8.681	4.998
1000	7.50E-13	189.2	1.70E-04	200.9	841.1	0.000	0.000

[1)] Average values determined in accordance with results of RRC KI and VNIIEF calculations

[2)] Maximum power value is 7120.5 kW (t=0.00594 s)

[3)] Average radial value

RT9

Table E-9.2. Radial energy characteristics of fuel rod # RT9*

Parameters	Coordinates of fuel radial layers (mm)			
	1 layer (0.825-2.777)	2 layer (2.777-3.454)	3 layer (3.454-3.747)	4 layer (3.747-3.840)
Number of fissions $x10^{-14}$ (fiss)	8.494	5.371	3.326	1.737
Fission density $x10^{-13}$ (fiss/g fuel)	2.567	2.705	3.349	5.230
Power** (kW)	3190	2020	1254	657.0
Energy deposition (cal/g fuel)	180.1	190.0	235.8	369.2
Energy deposition (J/g fuel)	754.0	795.6	987.1	1546
Energy deposition*** (per-unit)	0.488	0.515	0.639	1.000

* Average values were determined in accordance with results of RRC KI and VNIIEF calculations

** The power for the entire length of each layer at time 0.00594 s

*** Energy deposition in current layer/energy deposition in 4^{th} layer

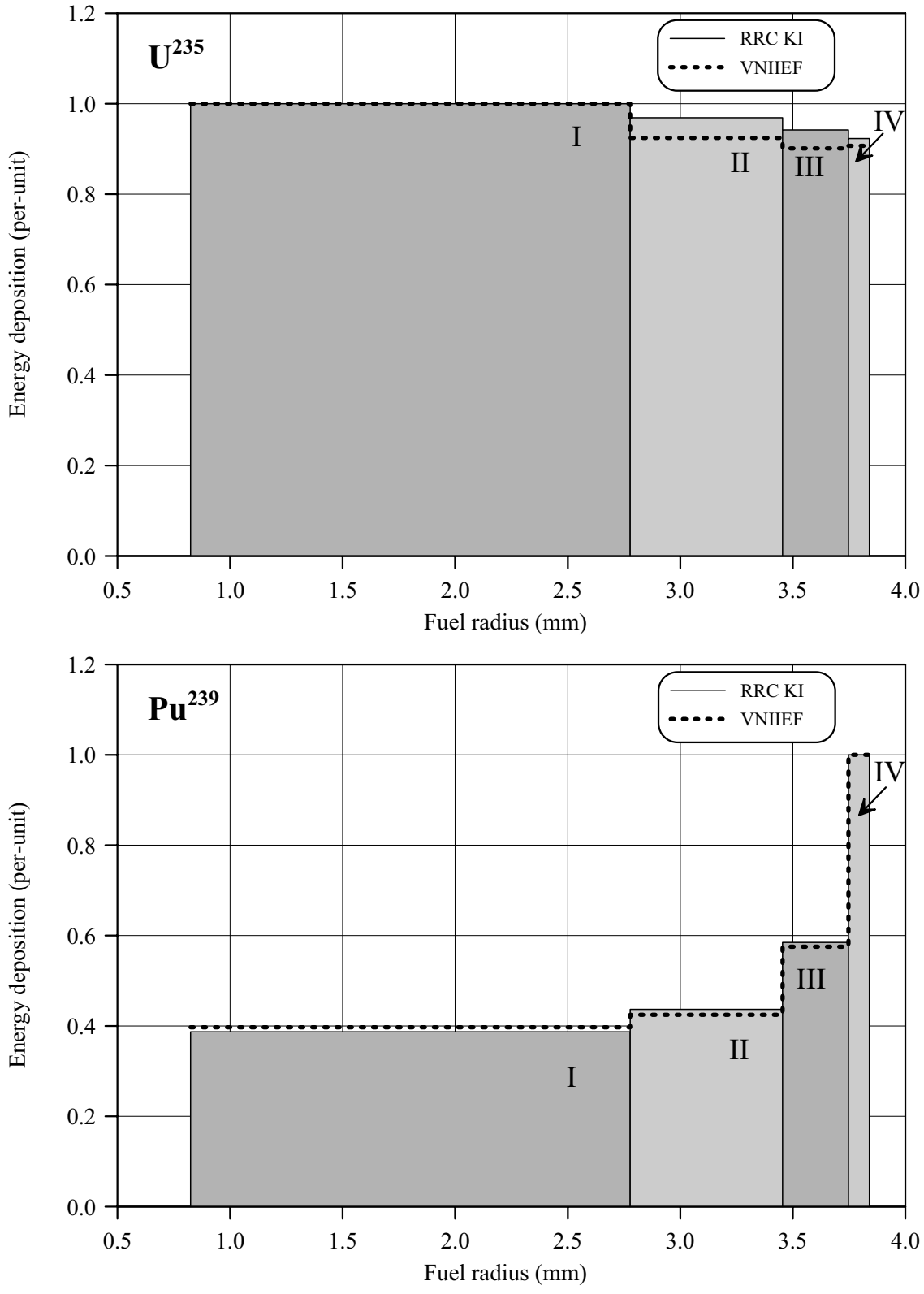


Fig.E-9.10. U^{235} and Pu^{239} radial distribution of energy deposition for fuel rod # RT9

RT9

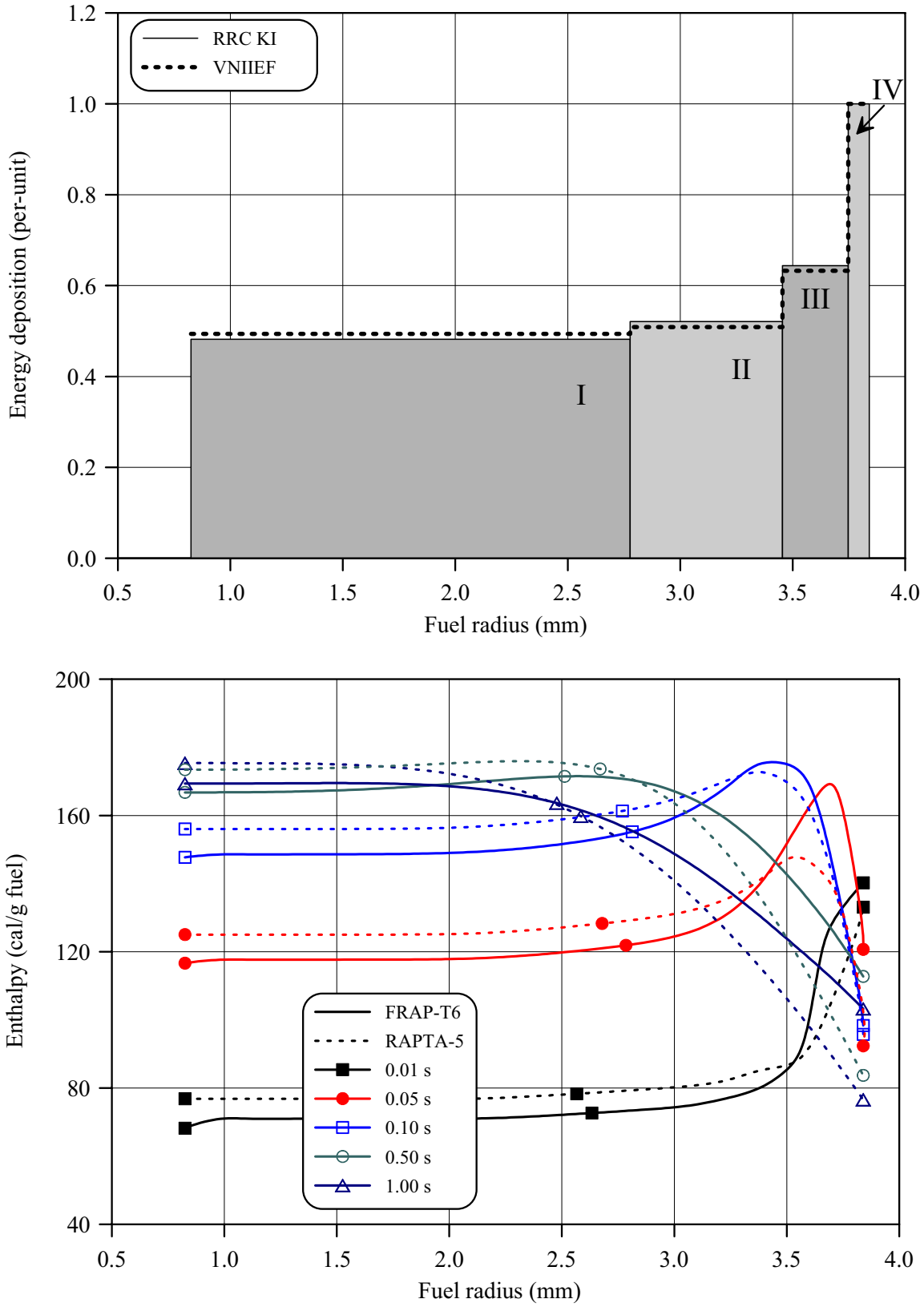


Fig.E-9.11. Radial distribution of energy deposition and fuel enthalpy for fuel rod # RT9

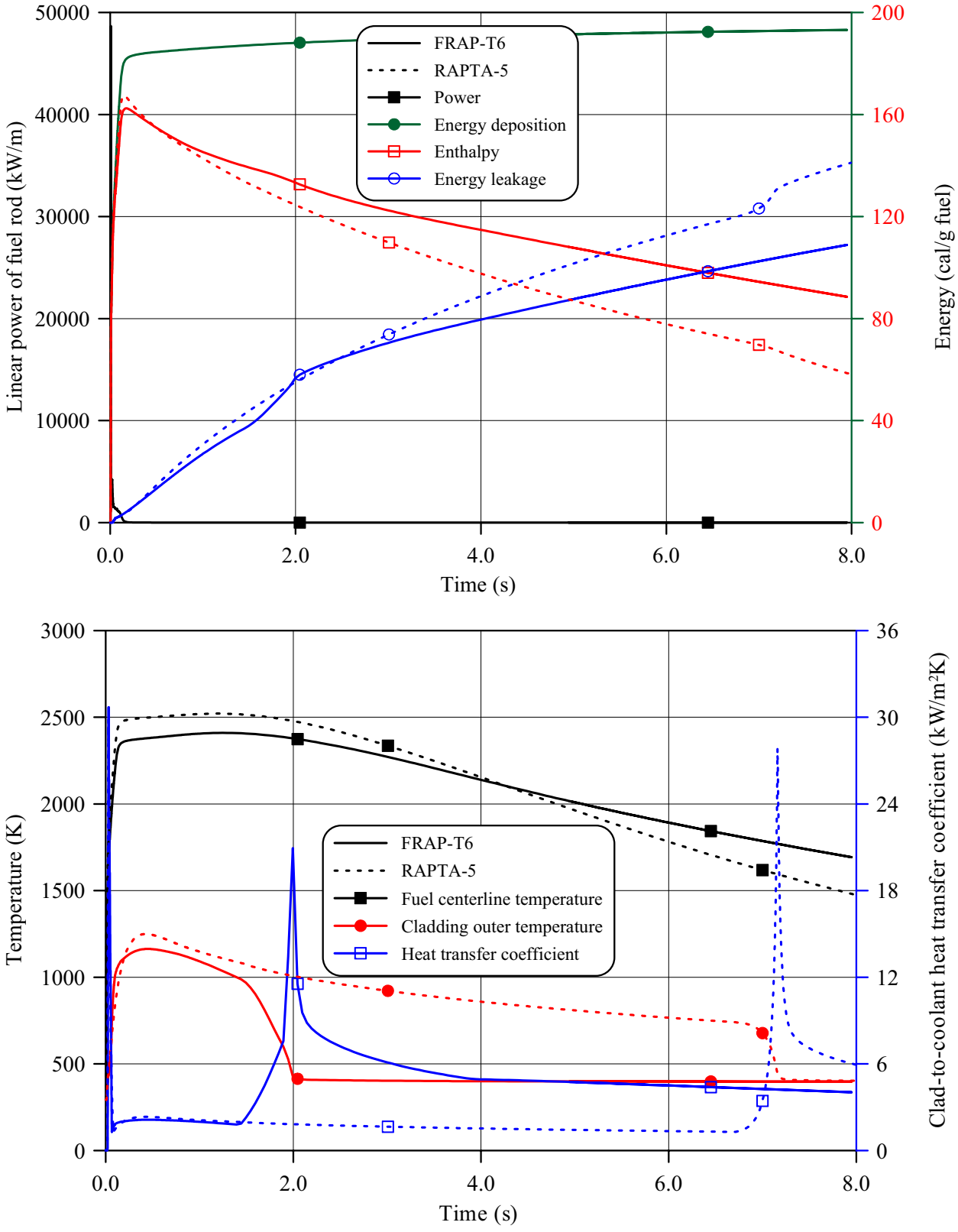


Fig.E-9.12. Thermal history of fuel rod # RT9 during the BIGR test in accordance with FRAP-T6/VVER and RAPTA-5 calculations

RT9

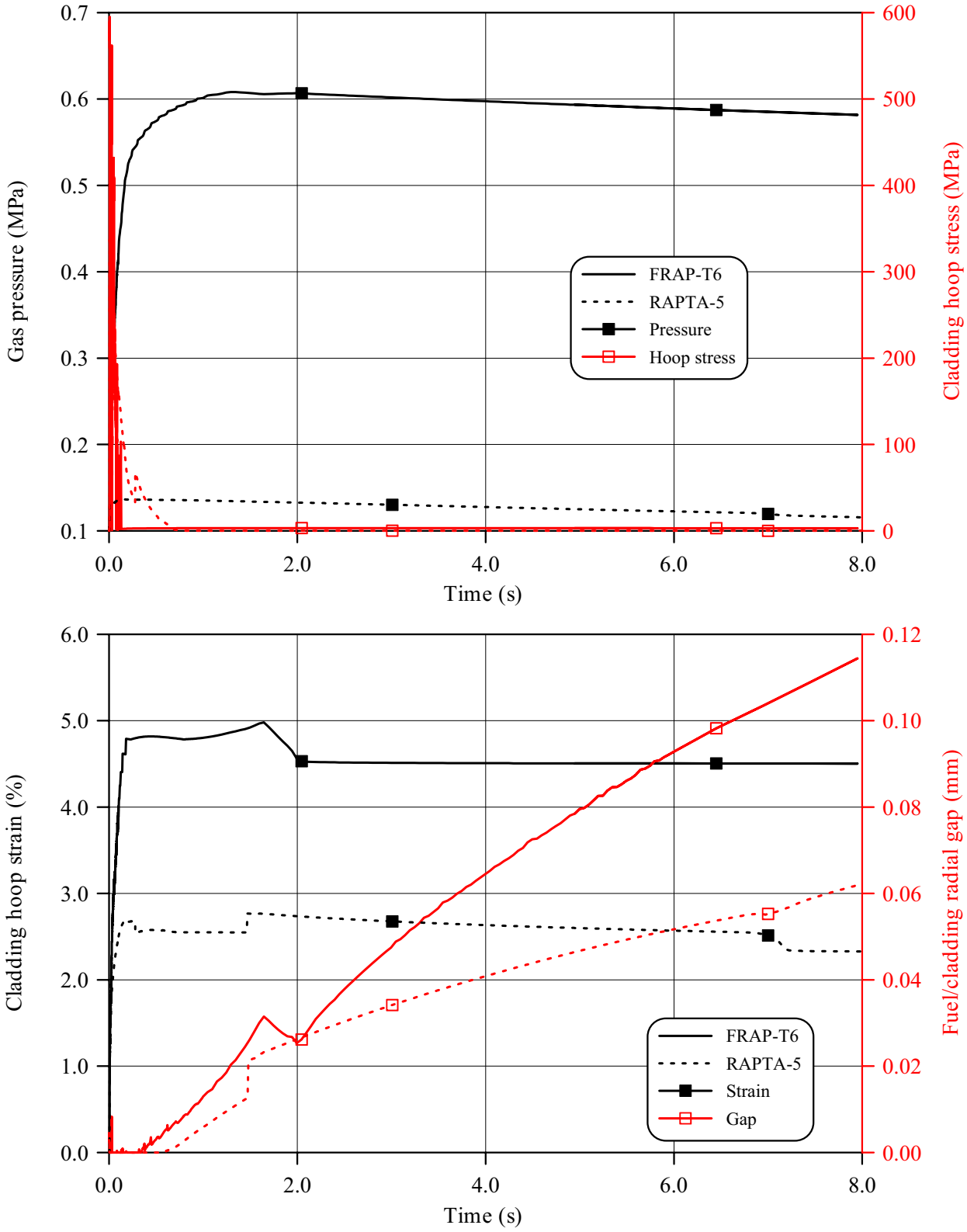


Fig.E-9.13. Mechanical behavior of fuel rod # RT9 during the BIGR test in accordance with FRAP-T6/VVER and RAPTA-5 calculations

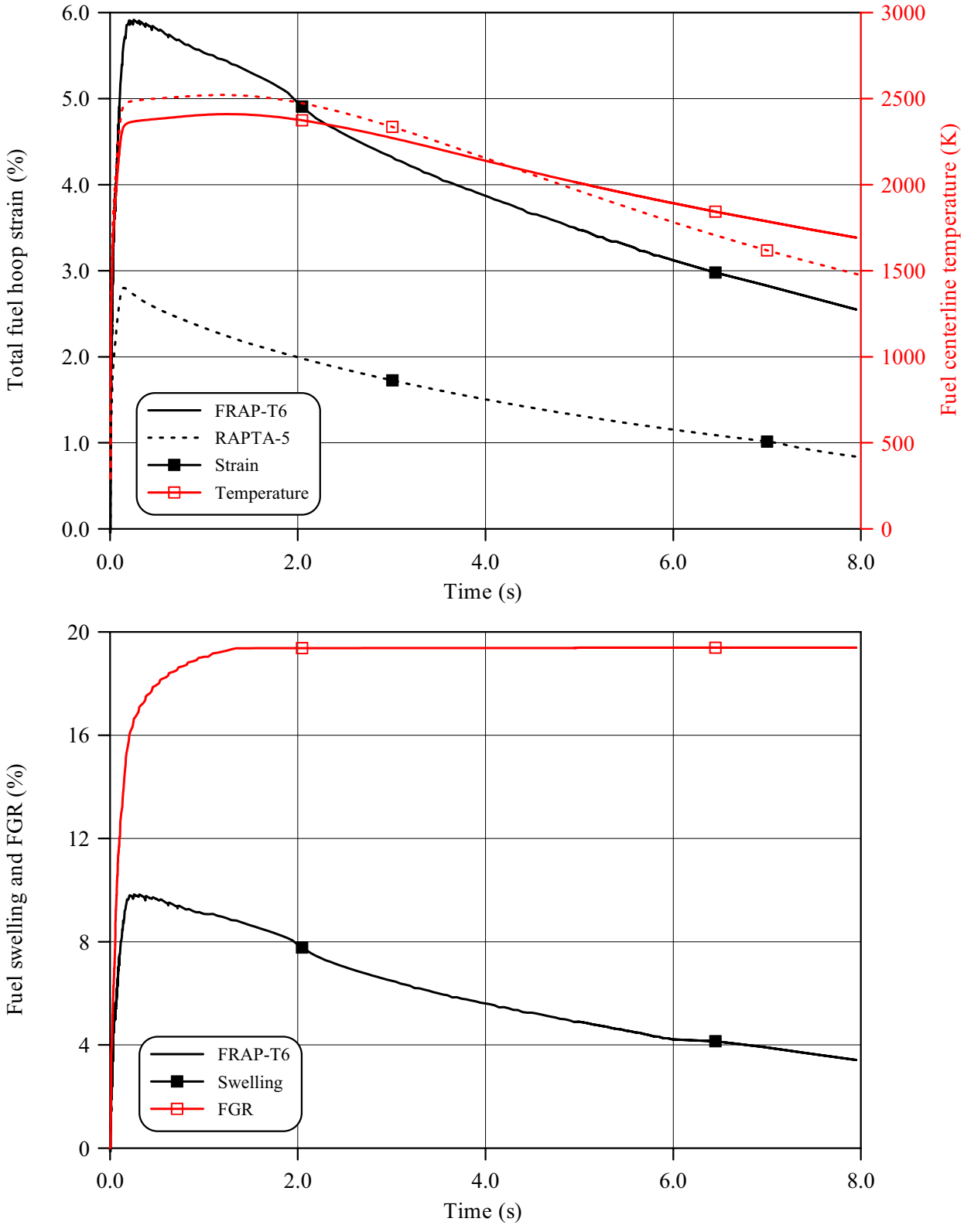


Fig.E-9.14. Fuel behavior during the BIGR test of fuel rod # RT9 in accordance with FRAP-T6/VVER and RAPTA-5 calculations

RT9

Table E-9.3. Axial distribution of cladding average outer diameter in fuel rod # RT9*

Axial coordinate (mm)	Cladding diameter (mm)	Axial coordinate (mm)	Cladding diameter (mm)	Axial coordinate (mm)	Cladding diameter (mm)	Axial coordinate (mm)	Cladding diameter (mm)
8	9.185	46	9.804	84	9.695	122	9.710
10	9.265	48	9.741	86	9.859	124	9.648
12	9.321	50	9.726	88	9.944	126	9.553
14	9.334	52	9.770	90	9.734	128	9.577
16	9.330	54	9.753	92	9.569	130	9.673
18	9.350	56	9.687	94	9.580	132	9.694
20	9.404	58	9.639	96	9.633	134	9.643
22	9.480	60	9.668	98	9.623	136	9.592
24	9.551	62	9.733	100	9.559	138	9.600
26	9.549	64	9.823	102	9.517	140	9.679
28	9.537	66	9.897	104	9.556	142	9.780
30	9.578	68	9.836	106	9.651	144	9.856
32	9.642	70	9.694	108	9.729	146	9.742
34	9.678	72	9.680	110	9.790	148	9.642
36	9.634	74	9.727	112	9.802	150	9.638
38	9.625	76	9.734	114	9.680	152	9.624
40	9.677	78	9.688	116	9.569	154	9.520
42	9.763	80	9.645	118	9.555	156	9.399
44	9.801	82	9.646	120	9.636	158	9.248

* Measured value determined on the basis of profilometry data (16 azimuthal directions)

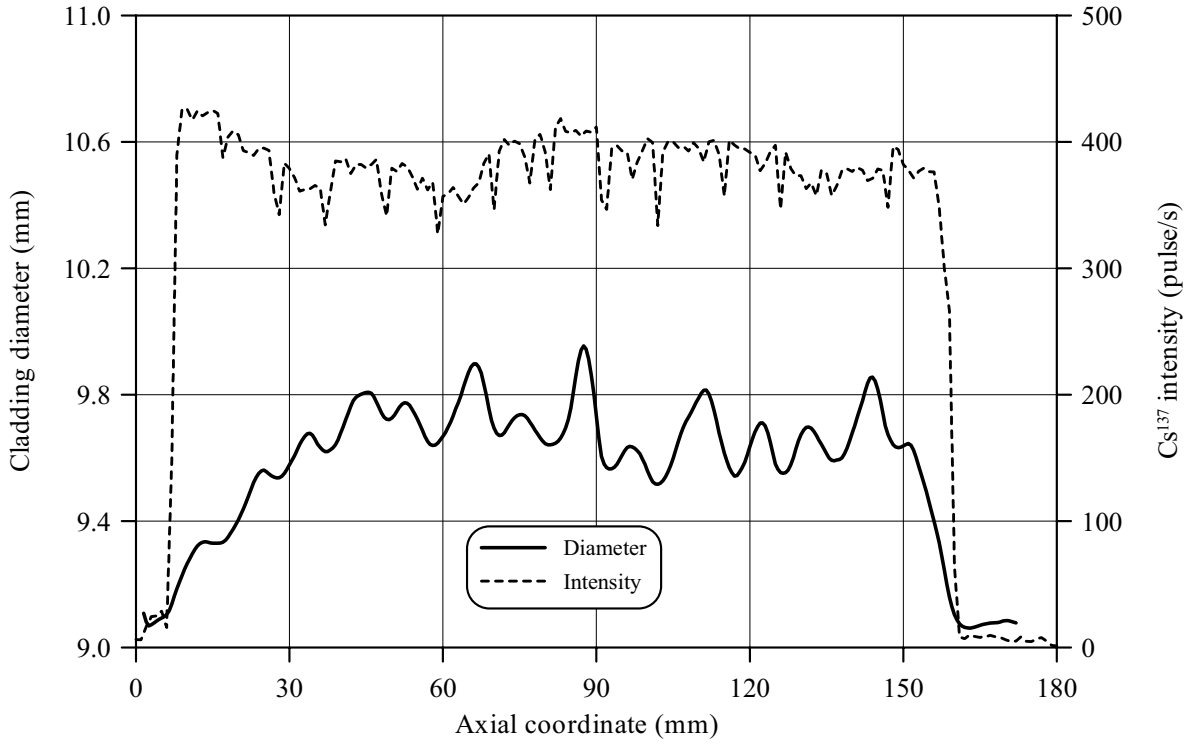


Fig.E-9.15. Cladding measured average diameter and γ-scanning results for fuel rod # RT9

Table E-9.4. The PIE results for fuel rod # RT9

	Parameter	Value
1.	Cladding outer diameter (mm):	
1.1.	Maximum diameter of the bidimensional data sample in "fuel rod length - azimuthal angle" coordinates (mm)	10.37
1.2.	Averaged azimuthal diameter and maximum diameter along the length selected from the sample of averaged azimuthal diameter (mm)	9.95
1.3.	Averaged diameter of the bidimensional data sample in "fuel rod length - azimuthal angle" coordinates (mm)	9.62
2.	Cladding residual hoop strain (%):	
2.1.	Maximum hoop strain	9.60
2.2.	Hoop strain at rupture	9.1; 9.6; 8.2; 8.6
3.	Fuel pellet conditional diameter (mm) in cross-section*:	
	at 69 mm elevation	8.21
	at 88 mm elevation	8.19
	at 110 mm elevation	8.24
	at 144 mm elevation	8.20
4.	ZrO_2 outer thickness (μm) in cross-section:	
	at 69, 88, 110, 144 mm elevations	5
5.	ZrO_2 inner thickness (μm) in cross-section:	
	at 69 mm elevation	8
	at 110 mm elevation	8
6.	Parameters characterizing FGR:	
6.1.	Gas composition (% by volume):	
	He	-
	N_2	-
	O_2	-
	Ar	-
	CO_2	-
	Kr	-
	Xe	-
6.2.	Free gas volume (cm^3)	-
6.3.	Gas volume under normal conditions (cm^3)	-
6.4.	Gas pressure under normal conditions (MPa)	-

* Reference value determined by the processing of fuel cross-section photographs

RT9

Table E-9.5. Organized BIGR test results for fuel rod # RT9

Parameter		Unit	Value		
			Measured	Calculated	
				FRAP-T6	RAPTA-5
1.	Fuel burnup	MW d/kg U	59.9	59.9	59.9
2.	Initial gas pressure	MPa	0.1	0.1	0.1
3.	Energy deposition	cal/g fuel	200.9	200.9	200.9
4.	Peak fuel enthalpy*	cal/g fuel	-	162.4	167.5
5.	Fuel maximum temperature	K	-	2524	2584
6.	Maximum temperature of cladding outer surface	K	-	1164	1249
7.	Cladding burst	Failed, Unfailed	Failed	-**	-**
8.	Cladding residual hoop strain				
	- average***	%	6.27	4.41	2.77
	- maximum	%	9.60	4.98	2.77

* Average value of peak fuel enthalpy 164.9 cal/g fuel

** This parameter was not calculated

*** Average value along the fuel stack length

Appendix E–10

Individual Characteristics of Fuel Rod # RT10

after the BIGR Test

RT10

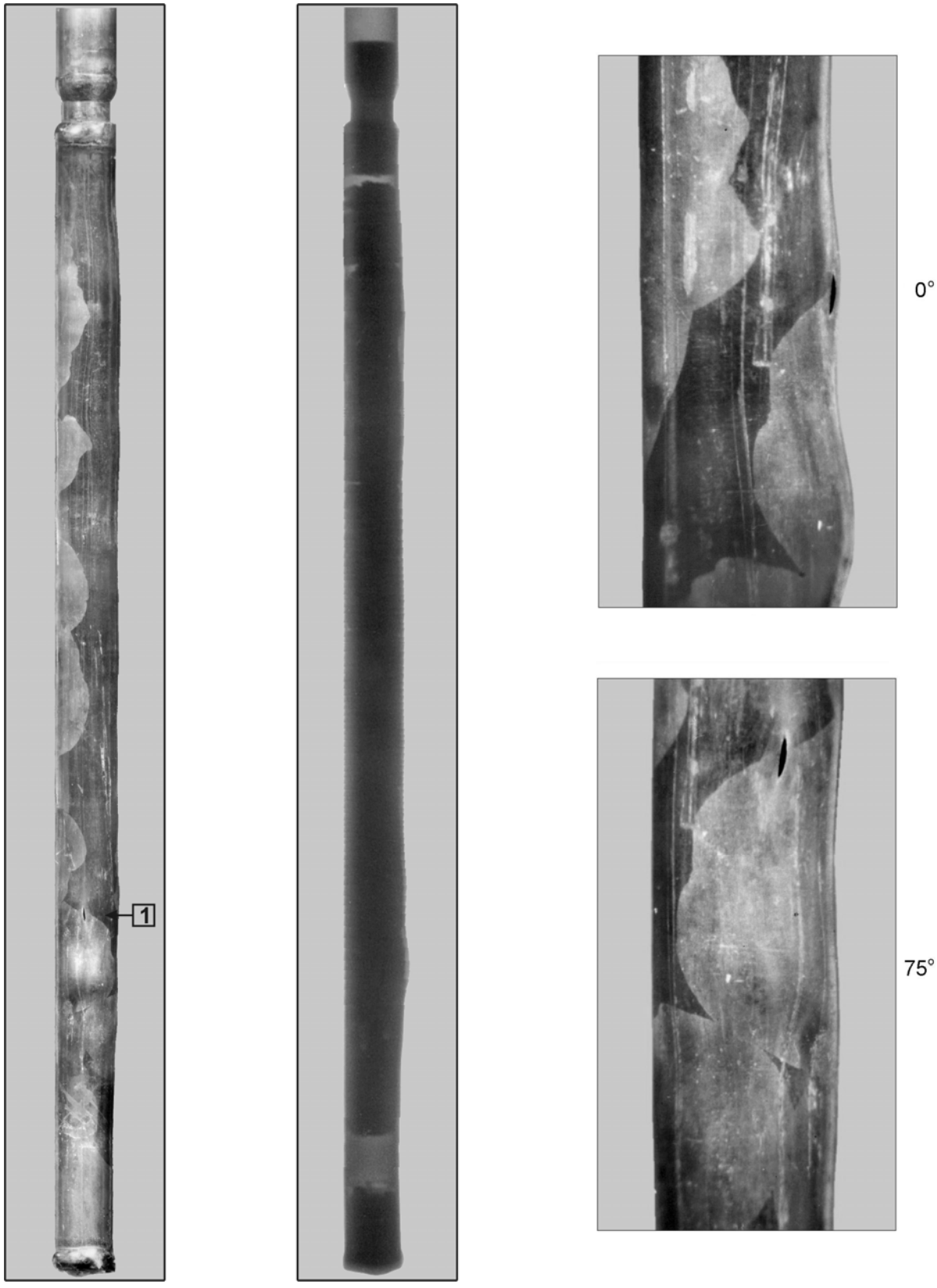


Fig.E-10.1. Appearance of failed fuel rod # RT10 after the BIGR test (photographs and X-ray photograph)

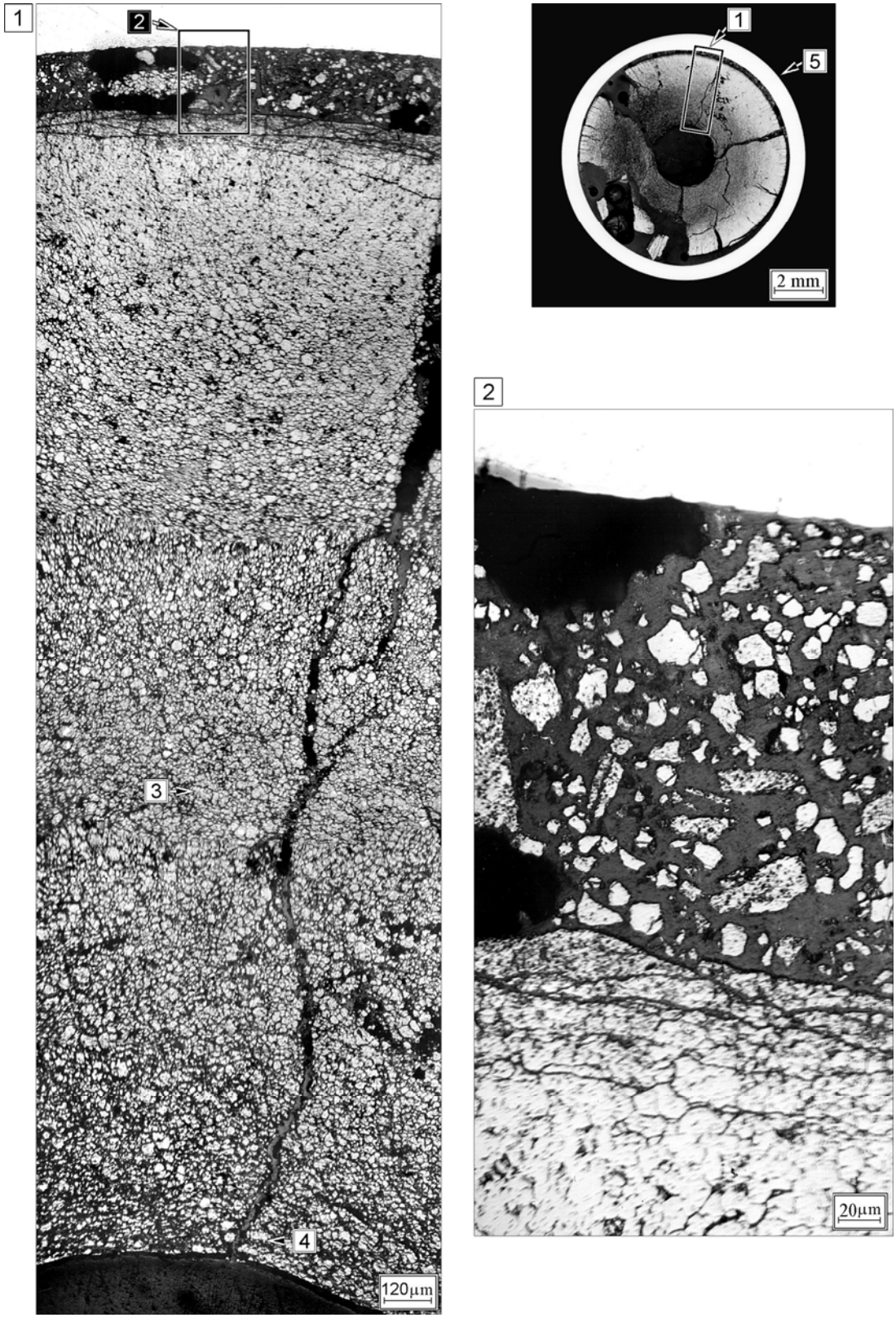


Fig.E-10.2. Cross-section and fuel microstructure of fuel rod # RT10 at 33 mm elevation (from low cap)

RT10

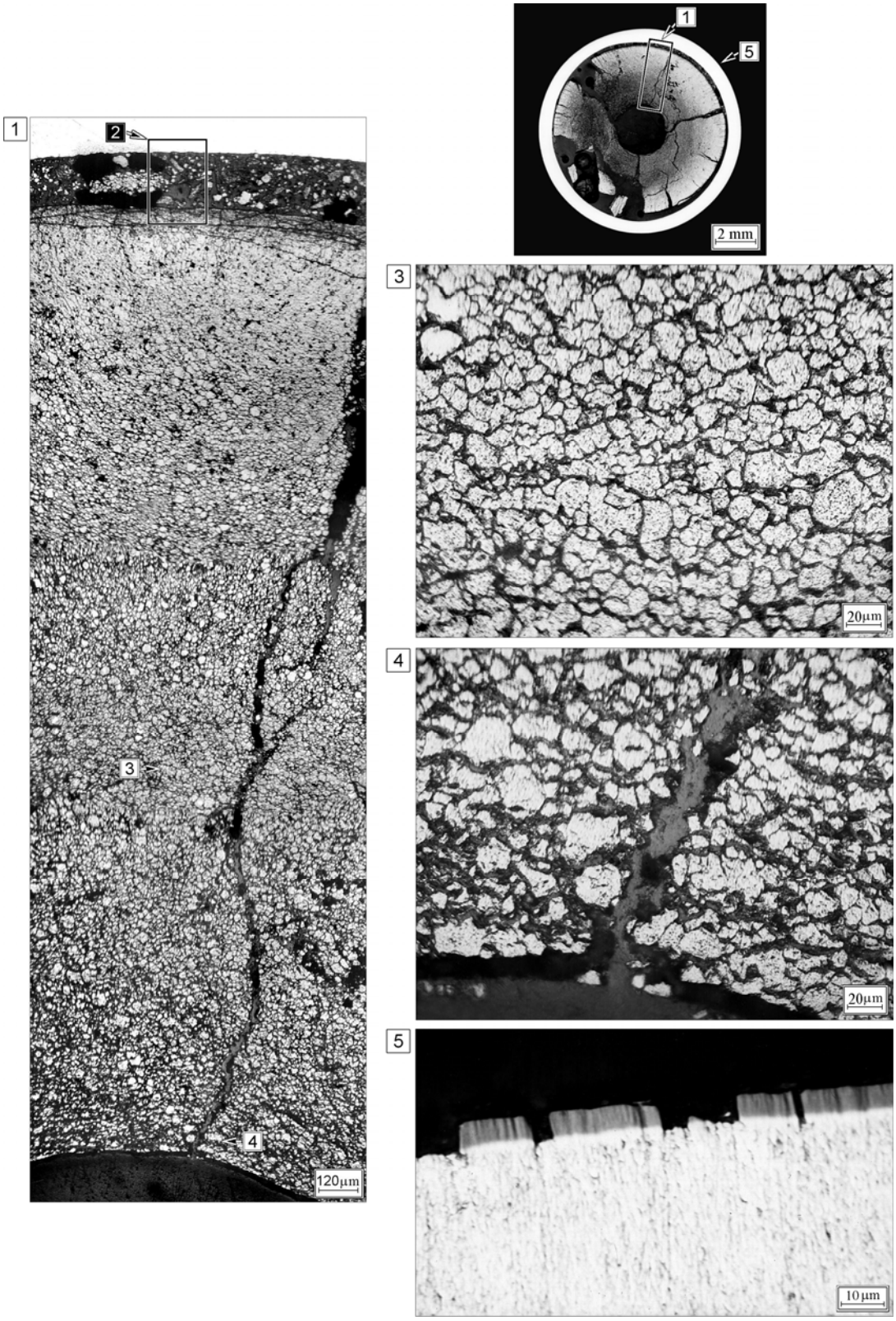
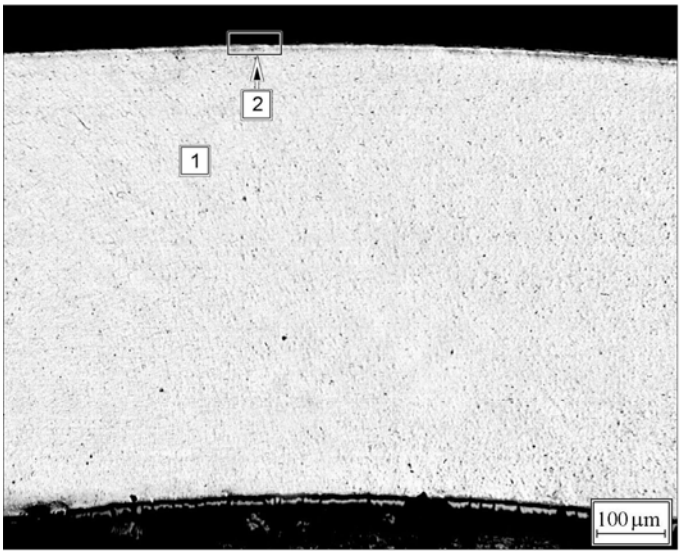
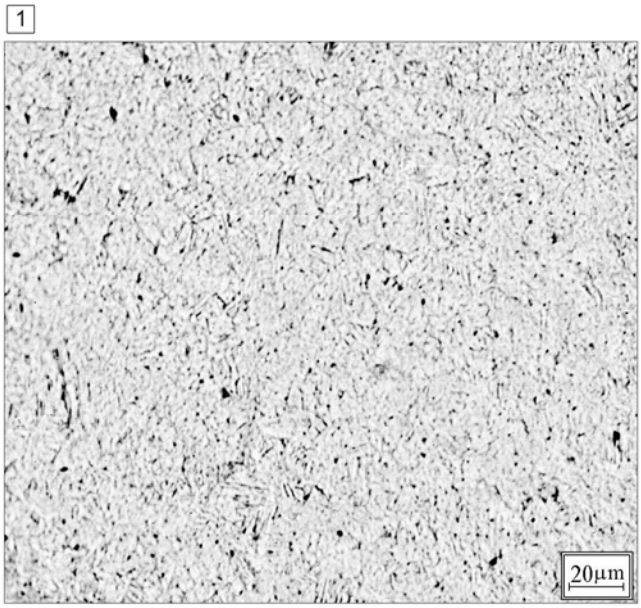


Fig.E-10.3. Cross-section and microstructure of fuel and cladding of fuel rod # RT10 at 33 mm elevation (from low cap)





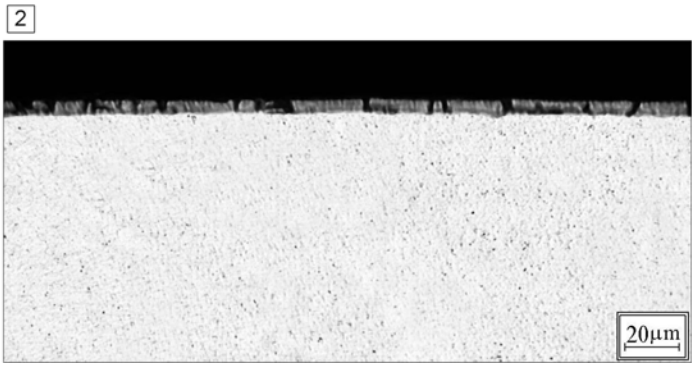


Fig.E-10.4. Cladding microstructure of fuel rod # RT10 at 33 mm elevation (from low cap)

RT10

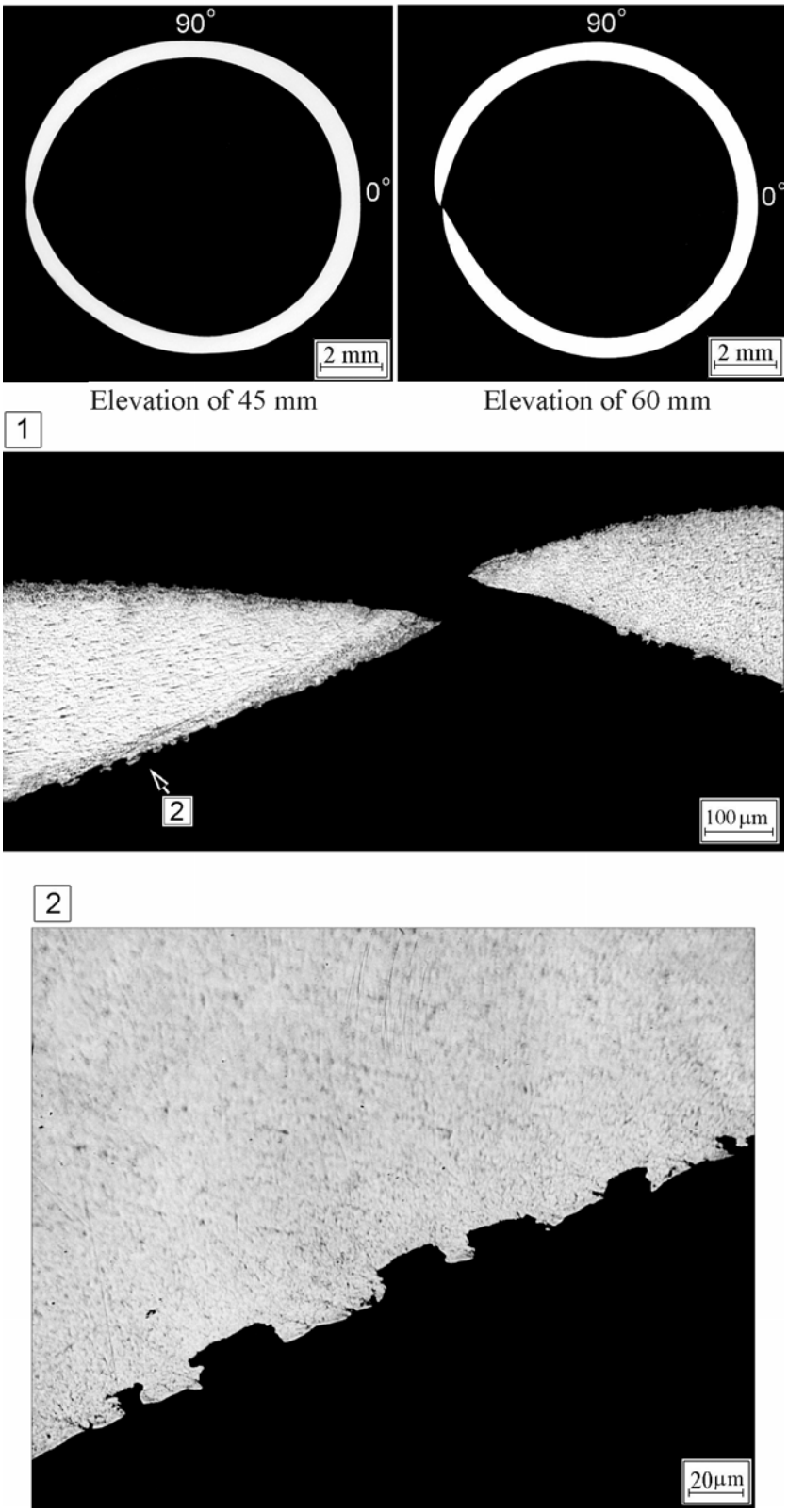


Fig.E-10.5. Cladding cross-sections at elevations 45 and 60 mm and cladding microstructure at 60 mm elevation (from low cap) for fuel rod # RT10

Table E-10.1. Time dependent energy characteristics of fuel rod # RT10

Time (s)	Relative reactor power (current/ maximum value) (per-unit)	Cumulative number of fissions in fuel rod (fiss) x10^{-14}	Power of fuel rod[1)2)] (kW)	Energy deposition		Fuel enthalpy[3)]	
				(cal/g fuel)	(J/g fuel)	FRAP-T6	RAPTA-5
0.000	0.00E+00	0.000	0.000	0.000	0.000	0.000	0.000
0.001	9.16E-03	0.140	75.14	0.151	0.634	0.671	0.008
0.002	4.13E-02	0.748	338.9	0.811	3.397	0.671	0.048
0.003	1.85E-01	3.508	1516	3.803	15.92	0.671	0.195
0.004	6.20E-01	14.31	5085	15.52	64.96	1.091	0.805
0.005	9.98E-01	39.15	8186	42.50	177.9	4.076	3.976
0.006	6.84E-01	64.62	5613	70.07	293.4	15.499	15.977
0.007	3.18E-01	78.53	2607	85.21	356.7	41.590	42.989
0.008	1.50E-01	84.89	1229	92.13	385.7	68.273	70.367
0.009	8.59E-02	88.17	705.1	95.67	400.5	82.848	85.261
0.010	6.22E-02	90.27	510.7	97.93	410.0	89.376	91.781
0.012	5.26E-02	93.44	431.1	101.4	424.4	94.495	96.818
0.014	5.67E-02	96.53	465.2	104.8	438.6	97.283	99.638
0.016	6.50E-02	99.88	533.4	108.6	454.5	100.010	102.487
0.018	6.93E-02	103.8	568.7	112.8	472.3	103.191	105.803
0.020	6.68E-02	107.7	547.9	117.1	490.1	106.810	109.590
0.022	5.90E-02	111.6	484.4	121.0	506.6	110.476	113.402
0.024	5.04E-02	114.6	413.3	124.5	521.1	113.842	116.911
0.026	4.19E-02	117.4	343.9	127.4	533.2	116.717	119.900
0.028	3.51E-02	119.5	288.4	129.7	543.2	119.070	122.357
0.030	3.09E-02	121.4	253.4	131.8	551.8	120.976	124.333
0.050	2.64E-02	137.3	217.2	149.1	624.3	134.540	138.386
0.070	2.21E-02	151.7	181.6	164.5	688.6	146.907	150.845
0.090	1.54E-02	162.6	126.8	176.3	738.0	154.873	160.149
0.110	6.66E-03	168.8	54.79	183.1	766.6	160.862	165.043
0.130	2.39E-03	170.9	19.80	185.7	777.4	162.471	165.870
0.150	1.23E-03	171.9	10.33	186.8	782.2	162.444	165.233
0.200	4.18E-04	172.9	3.614	188.0	787.1	160.937	162.802
1.000	6.97E-05	175.6	0.700	191.2	800.5	148.795	147.640
10.00	8.13E-06	181.6	0.093	199.5	835.3	61.291	66.612
100.0	1.64E-07	184.5	0.004	204.8	857.5	6.053	10.345
1000	6.45E-13	184.6	1.65E-04	206.7	865.2	0.000	0.000

[1)] Average values determined in accordance with results of RRC KI and VNIIEF calculations

[2)] Maximum power value is 8204 kW (t=0.00491 s)

[3)] Average radial value

RT10

Table E-10.2. Radial energy characteristics of fuel rod # RT10*

Parameters	Coordinates of fuel radial layers (mm)			
	1 layer (1.250-2.834)	2 layer (2.834-3.452)	3 layer (3.452-3.722)	4 layer (3.722-3.808)
Number of fissions $x10^{-14}$ (fiss)	8.317	5.305	3.238	1.607
Fission density $x10^{-13}$ (fiss/g fuel)	2.657	2.824	3.452	5.122
Power** (kW)	3688	2356	1442	718.6
Energy deposition (cal/g fuel)	185.8	197.7	242.4	360.8
Energy deposition (J/g fuel)	778.1	827.8	1015	1511
Energy deposition*** (per-unit)	0.515	0.548	0.672	1.000

* Average values were determined in accordance with results of RRC KI and VNIIEF calculations

** The power for the entire length of each layer at time 0.00491 s

*** Energy deposition in current layer/energy deposition in 4^{th} layer

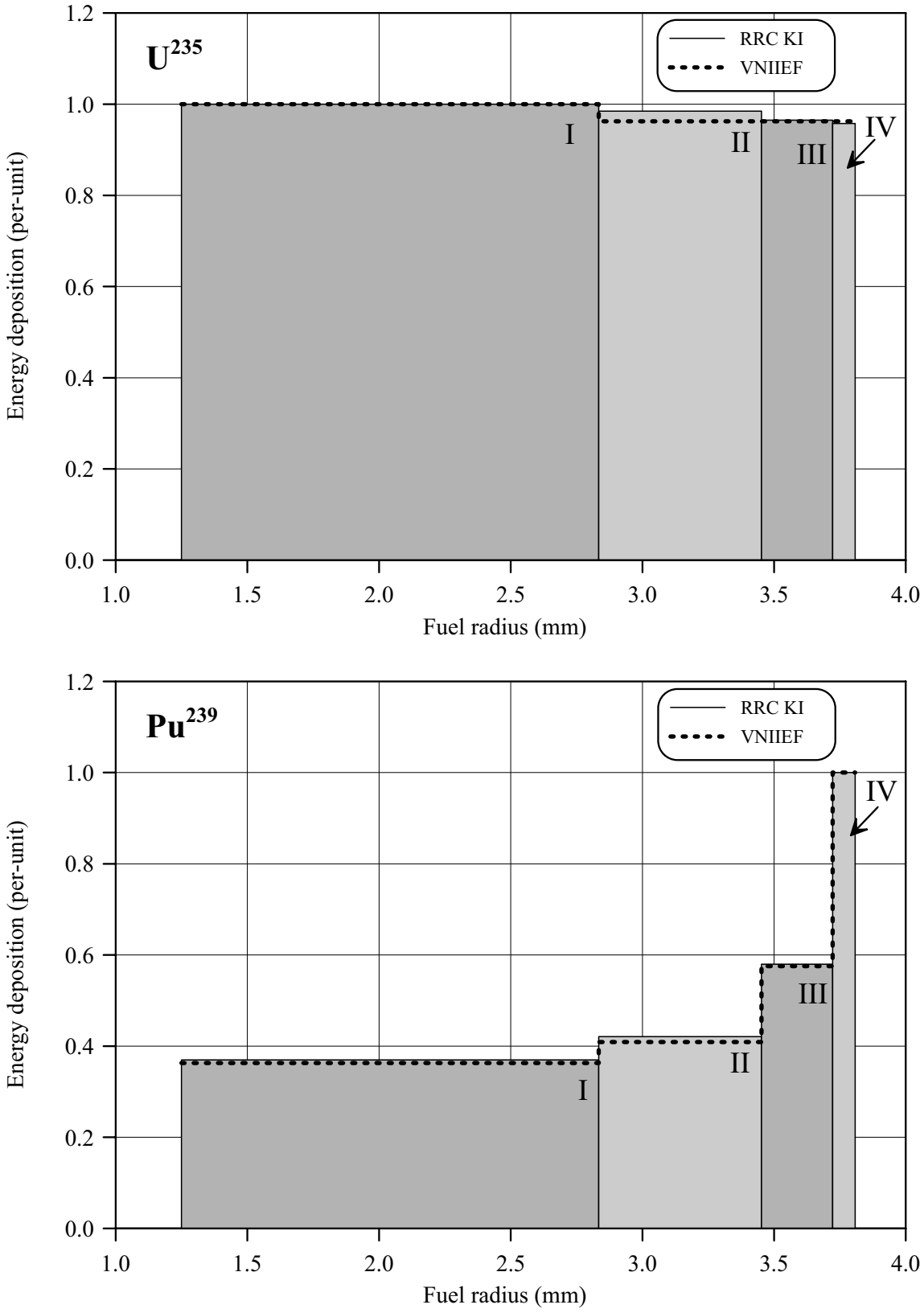


Fig.E-10.6. U^{235} and Pu^{239} radial distribution of energy deposition for fuel rod # RT10

RT10

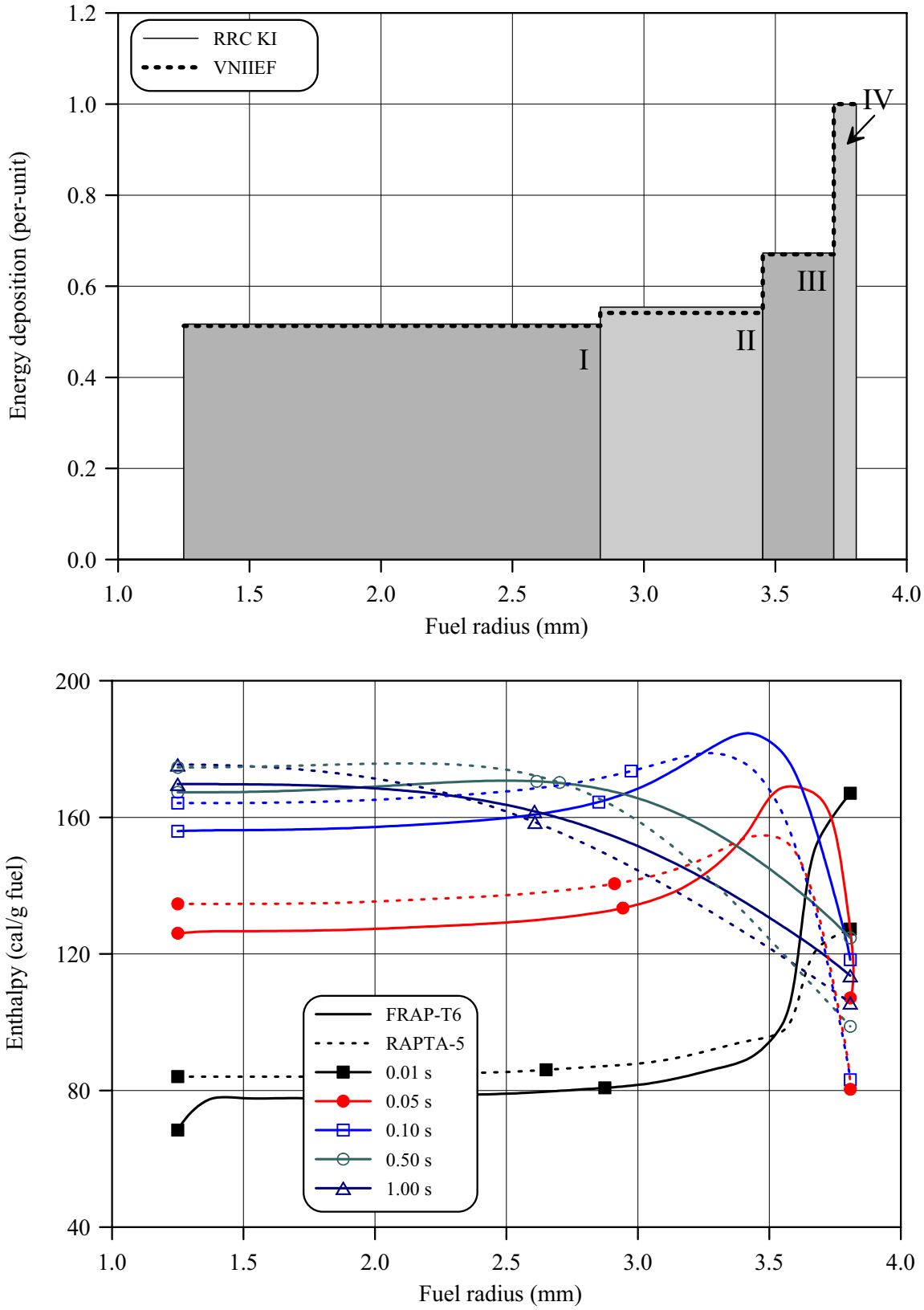


Fig.E-10.7. Radial distribution of energy deposition and fuel enthalpy for fuel rod # RT10

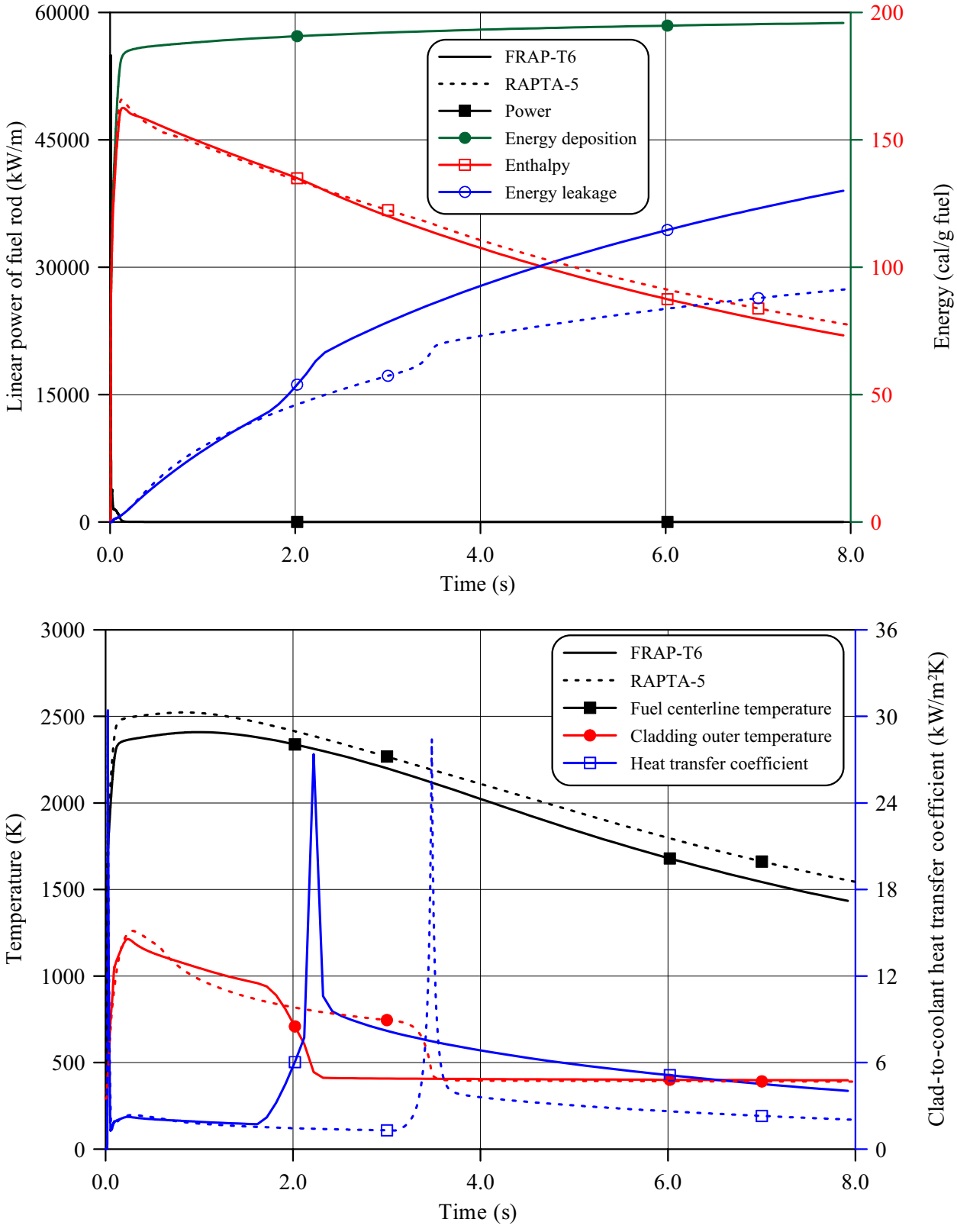


Fig.E-10.8. Thermal history of fuel rod # RT10 during the BIGR test in accordance with FRAP-T6/VVER and RAPTA-5 calculations

RT10

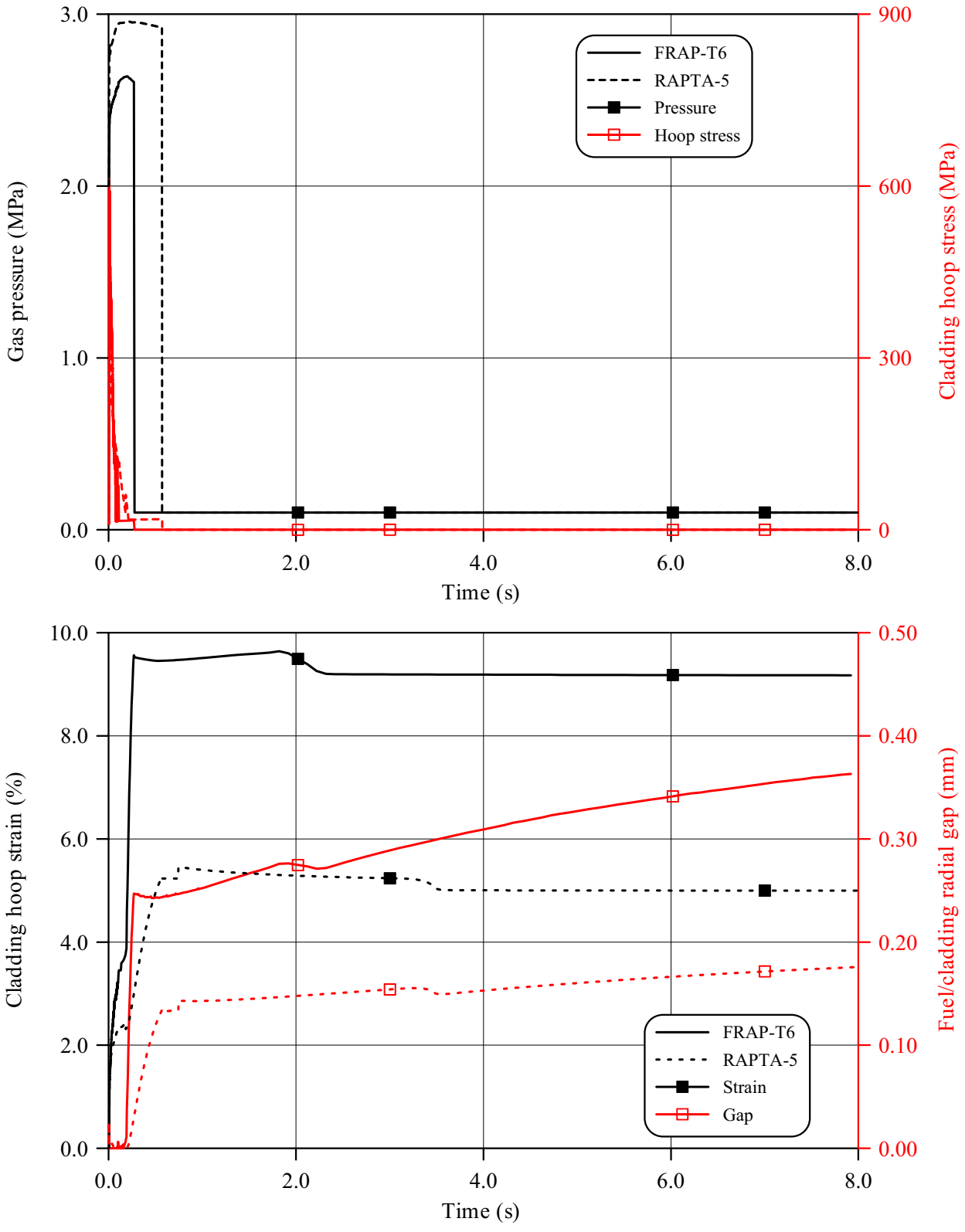


Fig.E-10.9. Mechanical behavior of fuel rod # RT10 during the BIGR test in accordance with FRAP-T6/VVER and RAPTA-5 calculations

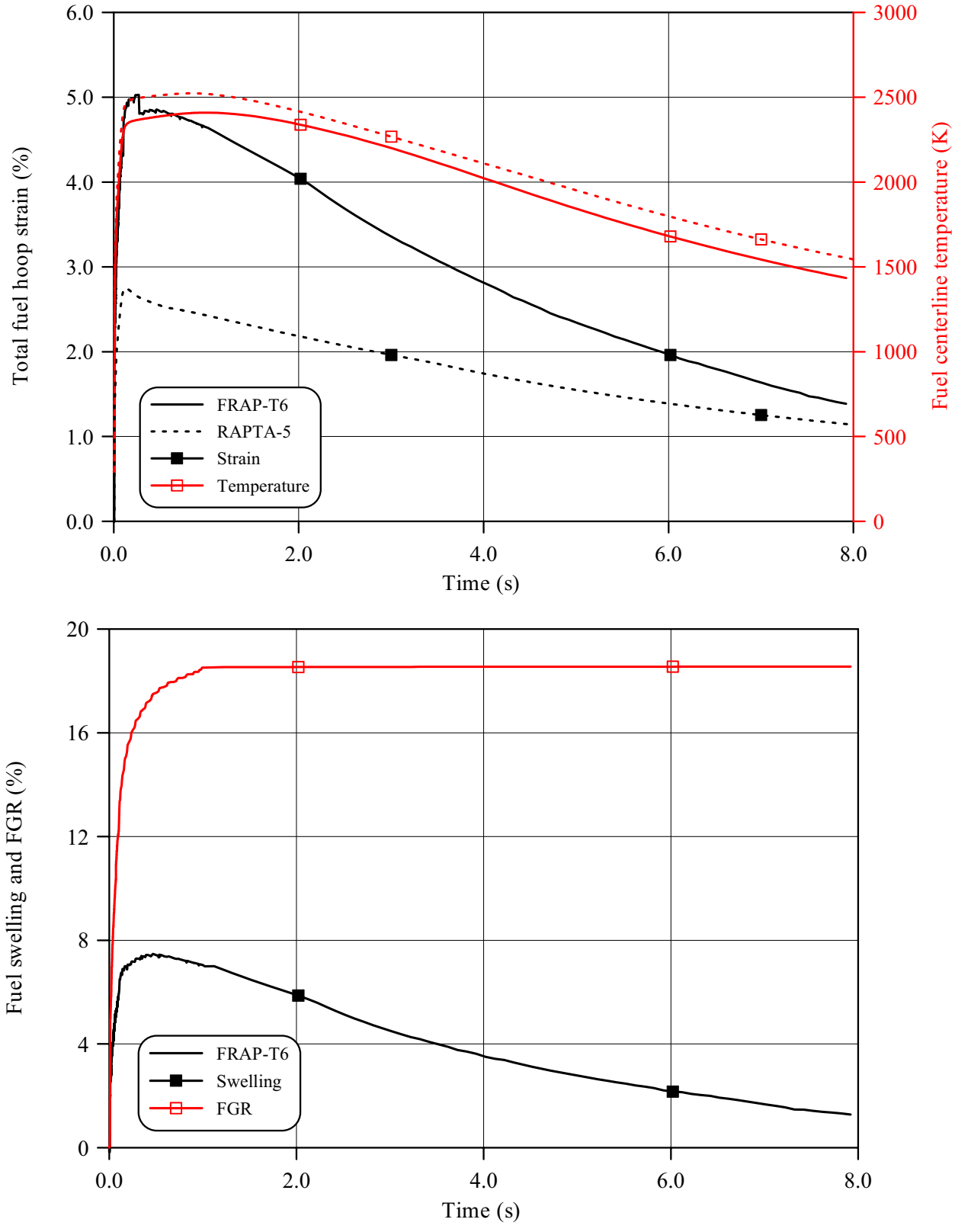


Fig.E-10.10. Fuel behavior during the BIGR test of fuel rod # RT10 in accordance with FRAP-T6/VVER and RAPTA-5 calculations

RT10

Table E-10.3. Axial distribution of cladding average outer diameter in fuel rod # RT10*

Axial coordinate (mm)	Cladding diameter (mm)	Axial coordinate (mm)	Cladding diameter (mm)	Axial coordinate (mm)	Cladding diameter (mm)	Axial coordinate (mm)	Cladding diameter (mm)
24	9.394	62	10.219	100	9.962	138	9.999
26	9.435	64	10.099	102	9.987	140	10.031
28	9.496	66	10.084	104	10.000	142	10.068
30	9.588	68	10.104	106	9.976	144	10.106
32	9.755	70	10.112	108	9.930	146	10.129
34	9.931	72	10.090	110	9.871	148	10.161
36	10.081	74	10.033	112	9.821	150	10.213
38	10.149	76	10.037	114	9.814	152	10.197
40	10.284	78	10.084	116	9.819	154	10.118
42	10.566	80	10.110	118	9.819	156	10.050
44	10.754	82	10.109	120	9.802	158	9.977
46	10.747	84	10.066	122	9.781	160	9.918
48	10.588	86	10.000	124	9.784	162	9.885
50	10.377	88	9.979	126	9.852	164	9.771
52	10.230	90	10.011	128	9.936	166	9.604
54	10.250	92	10.025	130	9.996	168	9.444
56	10.330	94	10.018	132	10.028	170	9.311
58	10.394	96	10.010	134	10.020	172	9.186
60	10.356	98	9.984	136	9.983	174	9.166

* Measured value determined on the basis of profilometry data (16 azimuthal directions)

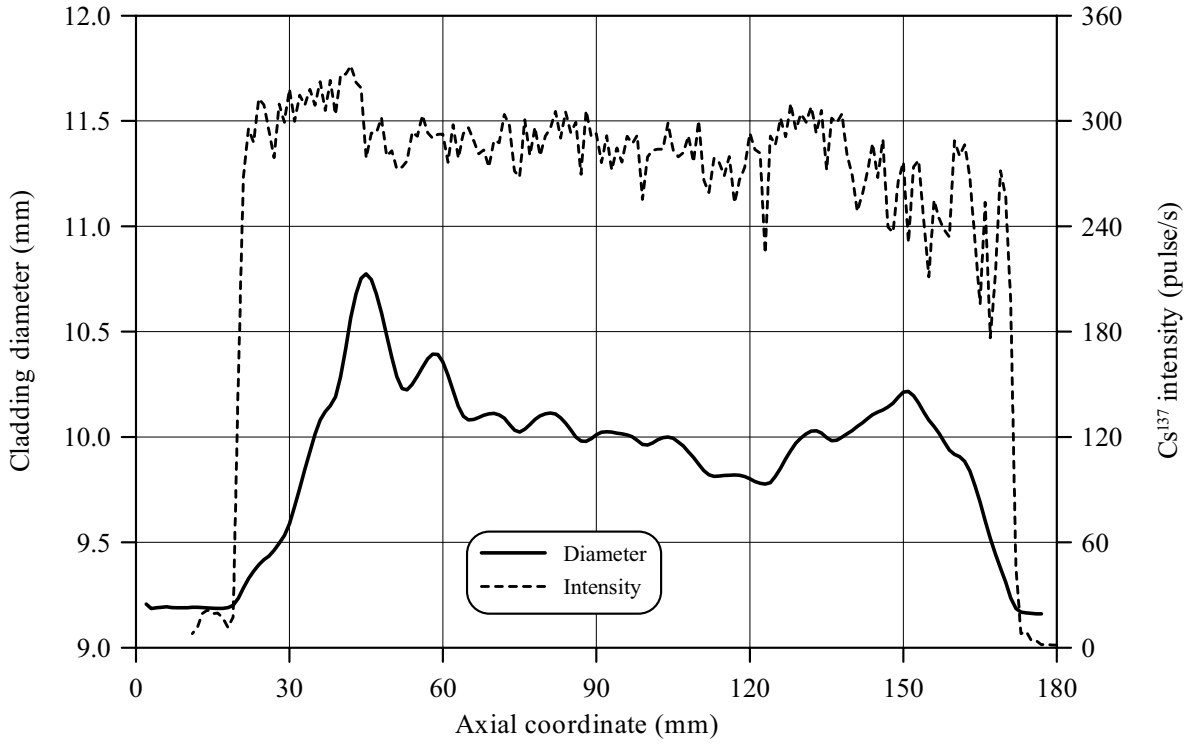


Fig.E-10.11. Cladding measured average diameter and γ-scanning results for fuel rod # RT10

Table E-10.4. The PIE results for fuel rod # RT10

	Parameter	Value
1.	Cladding outer diameter (mm):	
1.1.	Maximum diameter of the bidimensional data sample in "fuel rod length - azimuthal angle" coordinates (mm)	11.03
1.2.	Averaged azimuthal diameter and maximum diameter along the length selected from the sample of averaged azimuthal diameter (mm)	10.75
1.3.	Averaged diameter of the bidimensional data sample in "fuel rod length - azimuthal angle" coordinates (mm)	9.88
2.	Cladding residual hoop strain (%):	
2.1.	Maximum hoop strain	18.90
2.2.	Hoop strain at rupture	14.75
3.	Fuel pellet conditional diameter (mm) in cross-section*:	
	at 33 mm elevation	8.19
4.	ZrO_2 outer thickness (μm) in cross-section:	
	at 33, 45, 60 mm elevations	4–7
5.	ZrO_2 inner thickness (μm) in cross-section:	
	at 45, 60 mm elevations	0
6.	Parameters characterizing FGR:	
6.1.	Gas composition (% by volume):	
	He	-
	N_2	-
	O_2	-
	Ar	-
	CO_2	-
	Kr	-
	Xe	-
6.2.	Free gas volume (cm^3)	-
6.3.	Gas volume under normal conditions (cm^3)	-
6.4.	Gas pressure under normal conditions (MPa)	-

* Reference value determined by the processing of fuel cross-section photographs

RT10

Table E-10.5. Organized BIGR test results for fuel rod # RT10

Parameter		Unit	Value		
			Measured	Calculated	
				FRAP-T6	RAPTA-5
1.	Fuel burnup	MW d/kg U	47.0	47.0	47.0
2.	Initial gas pressure	MPa	2.0	2.0	2.0
3.	Energy deposition	cal/g fuel	206.7	206.7	206.7
4.	Peak fuel enthalpy*	cal/g fuel	-	162.5	165.9
5.	Fuel maximum temperature	K	-	2542	2578
6.	Maximum temperature of cladding outer surface	K	-	1214	1261
7.	Cladding burst	Failed, Unfailed	Failed	Failed	Failed
8.	Cladding residual hoop strain**				
	- average	%	8.94	6.12	5.45
	- maximum	%	18.90	9.09	5.45

* Average value of peak fuel enthalpy 164.2 cal/g fuel

** Average value along the fuel stack length

Appendix E–11

Individual Characteristics of Fuel Rod # RT11

after the BIGR Test

RT11

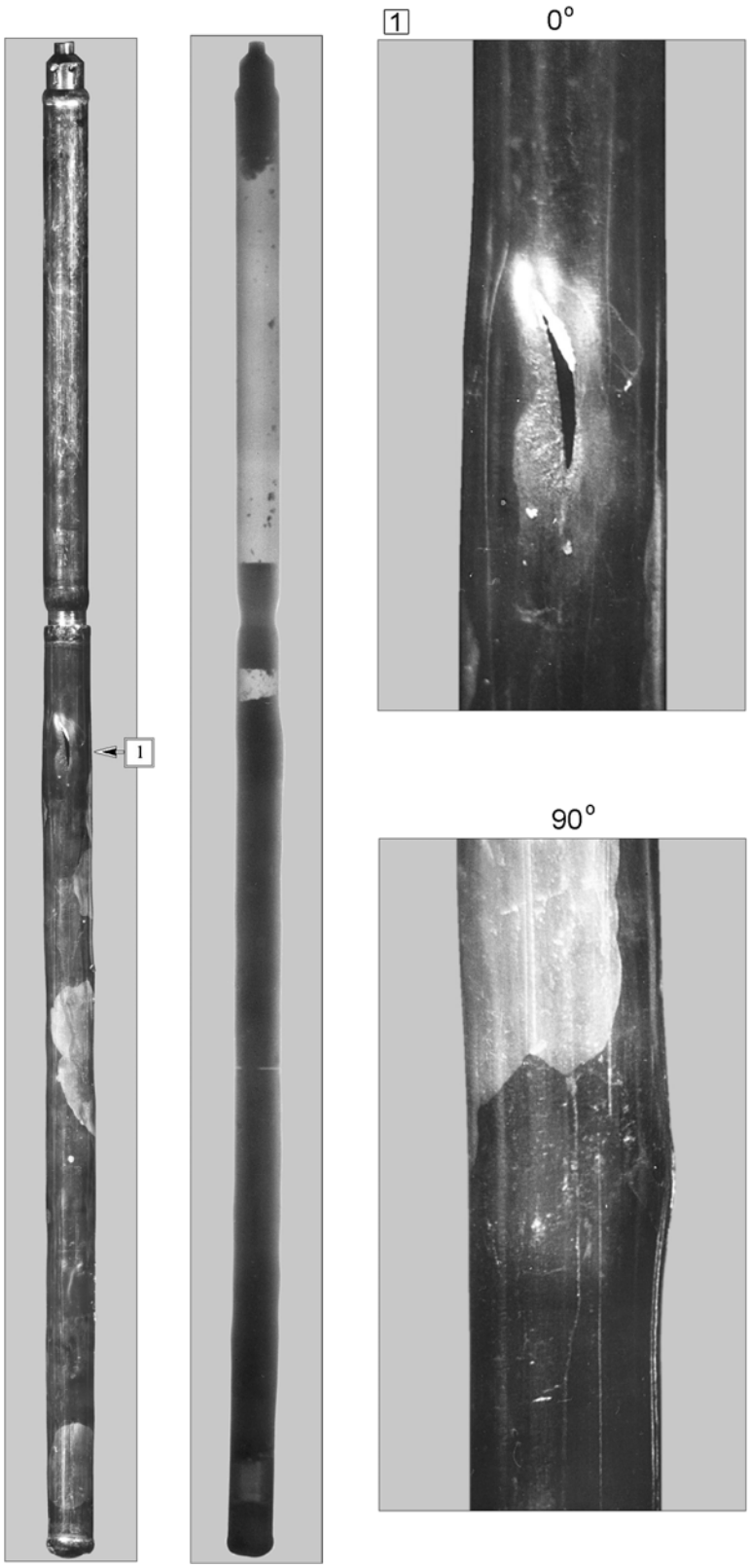


Fig.E-11.1. Appearance of failed fuel rod # RT11 after the BIGR test (photographs and X-ray photograph)

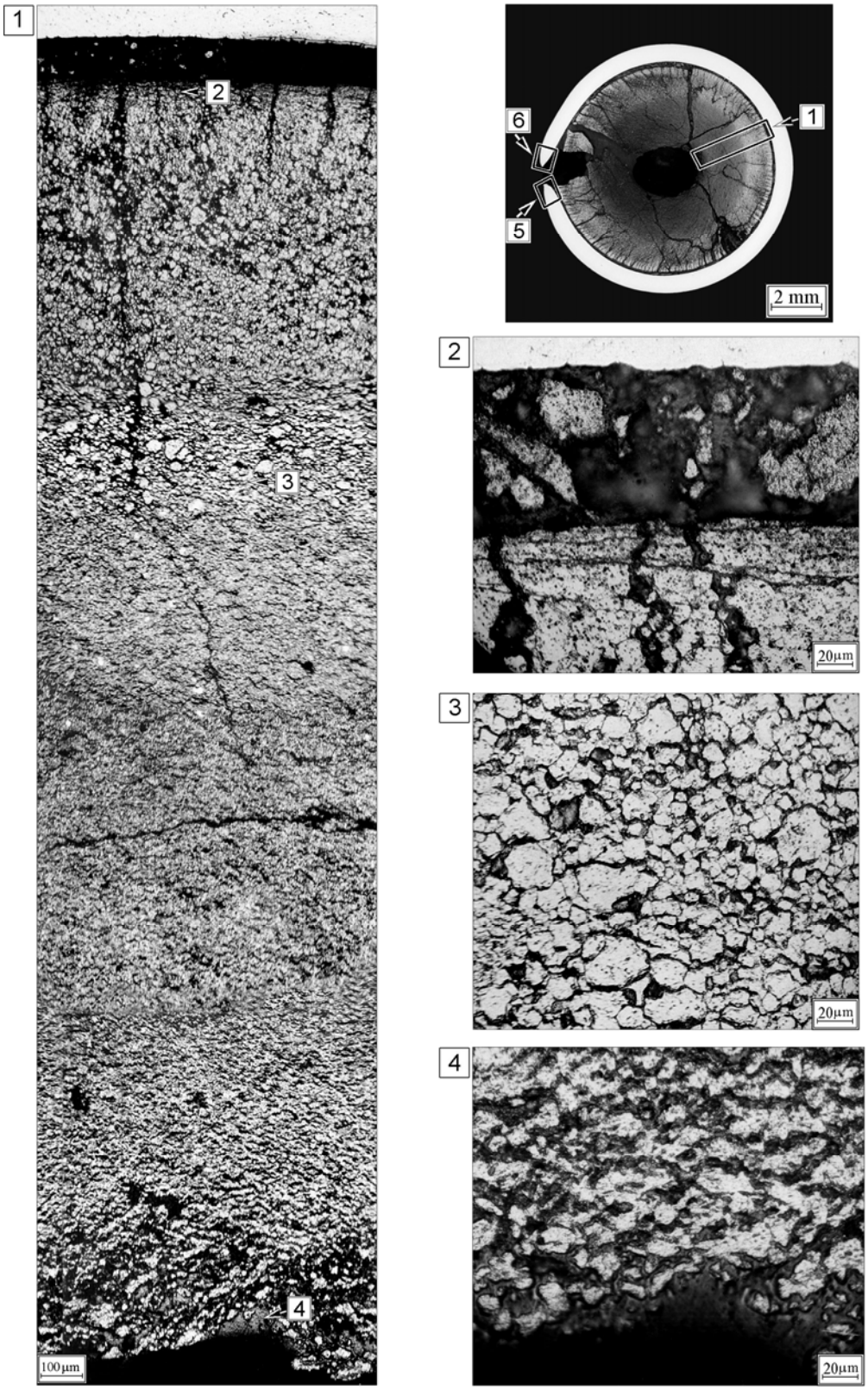
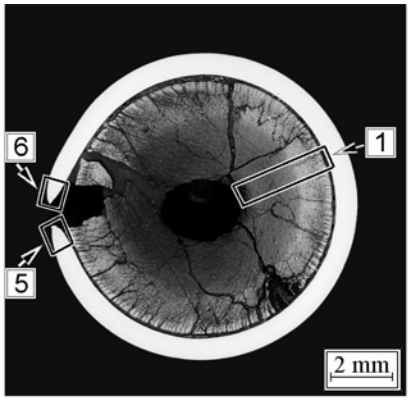


Fig.E-11.2. Cross-section and fuel microstructure of fuel rod # RT11 at 157 mm elevation (from low cap)





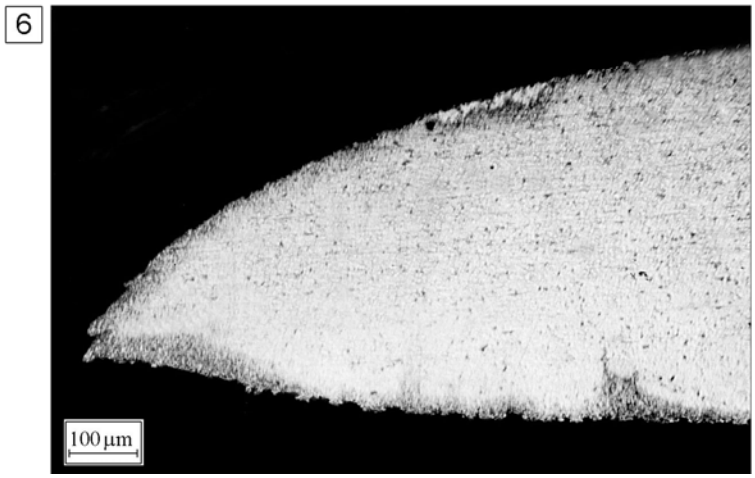


Fig.E-11.3. Cross-section and cladding microstructure of fuel rod # RT11 in the burst area at 157 mm elevation (from low cap)

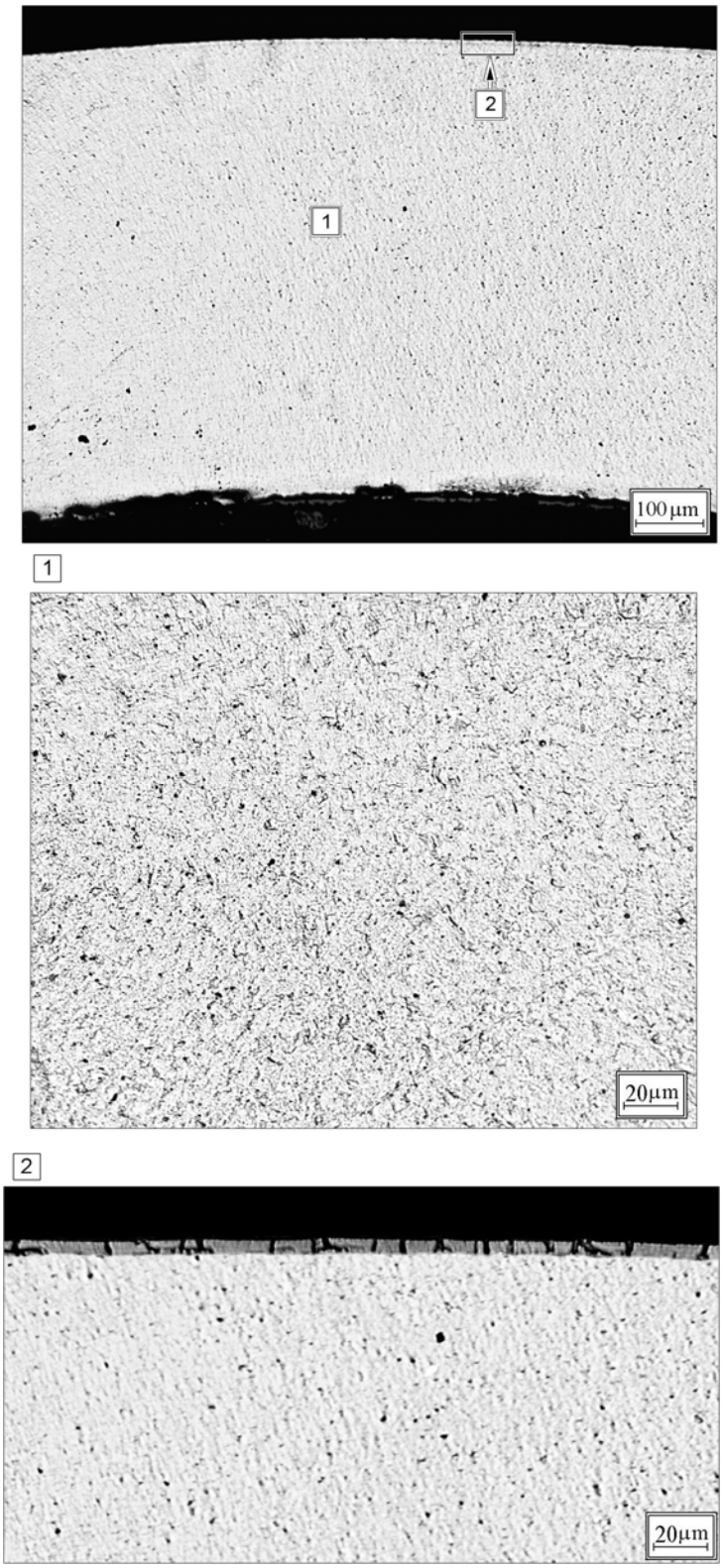


Fig.E-11.4. Cladding microstructure of fuel rod # RT11 at 157 mm elevation (from low cap)

RT11

Table E-11.1. Time dependent energy characteristics of fuel rod # RT11

Time (s)	Relative reactor power (current/ maximum value) (per-unit)	Cumulative number of fissions in fuel rod (fiss) x10^{-14}	Power of fuel rod[1)2)] (kW)	Energy deposition		Fuel enthalpy[3)]	
				(cal/g fuel)	(J/g fuel)	FRAP-T6	RAPTA-5
0.000	0.00E+00	0.000	0.000	0.000	0.000	0.000	0.000
0.001	2.61E-03	0.039	22.11	0.042	0.177	0.671	0.041
0.002	1.16E-02	0.217	98.28	0.235	0.983	0.671	0.226
0.003	5.28E-02	1.024	447.3	1.108	4.637	1.345	1.121
0.004	2.29E-01	4.652	1942	5.023	21.03	5.256	5.196
0.005	6.89E-01	17.65	5836	19.04	79.72	18.922	19.396
0.006	9.93E-01	44.50	8414	48.02	201.1	46.962	48.187
0.007	6.32E-01	69.48	5352	75.04	314.2	73.074	74.807
0.008	2.89E-01	82.68	2451	89.26	373.7	86.708	88.540
0.009	1.38E-01	88.68	1171	95.76	400.9	92.802	94.659
0.010	8.17E-02	91.83	692.7	99.15	415.1	96.005	97.592
0.012	5.36E-02	95.59	453.8	103.3	432.3	99.478	100.921
0.014	5.43E-02	98.76	460.0	106.6	446.5	102.185	103.704
0.016	6.37E-02	102.2	539.7	110.4	462.2	105.277	106.937
0.018	7.36E-02	106.3	623.5	114.9	480.9	109.043	110.867
0.020	7.85E-02	111.1	665.4	119.8	501.5	113.303	115.318
0.022	7.36E-02	115.3	623.5	124.7	522.1	117.572	119.748
0.024	6.17E-02	119.3	522.9	129.1	540.5	121.301	123.610
0.026	4.96E-02	123.0	420.3	132.7	555.4	124.284	126.707
0.028	4.02E-02	125.6	340.6	135.5	567.5	126.612	129.092
0.030	3.43E-02	127.8	290.4	137.9	577.4	128.479	131.024
0.050	2.75E-02	144.9	232.9	156.4	654.7	143.008	145.560
0.070	2.46E-02	160.1	208.8	173.1	724.6	154.413	158.770
0.090	2.16E-02	173.6	183.2	187.5	784.9	167.473	169.947
0.110	1.72E-02	185.5	146.1	200.2	838.2	178.630	179.596
0.130	8.76E-03	193.3	74.46	208.7	873.6	185.748	185.120
0.150	3.37E-03	196.7	28.83	212.2	888.5	188.096	186.670
0.200	7.24E-04	198.9	6.354	214.9	899.6	187.774	185.441
1.000	7.72E-05	202.2	0.801	218.9	916.6	164.951	170.085
10.00	8.95E-06	208.6	0.106	228.3	956.0	51.589	73.945
100.0	1.80E-07	212.3	0.004	234.4	981.2	5.968	11.422
1000	7.08E-13	212.4	1.89E-04	236.5	990.0	0.000	0.000

[1)] Average values determined in accordance with results of RRC KI and VNIIEF calculations

[2)] Maximum power value is 8470 kW (t=0.00588 s)

[3)] Average radial value

Table E-11.2. Radial energy characteristics of fuel rod # RT11*

Parameters	Coordinates of fuel radial layers (mm)			
	1 layer (1.250-2.834)	2 layer (2.834-3.452)	3 layer (3.452-3.722)	4 layer (3.722-3.808)
Number of fissions $x10^{-14}$ (fiss)	9.593	6.117	3.707	1.824
Fission density $x10^{-13}$ (fiss/g fuel)	3.050	3.239	3.937	5.793
Power** (kW)	3818	2438	1482	732.3
Energy deposition (cal/g fuel)	213.2	226.7	276.2	408.0
Energy deposition (J/g fuel)	892.7	949.0	1157	1708
Energy deposition*** (per-unit)	0.523	0.556	0.677	1.000

* Average values were determined in accordance with results of RRC KI and VNIIEF calculations

** The power for the entire length of each layer at time 0.00588 s

*** Energy deposition in current layer/energy deposition in 4^{th} layer

RT11

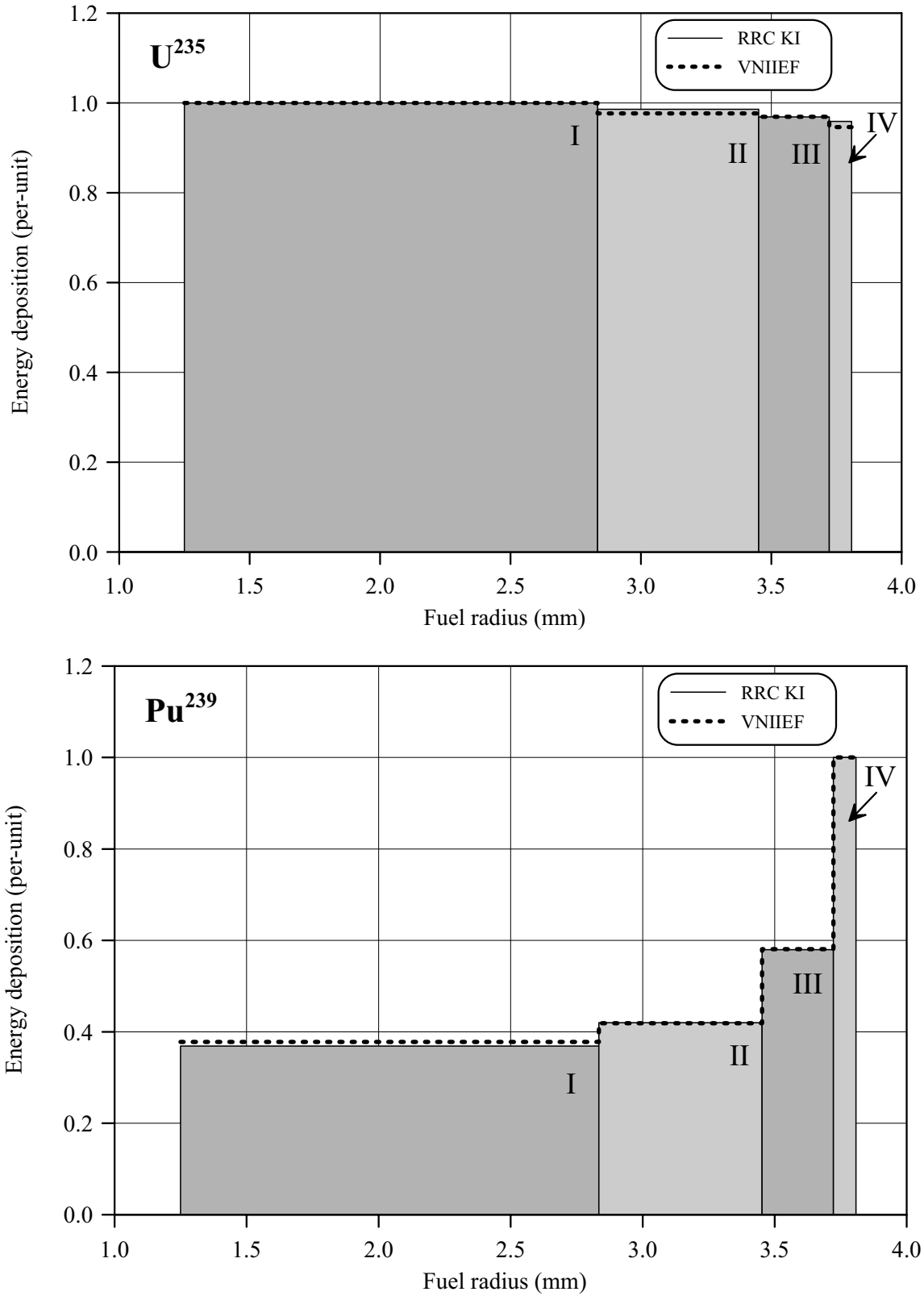


Fig.E-11.5. U^{235} and Pu^{239} radial distribution of energy deposition for fuel rod # RT11

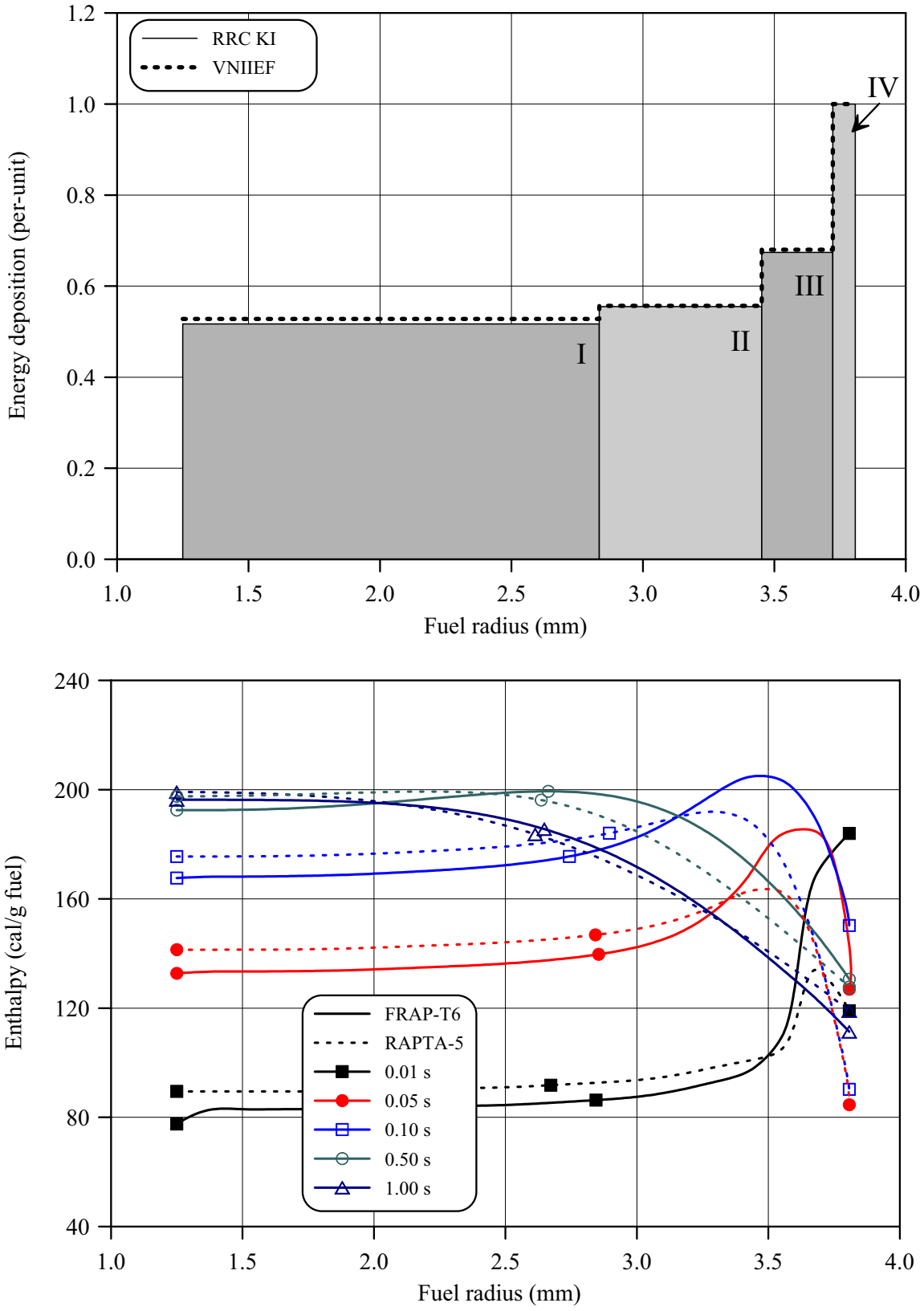


Fig.E-11.6. Radial distribution of energy deposition and fuel enthalpy for fuel rod # RT11

RT11

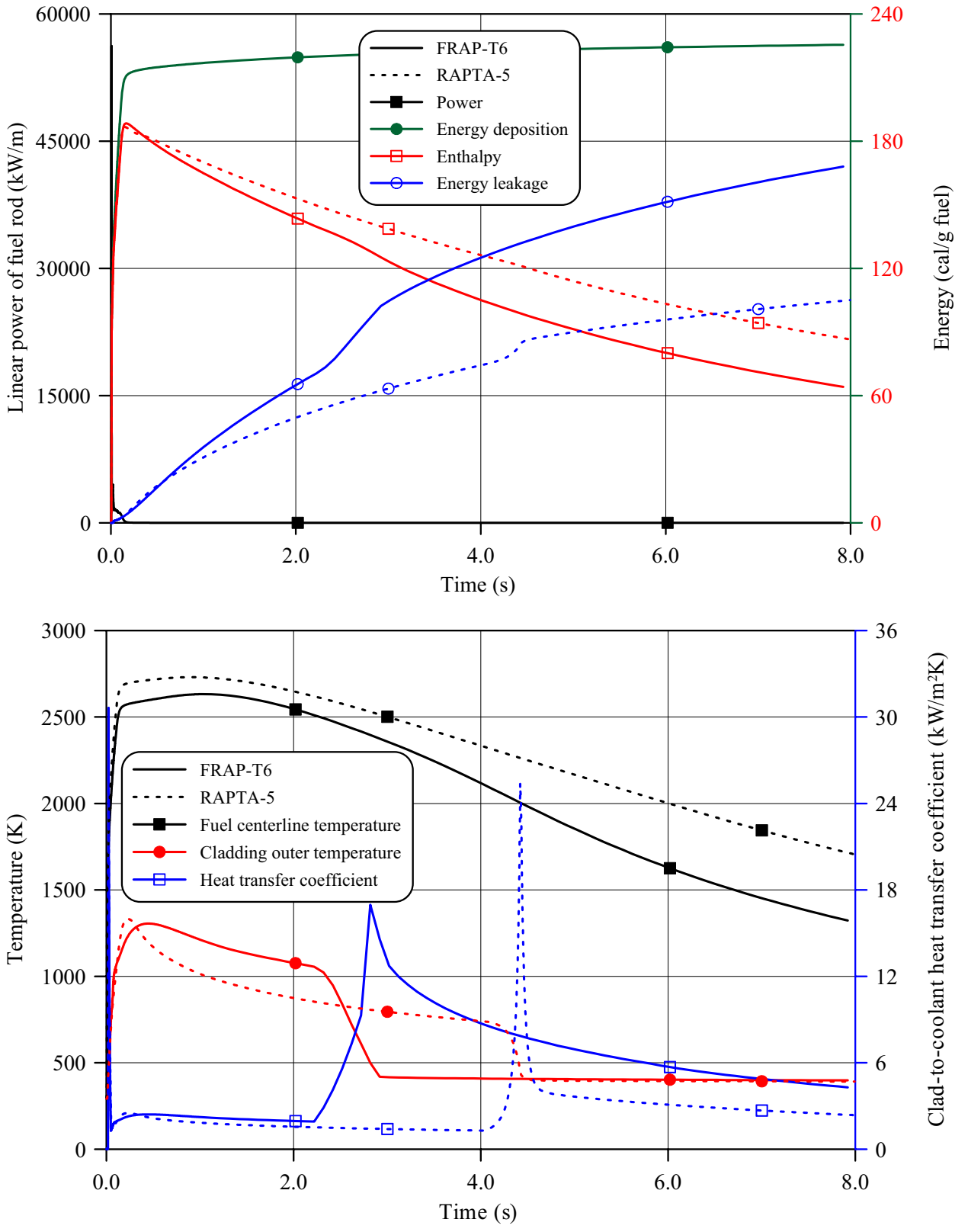


Fig.E-11.7. Thermal history of fuel rod # RT11 during the BIGR test in accordance with FRAP-T6/VVER and RAPTA-5 calculations

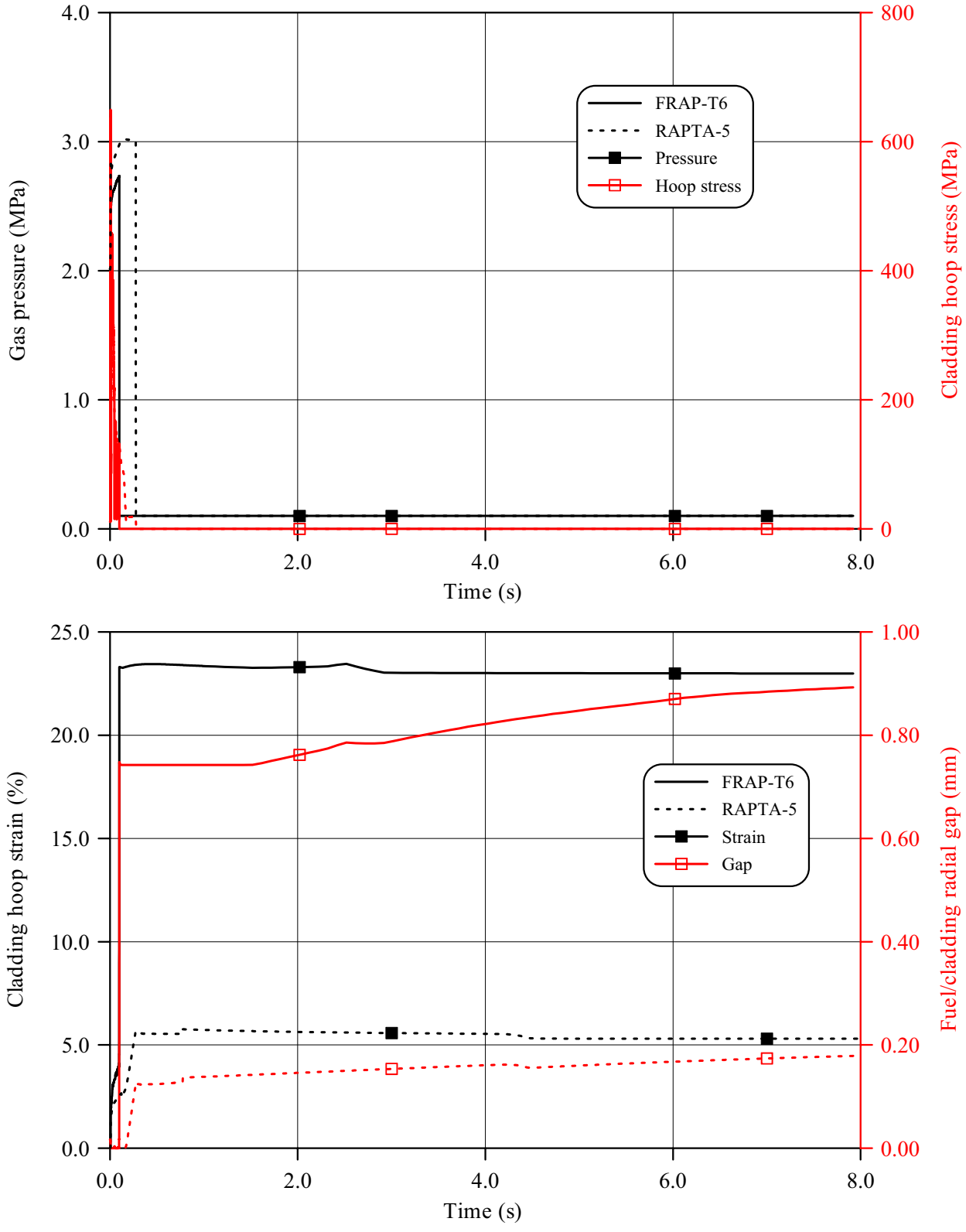


Fig.E-11.8. Mechanical behavior of fuel rod # RT11 during the BIGR test in accordance with FRAP-T6/VVER and RAPTA-5 calculations

RT11

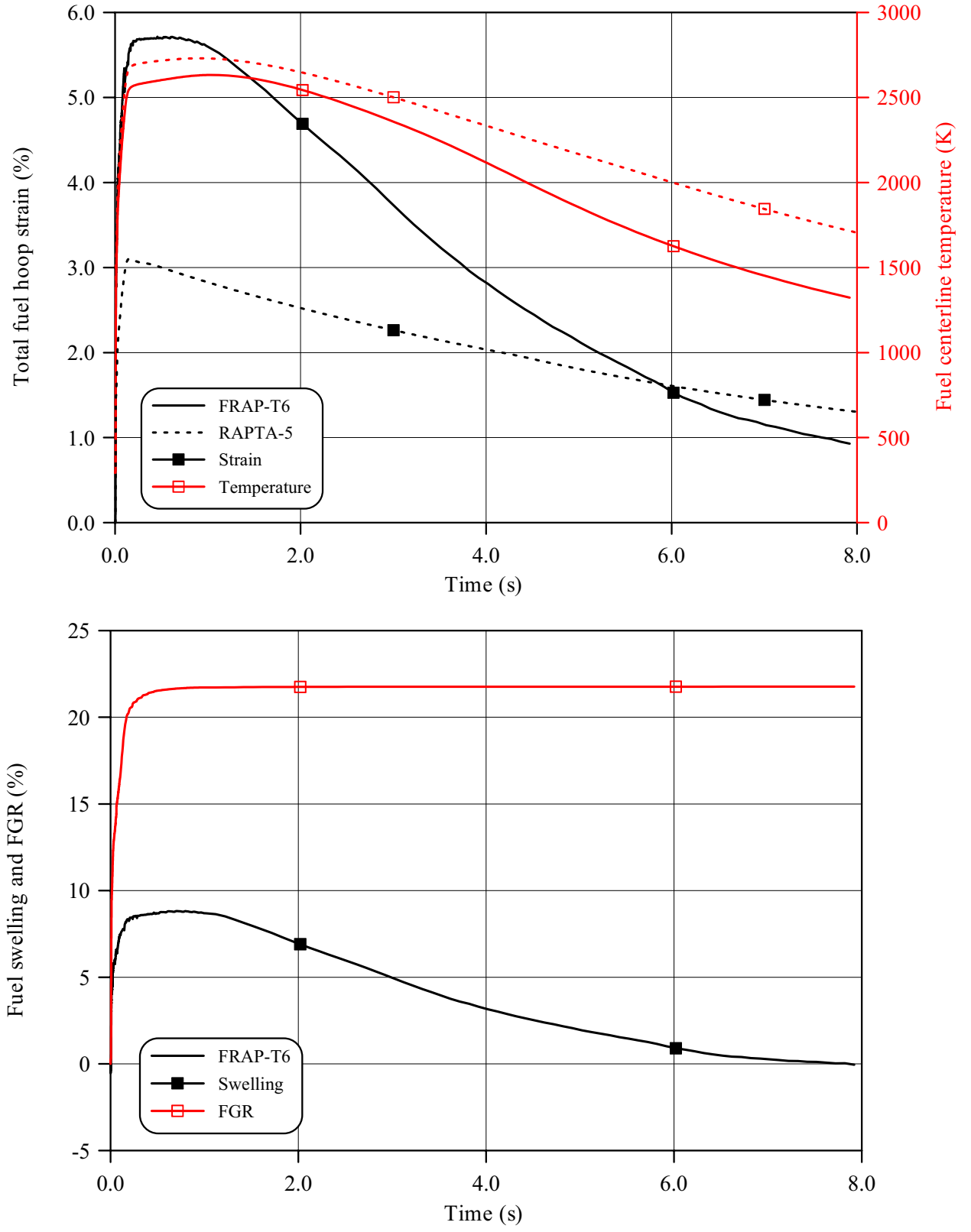


Fig.E-11.9. Fuel behavior during the BIGR test of fuel rod # RT11 in accordance with FRAP-T6/VVER and RAPTA-5 calculations

Table E-11.3. Axial distribution of cladding average outer diameter in fuel rod # RT11*

Axial coordinate (mm)	Cladding diameter (mm)	Axial coordinate (mm)	Cladding diameter (mm)	Axial coordinate (mm)	Cladding diameter (mm)	Axial coordinate (mm)	Cladding diameter (mm)
25	9.229	63	9.702	101	9.611	139	9.623
27	9.296	65	9.804	103	9.597	141	9.609
29	9.404	67	9.808	105	9.522	143	9.571
31	9.550	69	9.727	107	9.492	145	9.607
33	9.579	71	9.646	109	9.541	147	9.691
35	9.579	73	9.676	111	9.594	149	9.743
37	9.681	75	9.747	113	9.606	151	9.766
39	9.804	77	9.791	115	9.573	153	9.762
41	9.847	79	9.797	117	9.546	155	9.753
43	9.713	81	9.749	119	9.555	157	9.781
45	9.518	83	9.681	121	9.587	159	9.830
47	9.481	85	9.727	123	9.625	161	9.769
49	9.591	87	9.762	125	9.596	163	9.568
51	9.747	89	9.672	127	9.543	165	9.304
53	9.783	91	9.558	129	9.479	167	9.141
55	9.661	93	9.466	131	9.430	169	9.064
57	9.539	95	9.435	133	9.422	171	9.060
59	9.493	97	9.505	135	9.488	173	9.063
61	9.573	99	9.568	137	9.569	175	9.062

* Measured value determined on the basis of profilometry data (16 azimuthal directions)

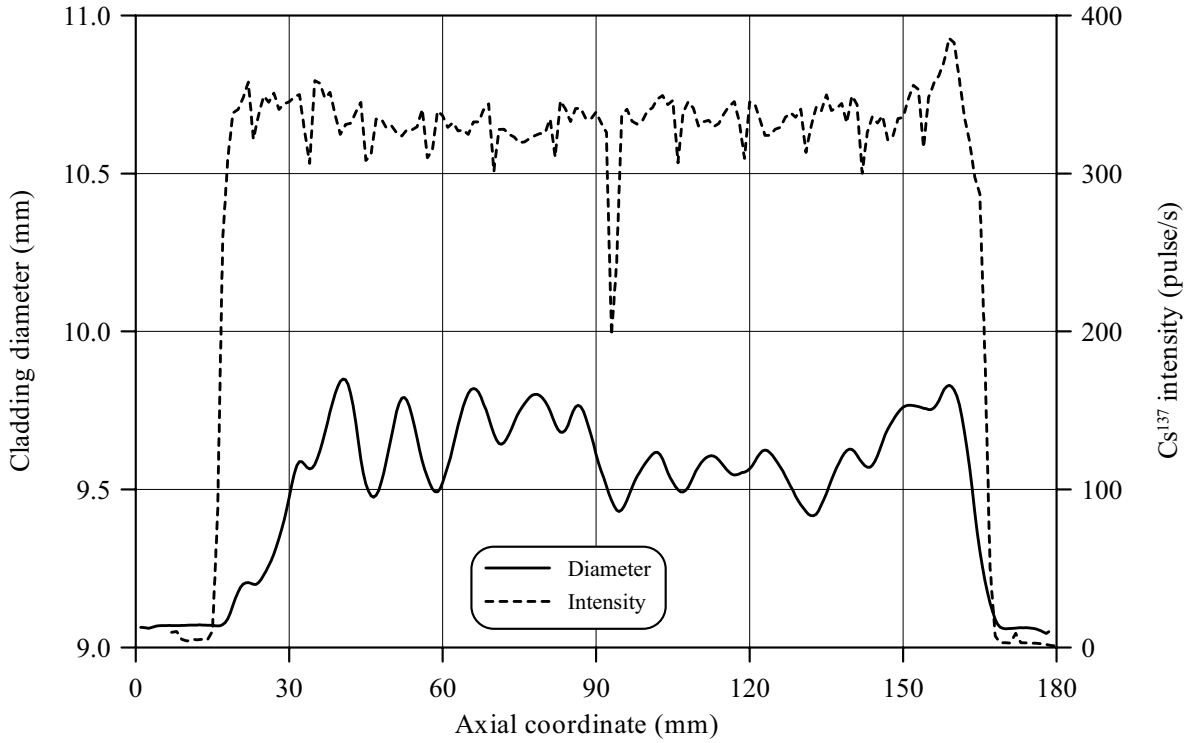


Fig.E-11.10. Cladding measured average diameter and γ-scanning results for fuel rod # RT11

RT11

Table E-11.4. The PIE results for fuel rod # RT11

	Parameter	Value
1.	Cladding outer diameter (mm):	
1.1.	Maximum diameter of the bidimensional data sample in "fuel rod length - azimuthal angle" coordinates (mm)	10.02
1.2.	Averaged azimuthal diameter and maximum diameter along the length selected from the sample of averaged azimuthal diameter (mm)	9.85
1.3.	Averaged diameter of the bidimensional data sample in "fuel rod length - azimuthal angle" coordinates (mm)	9.58
2.	Cladding maximum residual hoop strain (%)	8.20
3.	Fuel pellet conditional diameter (mm) in cross-section*:	
	at 157 mm elevation	8.31
4.	ZrO_2 outer thickness (μm) in cross-section:	
	at 157 mm elevation	4
5.	ZrO_2 inner thickness (μm) in cross-section:	
	at 157 mm elevation	0
6.	Parameters characterizing FGR:	
6.1.	Gas composition (% by volume):	
	He	-
	N_2	-
	O_2	-
	Ar	-
	CO_2	-
	Kr	-
	Xe	-
6.2.	Free gas volume (cm^3)	-
6.3.	Gas volume under normal conditions (cm^3)	-
6.4.	Gas pressure under normal conditions (MPa)	-

* Reference value determined by the processing of fuel cross-section photographs

Table E-11.5. Organized BIGR test results for fuel rod # RT11

Parameter		Unit	Value		
			Measured	Calculated	
				FRAP-T6	RAPTA-5
1.	Fuel burnup	MW d/kg U	47.2	47.2	47.2
2.	Initial gas pressure	MPa	2.0	2.0	2.0
3.	Energy deposition	cal/g fuel	236.5	236.5	236.5
4.	Peak fuel enthalpy*	cal/g fuel	-	188.4	186.7
5.	Fuel maximum temperature	K	-	2782	2774
6.	Maximum temperature of cladding outer surface	K	-	1306	1333
7.	Cladding burst	Failed, Unfailed	Failed	Failed	Failed
8.	Cladding residual hoop strain**				
	- average	%	5.45	3.68	5.76
	- maximum	%	8.20	22.90	5.76

* Average value of peak fuel enthalpy 187.5 cal/g fuel

** Average value along the fuel stack length

Appendix E–12

Individual Characteristics of Fuel Rod # RT12

after the BIGR Test

RT12

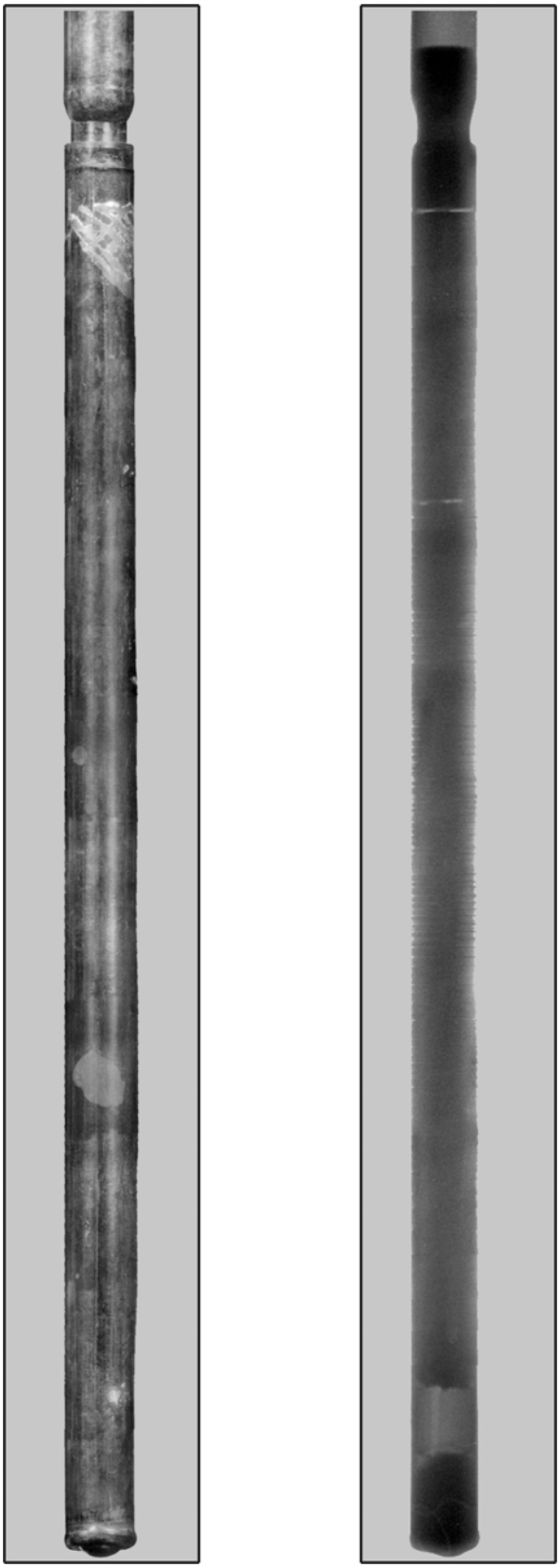


Fig.E-12.1. Appearance of unfailed fuel rod # RT12 after the BIGR test (photographs and X-ray photograph)

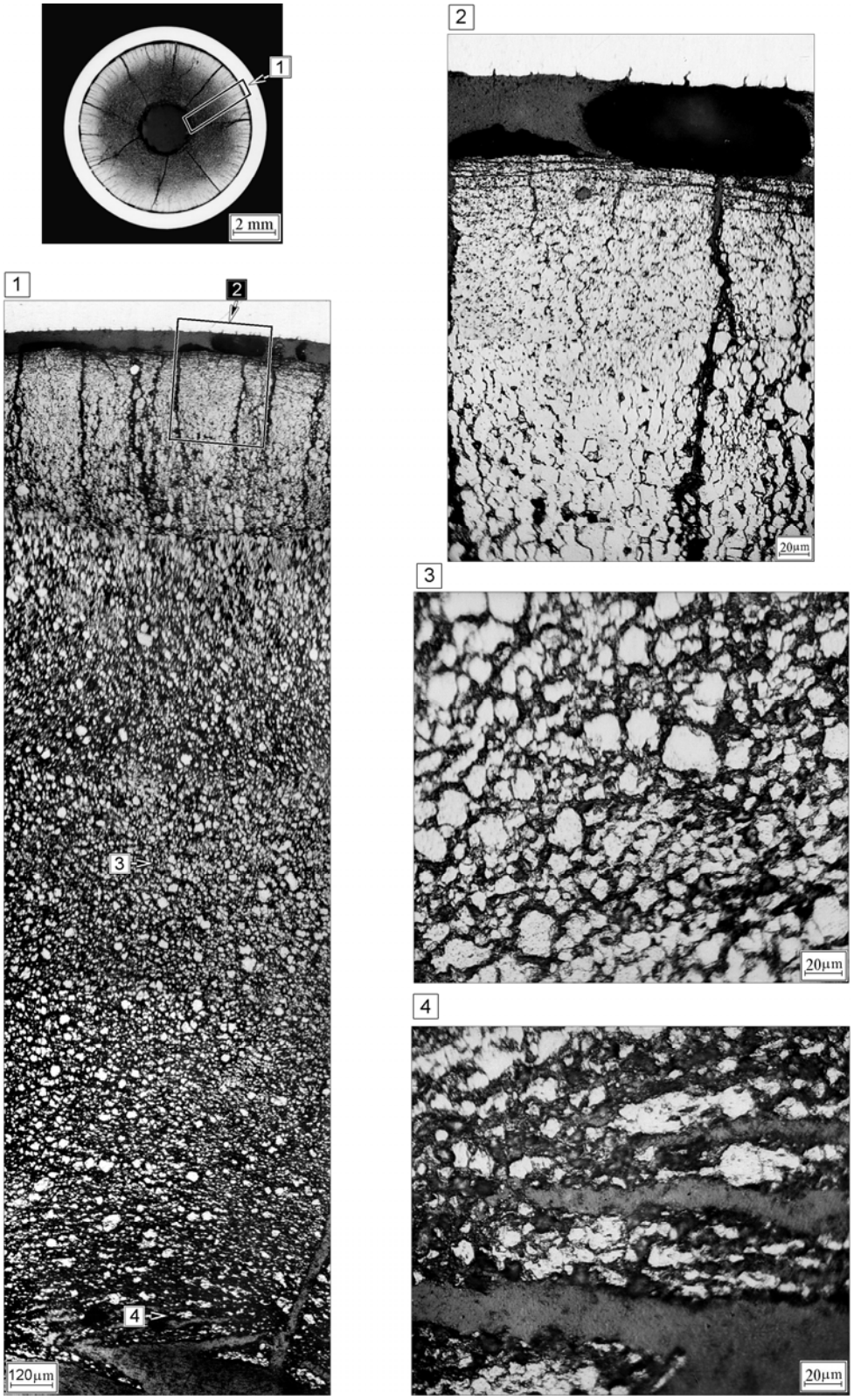


Fig.E-12.2. Cross-section and fuel microstructure of fuel rod # RT12 at 54 mm elevation (from low cap)

RT12

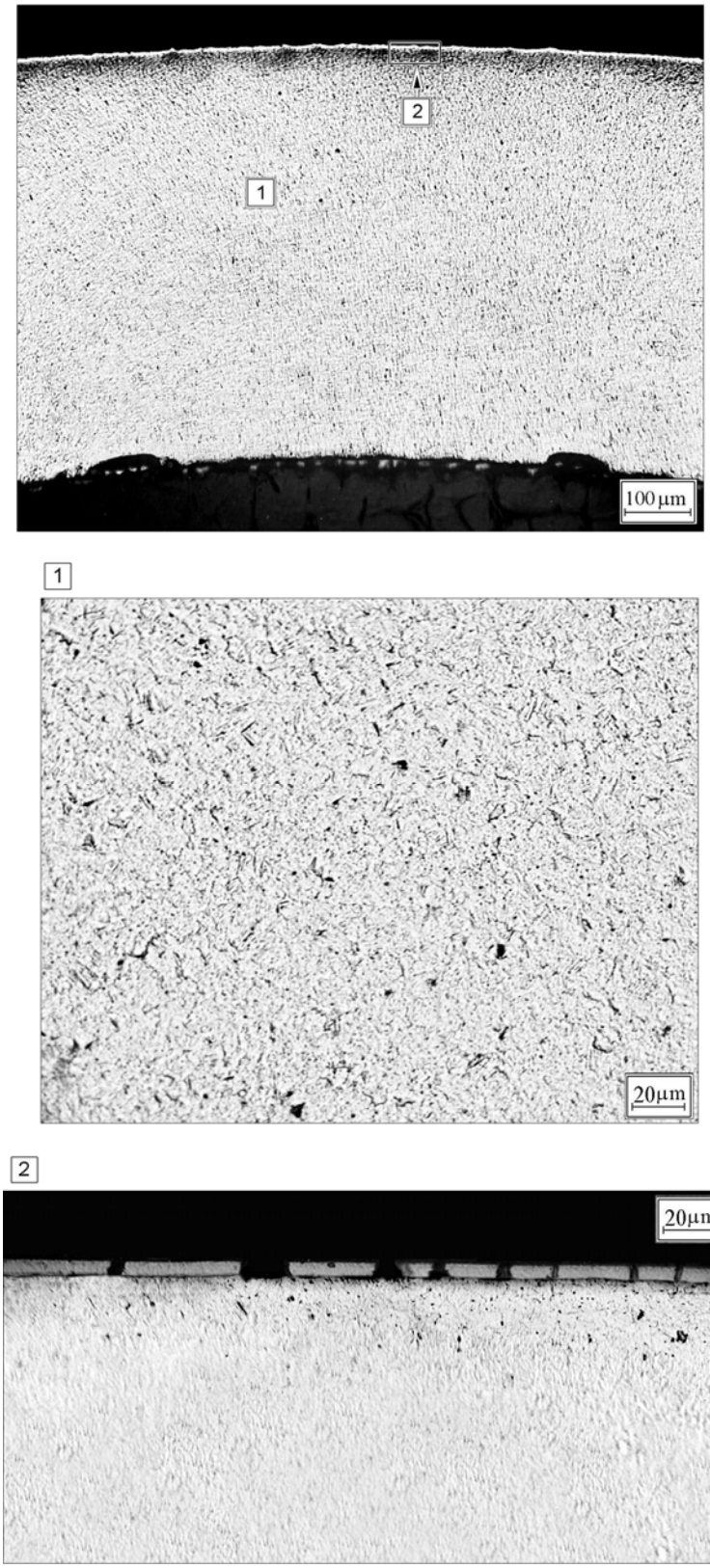


Fig.E-12.3. Cladding microstructure of fuel rod # RT12 at 54 mm elevation (from low cap)

Table E-12.1. Time dependent energy characteristics of fuel rod # RT12

Time (s)	Relative reactor power (current/ maximum value) (per-unit)	Cumulative number of fissions in fuel rod (fiss) x10^{-14}	Power of fuel rod[1)2)] (kW)	Energy deposition		Fuel enthalpy[3)]	
				(cal/g fuel)	(J/g fuel)	FRAP-T6	RAPTA-5
0.000	0.00E+00	0.000	0.000	0.000	0.000	0.000	0.000
0.001	2.98E-03	0.039	21.69	0.042	0.177	0.671	0.010
0.002	1.23E-02	0.208	89.58	0.225	0.941	0.671	0.048
0.003	4.92E-02	0.882	357.9	0.951	3.983	0.671	0.221
0.004	1.95E-01	3.617	1420	3.901	16.33	1.238	0.983
0.005	6.03E-01	13.21	4386	14.24	59.60	4.254	3.962
0.006	9.97E-01	34.62	7246	37.34	156.3	14.601	14.236
0.007	7.64E-01	58.23	5558	62.78	262.8	36.948	36.820
0.008	3.89E-01	72.66	2829	78.35	328.0	61.565	61.560
0.009	1.92E-01	79.71	1397	85.97	359.9	76.845	76.530
0.010	1.09E-01	83.35	791.2	89.94	376.6	84.231	83.649
0.012	6.29E-02	87.45	457.6	94.31	394.8	90.308	89.170
0.014	5.87E-02	90.53	426.7	97.58	408.6	93.524	92.025
0.016	6.41E-02	93.60	466.8	101.0	422.7	96.353	94.690
0.018	6.96E-02	97.03	506.3	104.7	438.2	99.400	97.679
0.020	6.95E-02	100.6	505.4	108.5	454.3	102.696	100.975
0.022	6.41E-02	104.0	466.1	112.2	469.8	106.008	104.271
0.024	5.57E-02	107.1	405.1	115.5	483.6	109.043	107.294
0.026	4.72E-02	109.9	342.9	118.4	495.6	111.652	109.884
0.028	3.99E-02	112.0	290.2	120.8	505.6	113.817	112.022
0.030	3.49E-02	114.0	253.8	122.8	514.1	115.607	113.796
0.050	3.13E-02	130.1	227.8	140.2	587.1	126.792	127.562
0.070	2.54E-02	144.4	184.9	155.7	652.0	138.170	139.931
0.090	1.83E-02	155.5	133.2	167.8	702.6	146.854	149.141
0.110	8.26E-03	162.4	60.22	175.1	732.9	152.608	153.953
0.130	3.11E-03	165.0	22.83	177.8	744.6	154.473	154.893
0.150	1.52E-03	166.0	11.21	179.1	749.8	154.714	154.282
0.200	4.74E-04	167.1	3.632	180.3	754.7	153.881	151.725
1.000	7.48E-05	169.6	0.667	183.4	767.8	135.980	128.738
10.00	8.71E-06	175.4	0.089	191.3	800.7	60.607	30.472
100.0	1.76E-07	177.8	0.003	196.3	821.7	10.376	5.051
1000	6.91E-13	177.9	1.59E-04	198.1	829.2	0.000	0.000

[1)] Average values determined in accordance with results of RRC KI and VNIIEF calculations

[2)] Maximum power value is 7270.5 kW (t=0.00606 s)

[3)] Average radial value

RT12

Table E-12.2. Radial energy characteristics of fuel rod # RT12*

Parameters	Coordinates of fuel radial layers (mm)			
	1 layer (1.250-2.834)	2 layer (2.834-3.452)	3 layer (3.452-3.722)	4 layer (3.722-3.808)
Number of fissions $x10^{-14}$ (fiss)	7.961	5.152	3.130	1.569
Fission density $x10^{-13}$ (fiss/g fuel)	2.528	2.723	3.318	4.974
Power** (kW)	3243	2102	1281	644.7
Energy deposition (cal/g fuel)	176.7	190.7	233.0	350.4
Energy deposition (J/g fuel)	740.0	798.3	975.4	1467
Energy deposition*** (per-unit)	0.505	0.544	0.665	1.000

* Average values were determined in accordance with results of RRC KI and VNIIEF calculations

** The power for the entire length of each layer at time 0.00606 s

*** Energy deposition in current layer/energy deposition in 4^{th} layer

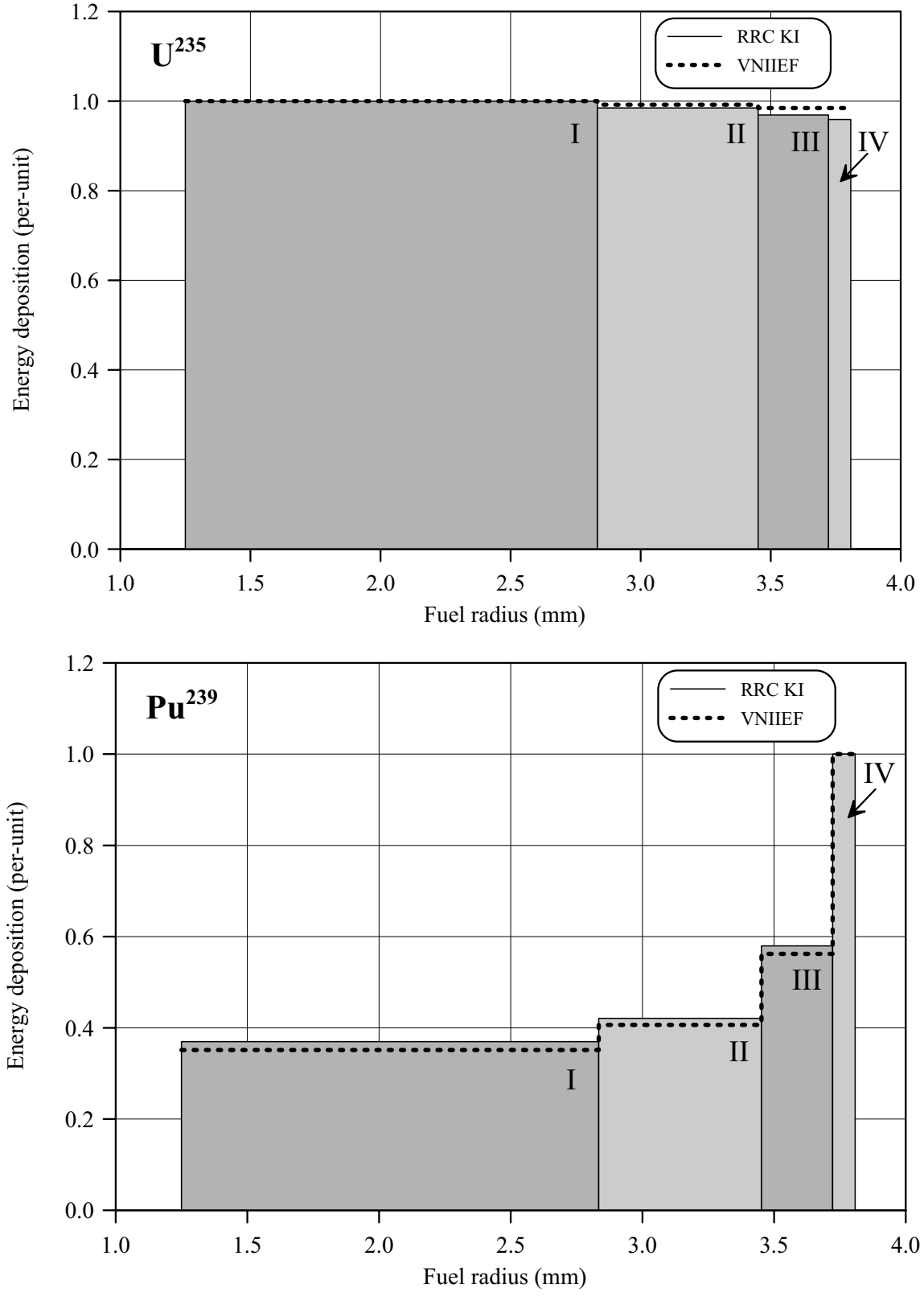


Fig.E-12.4. U^{235} and Pu^{239} radial distribution of energy deposition for fuel rod # RT12

RT12

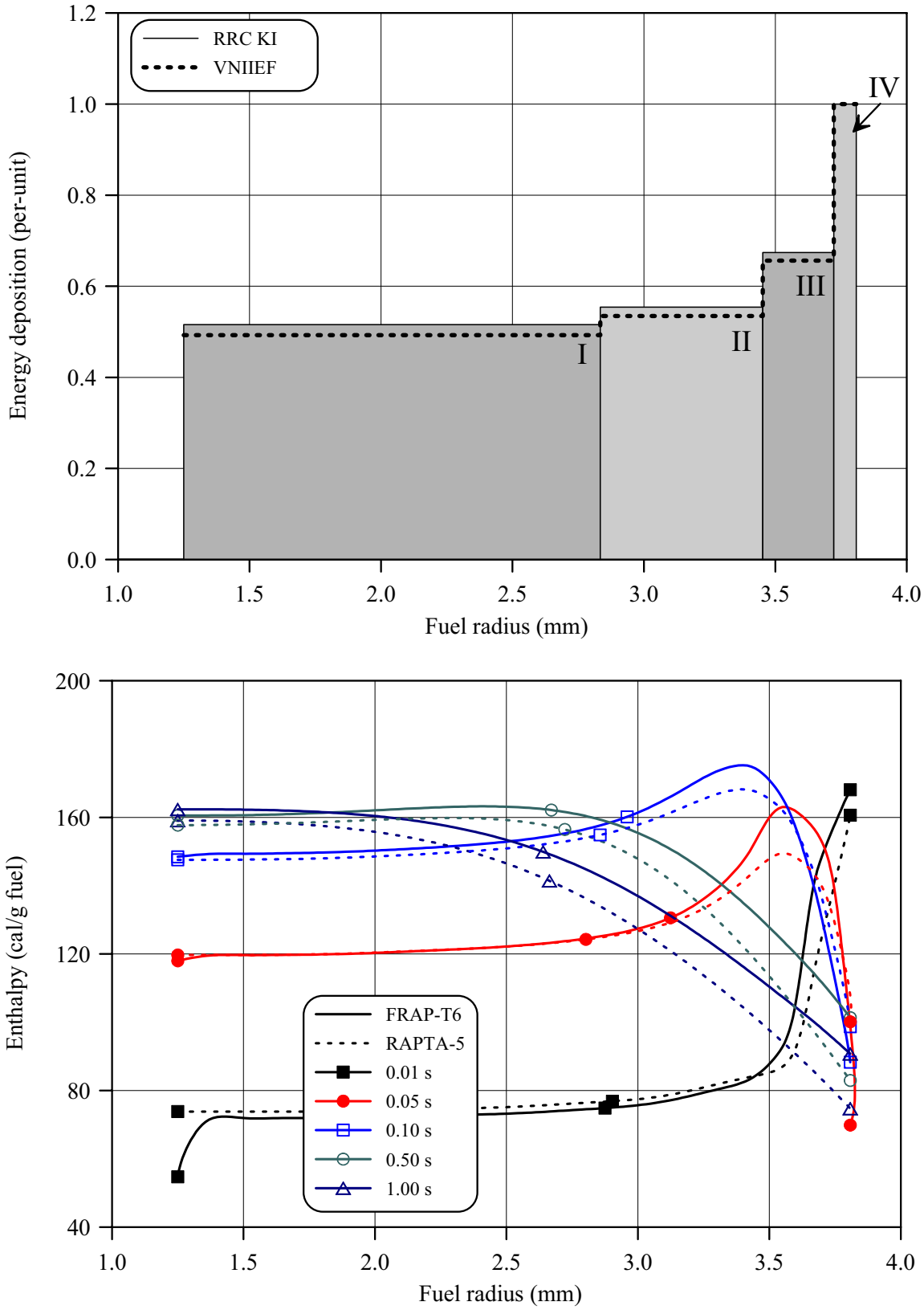


Fig.E-12.5. Radial distribution of energy deposition and fuel enthalpy for fuel rod # RT12

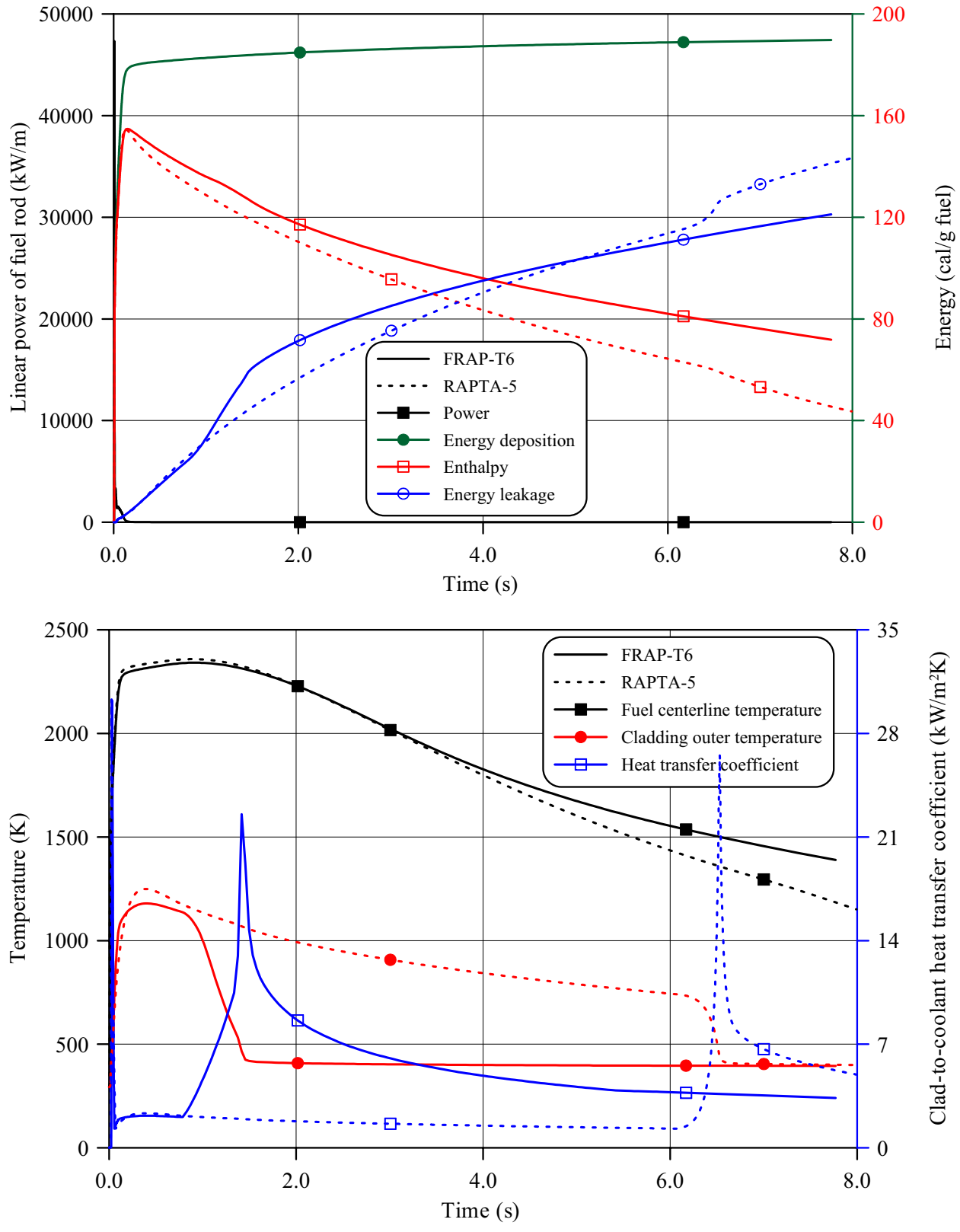


Fig.E-12.6. Thermal history of fuel rod # RT12 during the BIGR test in accordance with FRAP-T6/VVER and RAPTA-5 calculations

RT12

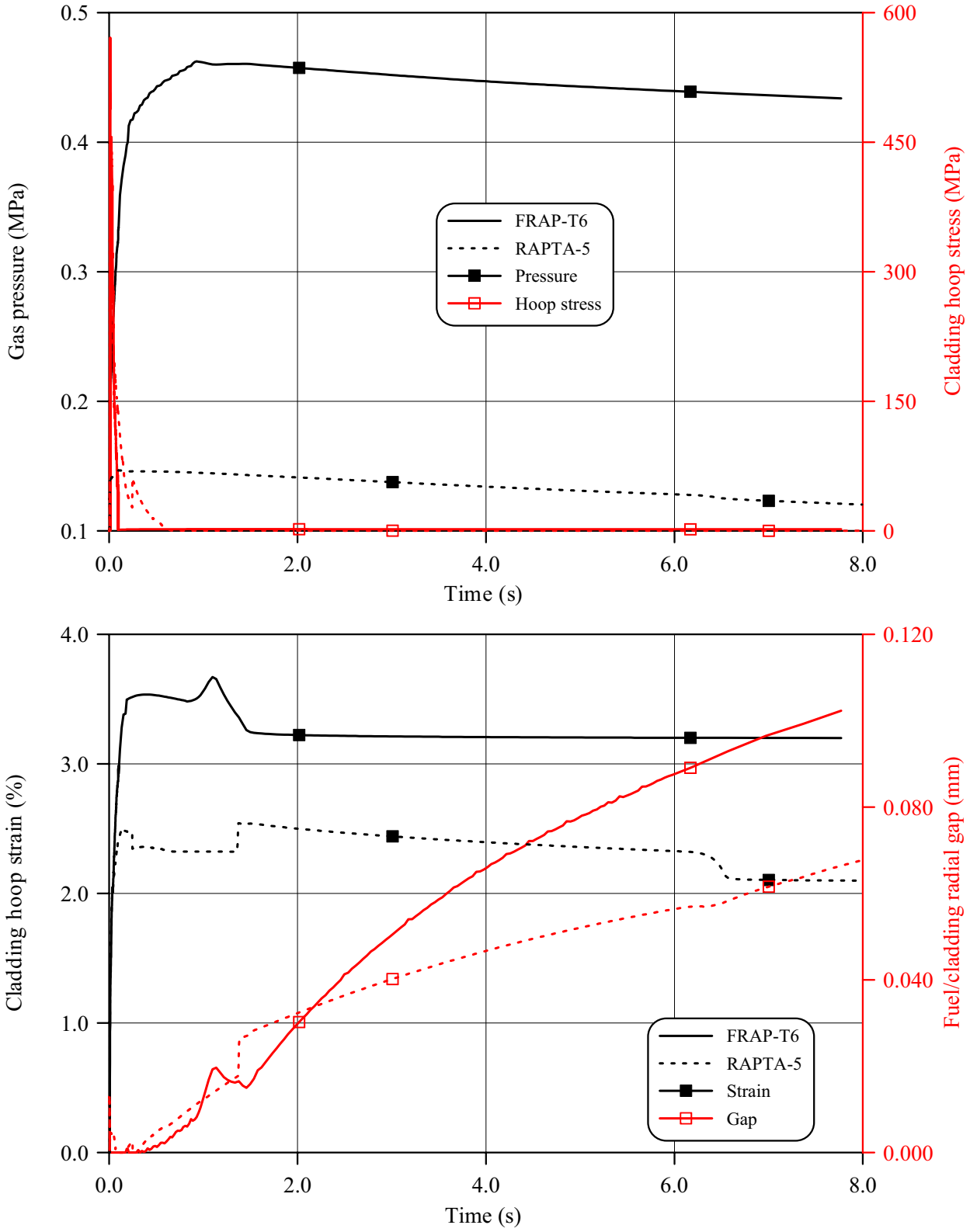


Fig.E-12.7. Mechanical behavior of fuel rod # RT12 during the BIGR test in accordance with FRAP-T6/VVER and RAPTA-5 calculations

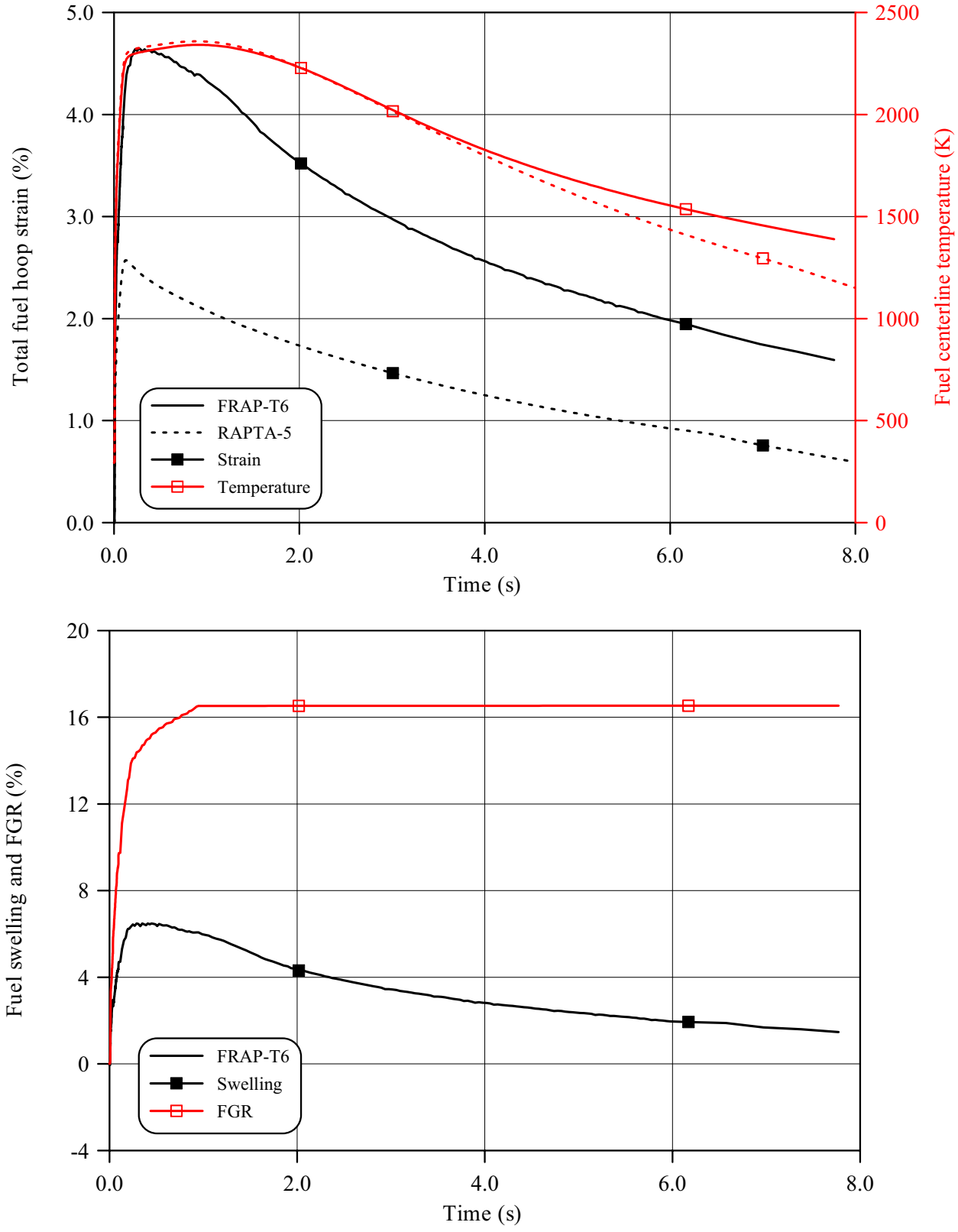


Fig.E-12.8. Fuel behavior during the BIGR test of fuel rod # RT12 in accordance with FRAP-T6/VVER and RAPTA-5 calculations

RT12

Table E-12.3. Axial distribution of cladding average outer diameter in fuel rod # RT12*

Axial coordinate (mm)	Cladding diameter (mm)	Axial coordinate (mm)	Cladding diameter (mm)	Axial coordinate (mm)	Cladding diameter (mm)	Axial coordinate (mm)	Cladding diameter (mm)
24	9.263	62	9.520	100	9.487	138	9.390
26	9.313	64	9.513	102	9.457	140	9.400
28	9.370	66	9.480	104	9.490	142	9.387
30	9.430	68	9.447	106	9.517	144	9.330
32	9.447	70	9.443	108	9.490	146	9.287
34	9.473	72	9.490	110	9.450	148	9.297
36	9.537	74	9.513	112	9.430	150	9.360
38	9.570	76	9.510	114	9.433	152	9.423
40	9.567	78	9.480	116	9.453	154	9.470
42	9.530	80	9.470	118	9.470	156	9.470
44	9.500	82	9.517	120	9.480	158	9.450
46	9.483	84	9.563	122	9.480	160	9.420
48	9.507	86	9.573	124	9.463	162	9.420
50	9.547	88	9.563	126	9.473	164	9.420
52	9.570	90	9.550	128	9.480	166	9.400
54	9.573	92	9.567	130	9.483	168	9.370
56	9.553	94	9.593	132	9.463	170	9.320
58	9.510	96	9.580	134	9.430	172	9.240
60	9.527	98	9.533	136	9.380	174	9.167

* Measured value determined on the basis of profilometry data (16 azimuthal directions)

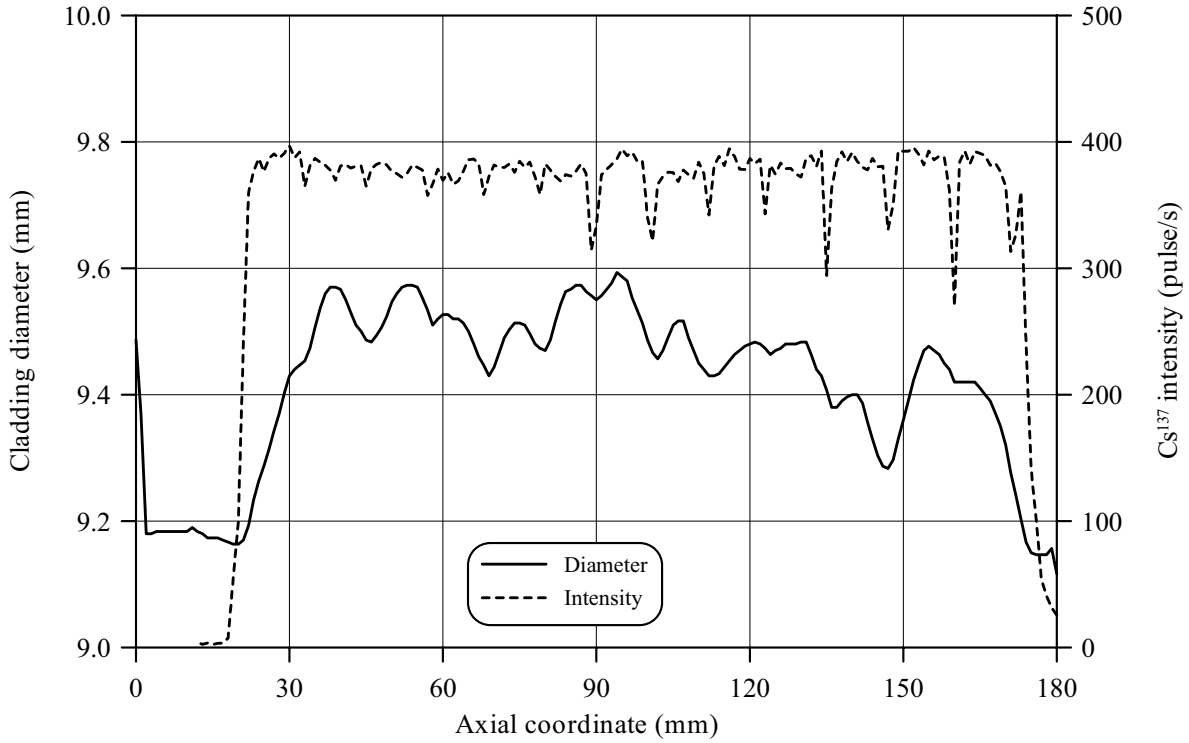


Fig.E-12.9. Cladding measured average diameter and γ-scanning results for fuel rod # RT12

Table E-12.4. The PIE results for fuel rod # RT12

	Parameter	Value
1.	Cladding outer diameter (mm):	
1.1.	Maximum diameter of the bidimensional data sample in "fuel rod length - azimuthal angle" coordinates (mm)	9.60
1.2.	Averaged azimuthal diameter and maximum diameter along the length selected from the sample of averaged azimuthal diameter (mm)	9.59
1.3.	Averaged diameter of the bidimensional data sample in "fuel rod length - azimuthal angle" coordinates (mm)	9.46
2.	Cladding maximum residual hoop strain (%)	5.78
3.	Fuel pellet conditional diameter (mm) in cross-section*:	
	at 54 mm elevation	8.05
4.	ZrO_2 outer thickness (μm) in cross-section:	
	at 54 mm elevation	3–5
5.	ZrO_2 inner thickness (μm) in cross-section:	
	at 54 mm elevation	0
6.	Parameters characterizing FGR:	
6.1.	Gas composition (% by volume):	
	He	35.13
	N_2	0.58
	O_2	0.08
	Ar	0.030
	CO_2	0.100
	Kr	5.78
	Xe	58.30
6.2.	Free gas volume (cm^3)	6.6
6.3.	Gas volume under normal conditions (cm^3)	32.7
6.4.	Gas pressure under normal conditions (MPa)	0.50
6.5.	FGR (%)	22.70

* Reference value determined by the processing of fuel cross-section photographs

RT12

Table E-12.5. Organized BIGR test results for fuel rod # RT12

Parameter		Unit	Value		
			Measured	Calculated	
				FRAP-T6	RAPTA-5
1.	Fuel burnup	MW d/kg U	47.4	47.4	47.4
2.	Initial gas pressure	MPa	0.1	0.1	0.1
3.	Energy deposition	cal/g fuel	198.1	198.1	198.1
4.	Peak fuel enthalpy*	cal/g fuel	-	154.7	154.9
5.	Fuel maximum temperature	K	-	2472	2466
6.	Maximum temperature of cladding outer surface	K	-	1180	1249
7.	Cladding burst	Failed, Unfailed	Unfailed	-**	-**
8.	Cladding residual hoop strain				
	- average***	%	4.35	3.11	2.54
	- maximum	%	5.78	3.11	2.54

* Average value of peak fuel enthalpy 154.8 cal/g fuel

** This parameter was not calculated

*** Average value along the fuel stack length

Appendix E–13

Azimuthal Distribution of Cladding Thickness for Fuel Rods

RT7–12

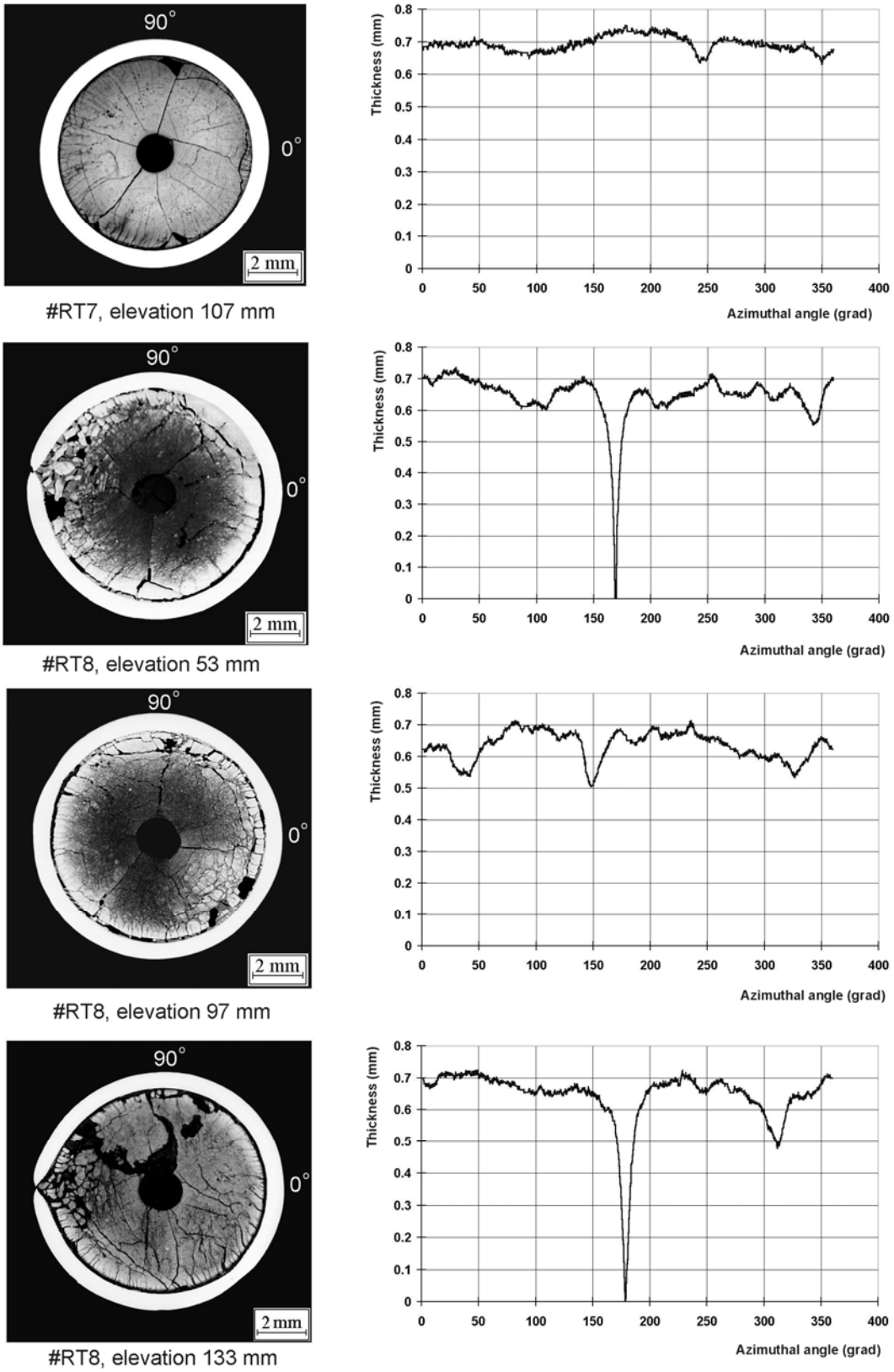


Fig.E-13.1. Cross-section and azimuthal distribution of cladding thickness in fuel rods ## RT7, 8 after the BIGR tests

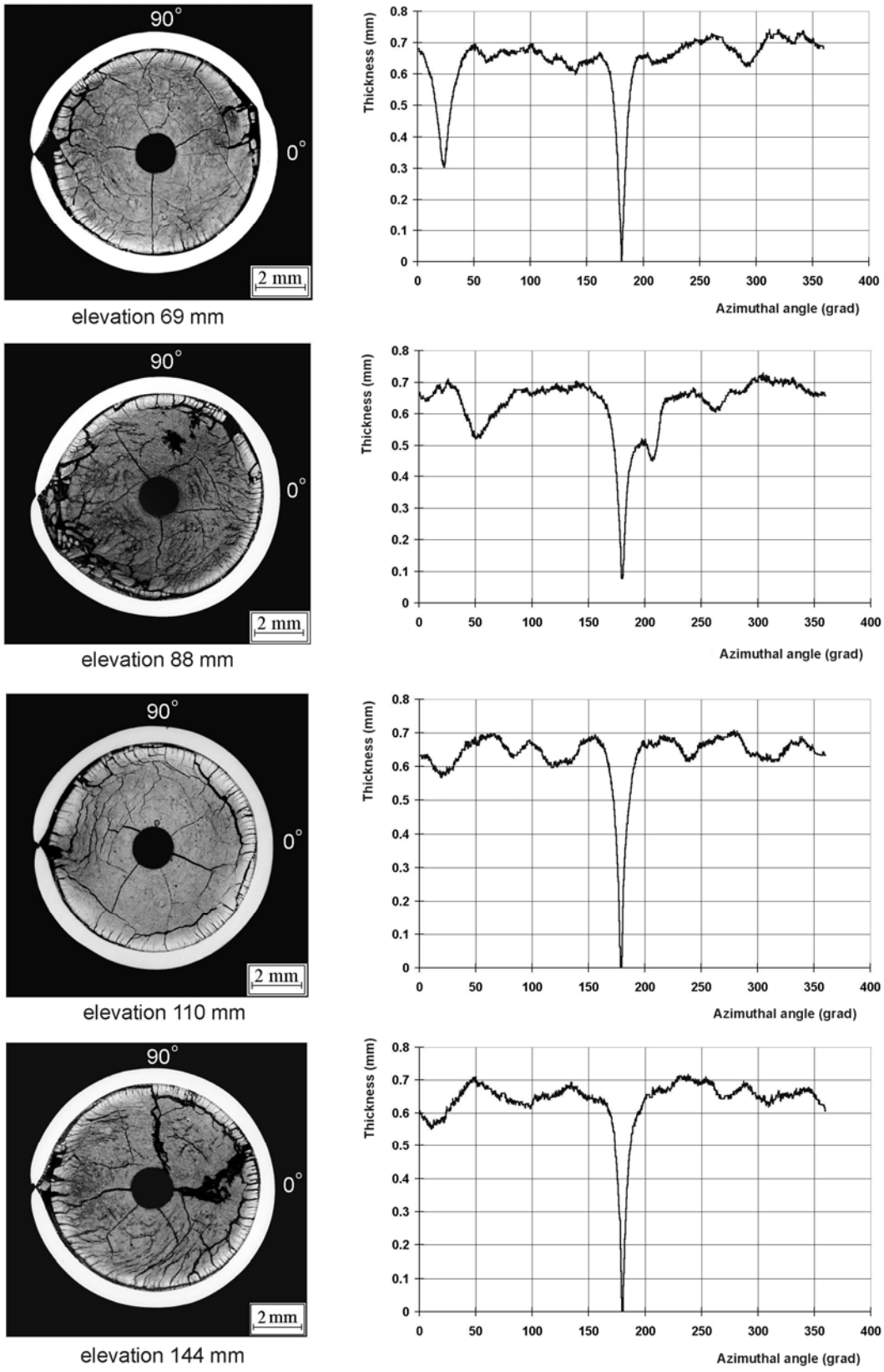


Fig.E-13.2. Cross-section and azimuthal distribution of cladding thickness in fuel rod # RT9 for different elevations after the BIGR tests

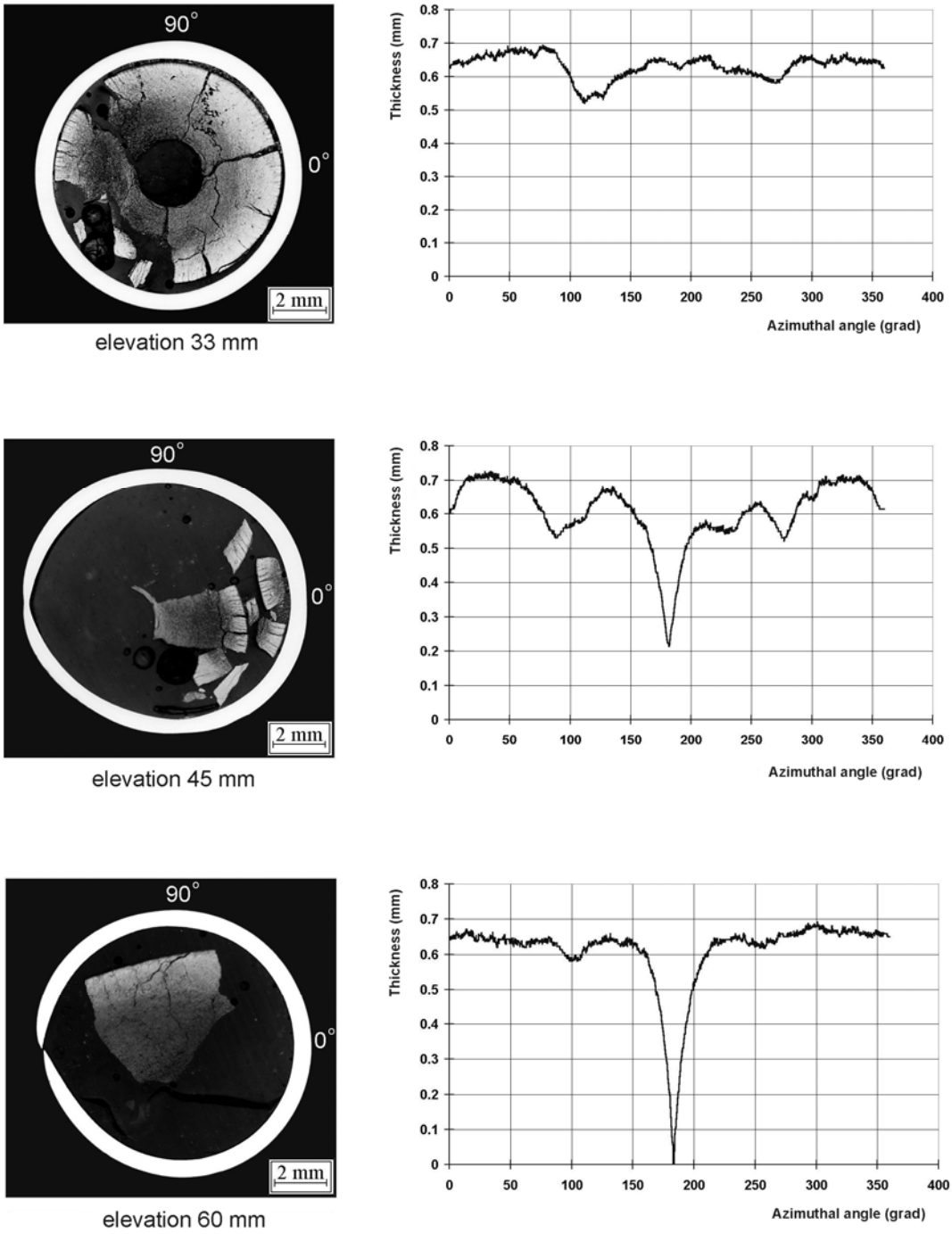
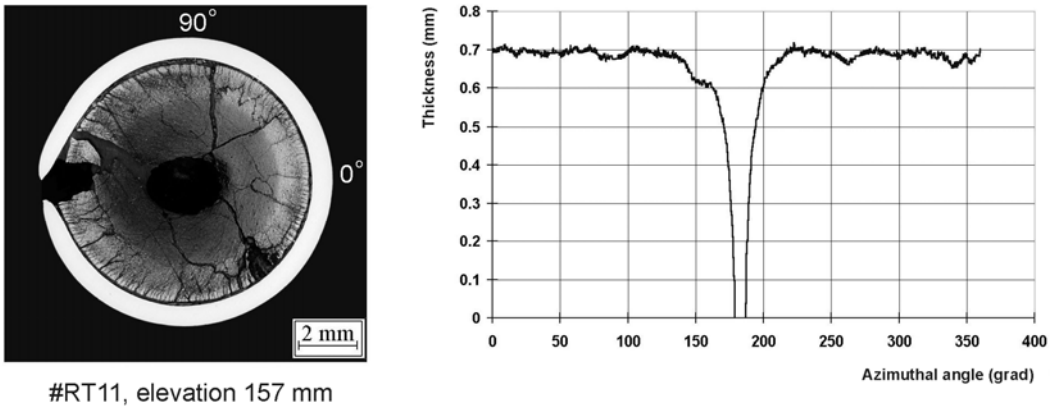
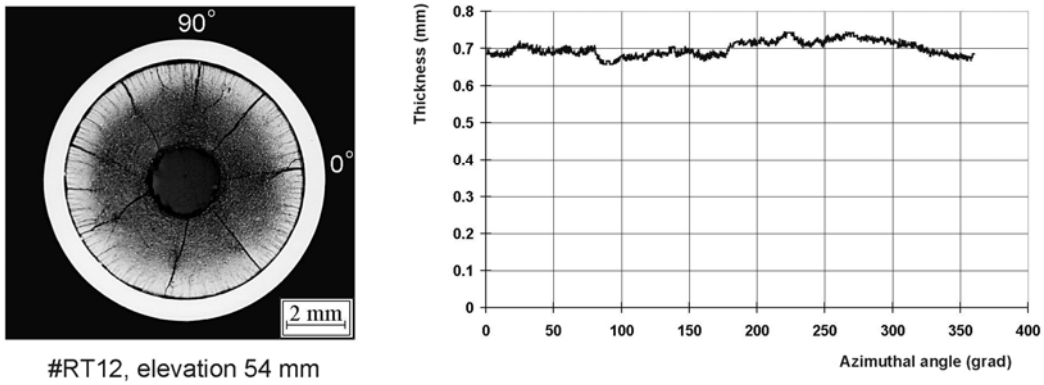


Fig.E-13.3. Cross-section and azimuthal distribution of cladding thickness in fuel rod # RT10 for different elevations after the BIGR tests



#RT11, elevation 157 mm



#RT12, elevation 54 mm

Fig.E-13.4. Cross-section and azimuthal distribution of cladding thickness in fuel rods ## RT11, 12 after the BIGR tests

NRC FORM 335 (9-2004) NRCMD 3.7

U.S. NUCLEAR REGULATORY COMMISSION

BIBLIOGRAPHIC DATA SHEET

(See instructions on the reverse)

1. REPORT NUMBER
(Assigned by NRC, Add Vol., Supp., Rev., and Addendum Numbers, if any.)

NUREG/IA-0213, Vol. 2
IRSN/DPAM 2005-275
NSI RRC KI3230

2. TITLE AND SUBTITLE

Experimental Study of Narrow Pulse Effects on the Behavior of High Burnup Fuel Rods with Zr-1%Nb Cladding and UO2 Fuel (VVER Type) under Reactivity-Initiated Accident Conditions: Test Conditions and Results

3. DATE REPORT PUBLISHED

MONTH	YEAR
March	2006

4. FIN OR GRANT NUMBER

Y6723

5. AUTHOR(S)

L. Yegorova, K. Lioutov, N. Jouravkova
O. Nechaeva, A. Salatov
V. Smirnov, A. Goryachev
V. Ustinenko, I. Smirnov

6. TYPE OF REPORT

International Agreement

7. PERIOD COVERED *(Inclusive Dates)*

8. PERFORMING ORGANIZATION - NAME AND ADDRESS *(If NRC, provide Division, Office or Region, U.S. Nuclear Regulatory Commission, and mailing address; if contractor, provide name and mailing address.)*

Nuclear Safety Institute of Russian Research Centre "Kurchatov Institute" Moscow, Russian Federation
A.A. Bochvar All-Russian Research Institute of Inorganic Materials Moscow, Russian Federation
State Research Centre "Research Institute of Atomic Reactors" Dimitrovgrad, Russian Federation
Russian Federal Nuclear Centre "All-Russian Research Institute of Experimental Physics" Sarov, Russian Federation

9. SPONSORING ORGANIZATION - NAME AND ADDRESS *(If NRC, type "Same as above"; if contractor, provide NRC Division, Office or Region, U.S. Nuclear Regulatory Commission, and mailing address.)*

Division of Systems Analysis and Regulatory Effectiveness
Office of Nuclear Regulatory Research
U.S. Nuclear Regulatory Commission
Wasington, DC 20555-0001

10. SUPPLEMENTARY NOTES

11. ABSTRACT *(200 words or less)*

This report contains a detailed description of calculation and test results obtained in the fast-pulse graphite-reactor (BIGR) tests of twelve fuel rods refabricated from the VVER-440 and VVER-1000 high burnup fuel elements (50 - 60 MWd/kgU).

12. KEY WORDS/DESCRIPTORS *(List words or phrases that will assist researchers in locating the report.)*

BIGR
Cladding
E110
Kurchatov Institute
Nuclear Fuel
Reactivity-Initiated Accident
Russian
Zirconium

13. AVAILABILITY STATEMENT

unlimited

14. SECURITY CLASSIFICATION

(This Page)
unclassified

(This Report)
unclassified

15. NUMBER OF PAGES

16. PRICE

PRINTED ON RECYCLED PAPER



Federal Recycling Program